

A PROBABILISTIC APPROACH TO THE
STABILITY OF ROCK SLOPES

by

EDWARD FRANCIS GLYNN

BCE, Villanova University
Villanova, Pennsylvania
(1969)

MSCE, Northeastern University
Boston, Massachusetts
(1972)

SUBMITTED IN PARTIAL FULFILLMENT
OF THE REQUIREMENTS FOR THE
DEGREE OF

DOCTOR OF PHILOSOPHY

at the

MASSACHUSETTS INSTITUTE OF TECHNOLOGY

September 1978

G.E. February 1971

Signature of Author.....
Department of Civil Engineering, September, 1978

Certified by.. Thesis Supervisor.....
n / - / / /

Accepted by.. Chairman, Department Committee on Graduate
Students of the Department of Civil Engineering

ARCHIVES

MASSACHUSETTS INSTITUTE
OF TECHNOLOGY

JUL 12 1979

LIBRARIES

A PROBABILISTIC APPROACH TO THE
STABILITY OF ROCK SLOPES

by

EDWARD FRANCIS GLYNN

Submitted to the Department of Civil Engineering
on September 18, 1978 in partial fulfillment of the
requirements for the Degree of Doctor of Philosophy

ABSTRACT

Probabilistic analyses provide an alternate approach to assessing the stability of rock slopes. In a probabilistic or reliability analysis the integrity of the slope is expressed as its probability of failure rather than its factor of safety. The primary advantage of reliability techniques is that they explicitly consider the uncertainty associated with engineering parameters.

There are a number of probabilistic techniques currently available; however, none of them provide a comprehensive treatment of the problem. This thesis presents a new method that eliminates some of the earlier limitations. In particular, the thesis concentrates on a few specific points and develops some tools to use in examining rock slope stability from a probabilistic standpoint.

The thesis presents a procedure that enables one to use the data from joint surveys i.e., the probability density functions (pdf's) of joint orientation to derive the pdf's of parameter that characterize the shape and orientation of possible rock wedges bounded by the joints.

The thesis developed an improved analytical model which describes the failure mode that consists of sliding along both joint planes. The model examines the influence of both in situ stresses and joint stiffnesses. It establishes the relationship between the two effects and extends the concepts to cover asymmetric wedges.

The thesis also presents a possible solution to one of the major unsolved problems in rock stability—joint persistence. The stochastic model developed in Chapter 5 provides a rational method for treating joint persistence. It uses Monte Carlo simulation to generate jointing patterns and then analyzes each pattern to identify the weakest failure path. The strength of the rock mass is characterized by a random "apparent persistence" parameter that can be used in probabilistic stability calculations.

Name and Title of Thesis Supervisor: Herbert H. Einstein
Associate Professor of Civil Engineering

ACKNOWLEDGEMENTS

I would like to extend my deepest gratitude to Professor Herbert Einstein who made this thesis a truly educational experience for me. Professor Einstein's patience and encouragement will be remembered long after the details of our work have been forgotten

I would also like to thank Professor Gregory Baecher for his discussions on applied probability and to Professor Daniele Veneziano for his assistance in the joint persistence model.

Elizabeth Manzi typed the final manuscript of the thesis and David MacNeill drafted most of the figures. I appreciate the long nights they spent in helping me meet my deadlines.

I want to thank my parents who as educators themselves taught me to appreciate the value of a good education.

Most of all, I would like to thank my wife Maggie for her untiring patience and assistance during my graduate studies.

Table of Contents

	<u>Page</u>
TITLE PAGE.	1
ABSTRACT.	2
ACKNOWLEDGEMENTS.	3
TABLE OF CONTENTS	4
LIST OF TABLES.	8
LIST OF FIGURES	9

Table of Contents

	<u>Page</u>
CHAPTER 1: INTRODUCTION.	16
1.0 Scope of Thesis	16
1.1 Outline of Thesis	17
CHAPTER 2: ROCK SLOPE RELIABILITY ANALYSIS: STATE OF THE ART.	20
2.0 Introduction.	20
2.1 Graphical Techniques.	24
2.2 Monte Carlo Simulations	35
2.3 Composite Models.	44
2.4 Stochastic Models	54
2.5 Summary	66
CHAPTER 3: KINEMATIC CONDITIONS -- COMPUTER PROGRAM DAYLITE	69
3.0 Introduction.	69
3.1 General Features of DAYLITE	71
3.2 Detailed Description of DAYLITE	82
3.2.1 Defining the Critical Zone	82
3.2.2 Partitioning the Critical Zone	83
3.2.3 Defining the Girdle.	88
3.2.4 Dividing the Girdle into Components.	90
3.2.5 Calculating $P [X_i]$	96
3.2.6 Identifying Wedges	97
3.2.7 Calculating $P [(\theta_o, \phi_o, \psi_o, (\beta_1)_o)]$	101

Table of Contents

	<u>Page</u>
3.3 Program Information.	103
CHAPTER 4: KINETIC CONDITIONS -- COMPUTER PROGRAM SWARS-2PM.	
4.0 Introduction	105
4.1 State of the Art - Stiffness and Stress Effects	107
4.2 Generalization of the Stiffness Approach	124
4.3 Stress Approach vs. Stiffness Approach	149
4.3.1 Introduction.	149
4.3.2 Detailed Discussion	152
4.4 The Factor of Safety	160
4.5 Computer Program SWARS-2PM	173
4.6 Computer Program SWARS-2MC	178
CHAPTER 5: INTERACTION BETWEEN DISCONTINUITIES AND INTACT ROCK -- COMPUTER PROGRAM JOINTSIM	
5.0 Introduction	179
5.1 General Features--Probabilistic Approach to Resistance of Jointed Rock	183
5.2 Stochastic Model of Joint Geometry	184
5.3 Mechanical Model	199
5.4 Computer Program JOINTSIM.	209
5.5 Results.	211
5.6 Summary.	221

Table of Contents

	<u>Page</u>
CHAPTER 6: AN INTEGRATED APPROACH TO RELIABILITY ANALYSIS.	224
6.0 Introduction.	224
6.1 Kinematic Restraints: $P[\theta_i, \phi_i]$	226
6.2 Kinetic Restraints: $P[U_i \theta_i, \phi_i]$	228
6.3 Calculating \bar{P}_f	235
6.4 Calculating P_f	236
6.5 Summary	245
CHAPTER 7: SUMMARY AND CONCLUSIONS	247
References.	252
Appendix A Spherical Distributions	257
Appendix B Two Problems in Vector Algebra.	278
Appendix C Computer Program DAYLITE.	289
Appendix D A Generalization of the Stiffness Approach.	316
Appendix E Computer Program SWARS-2PM.	328
Appendix F Computer Program SWARS-2MC.	363
Appendix G Strength Derivations for Mechanical Model.	395
Appendix H Computer Program JOINTSIM	426
Appendix I Sample Problem.	464

LIST OF TABLES

<u>Table</u>	<u>Title</u>	<u>Page</u>
5.1	Inputs to Computer Program JOINTSIM	210
A.1	Numerical Approximation of $f(\phi)$	263
A.2	Summary of Distributions	277

LIST OF FIGURES

<u>Fig. No.</u>	<u>Title</u>	<u>Page</u>
2.1	Sliding on a Single Plane	25
2.2	Kinematic Test for Sliding	26
2.3	Areas of Kinematic Instability on Stereonet	28
2.4	Kinetic Test for Sliding	29
2.5	Critical Zone for Sliding	31
2.6	Calculation of β_c	34
2.7	Probability of Failure	36
2.8	Use of Probability Density Function in Monte Carlo Simulation	37
2.9	Rock Slope Stability by Monte Carlo Simulation	39
2.10	Sample Problem--Major <u>et al.</u>	41
2.11	Marek & Savely Model	46
2.12	Call & Kim Model	48
2.13	Serrano & Castillo Model	51
2.14	Typical Results--Serrano & Castillo Model	53
2.15	Call & Nicholas Model--Definitions	56
2.16	Call & Nicholas Model--General Features	58
2.17	Baecher <u>et al.</u> Model	62
2.18	Veneziano Model	64
3.1	Critical Zone for Kinematic Instability	70
3.2	Flowchart for DAYLITE	73
3.3	Critical Zone Partitioned into Equal Area Cells	75
3.4	Two Intersecting Planes	76

LIST OF FIGURES

<u>Fig. No.</u>	<u>Title</u>	<u>Page</u>
3.5	Definition of ψ	77
3.6	Reference Cell and Its Girdle	78
3.7	Typical Girdle	80
3.8	Reduction of Critical Zone with α	84
3.9	Areas of Spherical Segments--Definition of δ	86
3.10	Spherical Segment Partitioned into Equal Area Cells	89
3.11	Meridonal vs. Polar Projection	91
3.12	Definition of δ	92
3.13	Location of I_0 on Polar Plane--Definition of η	94
3.14	Typical Component of Girdle	95
3.15	Renumbering of Characteristic Points on Girdle	98
4.1	Sliding Wedge--Reactions Perpendicular to the Joint Planes	108
4.2	Resolution of Weight Vector into Components	109
4.3	Force Diagram--Reactions Perpendicular to Joint Planes	110
4.4	Symmetric Wedge--Reactions with Components Tangent to Joint Planes	112
4.5	ϕ Required for FS = 1.0 vs. β	114
4.6	Stresses on Differential Area of the Joint Plane	116
4.7	Mohr Stress Circle for the Stress State Shown in Figure 4.6	118
4.8	<u>(FS) neglecting K</u> <u>(FS) including K</u> vs. β	120

LIST OF FIGURES

<u>Fig. No.</u>	<u>Title</u>	<u>Page</u>
4.9	Mohr Stress Circles for Active and Passive Cases	122
4.10	Generalized Stiffness Approach--Known Parameters	125
4.11	Generalized Stiffness Approach--Unknown Parameters	127
4.12	Notch in Infinite Slope	130
4.13	Wedge With Geometrically Similar Cross Sections	132
4.14	Direction of Displacement When $k_{1n} = k_{2n} \gg k_{1s} = k_{2s}$	135
4.15	Parameters Varied in Sensitivity Analyses	136
4.16	ϕ_R vs. β_1 For $\psi = 90^\circ$	138
4.17	ϕ_R vs. β For $\psi = 120^\circ$	140
4.18	ϕ_R vs. β For $\psi = 60^\circ$	141
4.19	Overhanging Joint Plane	142
4.20	R vs. β_{1cr} For $\psi = 60^\circ$	143
4.21	ϕ_R vs. β_1 For $\psi = 60^\circ$ and R = 1--Curves Reflect Different Reactions on Joint Plane 2	145
4.22	$\Delta\phi_{max}$ vs. ψ For $\theta = 45^\circ$	147
4.23	ϕ_R vs. β_1 For $\psi = 90^\circ$ and Varying S	148
4.24	Load, Stiffness and Stress vs. Time	151
4.25	Stiffness Approach--Idealized Case	153
4.26	Stresses on Differential Areas of the Joint Planes	156
4.27	Shear Forces on Joint Planes	161
4.28	$F_3/\tan \phi$ vs. K; $\beta_1 = 30^\circ$	164

LIST OF FIGURES

<u>Fig. No.</u>	<u>Title</u>	<u>Page</u>
4.29	$F_3/\tan \phi$ vs. K ; $\beta_1 = 45^\circ$	165
4.30	Schematic Failure Sequence	167
4.31	General Case-- \bar{D} and \bar{R} Not Parallel	171
4.32	A, B, C Coordinate System	175
4.33	Cross Section Perpendicular to \bar{A}	176
5.1	Typical Failure Surface	180
5.2	Persistence--Jennings' Relations	181
5.3	"En Echelon" Failure Surface	182
5.4	Coordinate System and Typical Jointing Pattern	185
5.5	Stochastic Model of Joint Geometry	186
5.6	Definitions of ψ_i , Ω_i , and d_i	188
5.7	Stochastic Model--Primary Process-- R^1 and R^2 Spaces	189
5.8	Stochastic Model--Primary Process-- P^3	191
5.9	Definition of f_i and Γ_i	192
5.10	Stochastic Model--Secondary Process-- R^1 and R^2 Spaces	194
5.11	Angles of Intersection Between Poisson Lines and an Arbitrary Line	195
5.12	Length of Joint Segment (Secondary and Tertiary Processes)	197
5.13	Typical Failure Paths	200
5.14	Principle of Minimum Resistance	202
5.15	Strength Determination--Path Through Intact Rock	204

LIST OF FIGURES

<u>Fig. No.</u>	<u>Title</u>	<u>Page</u>
5.16	Strength Determination--Path Along Joint Segment	206
5.17	% "En Echelon" Failures vs. σ	213
5.18	Histograms of Maximum Persistence and Apparent Persistence	216
5.19	Apparent Persistence vs. Magnitude of Stress	217
5.20	Apparent Persistence vs. Original Stress Ratio	218
5.21	Apparent Persistence vs. Inclination Angle	220
6.1	Typical Output from DAYLITE	227
6.2	Definition of H	230
6.3	Intersecting Poisson Planes--Derivation of $f_H(H)$	231
6.4	Influence of Slope Boundary	233
6.5	System Reliability of Slope	238
6.6	Derivation of $F_X(x)$ and $F_Y(y)$	242
6.7	Closely Spaced Joints From Set 1-- Correlation Between x's	244
A.1	Coordinate System For Joint Orientation	258
A.2	Spherical Surface Areas	259
A.3	Surface Area of a Spherical Segment	261
A.4	$f(\phi)$ vs. ϕ for the Uniform Distribution	264
A.5	Uniform Distribution	266
A.6	$f(\eta)$ vs. η for the Fisher Distribution	268
A.7	Fisher Distribution ($k = 5$)	269

LIST OF FIGURES

<u>Fig. No.</u>	<u>Title</u>	<u>Page</u>
A.8	Bingham Distribution ($k_1 = -5; k_2 = -3$)	272
A.9	Dershowitz Distribution ($k_1 = 5; k_2 = 3$)	274
A.10	Bivariate Normal Distribution--Projection on Plane	275
B.1	Definition of η	279
B.2	Law of Sines For Spherical Triangles	280
B.3	Derivation of z	282
B.4	Location of Points B, D and E	285
C.1	Definitions of θ and ϕ	290
C.2	Definitions of Ψ and β_1	291
C.3	Orientation of X, Y and Z Axes	293
D.1	Generalized Stiffness Approach--Known Parameters	317
D.2	Generalized Stiffness Approach--Unknown Parameters	319
D.3	Displacements--Left Joint	320
D.4	Displacements--Right Joint	322
E.1	Model Slope	330
E.2	Parameters For Rock Bolt Option	339
F.1	Model Slope	368
F.2	Definitions of Ψ and β_1	375
G.1	Failure Conditions--Intact Rock	396
G.2	Limitation on the Maximum Value of θ	398
G.3	Definition of γ	399
G.4	Circle With Dual Tangency	402
G.5	Failure Envelope With a Cusp	406

LIST OF FIGURES

<u>Fig. No.</u>	<u>Title</u>	<u>Page</u>
G.6	Failure Circle Tangent to Linear Envelope	408
G.7	Failure Circle Tangent to Parabolic Envelope at $\sigma = -a/2$ and $\tau = 0$	411
G.8	Failure Circle Touching Cusp	417
G.9	Failure Conditions--Joint	423
G.10	Typical Failure Circle for Joint	424
H.1	Coordinate System for JOINTSIM	427
H.2	Definition of DMIN	433

CHAPTER 1

INTRODUCTION

1.0 Scope of Thesis

The idea of analyzing the stability of rock slopes in a probabilistic framework is not new. McMahon developed a practicable approach in the early 1970's. His original model had a relatively limited range of applicability but it did introduce the notion of using the probability of failure rather than the factor of safety in rock slope stability analyses. Reliability techniques are now gaining popularity as their sophistication and range of applicability increases. As will be discussed in Chapter 2, the current models use a number of different approaches. Some combine deterministic models with Monte Carlo simulation so that some of the input parameters can be treated as random variables. Other models treat stability as a stochastic process that can be described mathematically. At the present time there is a wide gap between the two contrasting approaches. This thesis endeavors to establish an intermediate approach that is basically stochastic but does use Monte Carlo simulation to treat aspects of the problem that cannot presently be modeled stochastically.

A rigorous analysis should consider every aspect of the problem including the correlation among random variables and the interaction of failure bodies in the slope. It should also consider all possible modes of failure; toppling and

rotation as well as sliding should be examined. Some of the problems like correlation are probabilistic. Others like toppling are largely mechanical. None of these problems are well understood at the present time; furthermore, they may remain so for many years to come. This thesis does not address all the above problems but concentrates on a number of specific points. In particular, it presents a computer program that enables one to determine the shape and orientation of tetrahedral wedges through a numerical integration technique that uses the probability density functions of joint plane orientations. It also presents a detailed description of the mechanics of the failure mode that involves sliding along two planes. The mechanical model is incorporated into two computer programs that analyze the stability of wedges deterministically and probabilistically. The thesis introduces the concept of "apparent persistence" to characterize the shearing resistance of an echelon joint sets. Finally, the thesis shows how the individual techniques can be combined into a complete reliability analysis.

1.1 Outline of Thesis

The structure of the thesis reflects the same fundamental principle that underlies virtually all rock slope stability analyses. Slope stability is essentially a problem in discontinuum mechanics wherein both the wedge and its parent rock mass are treated as rigid bodies. Two conditions must

be met before failure can occur:

1. The wedge must be oriented in such a manner that movement towards a free face is physically possible - a kinematic condition.
2. The destabilizing forces must exceed the stabilizing forces - a kinetic condition.

The idea that failure depends on both the kinematic and kinetic conditions is reiterated throughout the thesis.

Chapter 2 presents a brief introduction to the concept of reliability analysis. It also reviews the state of the art of reliability analysis as applied to rock slope stability.

Chapter 3 discusses the kinematic aspects of the stability problem. It describes the computer program DAYLITE that enables the user to determine the probability density function of the orientation and shape of possible failure wedges.

Chapter 4 discusses the kinetic aspects of the stability problem. In particular, it discusses how the deterministic model for computing the factor of safety can be improved by incorporating joint stiffnesses and in situ lateral stresses into the analysis. The chapter presents two computer programs: SWARS-2PM, a modified version of SWARS-2P that includes the effects of joint stiffness and in situ stresses; and SWARS-2MC, a probabilistic version of SWARS-2PM that treats the input parameters as random variables through Monte Carlo simulation.

Chapter 5 presents a stochastic model that simulates the resistance of "en echelon" joints. It characterizes the resistance of jointed rock through an "apparent persistence"

parameter. This apparent persistence can be input directly into stability calculations.

Chapter 6 shows how the techniques described in Chapters 3 to 5 can be integrated into a complete reliability analysis. As indicated in Section 1.1, there are still many aspects of the analysis that are difficult to evaluate. The chapter outlines the limitations of the proposed analysis and notes the steps in the analysis that require additional refinement.

Chapter 7 presents a summary and conclusions.

CHAPTER 2

ROCK SLOPE RELIABILITY ANALYSIS: STATE OF THE ART

2.0 Introduction

The term "reliability analysis" is a relatively recent addition to the rock mechanics vocabulary. Engineers working in rock mechanics, like their counterparts in soil mechanics, are becoming aware of the advantages of using reliability theory. Unlike conventional approaches, reliability analyses explicitly consider the uncertainty associated with engineering judgments. The integrity of a structure is expressed in terms of its probability of failure rather than its factor of safety. Engineering parameters such as shear strength or pore pressure are treated as random variables i.e., quantities characterized by probability distributions.

The use of probability is not a totally radical departure from traditional approaches. Joint orientation data have always been analyzed statistically. Contour diagrams of joint poles correspond to probability density functions portrayed on a projected surface of a hemisphere. A deterministic analysis would be concerned primarily with the modal or central values of the distributions. The contour plots would serve to identify the modal values and perhaps influence the selection of a design factor of safety. (Diffuse diagrams may dictate a more conservative design criterion.) On the other hand, a probabilistic analysis would incorporate the dispersion or uncertainty of the

orientation data directly into the calculations.

Reliability theory is a useful tool in treating the innate variability of natural materials. It may prove to be even more valuable in examining another important source of uncertainty--incomplete information on design parameters. An engineer seldom has enough data to thoroughly describe all the inputs to his analysis. The shear strength parameters are frequently estimated from a limited number of tests. The location of the phreatic surface may be based on a very brief observation period. This same type of uncertainty pervades almost all the parameters on which an engineer predicates his design. In a reliability analysis he can quantify this uncertainty and treat the parameters as random variables with estimated probability density functions. The probability of failure will reflect the natural variability of material as well as the engineer's subjective assessment of parameters with scant data bases*.

The problem of rock slope stability provides an ideal subject for reliability studies. Most of the critical parameters such as joint persistence and cleft water pressures are difficult to evaluate deterministically. These parameters must be considered random variables to arrive at any realistic

* The distinction between natural variability and estimation error is a matter of interpretation. Natural variability can be considered a measure of the error associated with estimating the value of a parameter at a specific point. Theoretically, one could evaluate the parameter at every point and eliminate natural variability. Engineering analyses are based on a limited amount of data and should consider estimation error.

conclusions concerning the stability of a rock slope. A number of individuals have recognized the promise of such an approach and formulated probabilistic models. Most of the current models are relatively crude with limited applicability. These models may, however, form the foundations for more sophisticated versions.

The current models can be grouped into four broad categories:

Graphical Techniques

Monte Carlo Simulations

Composite Models

Stochastic Models

The groupings are rather arbitrary. Most of the models are based on the same fundamental principles and they share many features. The groupings serve primarily as a convenience to emphasize the similarity of certain models.

Many of the models are quite innovative. They can treat parameters like joint spacing or analyze stepped failure surfaces--effects which are difficult to assess deterministically. However, none of the current models provide a complete solution to slope stability problems. The question of which one to use in a particular situation is largely a matter of personal preference.

In examining the models one should evaluate them with respect to some objective criteria. An ideal model should fulfill three requirements:

Practicality The model should rely on input data which can be obtained from reasonably simple and inexpensive field surveys or laboratory techniques.

Rigorousness The model should be mathematically and probabilistically consistent. All bias in the input should be systematically eliminated. Correlation among the random variables should be explicitly considered.

Completeness The model should recognize the three-dimensional nature of rock wedges and investigate all possible modes of failure. It should be capable of handling diverse ground water conditions and wedge geometries.

None of the present models satisfy all the criteria. In fact no one is preeminent in all three categories. Most of them strike a compromise between practicality and rigorousness.

This section will examine a number of models or techniques. The discussions will highlight the advantages and limitations of each method. They will emphasize the probabilistic aspects of the models because engineers familiar with deterministic analyses may not be aware of the subtle probabilistic assumptions inherent to each model.

2.1 Graphical Techniques

McMahon (1971, 1974, 1975) has done an extensive amount of work in this field. His method is best suited for dry slopes where sliding occurs along a single discontinuity. The model does not require plane strain conditions. It can be used in cases where the strike of the joint plane is not parallel to the strike of the open face as long as there are tension joints present to isolate blocks and permit sliding along the major joints (Figure 2.1).

The technique developed by McMahon uses a lower hemisphere equal-area projection. The two critical steps in the analysis are to establish regions of kinematic and kinetic stability in the projection. The kinematic tests indicate whether a block is physically capable of movement. They consider the orientations of the joints relative to the slope. The kinetic tests indicate whether the driving forces exceed the resisting forces. They consider the shear strength of individual joints.

A block will not slide along a plane unless the line representing its direction of movement daylights on the slope. Figure 2.2 illustrates this concept for joint planes parallel (same strike) to the slope. Only those joints whose poles lie between A and B are joints on which movement can occur. The same type of analysis can be performed on any family of joints that share the same strike. In each case the locus of kinematically unstable joints includes all joints whose dip is undercut by the slope. (The analysis implicitly assumes

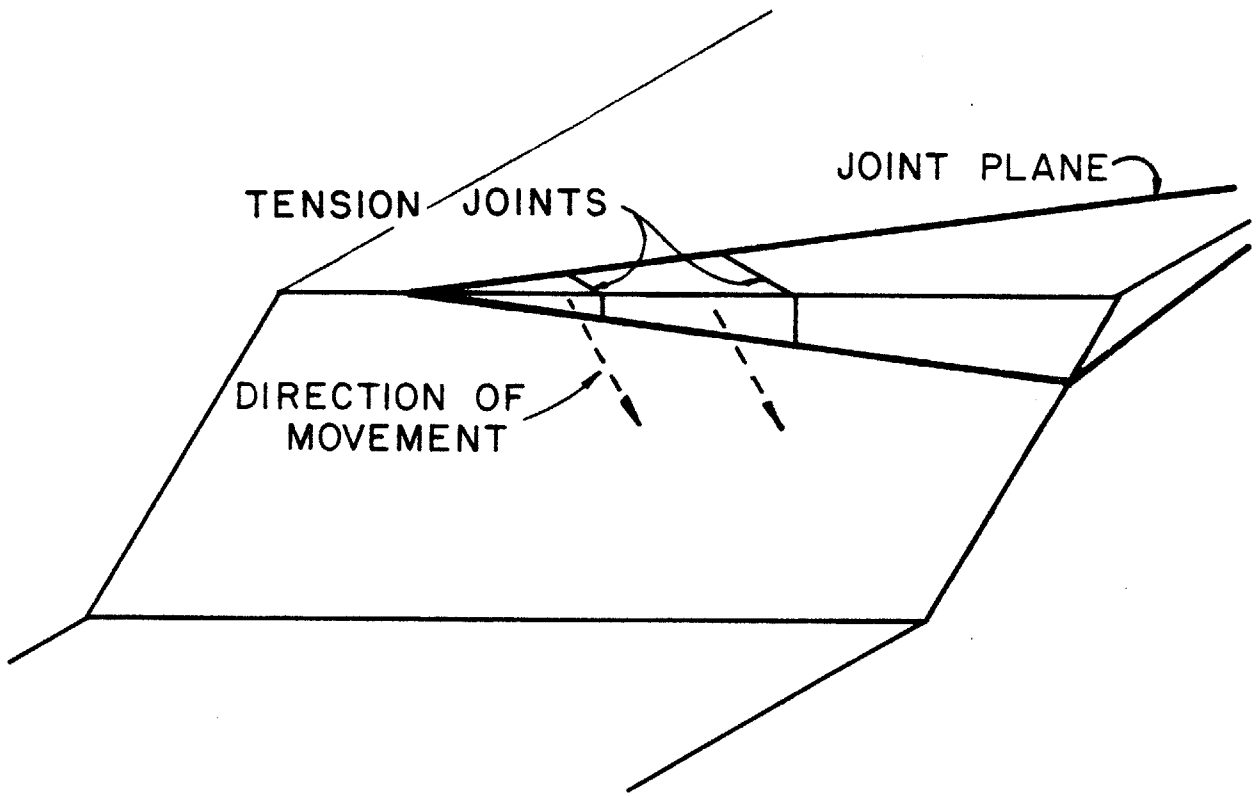


Figure 2.1 Sliding on a Single Plane
25

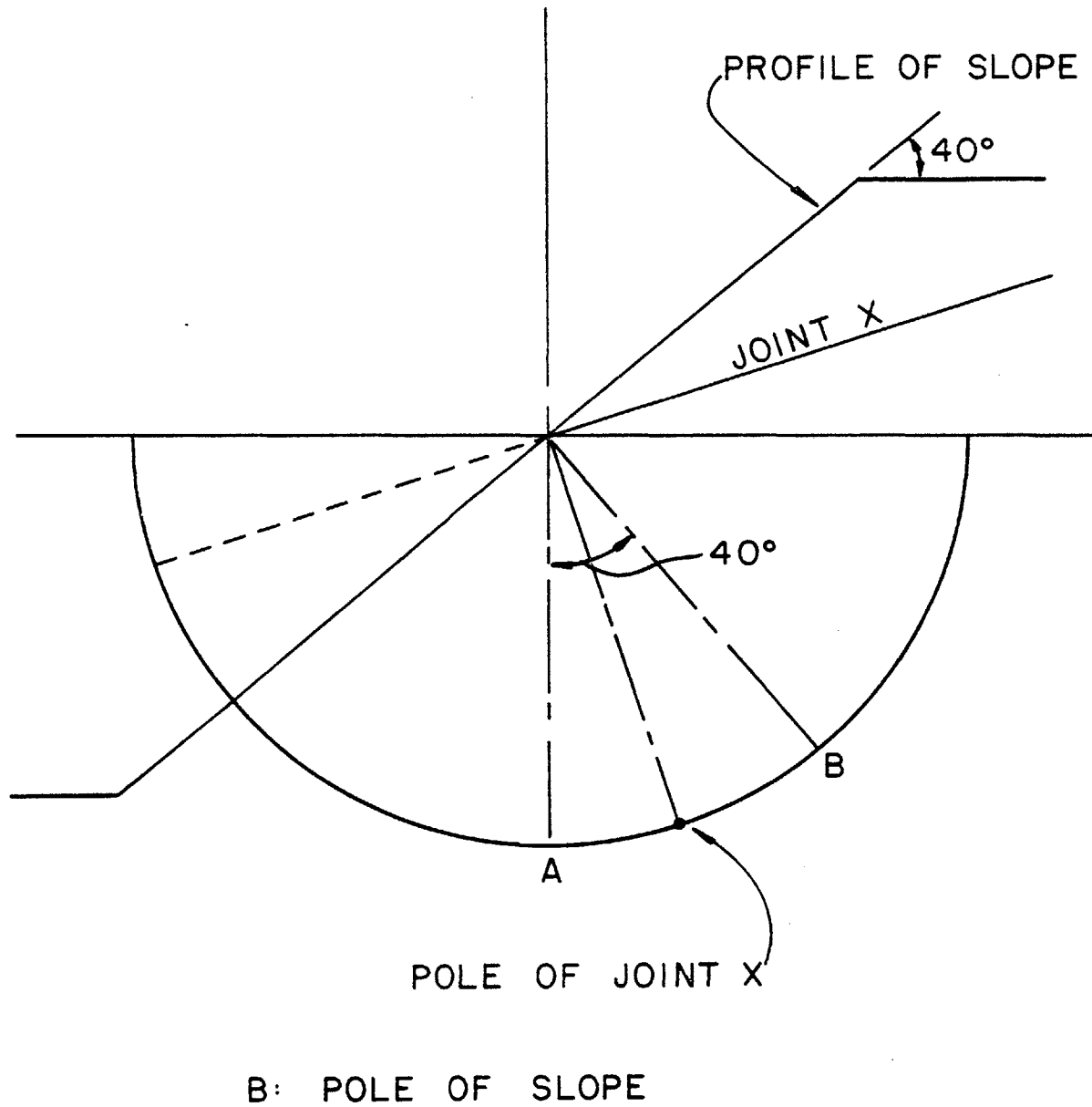


Figure 2.2 Kinematic Test for Sliding
26

that the dip of the joint corresponds to the direction of movement i.e., only hydrostatic and gravitational forces are present.) Figure 2.3 shows the locus of all unstable joints for slopes of various inclinations. The great circle on the right side of the figure are traces of the slopes and the closed curves on the left define the corresponding regions of kinematic instability; any joint whose pole lies within the curves will daylight. Points A and B correspond to those in Figure 2.2.

The fact that a joint may daylight does not imply that movement must occur. The shear strength of the joint may be sufficient to restrain movement. Kinetic tests must be imposed to resolve the question of stability. The case analyzed in Figure 2.4 involves a wedge whose resultant load consists solely of its weight. The wedge will not slide as long as the joint has a dip less than $\theta_{cr} = \phi$. All joints with poles between A and C are kinetically stable. The only joints along which sliding will occur in this simple case are those whose poles plot between C and B. The three dimensional representation of the region of kinetic stability is the area inside a circle of angular radius ϕ centered at the center of the projection (Figure 2.5). This circle is generated by revolving the circular sector defined by arc A-C (Figure 2.4) around the pole of the projections.

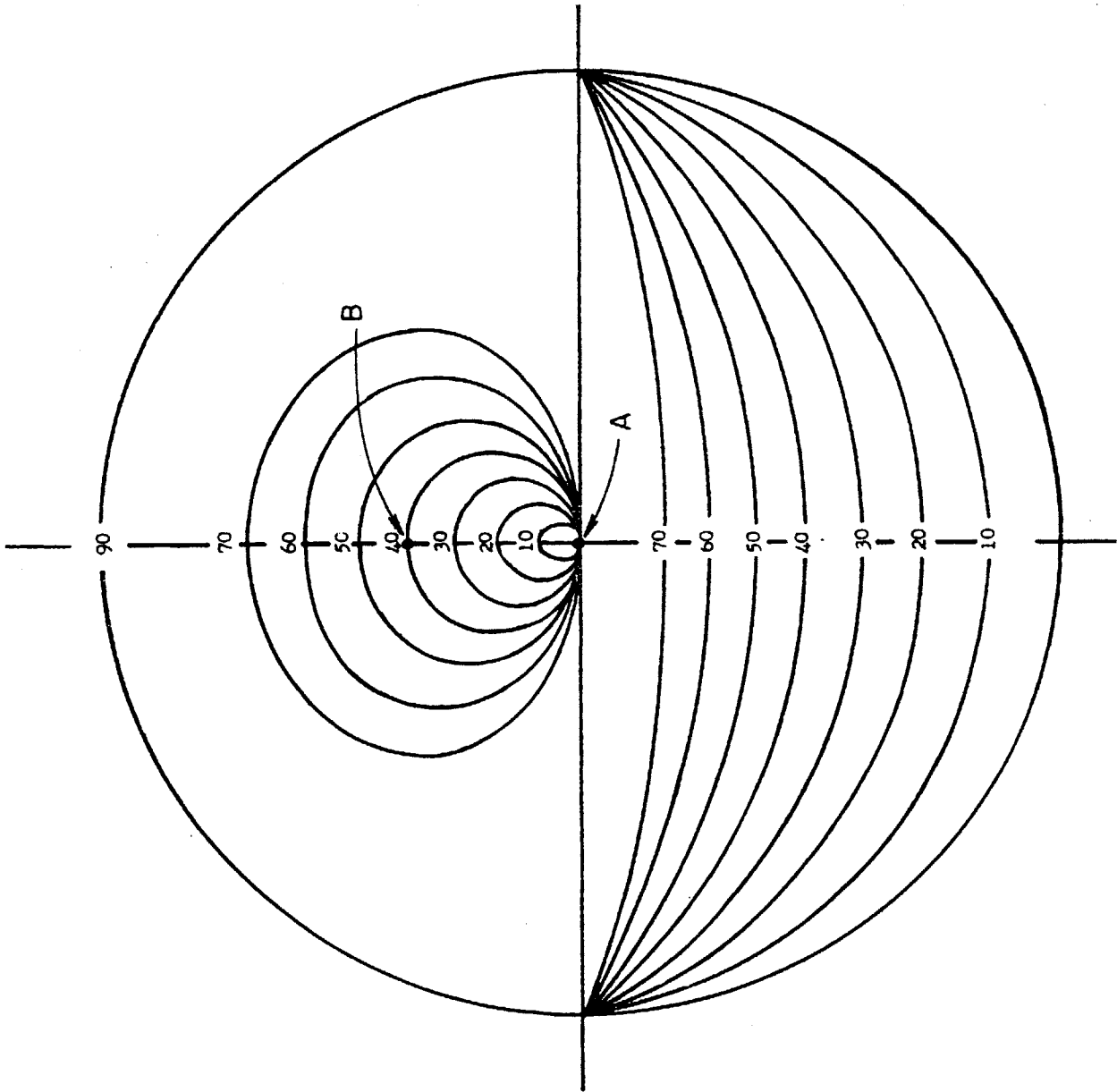
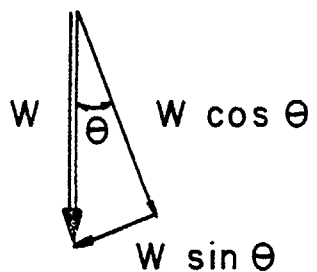
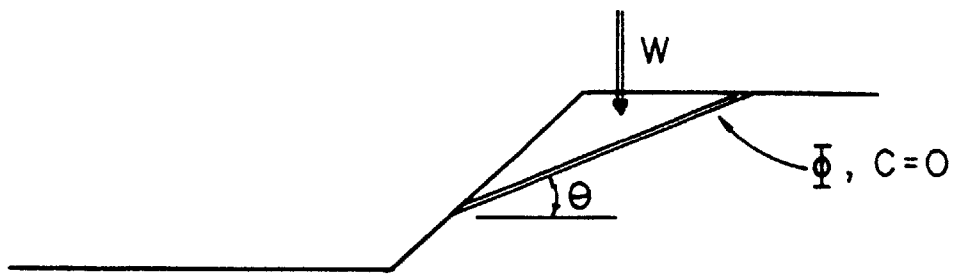


Figure 2.3 Areas of Kinematic Instability on Stereonet



$$F.S. = \frac{W \cos \theta \tan \phi}{W \sin \theta}$$

$$= \frac{\tan \phi}{\tan \theta}$$

$$\theta_{\text{critical}} = \phi$$

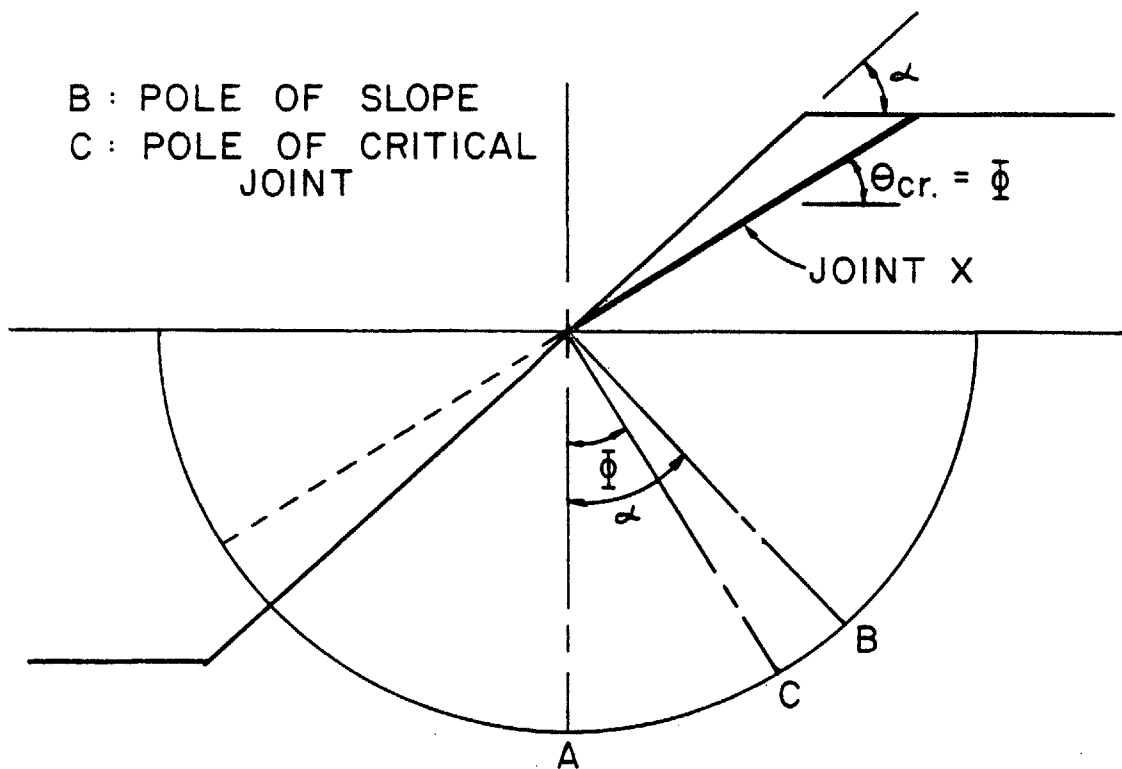


Figure 2.4 Kinetic Test for Sliding

The two stability regions just described provide a basis for applying probability theory. The reliability analysis of the slope reduces to a single decisive question: What is the probability that the slope will contain a joint (or joints) whose pole lies within the area of kinematic instability and outside the area of kinetic stability? This crucial crescent shaped zone is accentuated in Figure 2.5. McMahon (1971) discusses two limiting cases.

1. Uniform Distribution If the joints are uniformly distributed over the surface of the sphere P'_J , the probability of the occurrence of an unstable joint, is

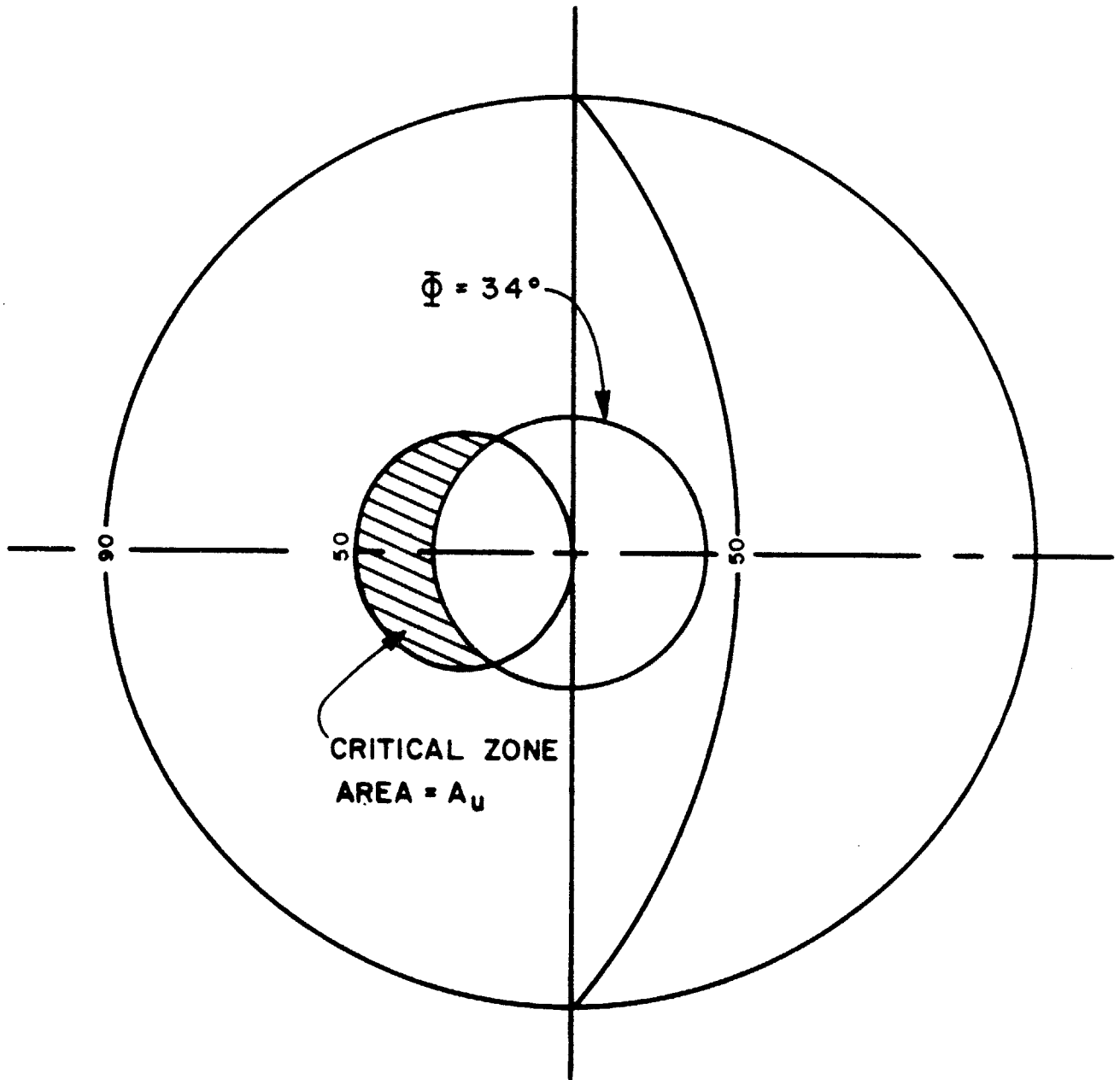
$$P'_J = \frac{A_u}{A_t}$$

Where A_u is the area of the critical zone shown in Figure 2.5 and A_t is the total area of the projection.

2. Indeterminate Distribution If the joint survey represents the best estimate of the sample population, P_J can be calculated as

$$P_J = \frac{N_u}{N_T}$$

Where N_u is the number of poles in the critical zone and N_T is the total number of poles or joints in the survey.



TOTAL AREA OF PROJECTION = A_t

Figure 2.5 Critical Zone for Sliding
 31

Most joint distributions do not correspond to either of these two extreme cases. If, however, the joint orientation has a mathematically describable probability density function (See Appendix A) P'_J can be found through numerical intergration techniques. McMahon (1971) describes a procedure for evaluating bevariate normal distributions with a rectangular normal probability chart. Herget (1978) also examined the bivariate normal distribution. He suggests sketching contours of constant standard deviation and then estimating the portion of each "ring" that lies in the critical zone.

P'_J is a conditional probability based on the assumption that only one joint is present. (P'_J = Probability of an unsafe joint given that only one joint is present.) If the joints are independently oriented P_J , the probability of the unsafe joint occurring, is:

$$P_J = 1 - (1 - P'_J)^N \quad (2.1)$$

where N is the number of joints in the slope. (In a rigorous analysis N should be treated as a random variable.) P_J corresponds to P_f , the probability of failure, for slopes in which the joint lengths are large relative to the size of the slope i.e., the joints will form a continuous failure plane. If only a portion of the joints are long enough to cause failure, P_f is computed as

$$P_f = P_J P_C \quad (2.2)$$

where P_C is the proportion of joints with the requisite

continuity to cause failure.

The graphical approach is not restricted to cases involving only gravitational loads. McMahon (1974) introduced the concept of critical dip (β_c) to treat hydrostatic and pseudo-static seismic loadings.* The critical dip is the dip of the flattest joint along which sliding takes place at limiting equilibrium. Dip is measured in the direction of movement. Figure 2.6 shows how β_c can be determined for the two loading conditions.** β_c is used in the same manner as ϕ in Figure 2.5. β_c is not necessarily a deterministic quantity. It can be treated as a function of time (temporal variations in ground water levels) or space (lateral variations in joint friction angles.)

McMahon's graphical approach is well suited to evaluate planar failures in cases where both the loads and the resistances are proportional to the weight of the block. When the proportionality occurs β_c is independent of H, i.e., the size

*McMahon's formulation of β_c includes a term to correct for lateral restraint in wedge failures:

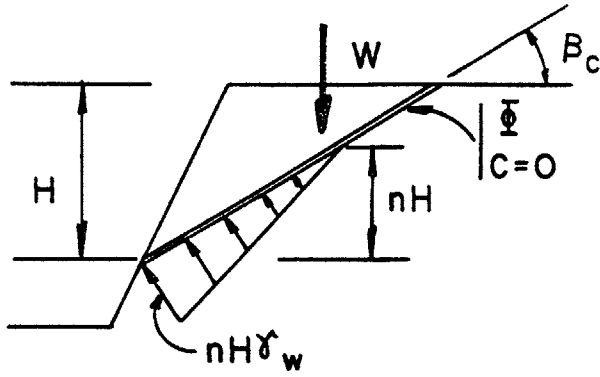
$$\tan\beta_c = K_s \tan(\phi - \alpha) \quad (2.3)$$

$$K_s = \frac{\sin\theta_1 + \sin\theta_2}{\sin(\theta_1 + \theta_2)}$$

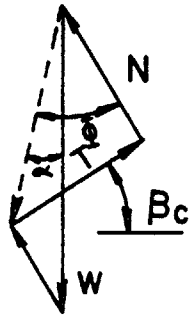
θ_1 and θ_2 are the apparent dips of the two planes bounding the wedge measured in a plane normal to their line of intersection. K_s is difficult to evaluate because both θ_1 and θ_2 are random variables. It may be more efficient to use McMahon's technique solely for planar failures ($K_s = 1.0$) and rely on other methods to investigate wedge failures.

**Note that the hydrostatic pressure is defined in terms of the quantity nH . β_c will be a function of n but not H because H^2 will appear in both the numerator (U) and the denominator (W). Also, U is a function of β_c . Since $\beta_c = \phi - \alpha$, the solution for α will require a reiterative approach.

HYDROSTATIC
LOAD



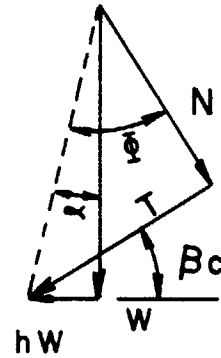
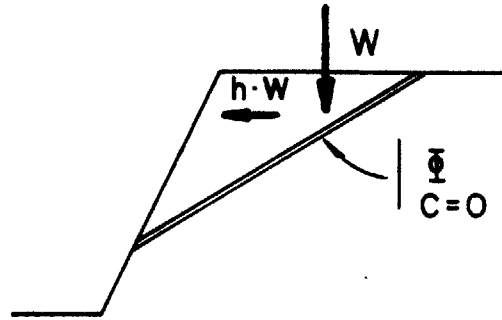
$$U = \frac{\pi}{2} H^2 \gamma_w \csc \beta_c$$



$$\sin \alpha = \frac{U \sin \phi}{W}$$

$$\beta_c = \phi - \alpha$$

PSEUDO - STATIC
SEISMIC LOAD



$$\sin \alpha = \frac{h}{1.0}$$

$$\beta_c = \phi - \alpha$$

Figure 2.6 Calculation of β_c

of the block does not affect its stability (Figure 2.6). Unfortunately β_c is a function of H for most hydrostatic loadings and for all cases in which the resistance includes a cohesive component. A varying β_c implies that the zone of kinetic stability changes with every combination of H and ϕ . The graphical approach is difficult to implement under these conditions. Stability problems involving cohesion or water pressures can, however, be analyzed with the methods outlined in the succeeding sections.

2.2 Monte Carlo Simulations

Monte Carlo simulations constitute an almost purely numerical approach to reliability analysis. They resemble sensitivity analyses cast in a probabilistic setting. In theory, the technique can be applied to virtually any problem that can be modelled deterministically. The factor of safety (FS) is computed for many sets of randomly selected input parameters. The probability of failure (P_f) is the proportion of FS values that fall below 1.0. A more formal definition of P_f is shown in Figure 2.7. The FS values are grouped to form a histogram which is used to delineate the probability density function (pdf) of FS. P_f is the area under the curve to the left of FS = 1.0.

The selection of input values is a critical step in the simulation technique. The values for each variable are chosen from the pdf of that variable. Figure 2.8 describes the procedure. $F_X(x)$, the cumulative distribution function

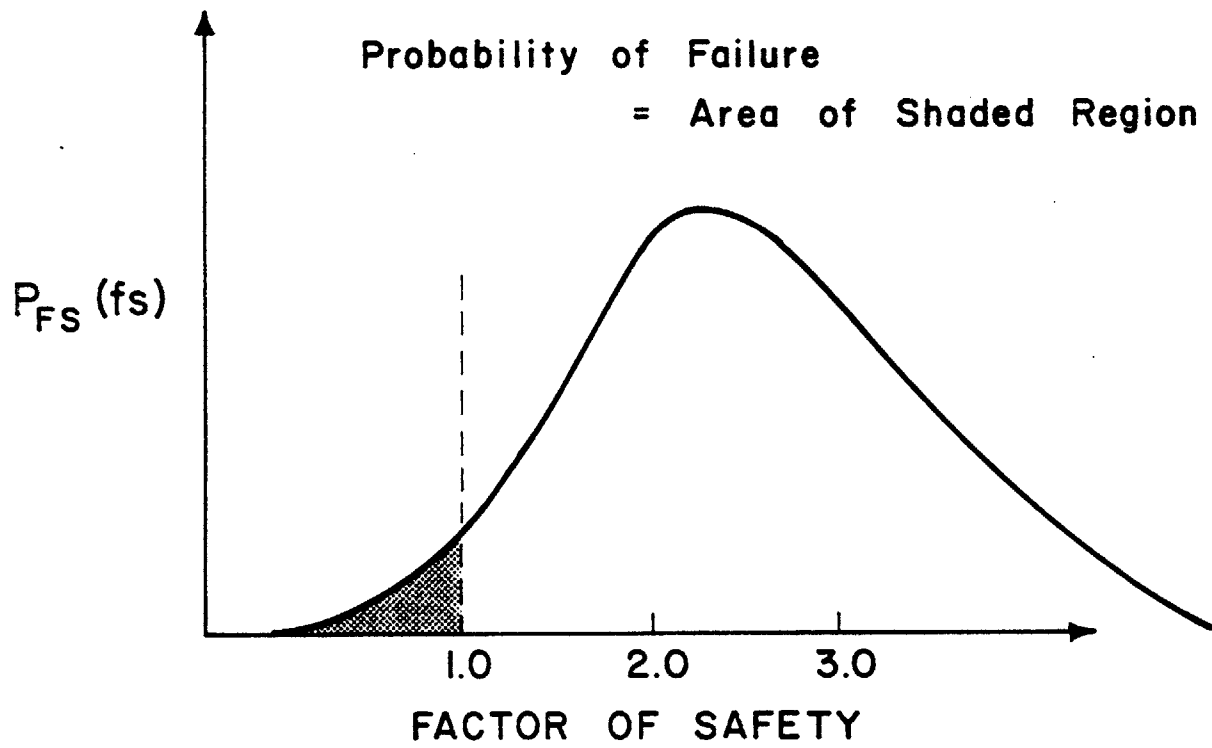


Figure 2.7 Probability of Failure

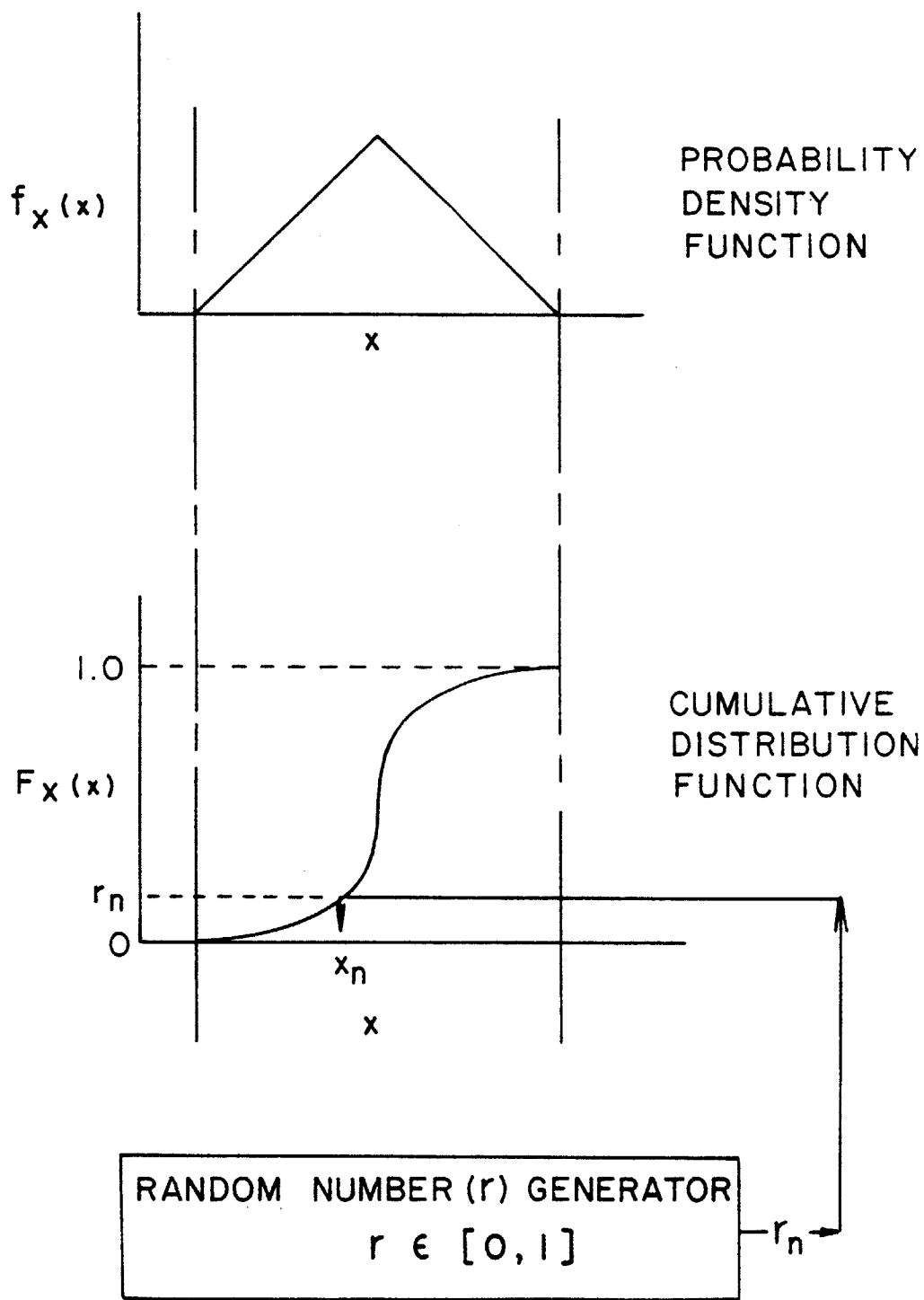


Figure 2.8 Use of Probability Density Function in Monte Carlo Simulation

of x , is the integral of $f_X(x)$. By definition, the domain of $F_X(x)$ is limited to the interval $[0,1]$. $F_X(x)$ will map any number r_n in that same interval $[0,1]$ to a value of x . If the r_n 's are the outputs of a random number generator the values of x will be randomly distributed i.e., the relative frequency with which values of x in the interval $[x + \Delta x, x - \Delta x]$ appear will be proportional to the area under the pdf in that same interval. A histogram of many x 's would resemble $f_X(x)$ in Figure 2.8.

Most Monte Carlo simulations involve several random variables. Figure 2.9 is a schematic representation of the technique applied to a rock slope stability problem. In general, the deterministic model is a limiting equilibrium analysis. Input parameters include the attitude and strength of the joint planes as well as ground water conditions and external loadings like rock bolts or surcharges. The analysis must be repeated for every set of input parameters. The volume of computations can become enormous; however, the simulation procedure can be readily programmed for a computer.

Monte Carlo techniques have been applied to numerous problems in rock mechanics. Su et al. (1970), used Monte Carlo simulations in conjunction with finite element methods to evaluate stress distributions around underground openings in rock strata. Pariseau (1973) extended their work to investigate the stability of roofs and pillars in mines. In the last few years Monte Carlo methods have been used to analyze rock slopes. In fact virtually all the reliability analyses to be discussed rely at least partially on simulation techniques.

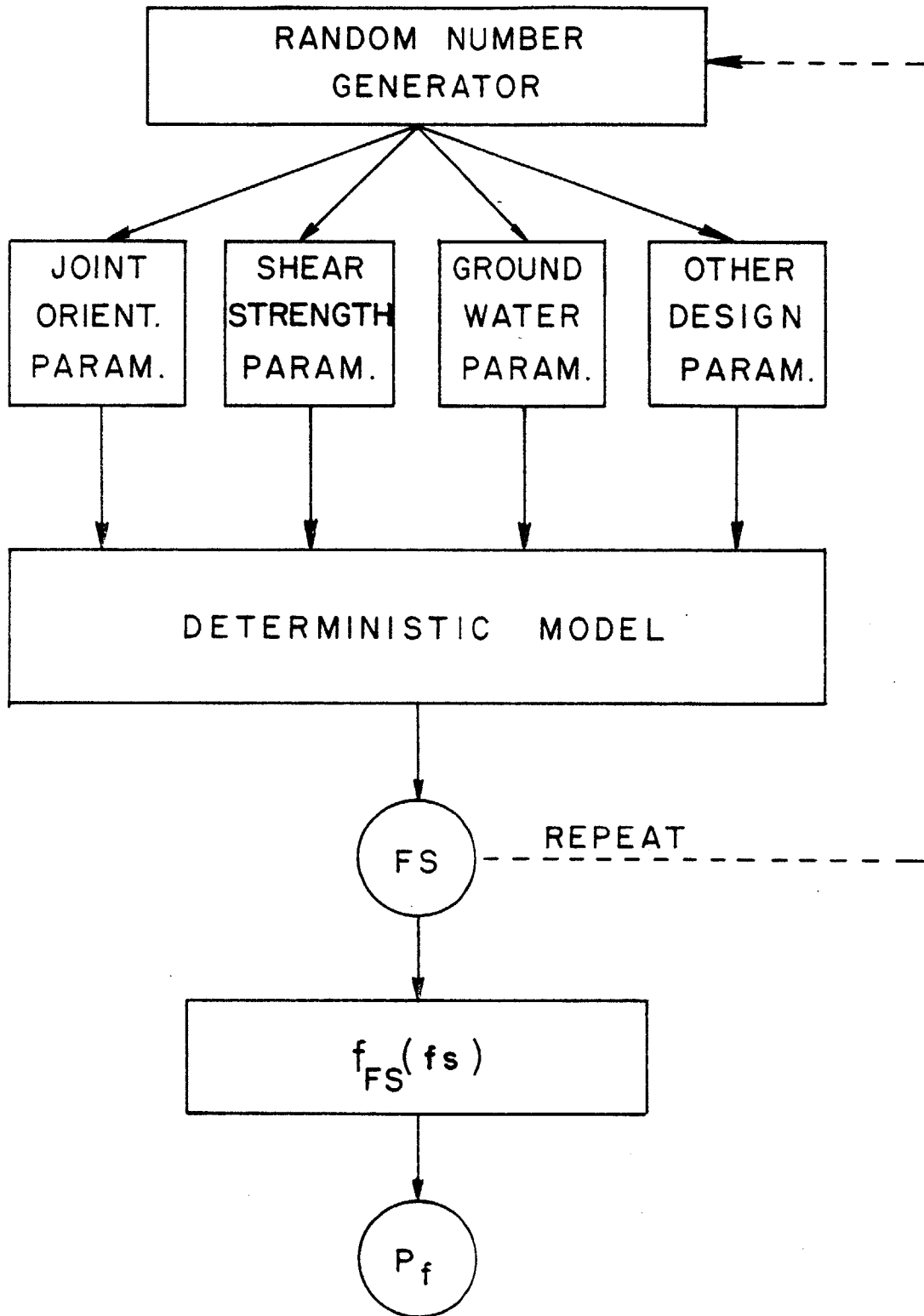


Figure 2.9 Rock Slope Stability by Monte Carlo Simulation

Major et al., (1978) have developed a probabilistic model that relies exclusively on Monte Carlo simulation. The core of their model is a deterministic algorithm that evaluates the stability of rock wedges as their FS against sliding. The wedges are formed by two intersecting discontinuities. The resulting tetrahedron may be truncated by a tension crack (Figure 2.10). Stability calculations are based on the conventional model that examines translational movement of a rigid body.* The analysis involves a maximum of 22 input parameters. Any combination (or all) of these parameters can be treated as random variables. Each random variable is characterized by one of five distributional forms: normal, truncated normal, uniform, triangular, and exponential. Figure 2.10 shows a sample problem presented by Major et al., with ten random variables. Two hundred sets of input parameters were used to find the distribution of FS. The simulations suggest that P_f is in the order of 0.07. (The authors did not document any attempt to estimate the standard error of P_f which may be fairly large.)

The value for P_f derived from the Major et al. computer program is actually a conditional probability based on the assumption that one and only one wedge forms i.e. precisely one joint from each set is present.** The true probability of

* In a companion paper (Kim et al., 1978) the authors briefly discuss other possible modes of failure.

** A similar conditioning problem was discussed earlier in connection with McMahon's graphical approach.

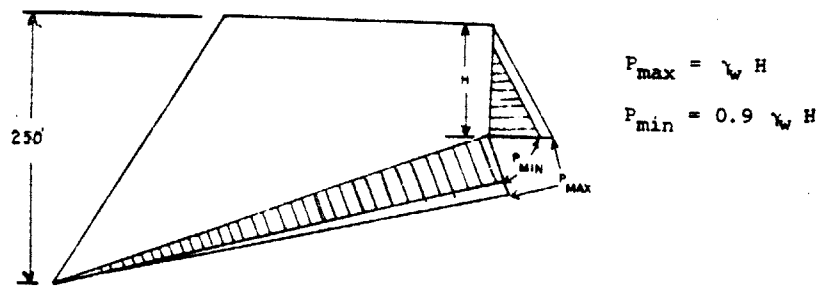
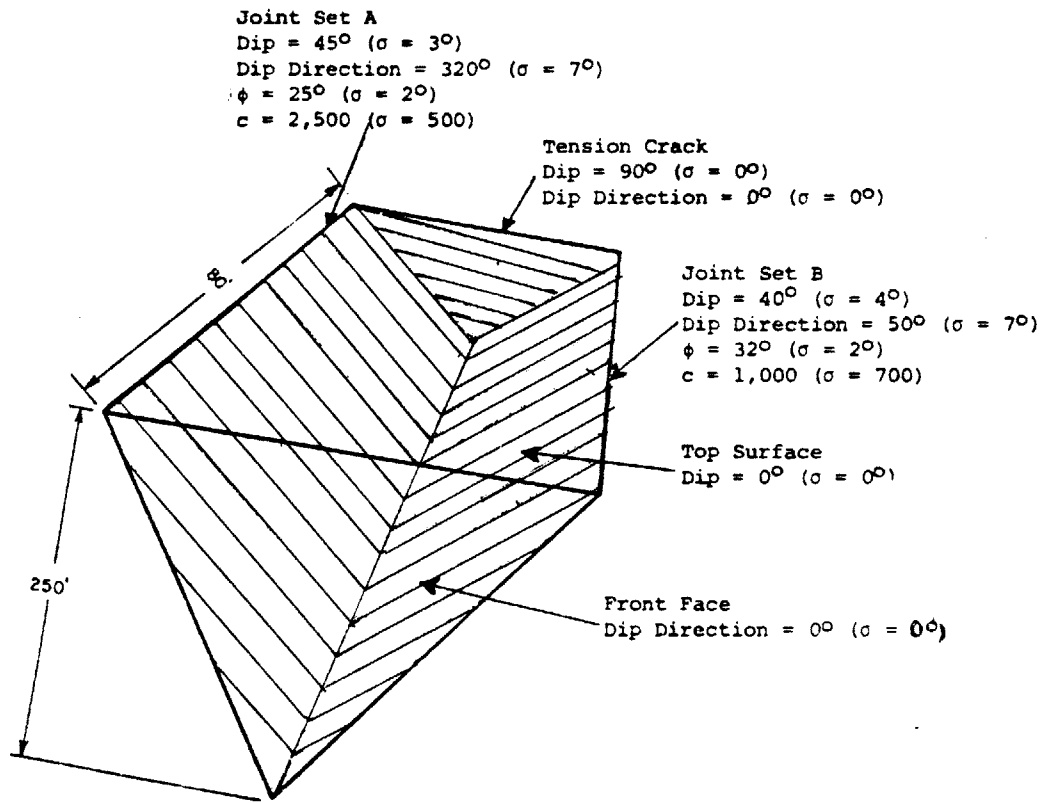


Figure 2.10 Sample Problem--Major et al.

failure is a function of the intensity of jointing. It may be lower than P_f if jointing is a relatively rare event. On the other hand, it may be considerably higher than P_f if the slope is highly jointed. Major et al. do not address this issue. However, the problem is not unique to their method. Virtually all the current reliability analyses must contend with this same problem. There is no simple solution. As will be shown, the joint model prepared by Veneziano (1978) may provide a tentative approach to the multiple wedge problem.

The Major et al. method can be a valuable tool in conducting reliability analyses. It does, however, have some difficulties which are common to all Monte Carlo methods. Simulation can be a computationally inefficient technique for highly reliable slopes. The number of trials required to determine P_f can be very large if P_f is small. The two hundred trials used in the example may be an optimistic figure. A P_f in the order of 0.001 may require several thousand simulations.*

Most Monte Carlo analyses neglect correlation among random variables. They treat each variable as if it were independently distributed. This assumption is frequently not justified. For example, strike and dip of joints might be correlated or extreme values of strength parameters might be

* P_f values in the order of 0.001 (or less) are very sensitive to the tails of the distributions of the input parameters. The tail behavior of these parameters is difficult to estimate at the present time.

associated with certain joint orientations. This correlation structure can become very complicated and difficult to incorporate in the analysis; however, neglecting the correlations can lead to erroneous results.

Monte Carlo methods are relatively easy to implement. Unfortunately this tractability often leads to their indiscriminate use. Monte Carlo simulation is not a panacea for probability analyses. It is subject to the same limitations as its deterministic algorithm. In addition, it requires a rigorously defined pdf for each random variable. The critical issue is whether one can rationally assign a pdf to all the important input parameters. For example, rock slope problems may have an extensive amount of information on joint orientation but virtually no data base for joint persistence or cleft water pressures. Yet, FS is much more sensitive to variations in joint persistence than to variations in joint strike. A poorly selected pdf for persistence will result in an unrealistic estimate of P_f . Major et al. present many options for selecting pdf's but give no hint as to typical distributions for each parameter. (Baecher et al., (1977) present a summary of current research on estimating pdf's for joint spacing and joint length.)

In using Monte Carlo techniques one tends to concentrate on the random variables with well defined pdf's. The ill-defined random variables are arbitrarily assigned disperse pdf's - often a uniform distribution is used. However, each random

variable contributes to the dispersion of FS values. The variable with uniform pdf's may have a much greater influence on the shape and location of the pdf of FS than the other variables. The sheer volume of computations and computer outputs can give one a false sense of security about the results.

2.3 Composite Models

Composite models include all the methods which endeavor to decompose the probability of failure into discrete components that can be analyzed independently. All the models have the same general form:

$$P_f = \sum P[A]P[B] \quad (2.5)$$

A is the event that a potentially unstable condition exists. B is the event that the destabilizing force exceeds the resistance. The product of their probabilities is summed over all possible unstable conditions. The two events are analagous to the kinematic and kinetic criteria in McMahan's model. In general A and B are treated as probabilistically independent events.

Composite models present an attractive concept. P_f is calculated as the joint probability of several conditions that lead to instability. A complex process is resolved into many simple components and each component is examined as a potential source of uncertainty. Many of the early reliability

models used this approach. Those models have evolved over the past few years to the point where they are now legitimate design tools. The two best examples of composite models are those developed by Marek and Savely (1978) and Serrano and Castillo (1974).

The Marek and Savely model examines two dimensional plane shear failures (Figure 2.11). The height is a deterministic quantity (H). The first step in the analysis is to discretise the dip angles (θ 's). The Gaussian distribution for θ shown in Figure 2.11 is divided into twelve cells.* The angle at the midpoint of each cell is considered representative of all dips within that cell. The probability that the dip will assume any one of the 12 discrete values is equal to the area of that particular cell. P_f is calculated as:

$$P_f = \sum_{j=1}^n P_{D_j} P_{L_j} P_{S_j} \quad (2.6)$$

n = number of cells

D_j = dip at midpoint of cell

P_{D_j} = P[dip is D_j]

P_{L_j} = P[discontinuity is continuous from A to B]

P_{S_j} = P[shear resistance is less than the driving force]

*Not all values of θ need to be analyzed. Values greater than the slope angle can be excluded--a kinematic restraint. Marek and Savely suggest neglecting all values less than ϕ minus 2 standard deviations of ϕ --a kinetic restraint.

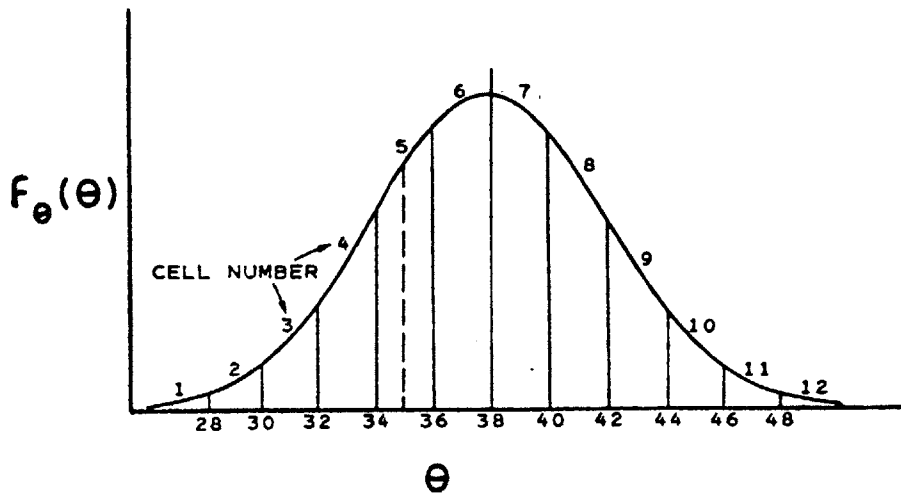
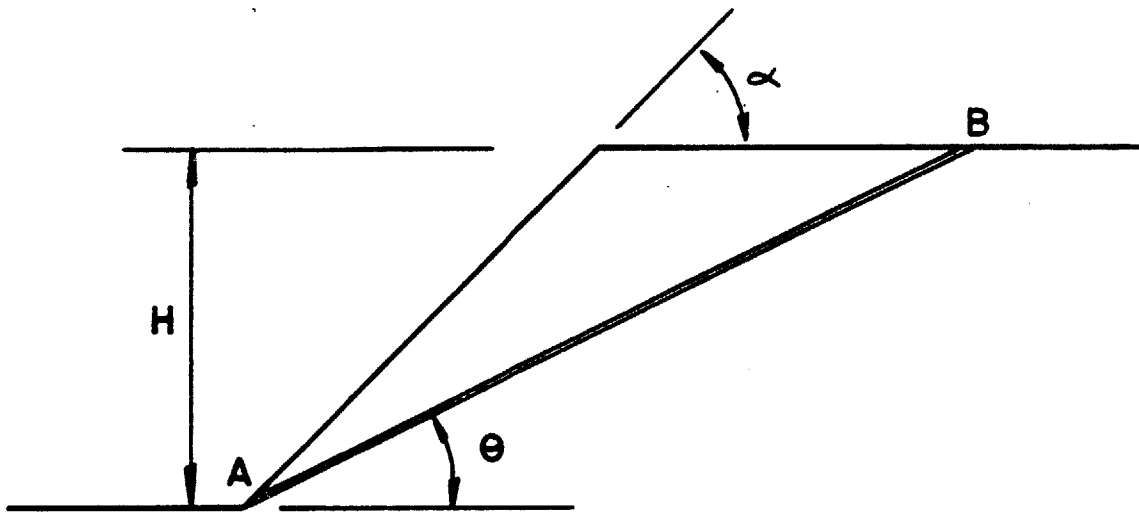


Figure 2.11 Marek & Savely Model

P_{L_j} can be determined from a cumulative distribution function of joint lengths. P_{S_j} is found through Monte Carlo simulation. Since α and H are deterministic, any value $\theta = D_j$ will completely describe the geometry and the weight (W) of the failure block as well as the shear ($W \sin D_j$) and normal forces ($W \cos D_j$) on the failure plane. Marek and Savely use Monte Carlo techniques to sample various sets of shear parameters (joint friction, ϕ , and joint roughness, i). P_{S_j} is the proportion of trials in which the shear force ($W \sin D_j$) exceeds the resistance $W \cos D_j \tan (\phi + i)$.

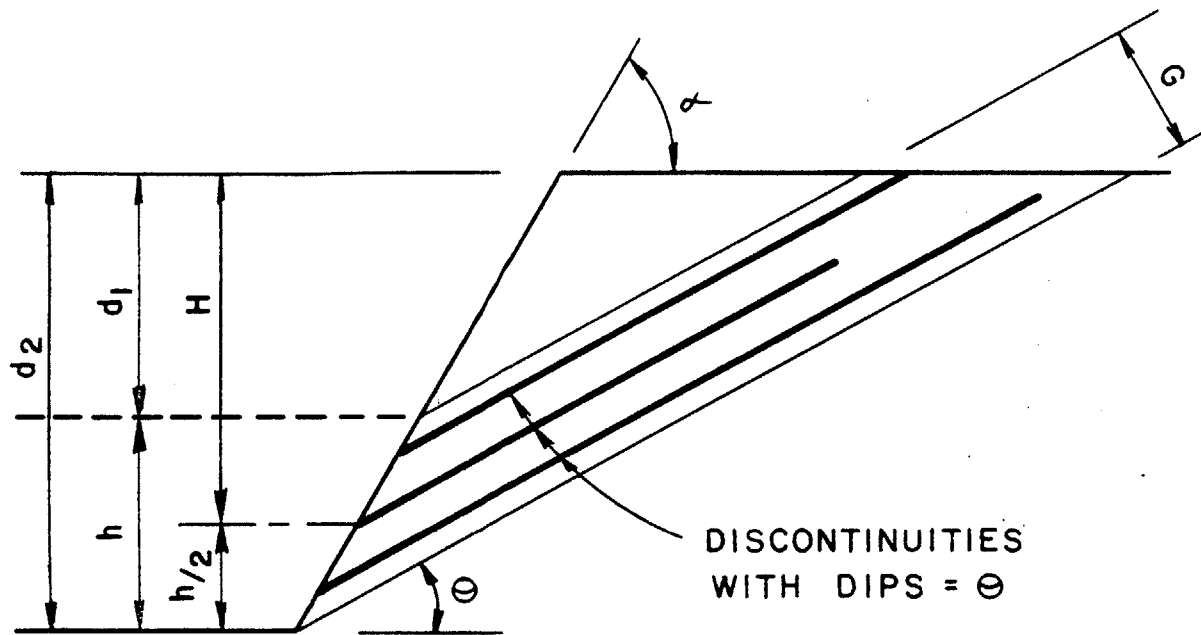
Call and Kim (1978) extended the Marek-Savely method to analyze slopes with numerous discontinuities. They considered the profile shown in Figure 2.12. It corresponds to an open pit mine which is to be deepened from d_1 to d_2 --a mining increment of h . N is the number of discontinuities that will be exposed during excavation. The expected value of N can be computed:

$$N = G/\lambda \quad (2.7)$$

$$G = \frac{h \sin(\alpha - \theta)}{\sin \alpha} \quad (2.8)$$

λ = mean fracture spacing

Call and Kim define PI , the probability of instability, as the probability that at least one unstable joint will be exposed. PI can be determined through a binomial expression:



$$G = \frac{h \sin(\alpha - \theta)}{\sin \alpha}$$

λ = MEAN JOINT SPACING

\bar{N} = MEAN # OF JOINTS

$$= \frac{G}{\lambda}$$

Figure 2.12 Call & Kim Model

$$PI = 1 - (1 - P_f)^N \quad (2.9)$$

P_f = probability of failure for a single fracture as computed by Marek and Savely.

The fact that N is actually a random variable can easily be incorporated into the analysis. If joint spacing is exponentially distributed N has a Poisson distribution:

$$f_N(n) = \frac{(G/\lambda)^n e^{-G/\lambda}}{n!} \quad (2.10)$$

PI can be conditioned on n and summed over all possible values of N .

$$PI = \sum_{\text{all } n} \left(f_N(n) \cdot (1 - (1 - P_f)^n) \right) \quad (2.11)$$

The Call-Kim model relies heavily on the assumption involving independence. It treats joint stability as a series of Bernoulli trials i.e., mutually independent experiments with a constant probability of failure. The fact that the n^{th} joint is stable does not influence the reliability (P_f) of the $(n + 1)^{\text{th}}$ joint. Even Marek and Savely's formulation of P_f is based on the assumption that joint orientation, length and frictional properties are independent parameters.* These assumptions do not necessarily invalidate the model. They should, however, be thoroughly investigated before the model is applied

*A careful search of the data bases for each pair of parameters may reveal correlations that can be introduced into the P_f calculations.

to a specific problem.

Serrano and Castillo (1974) use the same principles in their 3-dimensional model. The principal features of their model are shown in Figure 2.13. The figure is a front view of a rock slope that contains two sets of discontinuities.* Every intersection defines a potentially unstable wedge. Serrano and Castillo characterize the wedges by their surface areas or volumes. The triangles ABC and A'B'C' typify the largest wedges that can form. All wedges of that size will have a vertex that lies along the line BB'. Small wedges such as the family that is typified by ADE and D'E'C' are much more numerous. All the members of that particular family have vertices between D and D'.

The critical feature of the computerized model is a routine that identifies all possible combinations of joints that will produce a wedge whose area lies between the prescribed limits δ_n and δ_{n+1} . The problem is by no means trivial because the joint spacing is a random variable. P_f can be computed through the techniques described earlier. $P(\delta, F_0)$ is the probability that a wedge of volume δ will have a factor of safety less than F_0 .

$$P(\delta, F_0) = \sum_{i,j} \sum_R f_i^1 f_j^1 f_i^2 f_j^2 f_i^3 f_j^3 \quad (2.12)$$

* A more general version of the Serrano-Castillo model can accommodate 3 sets of discontinuities.

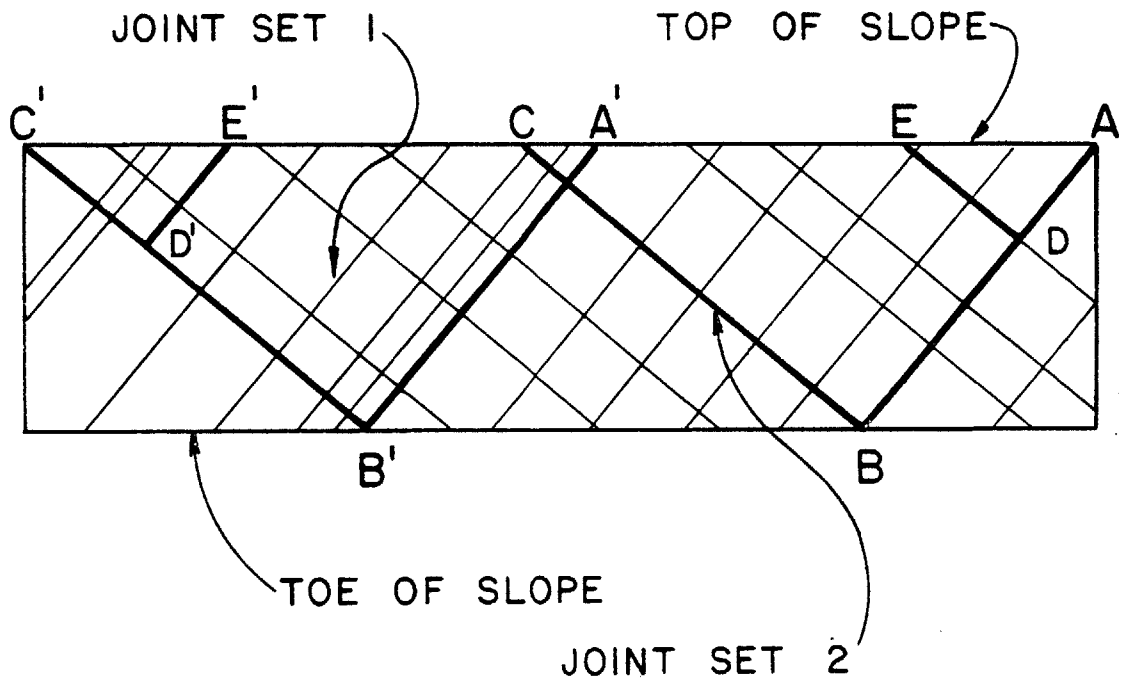


Figure 2.13 Serrano & Castillo Model

- i, j = all pairs of joints i and j that satisfy the volume = δ condition.
- R = subspace of all combinations of strength parameters that yield $FS < F_0$
- f_i^1, f_j^1 = density functions of the joint strength parameters
- f_i^2, f_j^2 = density functions of joint persistence
- f_i^3, f_j^3 = density functions of the intact rock strength parameters

The last step in the analysis is to construct the cumulative distribution function of F_0 for various values of δ . $F(\delta_0, F_0)$ is defined as the probability that some wedge with a volume equal to or larger than δ_0 will have a FS less than or equal to F_0 .

$$F(\delta_0, F_0) = 1 - \frac{\pi}{d_{\geq \delta_0}} (1 - P(\delta, F_0))^{n(\delta)} \quad (2.13)$$

$n(\delta)$ = number of wedges that have a volume of δ

Figure 2.14 shows some results that Serrano and Castillo obtained in their example. P_f is the value of $F(\delta_0, F_0)$ at $FS = 1.0$. It is a function of δ_0 and increases as the failure volume decreases.

The Serrano-Castillo model can be a versatile tool in the planning of pit mine slopes. The concept of explicitly

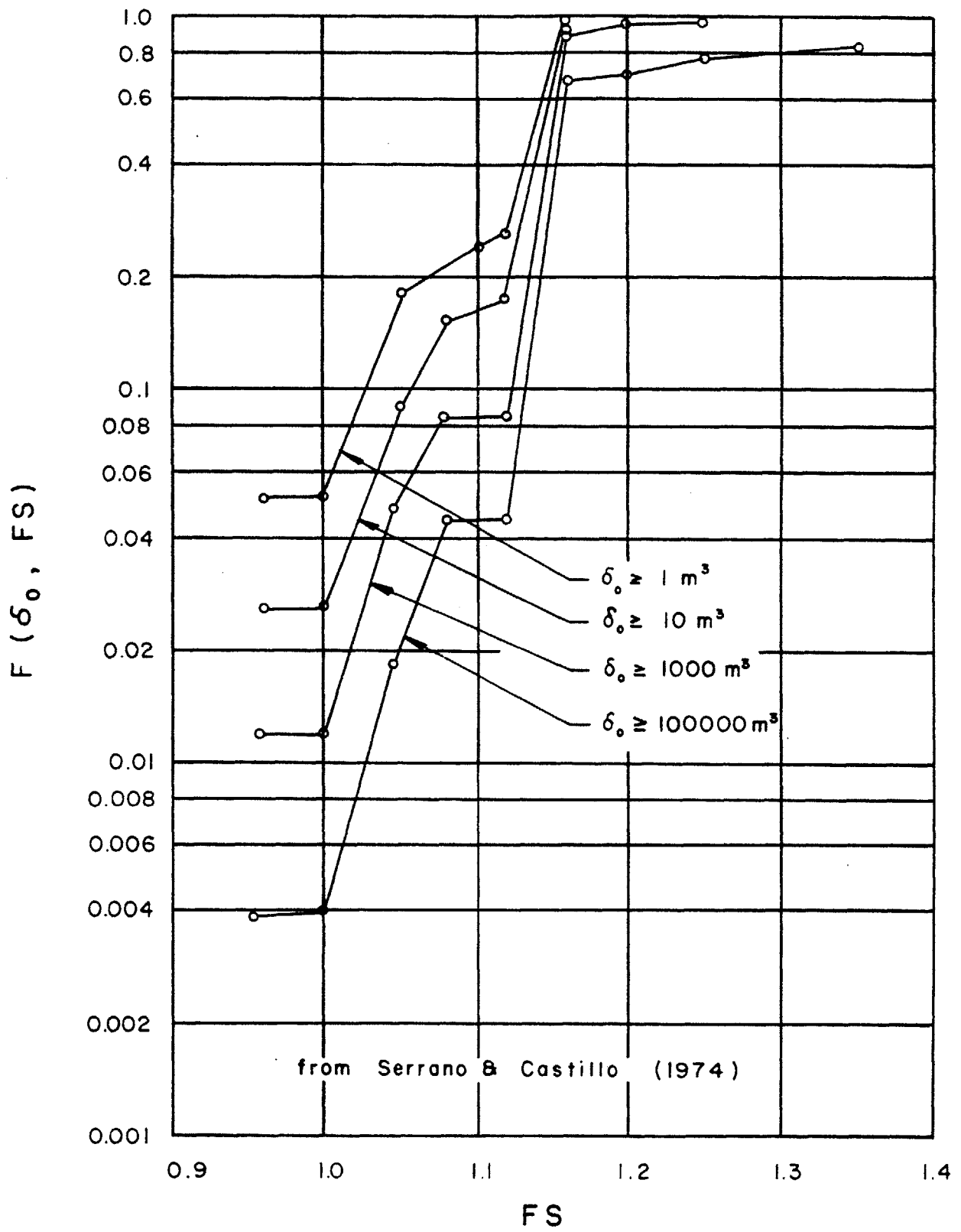


Figure 2.14 Typical Results--Serrano & Castillo Model

considering the size of the failure zone is an attractive approach because it enables a planner to evaluate the consequences of failure. However, the model is based on a number of assumptions concerning independence among parameters. As discussed earlier, these assumptions must be verified before the model is implemented. Finally, the model computes $F(\delta_o, F_o)$ through a long series of conditional probabilities. The volume of computations can become overwhelming for heavily jointed rock masses.

2.4 Stochastic Models

In many ways stochastic models constitute the most interesting approach to reliability analysis because they attempt to describe jointing as a random process. The models do not consider the mode of origin of the discontinuities but they do consider their attitude and location. The idea of treating any aspect of jointing as an analytically describable process is an innovative concept. Until recently joint data (orientation, length and spacing) has been analyzed on a strictly empirical basis. Various authors (Bridges, 1976; Barton, 1977; Call et al., 1976) have perceived some general properties i.e., the exponential nature of joint spacing, but no one has tried to interpret this behavior. Stochastic models present a unifying theory that accounts for these observed properties. However, the models do more than just enable one to visualize jointing patterns in a rock mass. They can be used to derive additional parameters which can

be valuable in stability analyses e.g., the mean number of wedge vertices on an excavated slope. The validity of the model can be measured by comparing predicted values with observed data.

Stochastic models can be either inductive or deductive. Inductive models find the pdf's for the inclination and persistence of failure surfaces by examining many continua--each of which contains a single failure path. Each path is pieced together from many individual joints whose length, orientation and spacing are treated as random variables. Inductive models infer the general properties of failure paths by investigating many specific examples. On the other hand, deductive models infer these properties by first generating joint patterns and then searching the pattern for possible failure surfaces. Deductive models populate a multi-dimensional space with a family of randomly generated joint planes. The entire joint system is examined to locate the path of minimum resistance.

Call and Nicholas (1978) developed an inductive stochastic model to investigate 2-dimensional stepped or "en echelon" failure surfaces. This failure mode occurs in slopes that contain two approximately orthogonal joint sets (Figure 2.15). The failure path is composed of many joint segments that coalesce to form a continuous surface. In some instances the joints may not form a complete path; the remaining rock bridges must rupture before the block can

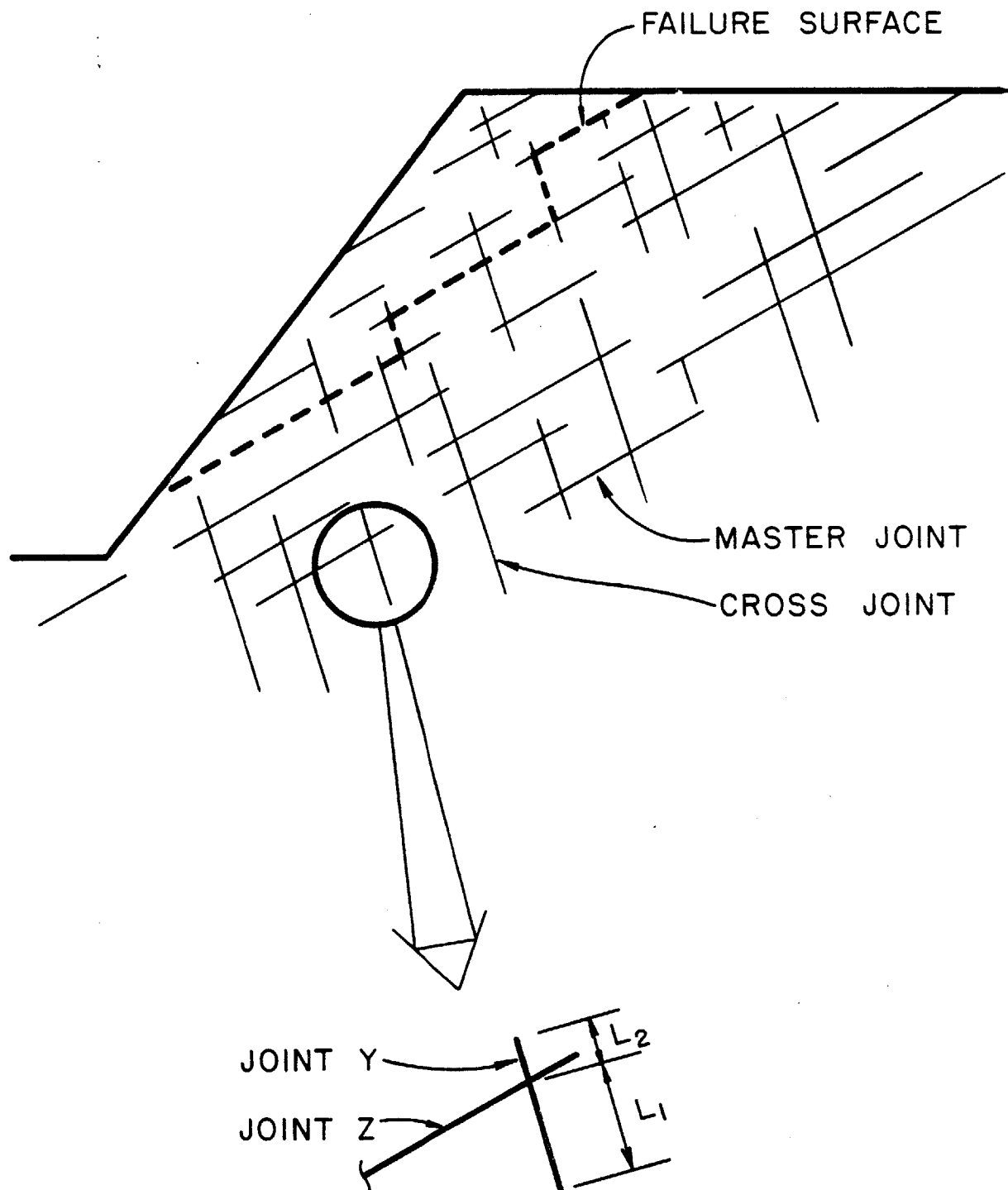


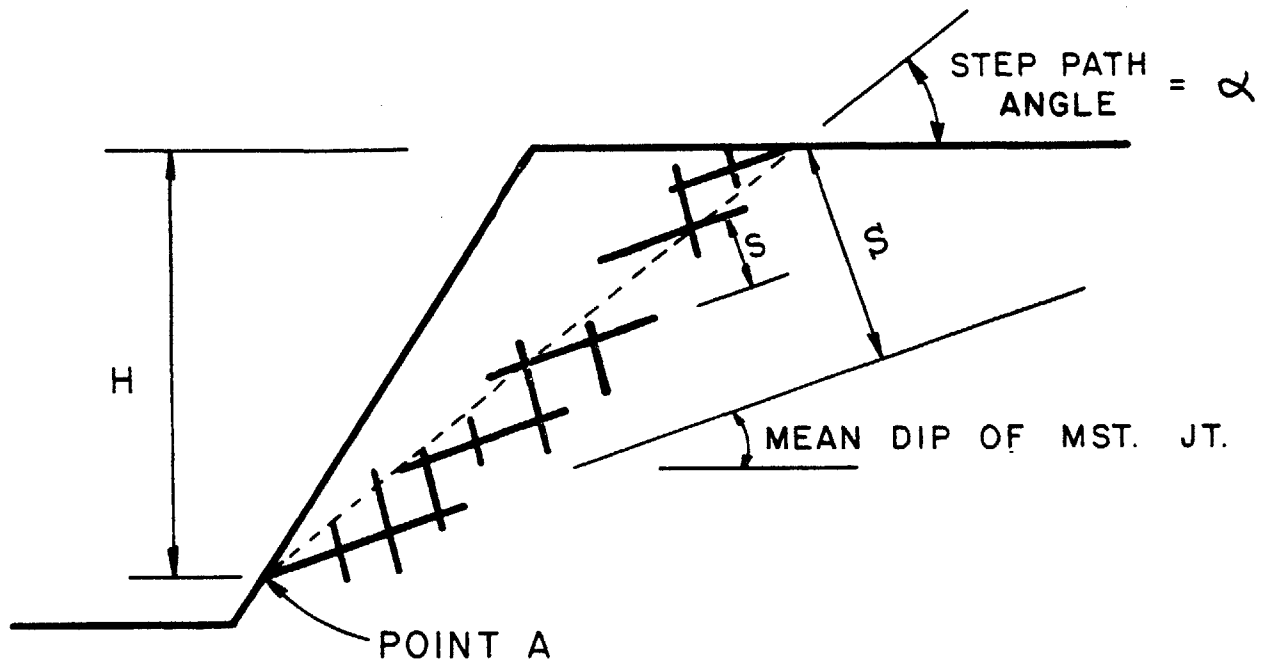
Figure 2.15 Call & Nicholas Model--Definitions

detach from its parent rock mass.

Call and Nicholas term the two joint sets "master joints" and "cross joints" (Figure 2.15). Each set is characterized by four random variables: dip, length, spacing and overlap. The last parameter describes the interaction between the two sets; it is defined in Figure 2.15. The overlap of joint Y is the ratio of L_1 , the distance that Y extends beyond joint Z to $(L_1 + L_2)$, the total length of Y^* .

The major features of the model are shown in Figure 2.16. The object is to fabricate a hypothetical failure path from an arbitrarily chosen point A to the top of the slope. Point A presumably locates a daylighting master joint and is defined by the distance H. A dip and length for this master joint is sampled from the appropriate pdf's through Monte Carlo techniques. A family of cross joints will intersect the master joint; the points of intersection are simulated by sampling random values from the pdf of cross joint spacing. Values are sampled until the sum of the N spacings exceeds the length of the master joint. The $(N-1)^{th}$ cross joint is the last one that actually intersects the master joint. The exact location of the $(N-1)^{th}$ joint is found by sampling values of dip, length, and overlap from the pdf's. The next master joint (the 2nd "stair") is located by sampling values

* Call and Nicholas indicate that their data suggest that overlap is uniformly distributed over the interval [0,1].



$$\% \text{ TENSILE FAILURE} = \frac{S}{S} 100$$

RANDOM VARIABLES

DIP	}	MASTER JOINT SET
LENGTH		CROSS JOINT SET
SPACING		
OVERLAP		

Figure 2.16 Call & Nicholas Model--General Features

of spacing, length, dip and overlap from the pdf's of master joints. The complete failure path is produced by alternately generating cross and master joints.

Occasionally the joints will not intersect. Whenever the path is interrupted the simulation process begins again as a new master joint is established. The interruption corresponds to a bridge of intact rock which must rupture before complete failure can occur. The size of the bridge(s) is expressed as "% tensile failure" (Figure 2.16). The entire failure path (including rock bridges) is characterized by α , its average inclination or "step path angle."

In their complete analysis Call and Nicholas generate a large number of failure surfaces and derive the pdf's of α and % tensile failure. The entire procedure is then repeated for various values of H. (In general, α decreases asymptotically with increasing H.) Call and Nicholas used this model to predict the inclination of failure slopes in an open pit mine. They found a good correlation between the distributions for predicted and observed values.

The Call-Nicholas approach is not a true reliability model in that it does not directly provide information on P_f . It can, however, be useful in predicting failure geometries in situations where the mere existence of a continuous failure path ensures failure. The restriction is important because the model ignores the kinetic conditions--it presumes that none of the joint surfaces develop enough resistance to

maintain stability along a continuous failure path. Under simple conditions (no water, no external loads) the master joints must have a mean dip that exceeds ϕ , the joint friction angle. (The mean dip of the master joints in the field study was 43° and the "% tensile failure" approached zero.) The kinetic conditions should be considered in analyzing slopes with flatter master joints. One practicable technique would involve sampling a value of ϕ from the corresponding pdf for each failure path. If $\alpha < \phi$ the path would not be considered in determining the pdf of α . The implementation of kinetic restraints would tend to shift the pdf of α to higher values because many potential failure paths with small step path angles would be stable.

The previous comments regarding Monte Carlo simulations also apply to the Call-Nicholas model. The selection of the proper pdf for each of the eight random variables is a critical requirement. The close comparison between predicted and observed failure paths suggests that the authors have chosen reasonable distributions.

Baecher et al., (1977) developed a deductive stachastic model for rock jointing. Their goal was to formulate a conceptual model that could explain two empirical observations:

1. joint lengths are lognormally distributed^{*}.
2. joint spacings are exponentially distributed.

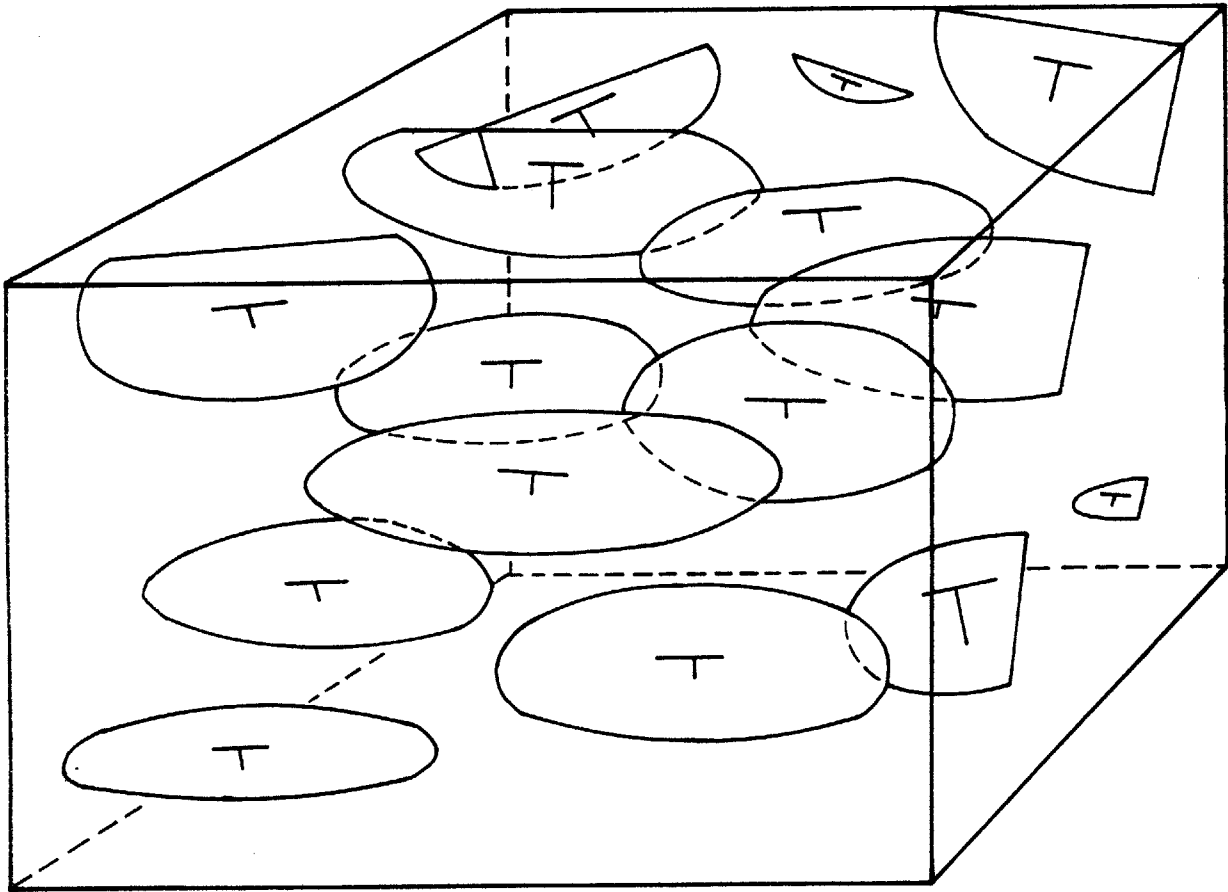
^{*} In a later work (Baecher and Lanney, 1978) the authors indicate that the underlying distribution for joint length may possibly be exponential. They identify a number of sampling biases which filter data from field surveys so that an underlying exponential (or gamma) distribution may appear to be lognormal.

Baecher et al., idealized joints as 2-dimensional convex disks randomly and independently positioned in space (Figure 2.17). The disks are circular with lognormally distributed radii. Joint radius and dip as well as joint radii and location are treated as statistically independent variables. (The independence assumptions are easier to justify if one only examines joints from a particular set of joints from a small zone.) The plan and profile shown in Figure 2.17 suggest what the joint traces might look like. The joint spacing and length characteristics are consistent with empirical observations.

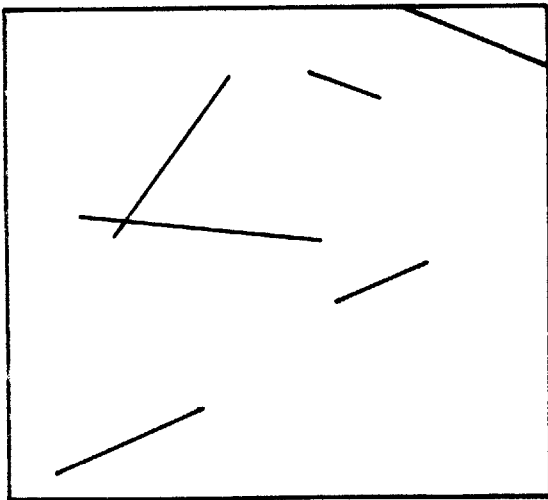
The model is an aid in visualizing the configuration of joints. However, it also describes a random process from which one can infer other properties. Baecher et al., have derived expressions for the mean and variance of the area of joints per unit volume. This parameter could be used as an index property in assessing the competency of a rock mass.

The Baecher et al. model is not a reliability model; in fact, it is not even concerned with slope stability. It does, however, provide a logical basis for approaching stability analyses. The model may be extended to furnish information on the location and shape of wedges at excavated faces.

The Veneziano model (Veneziano, 1978) is similar to the one proposed by Baecher et al. The latter model treats joints as isolated phenomena. Each disk is a solitary feature; the probability that any two disks will be coplanar is zero. The



PLAN



PROFILE

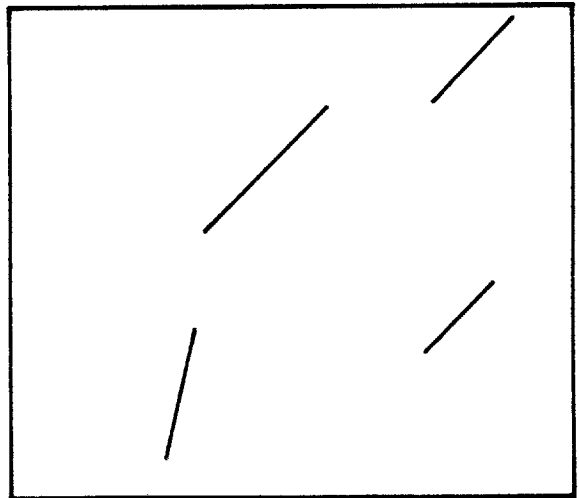


Figure 2.17 Baecher et al. Model
62

Veneziano model treats joints as bounded figures on Euclidean planes that extend to the borders of the rock mass. Each plane may contain several joints that are separated by zones of intact rock. The Baecher model is actually a special case of the Veneziano model in which each plane contains a single joint.

A detailed description of the Veneziano model will be presented in Chapter 5 so only the general features will be outlined here. Veneziano idealizes networks of joints as a Poisson process of planes in 3-dimensional space. The joints are generated through a three step sequence of random operations. First, Poisson planes or Poisson flats are generated in space to represent joint planes (Figure 2.18). Next, each plane is partitioned into random polygons by a family of Poisson lines. Finally, a specified proportion of the figures are shaded or colored. Shaded polygons correspond to joints while the remaining portions of the planes correspond to intact rock. In its most general form the model has five sets of input parameters: two density parameters (one of Poisson planes in space, the other of Poisson lines in each joint plane), two probability distributions (one of the orientation of planes and the other of the orientation of lines), and the shading probability. The parameters need not be constant; for example, the density of lines and the shading probability may depend upon the attitude of the joint plane. The same parameters may be uncertain and probabilistically dependent.

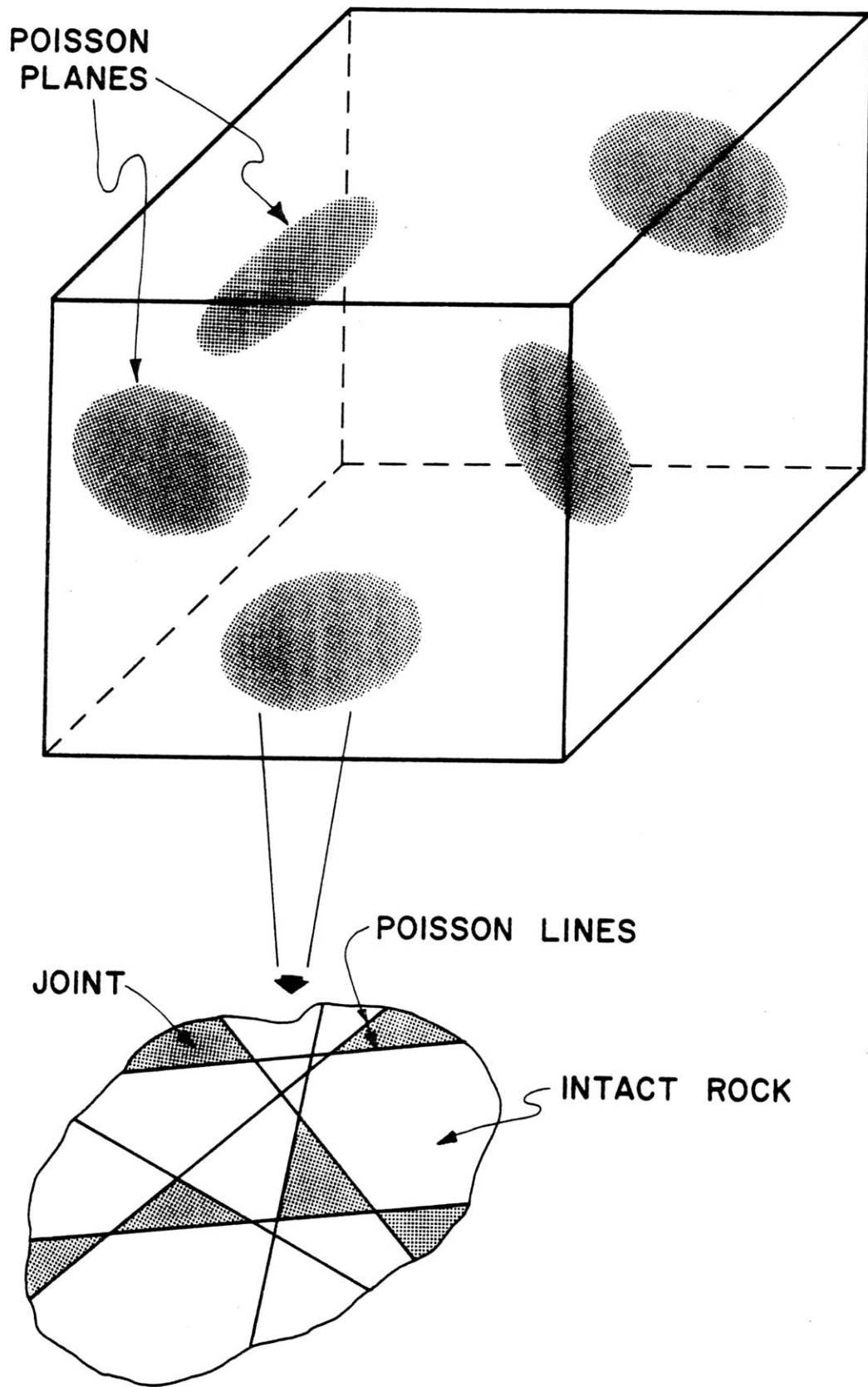


Figure 2.18 Veneziano Model
64

Veneziano used the model to derive a number of properties that are significant in stability analyses: the mean number of wedges that daylight in any particular region of a free face, the pdf's of the poles of the planes that define the wedges, the persistence along a specified failure surface and the area of joints per unit volume of rock. The first two properties are essentially the same parameters that Serrano and Castillo use in their analysis. Veneziano, however, has a closed form solution that greatly reduces the computational effort. These two parameters may provide the key to solving the multiple-wedge conditioning problem discussed earlier. The general approach could follow the technique developed by Serrano and Castillo: divide the excavated face into regions that contain wedges with similar sizes or volumes. Then each region can be analyzed individually and the resulting P_f values will actually be conditional probabilities based on the failure volume. The present version of the Veneziano model is not designed to compute P_f values. It is a conceptual model that hopefully will lead to a better understanding of the random process that control slope stability. The model may prove difficult to implement because of the unconventional nature of its input parameters. The five parameters that describe the Poisson and coloring processes must be derived from the data obtained in field surveys. Finally, the model may never realize its full potential. The model can handle correlations between various parameters. However, even the most

detailed field survey cannot provide enough information to define all these correlations. The model is simply much more powerful than the current state of the art in data acquisition and reduction.

2.5 Summary

All of the methods described in this chapter are recent additions to the rock mechanics literature and are currently undergoing improvements and modifications. The various authors have approached the reliability problem from many different directions. Despite the variety of techniques there are a number of observations that pertain to all the approaches:

1. All the methods demand accurately defined pdf's for the input parameters. Much more information is needed on typical distributional forms for such parameters as joint orientation and joint strength.
2. Information on correlation between random variables is almost totally lacking. For example, does ϕ depend on the joint length? This point raises two questions: How can field surveys be modified to deduce these correlations (if they exist)? How can the correlations be introduced into the analyses?
3. The assumption concerning the independence of joint planes must be carefully investigated. Do joints with particular orientations tend to congregate?

If a tetrahedral wedge is formed by one joint from set X and one joint from set Y does the fact that joint X_n from set X constitutes one boundary affect the marginal distribution of the member from set Y?

4. The multi-wedge problem needs to be examined as an exercise in system reliability. The binomial approach (Equation (2.11)) for calculating P_f may be too conservative. The P_f 's may be correlated i.e., adjacent wedges may have similar P_f 's because they share the same hydrostatic loads, etc.
5. Should all the uncertainty associated with a particular random variable be lumped together as if it had a common source? For example, a series of laboratory tests could be used to develop a pdf for ϕ . The pdf would reflect the imprecision of the tests as well as changes in the composition of the samples. However, this pdf is not necessarily the most appropriate one to use in stability calculations. The joint planes are so large that they tend to even out variations in composition. The pdf in the stability analysis should be less disperse than the laboratory one. (Vanmarcke (1977) examined this same problem in connection with fluctuations in soil properties.)

The comments outlined above span a wide range of disciplines. There are questions involving geology, random process

theory, systems engineering and geotechnical engineering. Some of the questions may not be answered for years to come. However, they should serve as a constant reminder that improvements in analytic techniques alone will never provide a complete solution to the problem of rock slope reliability.

CHAPTER 3

KINEMATIC CONDITIONS--COMPUTER PROGRAM DAYLITE

3.0 Introduction

The first step in analyzing the stability of a slope is to examine the kinematic restraints. Every pair of joints that intersect define a wedge; however, only a small number of these wedges may pose stability problems. The purpose of the kinematic tests is to isolate those potentially unstable wedges for further study. The tests are performed on a stereonet with constructions similar to the ones used in McMahon's (1971) approach.

A wedge will not be kinematically unstable unless the dip of its line of intersection is less than the apparent dip of the slope in the direction of the line's strike. From a graphical standpoint, only those lines of intersection which plot in the shaded area in Figure 3.1 will define potentially unstable wedges.

In a deterministic analysis where one is only interested in two specific planes the test is simple. Each pair of planes (and their corresponding line of intersection) can be checked individually. The tests will eliminate many wedges from further consideration.

LOWER HEMISPHERE EQUAL AREA STEREOCENTRIC

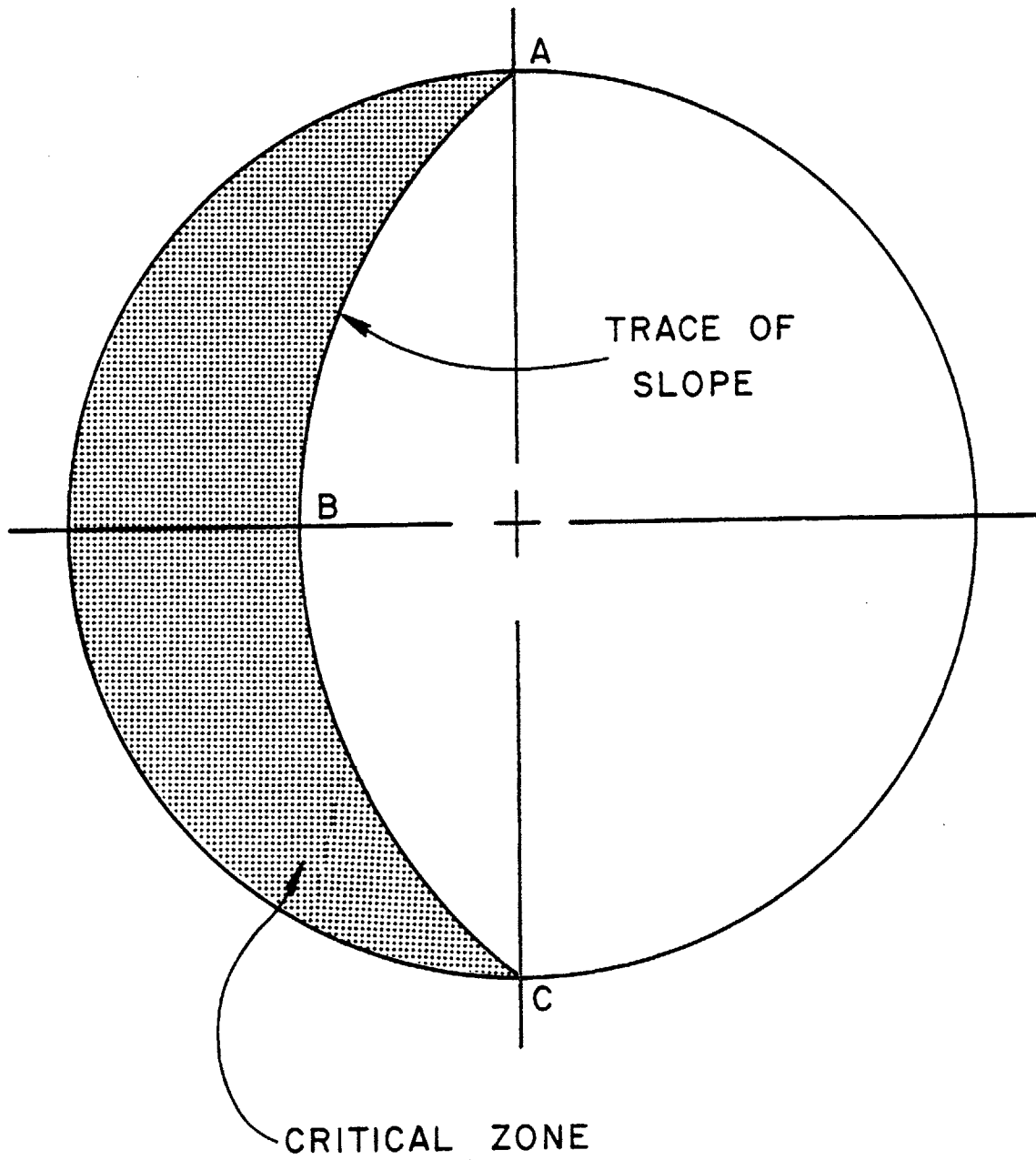


Figure 3.1 Critical Zone for Kinematic Instability

The kinematic tests are much more difficult to implement in reliability analyses because the orientations of planes are random variables. If, however, the pdf's of orientation can be described analytically it may be possible to derive the pdf of orientation for the lines of intersection. Knowing the position (and form) of this pdf in relation to the orientation of the slope face, one can compute some probabilities that may be useful in reliability analyses. For example, one can find the probability that any one wedge formed by two planes will be kinematically unstable--it is the volume* of the pdf that extends over the shaded area in Figure 3.1.

Unfortunately there is no closed form solution for obtaining the pdf of the lines of intersection given any arbitrary pair of pdf's that describe the orientation of joints. Therefore, the computer program DAYLITE was developed.

3.1 General Features of DAYLITE

DAYLITE derives the intersection pdf by computing $f(\theta, \phi)$ at specific points** in the critical zone. Each one of these points represents an orientation; the program identifies all possible combinations of joint planes which will have a line of intersection at that orientation. In essence, DAYLITE finds

* The pdf defined on the surface of a sphere is a 3 dimensional function. The integral of the curve over a region of the sphere ($\theta_1 < \theta < \theta_2$; $\phi_1 < \phi < \phi_2$) is the probability that the random variables (θ, ϕ) will be within the region.

**The program actually examines small incremental areas that can be characterized by a single point.

the pdf by addressing the question: Given an orientation (θ_o, ϕ_o) , what is the probability that two joints will combine to form a wedge whose line of intersection points in the (θ_o, ϕ_o) direction?

The solution procedure involves 3 steps:

1. Defining and partitioning the critical zone into cells.
2. Examining each cell to find pairs of joint planes that will have the appropriate line of intersection.
3. Calculating the probability that the slope will contain a requisite pair of joints.

Figure 3.2 lists the individual operations.

The remainder of this section presents an overview of the general procedure. Section 3.2 presents the details of each operation.

DAYLITE derives the intersection pdf numerically, but many of the mathematical operations can be visualized as graphical constructions on a stereonet. As indicated in Figure 3.1, the kinematically critical zone for wedge instability is bounded by the great circle that represents the trace of the slope on a lower hemisphere projection. The program partitions the zone into equal area spherical rectangles or cells. The boundaries of the rectangles constitute small circles of constant dip and great circles of constant strike so that the geometric figures

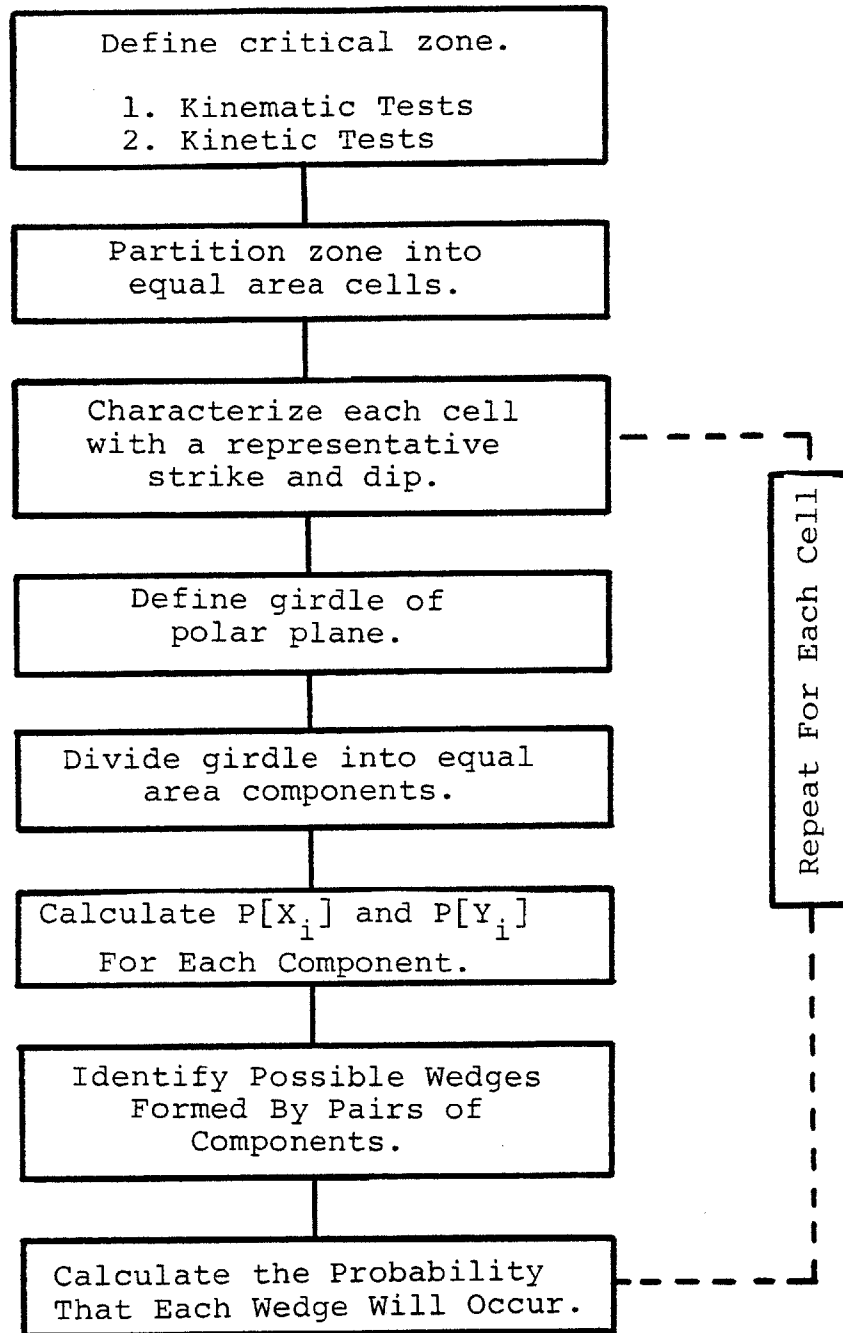


Figure 3.2 Flowchart for DAYLITE

correspond to the elements of a polar equal area stereonet (Figure 3.3). The purpose of the partitioning is to discretise the range of critical orientations into a number of representative values that can be studied on an individual basis. The value at the center of the cell characterizes all orientations within it. The program examines each of these cells and computes the probability that the line of intersection of two joint planes will be in that cell.

DAYLITE uses joint poles rather than joint planes. The line of intersection between two joints is the pole of the plane that contains the two joint poles (Figure 3.4). (This plane is termed the "polar plane".) AOB, the angle between the poles measured in the polar plane, is the dihedral angle between the joint planes. This dihedral angle is directly related* to the central angle or ψ angle of the wedge (Figure 3.5). There is a unique relationship between lines of intersection and polar planes. Each line of intersection corresponds to a different plane.

The colatitude** and latitude that characterize each cell define polar planes. Each cell represents a small range of orientations. If all the polar planes from a particular cell defined by (θ_o, ϕ_o) were plotted they would fall into a narrow

* In general, AOB and ψ are supplementary angles. However, under certain conditions, $\psi = \text{AOB}$. This discrepancy arises because all poles are plotted in the lower hemisphere. As will be shown in Section 3.2.6, the problem can be avoided by reverting back to planes to measure ψ angles.

**It is convenient to use spherical coordinates in developing computerized solutions. θ is the colatitude and corresponds to the azimuth. ϕ is the latitude and corresponds to the complement of the plunge angle.

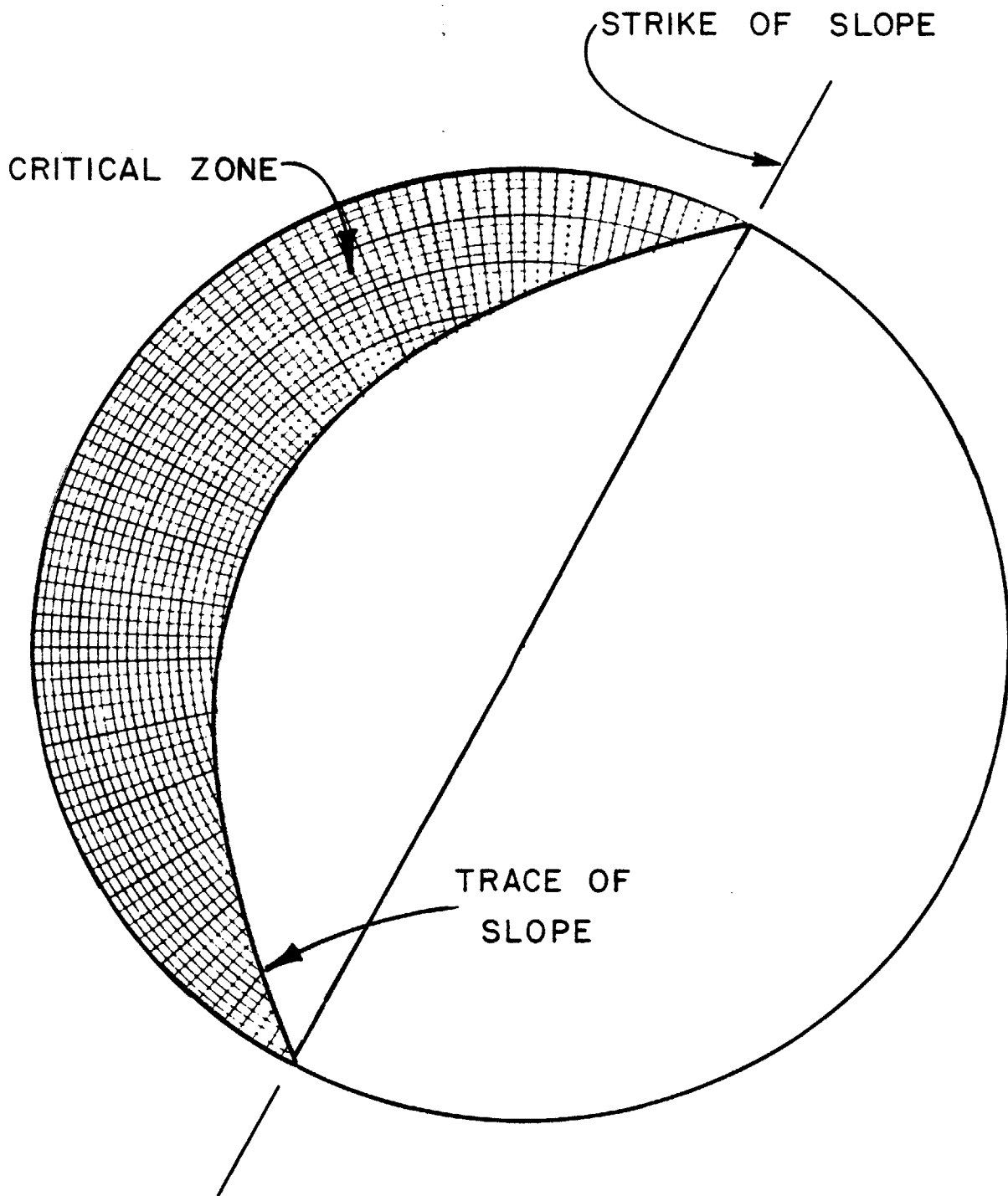
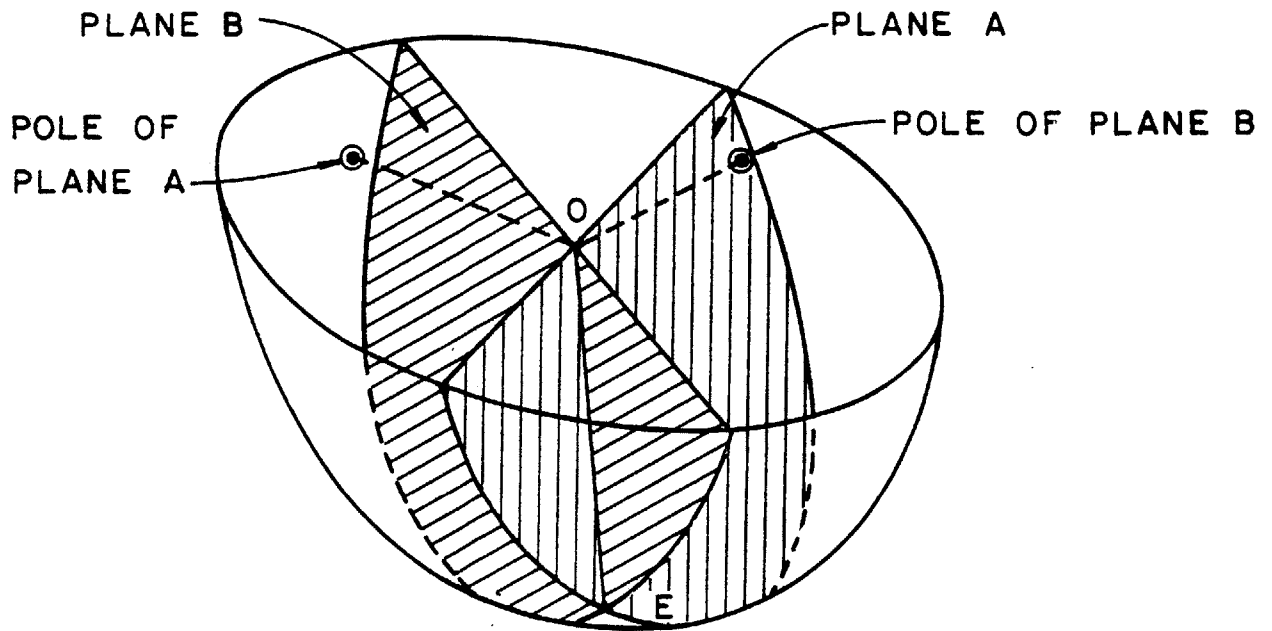
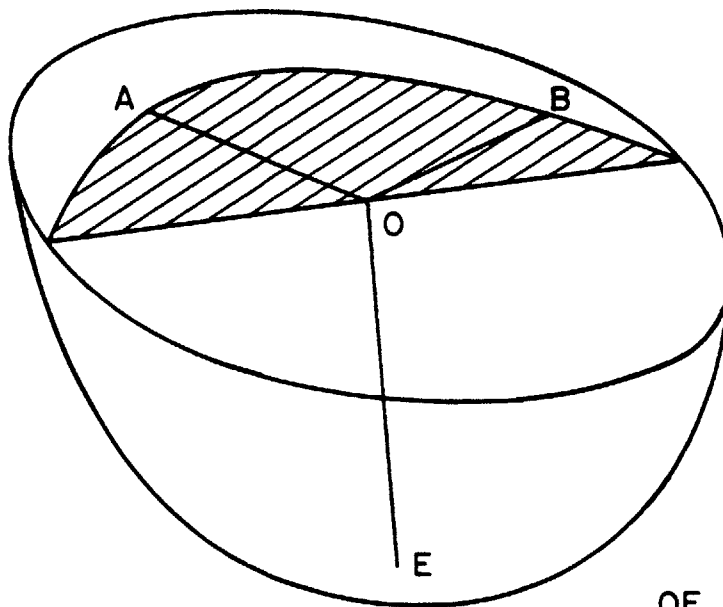


Figure 3.3 Critical Zone Partitioned into Equal Area Cells

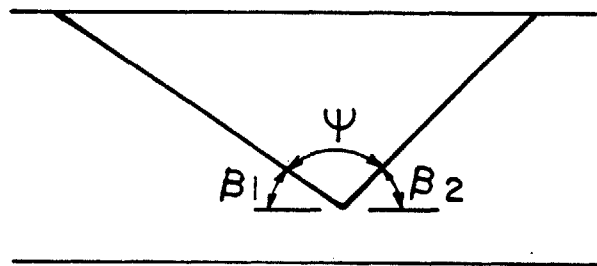
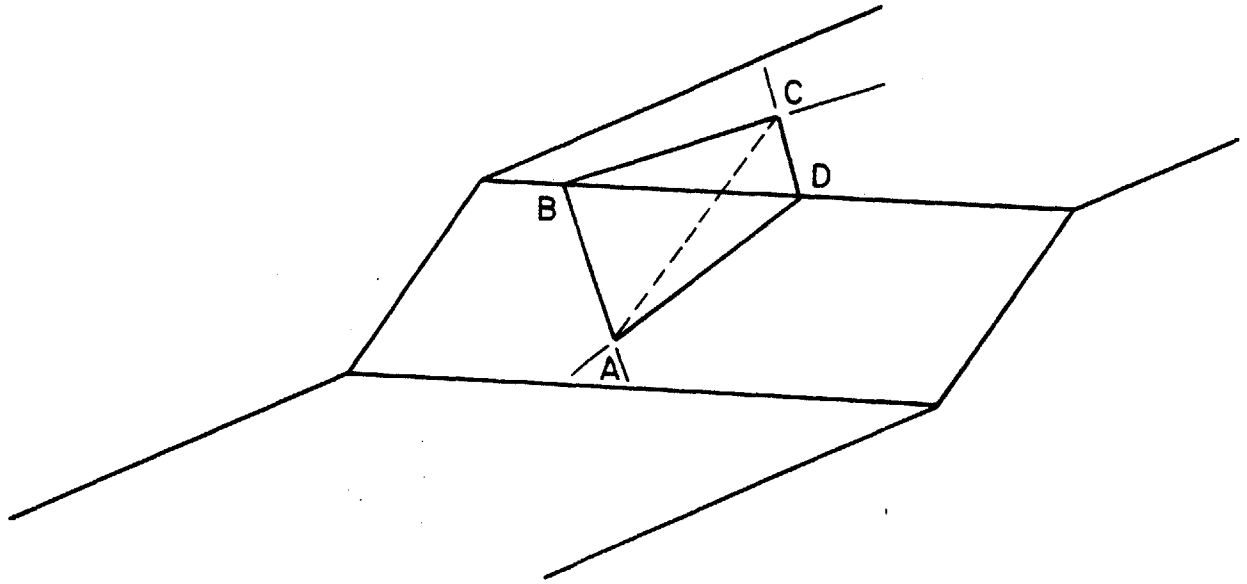


OE = LINE OF INTERSECTION



OE \perp PLANE AOB

Figure 3.4 Two Intersecting Planes



SECTION PERPENDICULAR TO AC

Figure 3.5 Definition of ψ

band or girdle* centered around the (θ_0, ϕ_0) polar plane (Figure 3.6). Figure 3.7 depicts the girdle from Figure 3.6 after it has been removed from the hemisphere and discretised into equal area components. Each component corresponds to a small area on the hemisphere. DAYLITE uses the pdf's of joint orientation to compute the probability that a joint pole will lie in any one component. $P[X_i]$ is defined as the probability that any one joint from set X will have a pole in component i; it is the integral of the pdf of set X over the spherical area of component i.

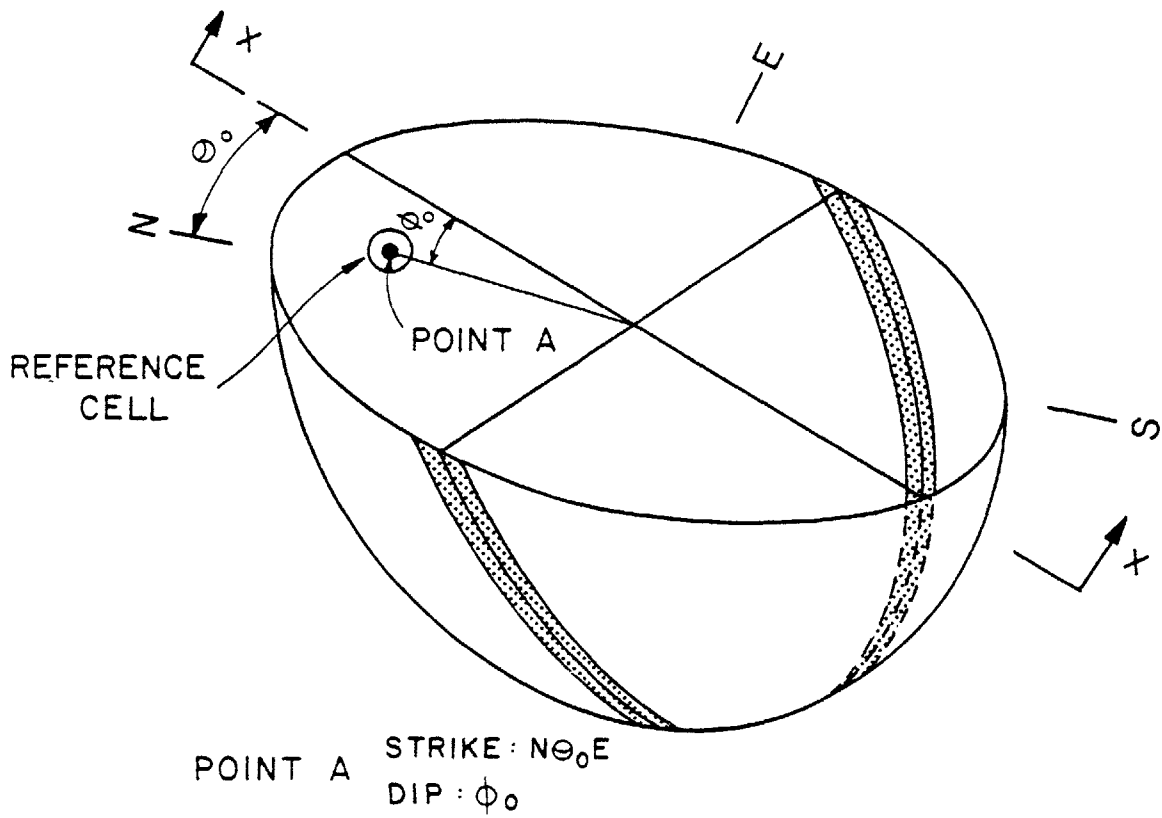
The partitioning operation on the girdle establishes n representative poles--one for each component. Each pair of poles (i,j) defines a wedge. The probability that a wedge defined by (i,j) will form is:

$$P[X_i]P[Y_j] + P[X_j]P[Y_i] \quad (3.1)$$

One joint must lie in component i while the other lies in component j.

As will be shown, the smallest wedge the program will consider has a ψ of $180/n$. The largest wedge has a ψ of $(n-1)180/n$. The program examines these extremes as well as all intermediate size wedges; in fact, the program investigates every possible combination of the n joint poles.

* Poles from a rectangular cell will not generate a true girdle i.e., a band of constant width. The actual band will be slightly wider at the ends.



δ = WIDTH OF CELL = WIDTH OF GIRDLE

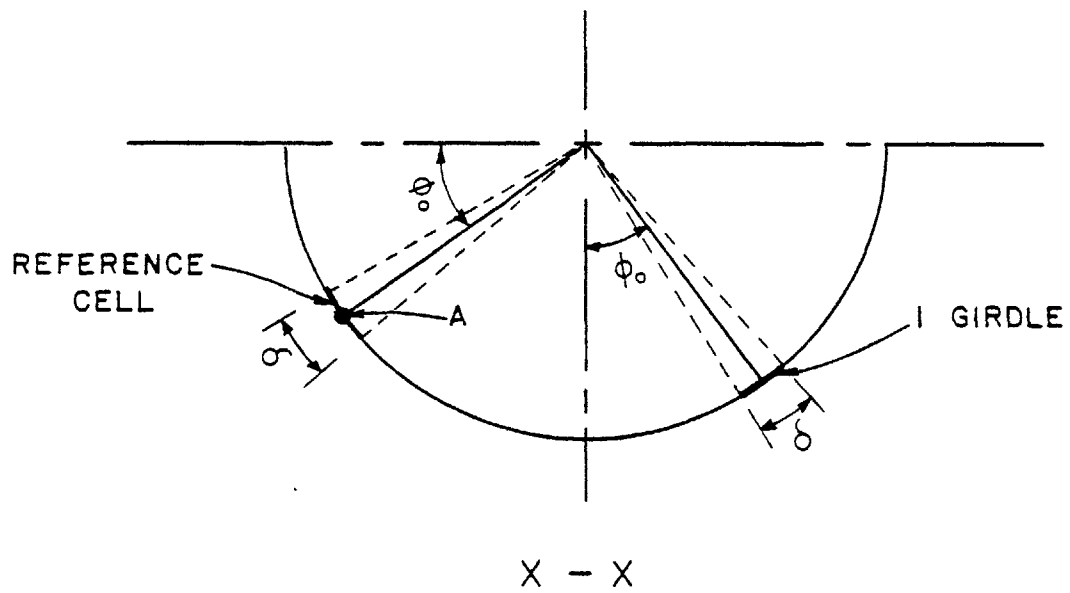
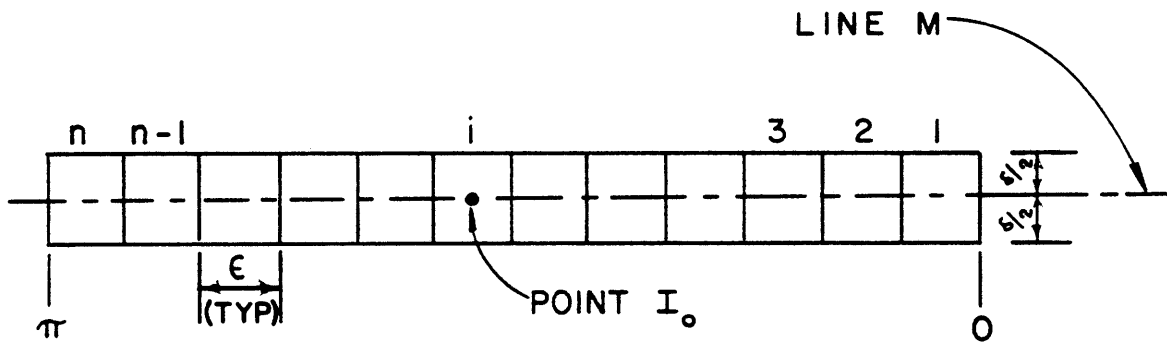


Figure 3.6 Reference Cell and Its Girdle



$$n = \text{NUMBER OF COMPONENTS} = \frac{\pi}{\epsilon}$$

Figure 3.7 Typical Girdle
80

The results of the analysis are expressed as $P[\theta_K, \phi_K, \psi_1]$, the probability that a wedge of central angle ψ_1 will have a line of intersection that daylight at (θ_K, ϕ_K) . (θ_K, ϕ_K) are the characteristic coordinates of cell in the critical zone and ψ_1 is a discrete variable with values $\frac{180}{n}, \frac{2(180)}{n}, \frac{3(180)}{n}$ $\frac{n-1}{n} 180$.

The two joints do not necessarily have to come from different sets. DAYLITE will calculate the probability that a particular wedge $(\theta_K, \phi_K, \psi_1)$ will be formed by two joints from set X (or two joints from set Y). The resulting probabilities are conditioned on the premise that only two joints from set X are present in the slope. The orientations of the two joints are treated as independent random variables i.e., the fact that one joint lies in a particular cell does not affect the pdf of the other joint. This same assumption of independence underlies the analysis involving joints from different sets. The assumption might be easier to justify in the latter case.

The critical step in the analysis is to assign values of $P[X_i]$ and $P[Y_i]$ to each component of the girdle. The operation requires that the pdf of joint orientation have an analytic form. Once the forms are determined the probability calculations become exercises in numerical integration. $P[X_i]$ is the volume of the pdf of X that lies over the i^{th} component.

DAYLITE will accept six different distributional forms:* Uniform, Fisher, Arnold, Bivariate Normal, Bingham, and Dershowitz. All these distributions are described in Appendix A. At the present time each set of joint orientation data must be studied to find the distribution which provides the closest fit. No one distribution appears to be universally applicable. Baecher et. al. (1978) made some preliminary studies on this subject and tentatively concluded that the Bivariate Normal and Bingham distributions are the most useful forms in describing orientation data.** Lanney (1978) and Dershowitz (19xx) provide some examples of fitting curves to actual data.

3.2.1 Defining the Critical Zone

The kinematically unstable zone consists of the entire region above the great circle ABC in Figure 3.1 because every point in that region represents a daylighting line of intersection. However, the fact that a line (or wedge) daylights does not necessarily imply that the wedge is unstable. Indeed, the second step in the reliability analysis is to examine resisting and driving forces to determine the probability that a daylighting wedge will fail. (This subject will be discussed in Chapters 4 and 6.) Nevertheless, wedges with shallow dips may have relatively small driving forces and, consequently,

* The current version of DAYLITE uses the six forms listed. The program can be modified to accept any spherical distribution that can be expressed analytically.

**The Dershowitz Distribution is a modified version of the Bingham and was formulated after the completion of the Baecher et al. study.

negligible probabilities of failure. The reliability analysis can be simplified by eliminating these wedges from further consideration at this early stage. The DAYLITE user can specify a minimum dip (α) which will reduce the critical zone. Figure 3.8 indicates that even a modest value of α can significantly reduce the critical zone.

In a rigorous reliability analysis α should be zero. Every wedge regardless of its orientation has a finite probability of failure; hence, every line of intersection should be examined. In choosing a non-zero α , the DAYLITE user opts to ignore some possible (albeit improbable) failure geometries involving wedges with shallow dips. The user elects to introduce some error into the analysis in order to reduce the volume of calculations. The selection of α requires some judgment. The parameter might be considered the lower bound of joint friction angles. From a physical standpoint it could represent the lowest practical coefficient of friction for mineral to mineral contact. From an analytical standpoint, α depends on the pdf of ϕ . If ϕ were normally distributed α might be defined as ϕ_{mean} minus 2 standard deviations of ϕ ; in this case, $P[\phi < \alpha] = 0.0228$.

3.2.2 Partitioning the Critical Zone

As mentioned in Section 3.1 and shown in Figure 3.3, the critical zone is partitioned into equal area cells to help one discern the location and shape of $f(\theta, \phi)$, the pdf of the line of intersection. θ and ϕ are continuous random variables;

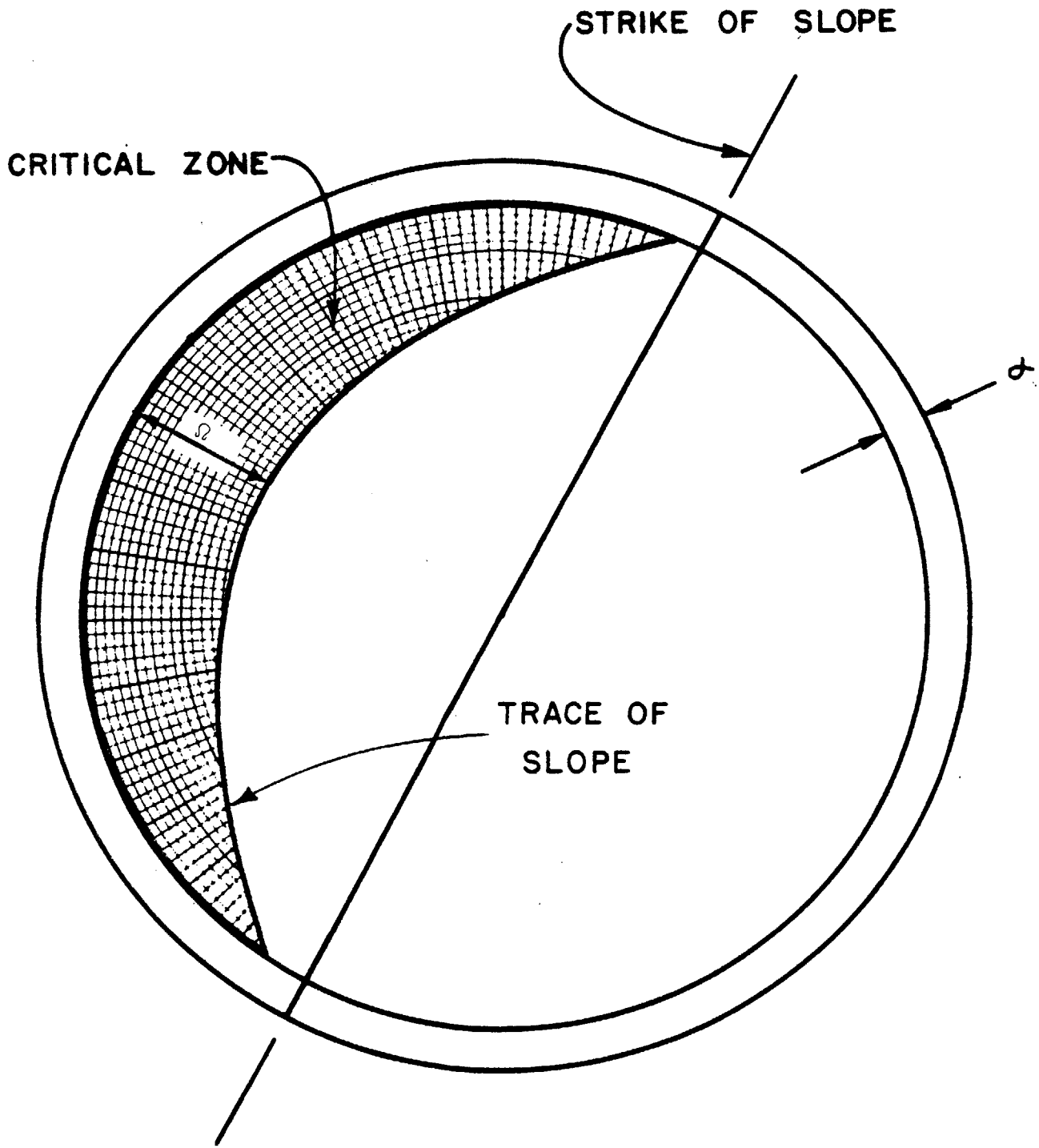


Figure 3.8 Reduction of Critical Zone with α

DAYLITE treats them as discrete random variables defined only at the characteristic coordinates of each cell, (θ_i, ϕ_i) . The program uses numerical techniques to compute $P[\theta_i, \phi_i]$, the probability that the line of intersection will lie in cell i . The method approximates the integral of $f(\theta, \phi)$ over A_i , the area of cell i .

$$P[\theta_i, \phi_i] = \int_{A_i} f(\theta, \phi) dA \quad (3.2)$$

As long as A_i is small,

$$P[\theta_i, \phi_i] = f(\theta_i, \phi_i) A_i \quad (3.3)$$

Or,

$$P[\theta_i, \phi_i]/A_i = f(\theta_i, \phi_i) \quad (3.4)$$

If A_i is a constant for all i ,

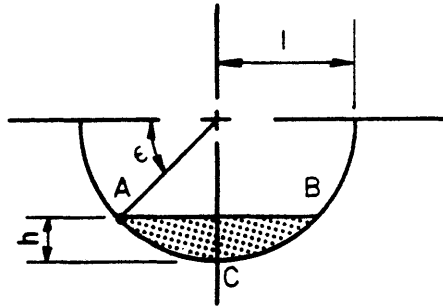
$$P[\theta_i, \phi_i] \propto f(\theta_i, \phi_i) \quad (3.5)$$

for all cells. Thus, the maximum(a) of $P[\theta_i, \phi_i]$ correspond to the mode(s) of $f(\theta, \phi)$.

The partitioning of the critical area is based on two parameters: Ω and ϵ . Ω , the maximum width of the zone, is defined as the dip of the slope (ϕ_s) minus α (Figure 3.8). ϵ is an angular value that controls the size of the unit cells. DAYLITE divides the spherical segment that lies between ϕ_s and α into $\frac{\Omega}{\epsilon}$ segments bounded by small circles.

The procedure is illustrated in Figure 3.9 which is a section through the hemisphere. The area of the spherical segment DEFG defined by Ω and α is $2\pi(\sin(\phi_s) - \sin\alpha)$; hence the area between any adjacent small circles should be:

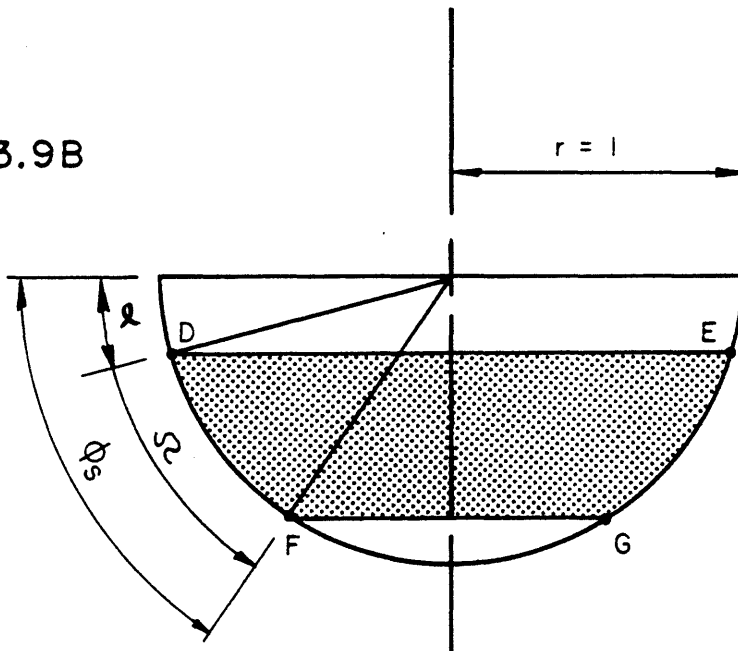
3.9A



AREA OF SEGMENT ABC

$$\begin{aligned}
 &= 2\pi r h \\
 &= 2\pi r^2(1 - \sin \omega) \\
 &= 2\pi (1 - \sin \omega) \\
 &\quad \text{for } r=1
 \end{aligned}$$

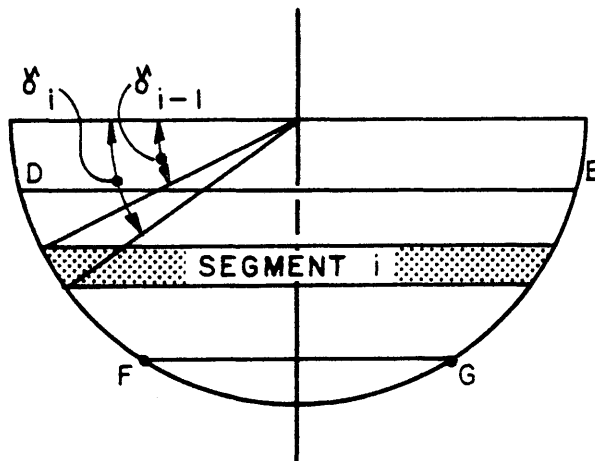
3.9B



AREA OF SEGMENT DEFG

$$= 2\pi (\sin(\phi_s) - \sin(\alpha))$$

3.9C



AREA OF SEGMENT i

$$= \frac{2\pi (\sin(\phi_s) - \sin(\alpha))}{\pi/\epsilon}$$

Figure 3.9 Areas of Spherical Segments--Definition of δ

$$\Delta A = 2\pi \frac{\sin(\phi_s) - \sin\alpha}{\frac{\Omega}{\varepsilon}} \quad (3.6)$$

The dips of the small circles can be computed from the surface areas. Let γ_{i-1} and γ_i ($\gamma_{i-1} < \gamma$) be the dips of the circles that bound the i^{th} spherical segment (Figure 3.9C):

$$A_t - (A_o + (i)\Delta A) = 2\pi(1 - \sin\gamma_i) \quad (3.7)$$

$$\begin{aligned} A_t &= \text{total area of the unit hemisphere} \\ &= 2\pi \end{aligned}$$

$$\begin{aligned} A_o &= \text{area of the spherical segment above the small} \\ &\quad \text{circle DE in Figure 3.9B} \\ &= 2\pi\sin\alpha \end{aligned}$$

Equation (3.7) can be rewritten as:

$$\gamma_i = \sin^{-1}\left(\sin\alpha + \frac{(i)\Delta A}{2\pi}\right) \quad (3.7A)$$

Let n = the number of segments. From Equation (3.7A):

$$\gamma_o = \alpha \quad (3.8)$$

$$\gamma_n = \Omega + \alpha \quad (3.9)$$

$$= \phi_s$$

The spherical segments of area ΔA are subdivided into cells of equal area by lines of constant strike. The angular

increment between adjacent strike lines is $\frac{\pi^*}{\epsilon}$. Figure 3.10 shows a segment bounded by α and ϕ_s that has been partitioned into cells. The area of each cell is $\frac{\Delta A}{\pi/\epsilon}$.

The method outlined above will partition the entire spherical segment. However, only those cells in the critical zone (Figure 3.8) must be studied. The great circle that defines the slope dissects some of the peripheral cells. DAYLITE examines all cells that lie even partially in the critical zone.

Each cell is characterized by a value of colatitude and latitude. The characteristic colatitude is the mean of the two colatitudes (or strikes) that border the cell. The characteristic latitude is the latitude that divides the cell into two parts with equal surface areas. It is computed in the same manner as γ_i :

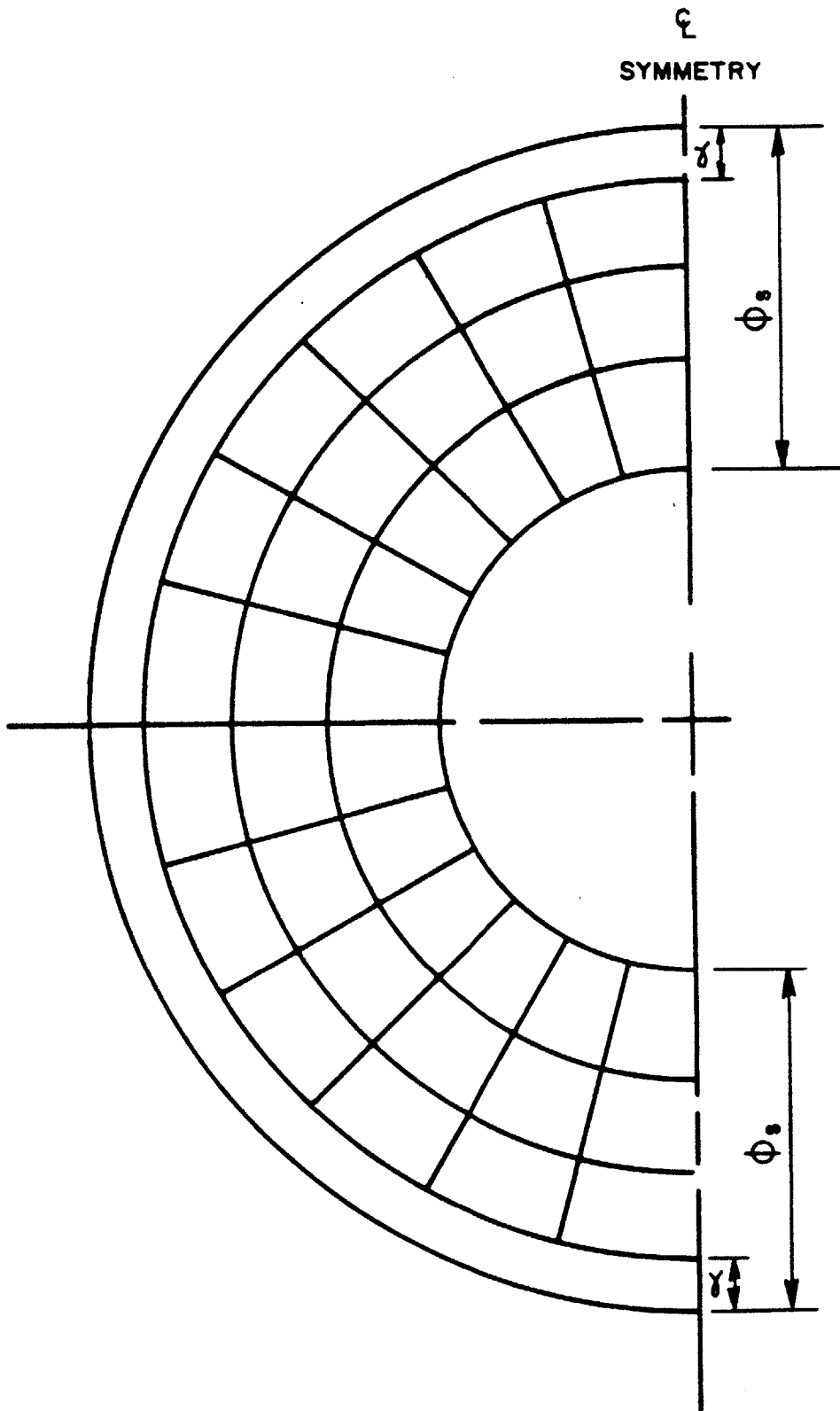
$$\begin{aligned} \phi_i &: = \text{characteristic latitude of cell bounded by } \gamma_{i-1} \text{ and } \gamma_i \\ &= \pi/2 - \text{characteristic dip} = \pi/2 - \hat{\gamma}_i \end{aligned} \quad (3.10)$$

$$= \pi/2 - \sin^{-1} \left(\sin \alpha + \frac{(i) \Delta A}{2\pi} - \frac{\Delta A}{2\pi} \frac{1}{2} \right) \quad (3.11)$$

3.2.3 Defining the Girdle

Each point in a cell defines a polar plane. All the polar planes from a single cell are located in a relatively

* ϵ should be chosen so that the quantities π/ϵ and $\frac{\Omega}{\epsilon}$ are integers. In addition, π/ϵ should be a positive integer. Smaller values of ϵ will define smaller cells; hence, result in better defined pdf's.



$$\text{AREA OF EACH CELL} = \frac{\Delta A}{(\pi/\epsilon)}$$

Figure 3.10 Spherical Segment Partitioned into Equal Area Cells

narrow band around the plane associated with the characteristic latitude and colatitude of the cell. If the cells were circular the locus of planes would form a girdle. In fact, the cells are spherical rectangles with aspect ratios that approach unity*. DAYLITE approximates the rectangles as circles with an equivalent area. The area of the cells is a constant:

$$A_{\text{cell}} = \frac{\Delta A}{(\pi/\epsilon)} \quad (3.12)$$

The diameter of the equivalent circle expressed as the spherical angle δ is shown in Figure 3.12:

$$\delta = 2 \cos^{-1} \left(1 - \frac{A_{\text{cell}}}{2\pi} \right) \quad (3.13)$$

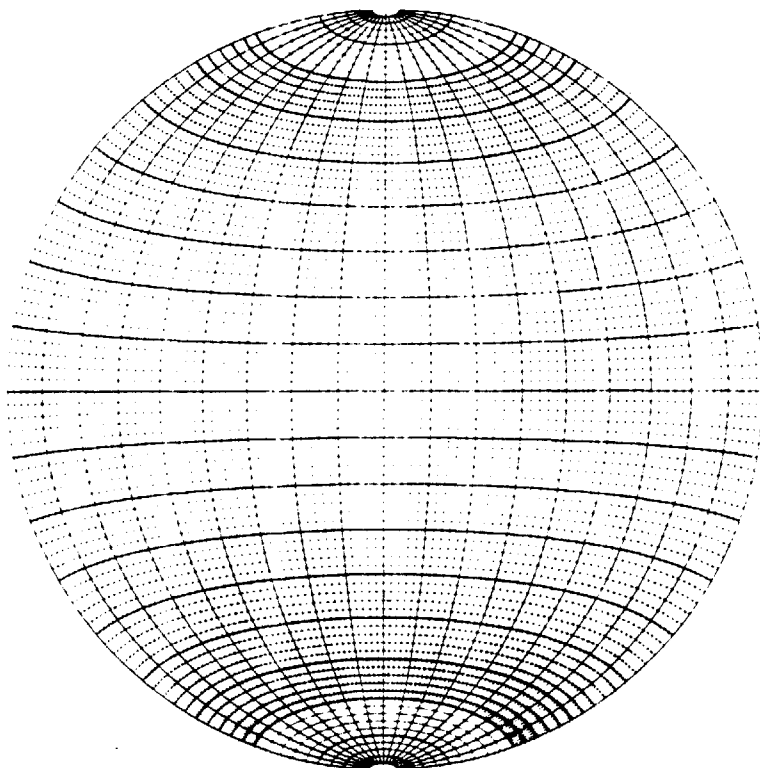
δ is also the width of the girdle that contains all the planes whose poles lie within the circle (see Figure 3.7).

3.2.4 Dividing the Girdle into Components

As shown in Figure 3.7, the dimensions of the girdle are δ by π . The girdle contains all the polar planes from a single cell in the critical zone. Line M which bisects the girdle is the trace of the polar plane defined by the characteristic colatitude and latitude of the cell (θ_0, ϕ_0). Every

* The ratio is not a constant. The cells in some regions of the hemisphere are more highly distorted. In a polar projection the maximum distortion occurs at the center whereas it occurs at the edge (along the strike direction) in meridonal projections (cf., Figure 3.11). The highly distorted region in a polar plot will not lie in the critical zone unless the slope is steep ($>60^\circ$).

Meridonal:



Polar:

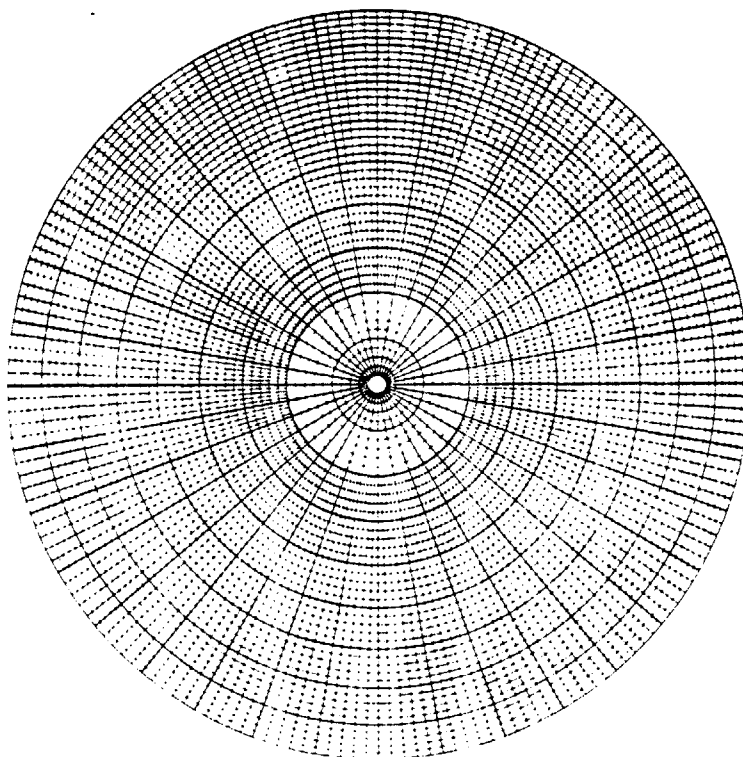
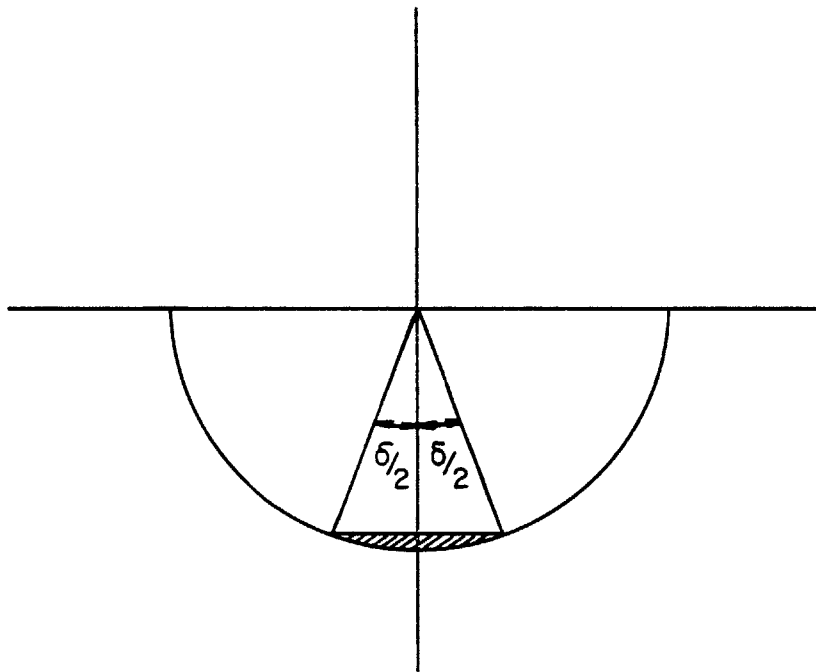
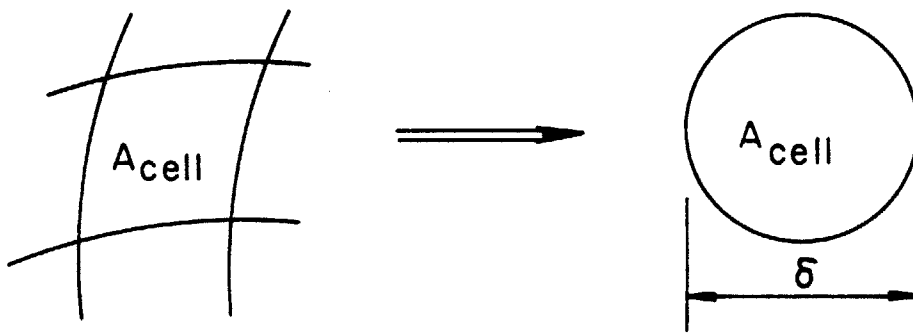


Figure 3.11 Meridonal vs. Polar Projection



$$A_{\text{cell}} = 2\pi \left(1 - \cos \frac{\delta}{2}\right)$$

Figure 3.12 Definition of δ

pair of points in the girdle represents a pair of joint orientations that could produce a requisite line of intersection i.e., any two joints whose poles lie in the girdle will define a wedge that has a line of intersection that pierces the unit hemisphere in the (θ_0, ϕ_0) cell.

Like the critical zone, the girdle is divided into a few discrete components that can be examined on an individual basis. The operation is based on ϵ , the parameter used to partition the critical zone. The girdle is separated into n equal area components where $n = \frac{\pi}{\epsilon}$; hence, each component has the dimensions ϵ by δ^* . The components are characterized by the coordinates of their midpoints e.g., point I_0 characterizes component i in Figure 3.7. All the midpoints lie along line M.

Figure 3.13 depicts the polar plane defined by the characteristic coordinates (θ_0, ϕ_0) or $(x_0, y_0, z_0)^{**}$ of a particular cell; this plane corresponds to line M of Figure 3.7. Point I_0 , the midpoint of the i^{th} component (Figure 3.14), is η radians from the strike direction $(x_1, y_1, 0)$ of the polar plane.

* The components will not be equidimensional. δ will always exceed ϵ , never by more than 13%. This disparity occurs because the rectangular cell in the critical zone is approximated by a circle.

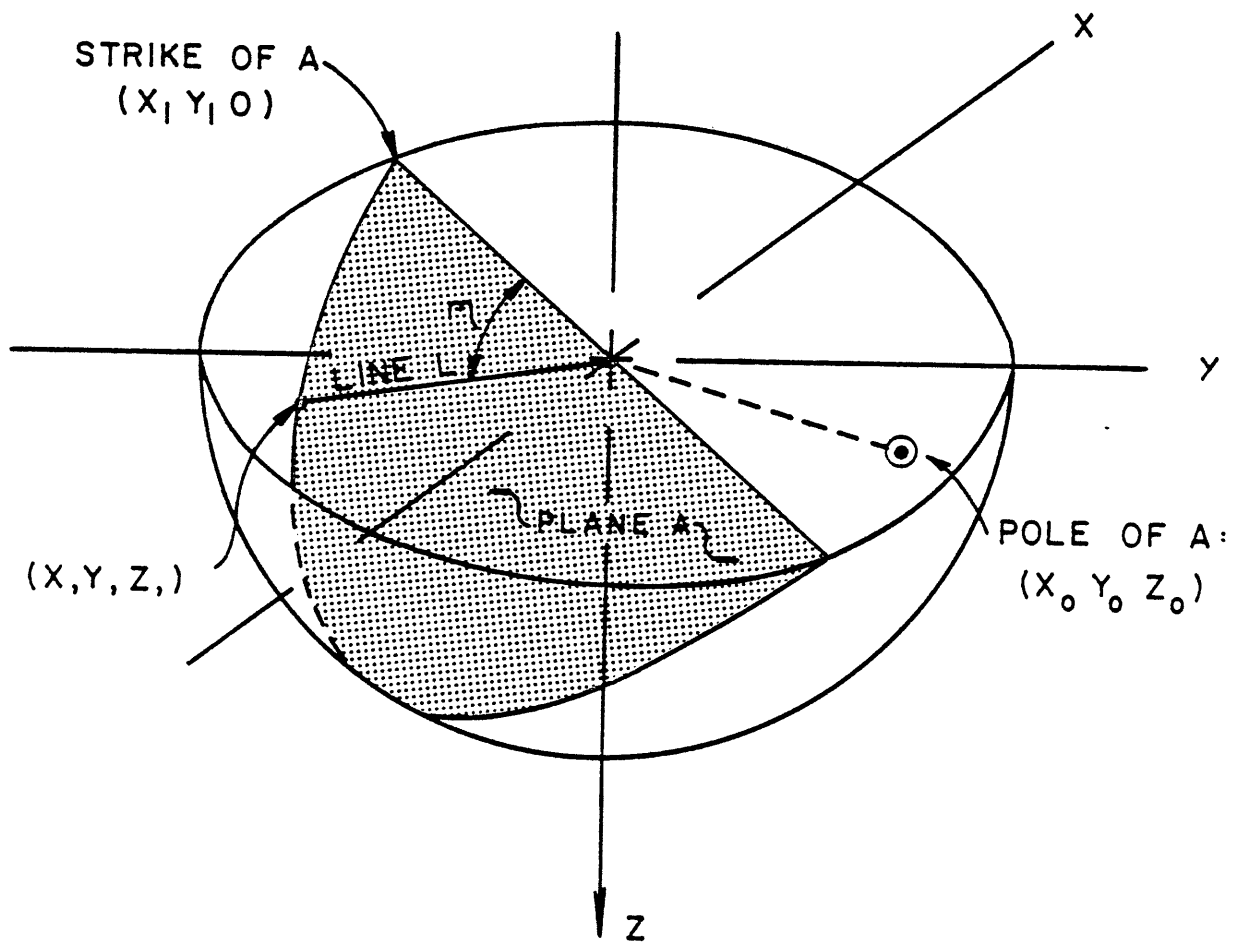
** The transformation from spherical to Cartesian coordinates can be made through the following relations:

$$x = \sin \theta \sin \phi$$

$$y = \cos \theta \sin \phi$$

$$z = \cos \phi$$

The positions of the x,y and z axis are shown in Figure 3.13

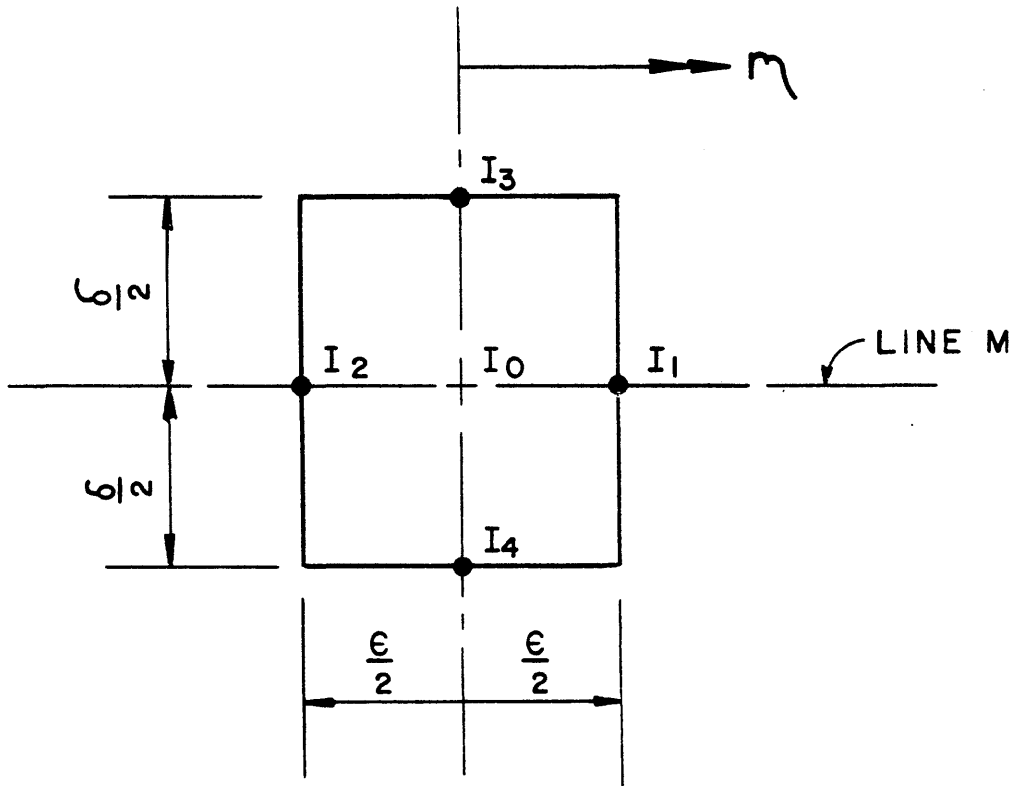


$$A = (X_0, Y_0, Z_0)$$

$$B = (X_1, Y_1, 0)$$

$$I_0 = (X, Y, Z)$$

Figure 3.13 Location of I_0 on Polar Plane--Definition of η



i^{th} COMPONENT OF GIRDLER

Figure 3.14 Typical Component of Girdle

The x, y and z coordinates of I_0 can be found by solving three simultaneous equations:

$$(x_0, y_0, z_0) \cdot (x, y, z) = x_0 x + y_0 y + z_0 z = \cos(\pi/2) = 0 \quad (3.14)$$

$$(x_1, y_1, 0) \cdot (x, y, z) = x_1 x + y_1 y = \cos \eta \quad (3.15)$$

$$x^2 + y^2 + z^2 = 1 \quad (3.16)$$

The solution to the equations is presented in Appendix B.

Points I_1 and I_2 (Figure 3.14) can be located by replacing η in Equation (3.15) with $\eta - \frac{\epsilon}{2}$ and $\eta + \frac{\epsilon}{2}$.

A similar set of equations can be used to determine the coordinates of points I_3 and I_4 (Figure 3.14) at the top and bottom of the girdle. This solution is also presented in Appendix B.

Thus, DAYLITE computes the coordinates of five points for every component of the girdle.

3.2.5 Calculating $P[X_i]$

$P[X_i]$ is the probability that any one joint pole from set X will be in the spherical area defined by component i of the girdle. It is the integral of the pdf of joint pole orientations over the area of the component. DAYLITE approximates this integral as

$$P[X_i] = \frac{A_c}{6} [2f(I_0) + f(I_1) + f(I_2) + f(I_3) + f(I_4)] \quad (3.17)$$

where A_c is the area of the girdle component - a constant for all components and $f(I_k)$ is the value of the pdf of joint pole orientations at point I_k shown in Figure 3.14.

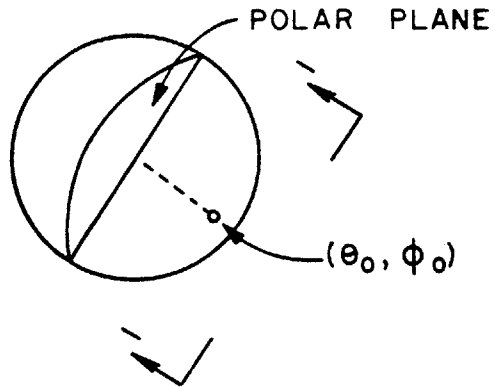
3.2.6 Identifying Wedges

The operations outlined in Sections 3.2.4 and 3.2.5 divide the girdle into n components and characterize each component by a single point. Thus, the area of the girdle is discretised into n representative points. Therefore all wedges which intersect the hemisphere in the (θ_o, ϕ_o) cell are formed by planes with poles coincident with two of the n points.

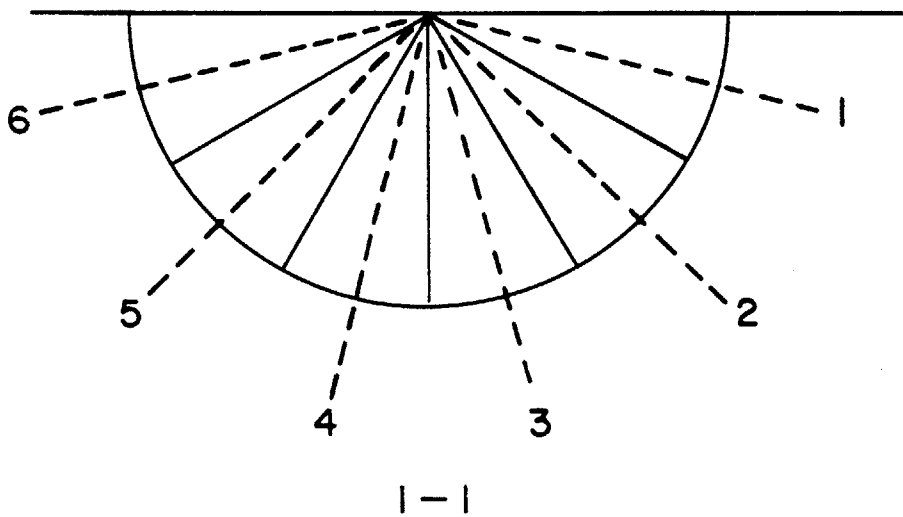
The easiest way to visualize the wedges is to examine the planes themselves rather than their poles. Figure 3.15B is a section perpendicular to the line of intersection that daylights at (θ_o, ϕ_o) . It depicts a typical polar plane that has been divided into 6 components*. The heavy lines labeled 1 through 6 indicate directions of representative poles for the respective components. Figure 3.15C shows the planes that correspond to the poles. (The planes are perpendicular to the section so only their linear traces appear.) The probability that plane i will occur is identical to the probability that its pole will intersect the sphere at point i .

* A plane with 6 components is used to illustrate the concept. The actual number of components (n) depends on ϵ i.e., $n = \pi/\epsilon$. n should be an even integer to facilitate the computations.

3.15A



3.15 B



3.15 C

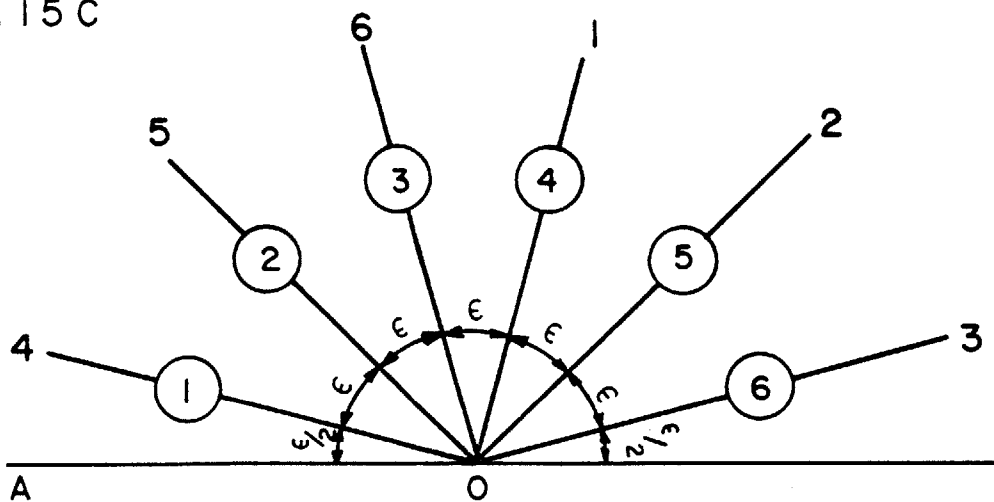


Figure 3.15 Renumbering of Characteristic Points on Girdle

The planes can be renumbered so that they become consecutive in a clockwise direction from the line segment OA. (The new numbering system is shown in Figure 3.15C as (i) .) n is the number of poles (or planes) and $()_{old}$ and $()_{new}$ refer to the plane designations in the two respective systems.

$$1 \leq (j)_{new} \leq \frac{n}{2} \quad (j)_{new} = \left[(j)_{old} + \frac{n}{2} \right] \quad (3.18)$$

$$\frac{n}{2} < (j)_{new} \leq n \quad (j)_{new} = \left[(j)_{old} - \frac{n}{2} \right] \quad (3.19)$$

The algorithm is different for the two quadrants.

The largest wedge that can form has a central angle or ψ of $\frac{n-1}{n} 180^\circ$ while the smallest wedge has a ψ of $\frac{180^\circ}{n}$. If $\bar{\epsilon}$ is ϵ expressed in degrees i.e., $\bar{\epsilon} = \epsilon \frac{180}{n}$:

$$\psi_{max} = (n-1)\bar{\epsilon} \quad (3.20)$$

$$\psi_{min} = \bar{\epsilon} \quad (3.21)$$

The angle between any adjacent pair of planes is $\bar{\epsilon}$; hence, the angle between any two planes must be $k\bar{\epsilon}$ where k is an integer between 1 and $n-1$. Thus, the wedges defined by DAYLITE have ψ 's that are multiples of $\bar{\epsilon}$.

$$\psi_{\min} = \psi_1 = \bar{\epsilon} \quad (3.22)$$

$$\psi_2 = 2\bar{\epsilon} \quad (3.23)$$

$$\psi_k = k\bar{\epsilon} \quad (3.24)$$

$$\psi_{\max} = \psi_{n-1} = (n - 1)\bar{\epsilon} \quad (3.25)$$

DAYLITE computes each ψ_k and identifies all possible combinations of planes that will produce a wedge with a central angle of ψ_k . Each combination consists of two planes that are separated by an angle of $k\bar{\epsilon}$. Thus, ψ_k will have $n-k$ combinations:

$$(1, 1 + k)$$

$$(2, 2 + k)$$

$$(n - k, n)$$

The larger the ψ_k , the fewer the combinations. ψ_{\max} has only one pair of points i.e., $(1, n)$ whereas ψ_{\min} has $n-1$ pairs.

DAYLITE also computes the β_1 angle (Figure 3.5) associated with each wedge. As shown in Figure 3.15, the incremental angle between any adjacent planes is $\bar{\epsilon}$. Hence, for any wedge:

$$\beta_1 = \frac{\bar{\epsilon}}{2} + \left[(j)_{\text{new}} - 1 \right] \bar{\epsilon} \quad (3.26)$$

where $(j)_{\text{new}}$ is the number of the plane which forms the right boundary of the wedge.

The four parameters ϕ, θ, ψ and β_1 completely define the orientation of a wedge.

3.2.7 Calculating $P[(\theta_o, \phi_o, \psi_o, (\beta_1)_o)]$

The results of the analysis performed by DAYLITE are expressed as the probability that a particular wedge $(\theta_o, \phi_o, \psi_o, (\beta_1)_o)$ will form. The program examines every pair of girdle components and, in doing so, identifies every possible wedge geometry. For example, all wedges in Figure 3.15C have a line of intersection oriented at (θ_o, ϕ_o) but the only two joints which form a wedge with $\psi = 2\varepsilon$ and $\beta_1 = \frac{3\varepsilon}{2}$ are joints 2 and 4. One joint pole must lie in girdle component 5 while the other lies in component 1. Thus, the probability that one joint from set X and one joint from set Y will combine to form a $(\theta_o, \phi_o, \psi_o, (\beta_1)_o)$ wedge is:

$$P[(\theta_o, \phi_o, \psi_o, (\beta_1)_o)] = P[X_1]P[Y_5] + P[X_5]P[Y_1] \quad (3.27)$$

$$P[X_i] = P[\text{set X will have a pole in girdle compent i}]$$

The output from DAYLITE includes three different probability calculations:

$P[\theta_i, \phi_i]$ - the probability that a wedge (regardless of its shape) will have a line of intersection oriented in the (θ_i, ϕ_i) direction.

$P[\theta_i, \phi_i, \psi_j]$ - the probability that a wedge with a central angle of ψ_j (regardless of β_1) will have a line of intersection oriented in the (θ_i, ϕ_i) direction.

$P[\theta_i, \phi_i, \psi_j, (\beta_1)_k]$ - the probability that a wedge with a central angle of ψ_j and a β_1 of $(\beta_1)_k$ will have a line of intersection oriented in the (θ_i, ϕ_i) direction.

The probabilities are related:

$$P[\theta_i, \phi_i, \psi_j] = \sum_k P[\theta_i, \phi_i, \psi_j, (\beta_1)_k] \quad (3.28)$$

$$P[\theta_i, \phi_i] = \sum_j P[\theta_i, \phi_i, \psi_j] \quad (3.29)$$

As indicated in Section 3.1, the user can specify that the two joints belong to different sets (as in Equation (3.27)) or that both joints belong to the same set--either set X or set Y.

$P[\theta_i, \phi_i]$ is useful in the early stages of the analysis because it provides an overview of the problem. It enables one to determine the most likely orientations for wedges independent of their shape. The other two probabilities are used in the detailed analysis. They give specific information on the shapes of wedges.

3.3 Program Information

The input parameters to DAYLITE include the orientation of the open face and the distributional parameters of the two joint sets. The user must also prescribe the accuracy desired in the numerical integration procedure. He must specify four angular values: $\epsilon, \alpha, \hat{\psi}$ and $\Delta\psi$.

ϵ controls the size of the unit cell in the critical zone and the width of girdle components. The parameter was discussed in Section 3.2.2.

α reduces the critical zone. The program will not examine any lines of intersection that have a dip less than α . The parameter was discussed in Section 3.2.1.

$\hat{\psi}$ is a parameter that controls the minimum size wedge. The smallest wedge the program identifies has a central angle of $\bar{\epsilon}$ (Section 3.2.6). The user may not be interested in very narrow wedges because they tend to have high FS's (or low P_f 's). The narrow geometry induces high normal stresses in the joint planes - thus, high resistances. The user can opt to ignore these narrow wedges by specifying a value for ψ . The program will not examine any wedge with a central angle smaller than ψ . (The program will investigate all wedges larger than $\bar{\epsilon}$ if ψ is not specified.)

$\Delta\psi$ enables the user to reduce the volume of output without sacrificing too much information. The program will sum values of $P[\theta_i, \phi_i, \psi_j]$ and express the results as $P[\theta_i, \phi_i, \psi_A \leq \psi_j \leq \psi_B]$ where $\psi_B - \psi_A = \Delta\psi$ thus,

$$P[\theta_i, \phi_i, \psi_A \leq \psi_j \leq \psi_B] = \sum_{\substack{\text{all } \psi_j \\ \text{such that} \\ \psi_A \leq \psi_j \leq \psi_B}} P[\theta_i, \phi_i, \psi_j] \quad (3.30)$$

The program computes $P_{\theta_i, \phi_i, \psi_j}$ for ψ_j values of $\psi_A, \psi_A + \bar{\epsilon}, \psi_A + 2\bar{\epsilon}, \dots, \psi_B$.

It then sums the probabilities as prescribed by Equation (3.30). Thus, the output describes ψ in terms of a range of central angles rather than specific angles.

$\epsilon, \alpha, \hat{\psi}$ and $\Delta\psi$ cannot be chosen arbitrarily. DAYLITE partitions various angular dimensions and there must be an integral number of subdivisions in each instance. The 4 parameters must conform to the following criteria:

$$1. \frac{\Omega}{\epsilon} = \text{an integer} \quad (3.31)$$

$$2. \frac{\pi}{\epsilon \hat{\psi}} = \text{an even integer} \quad (3.32)$$

$$3. \frac{\psi}{\epsilon} = \text{an integer} \quad (3.33)$$

$$4. \frac{\Delta\psi}{\hat{\psi}} = \text{an integer} \quad (3.34)$$

The program will notify the user if any of the criteria are violated.

Appendix C presents a user's manual and a program listing for DAYLITE. A sample output is shown in Appendix I.

CHAPTER 4

KINETIC CONDITIONS - COMPUTER PROGRAM SWARS-2PM

4.0 Introduction

Chapter 3 discussed the kinematic aspects of rock slope stability. The kinematic tests only provide part of the answer to the question of stability. They narrow the scope of the problem by focusing attention on the wedges which daylight. However, the fact that a wedge is physically capable of movement does not necessarily imply that it will fail. The resistance along joint planes may inhibit movement. The critical question is: What are the relative magnitudes of the driving and resisting forces? This chapter will examine this kinetic aspect of wedge stability.

A number of individuals (Wittke (1965A, 1965B), John (1968), Hendron et al. (1971), Hoek and Bray (1974)) have developed deterministic models to assess the stability of wedges. They all use a limiting equilibrium approach and define the factor of safety as the ratio of resisting to driving forces. All the techniques treat both the wedge and its parent rock mass as rigid bodies and assume the two bodies are separated by discontinuities that can be idealized as thin zones of relatively deformable material. The factor of safety is a function of the stresses acting on the discontinuities or joint planes. The reactions are indeterminate so all the techniques make some assumptions to simplify the problem. The

most common assumptions are:

1. Moments can be neglected - failure occurs as translational sliding.
2. In the joint plane there are no shear stresses that act perpendicular to the line of intersection of the wedge - all the reactions on the wedge are either parallel to the line of intersection or perpendicular to joint planes.
3. Lateral in situ stresses do not affect the reactions in the joint planes.
4. The strength parameters which characterize the joint plane can be expressed as deterministic values which are essentially constant over the entire joint surface.

The first three assumptions concern the mechanics of the model while the last one concerns the uncertainty (or certainty) associated with geologic parameters.

This chapter presents a model that relaxes some of these assumptions--particularly the last three. The new model modifies the analytic technique developed by Hendron et al.* by incorporating the effects of joint stiffness and in situ stresses into the stability calculations (Sections 4.2 through 4.5). This improved deterministic model is then converted into a probabilistic model by treating the input parameters as random variables through Monte Carlo simulation (Section 4.6).

The chapter begins by reviewing the state of the art in stiffness and stress effects.

* Campbell (1974) programmed the Hendron et al. technique for a computer. The Campbell program (SWARS-2P) will serve as a basis for a computerized version of the modified analysis.

4.1 State of The Art - Stiffness and Stress Effects

Most present approaches to rigid body analysis assume that the reactions between the wedge and the parent rock mass are perpendicular to the two** joint planes (Figure 4.1). Figure 4.2 shows a typical wedge and two sections - one perpendicular to the line AC, the line of intersection, and one parallel to line AC. The assumption regarding the orientation of the reactions in the joint planes leads to the force diagram in Figure 4.3. The two reactions, R_1 and R_2 , can be derived by solving two equations of force equilibrium:

$$W \cos \theta = R_1 \cos \beta_1 + R_2 \cos \beta_2 \quad (4.1)$$

$$R_1 \sin \beta_1 = R_2 \sin \beta_2 \quad (4.2)$$

If $\beta_1 = \beta_2 = \beta$:

$$R_1 = R_2 = \frac{W \cos \theta}{2 \cos \beta} \quad (4.3)$$

The assumption concerning the normality of the reactions simplifies the analysis, but is it a realistic approach? The shear stresses on the joint planes have been investigated by Mahtab and Goodman (1970) and St. John (1971) through

** All the wedges discussed in this chapter are "two-joint wedges" i.e., tetrahedrons formed by two intersecting joints and two free surfaces.

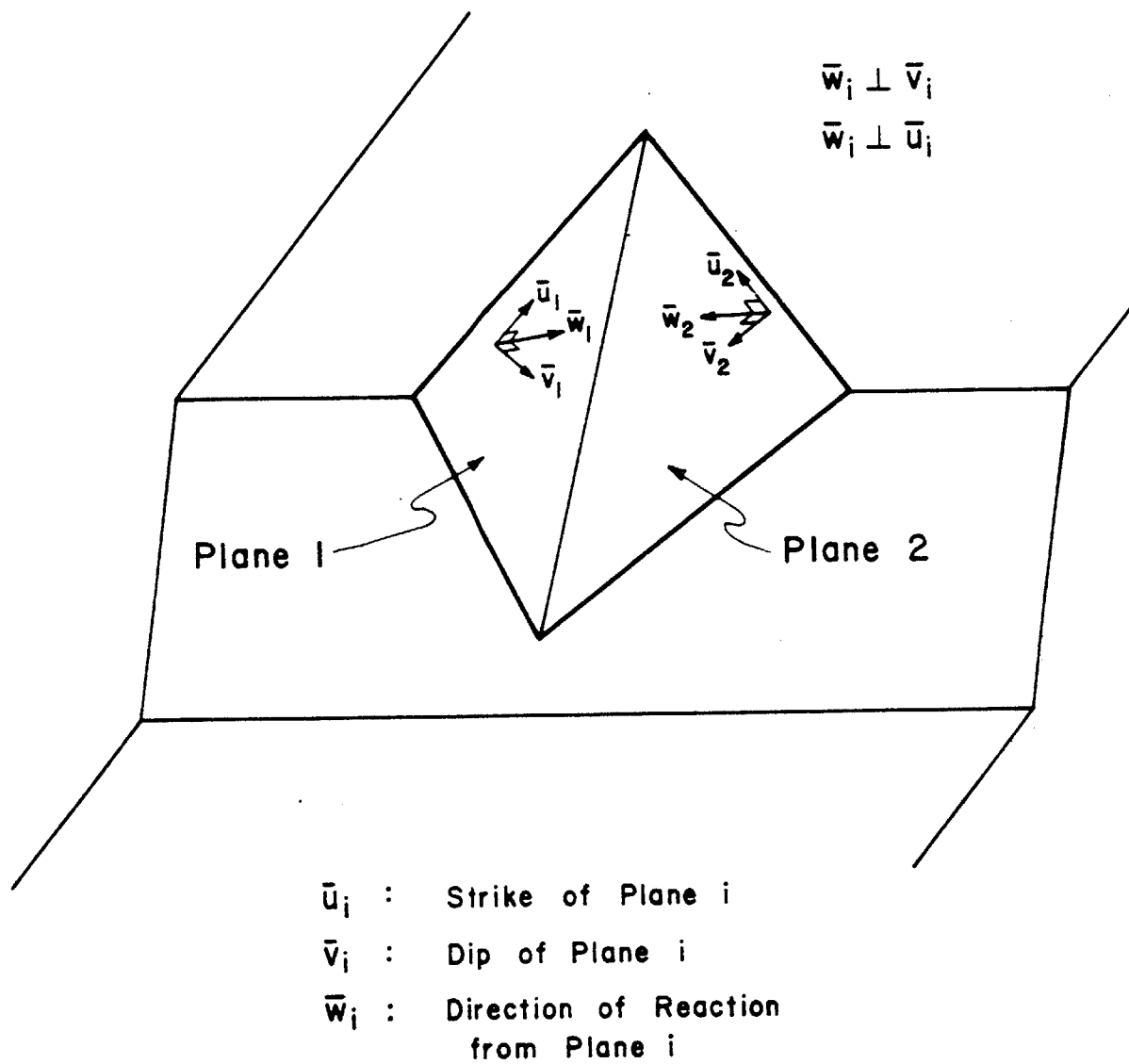


Figure 4.1 Sliding Wedge--Reactions Perpendicular to the Joint Planes

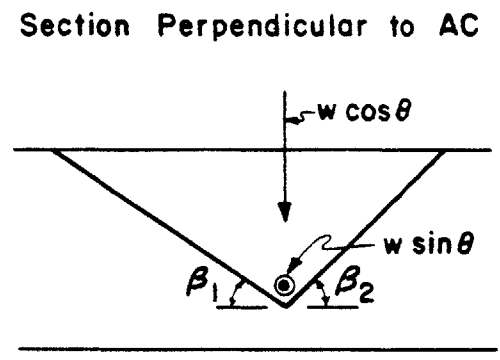
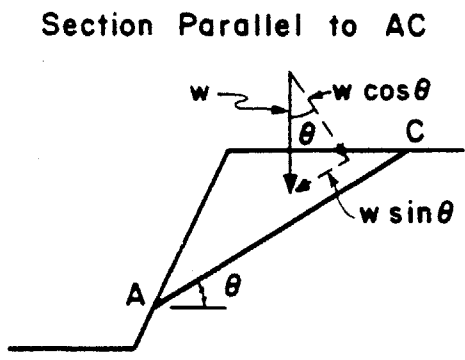
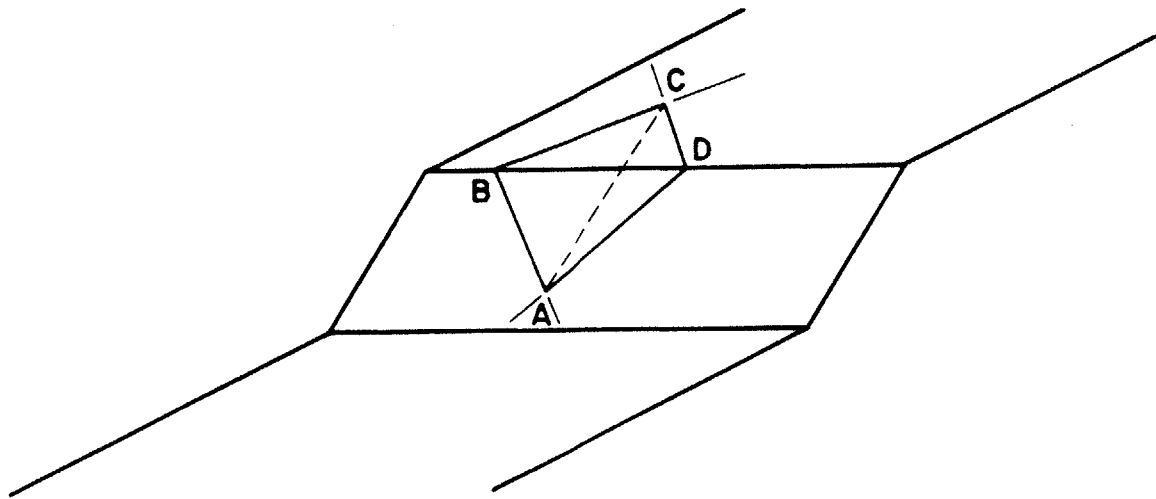


Figure 4.2 Resolution of Weight Vector into Components

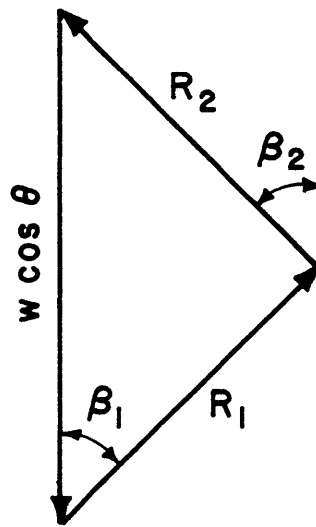


Figure 4.3 Force Diagram--Reactions Perpendicular to Joint Planes

the use of joint shear and normal stresses and by Steiner (1977) through the use of the ratio of horizontal to vertical stresses.

The stiffness approach introduces (Figure 4.4A) the tangential force T_i in addition to the normal forces N_i to represent the reactions on the sliding planes. N_i and T_i can be determined if the shear stiffness $(k_s)^*$ and normal stiffness $(k_n)^*$ of the joint or their ratio $R = \frac{k_n}{k_s}$ is known. For a symmetric wedge the ratio T_1/N_1 can be calculated as

$$\frac{T_1}{N_1} = \frac{\tau_1}{\sigma_{n_1}} = \frac{k_s \sin \beta \delta_r}{k_n \cos \beta \delta_r} = \frac{\tan \beta}{R} \quad (4.4)$$

From the force diagram shown in Figure 4.4C:

$$W \cos \theta = N_1 \cos \beta + N_2 \cos \beta + T_1 \sin \beta + T_2 \sin \beta \quad (4.5)$$

and

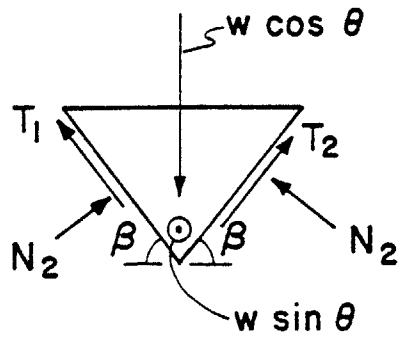
$$N_1 = N_2 = \frac{R \cos \beta}{2(\sin^2 \beta + R \cos^2 \beta)} W \cos \theta \quad (4.6)$$

$$T_1 = T_2 = \frac{\sin \beta}{2(\sin^2 \beta + R \cos^2 \beta)} W \cos \theta \quad (4.7)$$

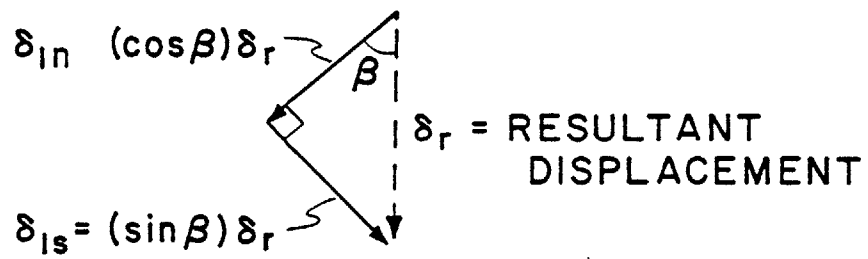
For $R = \infty$, i.e., for zero shear stiffness:

$$N_1 = \frac{W \cos \theta}{2 \cos \beta} \text{ and } T_1 = 0$$

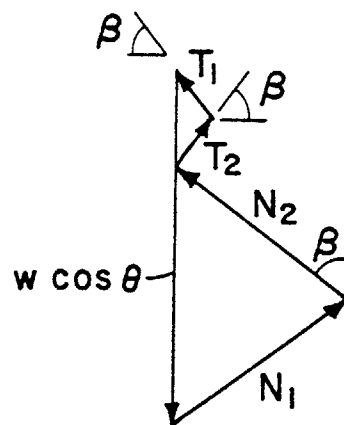
* $k_s = \frac{\tau}{\delta_s}$; $k_n = \frac{\sigma_n}{\delta_n}$ where τ and σ_n are the shear and normal stresses; δ_s and δ_n are the shear and normal displacements.



4.4 A



4.4 B



4.4 C

Figure 4.4 Symmetric Wedge--Reactions with Components Tangent to Joint Planes

These are the values derived earlier with the standard assumption regarding the normality of reactions.

The forces T_i and N_i can be used in the limit equilibrium equation for the wedge:

$$\text{Factor of Safety} = FS = \frac{2N_1 \tan \phi}{T} \quad (4.8)$$

where $2N_1 \tan \phi$ is the resisting factor (assuming only frictional resistance is present) and T is the driving force which is the vectorial addition of the shear forces perpendicular and parallel to the line of intersecting (Figure 4.4A).

$$T = \sqrt{(2T_1)^2 + (W \sin \theta)^2} \quad (4.9)$$

If only the shear force in the direction of wedge movement, i.e., parallel to the line of interaction AD is considered,*

$$FS = \frac{2N_1 \tan \phi}{W \sin \theta} \quad (4.10)$$

To show the effect of different shear and normal stiffnesses ϕ_R (the "required friction angle" to obtain $FS = 1.0$) has been plotted versus the angle β (for a symmetrical wedge) in Figure 4.5.

Decreasing R , i.e., increasing k_s relative to k_n , leads to a greater required friction angle.

* Section 4.4 examines the question of what constitutes failure and how to define the factor of safety.

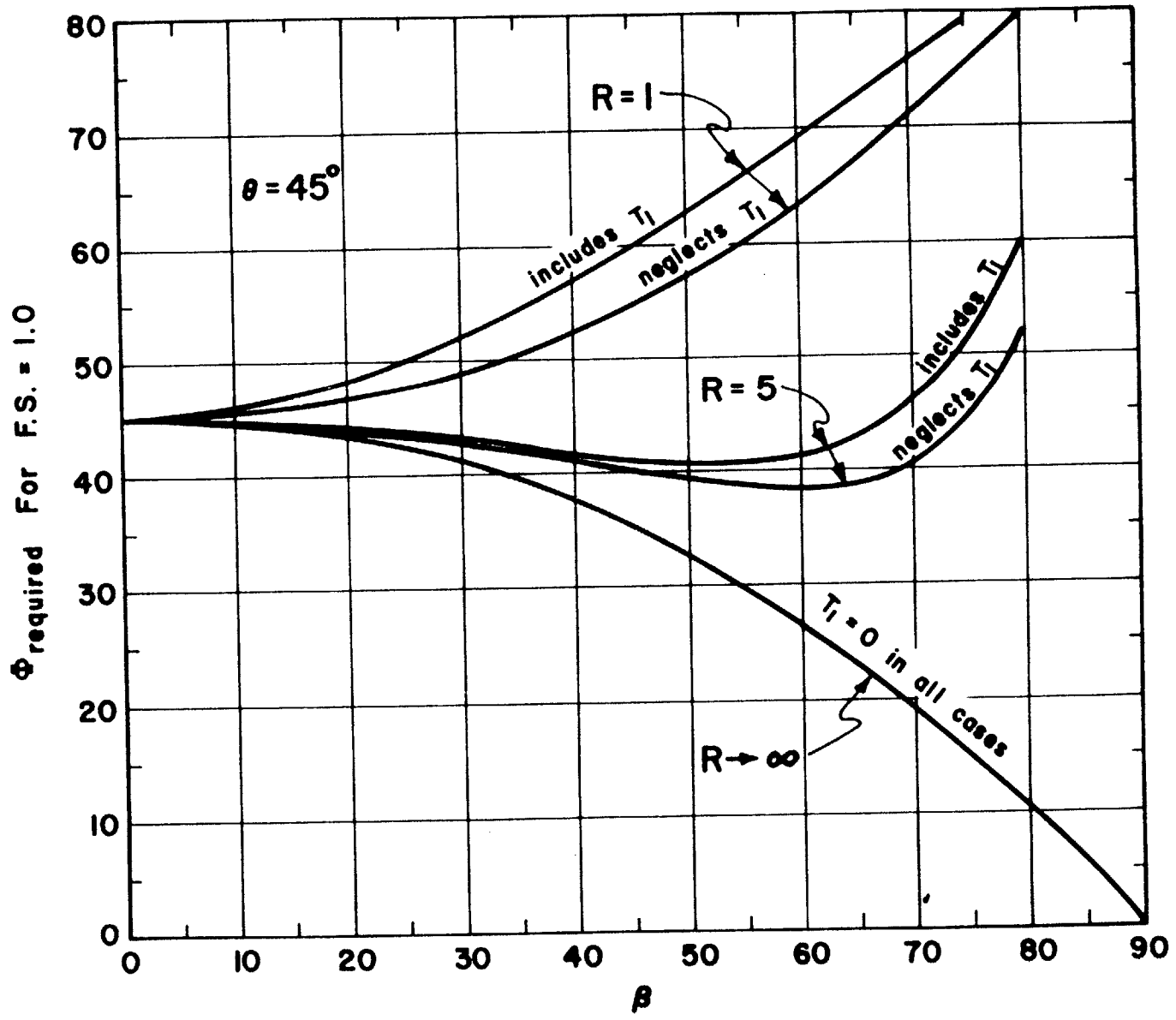


Figure 4.5 ϕ Required For F.S. = 1.0 vs. β

The importance of R raises the question what values of R do occur in nature? Several investigations have been conducted by Goodman (1972), Kulhawy (1975), Rosso (1976) and Barton (1972). Although the number of test results (especially concerning normal stiffness) has been increasing it is not yet possible to correlate stiffness values with particular rocks, with particular surface characteristics or with a combination of both. The references listed above quote R values that range from 0.5 to 1000. Unweathered joints usually fall in the upper (500-1000) portion of the range while joints with fillers usually have R values below 50. Additional research on joint stiffness values and possible correlations with other rock joint parameters is necessary.

Several improvements of the stiffness approach should be made. The St. John model is based on a symmetric wedge with identical stiffness ratios on the two sliding planes. The strength of the joint is characterized solely in terms of frictional resistance with no provisions for cohesive resistance. Some of these limitations have been eliminated in an extended version of the model that will be discussed in Section 4.2.

The stress approach as introduced by Steiner relaxes the force direction assumptions by explicitly including the horizontal stress acting on the wedge. From the stresses acting on a small element of the wedge (Figure 4.6), one can establish a force equilibrium:

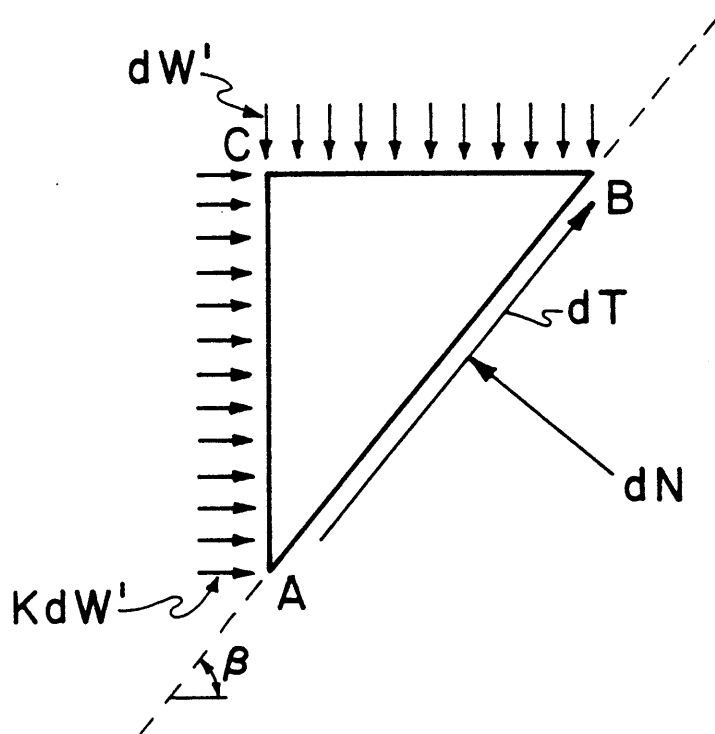


Figure 4.6 Stresses on Differential Area of the Joint Plane

$$dN = (dW') \cos \beta (L_{CB}) + (KdW') \sin \beta (L_{CA}) \quad (4.11)$$

where $L_{CB} = \text{distance CB}$

and $L_{CA} = \text{distance CA,}$

when $L_{CB} = 1$

$$L_{CA} = \tan \beta \quad (4.12)$$

and thus

$$dN = dW' \cos \beta + KdW' \sin \beta \tan \beta \quad (4.13)$$

Since dW' and KdW' are constant along the entire length of the joint the equation can be integrated to yield the normal force on the joint.

$$N = W' (\cos \beta + K \sin \beta \tan \beta) \quad (4.14)$$

(Instead of the differential force equilibrium described above, one could arrive at the same result using the Mohr stress circle, Figure 4.7.) If $W' = \frac{1}{2}W \cos \theta$, i.e., one half the weight component in a direction perpendicular to the line of intersection (see Figure 4.3),

$$N_1 = N_2 = \frac{1}{2}W \cos \theta (\cos \beta + K \sin \beta \tan \beta) \quad (4.15)$$

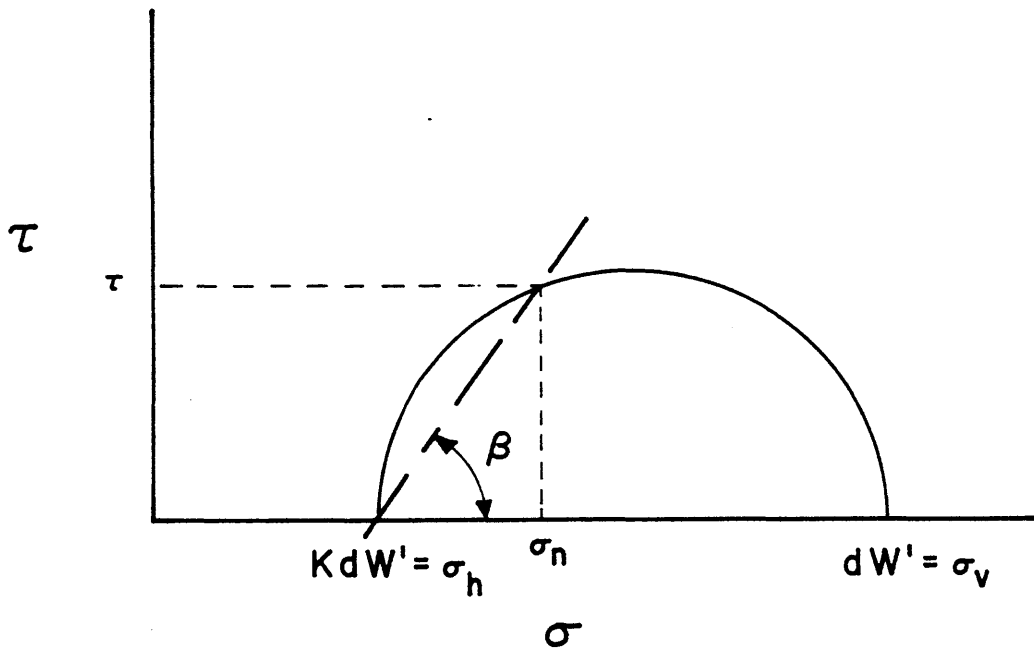


Figure 4.7 Mohr Stress Circle for the Stress State Shown
in Figure 4.6

and

$$T_1 = T_2 = \frac{1}{2} W \cos \theta (\sin \beta - K \cos \beta \tan \beta) \quad (4.16)$$

for $K = 1$, the forces become:

$$N_1 = \frac{W \cos \theta}{2 \cos \beta} \text{ and } T_1 = 0 \quad (4.17)$$

i.e., the values for the standard normal reaction assumption. This standard assumption includes implicitly the equality of vertical and horizontal stresses.

Factors of safety can be derived either by considering the tangential forces parallel and perpendicular to the wedge movement direction or by only considering those parallel to the movement:

$$FS = \frac{2N_1 \tan \theta}{\sqrt{(2T_1)^2 + (W \sin \theta)^2}} \quad (4.18)$$

$$FS = \frac{2N_1 \tan \phi}{W \sin \theta} \quad (4.19)$$

The effect of introducing a factor $K \neq 1$ in the computation of factors of safety is presented in Figure 4.8, where

$$\frac{FS \text{ with } K \neq 1}{FS \text{ with } K = 1} = \frac{\frac{W \cos \theta}{W \sin \theta} \tan \phi}{\frac{W \cos \theta}{W \sin \theta} \tan \phi} \cdot \frac{\frac{1}{\cos \beta} (\cos^2 \beta + K \sin^2 \beta)}{\frac{1}{\cos \beta}} \quad (4.20)$$

$$= \cos^2 \beta + K \sin^2 \beta \quad (4.21)$$

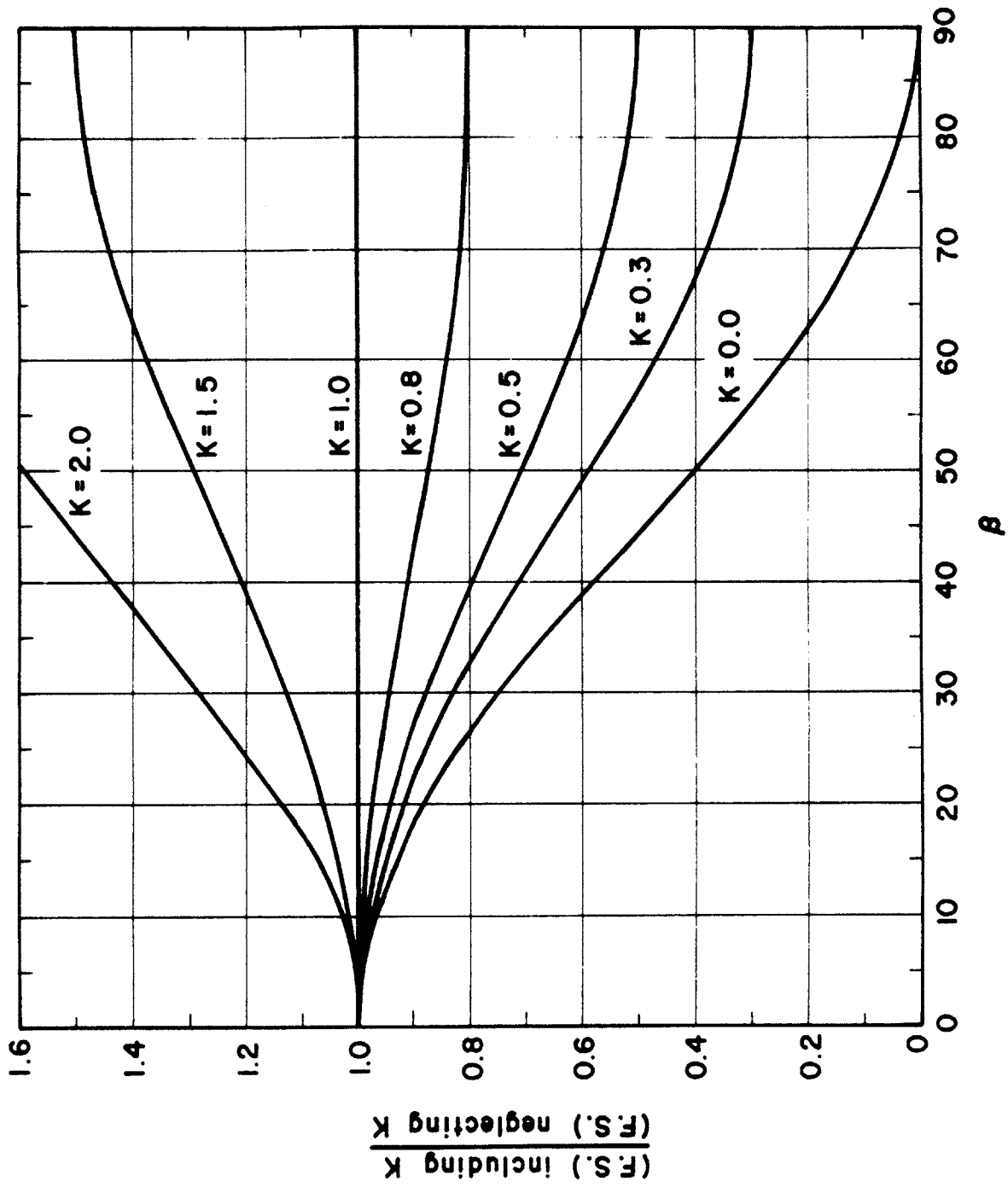


Figure 4.8 $\frac{\text{(FS) neglecting } K}{\text{(FS) including } K}$ vs. β

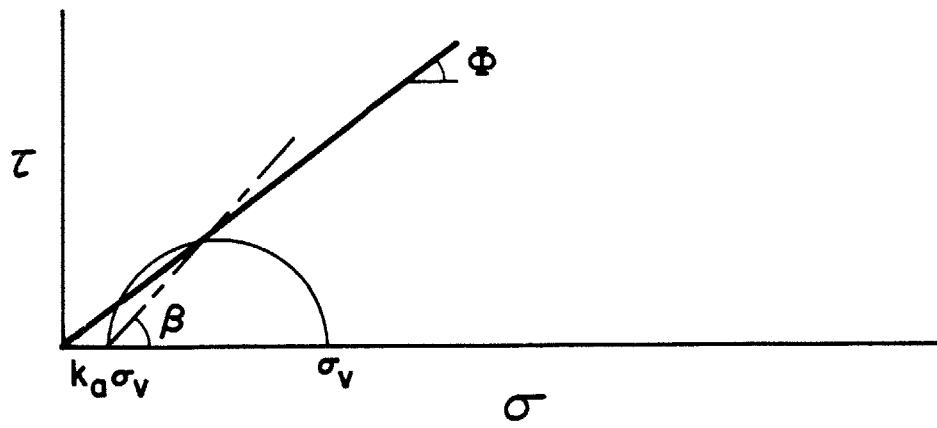
Figure 4.8 shows that with $K > 1$ the traditional assumption ($K = 1$ and thus a reaction normal to the sliding plane only) underestimates the factor of safety and for $K < 1$ it overestimates it.

The notion of the stress ratio K needs some further clarification particularly in the context of a jointed rock mass. The K used by Steiner refers to the state of stress within the wedge which may or may not be equal to the stress state in the remainder of the rock mass. A change or discontinuity in the material properties of a medium does not necessarily create a discontinuity in the state of stress existing in the medium. The question that arises is, what created the discontinuity in the first place or (more generally formulated) what is the stress history at the particular location? Depending on the stress history of the joint, one can often assume that K in the wedge is identical to K in the entire rock mass.

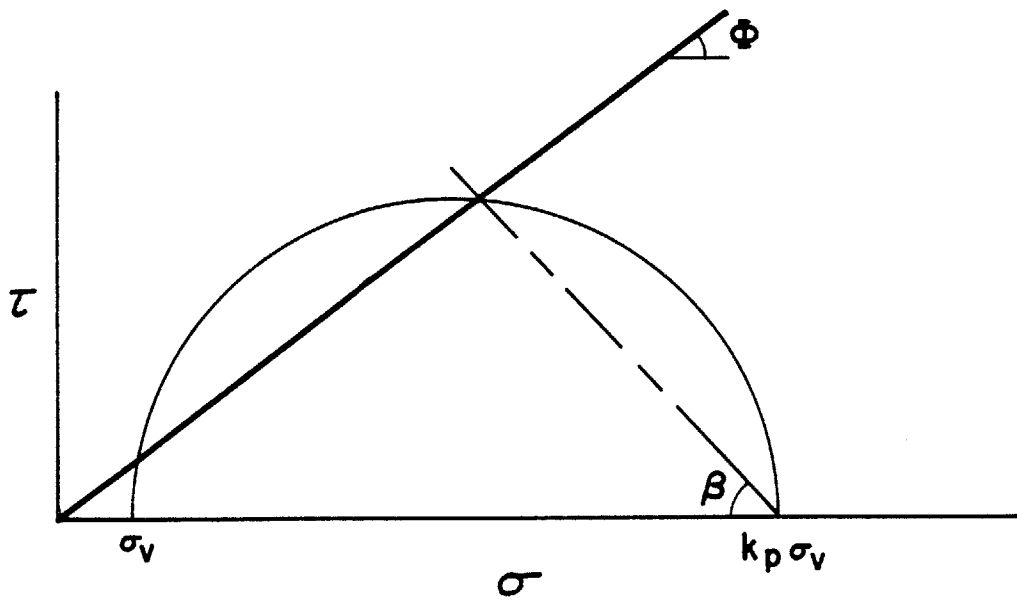
The use of the stress ratio K in wedge stability analysis introduces the possibility of active or passive failure modes of a wedge in the direction perpendicular to the line of intersection. As shown in Figure 4.9A, the active case is:

$$\tan \phi = \frac{\tau}{\sigma_n} = \frac{T}{N} = \frac{\sin \beta - K \sin \beta}{\cos \beta + K \sin \beta \tan \beta} = \frac{(1 - K)}{\text{ctn } \beta + K \tan \beta} \quad (4.22)$$

Thus,



4.9 A



4.9 B

Figure 4.9 Mohr Stress Circles for Active and Passive Cases

$$K_a = \frac{1 - \tan \phi \operatorname{ctn} \beta}{1 + \tan \phi \tan \beta} \quad (4.23)$$

In the passive case (Figure 4.9B) the direction of T reverses; therefore, a minus sign must be introduced into Equations (4.16) and (4.22).

$$\tan \phi = \frac{-T}{N} = \frac{-(1 - K)}{\operatorname{ctn} \beta + K \tan \beta} \quad (4.24)$$

Thus,

$$K_p = \frac{1 + \tan \phi \tan \beta}{1 - \tan \phi \operatorname{ctn} \beta} \quad (4.25)$$

The practical significance of these two failure modes will be discussed in Section 4.4. Although the joint shear strength is exceeded in both cases it does not imply sliding failure along the line of intersection. It simply means that in the active case the wedge will settle and in the passive case the wedge will be lifted up until equilibrium is reached. These represent cases where the overall stress field in the rock mass will be different from the stress field in the wedge. In the wedge, K can only vary between the limits K_a and K_p as determined by ϕ and β (see Equations 4.23 and 4.25) whereas in the rock mass K values smaller and greater respectively than these K_a and K_p can exist; K in such a rock mass will be inhomogeneously distributed.

In this section both the stiffness and the stress

approaches were presented as methods for determining reactions at the joint planes. Section 4.3 discusses the relationship between the two approaches.

4.2 Generalization of the Stiffness Approach

The stiffness approach outlined by St. John can be generalized to include asymmetric wedges and arbitrary loads such as those shown in Figure 4.10. (The figure is a cross-section taken perpendicular to the line of intersection between two joint planes.) The generalized problem can be treated in a manner very similar to the one used by St. John. The fundamental assumption in the approach is that the wedge behaves as a rigid body resting on a deformable medium (the joint planes). The deformational characteristics of the joints can be expressed in terms of two stiffness values: k_n and k_s .

$$k_n = \frac{\text{normal stress}}{\text{normal displacement}} = \frac{\sigma_n}{\delta_n} \quad (4.26)$$

$$k_s = \frac{\text{shear stress}}{\text{shear displacement}} = \frac{\tau}{\delta_s} \quad (4.27)$$

k_n and k_s are material properties which are assumed constant throughout the range of stresses encountered in engineering practice. The method implicitly assumes that σ_n and δ_s as well as τ and δ_n are unrelated, i.e., the off-diagonal terms in the stiffness matrix are zero.

X, Y: RESULTANT LOADS

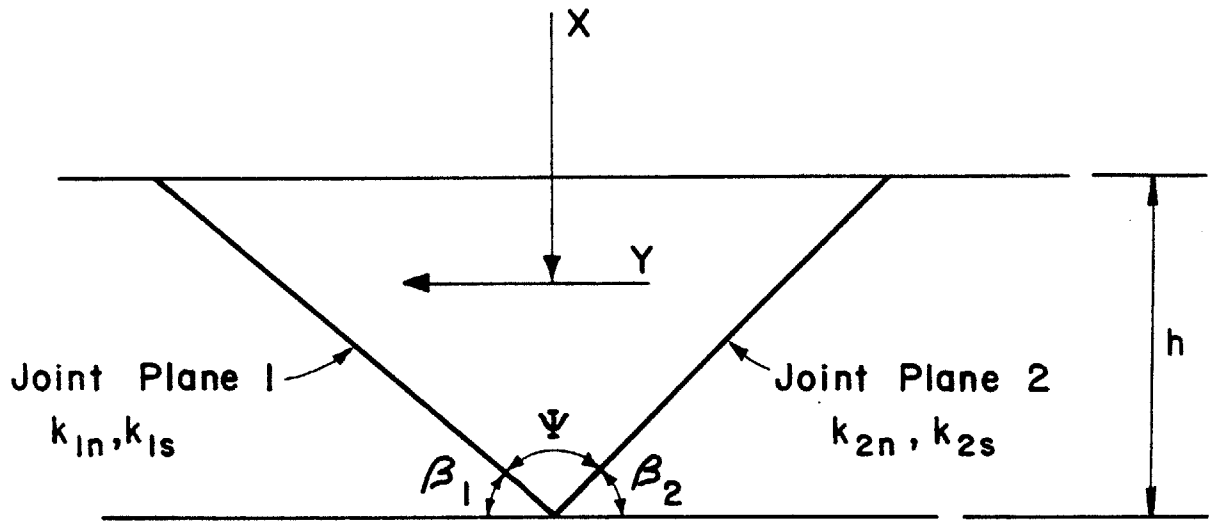


Figure 4.10 Generalized Stiffness Approach--Known Parameters

$$\begin{pmatrix} \sigma_n \\ \tau \end{pmatrix} = \begin{bmatrix} k_n & 0 \\ 0 & k_s \end{bmatrix} \begin{pmatrix} \delta_n \\ \delta_s \end{pmatrix} \quad (4.28)$$

As indicated in Figure 4.11, the problem involves six unknowns: N_1 , T_1 , N_2 , T_2 , δ_t and α . There are also six independent equations. Two equations are the force equilibrium equations in the x and y directions:

$$N_1 \cos \beta_1 + T_1 \sin \beta_1 + N_2 \cos \beta_2 + T_2 \sin \beta_2 = X \quad (4.29)$$

$$N_1 \sin \beta_1 - T_1 \cos \beta_1 - N_2 \sin \beta_2 + T_2 \cos \beta_2 = Y \quad (4.30)$$

The other four equations relate the shear and normal stresses to the magnitude and direction of the resultant displacement:

$$\delta_t h = \frac{N_1}{(\sin \alpha + \cos \alpha \operatorname{ctn} \beta_1) k_{1n}} \quad (4.31)$$

$$= \frac{T_1}{(\cos \alpha - \sin \alpha \operatorname{ctn} \beta_1) k_{1s}} \quad (4.32)$$

$$= \frac{N_2}{(\cos \alpha \operatorname{ctn} \beta_2 - \sin \alpha) k_{2n}} \quad (4.33)$$

$$= \frac{T_2}{(\cos \alpha + \sin \alpha \operatorname{ctn} \beta_2) k_{2s}} \quad (4.34)$$

$\delta_T = \text{Resultant Displacement}$

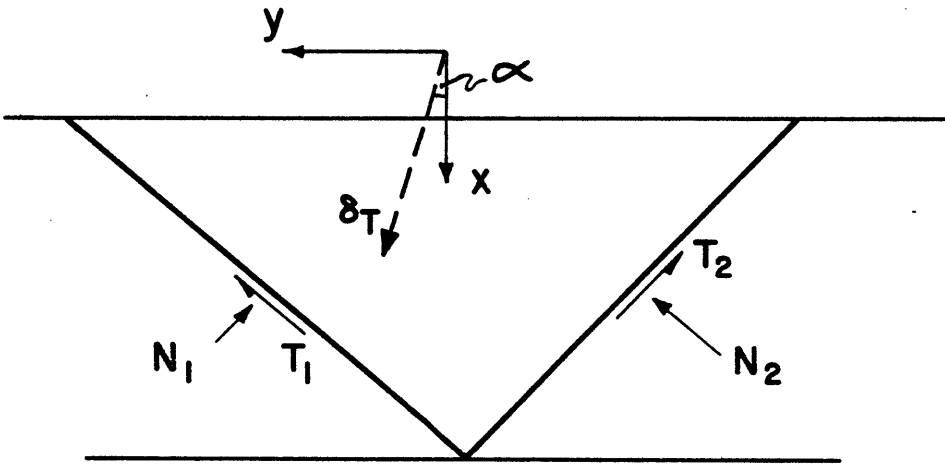


Figure 4.11 Generalized Stiffness Approach--Unknown Parameters

All of the above expressions are derived in Appendix D.

The six equations can be reduced to two if T_1 , T_2 and N_2 are expressed in terms of T_1 and substituted into the force equilibrium equations:

$$\cos \beta_1 + \frac{ak_{1s} \sin \beta_1 + bk_{2n} \cos \beta_2 + ck_{2s} \sin \beta_2}{(\sin \alpha + \cos \alpha \operatorname{ctn} \beta_1)k_{1n}} = \frac{X}{N_1} \quad (4.35)$$

$$\sin \beta_1 - \frac{ak_{1s} \cos \beta_1 + bk_{2n} \sin \beta_2 - ck_{2s} \cos \beta_2}{(\sin \alpha + \cos \alpha \operatorname{ctn} \beta_1)k_{1n}} = \frac{Y}{N_1} \quad (4.36)$$

where $a = \cos \alpha - \sin \alpha \operatorname{ctn} \beta_1$

$b = \cos \alpha \operatorname{ctn} \beta_2 - \sin \alpha$

$c = \cos \alpha + \sin \alpha \operatorname{ctn} \beta_2$

The two equations involve only two unknowns (N_1 and α).

They can be solved for α :

$$\alpha = \tan^{-1} \left[\frac{YB - XA}{XC - YA} \right] \quad (4.37)$$

$$A = (k_{1n} - k_{1s}) \cos \beta_1 + (k_{2s} - k_{2n}) \cos \beta_2$$

$$B = k_{1n} \frac{\cos^2 \beta_1}{\sin \beta_1} + k_{1s} \sin \beta_1 + k_{2n} \frac{\cos^2 \beta_2}{\sin \beta_2} + k_{2s} \sin \beta_2$$

$$C = k_{1n} \sin \beta_1 + k_{1s} \frac{\cos^2 \beta_1}{\sin \beta_1} + k_{2n} \sin \beta_2 + k_{2s} \frac{\cos^2 \beta_2}{\sin \beta_2}$$

All the remaining unknowns can be found by substituting back into the various equations. The solution procedure is a

cumbersome operation to perform by hand, but it can be easily programmed for a computer.

All the expressions shown above were based on a two dimensional cross section; hence, the analysis implicitly assumed the wedge has a length of unity along the line of interaction. Strictly speaking, the equations are valid only for cases involving an infinitely long wedge of constant dimensions in an infinitely high rock slope (Figure 4.12). The joint planes bounding the wedge form a notch in the slope; X and Y correspond to loads per unit length along the notch. All of the reactions at the joint planes are constant along the slope. Obviously, these conditions are seldom even approximated in the field.

Fortunately, the physical interpretation of the results need not be quite so restrictive. The left side of Equations (4.35) and (4.36) depend only on stiffnesses and the shape of the wedge; they do not contain any terms involving h , the height of the wedge. Thus, the ratios X/N_1 and Y/N_1 are constant for geometrically similar cross sections even though X, Y and N_1 may each be functions of h . This independence can be used to generalize the applicability of Equations (4.35) and (4.36). They are valid for finite wedges as long as all cross sections perpendicular to the line of intersection are geometrically similar. This situation occurs whenever the

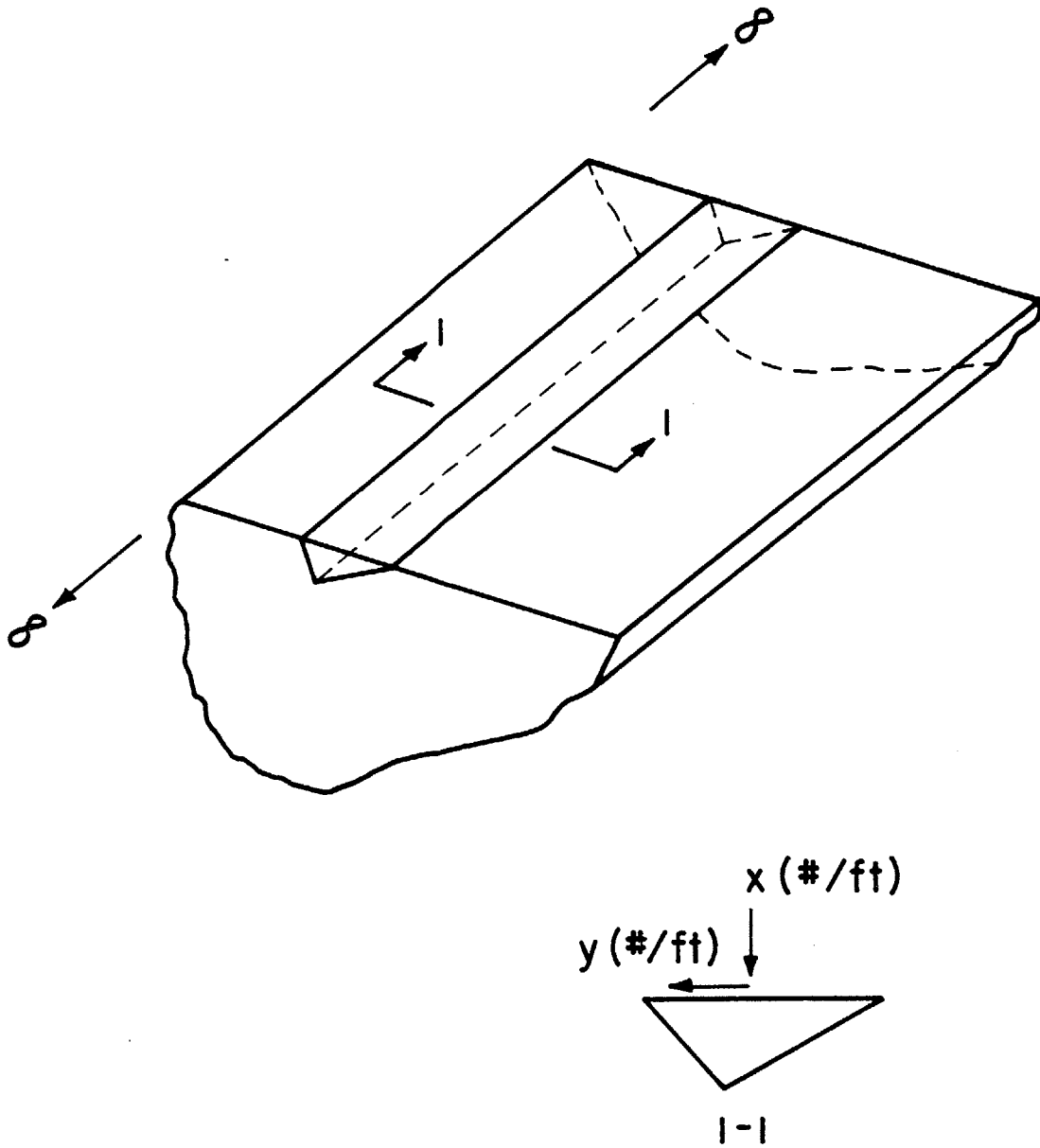


Figure 4.12 Notch in Infinite Slope

line of intersection of the joint planes intersects the slope at a right angle (Figure 4.13). The proof of this generalized relationship is relatively straightforward:

Equation (4.35) can be rewritten in terms of differentials

$$dN_1 = \frac{dX}{e} \quad (4.38)$$

$$\text{where } e = (\cos \beta_1 + \frac{ak_{1s} \sin \beta_1 + bk_{2n} \cos \beta_2 + ck_{2s} \sin \beta_2}{(\sin \alpha + \cos \alpha \operatorname{ctn} \beta_1)k_{1n}})$$

N_1 is the total force in joint plane 1.

$$N_1 = \int_{\text{entire wedge}} dN_1 = \frac{1}{e} \int_{\text{entire wedge}} dX \quad (4.39)$$

$$N_1 = \frac{X}{e} \quad (4.40)$$

$$\text{Similarly, } N_1 = \frac{Y}{f} \quad (4.41)$$

$$\text{where } f = (\sin \beta_1 - \frac{ak_{1s} \cos \beta_1 + bk_{2n} \sin \beta_2 - ck_{2s} \cos \beta_2}{(\sin \alpha + \cos \alpha \operatorname{ctn} \beta_1)k_{1n}})$$

Equations (4.40) and (4.41) are mathematically identical to (4.35) and (4.36); however, X and Y represent the total applied forces in the x and y direction rather than unit loads as in Equations (4.35) and (4.36).

Analyses involving asymmetrical wedges must be handled on an individual basis. The gross contact areas between the wedge and its parent rock mass must be calculated for each

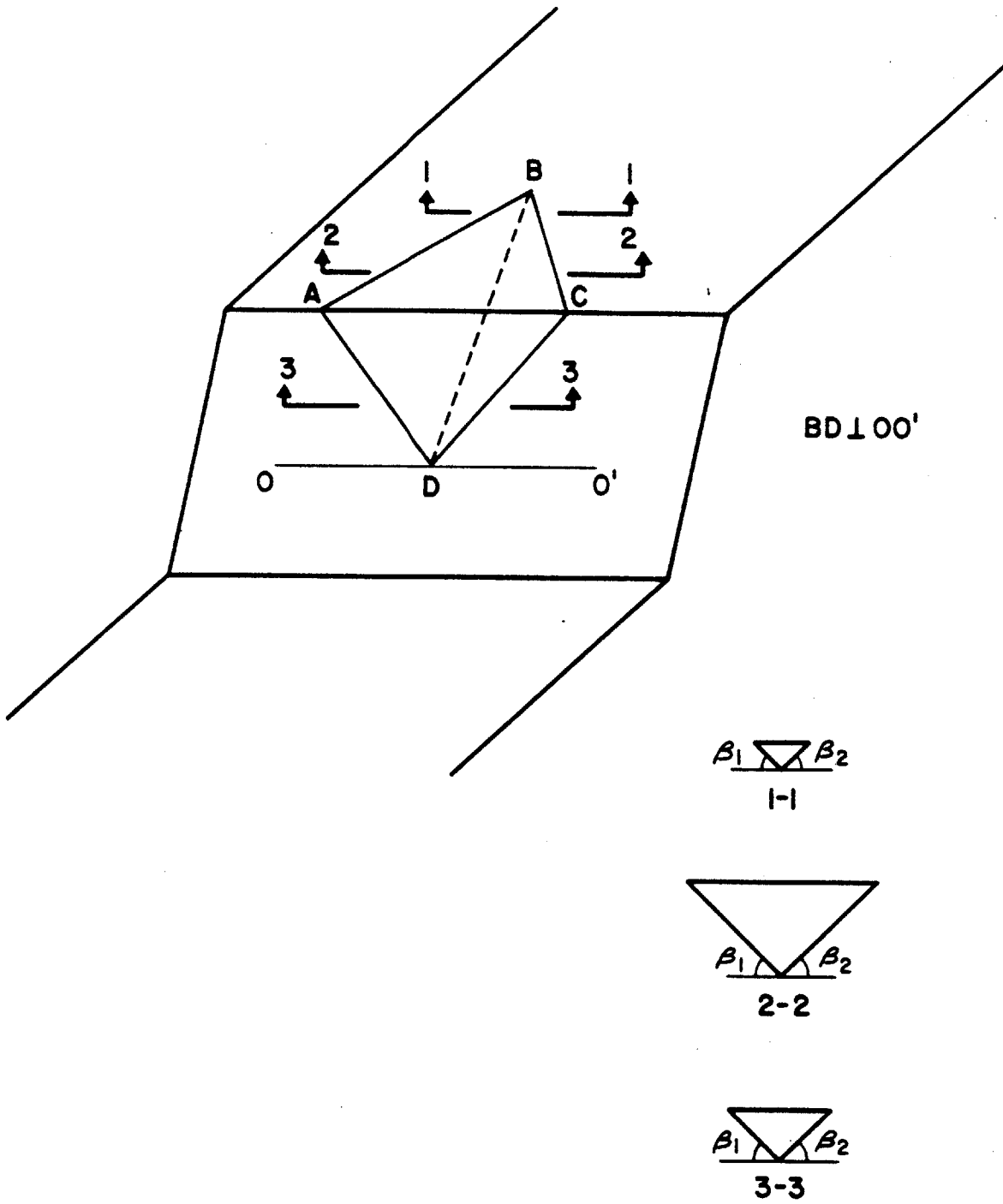


Figure 4.13 Wedge With Geometrically Similar Cross Sections
132

joint plane. As will be discussed later, the analysis can easily be programmed for computerized solutions.

Special Conditions

There are some special situations where it is possible to simplify the analysis. If there is no load in the y direction, i.e., $Y = 0$ the expression for α (Equation (4.37)) simplifies to:

$$\alpha = \tan^{-1} \left[\frac{(k_{1s} - k_{1n}) \cos \beta_1 + (k_{2n} - k_{2s}) \cos \beta_2}{k_{1n} \sin \beta_1 + k_{1s} \frac{\cos^2 \beta_1}{\sin \beta_2} + k_{2n} \sin \beta_2 + k_{2s} \frac{\cos^2 \beta_2}{\sin \beta_1}} \right] \quad (4.42)$$

Case 1: $Y = 0 \quad k_{1n} = k_{2n} = k_{1s} = k_{2s}$

When all the stiffnesses are equal the numerator of the equation reduces to 0 and α becomes 0. The equality of stiffness (together with $Y = 0$) implies that the resultant displacement of the wedge will be in the x direction.

Case 2: $Y = 0 \quad k_{1n} = k_{2n} \gg k_{1s} = k_{2s}$

These conditions correspond to the assumptions implicitly made in conventional stability analyses. The equation for α becomes:

$$\alpha = \tan^{-1} \left[\frac{\cos \beta_2 - \cos \beta_1}{\sin \beta_1 + \sin \beta_2} \right] = \frac{\beta_1 - \beta_2}{2} \quad (4.43)$$

Thus, the resultant displacement will occur at an inclination equal to half the difference between β values (Figure 4.14).

Results

The solution procedure outlined above has been used to develop several plots that illustrate the sensitivity of the results (particularly N_1 and N_2) to changes in the input parameters ($\beta_1, \beta_2, k_{1n}, k_{2n}, k_{1s}, k_{2s}$). The results are valid for a wedge in a infinitely long notch or a wedge whose line of intersection is orthogonal to the strike of the slope face. In all cases, $Y = 0$ and $X =$ weight of the wedge. The results are expressed in the same manner as those presented in Section 4.1 i.e., the dependent variable is ϕ_R (the value of ϕ required to produce a factor of safety equal to 1.0):

$$\phi_R = \tan^{-1} \frac{W \sin \theta}{N_1 + N_2} \quad (4.44)$$

θ = angle between the line of intersection of joint planes and the horizontal (Figure 4.15).

W = weight of wedge.

Figure 4.15 shows a typical wedge and identifies the parameters selected for study in the sensitivity analyses.

Case 1: $k_{1n} = k_{2n}; k_{1s} = k_{2s}; \psi = 90^\circ$

$$0^\circ \leq \beta_1 \leq 90^\circ$$

$$0^\circ \leq \beta_2 \leq 90^\circ$$

$$k_{1n} = k_{2n} \gg k_{1s} = k_{2s}$$

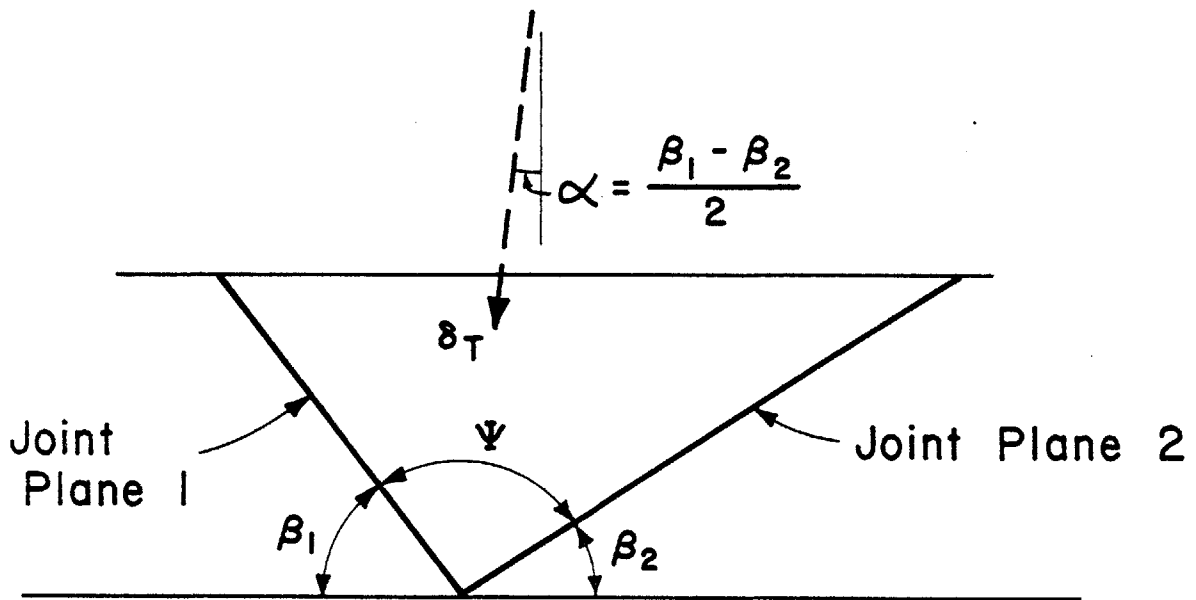


Figure 4.14 Direction of Displacement When $k_{1n} = k_{2n} \gg k_{1s} = k_{2s}$

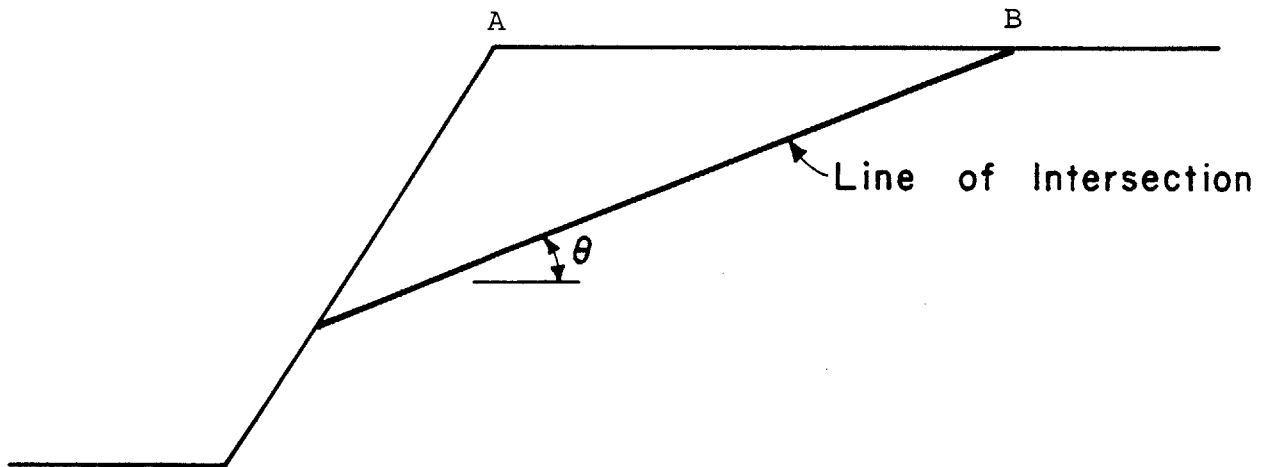
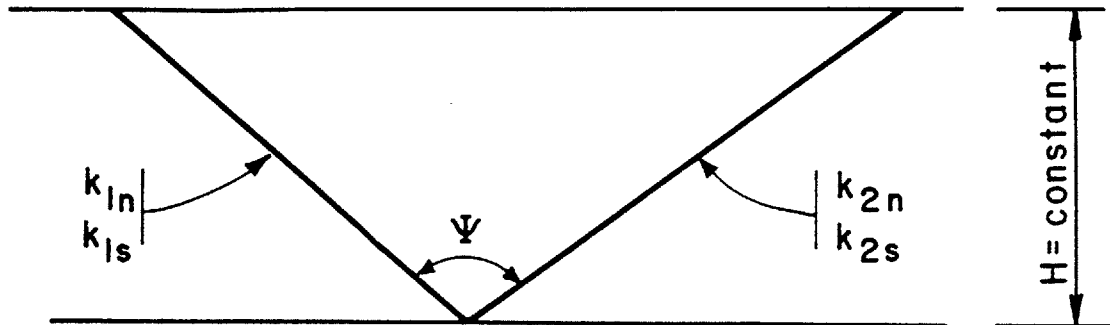


Figure 4.15 Parameters Varied in Sensitivity Analyses

Figure 4.16 illustrates the functional relationship between β_1 and ϕ_R (β_1 and β_2 are complementary angles as $\beta_2 = 180^\circ - \psi - \beta_1 = 90^\circ - \beta_1$). Two families of curves were developed for $\theta = 30^\circ$ and $\theta = 45^\circ$ respectively. Each family is composed of several members that represent different values of R, the stiffness ratio:

$$R = \frac{k_{1n}}{k_{1s}} = \frac{k_{2n}}{k_{2s}} \quad (4.45)$$

All the curves are symmetrical about the line $\beta_1 = \beta_2 = 45^\circ$.

$R = \infty$ and $R = 1$ represent conditions that are tentatively considered to be the upper and lower bounds for natural rock joints. The curve for $R = \infty$ reflects the effect of "wedging" (Hoek and Bray, 1972) as ϕ_R decreases with increasing β_1 . The curve for $R = 1$ shows just the opposite trend as ϕ_R increases strongly with β_1 . (The two curves seem to be symmetrical about the line $\phi_R = \theta$. However, this apparent symmetry has not been analytically proven. There is no readily discernible explanation for this effect from a mechanical standpoint). A stiffness ratio of 2.5 yields a virtually constant value of friction angle that is approximately equal to θ .

Case 2 : $k_{1n} = k_{2n}$; $k_{1s} = k_{2s}$ $\psi = 120^\circ$

$$0^\circ \leq \beta_1 \leq 60^\circ$$

$$0^\circ \leq \beta_2 \leq 60^\circ$$

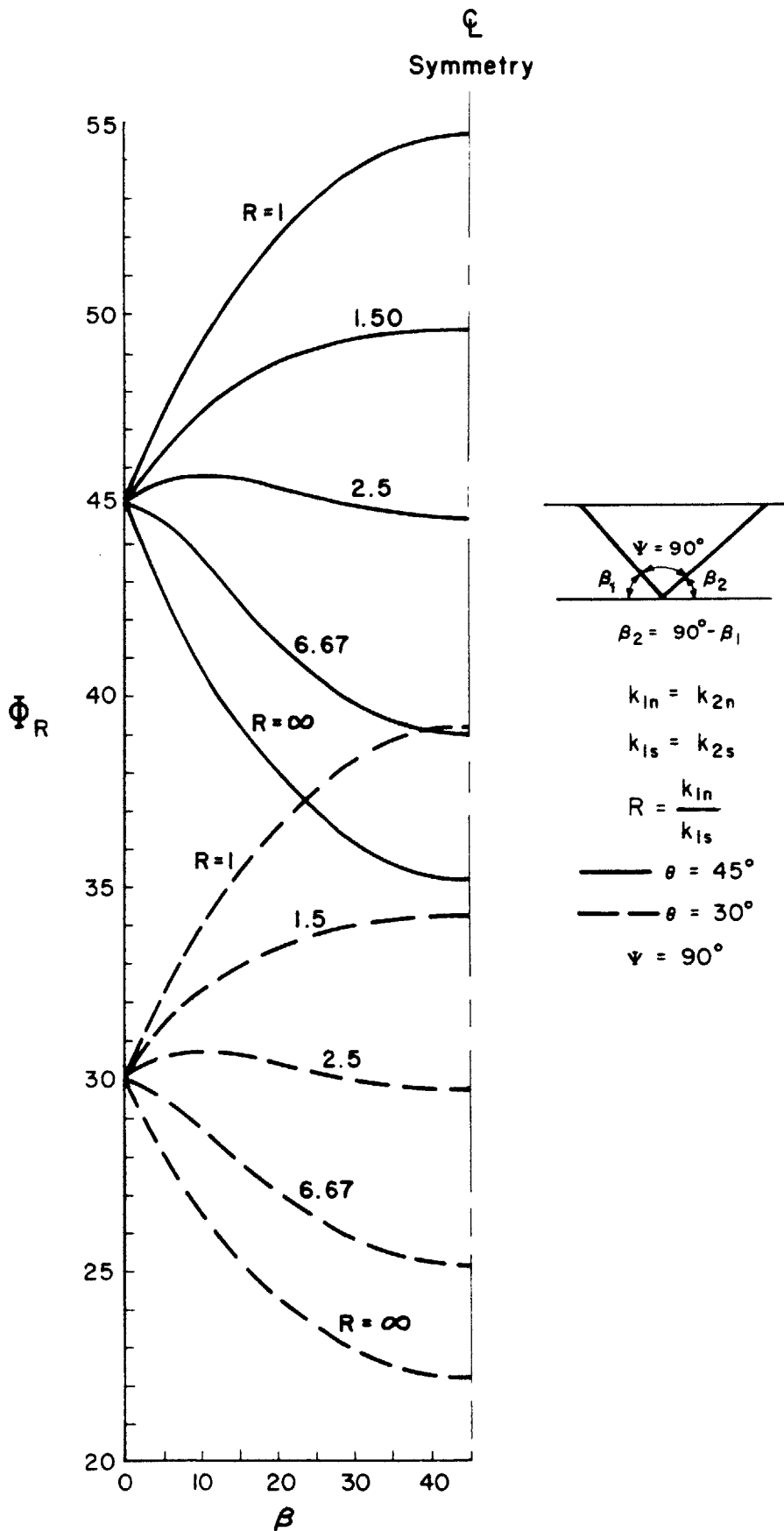


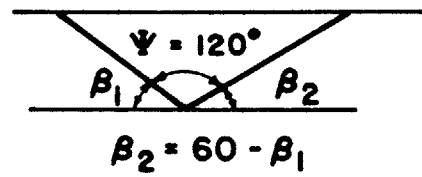
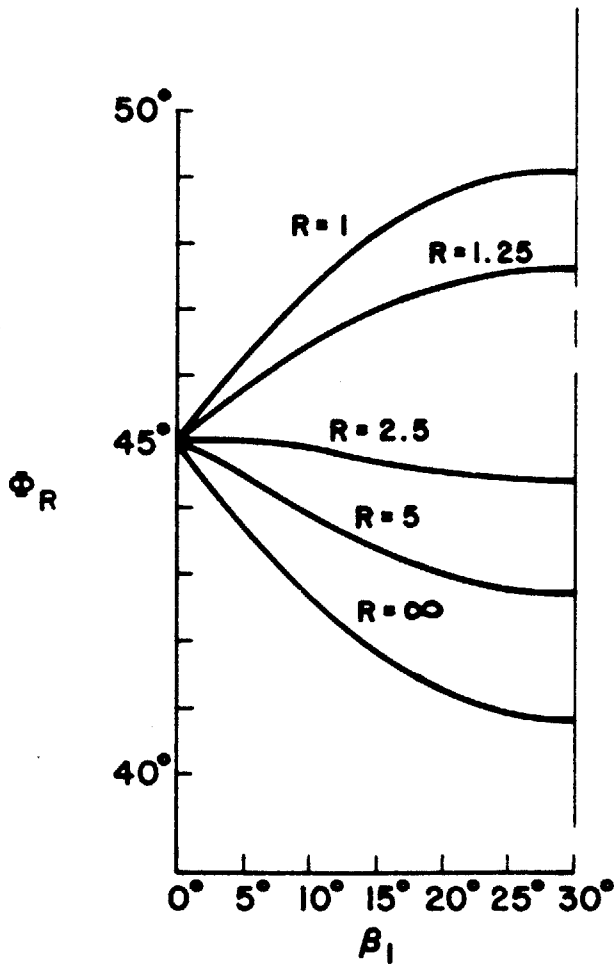
Figure 4.16 Φ_R vs. β_1 For $\Psi = 90^\circ$

The curves for $\psi = 120^\circ$ (Figure 4.17) look quite similar to those for $\psi = 90^\circ$ (Figure 4.16). They have an axis of symmetry and they diverge as β_1 increases. However, the divergence is not as pronounced for $\psi = 120^\circ$. The difference in ϕ_R values is approximately 8.2 at $\beta = \beta_1 = 30^\circ$. Once again, a value of $R = 2.5$ yields $\phi_R \sim \theta$ regardless of the value of β_1 .

Case 3: $k_{1n} = k_{2n}; k_{1s} = k_{2s}; \psi = 60^\circ$
 $0^\circ \leq \beta_1 \leq 120^\circ$
 $0^\circ \leq \beta_2 \leq 120^\circ$

Figure 4.18 presents results for the case $\psi = 60^\circ$. Near the axis of symmetry ($\beta_1 = 60^\circ$) the curves behave much like the ones examined earlier. However, as β_1 approaches 0 the curves become irregular. A problem arises in that region because β_2 ($\beta_2 = 120^\circ - \beta_1$) becomes greater than 90° , i.e., joint plane 2 overhangs the wedge (Figure 4.19). The overhang does not pose any difficulties from an analytical standpoint; however, the physical interpretation of the results demands some close scrutiny. For every R there is a critical value of β_1 (defined as β_{1cr}) such that for all $\beta_1 < \beta_{1cr}$ the normal force on joint plane 2 is tensile. This value β_{1cr} occurs when the direction of the wedge's resultant displacement is parallel to joint plane 2 (Figure 4.19). Figure 4.20 shows the relationship between β_{1cr} and R . If $\beta_1 \leq \beta_{1cr}$ the

ζ
 Symmetry



$$k_{1n} = k_{2n}$$

$$k_{1s} = k_{2s}$$

$$R = \frac{k_{1n}}{k_{1s}}$$

$$\theta = 45^\circ$$

$$\Psi = 120^\circ$$

Figure 4.17 Φ_R vs. β_1 For $\Psi = 120^\circ$

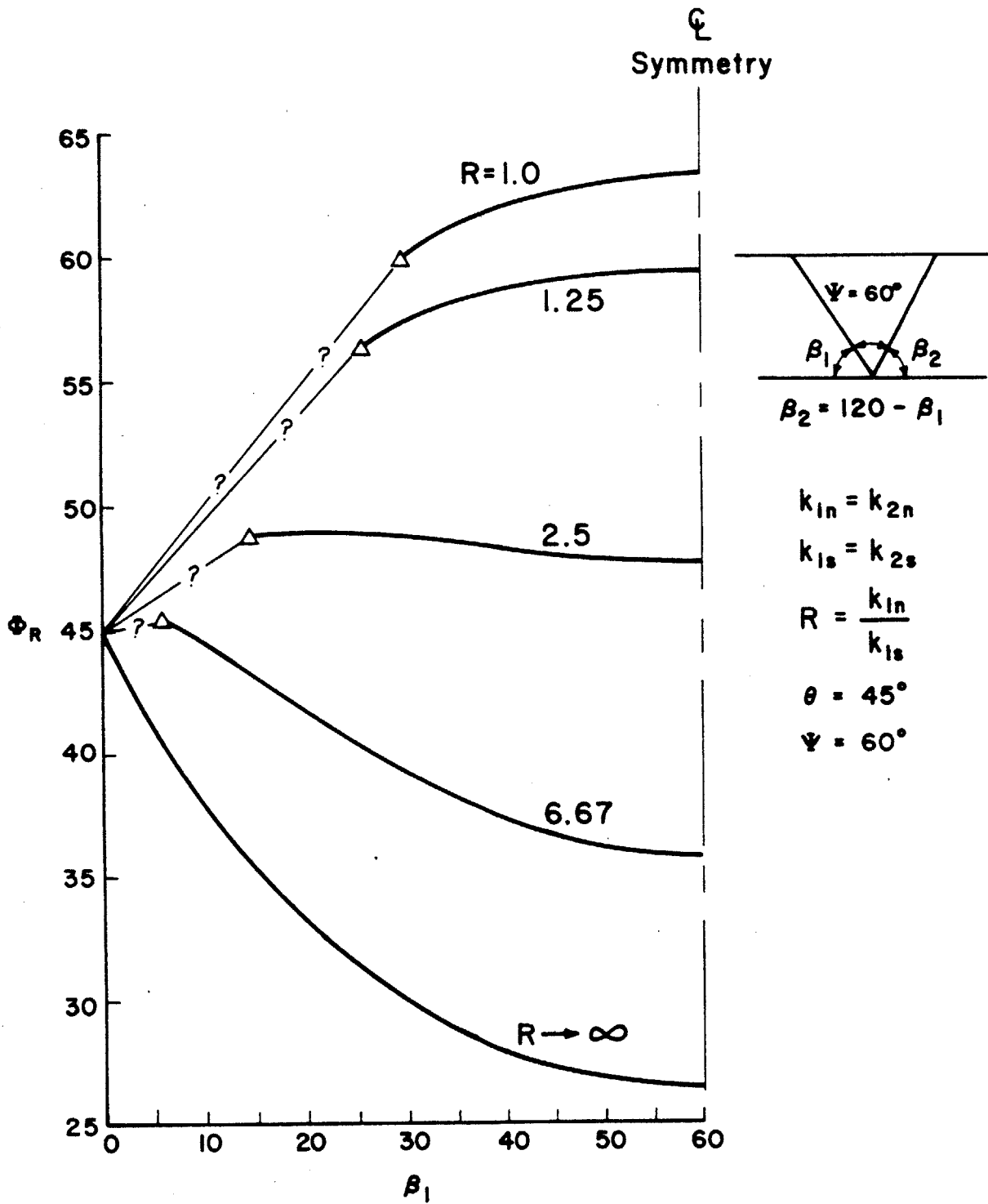


Figure 4.18 Φ_R vs. β_1 For $\Psi = 60^\circ$

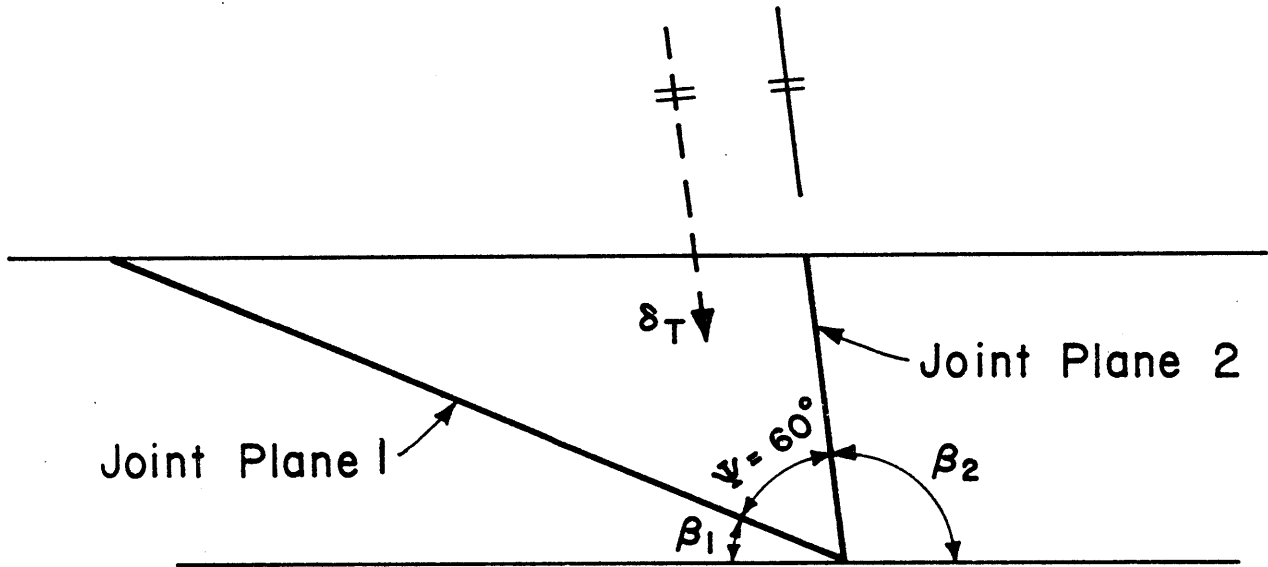


Figure 4.19 Overhanging Joint Plane

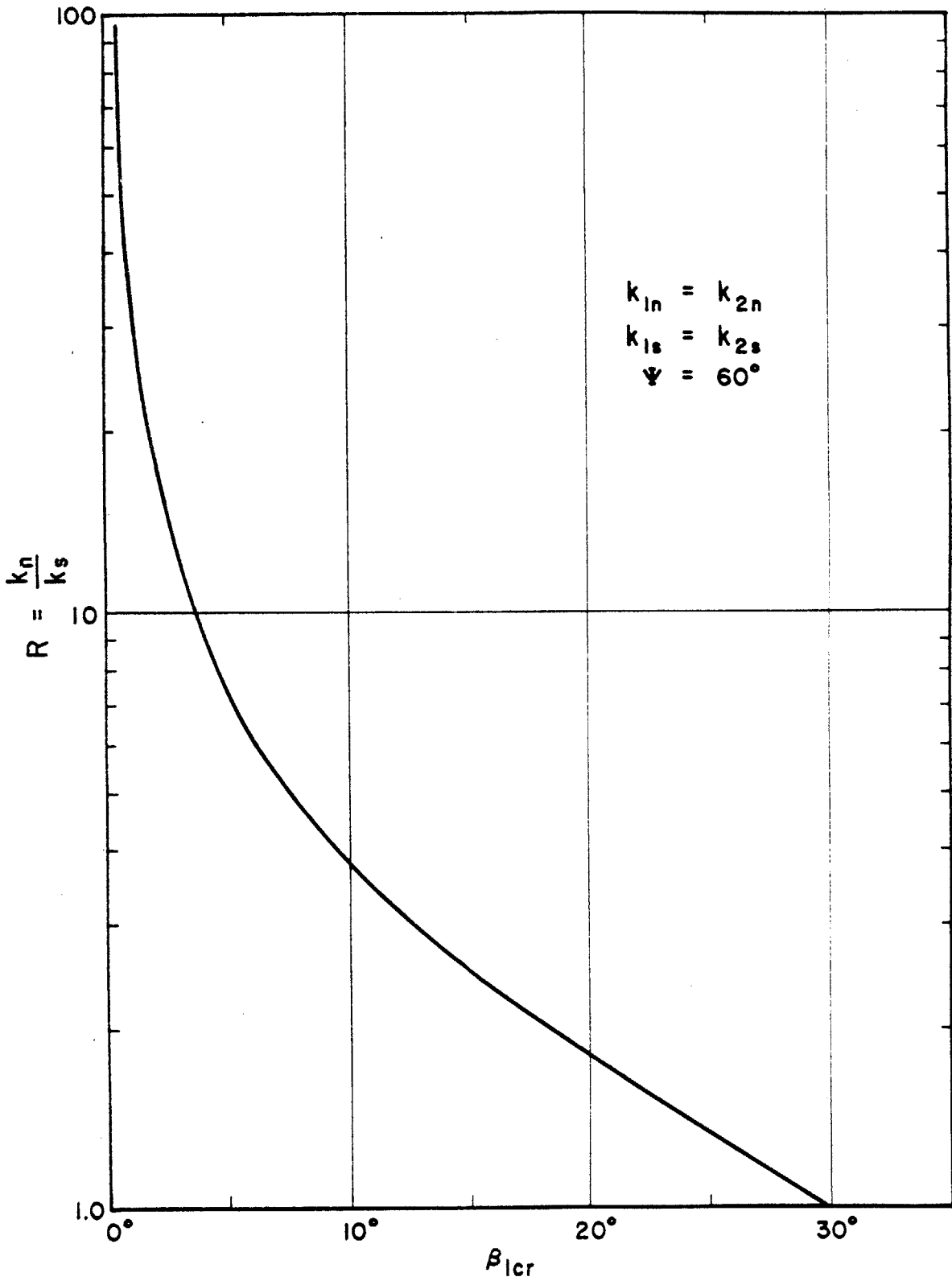


Figure 4.20 R vs. β_{lcr} for $\Psi = 60^\circ$

wedge tends to pull away from joint plane 2. Continuous rock joints cannot sustain a tensile load so the curves for ϕ_R must be modified to reflect the change in N_2 . The exact form of the curve depends on the shape and deformational characteristics of the asperities in the joint plane. It is conceivable that even in the absence of a normal force some asperities may interlock and generate a shear force in the overhanging joint plane. On the other hand, if the plane is relatively smooth, T_2 (as well as N_2) may reduce to 0 as soon as β_1 is less than β_{1cr} . Figure 4.21 illustrates schematically some of the typical forms the curve for $R = 1$ may assume. Curve B ignores the tension problem. It is merely a mathematical extension of Curve A into tensile region of N_2 . Curve C represents the other extreme. A severe discontinuity occurs at $\beta_1 = \beta_{1cr} = 30^\circ$ as both N_2 and T_2 drop to 0. The portion of Curve C that lies to the right of point 0 represents sliding along a single plane--plane 1. Curve D recognizes the existence of some shear forces in the joint plane for $0 < \beta < \beta_{1cr}$. Most natural joint planes would probably have curves that plot between C and D. It is interesting to note that the inability of overhanging joints to maintain tensile loads can be helpful from a stability standpoint in that it reduces ϕ_R (compare Curves B and D in Figure 4.21). (Joints with bridges of

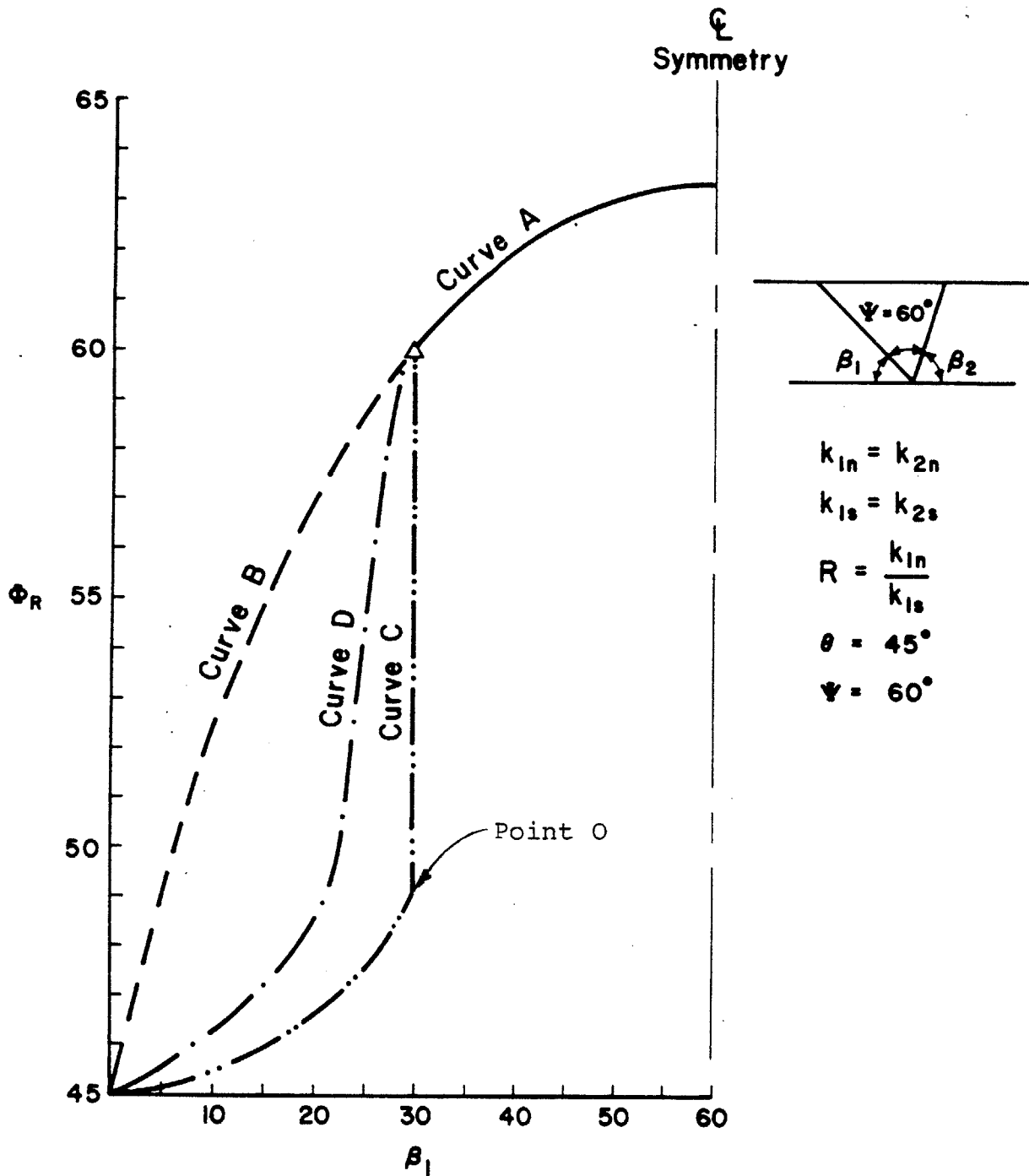


Figure 4.21 Φ_R vs. β_1 For $\Psi = 60^\circ$ and $R = 1$ --Curves Reflect Different Reactions on Joint Plane 2

intact rock may be capable of maintaining tensile forces; the tensile capacity would depend on the persistence of the respective joints.)

When $\beta_1 > \beta_{1cr}$, the curves for $R = 1$ and $R = \infty$ seem to be symmetrical--a property which is apparently shared by all such pairs of curves. For $\psi = 60^\circ$, the maximum difference ($\Delta\phi_{\max}$) between the curves is 30° . This difference always reaches a maximum at $\beta_1 = \beta_2$ and is a function of ψ . Figure 4.22 shows that $\Delta\phi_{\max}$ is a very strong function of ψ and decreases rapidly as ψ increases.

Case 4: $k_{1s} = k_{1n}$; $k_{2s} = k_{2n}$ $\psi = 90^\circ$

$$0^\circ \leq \beta_1 \leq 90^\circ$$

$$0^\circ \leq \beta_2 \leq 90^\circ$$

$$S = \frac{k_{2s}}{k_{1s}} = \frac{k_{2n}}{k_{1n}}$$

The effect of different stiffnesses in the joint planes is shown in Figure 4.23. The curves become more skewed as S increases. The changes in shape reflect the fact that in Equation (4.44) the numerator ($W \sin \theta$) is a constant while the denominator ($N_1 + N_2$) varies with geometry of the wedge. A high value of S suggests that joint plane 2 bears a disproportionately large share of the weight of the wedge. The reaction at joint plane 2 consists of N_2 and T_2 . Since β_1

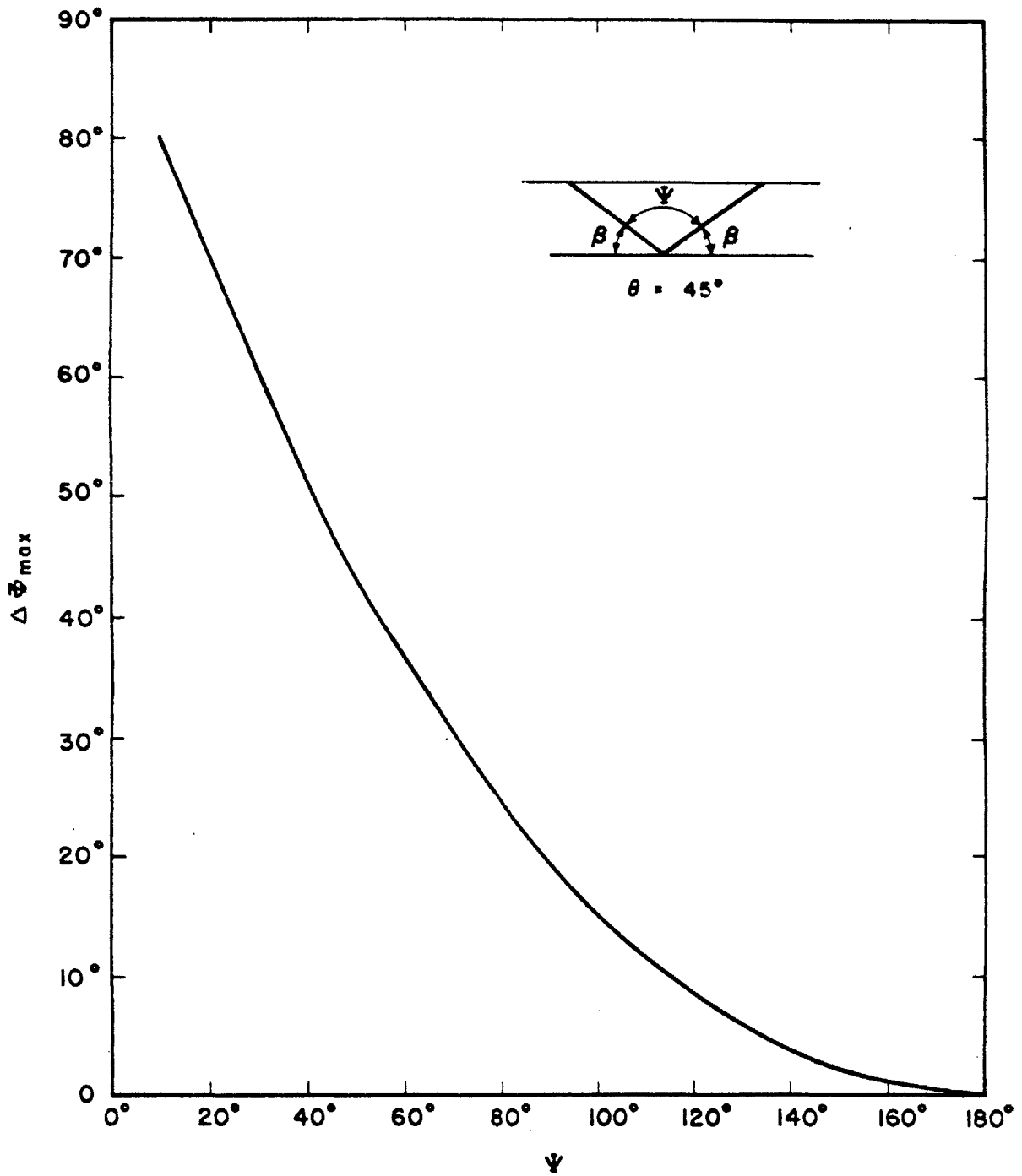


Figure 4.22 $\Delta\phi_{\max}$ vs. Ψ for $\theta = 45^\circ$

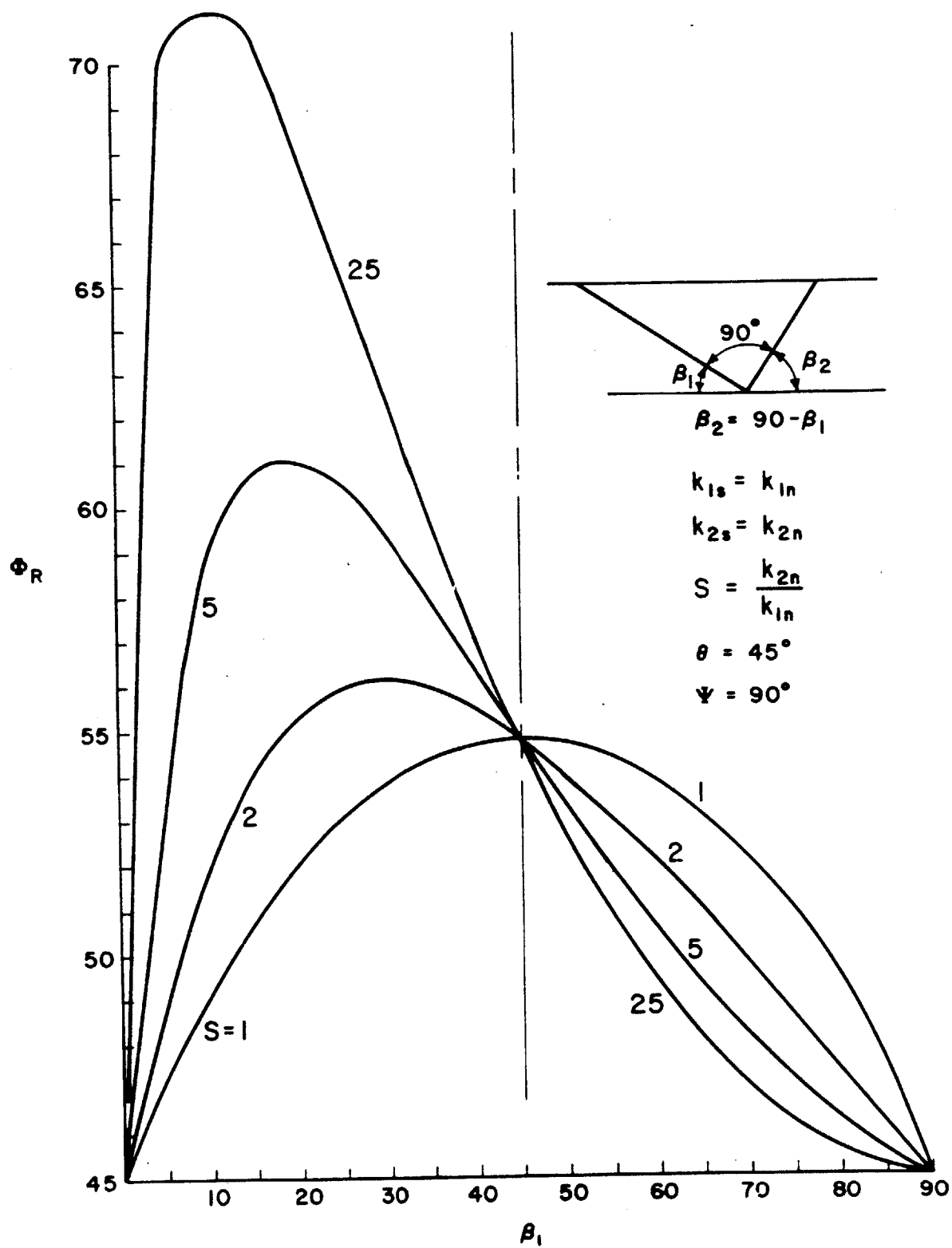


Figure 4.23 Φ_R vs. β_1 For $\Psi = 90^\circ$ and Varying S

and β_2 are complementary angles, β_1 values near 0° are associated with β_2 values near 90° . When β_2 approaches 90° most of the reaction is supplied by T_2 . Under these conditions (low β_1 and high S), N_1 and N_2 are low and a high ϕ_R is required to maintain equilibrium. The argument can be reversed for cases involving β_1 near 90° . β_2 near 0° implies a high N_2 and a correspondingly low ϕ_R .

All of the curves pass through the point $\beta_1 = 45^\circ$ and $\phi_R = 54.75$. Since ψ equals 90° , β_1 of 45° defines a symmetrical wedge. Under this special condition, the sum $N_1 + N_2$ is a constant regardless of the value of S .

All of the results summarized in this section are based on wedges that have geometrically similar cross sections along their entire lengths. The physical significance of this assumption was discussed earlier. The method can be generalized to handle wedges with arbitrary geometries. The technique is discussed in Section 4.5 in connection with the computer program SWARS-2PM.

4.3 Stress Approach Vs. Stiffness Approach

4.3.1 Introduction

Section 4.1 showed that the stresses on the joint planes is a critical input to the stability analysis. That same section discussed two alternate methods for computing the stresses. An obvious question arises: How does one determine the stresses on the joint planes? The question is difficult to answer because the stresses depend on

cumulative effects of loads and joint stiffnesses - both of which can change as time progresses. Figure 4.24 illustrates the concept. It is a schematic representation of the temporal variations in loads, joint stiffnesses and stresses that occurred during the existence of a hypothetical wedge.

The stresses are a function of the loads and stiffnesses. During any small time increment Δt there is a direct relationship between incremental loads (ΔL) and incremental stresses (ΔS). ΔS is related to ΔL through the stiffness equations presented in Section 4.3. The precise relationship between ΔS and ΔL depends on the values of the stiffnesses during that time interval. An incremental load applied at t_1 will not necessarily produce the same change in stresses as the same load applied at t_2 because the stiffnesses at t_1 and t_2 may be different. The stresses at any time t reflect the original stresses (at t_0) plus all the changes that have occurred since t_0 . (The model presumes that the principle of superposition is valid at least in a crude sense.) Thus, S_p , the present state of stress, is a function of the cumulative interaction between loads and stiffnesses; S_p is not directly related to the current stiffnesses. The current stiffnesses are instrumental in determining the effects of additional loads, but yield no information concerning S_p .

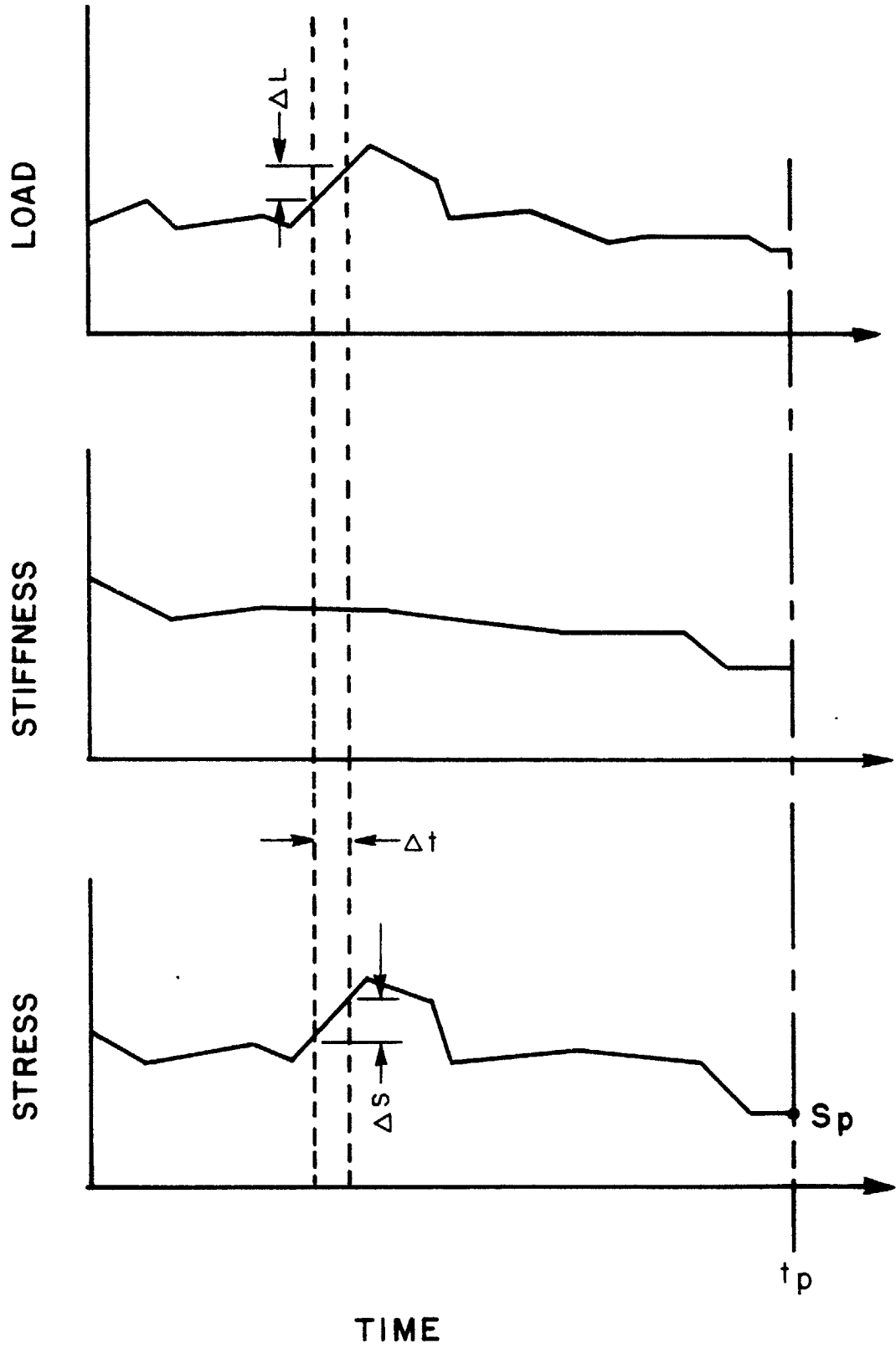


Figure 4.24 Load, Stiffness and Stress vs. Time

This discussion raises an interesting point about the stiffness plots presented in Section 4.1 (Figures 4.16 through 4.18). These plots describe a highly idealized situation that is portrayed in Figure 4.25. They treat the weight of the wedge as an external load that is not applied until after the stiffnesses have reached their current values. In effect, the wedge is placed in a preconditioned notch at t_p , the present time. Nevertheless, the plots can provide some useful information that will be discussed later in this section.

4.3.2 Detailed Discussion

The joints which define a rock wedge formed when the intact rock mass became overstressed.* The creation of the joints changed the stress field near the joints as the rock mass re-established equilibrium. Once formed, the joints may have been subjected to a variety of geologic processes. Some processes such as glaciation or erosion can be active for thousands of years. Others such as seismic activity or rainwater infiltration can be intermittent. Regardless of the process, the joints interact with their evolving environment. The stresses on the joints change to satisfy new loading conditions. The stresses at any one time reflect not only the current conditions but also the entire loading history of the joints.

K, the ratio of horizontal to vertical stresses in

* The joints may not have formed simultaneously. The time of formation is not an important feature of the argument.

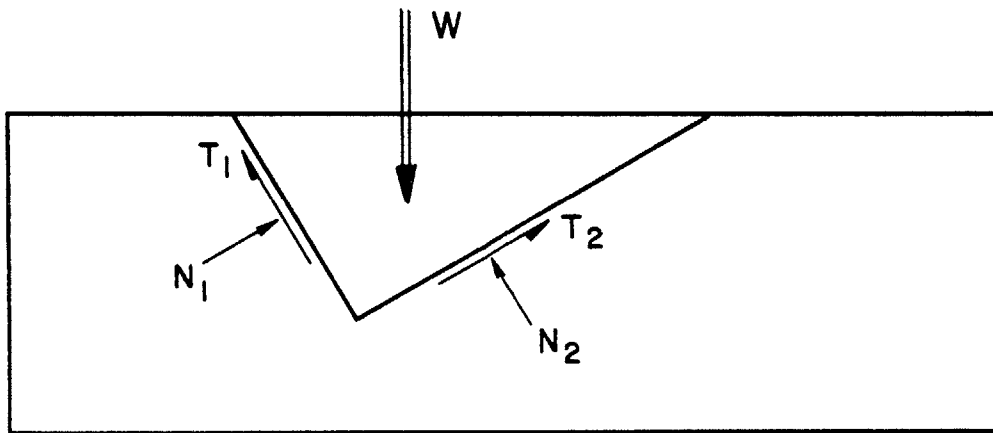
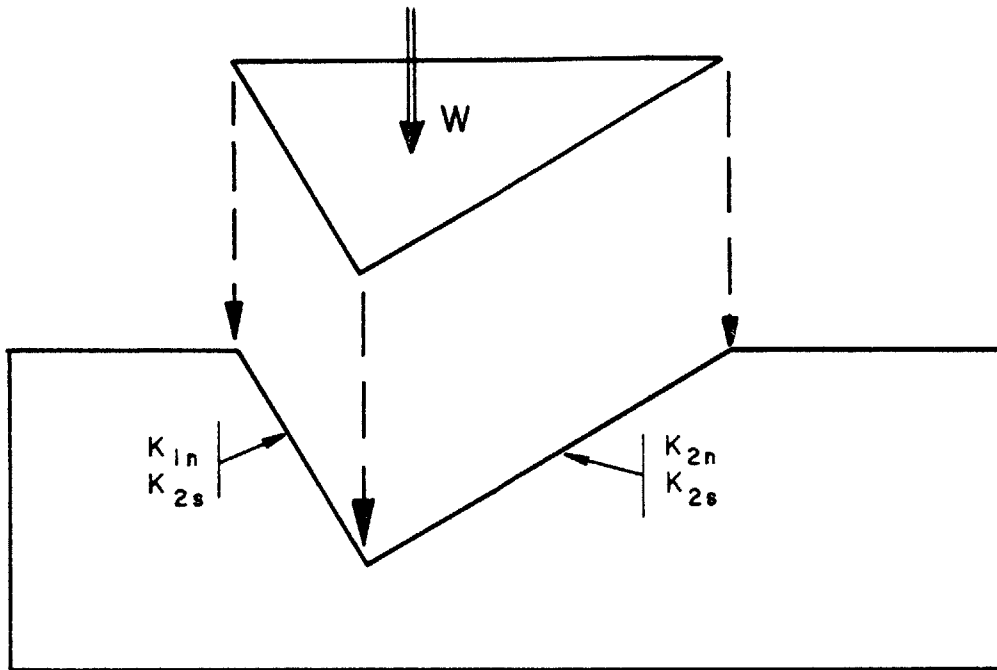


Figure 4.25 Stiffness Approach--Idealized Case

the wedge bounded by the joints, can be considered a parameter that describes the net effect of all the loadings during the wedge's existence. It is not necessarily identical to the ratio of in situ stresses in the parent rock mass. The joint is a discontinuity in the physical properties of the rock and may create irregularities in the ambient stress field that characterize the rock mass. The joints may isolate the wedge from the remainder of the rock mass. On the other hand, the stress field may be continuous across the joint.

The idea that K characterizes the stresses in the joint planes provides some insight into the parameter, but the critical question remains: How does one measure K ? K is intimately linked to the geologic history of the wedge so it is almost impossible to determine the value a priori. However, there are limits to the range of values that K can assume. K must lie between K_a and K_p^* which represent the active and passive states of failure described in Section 4.1. The only way to determine K for a specific wedge is to actually measure the stresses in the wedge. Unfortunately, the techniques for measuring in situ stresses are too complicated and too expensive to use for all wedges. At the present time K is usually estimated. The most realistic approach is to treat K as a random variable and perform a reliability analysis on the wedge. The uncertainty associated

* The derivations in Section 4.1 assumed that the strength of the joint consisted solely of frictional resistance.

with K can be incorporated directly into the stability analysis.

The discussion in Section 4.1 treated symmetric wedges. The concept can be extended to handle asymmetric wedges. Figure 4.26 is a section taken perpendicular to the line of intersection of a typical asymmetrical wedge. Each differential segment along the joint plane can be treated like the element shown in Figure 4.6. The K parameter relates the shear and normal stresses on the joint planes (Equations (4.15) and (4.16)). The stresses can be integrated to yield the following expressions:*

$$\frac{T_1}{N_1} = \frac{(1-K)}{\text{ctn } \beta_1 + K \tan \beta_1} = \lambda_1 \quad (4.46)$$

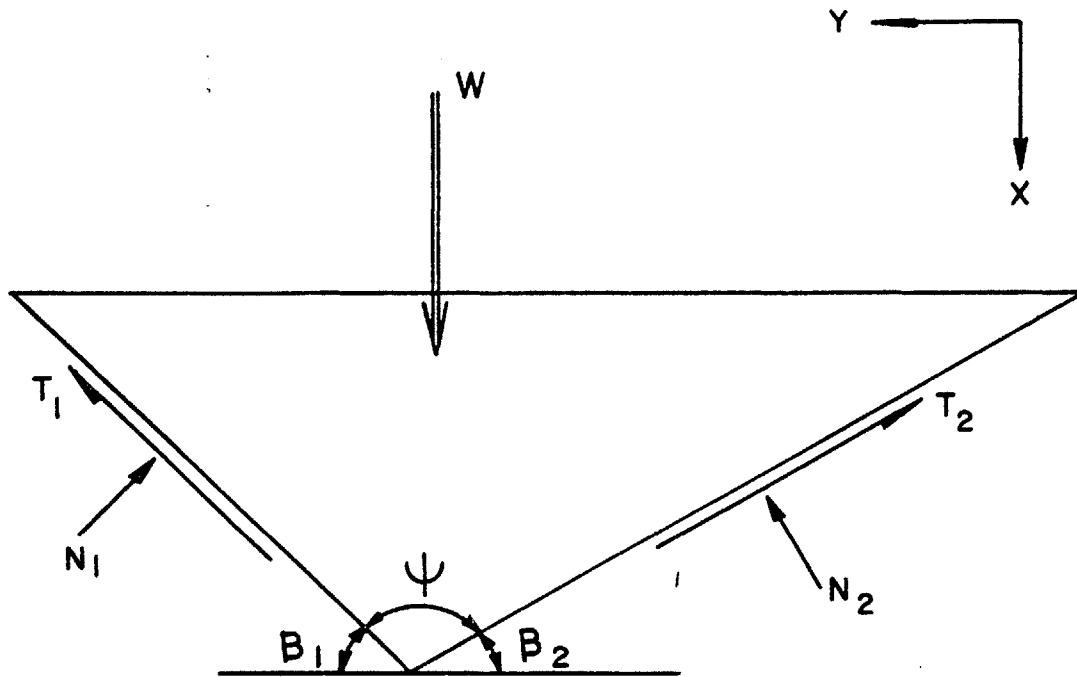
$$\frac{T_2}{N_2} = \frac{(1-K)}{\text{ctn } \beta_2 + K \tan \beta_2} = \lambda_2 \quad (4.47)$$

Equations (4.46) and (4.47) can be used in conjunction with the equations of force equilibrium to evaluate N_1 , T_1 , N_2 , T_2 .

Summing forces in the x direction (Figure 4.26):

$$N_1 \cos \beta_1 + \lambda_1 N_1 \sin \beta_1 + N_2 \cos \beta_2 + \lambda_2 N_2 \sin \beta_2 = W^1 \quad (4.48)$$

*K may vary over the height of the wedge. If K does vary, the parameter shown in Equations (4.46) and (4.47) is the mean value of K for the entire height.



$$\frac{dT_j}{dN_j} = \frac{1 - K}{\cot \beta_j + K \tan \beta_j}$$

Figure 4.26 Stresses on Differential Areas of the Joint Planes

w^1 is the component of the weight acting perpendicular to the line of intersection. As shown in Figure 4.2, $w^1 = W \cos \theta$.
Summing forces in the y direction:

$$N_1 \sin \beta_1 - \lambda_1 N_1 \cos \beta_1 - N_2 \sin \beta_2 + \lambda_2 N_2 \cos \beta_2 = 0 \quad (4.49)$$

Rearranging Equation 4.49:

$$\frac{N_1}{N_2} = \frac{(\sin \beta_2 - \lambda_2 \cos \beta_2)}{(\sin \beta_1 - \lambda_1 \cos \beta_1)} = \lambda_3 \quad (4.49A)$$

Equations (4.49A) and (4.48) can be solved for N_2 :

$$N_2 = \frac{W \cos \theta}{\lambda_3 (\cos \beta_1 + \lambda_1 \sin \beta_1) + (\cos \beta_2 + \lambda_2 \sin \beta_2)} \quad (4.50)$$

Finally,

$$N_1 = \lambda_3 N_2 \quad (4.49B)$$

$$T_1 = \lambda_1 N_1 \quad (4.46A)$$

$$T_2 = \lambda_2 N_2 \quad (4.47A)$$

The equilibrium analysis outlined above did not explicitly consider joint stiffnesses. It was concerned solely with the current state of stress on the joint planes. The stiffnesses enter the problem indirectly through the K parameter.

K reflects the response of the wedge to a series of loadings. The response for any particular load depends on the material properties of the joints. However, these properties (the shear and normal stiffnesses) can change with time.* The incremental stresses that develop during each loading are a function of the joint properties at the time of the loading. There is no unique relationship between the current stresses and current stiffnesses.

Although the stiffnesses are not helpful in determining the current state of stress they can be used to determine the additional stresses due external loadings like rock bolts or surcharges. In fact any "current loading" can be analyzed with the stiffness approach presented in Section 4.2. The procedure is consistent with the concept proposed earlier: loads should be analyzed in terms of the stiffnesses that existed at the time of their application.

Thus, the stability analysis that will be described in Sections 4.4 and 4.5 combines the stress and stiffness approaches in the following manner:

1. The stress approach is used to calculate the reactions (N_1, N_2, T_1, T_2) due to the weight of the wedge.
2. The stiffness approach is used to calculate the reactions due to all other loads.

* There are many mechanisms that can change the joint properties. The stiffnesses may decrease during extreme loadings because aspartities shear off. Ground water percolation through the joints can either decrease (through leaching) or increase (through cementation) the stiffnesses.

The procedure is admittedly a simplification of actual conditions but it does present a consistent methodology for treating rock wedges.

The weight of the wedge should be analyzed through the stress approach. The stiffness plots shown as Figures 4.16 to 4.18 are a direct violation of this principle. As shown earlier, the stiffness approach should only treat "current" loads. Although the plots should not be used to examine gravitational loads they can be used to examine any other loading that is directly proportional to the size of the wedge. The plots were based on cross sections with different shapes (β_1 varied) but with a constant height (Figure 4.15). N_1 and N_2 are directly proportional to the weight of the unit cross section (Equation (4.40); $X = W \cos \theta$). Equation (4.44) indicates that ϕ_R , the ordinate of the plots, is a function of $\frac{W}{N_1 + N_2}$; hence, any loading that is directly proportional to the weight should yield the same values of ϕ_R . Since the wedges have a constant height the distance AB in Figure 4.15 is directly related to the area or to the weight of the section. A uniform loading along AB would be directly related to the weight of the wedge. Therefore, Figures 4.16 to 4.19 show the effect of a uniform surcharge on the top (and front) faces of the wedge.

4.4 The Factor of Safety

The presence of shear forces on the joint planes in a direction perpendicular to the line of intersection presents some difficulties in defining the factor of safety (FS). This problem was alluded to in Section 4.1 where FS was calculated two different ways. In rock slope analyses FS is usually defined as the ratio of resisting to driving forces. However, the definition assumes that both forces act in the same direction. The condition is seldom fulfilled in real problems.

Figure 4.27 shows the shear forces that should be considered in a typical stability analysis. As derived in Figure 4.2, the shear force along the line of intersection is $W \sin \theta^*$. T_1 and T_2 are shear forces perpendicular to the line of intersection. In the special case where $K = 1$ (the situation considered in conventional analyses) T_1 and T_2 are both zero; therefore, the entire shear resistance along the joint planes counteracts $W \sin \theta$. Whenever K does not equal unity the shear resistance must counteract T_1 and T_2 in addition to $W \sin \theta$. In fact, the effect is magnified because the presence of T_1 and T_2 actually decreases the shear resistance. As indicated in Section 4.1, T_1 and T_2 increase at the expense of N_1 and N_2 . As N_1 and N_2 decrease the frictional resistance declines. The crucial questions are:
* This simplified model presumes that gravity is the only force acting on the wedge.

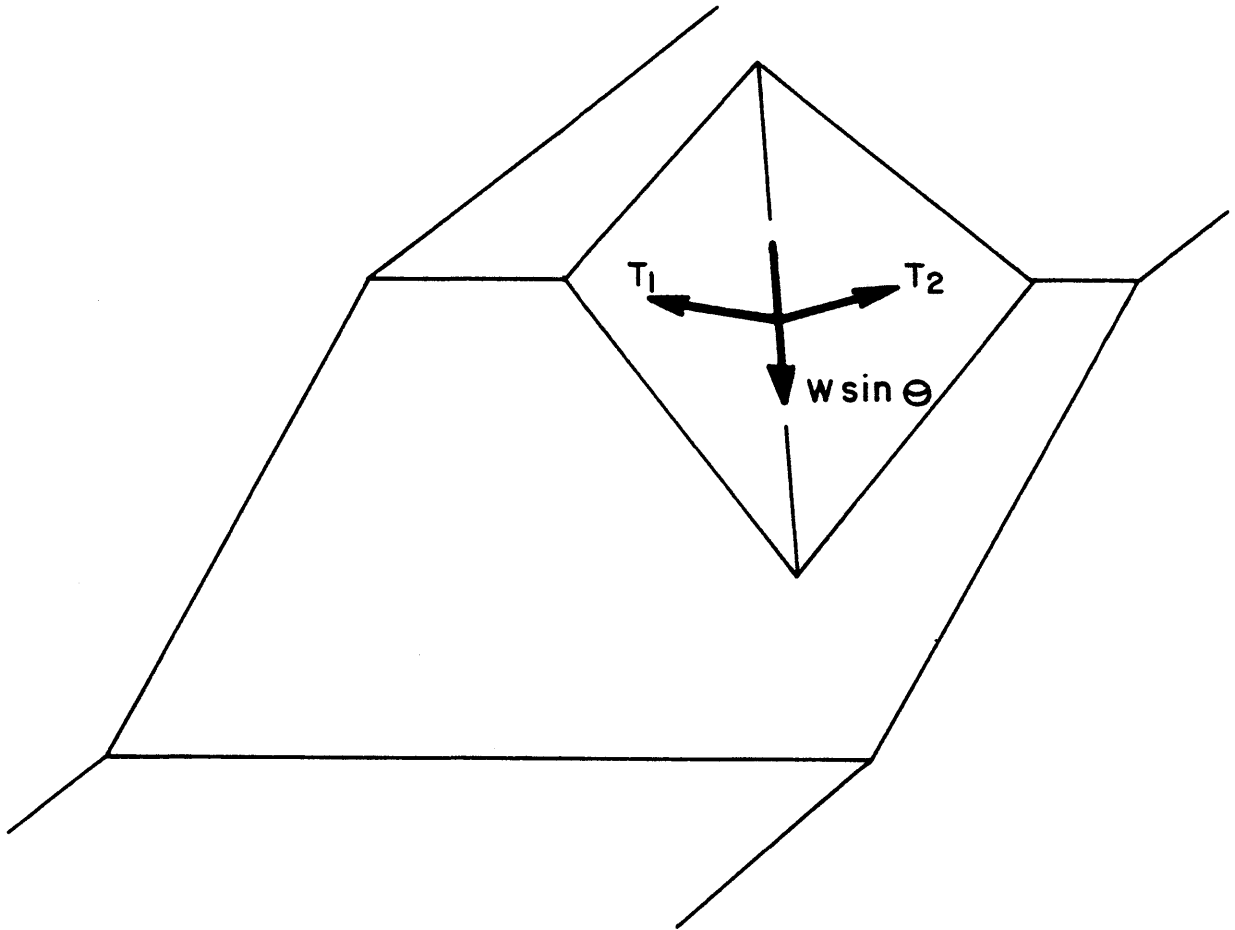


Figure 4.27 Shear Forces on Joint Planes

How do T_1 and T_2 affect the stability of the block and how can they be incorporated into stability calculations?

St. John addressed this problem in analyzing symmetric wedges with purely frictional resistance. As indicated in Section 4.1, St. John defined the factor of safety as:

$$FS = \frac{2N \tan \phi}{\sqrt{(2T)^2 + (W \sin \theta)^2}} \quad (4.51)$$

Thus, the driving force was considered the vectorial sum of the shear forces* in the joint planes. The resultant shear forces in the two planes are mirror images of one another because the wedge is symmetric. At limiting equilibrium the direction of impending motion is down the line of intersection and into the notch i.e., the wedge has a tendency to "settle" in the notch as well as move down the line of intersection.

The direction of motion is an important consideration in examining stability problems. What are the practical implications of a wedge settling in its notch? Surely there is a limit to the amount of movement that can occur in this direction. A minor amount of settlement may not be significant from an engineering standpoint. The important question is what happens after failure? Settlement

may be tolerable but sliding down the line of intersection

* St. John computed the T forces through a stiffness analysis; however, the derivation of T is not a salient feature of the current discussion.

is clearly unacceptable. Strictly speaking, limiting equilibrium cannot provide any insight into post-failure behavior because it is concerned solely with the condition of the system just at failure. Baligh et al. (19xx) have done some interesting work in this area.

Baligh et al. investigated the influence of K , the stress ratio, on the stability of symmetric wedges. They used the stress approach developed by Steiner (as presented in Section 4.1) to determine the forces on the joint planes; hence, both T and N are functions of K . Like St. John, Baligh et al. treated the driving force as the vectorial sum of the two shear components on each plane. They define the factor of safety as F_3 :

$$FS = F_3 = \frac{2N \tan \phi}{\sqrt{(2T)^2 + (W \sin \theta)^2}} \quad (4.51)$$

The equation can be rewritten as:

$$\frac{F_3}{\tan \phi} = \frac{2N}{\sqrt{(2T)^2 + (W \sin \theta)^2}} \quad (4.51A)$$

As shown in Figures 4.28 and 4.29, the quantity $F_3/\tan \phi$ can be plotted as a function of K . The three curves in each figure correspond to wedges whose lines of intersection plunge at 5° , 15° and 45° . Figure 4.28 and Figure 4.29 were

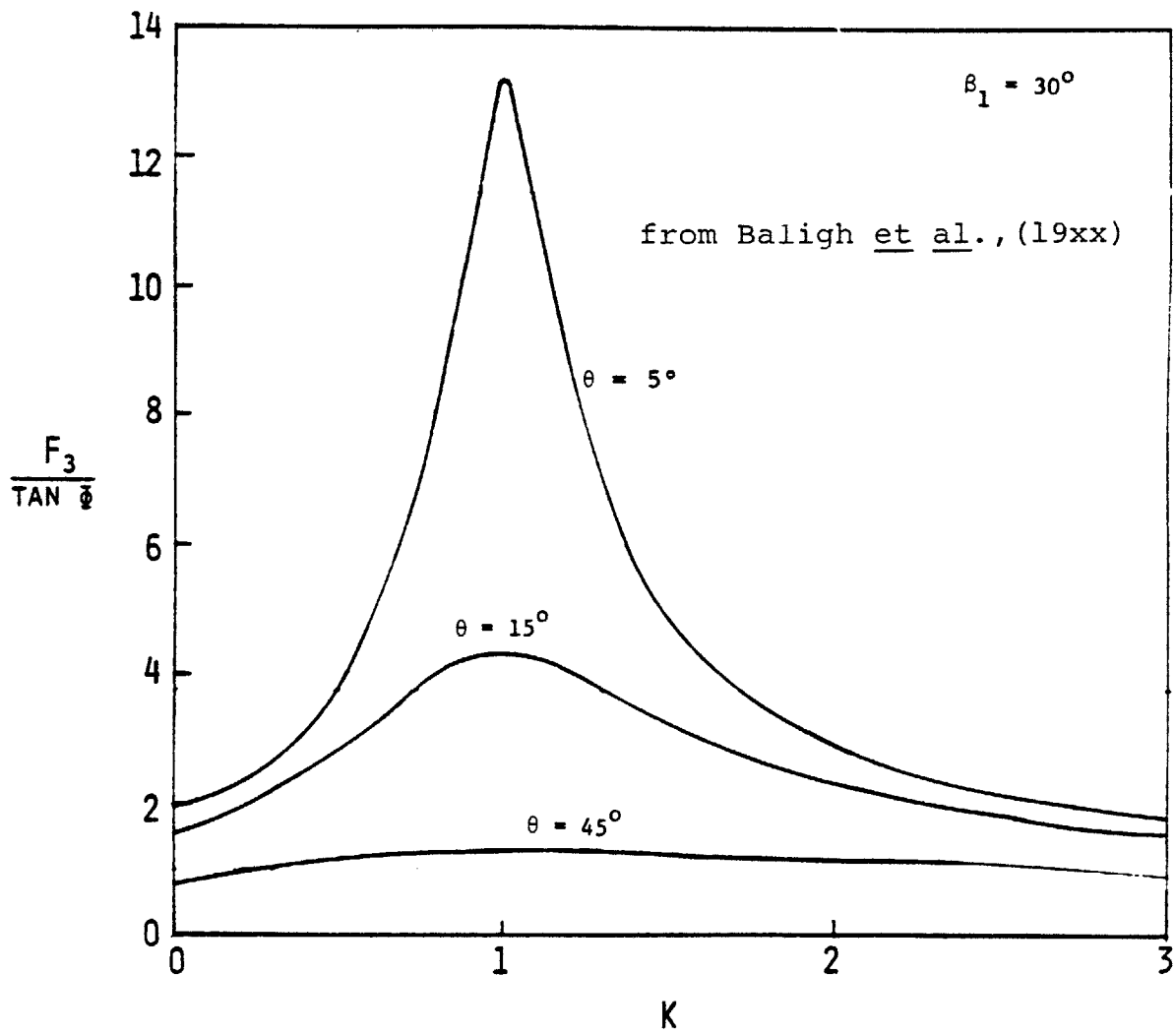


Figure 4.28 $F_3/\tan \phi$ vs. K ; $\beta_1 = 30^\circ$

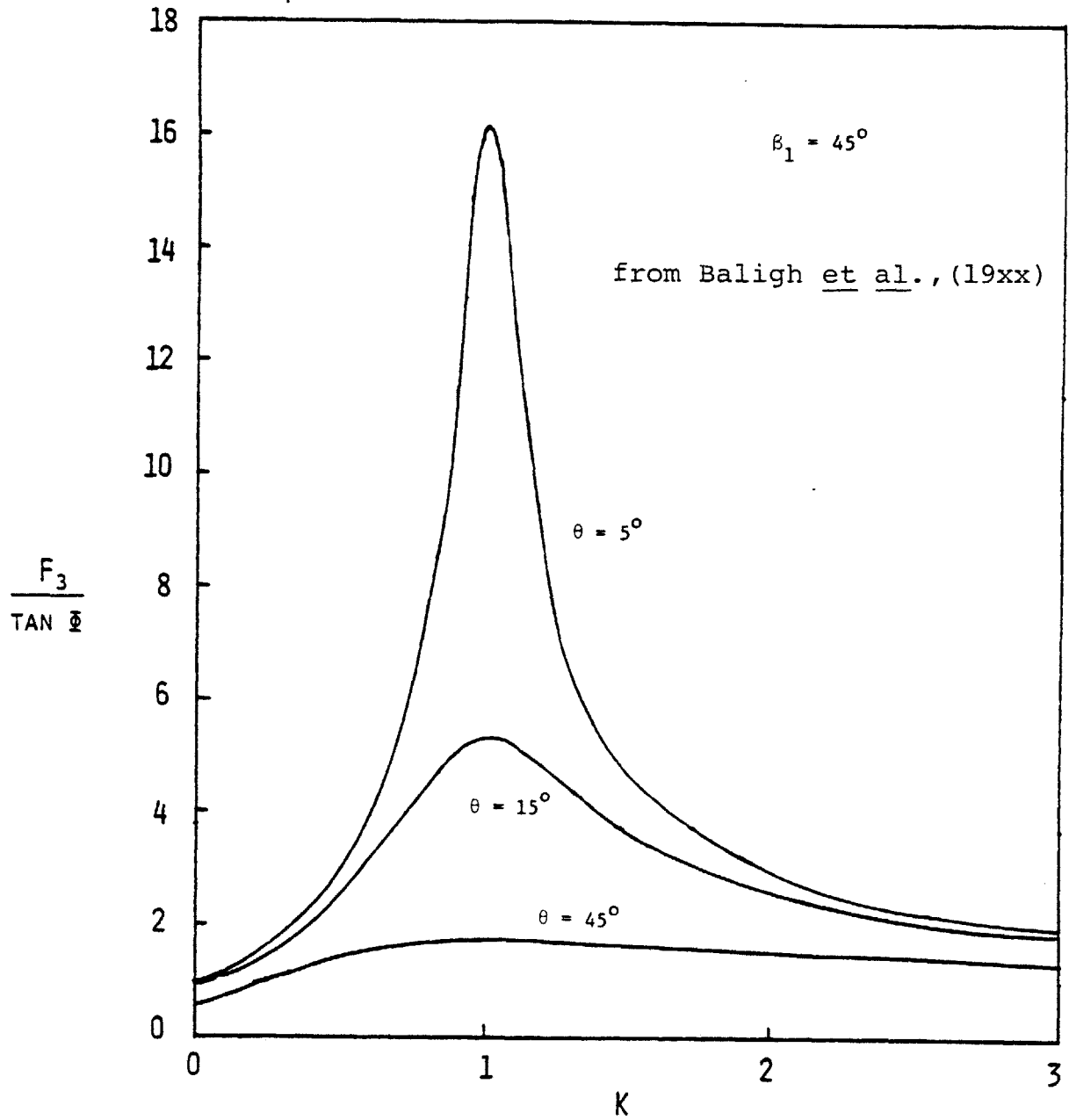


Figure 4.29 $F_3/\tan \Phi$ vs. K ; $\beta_1 = 45^\circ$

developed for β 's of 30° and 45° respectively.

All of the curves have a maximum at $K = 1.0$. When $K = 1.0$, T is zero and the impending motion is down the line of intersection. Also,

$$\frac{F_3}{\tan \phi} = \frac{1}{\tan \theta \cos \beta} \quad (4.52)$$

The plots are helpful in visualizing how rock wedges fail. Figure 4.30 is a schematic representation of an F curve similar to the ones in Figures 4.28 and 4.29. (The term $\tan \phi$ will be considered a constant. It can be factored into the ordinate scale.) At some arbitrary time (say t_p in Figure 4.24) the stresses on the joint planes correspond to point A. If some additional loads are placed on the wedge the stresses on the joint planes will change - the incremental stresses will depend on the stiffnesses as discussed in Section 4.3. Let the new stress state correspond to point B. At B the wedge is at limiting equilibrium; any additional loads will initiate movement. The direction of movement will be along the line of intersection and into the notch. However, as soon as the wedge begins to settle into its notch the lateral stresses will increase. This "wedging" action increases K which in turn increases N and decreases T . According to this conceptual model the wedge can sustain additional loadings and pass from point B to C

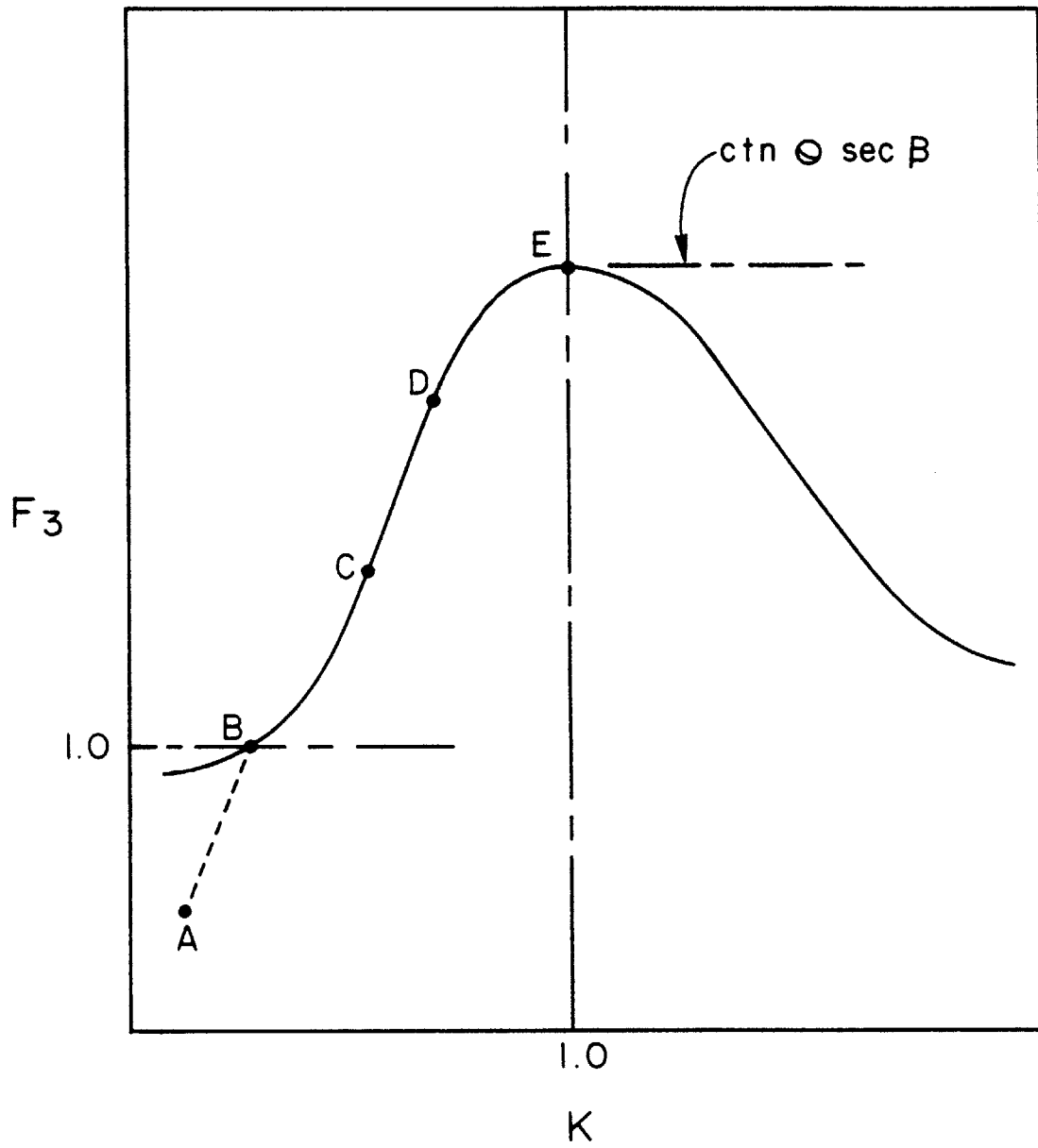


Figure 4.30 Schematic Failure Sequence

and D.* With each incremental load the wedge settles a little more and K increases. Finally, the wedge reaches point E where T is zero. At E i.e., $K = 1.0$ the direction of movement is exclusively along the line of intersection. Theoretically, there is nothing to prevent the wedge from sliding along the line of intersection out of its notch.

A similar effect occurs when $K > 1.0$ i.e., to the right of the maximum. This situation would correspond to passive conditions and the initial movement would be out of the notch and along the line of intersection. K would eventually reach 1.0 as the load increased.

Thus, it is possible to define two factors of safety: FS_I , the initial factor of safety, corresponds to point B; FS_U , the ultimate factor of safety, corresponds to point E. FS_U is the value used in traditional stability calculations. The engineer must use his judgement in deciding whether to use FS_I or FS_U as a design criterion in a particular situation. If movements must be kept to an absolute minimum FS_I would be the more appropriate choice. If he merely wanted to design against catastrophic movements, FS_U would be the better choice.

* In the model $\tan \phi$ is assumed to be constant even after initial failure (point B).

The distinction between the two factors of safety is clear in Figure 4.30. However, that figure is a highly idealized model that ignores some important effects. In particular, it assumes that the shear strength of the joint planes consists solely of frictional resistance that can be expressed with a constant ϕ . In reality ϕ may be composed of interlocking asperities as well as mineral to mineral friction. The asperities may shear off as movement occurs. In effect, ϕ should decrease as the wedge is loaded beyond initial failure. Also, the model neglects cohesion along the joints. This cohesion may consist of bridges of intact rock which will shear when movement commences. One simplistic method for treating these effects is to neglect the cohesion and asperities in computing FS_U . (This is the approach that is used in the computer program that will be described in Section 4.5.)

All the wedges considered in the discussion of factor(s) of safety have been symmetric with respect to their geometric, stiffness, and frictional characteristics. Under these conditions i.e.

$$\beta_1 = \beta_2 \quad (4.53)$$

$$\phi_1 = \phi_2 \quad (4.54)$$

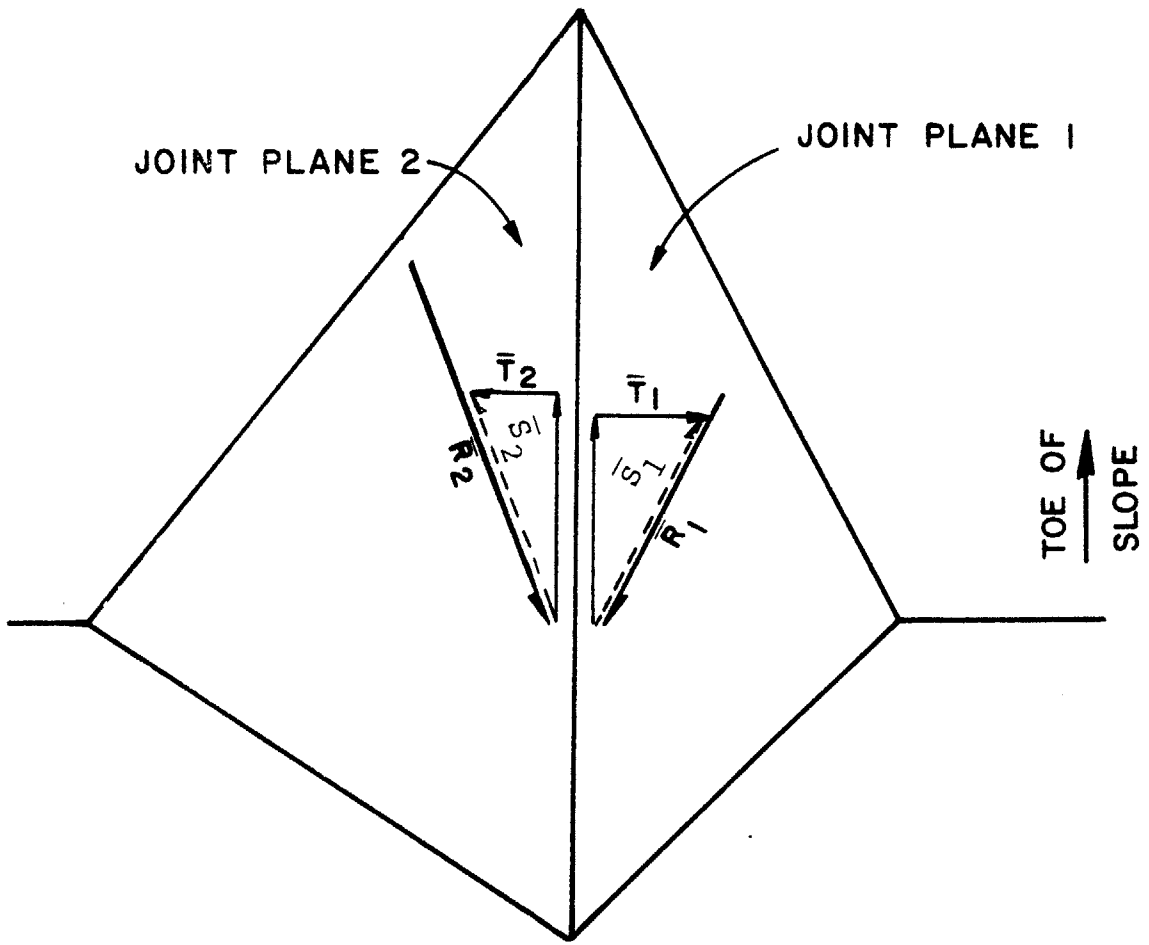
$$k_{1s} = k_{2s} \quad (4.55)$$

$$k_{1n} = k_{2n} \quad (4.56)$$

the impending motion is in the vertical plane that contains the line of intersection. The resultant of all the driving forces and the resultant of the shear resistances are in that same plane; in fact, the two resultants are colinear. Thus, the FS used by St. John and Baligh et al. is a direct comparison of colinear forces. Given the assumption of rigid body movement FS is rigorously defined from the standpoint of mechanics or statics.

FS is much more difficult to define if the wedge is asymmetric i.e., any of the conditions prescribed by Equations (4.53) to 4.56) are violated. Most asymmetric conditions will introduce a displacement component out of the vertical plane that contains the line of intersection. (The situation is shown in Figure 4.11. α is generally non zero for asymmetric conditions.) Also, the resultant of all the driving forces will no longer be colinear with the resultant of all the resisting forces.

The forces (and resultants) are shown in Figure 4.31 which is a plan view of the notch. Each joint plane has a shear component in the direction parallel to the line of intersection. The two components add up to $W \sin \theta$. The components in planes 1 and 2 are $n \cdot W \sin \theta$ and $(1 - n) \cdot \sin \theta$ respectively. Each plane also has a shear force perpendicular to the line of intersection (T_1 and T_2).



Note: $\bar{s}_1 + \bar{s}_2 = \bar{D}$

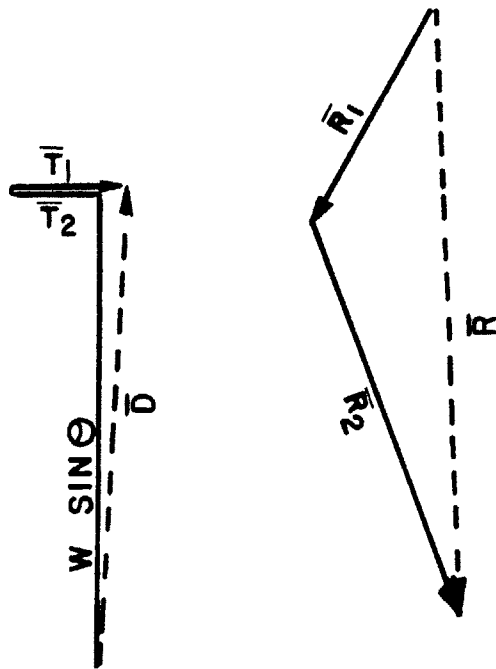


Figure 4.31 General Case-- \bar{D} and \bar{R} Not Parallel

The resultants of $(T_1 + n w \sin \theta = \bar{S}_1)$ and $(T_2 + (1-n) W \sin \theta = \bar{S}_2)$ are shown in Figure 4.31. The shear resistance in each plane is in the direction of the respective resultant. Thus, \bar{R}_1 is in the direction of \bar{S}_1 and \bar{R}_2 is in the direction of \bar{S}_2 . Both \bar{R}_1 and \bar{R}_2 represent the maximum possible shear resistance that can be mobilized; therefore, their magnitudes (but not directions) may differ from \bar{S}_1 and \bar{S}_2 . Figure 4.31 indicates that the sum of the resistances $(\bar{R}_1 + \bar{R}_2)$ is not in the same direction as the sum of the driving forces $(\bar{S}_1 + \bar{S}_2)$. $(\bar{R}_1 + \bar{R}_2)$ cannot be compared directly with $(\bar{S}_1 + \bar{S}_2)$ because of the disparity in directions. Thus, FS must be defined in terms of some arbitrary criterion; there is no unequivocal definition.

The computer program that will be described in Section 4.5 uses the following definition:

$$FS = \frac{\bar{R} \cdot \bar{\Delta}}{\bar{D} \cdot \bar{\Delta}} \quad (4.57)$$

\bar{R} is the resultant vector of all resisting forces

\bar{D} is the resultant vector of all driving forces

$\bar{\Delta}$ is the direction of impending motion

FS is considered the ratio of the components of \bar{R} and \bar{D} in the direction of $\bar{\Delta}$.

The definition of $\bar{\Delta}$ is somewhat ambiguous because the "direction of impending motion" is considered the direction of displacement due to an imposed load. Thus, $\bar{\Delta}$ will not

correspond to failure conditions unless the load creates a condition where $FS = 1.0$. Different loads will produce different Δ 's. The program offers the user two options:

1. $\bar{\Delta}$ is displacement that would occur under a purely vertical load i.e., in what direction would the wedge move if its unit weight suddenly increased by a small percentage? $\bar{\Delta}$ is based on the current stiffness.
2. $\bar{\Delta}$ is the displacement that occurs under all the "current loads." Current loads include all loads except the weight of block; they are the loads that are analyzed using the stiffness approach.

In the special case where there is total symmetry Equation (4.57) will yield the same FS as Equation (4.51).

4.5 Computer Program SWARS-2PM

The stiffness and stress approaches discussed in Sections 4.1 to 4.4 and in Appendix D have been incorporated into a computer program, SWARS-2PM. SWARS-2PM is actually a modified version of SWARS-2P which was originally developed by Campbell (1974) using the conventional assumption regarding the absence of T_1 and T_2 forces on the joint planes. SWARS-2PM retains all the versatility of its predecessor with respect to

loading conditions and ground water options; however, it determines the reactions on the joint planes according to the method prescribed in Section 4.3. If the failure mode involves sliding on both planes*, the program computes the two factors of safety defined in Section 4.4: FS_I and FS_U .

The stress approach is used to calculate the reactions on the joint planes due to the weight of the wedge. The generalized stiffness approach is used to calculate the reactions due to all other loads. In implementing the generalized stiffness approach, SWARS-2PM utilizes the relations developed in Appendix D with two modifications:

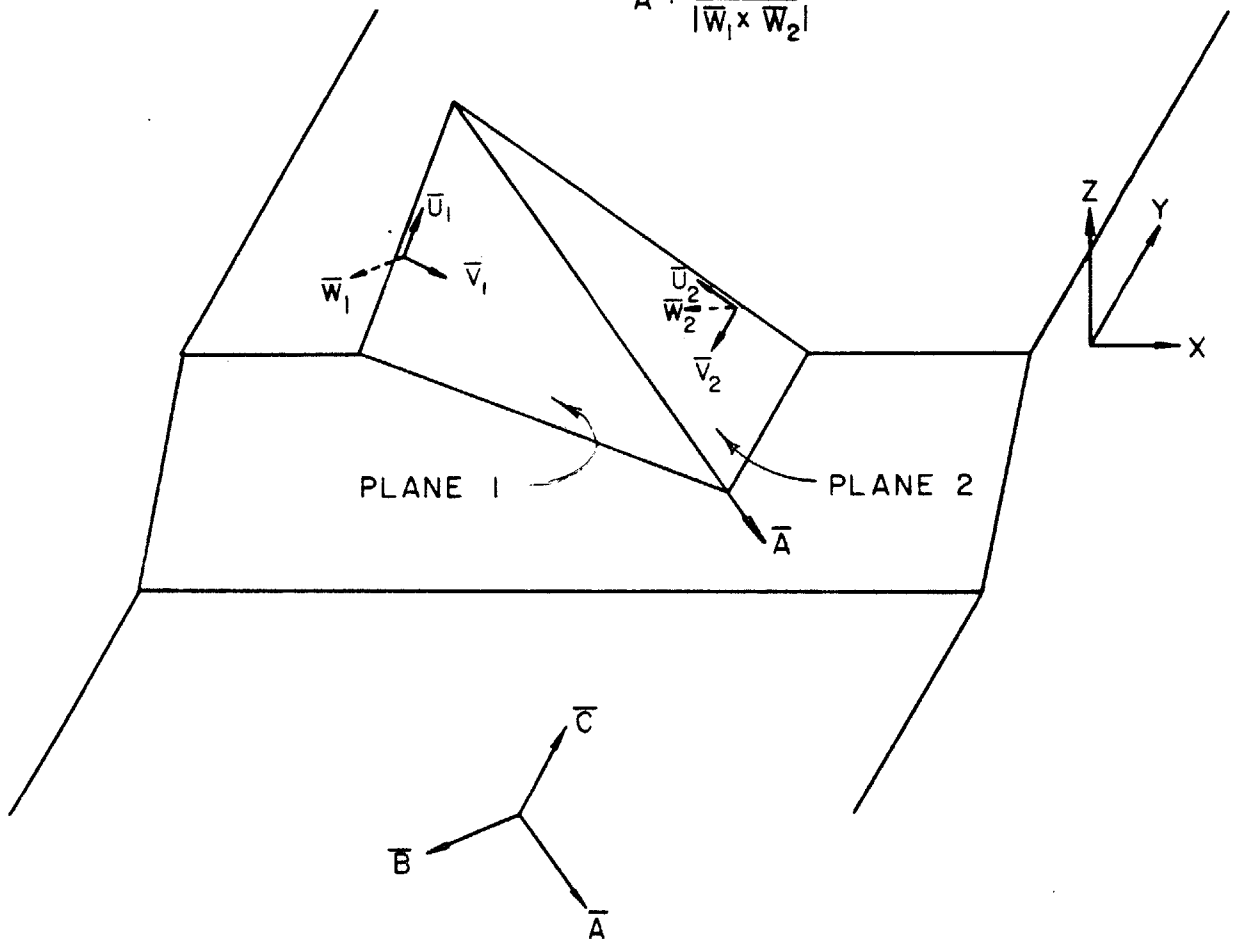
1. A_1 , the area of joint plane 1, replaces the term $h \csc \beta_1$ in Equation (D.3).
2. A_2 , the area of joint plane 2, replaces the term $h \csc \beta_2$ in Equation (D.6).

The program resolves the resultant of all "stiffness" loads into components along the A,B and C axes shown in Figure 4.32. The B and C components (Figure 4.33) correspond to the respective Y and X forces in Equations (D.10) and (D.9). The A component that lies along the line of intersection is part of \bar{D} , the driving vector, that appears in the denominator of the FS equation:

$$FS = \frac{\bar{R} \cdot \bar{\Delta}}{\bar{D} \cdot \bar{\Delta}} \quad (4.57)$$

* If the failure mode involves sliding on a single plane, SWARS-2PM will perform exactly the same analysis as SWARS-2P.

\bar{U}_i : STRIKE
 \bar{V}_i : DIP
 $\bar{W}_i: \bar{U}_i \times \bar{V}_i$
 $\bar{A}: \frac{\bar{W}_1 \times \bar{W}_2}{|\bar{W}_1 \times \bar{W}_2|}$



$\bar{A}, \bar{B}, \bar{C}$: UNIT VECTORS FORMING SETS OF ORTHAGONAL AXES

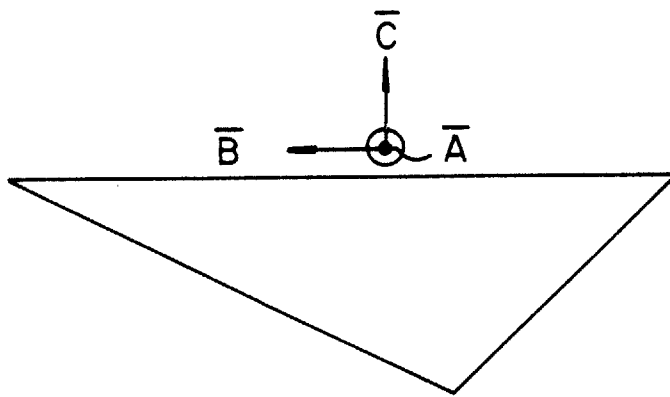
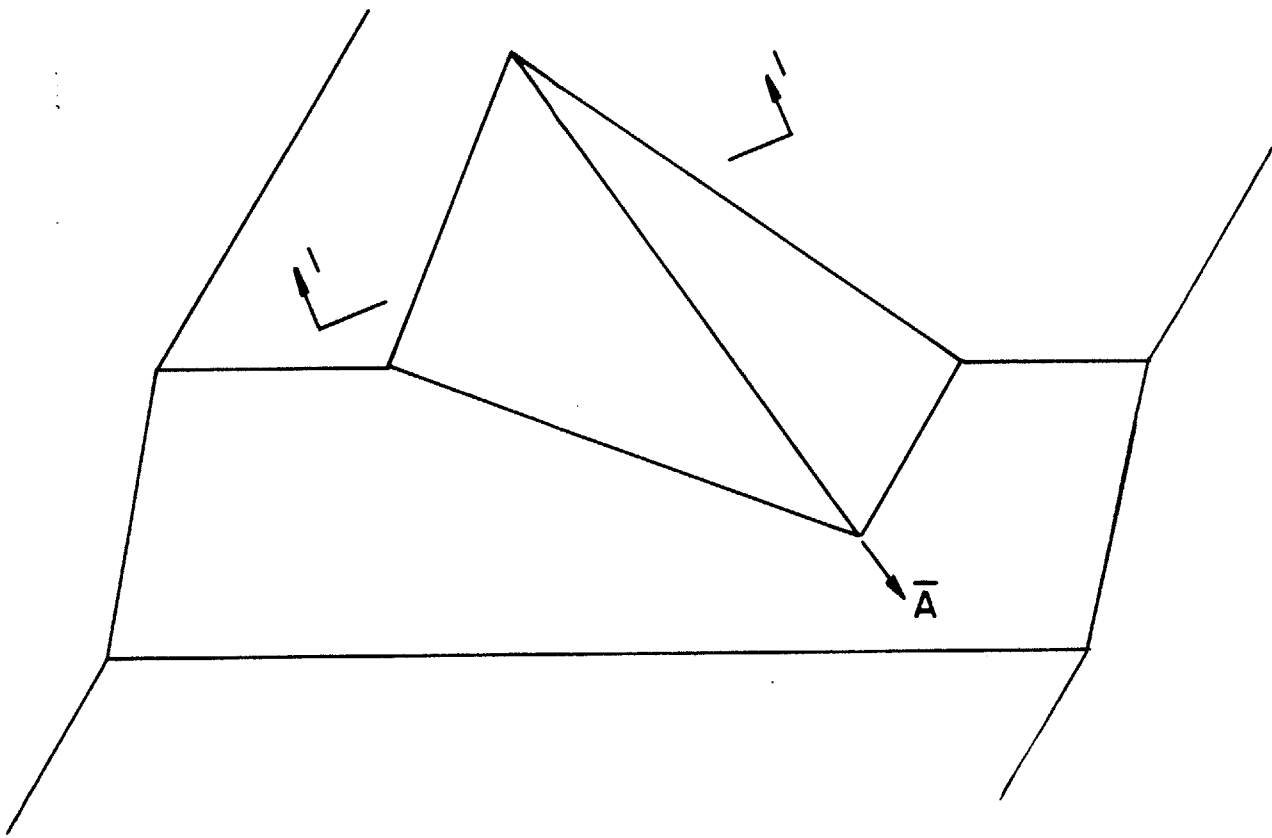
\bar{A} : LINE OF INTERSECTION

\bar{B} : $\bar{B} \perp \bar{A}$; $\bar{B} \perp Z$ AXIS

$$\bar{B} = \frac{\bar{A} \times (0,0,1)}{|\bar{A} \times (0,0,1)|}$$

$$\bar{C} = \bar{B} \times \bar{A}$$

Figure 4.32 A, B, C Coordinate System



SECTION 1-1 \perp \bar{A}

Figure 4.33 Cross Section Perpendicular to \bar{A}

$\bar{\Delta}$, the direction of impending motion, is composed of components along the A, B and C axes. Δ_B and Δ_C are related to δ_t and δ , the magnitude and direction of the displacement, in the generalized stiffness approach:

$$\Delta_B = \delta_t \sin \alpha \quad (4.58)$$

$$\Delta_C = -\delta_t \cos \alpha \quad (4.59)$$

In computing Δ_A , the program assumes that the shear stiffness in the direction parallel to the line of intersection is identical to the shear stiffness in the direction perpendicular to the line of intersection.* Thus,

$$\Delta_A = \frac{F_A}{A_1 K_{1s} + A_2 K_{2s}} \quad (4.60)$$

where F_A is the load component in the A direction

If the user selects the option wherein Δ is considered the displacement that would occur in response to a purely vertical load, the program computes the Δ_A , Δ_B and Δ_C that would occur under an imaginary vertical load of unity. (The imaginary load is not considered in the \bar{R} or \bar{D} computations.)

Appendix E contains a complete listing of SWARS-2PM as well as a user's manual.

* The program can easily be modified to accept two shear stiffness for each joint plane but such a refinement is probably unwarranted given the state of the art concerning the measurement of stiffness values.

4.6 Computer Program SWARS-2MC

SWARS-2MC is a modified version of SWARS-2PM that enables the user to determine the probability of failure (P_f) through Monte Carlo simulation. The program will compute the factor of safety for many sets of input parameters -- P_f is the proportion of FS values that fall below 1.0. Any (or all) of the parameters that define the shape and size of the wedge or characterize the shear resistance along the joint planes can be considered random variables. The values for these random variables should be selected in accordance with their respective probability density functions.*

SWARS-2PM and SWARS-2MC use precisely the same algorithms for computing the factor(s) of safety. There are, however, some differences in the manner in which information is input to the two programs. In particular, SWARS-2MC is designed so that its input parameters are compatible with the output from DAYLITE i.e., wedges are defined in terms of θ_o , ϕ_o , ψ and β_1 (Section 3.2.6). Thus, the conditional probabilities of ψ and β_1 calculated in DAYLITE can serve as a basis for Monte Carlo simulation.

Appendix F describes the features of SWARS-2MC and summarizes the differences between the SWARS-2MC and SWARS-2PM. Appendix F also contains a users' manual and program listing for SWARS-2MC.

* Section 2.2 reviews the principles of Monte Carlo simulation.

CHAPTER 5

INTERACTION BETWEEN DISCONTINUITIES AND INTACT ROCK--

COMPUTER PROGRAM JOINTSIM

5.0 Introduction

A typical rock mass is characterized by several sets of discontinuities. The spacings between discontinuities within each set vary; each discontinuity is a planar feature that consists of intact rock bridges as well as truly discontinuous zones. Traditional slope stability analyses are performed by examining the stability of bodies that are bounded by planes that are oriented in the mean direction of each set of discontinuities (Figure 5.1). Persistence* and (to a lesser extent) spacing are considered by assigning different cohesion and friction parameters to the intact and discontinuous portions of the discontinuity plane as proposed by Jennings (1970). The real failure surface may actually have the shape shown in Figure 5.1 or an "en echelon" shape as shown in Figure 5.3. The failure surface forms along the path of minimum resistance. Clearly the interaction between discontinuities and intact rock plays a major role. The "intact portions" of the failure surface usually control its shape and location because of the high resistance of intact rock. Traditional slope stability analyses recognize this fact and frequently assign persistences of 100% to the failure planes to be conservative. Such an approach is

* Persistence of a joint plane is defined in Figure 5.2.

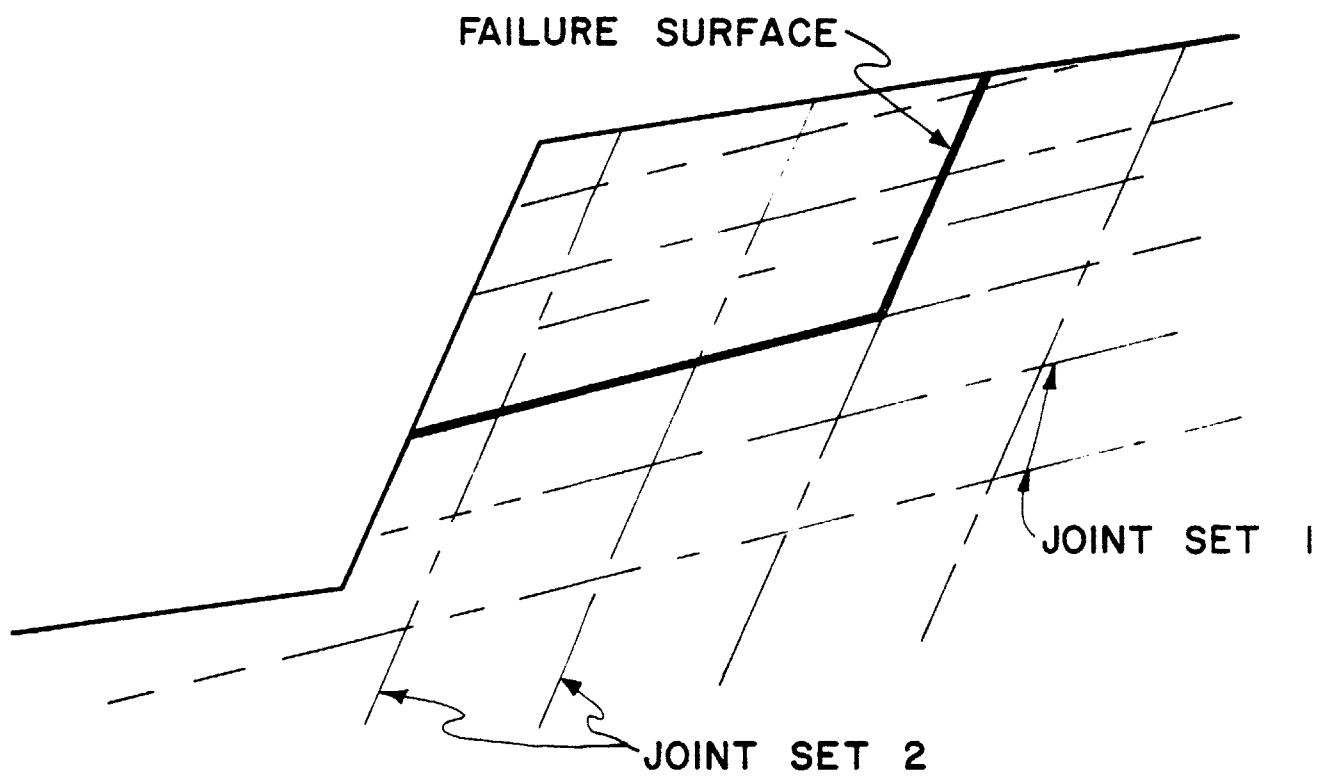
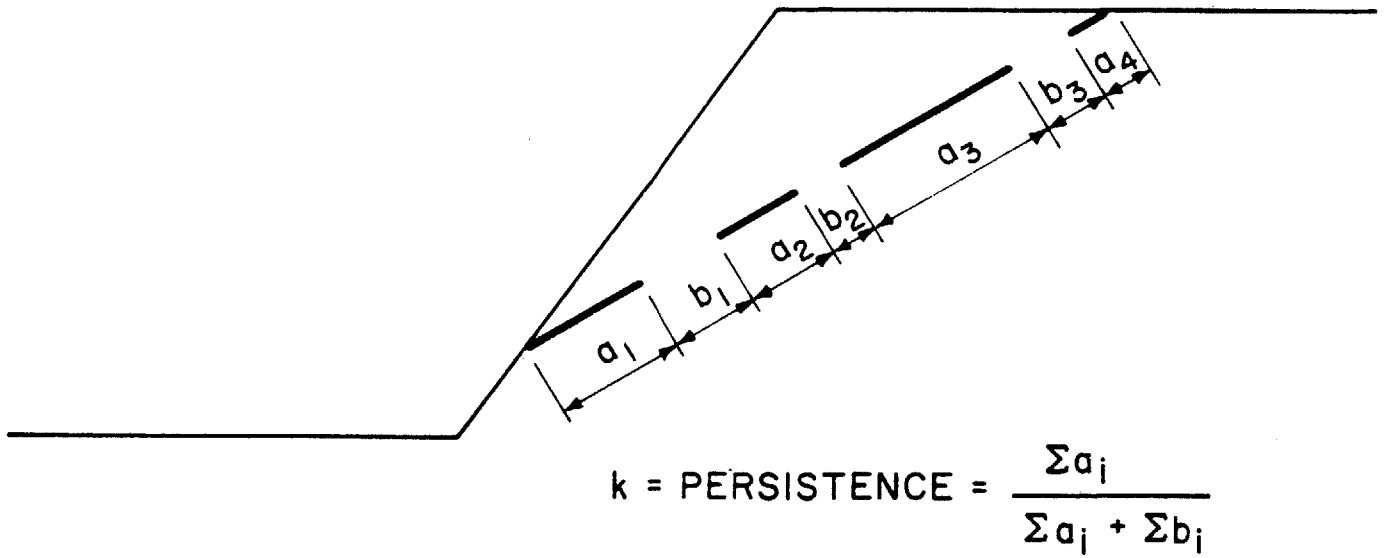


Figure 5.1 Typical Failure Surface



$$c_a = (1 - k)c_r + (k)c_j$$

$$\tan \phi_a = (1 - k)\tan \phi_r + (k)\tan \phi_j$$

Figure 5.2 Persistence--Jennings' Relations

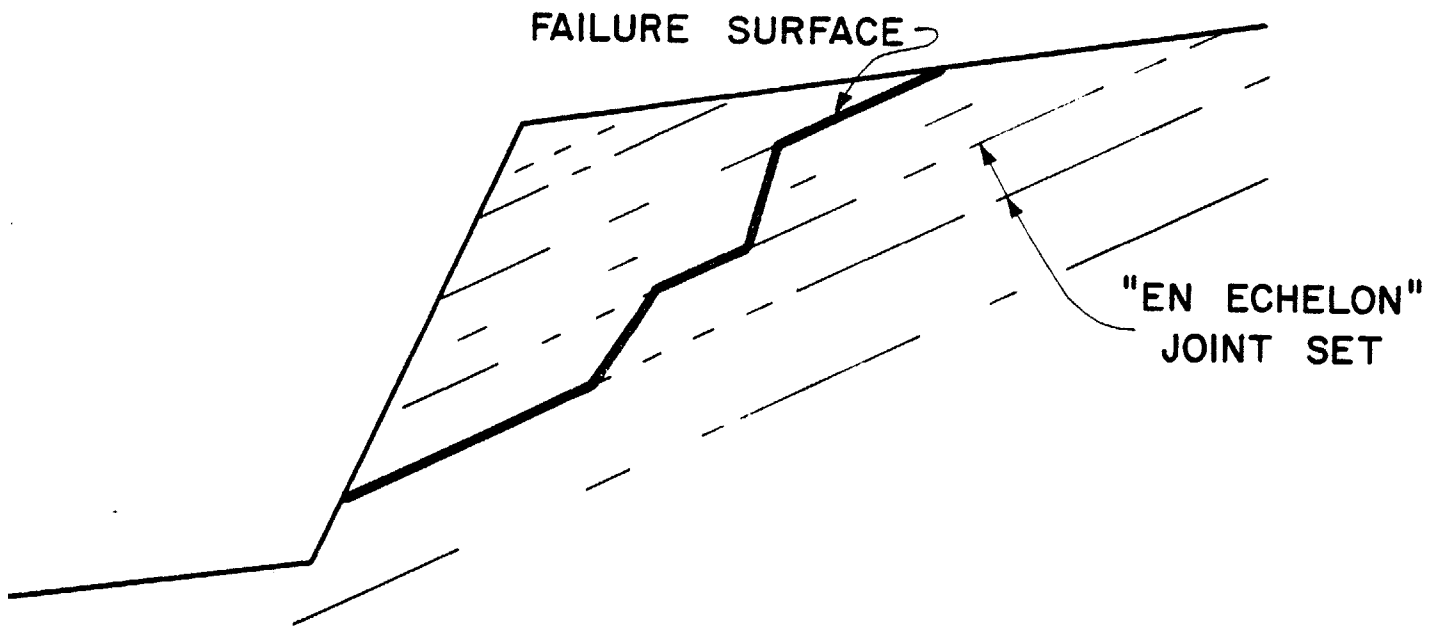


Figure 5.3 "En Echelon" Failure Surface

overly conservative and frequently uneconomical. However, it is the only rational procedure because information on persistence is seldom available. Even if information on persistence were available it would have only limited value because the persistence of the various possible "en echelon" failure surfaces would remain unknown. The inability of deterministic approaches to treat the interaction between intact rock and discontinuities is a major weakness in traditional rock slope stability analysis. This interaction must be rationally incorporated into any model that attempts to simulate the real behavior of rock slopes. The probabilistic approach that will be presented in this chapter can treat the discontinuity-intact rock interaction in a satisfactory manner.

5.1 General Features--Probabilistic Approach to Resistance of Jointed Rock

The rock mass under consideration is analyzed by first simulating joint geometries from a stochastic model. The geometries represent a distribution of joint patterns that might occur in a particular rock mass. Each geometric realization has many possible failure surfaces. The resistances of the various failure surfaces to a standard loading sequence are computed and the minimum resistance is determined. The minimum resistance characterizes that particular realization of joints. By repeating this operation for many simulated joint networks one can estimate the probability of

distribution of minimum resistance and hence, the probability of failure.

Specifically, each simulation generates a single set of parallel discontinuities with intact and discontinuous portions (Figure 5.4). The spacing and the persistence of the discontinuities are random variables. The jointing patterns are simulated through the stochastic model described in Section 5.2. The distribution of minimum resistance is found by analyzing each pattern with the mechanical model described in Section 5.3. These resistance distributions can then be expressed as distributions of strength parameters e.g. cohesion and friction in a Mohr-Coulomb expression.

5.2 Stochastic Model of Joint Geometry

The network of discontinuities is idealized as a Poisson process of planes in space. The abstract mathematical process was conceived and refined by a number of individuals over the past fifteen years (Matheron, 1975; Miles, 1964, 1969, 1971, 1972; Switzer, 1965). Veneziano (19xx) adapted it to simulate rock jointing and used it to derive other properties of geotechnical significance.

Discontinuities and particularly joints within a rock mass are generated through a three step sequence of random operations. The primary process generates Poisson planes which are taken to represent joint planes (Figure 5.5). The

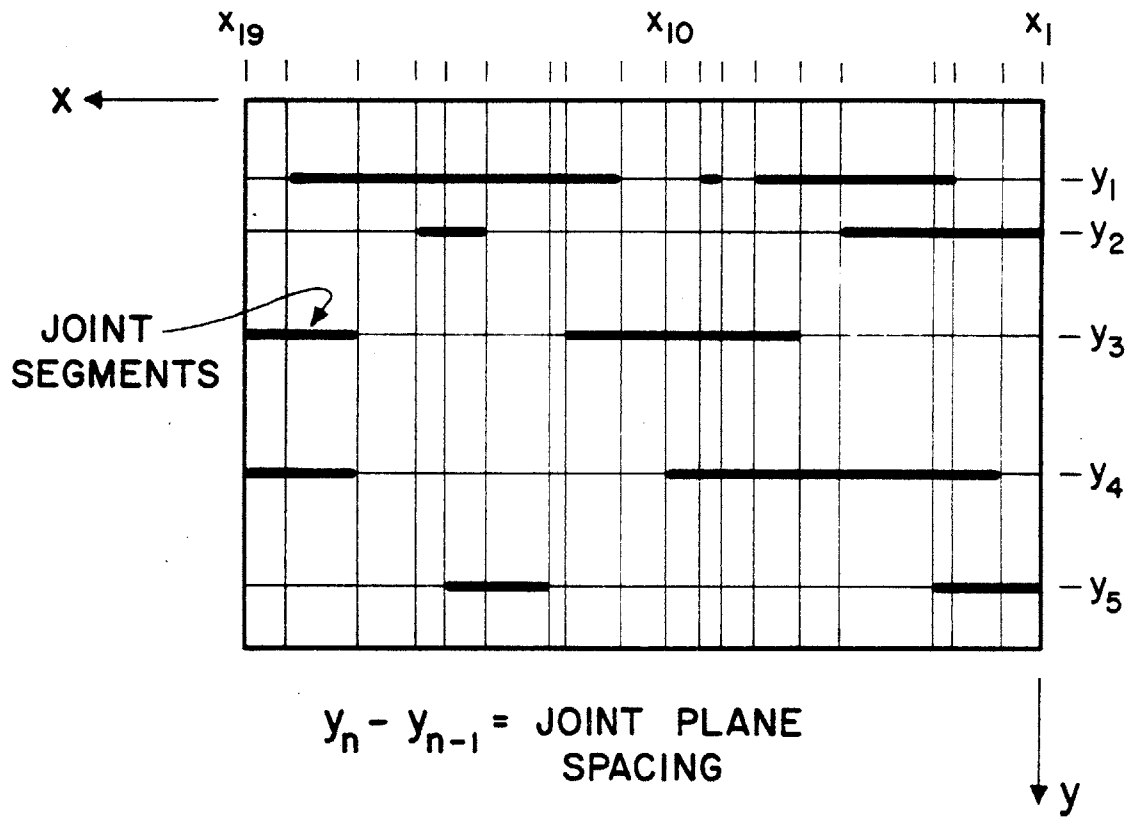


Figure 5.4 Coordinate System and Typical Jointing Pattern

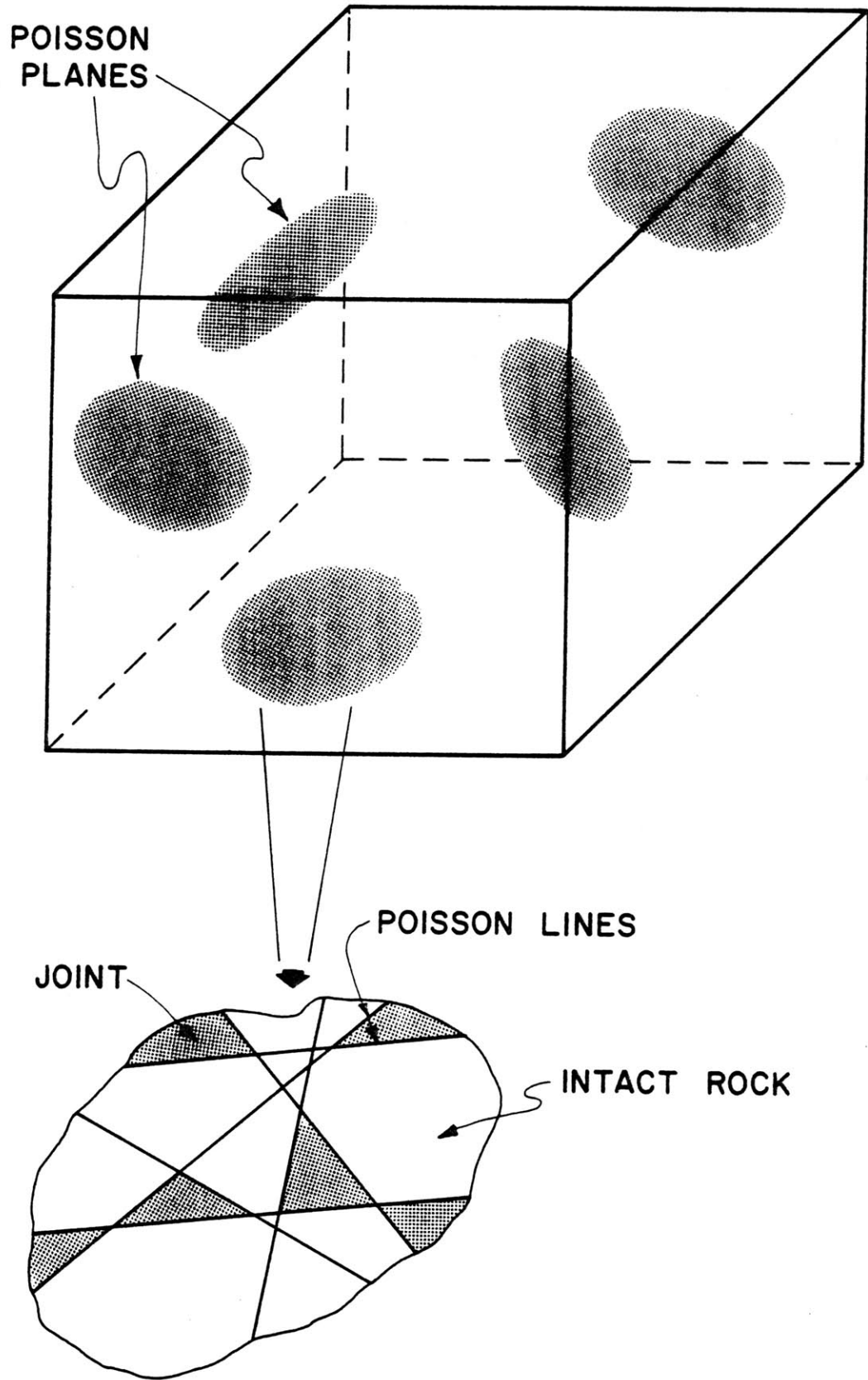


Figure 5.5 Stochastic Model of Joint Geometry
186

secondary process partitions each plane into random polygons by a family of Poisson lines. The tertiary process shades (or colors) a certain proportion of these figures. Shaded polygons represent joints while the remaining portions of the plane represent intact rock.

Primary Process

The stochastic model treats joint planes as Poisson flats in R^3 , the three dimensional space that corresponds to the rock mass. Let X_1 , X_2 and X_3 be orthogonal axes in R^3 that meet at point 0. Any arbitrary plane in R^3 can be expressed as an equation of the form:

$$X_1 \sin \psi_i \cos \Omega_i + X_2 \sin \psi_i \sin \Omega_i + X_3 \cos \psi_i = d_i \quad (5.1)$$

As shown in Figure 5.6, d_i represents the signed distance from the plane to the origin while ψ_i and Ω_i are orientation angles.

$$-\infty < d_i < \infty$$

$$0 \leq \psi_i \leq \pi$$

$$0 \leq \Omega_i \leq \pi$$

Each plane in R^3 is characterized by a unique set of parameters (d_i, ψ_i, Ω_i) .

If the d_i 's are marked on the real line (the R^1 space) the resulting point process (Figure 5.7) is Poisson with constant intensity $1/\rho_3$ where ρ_3 is the mean distance between neighboring points.

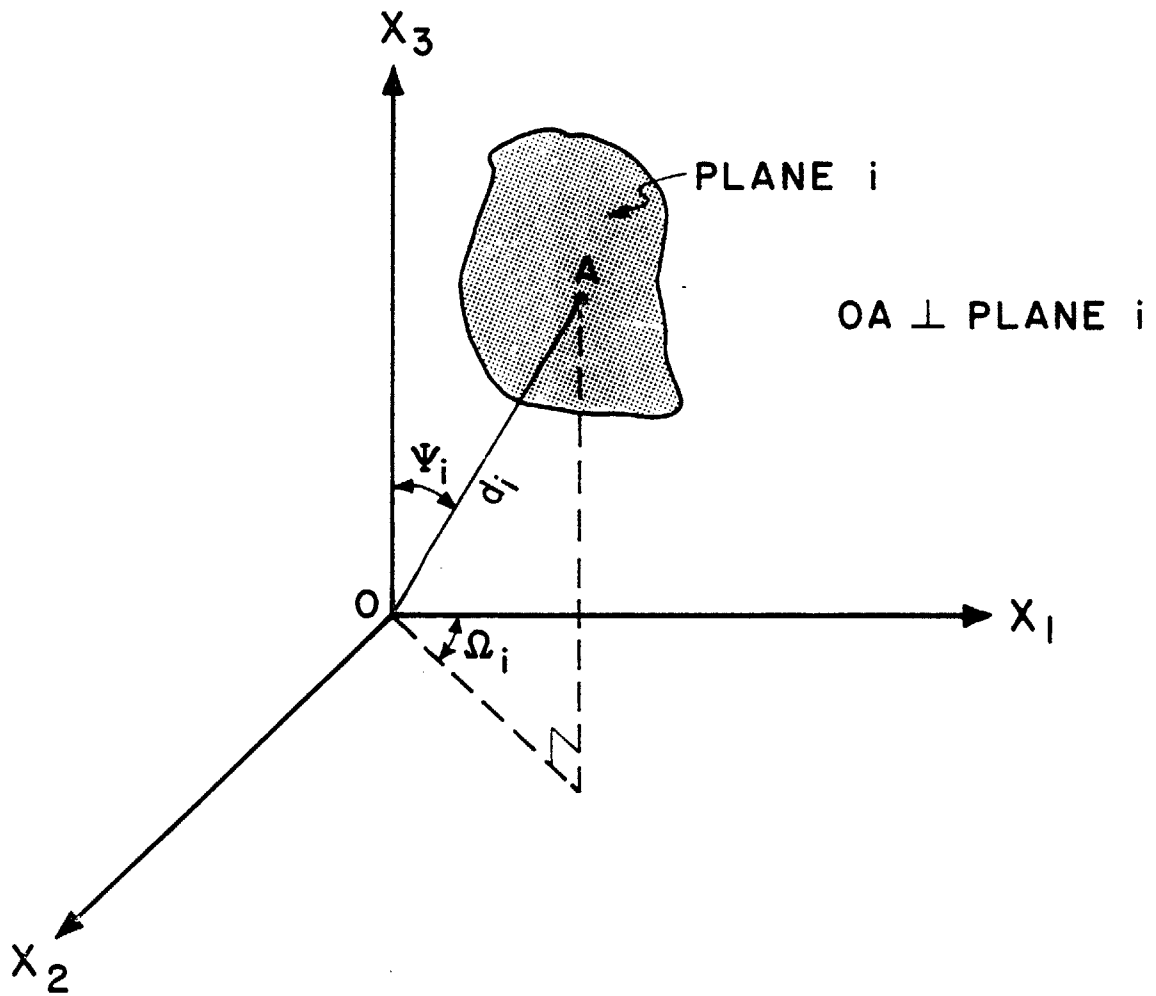
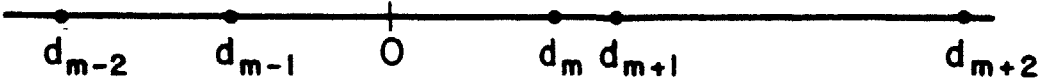


Figure 5.6 Definitions of ψ_i , Ω_i , and d_i

R^1 Space



R^2 Space

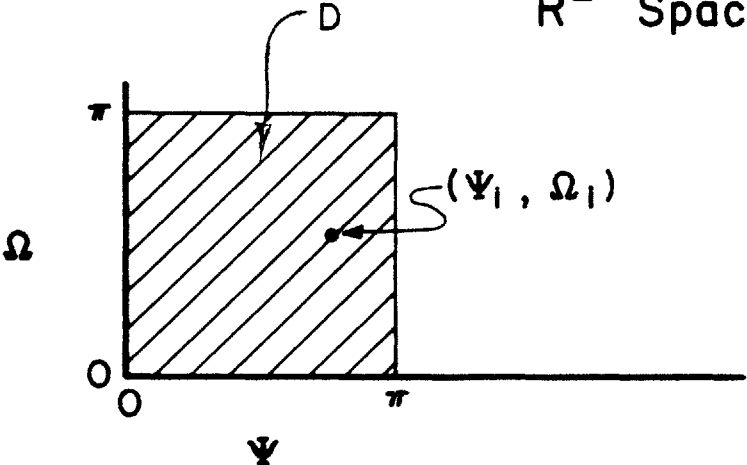


Figure 5.7 Stochastic Model--Primary Process-- R^1 and R^2 Spaces

In a similar manner, the pair of orientation angles can be mapped in D , a square region of the real plane (the R^2 space), as shown in Figure 5.7. Each point in the region represents a unique orientation.

The plane region D can be combined with the real line R^1 to form P^3 , a cylinder in R^3 (Figure 5.8). Miles (1972) showed that homogeneous Poisson networks in R^3 can be generated from Poisson point processes in P^3 . Homogeneity implies that the process is invariant with respect to translation of the origin.

Secondary Process

The Poisson process of lines on each joint plane is similar to the Poisson process of planes in R^3 . Figure 5.9 shows a typical joint plane that has been partitioned by a family of Poisson lines. Let Y_1 and Y_2 be orthogonal axes that meet at O' . Any line in the plane can be expressed as a linear equation:

$$Y_1 \cos \Gamma_i + Y_2 \sin \Gamma_i = f_i \quad (5.2)$$

The distance f_i and the angle Γ_i are shown in Figure 5.9.

$$-\infty < f_i < \infty$$

$$0 \leq \Gamma_i \leq \pi$$

Each line is identified by a unique pair of parameters (f_i, Γ_i) . The ordered sequence

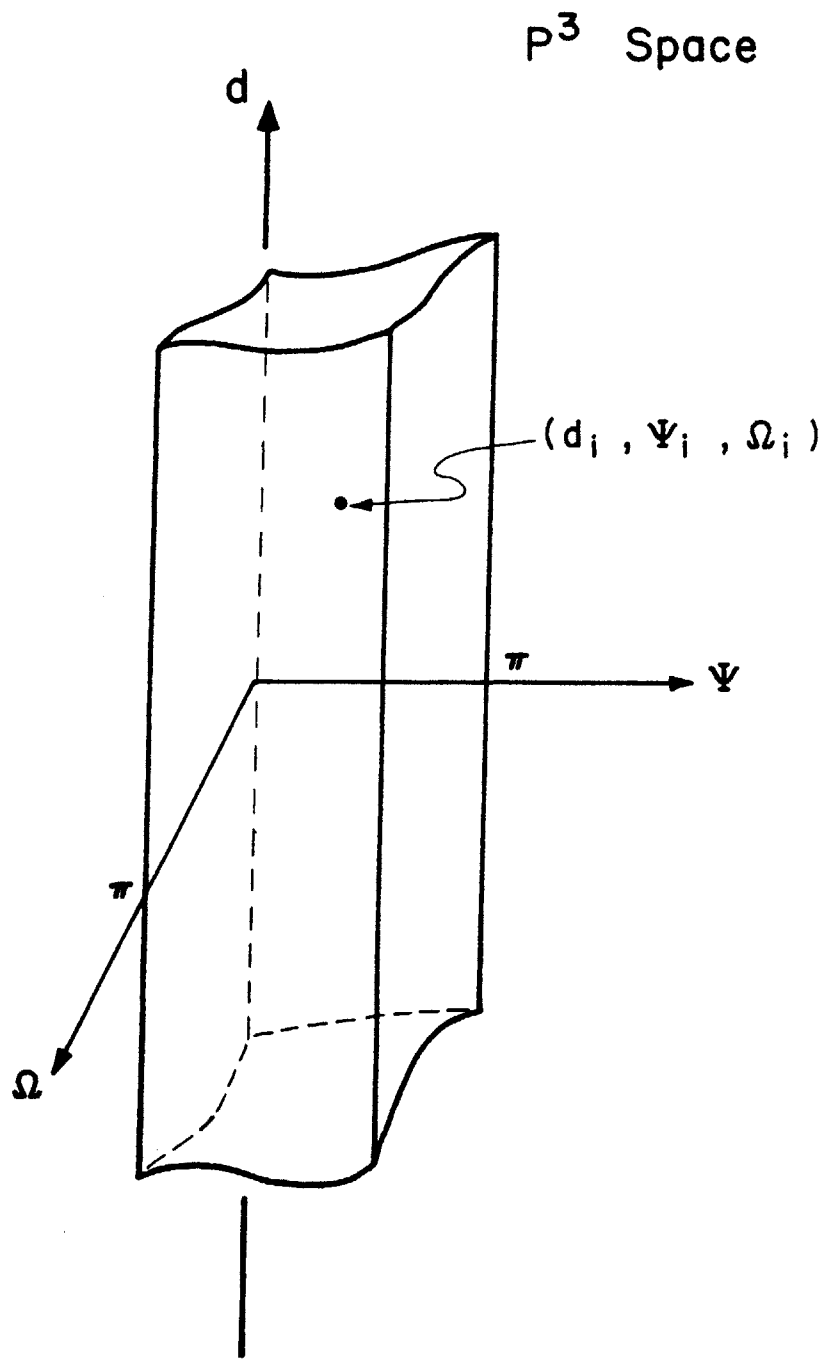


Figure 5.8 Stochastic Model--Primary Process-- P^3 Space

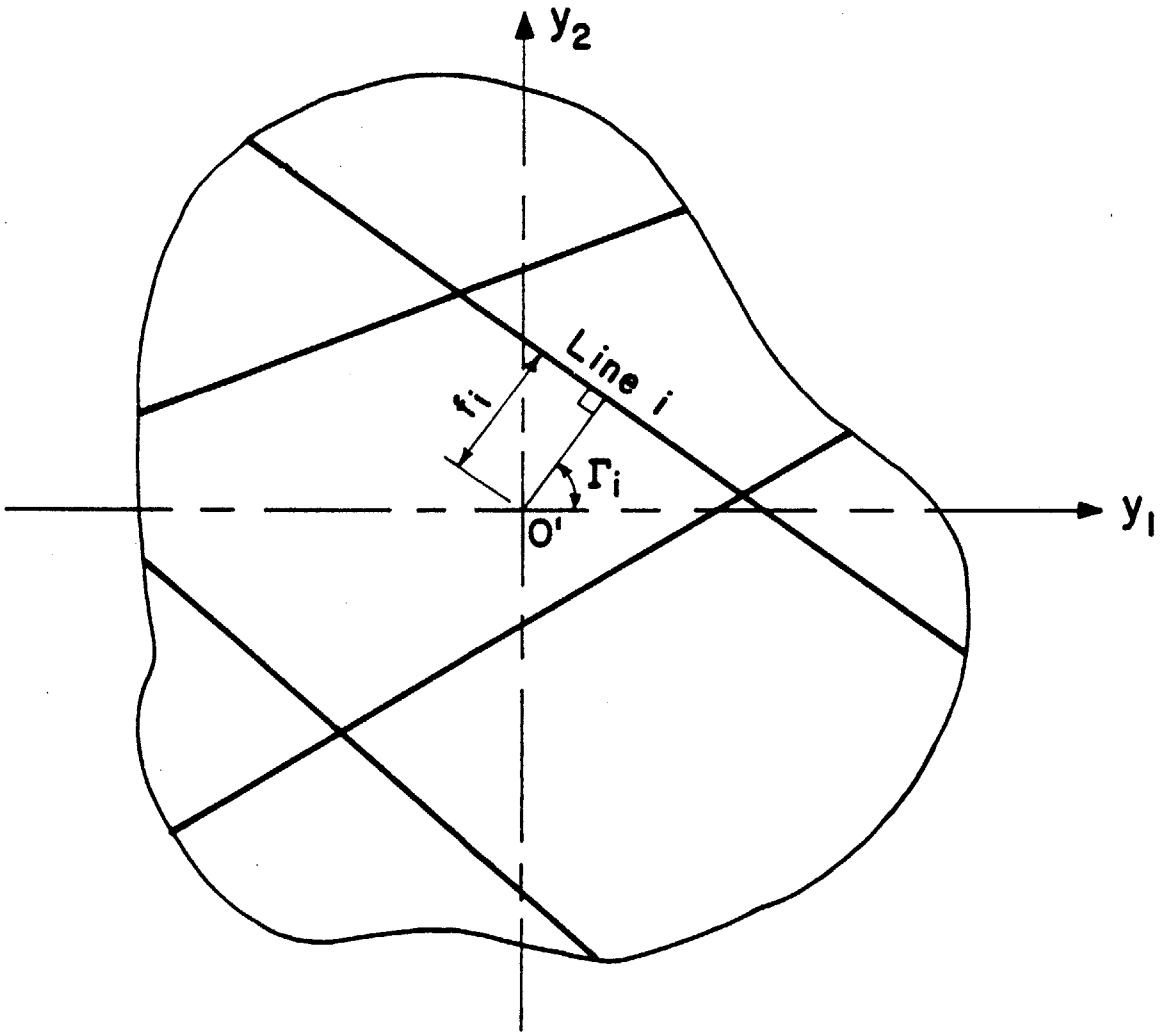


Figure 5.9 Definitions of f_i and Γ_i

$$\dots f_{m-2} < f_{m-1} < f_m < f_{m+1} < f_{m+2} \dots$$

corresponds to a Poisson process of points along the R^1 space with intensity $1/\rho_2$ (Figure 5.10). The distances between neighboring points are exponentially distributed with mean value ρ_2 . The points (f_i, Γ_i) constitute a Poisson process of points within the infinite rectangle shown in Figure 5.10. If Γ is uniformly distributed over the interval $0 \leq \Gamma \leq \pi$ the Poisson process has a constant density, $\frac{1}{\rho_2 \pi}$

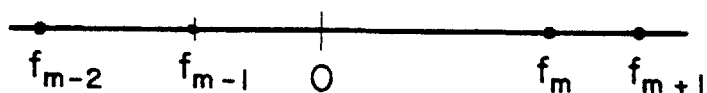
Miles (1964) studied the associated isotropic process of Poisson lines on the plane and developed a number of useful relationships. In particular, he found that:

1. The expected number of intersections between Poisson lines per unit area is $\frac{1}{\pi(\rho_2)^2}$
2. The intersections between any arbitrary line and the Poisson lines constitute a Poisson process with constant intensity $\frac{2}{\rho_2 \pi}$,
3. The angles of intersection (Figure 5.11) are independently distributed with identical pdf's:

$$f_A(a) = \frac{1}{2} \sin a \quad 0 \leq a \leq \pi \quad (5.3)$$

The process may not be isotropic. Anisotropy can be treated in a fairly straightforward manner. It involves cases where the pdf for Γ is non-uniform. Miles (1964) considered this case and developed some expressions similar to those for the isotropic case.

R^1 Space



R^2 Space

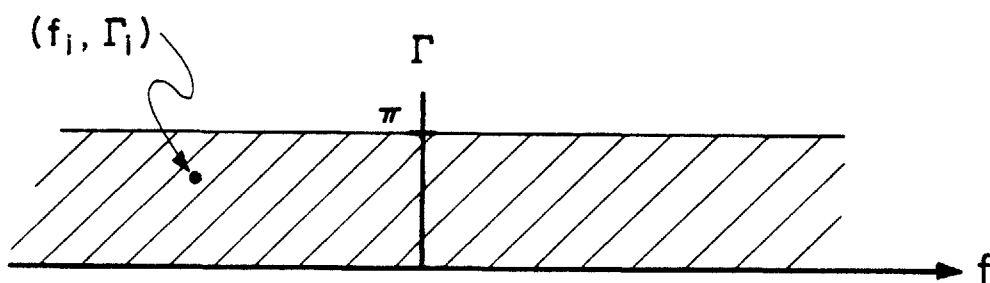


Figure 5.10 Stochastic Model--Secondary Process-- R^1 and R^2 Spaces

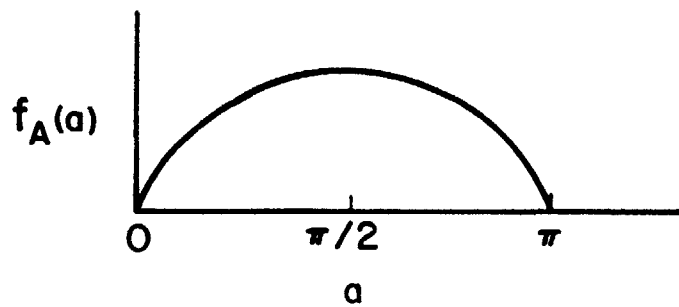
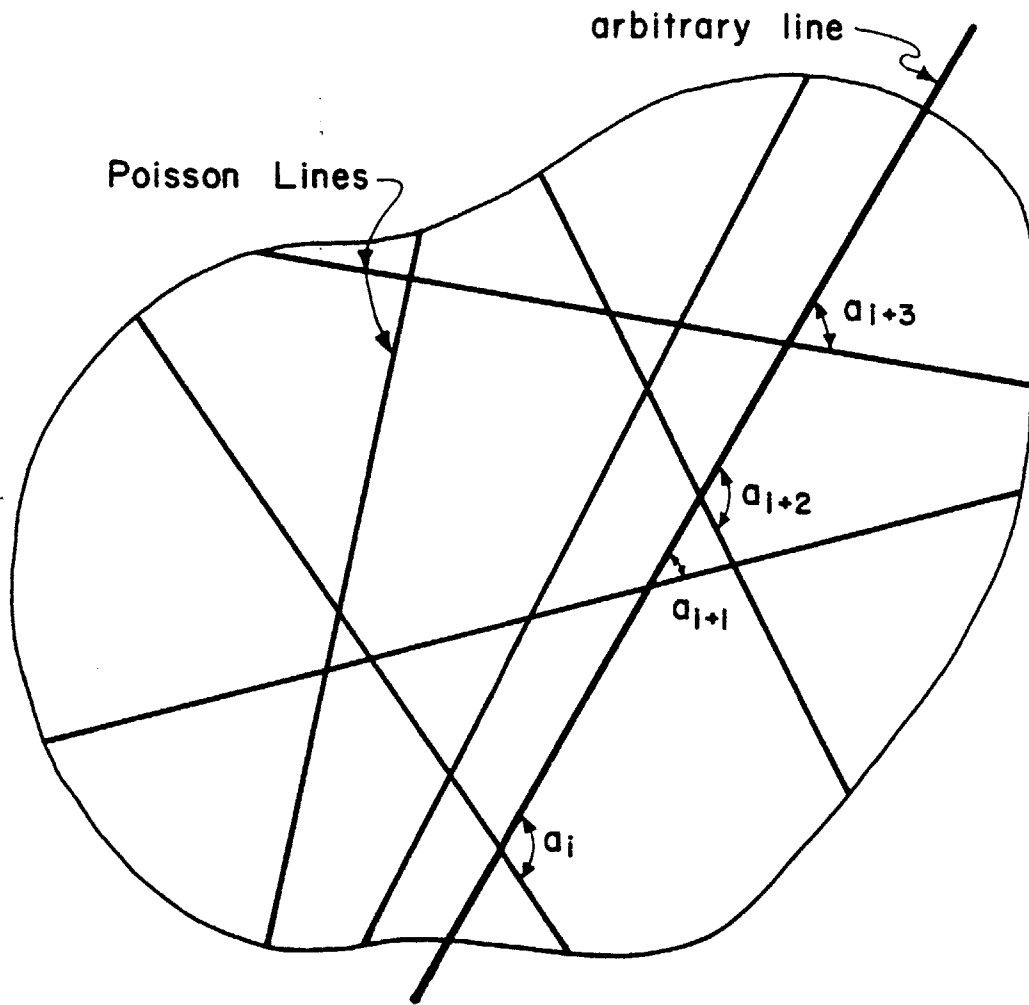


Figure 5.11 Angles of Intersection Between Poisson Lines
and an Arbitrary Line
195

Tertiary Process

The last operation involves the shading or "jointing" of individual polygons. The probability of shading has a constant value (p) and the shading operation is performed independently on each polygon i.e., the fact the one polygon is shaded does not affect the probability that an adjacent polygon will be shaded. Switzer (1965) has shown that the resulting binary random field has Markovian properties along straight lines.

Figure 5.12 shows a typical realization on a joint plane. The arbitrary line A-A' intersects numerous Poisson lines and traverses both shaded and unshaded regions. As mentioned earlier, the distance between consecutive intersections is exponentially distributed with mean value $\frac{\rho_2 \pi}{2}$. However, only those intersections that involve a transition between jointed and unjointed polygons have practical significance. For example, the polygons "G" and "H" in Figure 5.12 are both shaded so that the aggregate joint length along A-A' extends from point m to point n. Thus, the shading probability can be considered a "random selection" parameter for the Poisson polygons so that only those intersections involving color transitions are observed. Therefore, the mean values for jointed and unjointed lengths become

$$\delta_j = \frac{\rho_2 \pi}{2(1-p)} \quad (5.4)$$

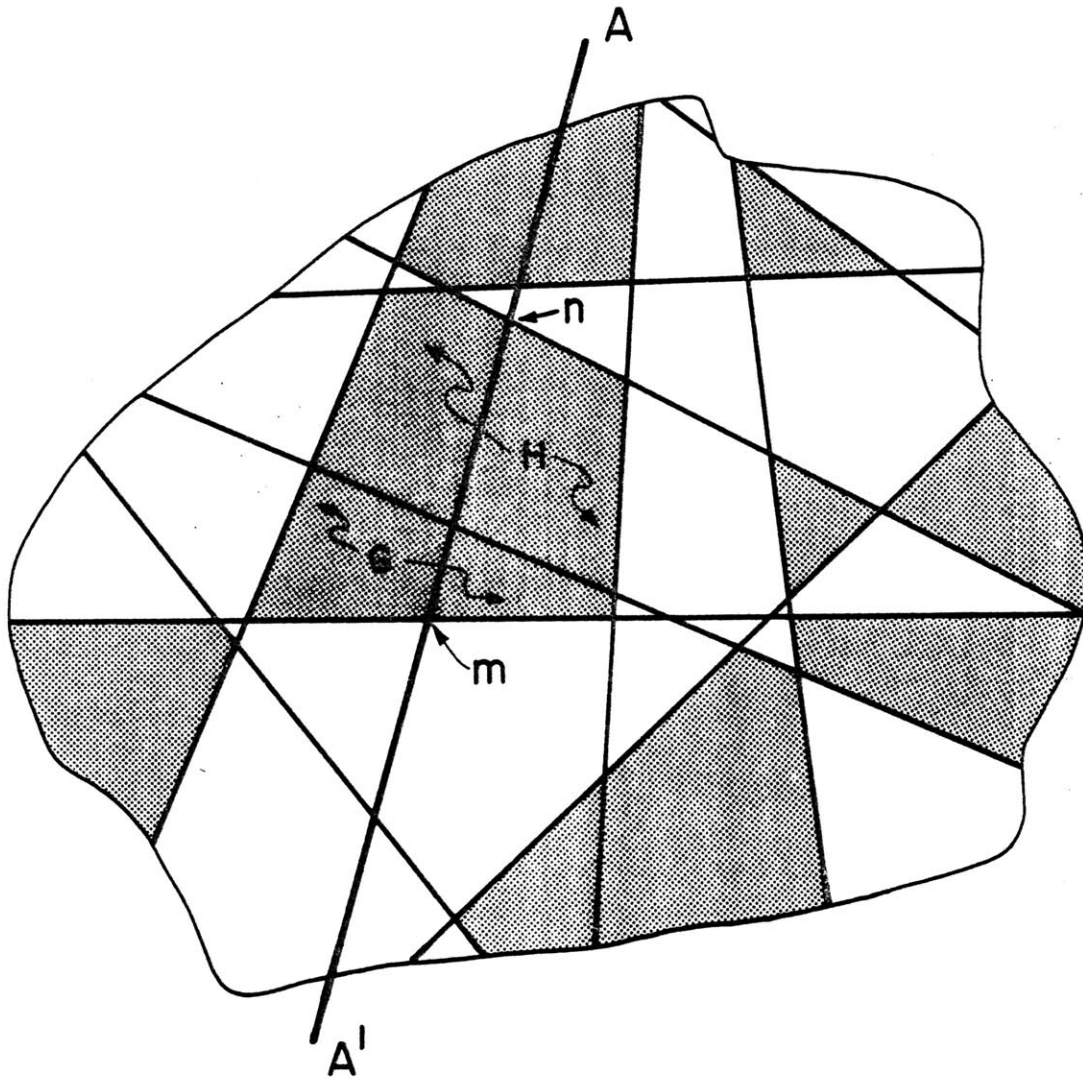


Figure 5.12 Length of Joint Segment (Secondary and Tertiary Processes)

$$\text{and } \delta_r = \frac{\rho 2\pi}{2p} \text{ respectively, where } p \text{ is} \quad (5.5)$$

the shading probability of each polygon.

The stochastic model for joint geometry consists of the three processes just described. Thus, in its most general form, the model has five sets of input parameters: two density parameters (one of Poisson planes in space, the other of Poisson lines in each joint plane), two probability distributions (one of the orientation of planes and the other of the orientation of lines), and the shading probability. The parameters need not be constant; for example, the density of lines and the shading probability may depend upon the orientation of the joint plane. The same parameters may be uncertain and probabilistically dependent.

"En Echelon" Joints

The number of variables can be reduced if one concentrates on the problem of "en echelon" jointing. Since joint planes are assumed to be parallel and to have a known orientation their orientation distribution becomes trivial and the density parameter of planes is simply $1/\lambda$ where λ is the mean spacing between planes. In addition, $1/\rho$, the density of lines in a plane, is assumed the same for all planes and the distribution of line orientations is considered uniform. Under these assumptions the model requires three scalar parameters: λ , ρ and p .

Figure 5.4 is a cross-section through a hypothetical rock mass whose jointing patterns can be generated by the model

just described. On a cross-section perpendicular to the joint planes (like Figure 5.4), the planes are exponentially distributed with mean value λ . The jointed and unjointed segments within each plane have identical independent exponential distributions with mean values $\delta_j = \frac{\rho\pi}{2(1-p)}$ and $\delta_r = \frac{\rho\pi}{2p}$, respectively.

5.3 Mechanical Model

An analytical method has been developed to evaluate the strength of a rock mass containing "en echelon" joints. Input parameters include the ambient stress field and the strength characteristics of both the intact rock and of the joints, as well as the joint network simulation.

Path of Minimum Resistance

Figure 5.4 can be considered a typical example of the joints in one realization. The objective is to find the path of minimum resistance for all possible failure paths which proceed from the left boundary upwards across the jointed mass and reach the right boundary. Hence paths A, B, and C in Figure 5.13 are acceptable failure routes whereas D and E are not. Continuous paths along joint planes (such as A in Figure 5.13) constitute one obvious and relatively small family of failure paths. Routes that involve transitions between planes (such as B and C) comprise a much larger family.

The critical path is found by means of dynamic programming. Each jointing pattern is characterized by a grid formed

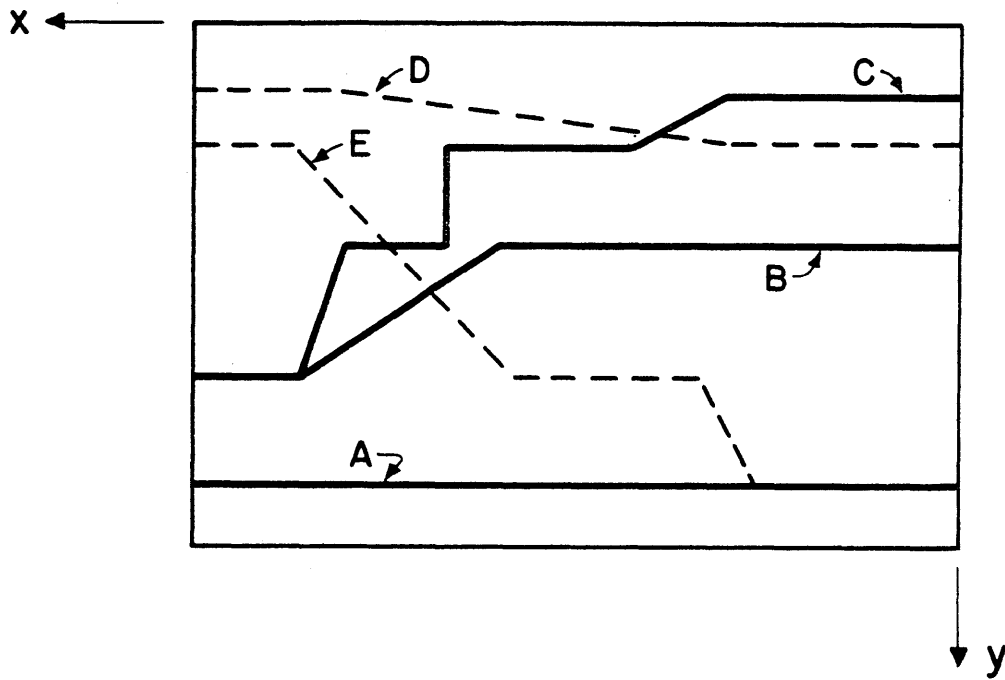
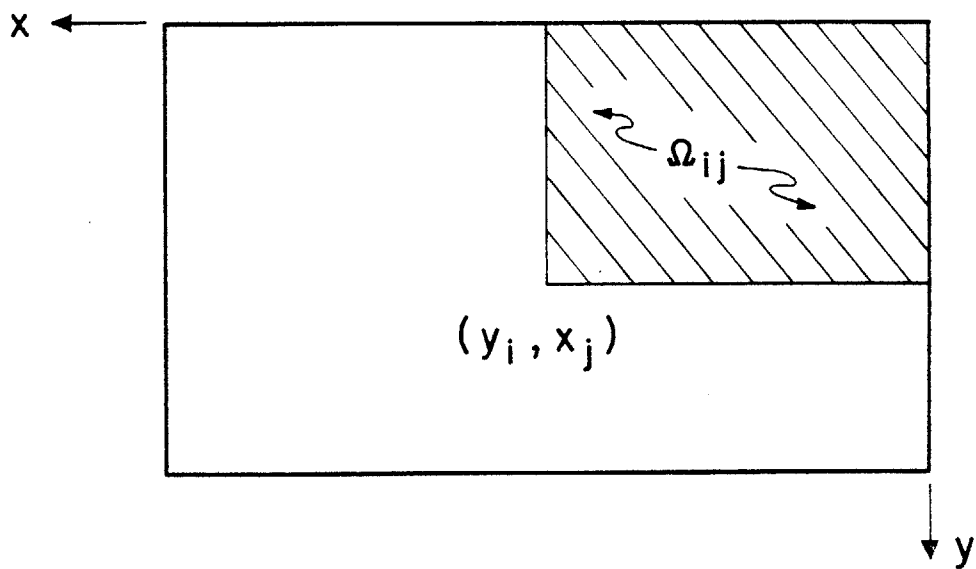


Figure 5.13 Typical Failure Paths

by pairing all possible combinations of x and y where the y 's are the coordinates of the joint planes and the x 's are the coordinates of all tips of joint segments (Figure 5.4). The grid points represent possible junction points for failure paths between joint sections on one plane and between planes (see Figure 5.4). Transitions always occur from (x_i, y_i) to (x_j, y_j) such that $x_i \geq x_j$ and $y_i \geq y_j$. In order to identify the critical path each point is examined to find the minimum strength path between that point and the right boundary of the jointed mass. The analysis begins at the upper right corner. The first point, $x = x_1 = 0$ and $y = y_1$ has zero strength because it lies on the right boundary. The algorithm proceeds to check all the points along the top row where $y = y_1$ and then examines progressively higher y 's always working from right to left along the rows. For each point all paths through grid points above and to the right are screened. In effect, the program constructs a resistance matrix, \underline{R} , of order n by m where n is the number of planes and m is the total number of joint tips. The (i,j) th element, $R_{i,j}$, is the resistance of the upper right portion of the rock mass, $\Omega_{i,j}$, with respect to (i,j) given that the failure route passes through (i,j) and terminates somewhere along the right edge (Figure 5.14). Once all the coefficients in the matrix \underline{R} have been evaluated, the minimum resistance R , can be found:

$$R = \min R_{i,m} \text{ for } i = 1, n \quad (5.6)$$



$R_{i,j}$ = minimum resistance of block $\Omega_{i,j}$

Figure 5.14 Principle of Minimum Resistance

Strength Derivation

The strength of the material between grid points is calculated using a Griffith-Modified Griffith envelope for the intact rock and a linear Mohr-Coulomb envelope for the joints. The Griffith-Modified Griffith envelope is parabolic in the tensile range and linear in the compressive range (Figure 5.15C). It is completely defined by two parameters: σ_t , the tensile strength of the rock, and ϕ_r , the friction angle. The Griffith-Modified Griffith envelope defines the critical stresses for crack initiation and thus gives a lower bound to the resistance of intact rock. An upper bound would be defined by the stress conditions which characterize complete failure with cracks propagating through the entire specimen. The most appropriate envelope for the problem under study may be one between these two extremes; however, the lower bound was chosen as a realistic albeit conservative estimate of resistance.

The details of the resistance determination and particularly the analytical formulations are presented in Appendix G. Figure 5.15 summarizes the resistance determination for failure through intact rock. The jointing pattern and the orientation of the joints relative to the initial state of stress are shown in Figure 5.15A. (In general, the joints are not parallel to either of the principal stress axes.) The objective is to find the resistance which must be overcome to

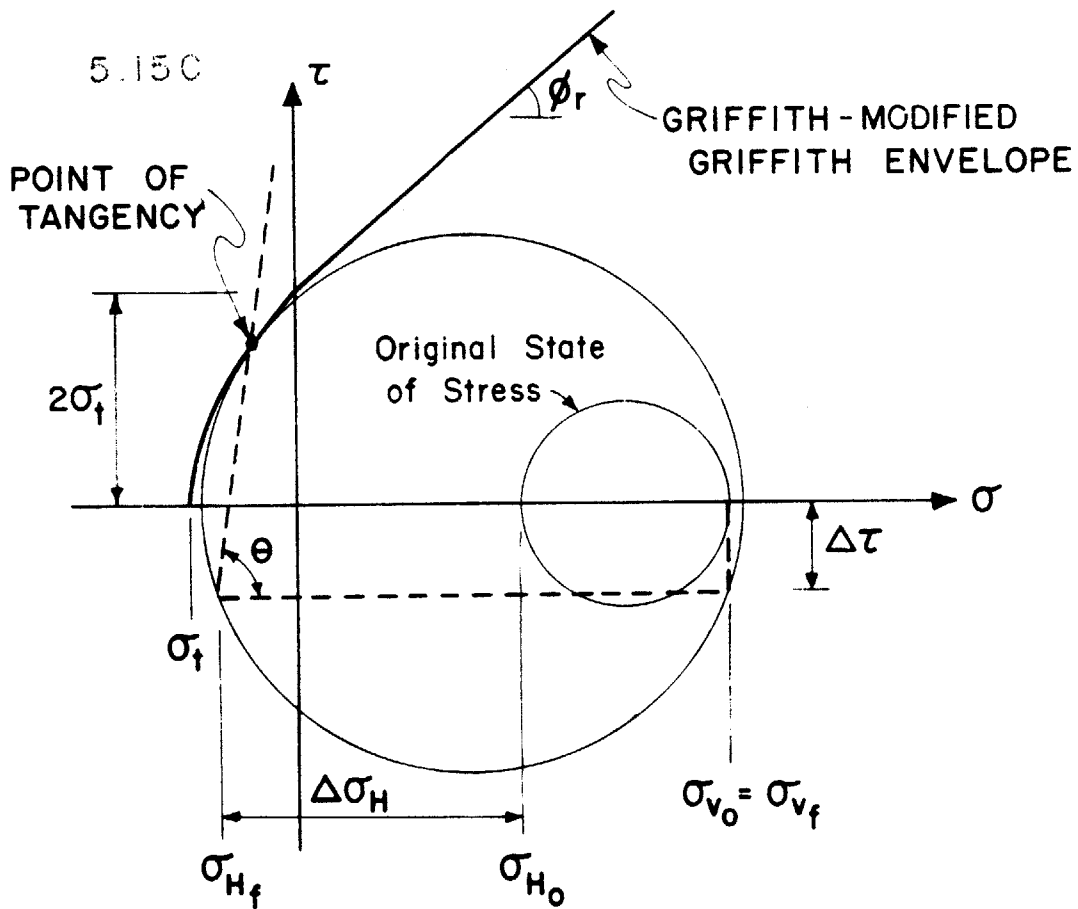
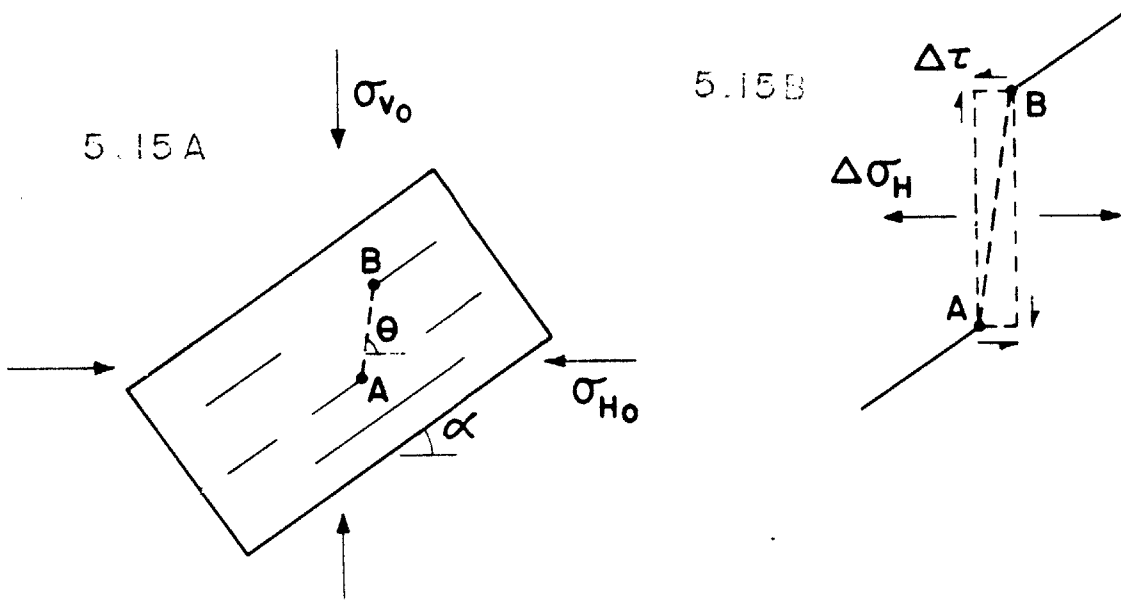


Figure 5.15 Strength Determination--Path Through Intact Rock
204

create a failure path from point A to point B. This path will eventually be combined with other segments to form failure routes through the entire "rock mass". Figure 5.15B is a more detailed illustration of the region near points A and B. The rectangular area bounded by the dashed lines represents a small mass of intact rock about to undergo failure. The prescribed failure path (A to B) has a definite orientation with respect to the stress field. The additional stresses required to cause failure must be applied in such a manner that failure occurs along A-B (Figure 5.15B). Specifically, the Mohr circle for the state of stress at failure must be tangent to the Griffith-Modified Griffith envelope at a point such that the failure plane develops in the direction A-B. The critical stress condition is obtained by superimposing upon the ambient stress field both negative horizontal stresses ($\Delta\sigma_h$) and shear stresses ($\Delta\tau$) in the horizontal and vertical planes (Figure 5.15B). Intact rock will generally undergo tensile failure in the stress ranges normally encountered in engineering practice.

If the two points under consideration lie in the same joint segment the strength computation is somewhat simpler (Figure 5.16). Failure along a joint (C to D) occurs when one of the points of intersection between the Mohr circle and the failure envelope is the point that represents the state of stress at the orientation of the joint. In general, the initial horizontal stress will be reduced through the

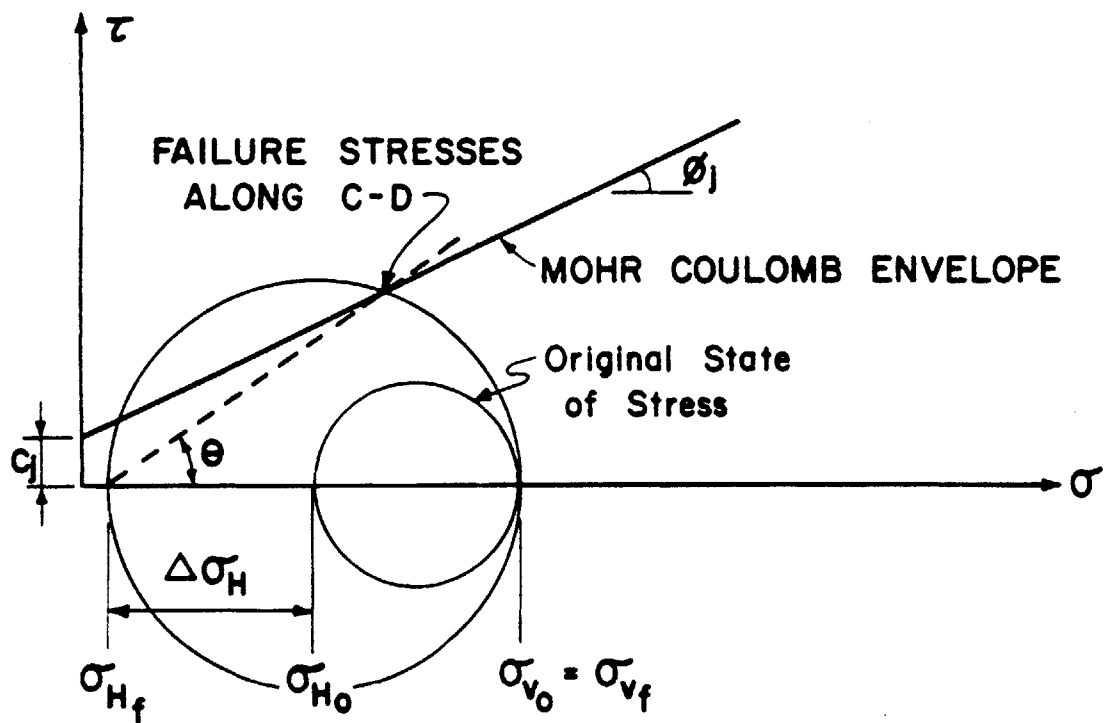
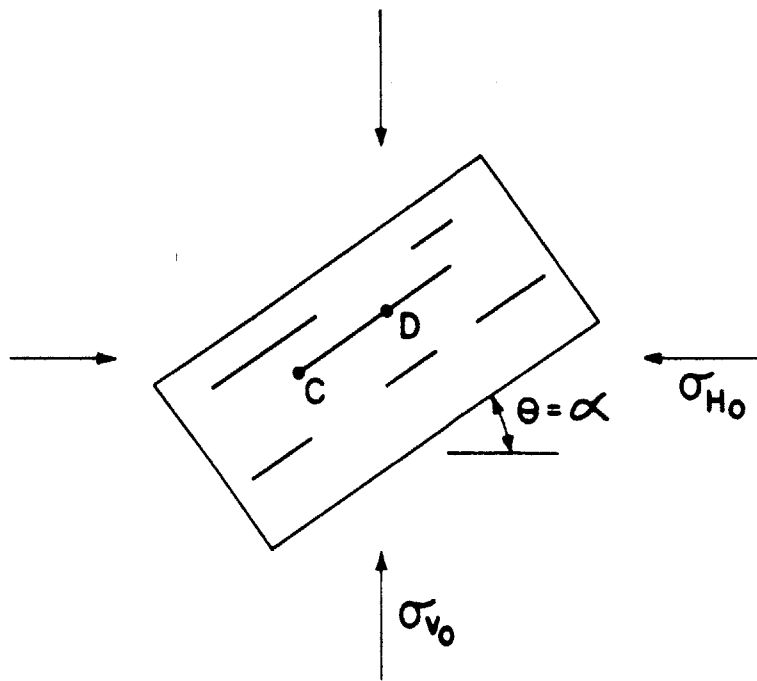


Figure 5.16 Strength Determination--Path Along Joint Segment
206

application of a negative horizontal stress ($\Delta\sigma_h$) in order to produce these failure conditions.

Once the strength of segments such as A-B and C-D have been calculated they are combined to determine the resistance for composite paths. The primary concern of the entire analysis is to find the composite path with the minimum strength. The strengths for individual path segments are combined by transforming the superimposed stresses into force components parallel and perpendicular to the orientation of the joint planes. Forces in the same direction are added to yield two aggregate forces: S (parallel to the joint plane) and N (perpendicular to the joint plane). Finally, S and N are combined to give the Apparent Resistance, AR, where,

$$AR = S + N(\tan \phi_j) \quad (5.7)$$

The path with the minimum AR is the critical one. In essence, the resistance of a failure path (not necessarily coplanar with one of the joint planes) is characterized by the shear force which must be applied in the direction of the joint planes to cause failure.

Apparent Persistence

The minimum AR of a jointed rock mass is not a particularly useful parameter for engineering calculations. A better way to express the results is in terms of apparent strength

parameters. Jennings (1970) proposed that a planar failure surface involving both intact rock and joints be treated as if it were composed of a single hypothetical material with an apparent cohesion, c_a , and an apparent friction angle, ϕ_a . Jennings' relations can be modified to yield the following expressions:

$$c_a = (1 - k)c_r + (k)c_j \quad (5.8)$$

$$\tan \phi_a = (1 - k)\tan \phi_r + (k)\tan \phi_j \quad (5.9)$$

where subscript "r" denotes rock
 subscript "j" denotes joint
 k = persistence (Figure 5.2)

The concept of apparent persistence is proposed in this paper. Apparent persistence is the value of persistence along a joint plane that has the same value of AR as the critical failure path. One can compute the AR_0 and the AR_{100} which are the values of AR for a failure path that extends along planes having a persistence of 0% and 100% respectively. AR_{cr} , the value for the critical failure surface (which is typically nonplanar), is between the two extremes. The apparent persistence, w , is defined as

$$w = \frac{AR_0 - AR_{cr}}{AR_0 - AR_{100}} (100) \quad (5.10)$$

Apparent persistence is a measure of the proximity of AR_{cr} to AR_{100} . It is concerned solely with the strength along the critical path and ignores the location and configuration of the failure surface. Apparent persistence compares the strength of the critical path to the strengths of paths solely through intact rock or solely along a joint. It expresses the strength of the critical path in terms of apparent persistence. This concept is more fully developed in Section 5.5.

5.4 Computer Program DAYLITE

The analytical models derived in Sections 5.2 and 5.3 and Appendix G are incorporated in a computer program. The primary input parameters to the program are those listed in Table 5.1. They include the general attitude of the joints, the distributional parameters of the joints, the strength characteristics of both the joints and intact rock and the in situ stress field. The program generates a specified number of random jointing patterns (or "realizations") and analyzes each pattern to locate the path of minimum resistance. Finally, it computes the value of apparent persistence. (The program uses three different techniques to interpret the minimum resistance strength. The "Reduction Option #1" corresponds to apparent persistence as defined in the previous section.)

Table 5.1

Generic Group	Symbol	Definition	Value*
Geometry of Block	α	Angle of Inclination	30°
	h	Height	40°
	l	Width	80°
Strength Parameters	ϕ_r	Friction Angle of Intact Rock	30°
	c_r	Cohesion of Intact Rock	80**
	ϕ_j	Friction Angle of Joint	30°
	c_j	Cohesion of Joint	2**
Distribution Parameters	ρ	Mean Joint Plane Spacing	4**
	δ_j	Mean Length of Joint Segment	10**
	δ_r	Mean Length of Rock Bridge	20**
Original Stress	σ_{v_0}	Vertical Stress	varies
	σ_{h_0}	Horizontal Stress	varies

* The values listed were used in the sensitivity analyses discussed in Section 5.5. Unless otherwise noted in plots the values listed were used in all computer runs.

** Any set of dimensionally consistent units will yield the same values of apparent persistence.

TABLE 5.1 Inputs to computer program JOINTSIM

The program is designed to handle up to 400 realizations; however, the capacity can easily be expanded. The basic output consists of a recapitulation of the inputs, a listing of the more important output parameters for each realization and a statistical summary of the inclinations of the failure path, the maximum persistence and the apparent persistence for all realizations. The program has a series of options that enable one to obtain a much more detailed output. For example, one can get the coordinates of each joint segment, a listing of the strengths of all possible failure paths from each point (x_i, y_i) or the precise location of the minimum resistance path.

A typical output (in its abbreviated form) is presented in Appendix H. The appendix also contains a complete listing of the program as well as a users' manual.

5.5 Results

The analytical procedure and the computer program were tested by investigating the sensitivity of the resulting strength parameters relative to the input parameters. In particular, the effect of changes in the magnitude and in the horizontal to vertical ratio $(\sigma_{ho}/\sigma_{vo})$ of original stresses and the effects of variations in the joint orientation were examined. The set of input parameters used as a basis for comparison is listed in Table 5.1.

En Echelon or Multi-Planar Failure Paths

The sensitivity study was concerned primarily with parameter values that are likely to generate "en echelon" failures, i.e., failures that involve at least one transition between joint planes. Jointed rock masses which have relatively large mean spacings between planes or relatively high strength parameters for intact rock tend to fail along a single joint plane. Figure 5.17 suggests this relationship between mean spacing and frequency of "en echelon" failures. Since the number of realizations (1 realization = 1 jointing pattern) is quite small (40) the curve serves to identify a trend rather than a definitive relationship.

Maximum Persistence Vs. Apparent Persistence

The number of joint planes in each realization of the simulation procedure is a Poisson random variable, S^* , with a probability mass function:

$$P_S(s) = \frac{(h/\rho)^s e^{-(h/\rho)}}{s!} \quad (5.11)$$

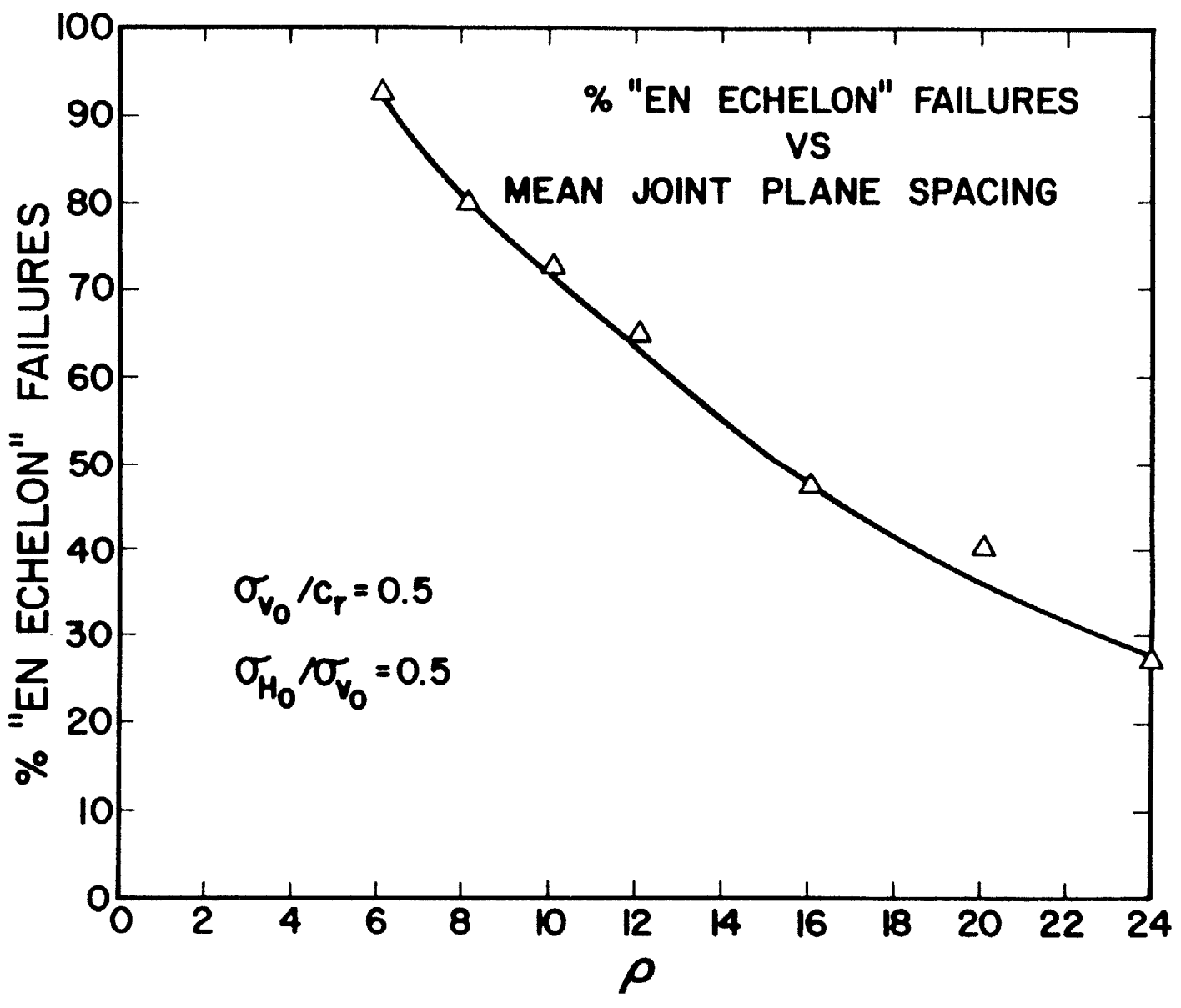
and mean $m_S = h/\rho$.

From the parameters of Table 5.1: $m_S = 40/4 = 10$.

The persistence of each joint plane is also a random variable, T , with mean:

* Upper case notation is used for random variables and a lower case notation for specific values of the variable.

Figure 5.17 % "En Echelon" Failures vs. ρ



$$m_T = \frac{\delta_j}{\delta_j + \delta_r} (100) \quad (5.12)$$

where δ_j is the mean length of joint segments

δ_r is the mean length of rock bridges.

From Table 5.1: $m_T = \frac{10}{10 + 20} (100) = 33.3\%$

The maximum persistence along the joint planes in each realization is a random variable, Q . There is no simple analytical expression for the mean, m_Q . It depends on the dimensions of the jointed rock block as well as on the distributional parameters of the jointing process. In any case, m_Q is not less than m_T . Using the parameter values in Table 5.1 one finds from simulation an m_Q of 63.1%.

The apparent persistence, W , defined in Section 5.4 reflects both the persistence of individual joint planes and possible transitions between joint planes. If the joint planes are widely spaced, the critical path will follow a single joint plane--the one with the maximum persistence and $w = q$. w is actually a lower bound for q because if there were no transitions between joint planes the critical path would follow the joint plane with the maximum persistence. When the critical path involves a transition it must have "found" a route that has less resistance than the plane with maximum persistence. In general, $w > q$ with the difference $m_W - m_Q$ reflecting plane to plane transitions in critical paths.

Figure 5.18 shows a pair of histograms that summarize the results of 250 realizations in terms of W and Q . The histograms of apparent persistence is shifted to the right with respect to that of maximum persistence because of the aforementioned effect (causing a different $m_W - m_Q$) of transitions between planes. The maximum persistence histogram is more dispersed and has a more pronounced peak.

Magnitude of Stress

The magnitude of the stress field does not appear to exert a major influence on the apparent persistence. Figure 5.19 presents the results of a series of computer runs in which the stress ratio (σ_{ho}/σ_{vo}) was held constant (0.25 or 1.0) while the magnitude of stress (σ_{vo}/c_r) varied from 0.125 to 1.00. Each run involved 250 simulations. The curve for $\sigma_{ho}/\sigma_{vo} = 0.25$ indicates that m_W increases as σ_v increases. However, the curve for isotropic stresses suggests the m_W is virtually independent of σ_{vo} . It seems that the influence of magnitude of stress increases as the stress ratio decreases. The histogram of W for the six parameter combinations have approximately the same dispersion with sample standard deviations in the range of 11.3 to 12.7.

Stress Ratio

The effect of stress ratio on apparent persistence is shown in Figure 5.20. There is a small but steady decrease in m_W (and increase in σ_w^2) as the stress ratio increases from

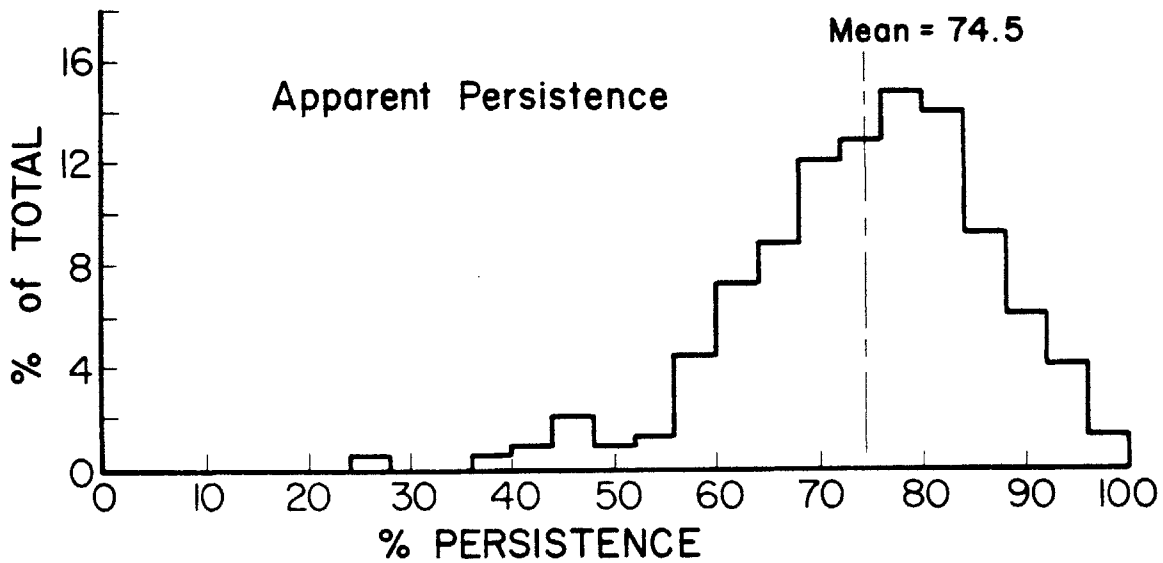
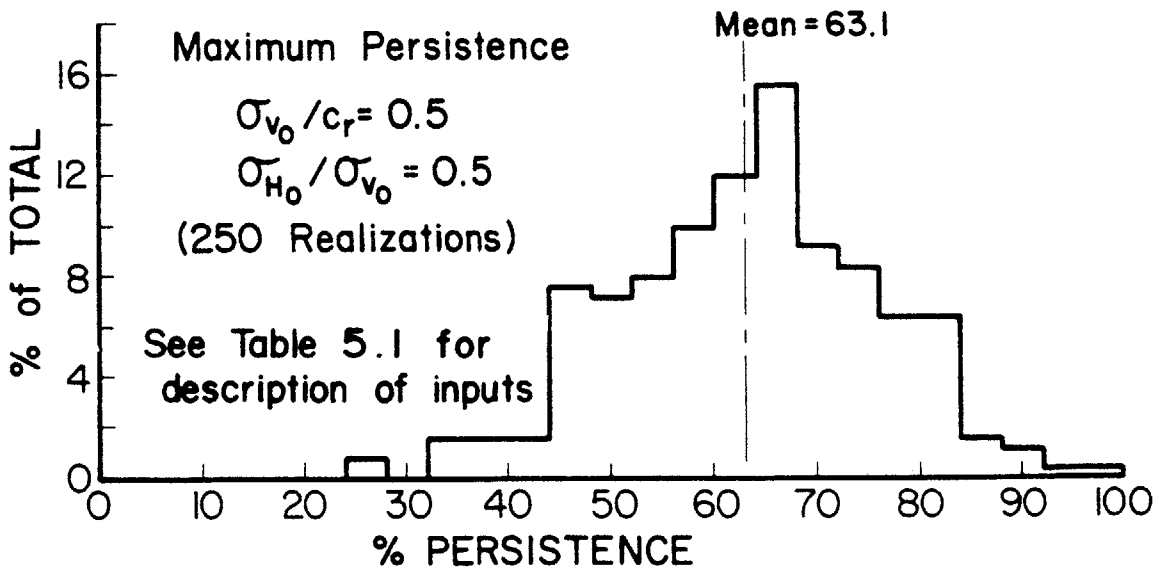


Figure 5.18 Histograms of Maximum Persistence and Apparent Persistence

216

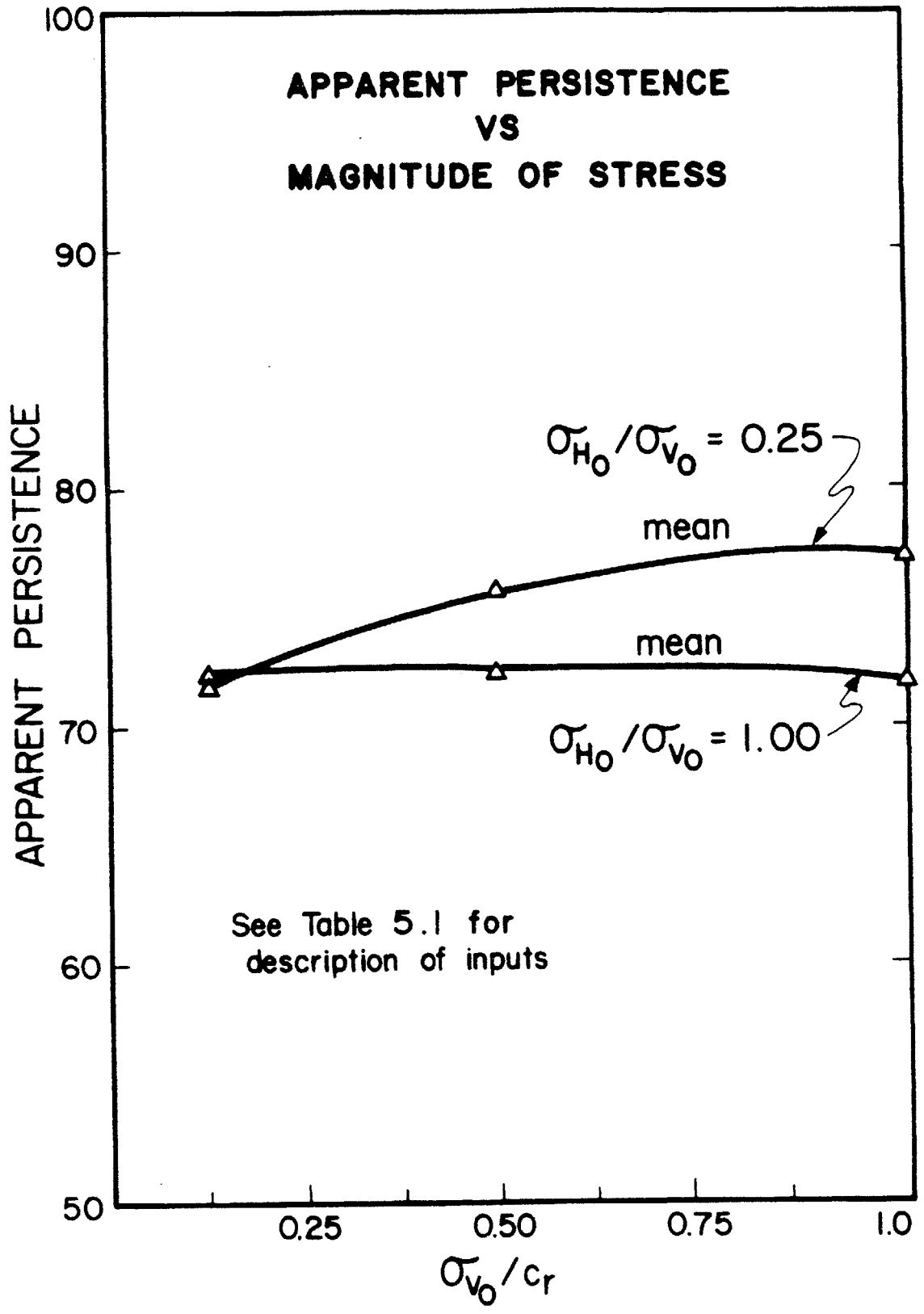


Figure 5.19 Apparent Persistence vs. Magnitude of Stress
217

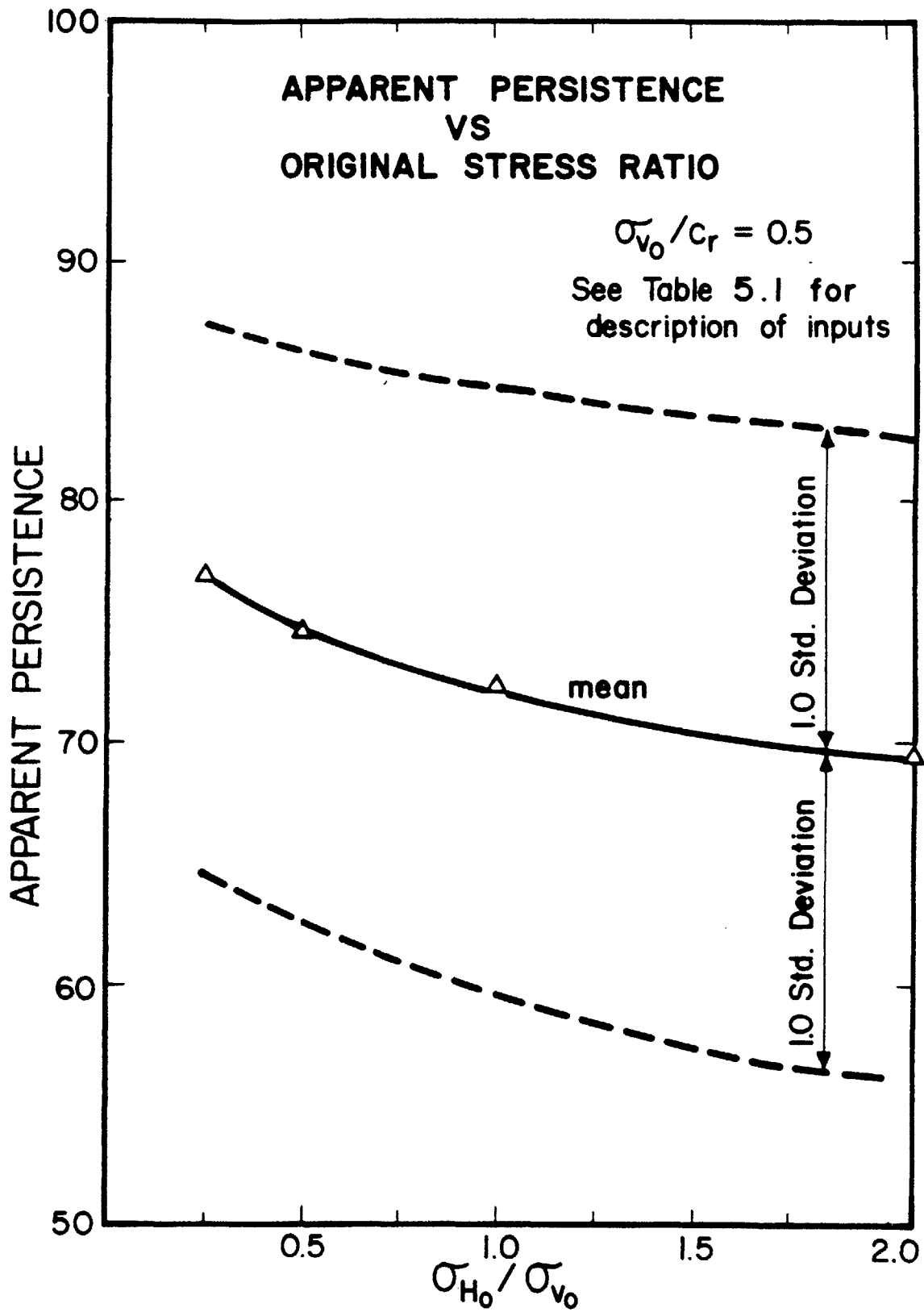


Figure 5.20 Apparent Persistence vs. Original Stress Ratio
218

0.25 to 2.0. The total change in m_W over that range is approximately 9%.

Orientation of Joints

Three computer runs were used to investigate the relationship between apparent persistence and the joint inclination, α . This limited data suggests that m_W is only moderately sensitive to changes in α (Figure 5.21); m_W decreases with increasing α whereas σ_W^2 is essentially constant. The change of m_W for the range of $15^\circ < \alpha < 45^\circ$ does not exceed the standard deviation. In this sense one may say that the apparent persistence, W , is not very sensitive to α .

This insensitivity can be a very useful result. It suggests that computations of m_W for a particular joint inclination can be used for other α 's without introducing appreciable error. The fact that m_W is not a strong function of α does not imply that the absolute strength of rock masses with dissimilar joint orientations is the same. As defined in Equation (5.10), apparent persistence is a ratio of strengths. Thus, two realizations with different α 's may have the same apparent persistence even though their respective A_0 's, A_{cr} 's and A_{100} 's are different. As long as the respective values are proportionate, the two apparent persistences will be identical. Figure 5.21 suggests that the proportionality (almost) occurs as α varies as long as all the other parameters are identical.

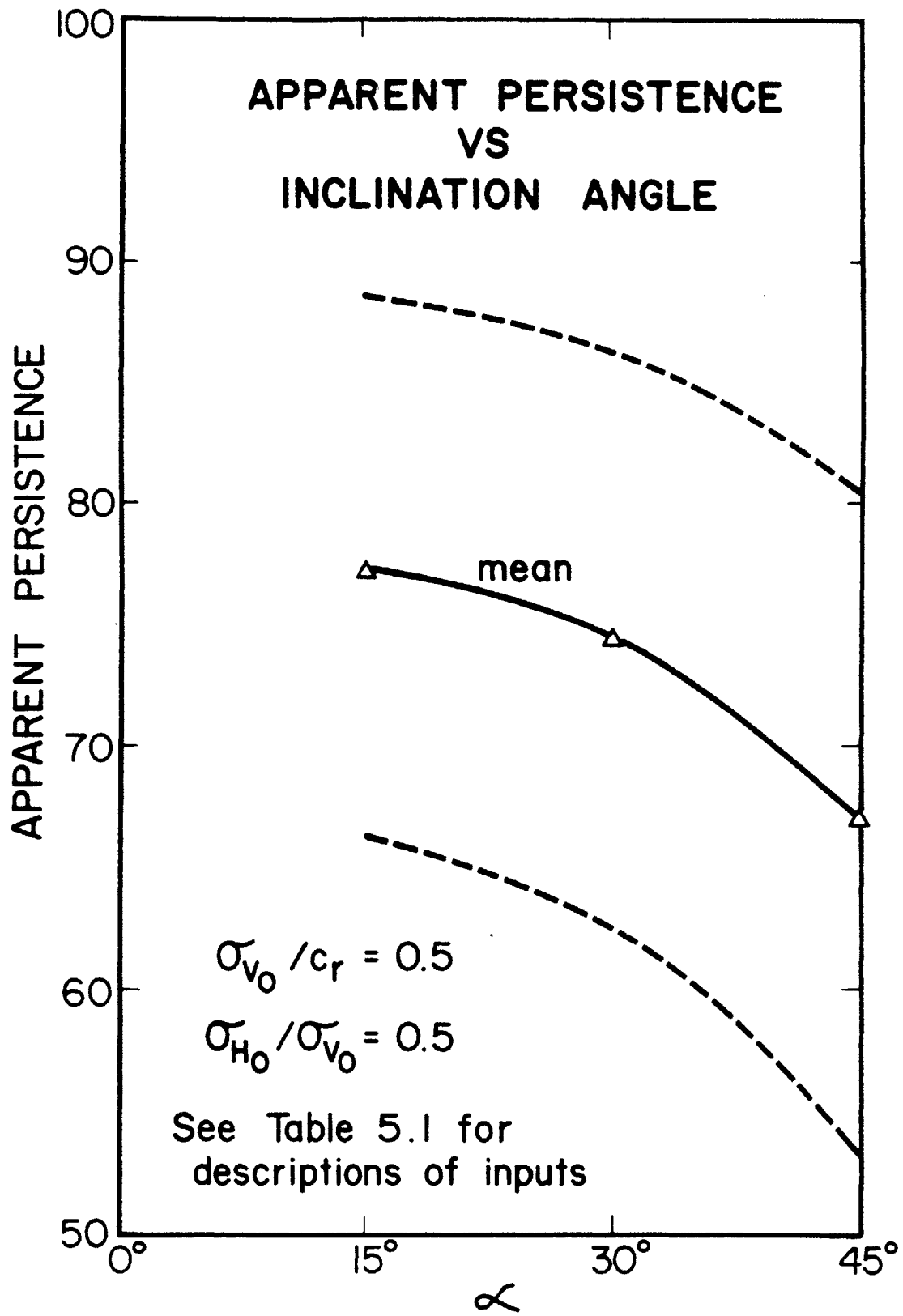


Figure 5.21 Apparent Persistence vs. Inclination Angle

In stability analyses, values of apparent persistence would be used in conjunction with the proper α 's to yield different strengths.

5.6 Summary

The probabilistic model for shearing resistance of jointed rock is a step in the development of a comprehensive technique for analyzing the reliability of rock slopes. It represents a possible solution to one of the major unsolved problems in rock slope stability analysis -- the interaction between intact rock and discontinuities. The model provides a rational method for treating joint persistence; the method is based on information that can be obtained from field surveys.

The most important feature of the model is that it characterizes the strength of a jointed rock mass through an apparent persistence parameter. Apparent persistence is not a measure of absolute strength; it is an index that compares the strength of the critical path to the strength of a path through intact rock. Apparent persistence is a geometric interpretation of the interaction that occurs between the jointed and unjointed segments of an echelon joint planes.

Apparent persistence can be used in conjunction with Jennings' relations to describe the strength along failure surfaces in stability analyses involving an echelon failure planes. In analyses that consider tetrahedral wedges bounded by two joint planes the apparent persistences on the two planes are

treated as independent random variables.

The current model as described in this chapter is merely the first step in treating the persistence problem. The model examines a fairly simple (albeit common) jointing system. Some of the limitations in the model can be eliminated through conditioning; however, other restrictions can only be relaxed by modifying and extending the present version of the model.

The apparent persistence calculations presented in the chapter were based on a deterministic set of strength parameters. It is possible to treat the strength parameters as random variables by conditioning the apparent persistence on the strength parameters. For example, the pdf's of ϕ_r and c_r could be discretised into a limited number of values each of which would have a finite probability of occurrence. A series of simulations (and apparent persistence computations) could be performed on each pair of ϕ_r and c_r values. If ϕ_r and c_r were independent random variables, the (unconditional) apparent persistence would be:

$$w = \sum_i \sum_j W_{ij} P[\phi_{r_i}] P[c_{r_j}] \quad (5.13)$$

where W_{ij} is the apparent persistence based on ϕ_{r_i}
and c_{r_j}
 $P[\phi_{r_i}]$ is the probability that ϕ_r is ϕ_{r_i}
 $P[c_{r_j}]$ is the probability that c_r is c_{r_j}

The shape of the strength for intact rock is not a critical feature of the model. The model defined strength in terms of a Griffith-Modified Griffith envelope, but other strength criteria could be used. In particular, one might want to use the upper bound envelope that characterizes crack propagation through the entire specimen (Section 5.3). Since apparent persistence is a relative measure of strength it should not be highly sensitive to the shape of the intact failure envelope*.

The stochastic model can (and should) be expanded to consider the three dimensional aspects of persistence i.e., the model should examine the joint planes as three-dimensional features rather than just their traces on a two-dimensional cross section. Also, the model should consider cases involving non-parallel joints and recognize possible correlations between the geometric parameters of different joint sets.

* Apparent persistence is virtually insensitive to the strength parameters along the joints because the intact segments have such a dominant effect on the location of the critical path. The resistance along jointed segments is almost negligible compared to the resistance through intact material regardless of ϕ_j and c_j .

CHAPTER 6

AN INTEGRATED APPROACH TO RELIABILITY ANALYSIS

6.0 Introduction

The earlier chapters discussed various aspects of reliability analysis in rock slopes. Chapters 3 to 5 presented some tools to use in reliability analysis but each technique was developed as an independent component. This chapter will endeavor to show how the individual elements can be combined into a complete analysis.

The reliability analysis is based on a concept that underlies all rock slope analyses: Failure cannot occur unless both kinematic and kinetic conditions are met. Chapter 3 discussed the kinematic aspects and presented the computer program DAYLITE. Chapter 4 discussed the kinetic aspects and presented the computer program SWARS-2MC. The results from the two programs can be combined to provide a complete reliability analysis. The two operations are combined in a manner similar to that used in composite models (Section 2.3) i.e.,

$$P_f = P[A]P[B] \quad (6.1)$$

$P[A]$: the probability that a wedge daylights

$P[B]$: the probability that the driving
forces exceed the resisting forces.

The analysis proceeds as follows:

1. Examine each cell in the critical zone and determine $P[\theta_i, \phi_i]$, the probability that a

line of intersection for any two joints will be in the cell characterized by the coordinates (θ_i, ϕ_i) .

2. Use Monte Carlo simulation to determine $P[U_i | \theta_i, \phi_i]$ the probability that a wedge daylighting in cell (θ_i, ϕ_i) will be kinetically unstable.

3. Calculate \bar{P}_f for any two joints as;

$$\bar{P}_f = \sum_{\text{all } i} P[U_i | \theta_i, \phi_i] P[\theta_i, \phi_i] \quad (6.2)$$

4. Adjust \bar{P}_f to reflect the fact that the slope may contain more than one potentially unstable wedge, i.e.,

$$\begin{aligned} P_f &= \text{Probability of failure for the entire slope} \\ &= f(\bar{P}_f, k) \end{aligned} \quad (6.3)$$

where \bar{P}_f is the probability of failure for a single wedge and k is the number of wedges on the slope.

The four-step procedure outlined above will provide a P_f value that approximates the reliability of the slope. The procedure does not provide a rigorous solution to the stability problem; there are a number of areas that require development. The purpose of this chapter is not to present a definitive solution but rather to show where the techniques developed in the earlier chapters fit into the solution. The remainder of this chapter examines each of the four steps

and in doing so emphasizes two points:

1. What assumptions are involved in each step?
2. Which steps require additional development?

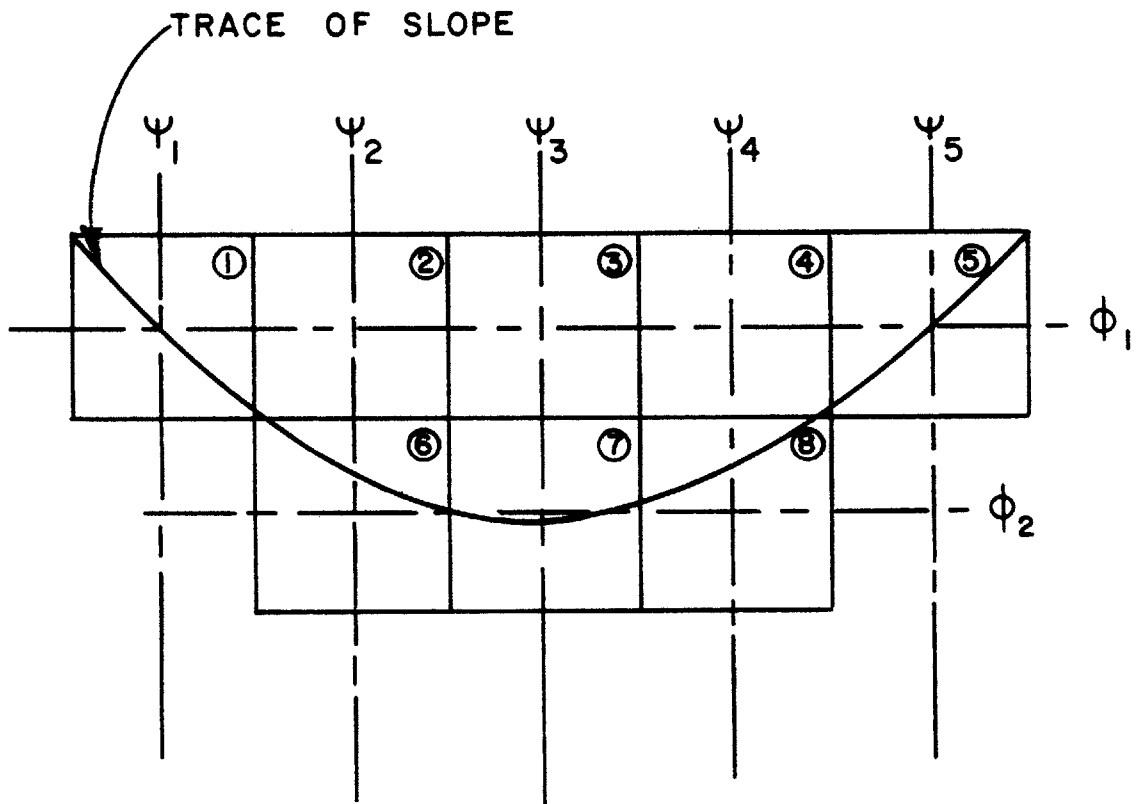
6.1 Kinematic Restraints: $P[\theta_i, \phi_i]$

Figure 6.1 shows the results from a hypothetical DAYLITE run in which the critical zone was partitioned into 8 cells* each of which is characterized by a pair of spherical coordinates (θ_i, ϕ_i) . Values of $P[\theta_i, \phi_i]$ for each cell are tabulated in Figure 6.1. The values represent the probability that a joint from set 1 will combine with a joint from set 2 to form a wedge whose line of intersection daylights in the respective cell.** The values are the kinematic probabilities that will be used in reliability analysis. They were computed in accordance with the procedures described in Chapter 3 which assumed that the orientations of joint planes were independent random variables.

Some of the cells may have very low $P[\theta_i, \phi_i]$'s. The low values indicate that it is highly unlikely that a wedge will daylight at those orientations. The analysis can be shortened if these cells are eliminated from further

* 8 cells are used to illustrate the concept. A considerably larger number of cells would be used in any real problem.

**DAYLITE will also compute the probability that two joints from the same set will combine to form wedges.



<u>Cell</u>	<u>P[θ_i, φ_i]</u>
1	0.056
2	0.078
3	0.096
4	0.032
5	0.009
6	0.066
7	0.088
8	0.044

Figure 6.1 Typical Output from DAYLITE
227

consideration at this early stage in the analysis. In ignoring cells, one introduces some errors into the analysis because every cell in the critical zone, regardless of its orientation, has a finite probability of representing a potentially unstable wedge. However, if the cell has a $P[\theta_i, \phi_i]$ that is several orders of magnitude lower than the modal value of $P[\theta, \phi]$, the error will be small. (The decision to ignore a cell is actually a judgement on $P_f = P[U_i | \theta_i, \phi_i]$ rather than just on the $P[\theta_i, \phi_i]$ term. If $P[\theta_i, \phi_i]$ is very small, P_f will also be very small.)

6.2 Kinetic Restraints: $P[U_i | \theta_i, \phi_i]$

The discussion on kinetic restraints will first present some general comments on how $P[U_i | \theta_i, \phi_i]$ is obtained for each cell in the critical zone. Next, the section examines one of the inputs to that calculation, the pdf of the height of failure wedges. Finally, the section shows that the calculations for kinetic instability must be performed on each cell in the critical zone.

$P[U_i | \theta_i, \phi_i]$ for each cell is obtained through Monte Carlo simulation with the computer program SWARS-2MC (Section 4.6). θ and ϕ are the only two deterministic parameters in the analysis. ψ and β_1 define the shape of the wedge; their pdf's can be obtained from the DAYLITE output for the (θ_i, ϕ_i) cell. The mechanical properties (stiffness and strength) of

each joint set and the location of the piezometric surface must be characterized in terms of pdf's.* If the joints in a particular set are relatively closely spaced the strength of an echelon failure paths can be expressed through the apparent persistence parameters introduced in Chapter 5.

The height of the wedge, H , is the vertical distance from the top of the slope to the vertex of the wedge (Figure 6.2). If there are no cleft water pressures in the joints and there is no cohesion on either joint, the factor of safety is independent of H . If either cleft water pressure or cohesion is present H must be treated as a random variable. One reasonable approximation of the pdf of H would be the uniform distribution over the entire height of the slope. The derivation is based on the assumption that joint planes can be treated as Poisson planes in space (Section 5.2).** Figure 6.3A depicts a rock slope that contains two sets of discontinuities. Line OA is the trace on the slope of joint A from set 1. Joints from set 2 intersect joint A to form various size wedges. If the joints from set 2 are Poisson their spacing in exponentially distributed in all directions--

* At the present time little is known about typical pdf's for the mechanical properties of joints or ground water conditions. Research is currently underway at M.I.T. to establish typical pdf's for strength parameters. The results will be published in a report authored by Baecher and Einstein, et al., (19xx).

**A number of authors (e.g., Baecher et al., 1977) have presented empirical evidence that suggests that the assumption is valid.

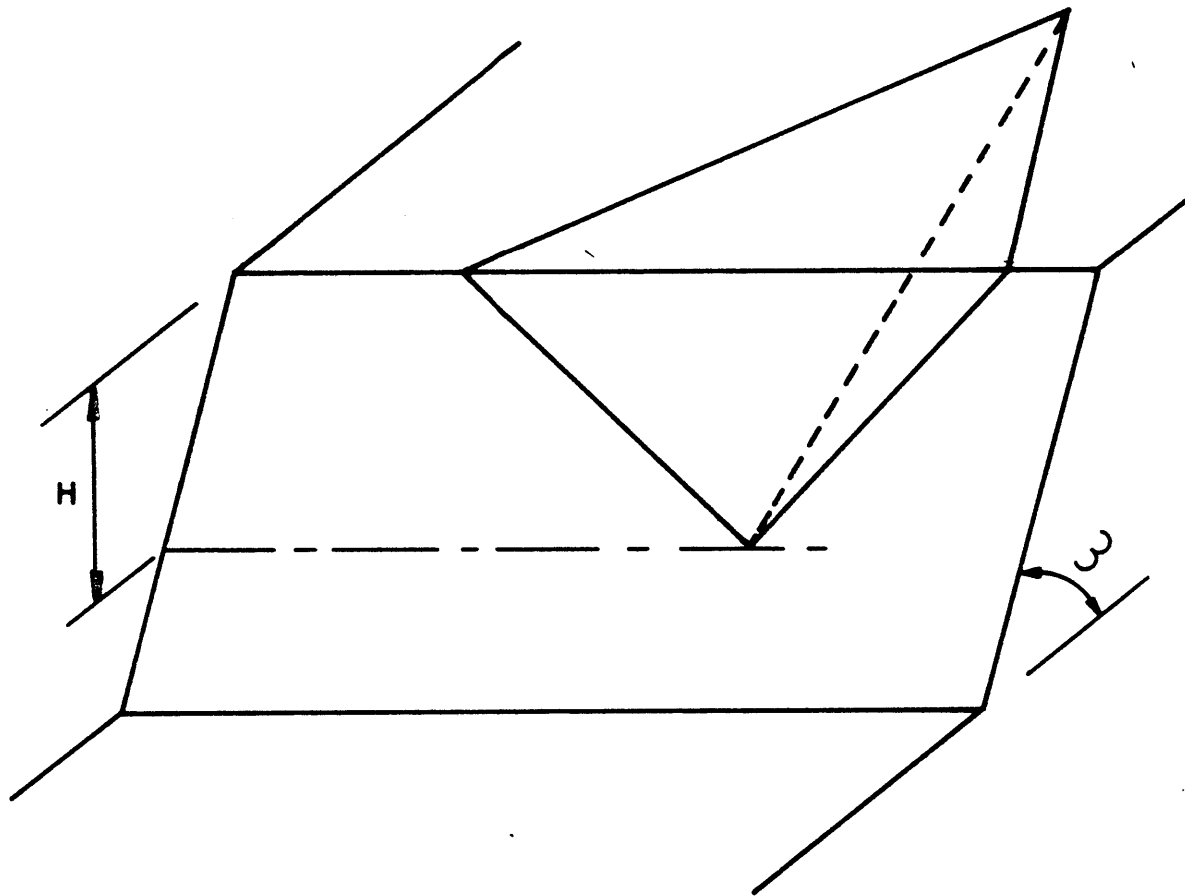
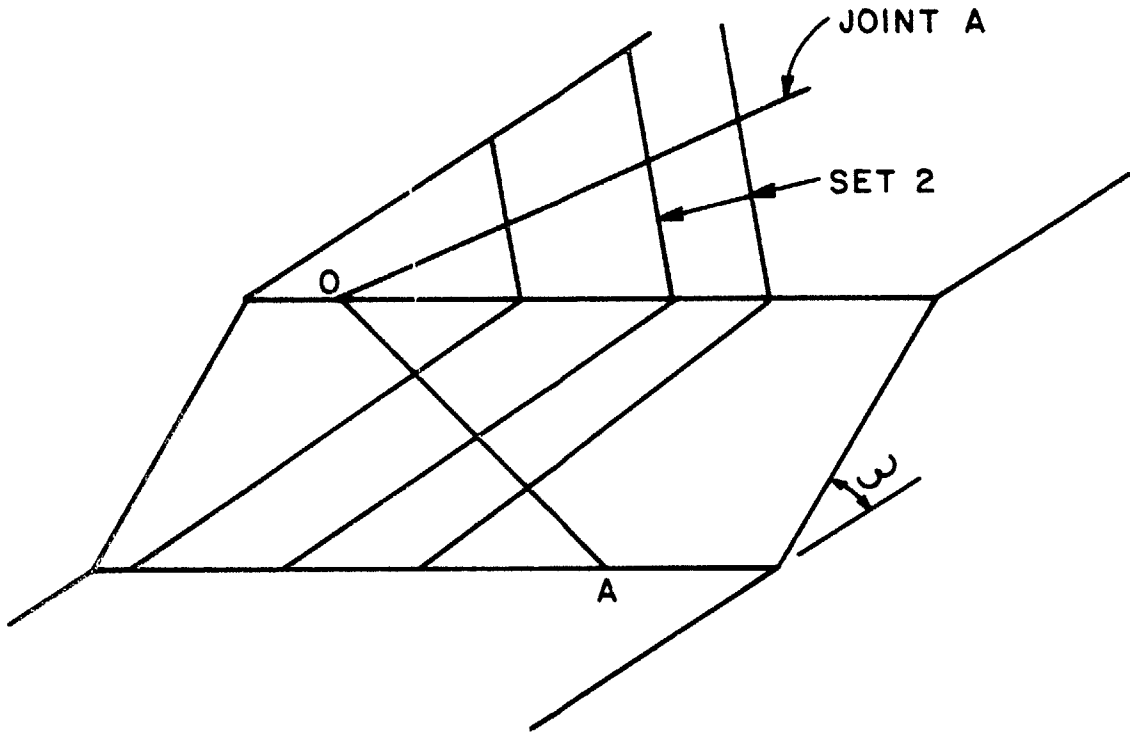
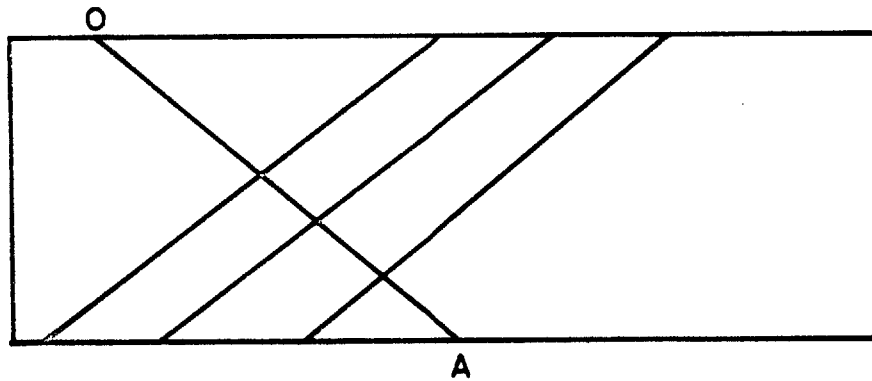


Figure 6.2 Definition of H



6.3 A



6.3 B

Figure 6.3 Intersecting Poisson Planes--Derivation of $f_H(H)$

including the direction along OA. (The mean spacing will vary with direction but the exponential nature of the distribution will not.) Thus, the points of intersection between joints from set 2 and the line OA constitute a Poisson process (Figure 6.3B). Since the intersections are Poisson every differential segment on OA has an equal probability of containing an intersection. In a similar manner, every distance d_i from point 0 to the i^{th} differential segment has an equal probability of locating an intersection. Thus, $f_D(d)$ has a uniform distribution. The intersection points represent the vertices of wedges and the d_i distances are directly related to the wedge heights (H's) through a trigonometric constant. Since $f_D(d)$ is uniform, $f_H(H)$ must also be uniform.

The pdf for H is not perfectly uniform because the preceding argument ignored the lateral boundaries of the slope. Figure 6.4 is a front view of a slope. None of the joints from set 1 that lie to the right of joint B can form a wedge of height H because joint set 2 is restricted by the right boundary. As joints from set 1 approach the boundary they form smaller and smaller wedges. Thus, for the whole slope, small wedges are somewhat more likely to occur than large ones. Nevertheless, the uniform distribution should provide a reasonable approximation* for the pdf of H.

* Veneziano (19xx) used his model (Sections 1.5 and 5.1) to examine a related problem--the distribution of vertices on the plane of the slope. He concluded that the location of vertices did not constitute a Poisson process.

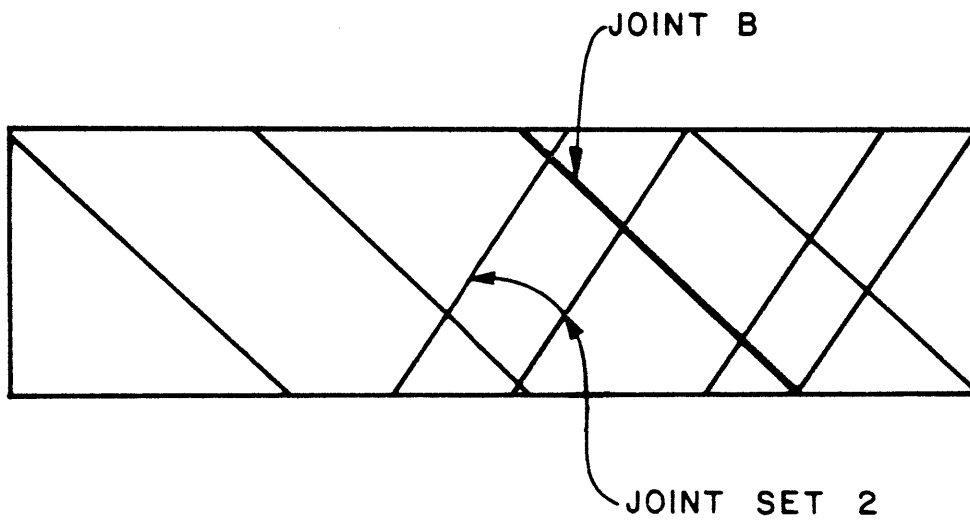


Figure 6.4 Influence of Slope Boundary

Once all the pdf's for the appropriate input parameters have been established $P[U_i | \theta_i, \phi_i]$ can be found through Monte Carlo simulation. $P[U_i | \theta_i, \phi_i]$ is the proportion of trials that have an FS that falls below 1.0. In defining failure, one must differentiate between FS_I and FS_U . As discussed in Section 4.4, FS_I corresponds to initial movement (in any direction) while FS_U corresponds to movement down the line of intersection. FS_U may be more suitable for simulation because there are fewer variables (and fewer pdf's) to define; however, either definition can be used in the analysis.

Every cell in the critical zone is characterized by a unique pair of θ and ϕ values. The simulation procedure that examines kinetic instability must be repeated for each of these orientations. The pdf's for ψ and β_1 (as determined by DAYLITE) will vary for each (θ_i, ϕ_i) ; the pdf's for the other random variables may be varied at the discretion of the individual performing the analysis.

As discussed in Section 2.2, Monte Carlo simulations have a number of limitations. In particular, the simulations are usually based on a number of assumptions concerning the independence of random variables. The procedure described above (and implemented in the SWARS-2MC program) relies on many independence assumptions. The most important ones are:

1. Joints from different sets are uncorrelated. The fact that a particular joint from set A is present does not affect the marginal distribution of set B.

(DAYLITE is based on this assumption.)

2. Joint orientation and joint strength parameters are uncorrelated. Low strengths are not associated with any particular joint orientation.

3. Joint length and joint spacing are uncorrelated.

(JOINTSIM, the program that computes apparent persistence, is based on this assumption; however, the program can be modified to accommodate such correlation.)

Very little information is available to verify (or contradict) these assumptions. In some instances (like strength parameter) the data base is too small to discern correlations. In other instances (like orientation) the data base is adequate but the data is not usually gathered or recorded in a manner that would disclose correlations. Improvements in sampling techniques may provide some insight into the correlation structure of the random variables that describe the orientation and shape of wedges. Correlations involving the mechanical properties of joints present a much more difficult problem that may remain unsolved for the foreseeable future.

6.3 Calculating \bar{P}_f

\bar{P}_f is defined as the probability that any two intersecting joints will form an unstable wedge. The wedge must be both kinematically and kinetically unstable; hence, \bar{P}_f is computed as the product of the kinematic ($P[\theta_i, \phi_i]$) and

kinetic ($P[U_i | \theta_i, \phi_i]$) probabilities. The product is summed over all cells in the critical zone:

$$\bar{P}_f = \sum_{\text{all } i} P[U_i | \theta_i, \phi_i] P[\theta_i, \phi_i] \quad (6.4)$$

\bar{P}_f is actually a conditional probability based on the premise that two and only two joints intersect to form a wedge. P_f , the probability of failure for the entire slope, could be either less than or more than \bar{P}_f . If the rock mass has widely spaced joints relative to the dimensions of the slope there may be a high probability that no wedges form. On the other hand, there are usually many intersections and each one defines a potentially unstable wedge. \bar{P}_f must be adjusted to reflect the fact that there are many possible failures.

6.4 Calculating P_f

P_f , the probability of failure for the entire slope, is a function of \bar{P}_f as well as k , the number of wedges in the slope. Calculating P_f is a two-fold problem:

1. Determining the functional relationship between k and \bar{P}_f .
2. Determining the distribution of the random variable k .

The first problem is the more difficult one to solve because it is a problem in system reliability in which the entire rock slope is treated as an engineering system. The second problem can be handled (at least crudely) with the approximation technique presented later in this chapter.

Figure 6.5 shows two hypothetical slopes each of which contains joints from two sets. In Figure 6.5A there are two joints from each set and they form two distinct wedges. If the wedges were independent and their \bar{P}_f 's were \bar{P}_{f1} and \bar{P}_{f2} respectively, P_f , the reliability of the entire slope, would be

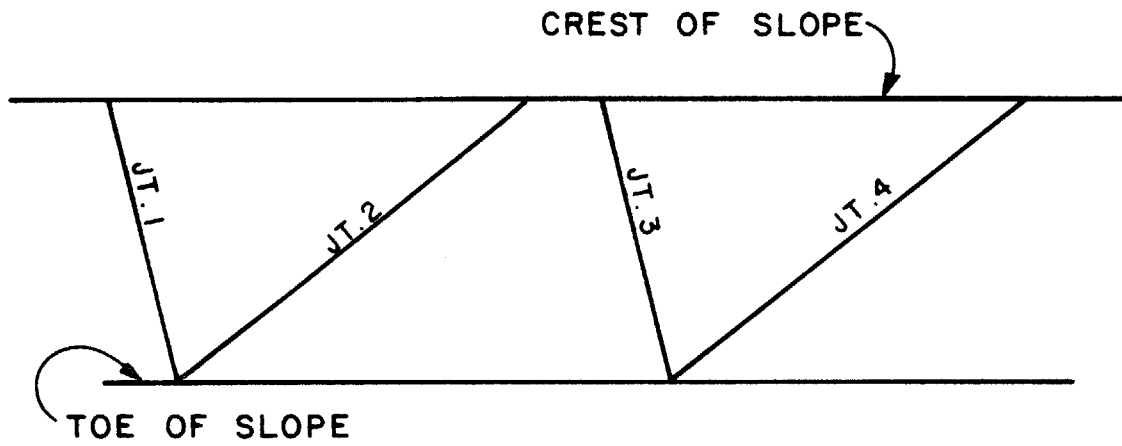
$$P_f = 1 - (1 - \bar{P}_{f1})(1 - \bar{P}_{f2}) \quad (6.5)$$

if $\bar{P}_{f1} = \bar{P}_{f2} = \bar{P}_f$:

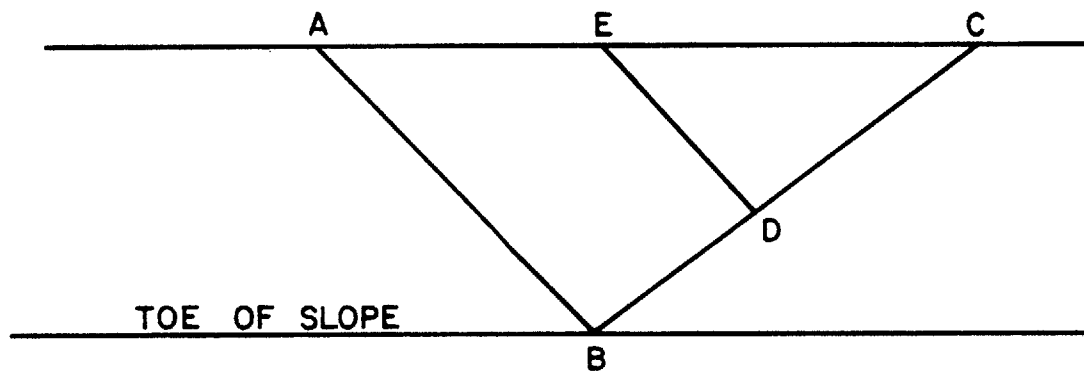
$$P_f = 1 - (1 - \bar{P}_f)^2 \quad (6.6)$$

On the other hand, if the wedges were perfectly correlated i.e. joints 1 and 3 (as well as the pair 2 and 4) were identical in orientation and strength parameters,

$$P_f = \bar{P}_f = (1 - \bar{P}_f)^1 \quad (6.7)$$



6.5 A



6.5 B

Figure 6.5 System Reliability of Slope

The fact that one wedge fails necessarily implies that its twin must fail.

Equations (6.6) and (6.7) represent two limiting cases. If the wedges were imperfectly correlated:

$$P_f = 1 - (1 - \bar{P}_f)^r \quad (6.8)$$

where $1 < r < 2$

The argument can be extended to systems involving n wedges. The two limiting values for P_f would be:

$$P_f = 1 - (1 - \bar{P}_f)^n \quad (\text{independent wedges}) \quad (6.9)$$

$$P_f = \bar{P}_f \quad (\text{perfect correlation}) \quad (6.10)$$

There are at least two forms of correlation: spatial and functional. Spatial correlation implies that the variation in properties between two different joints is a function of the distance between the two joints. In other words, given joint A and its attendant properties, the marginal distribution of the properties of joint B depends on the distance between A and B. At the present time little is known about the spatial correlation of mechanical properties. They are generally assumed to be uncorrelated.

Even if the joints are not spatially correlated the wedges they form may be functionally correlated. Figure 6.5B shows a typical case. Wedges ABC and CDE are related because they are both bounded by the same joint plane. The \bar{P}_f 's for the wedges are also related; the degree of dependence depends on the relative importance of joint plane BDC in determining the stability of the wedge. If, for example, BCD contributes most of the resistance to both wedges, the \bar{P}_f 's may be highly correlated. If BCD contributes little to the respective resistances, the \bar{P}_f 's may be virtually uncorrelated.

As evidenced by Equations (6.9) and (6.10), correlation among wedges can have an enormous impact on reliability calculations. The difference between the upper bound (Equation (6.9)) and the lower bound (Equation (6.10)) of P_f can easily reach orders of magnitude in a heavily jointed rock mass i.e., large n . The system reliability of a slope is a complicated problem that depends on wedge geometries as well as the correlations among individual parameters. At the present time there is no rational method for assessing the system reliability of a rock slope. The solution to this problem is one of the crucial steps in developing a rigorous reliability analysis technique.

A conservative approach would be to assume independence and use the upper bound i.e.,

$$P_f = 1 - (1 - \bar{P}_f)^n \quad (6.9)$$

However, n is not a deterministic parameter; it is a random variable. The term $(1 - (1 - \bar{P}_f)^n)$ can be conditioned on n :

$$P_f = (1 - (1 - \bar{P}_f)^n) P[n] \quad (6.11)$$

where $P[n]$ is the probability that the number of vertices is n .

Determining the pdf of n is no trivial matter. The following procedure illustrates how the problem might be approached. The procedure should provide a rough approximation of the pdf for some rather restrictive conditions.

There are a number of assumptions:

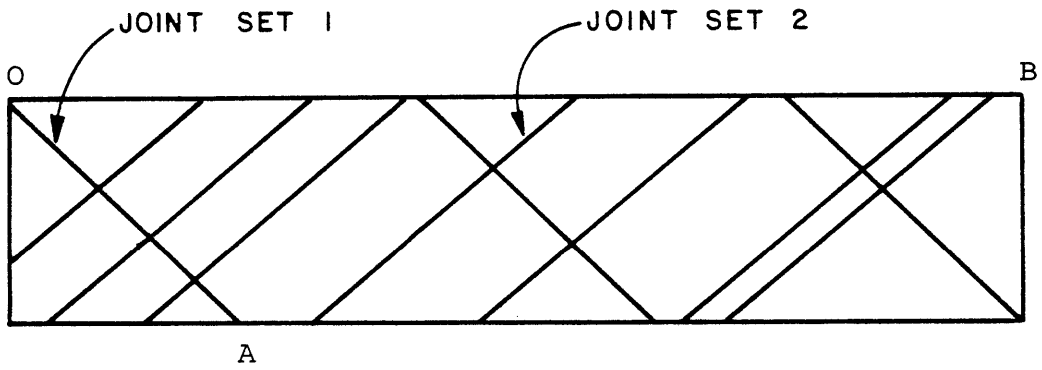
1. Joint planes are Poisson.
2. The pdf of joint plane orientation (for both joint sets) has a relatively small dispersion.
3. The joint sets are roughly orthogonal.
4. The slope is relatively lightly jointed.

The pdf for n can be approximated as follows (Figure 6.6):

ρ_1 = mean spacing of joint set 1 along the line OB

ρ_2 = mean spacing of joint set 2 along the line OA which is the trace of the mean joint from set 1.

x , the number of intersections of joints from set 2 with the line OA, has a Poisson distribution.



Distance O-A = L

Distance O-B = b

Figure 6.6 Derivation of $f_X(x)$ and $f_Y(y)$
242

$$f_X(x) = \frac{(L\rho_2)^x e^{-L\rho_2}}{x!} \quad (6.12)$$

where L is the distance along OA from the crest to the toe of the slope

y, the number of traces that appear on the slope also has a Poisson distribution:

$$f_Y(y) = \frac{(b\rho_1)^y e^{-b\rho_1}}{y!} \quad (6.13)$$

where b is the width of the slope.

Finally,

$$n \sim x \cdot y^* \quad (6.14)$$

Knowing the pdf's for X and Y one can compute the pdf for n. The approximation is crude and can become quite inaccurate for closely jointed rock masses. Equation (6.14) assumes that x, the number of intersections along any particular joint in set 1, is an independent random variable for all joints in set 1. If, however, two joints from set 1 are closely spaced (Figure 6.7) the number of intersections for the two joints are highly correlated.

* The derivation suggests that all joints must extend from the crest to the toe of the slope. The assumption can be justified if one treats joints as planar features with persistences less than 100% i.e., all joints in set 1 have a length L but their persistences vary. The persistence is a random variable that would be incorporated into the kinetic stability calculations.

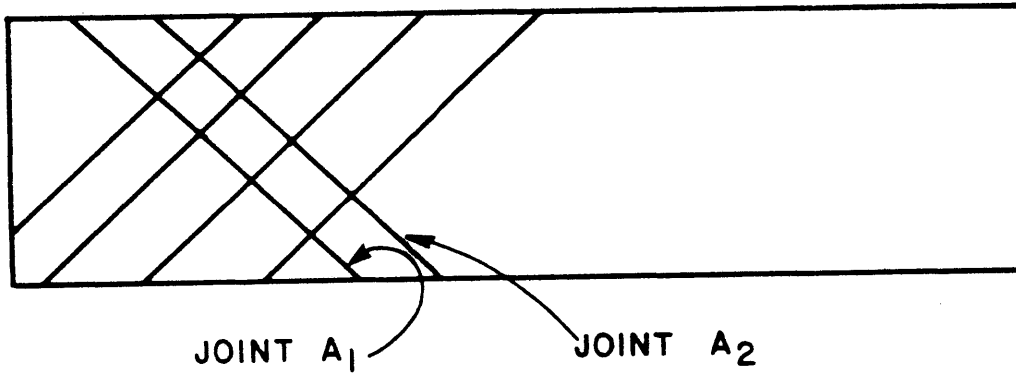


Figure 6.7 Closely Spaced Joints From Set 1--

Correlation Between x's

The procedure outlined above is not intended to serve as a design guide; it merely illustrates the concept. The method can (and should) be generalized to relax some of the limitations.* However, even a precise knowledge of $f_N(n)$ will not guarantee a reasonable estimate of P_f . $F_N(n)$ can be used to calculate the upper bound of P_f but provides no information as to the proximity of P_f to that upper bound. P_f cannot be accurately determined until the system reliability problem is resolved.

6.5 Summary

The purpose of this chapter was to show how the techniques developed in Chapters 3 to 5 could be incorporated into a reliability analysis. The techniques in themselves do not provide a complete treatment of the problem; however, they do represent an improvement over existing methods. In particular, the DAYLITE program provides information on the shape and orientation of potentially unstable wedges. The SWARS-2PM program gives some insight into the failure mode that involves sliding along two planes. Finally, the JOINTSIM program presents a rational method for evaluating the resistance of jointed rock masses.

There are still many problems in reliability analyses that are not well understood. As indicated in the earlier sections

* The method presented in this section was concerned with intersections between joints from different sets. Veneziano (19xx) used his model to examine the distribution of vertices when both of the intersecting joints come from the same set.

of this chapter, two related problems are particularly troublesome: possible correlations among random variables and a systems approach to the reliability of a multiply jointed rock slope. The problems are actually twofold: how can the correlation information be obtained from survey data and how can it be incorporated into the analysis? None of the current reliability analyses (including those presented in Chapter 2) directly address these questions. All the methods rely on assumptions (usually involving independence of parameters) to render the problem manageable. The P_f value calculated in each case is necessarily an approximation of the reliability of the slope. The credibility of P_f is directly related to the validity of the respective assumptions i.e., how closely they conform to reality. Unfortunately it is difficult to judge the validity of some of the assumptions at the present time. Many of the parameters used in rock slope stability have very limited data bases. It is hard to establish typical distributions or correlation coefficients for these variables. The statistical properties of these parameters should become more evident as additional data (and better procurement techniques) become available. The system reliability problem can be examined once the underlying correlation structure is found.

CHAPTER 7

SUMMARY AND CONCLUSIONS

Probabilistic analyses provide an alternate approach to assessing the stability of rock slopes. In a probabilistic or reliability analysis the integrity of the slope is expressed as its probability of failure rather than its factor of safety. The primary advantage of reliability techniques is that they explicitly consider the uncertainty associated with engineering parameters. The parameters are treated as random variables that can be characterized with probability distributions. The method is ideally suited for rock slope analysis because many of the critical parameters such as joint persistence are difficult to evaluate deterministically. These parameters must be considered random variables to arrive at any realistic conclusions concerning the stability of a rock slope.

Reliability analysis for rock slopes is still a relatively new concept. As indicated in Chapter 2, there are a number of analysis techniques currently available; however, none of the methods provide a comprehensive treatment of the problem. This thesis presents a new method that eliminates some of the limitations of earlier techniques. In particular, the thesis concentrates on a few specific points and develops some tools to use in examining slope stability from a probabilistic standpoint.

The method presented in this thesis uses a limiting equilibrium approach as both the rock wedge and its parent

rock mass are treated as rigid bodies. In such an approach, two conditions must be met before failure can occur:

1. The wedge must be oriented in such a manner that movement towards a free face is physically possible--a kinematic condition.
2. The destabilizing forces must exceed the stabilizing forces--a kinetic condition.

The problem can be formulated probabistically as:

$$\begin{aligned} P_f &= \text{Probability of Failure} \\ &= \sum P[A]P[B] \end{aligned} \quad (7.1)$$

where $P[A]$ is the probability that a wedge is kinematically unstable and $P[B]$ is the probability that the wedge is kinetically unstable. The product of the probabilities is summed over all potentially unstable conditions.

$P[A]$ is determined through a numerical procedure that examines the zone of kinematic instability as defined on a stereographic projection. The technique partitions the zone into equal area cells and calculates the probability that the line of intersection of two joint planes will pierce the reference hemisphere in each cell. The technique also provides information on the shapes of possible tetrahedrons that are associated with each line of intersection.

$P[B]$ is calculated through Monte Carlo simulation. The simulation is based on an improved version of the conventional

deterministic model for wedge stability. The conventional model was modified by incorporating the effects of joint stiffnesses and in situ stresses into the stability calculations. In a Monte Carlo simulation the input parameters must be characterized by probability density functions (pdf's). The pdf's for the orientation and shape of wedges can be derived from the algorithm that examines kinematic instability. The strength of a jointed rock mass (specifically, a rock mass with an echelon joints) can be described through an "apparent persistence" parameter which is obtained through a stochastic model discussed in the thesis.

$P[A]$ and $P[B]$ must be calculated for each cell in the zone of kinematic instability. The product summed over all cells is P_f --the probability that two joints will intersect to form an unstable wedge. P_f is conditioned on the premise that two and only two joints occur on the slope. The final step in the analysis is to "adjust" P_f to reflect the fact that the slope may contain many potentially unstable wedges. Evaluating the behavior of a multiply jointed rock mass is actually a problem in system reliability in which the entire slope is considered an engineering system. The problem is discussed briefly in Chapter 6.

As indicated earlier, this thesis addresses a number of specific points that must be considered in formulating a general method to evaluate the reliability of rock slopes. The techniques presented in the thesis do not, in themselves, constitute a complete analysis; however, they do clarify certain aspects of

the reliability problem. Each individual technique provides some new insight into the behavior of jointed rock masses. The cumulative effect of all the techniques is to advance the state of the art of rock slope stability analysis.

The procedure developed in Chapter 3 enables one to use the data from joint surveys i.e., the pdf's of joint orientation, to derive the pdf's of parameters that characterize the shape and orientation of tetrahedral wedges. The latter distribution is particularly useful because the orientation of the wedge is an input to the test for kinematic stability. The procedure involves a series a repetitive calculations because the pdf's are derived through numerical integration; however, the entire procedure has been programmed for use with a computer.

The thesis also presents an improved analytical model which describes the failure mode that consists of sliding along both joint planes. The model examines the influence of both in situ stresses and joint stiffnesses. As indicated in Chapter 4, earlier researchers had investigated the effects of both stresses and stiffnesses, but no one had established the relationship between the two. The model unifies the two approaches and extends the concepts to cover asymmetric wedges. The model distinguishes between two factor of safety: FS_I , the factor of safety against initial movement, and FS_U , the factor of safety against ultimate failure wherein the wedge slides down its line of intersection. In general, the initial

movement is not parallel to the line of intersection; it has a component into or out of the notch bounded by the joint planes.

The thesis also presents a possible solution to one of the major unsolved problems in rock stability--joint persistence. The stochastic model developed in Chapter 5 provides a rational method for treating joint persistence. The model uses Monte Carlo simulation to generate jointing patterns and then analyzes each pattern to identify the weakest failure path. The strength of the jointed rock mass is characterized by a random "apparent persistence" parameter that can be used in probabilistic stability calculations. Apparent persistence is not a measure of absolute strength, it is an index that compares the strength of the weakest path to the strength of paths through intact rock. Apparent persistence appears to be relatively insensitive to variations in the magnitude and orientation of the stress field; however, it is sensitive to the cohesion of intact rock as well as the distribution parameters of joint spacing and joint length.

References

ASCE: American Society of Civil Engineers

CISRM: Congress of the International Society for Rock Mechanics

USSRM: U.S. Symposium on Rock Mechanics

- Baecher, G.B., N.A. Lanney and H.H. Einstein (1977), "Statistical Description of Rock Properties and Sampling," 18th USSRM, pp. 5C1-5C6.
- Baecher, G.B. and N. A. Lanney (1978), "Trace Length Biases in Joint Surveys," 19th USSRM, pp. 56-65.
- Baecher, G. B., et al. (1978), Risk Analysis for Rock Slopes in Open Pit Mines - Annual Technical Report, M.I.T. Department of Civil Engineering Report, 295 pp.
- Baecher, G.B., et al. (19xx), Risk Analysis for Rock Slopes in Open Pit Mines - Final Report, M.I.T. Department of Civil Engineering Report.
- Baligh, M.M. et al. (19xx), "Effect of Longitudinal Stresses on Slope Stability," Manuscript submitted to ASCE Journal of the Geotechnical Engineering Division.
- Barton, C.M. (1977), "Geotechnical Analysis of Rock Structure and Fabric in C.S.A. Mine, Cabar, New South Wales," Applied Geomechanics Technical Paper 24, Commonwealth Scientific and Industrial Research Organization, Australia.
- Barton, N. (1972), "A Model Study of Rock-Joint Deformation," International Journal of Rock Mechanics and Mining Sciences, Vol. 9, No. 5, pp. 579-602.
- Bridges, M.C. (1977), "Presentation of Fracture Data for Rock Mechanics," 2nd Australian-New Zealand Conference on Geomechanics, pp. 144-148.
- Bridges, M.C. (1977), "Statistical Analysis of Clusters of Orientations," from unpublished doctoral thesis.
- Call, R.B., J. Savely and D.E. Nicholas (1976), "Estimation of Joint Set Characteristics from Surface Mapping Data," 17th USSRM, pp. 2B2-1 - 2B2-9.

- Call, R.D. and D.E. Nicholas (1978), "Prediction of Step Path Failure Geometry for Slope Stability Analysis," 19th USSRM.
- Call, R.D. and Y.C. Kim (1978), "Composite Probability of Instability for Optimizing Pit Slope Design," 19th USSRM.
- Campbell, D.S. (1974), Analytical Method for Analysis of Stability of Rock Slopes, SM Thesis, M.I.T., 134 pp.
- Dershowitz, W.S. (19xx), Probabilistic Models for Prediction of the Deformation of Jointed Rock Masses, SM Thesis, M.I.T.
- Glynn, E.F., D. Veneziano and H.H. Einstein (1978), "Probabilistic Model For Shearing Resistance of Jointed Rock," 19th USSRM, pp. 66-76.
- Goodman, R.E., F.E. Heuze and Y. Ohnishi (1972), "Research on the Strength-Deformability-Water Pressure Relationships for Faults in Direct Shear," Final Report - Contract ARPA No. H0210020, Advanced Research Projects Agency.
- Hendron, A.J., E.J. Cording and A.K. Aiyer (1971), "Analytical and Graphical Methods for the Analysis of Slopes in Rock Masses," NCG Technical Report No. 36 162 pp.
- Herget, G. (1978), "Analysis of Discontinuity Orientation for a Probabilistic Slope Stability Design," 19th USSRM pp. 42-50.
- Hoek, E and J. Bray (1974), Rock Slope Engineering, Institution of Mining and Metallurgy. London.
- Hoek, E. (1968), "Brittle Failure of Rock," Rock Mechanics in Engineering Practice (eds. K.G. Stagg and O.C. Zienkiewicz), John Wiley and Sons, New York, pp. 99-124.
- Jennings, J.E. (1970), "A Mathematical Theory for the Calculation of the Stability in Open Cast Mines," Symposium on the Theoretical Background to the Planning of Open Pit Mines With Special Reference to Slope Stability, pp. 87-102.
- John, K.W. (1968), "Graphical Stability of Slopes in Jointed Rock," ASCE Journal of the Soil Mechanics and Foundation Division, Vol 94, SM2, pp. 497-526.

- Kim, H., G. Major and D. Ross-Brown (1978), "Application of Monte Carlo Techniques to Slope Stability Analyses," Supplement to 19th USSRM, pp. 28-39.
- Kulhawry, F. (1975), "Stress Deformation Properties of Rock and Rock Discontinuities," Engineering Geology, Vol. 9. No. 4. pp. 327-350.
- Lanney, N.A. (1978), Statistical Description of Rock Properties and Sampling, SM Thesis, M.I.T., 253 pp.
- Mahtab, M. and R.E. Goodman (1970), "Three-Dimensional Analysis of Jointed Rock Slopes," 2nd CISRM, pp. 353-360.
- Major, G., D. Ross-Brown and H. Kim (1978), "A General Probabilistic Analysis for Three-Dimensional Wedge Failures," Supplement to 19th USSRM, pp. 45-56.
- Maloney, G.L. (1977), Computer Technique for Analysis of Rigid Blocks Formed by Three Sets of Intersecting Discontinuities in a Rock Slope, SM Thesis, M.I.T. 157 pp.
- Mardia, K.V. (1972), Statistics of Directional Data, Academic Press, New York, 357 pp.
- Marek, J.M. and J.P. Savely (1978), "Probabilistic Analysis of the Plane Shear Failure Mode," Supplement to 19th USSRM, pp. 40-44.
- Matheron, G. (1975), Random Sets and Integral Geometry, John Wiley and Sons, New York.
- McMahon. B. (1971), "A Statistical Method for the Design of Rock Slopes," 1st Australia-New Zealand Conference on Geomechanics, pp. 314-321.
- McMahon, B. (1974), "Design of Rock Slopes Against Sliding on Pre-existing Fractures," 3rd CISRM, Vol. II-B, pp. 803-808.
- McMahon, B. (1975), "Probability of Failure and Expected Volume of Failure in High Rock Slopes," 2nd Australia-New Zealand Conference on Geomechanics, pp. 308-313.
- Miles, R.E. (1964), "Random Polygons Determined by Random Lines in a Plane," Proceedings, National Academy of Sciences, (USA), Vol 52, pp. 901-907 and 1157-1160.
- Miles, R.E. (1969), "Poisson Flats in Euclidean Space," Advanced Application Problems, Vol. 1 pp. 211-237.

- Miles, R.E. (1971), "Poisson Flats in Euclidean Space, Part II," Advanced Application Problems, Vol. 3, pp. 1-43.
- Miles, R.E. (1972), "The Random Division of Space," Supplement, Advanced Application Problems, pp. 243-266.
- Pariseau, W.G. (1973), "Influence of Rock Properties Variability on Mine Opening Stability," 9th Canadian Rock Mechanics Symposium, pp. 141-165.
- Rosso, R. (1976), "A Comparison of Joint Stiffness Measurements in Direct Shear, Triaxial Compression and In Situ," International Journal of Rock Mechanics and Mining Sciences, Vol. 13, No. 6, pp. 167-172.
- St. John, C. (1971). "Three-Dimensional Analysis of Jointed Rock Slopes," CISRM at Nancy, Paper II-9.
- Serrano, A.A. and E. Castillo (1974) "A New Concept About the Stability of Rock Masses," 3rd CISRM, Vol. II-B, pp. 829-826.
- Steffen, O.K.H. and J.E. Jennings (1974), "Definition of Design Joints for Two-Dimensional Rock Slope Analyses," 3rd CISRM, Vol. II-B, pp. 827-832.
- Steiner, W. (1977), Three-Dimensional Stability of Frictional Slopes, SM Thesis, M.I.T., 111 pp.
- Su, W.L., W.J. Wang and R. Stefanko (1970), "Finite Element Analysis of Underground Stresses Utilizing Stochastically Simulated Material Properties," Rock Mechanics Theory and Practice (ed. W.H. Somerton), SME/AIME, New York, pp. 253-266.
- Switzer, P. (1965), "A Random Set Process in the Plane with Markovian Property," Annals of Mathematical Statistics, Vol. 36, No. 6, pp. 1853-1863.
- Vanmarcke, E.H. (1977), "Probabilistic Modeling of Soil Profiles," ASCE Journal of the Geotechnical Engineering Division, Vol. 103, No. GT11, pp. 1227-1246.
- Veneziano, D. (19xx), "Probabilistic Model of Joints in Rock," Manuscript submitted to Geotechnique.

- Wittke, W. (1964), "Ein rechnerischer Weg zur Ermittlung der Standsicherheit von Böschungen in Fels mit durchgehenden, ebenen Absonderungsflächen," Principles in the Field of Geomechanics, Rock Mechanics and Engineering Geology, Supplementum I, 14th Symposium of the Austrian Regional Group of the International Society for Rock Mechanics, pp. 101-129.
- Wittke, W. (1965a) "Verfahren zur Berechnung der Standsicherheit belasteter und unbelasteter Felsböschungen," Rock Mechanics and Engineering Geology, Supplementum II, pp. 52-79.
- Wittke, W. (1965b) "Verfahren zur Standsicherheitsberechnung starrer, auf ebenen Flächen gelagerter Körper und die Anwendung der Ergebnisse auf die Standsicherheitsberechnung von Felsböschungen," Veröffentlichungen, des Technischen Hochschule Fridericiana in Karlsruhe, Heft 20.

Appendix A

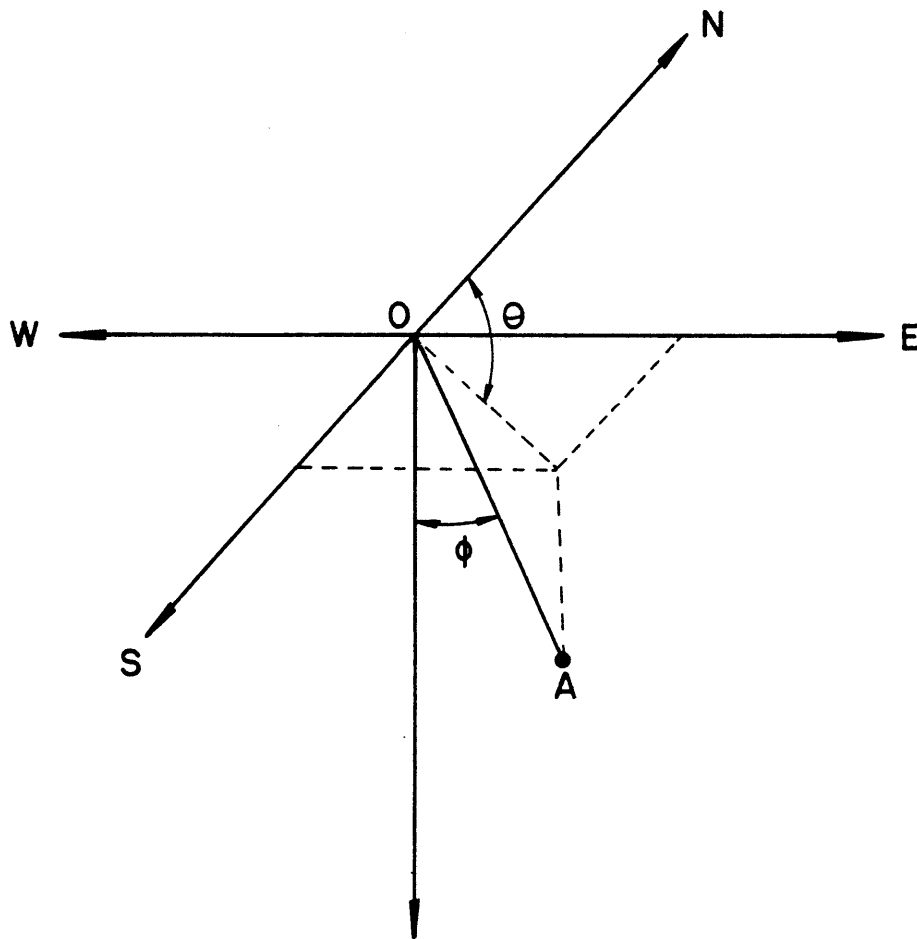
Spherical Distributions

A.0 Introduction

One of the inputs to DAYLITE is the pdf of joint orientation for each joint set. The user can choose from the six distributional forms described in this appendix. None of the six seem to be general enough to provide a good fit for any arbitrary compilation of real orientation data. The choice of an analytic form for a particular joint set should be based on the specific characteristics of its data base. Der-showitz (19xx) has developed a computer program that examines orientation data to find the best fitting distribution (and its requisite constants) from the six general forms.

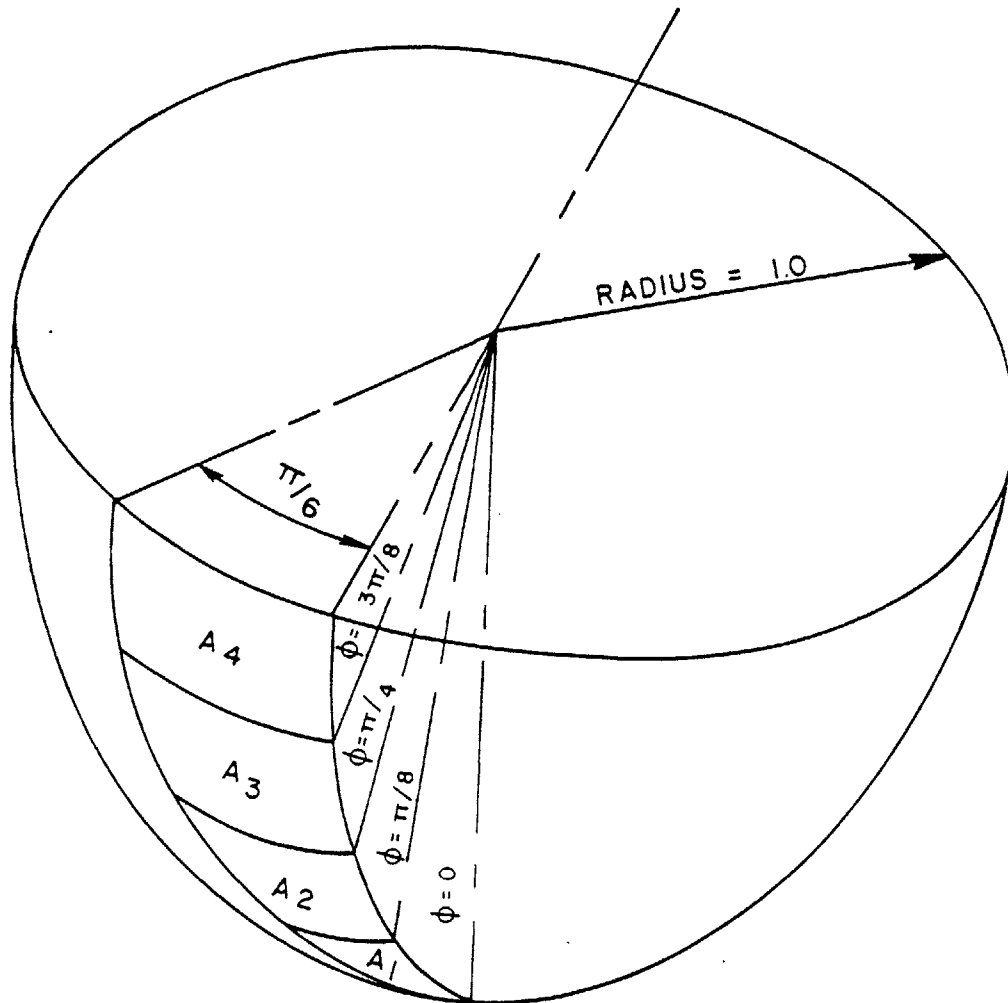
Figure A.1 shows the coordinate system used to describe orientation data. Joint planes are defined by the lower hemisphere projection of their poles. ϕ is the latitude while θ is the colatitude. θ is usually measured clockwise from North but other conventions are admissible.

Spherical coordinates are useful for describing joint orientations; however, they can become troublesome in interpreting or visualizing pdf's. The problem involves spherical surface areas: equal increments of latitude do not produce equal increments of surface areas. Figure A.2 depicts a spherical wedge of width $\frac{\pi}{6}$. The wedge is divided into four sections by small circles corresponding to ϕ values of $\frac{\pi}{8}$, $\frac{\pi}{4}$



OA = JOINT POLE

Figure A.1 Coordinate System For Joint Orientation



$$A_1 = 0.040$$

$$A_2 = 0.114$$

$$A_3 = 0.170$$

$$A_4 = 0.200$$

Figure A.2 Spherical Surface Areas

and $\frac{3\pi}{8}$. $\Delta\phi$ is a constant between any two circles, but the area between adjacent circles increases as ϕ increases.

Figure A.3 derives the general formula for the area of a spherical segment on a unit hemisphere:

$$A_s = 2\pi(1 - \cos \phi) \quad (\text{A.1})$$

A_s is the area of the entire segment ($\theta = 2\pi$). A , the area of a wedge of width θ , is:

$$A = 2\pi(1 - \cos \phi) \frac{\theta}{2\pi} \quad (\text{A.2})$$

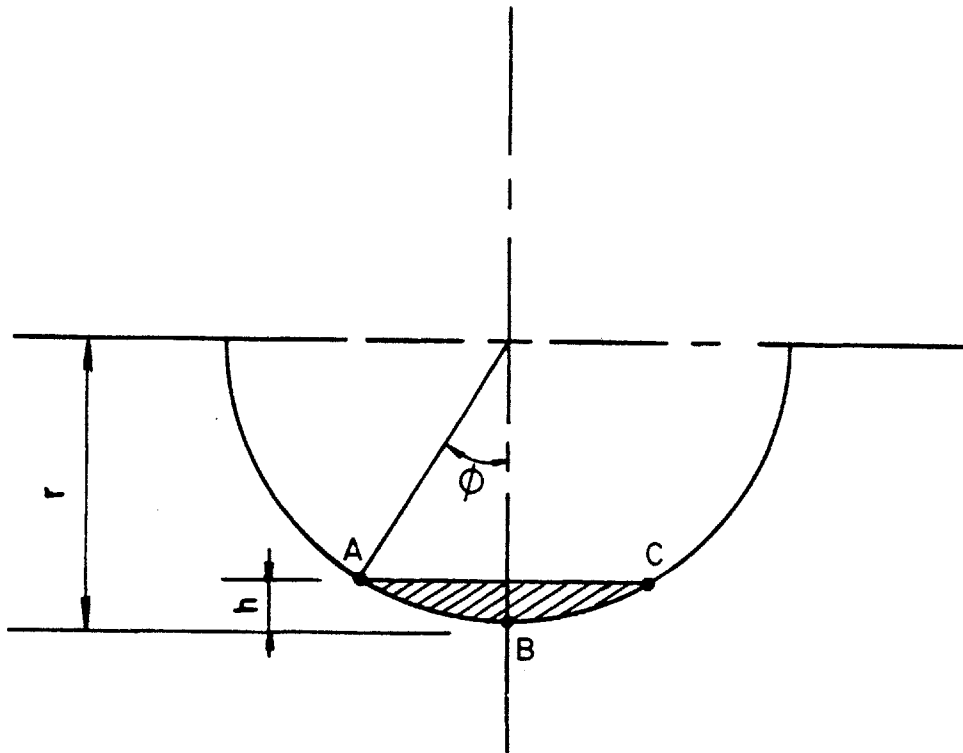
Taking the differential of each side:

$$dA = \sin \phi \, d\phi d\theta \quad (\text{A.3})$$

Thus, a differential increment of surface area is not merely the product of $d\phi$ and $d\theta$. It is a function of ϕ i.e., where the differential area is located on the hemisphere.

$\sin \phi$ is a correction factor that compensates for the fact that differential spherical segments defined by constant $d\phi$'s do not have equivalent areas. The $\sin \phi$ term appears in almost all the distributions discussed in this appendix. The lone exception is the bivariate normal which is actually defined on a plane rather than on a sphere.

The implications of the $\sin \phi$ term become apparent when one examines specific pdf's. The simplest pdf to examine is



AREA OF SPHERICAL SEGMENT A B C =

$$2 \pi r h = 2 \pi r^2 (1 - \cos \phi)$$

FOR $r = 1$: AREA = $2 \pi (1 - \cos \phi)$

Figure A.3 Surface Area of a Spherical Segment

the uniform distribution. In the uniform distribution every infinitesimal element on the surface of the hemisphere has an equal probability of containing a joint pole. The pdf has a constant value of $\frac{1}{2\pi}$ over the entire surface. Consider the marginal pdf of ϕ . By definition:

$$f(\phi) = \lim_{\Delta\phi \rightarrow 0} \frac{P[\phi - \Delta\phi < \phi < \phi + \Delta\phi]}{\Delta\phi} \quad (\text{A.4})$$

Table A.1 approximates $f(\phi)$ by dividing the domain of ϕ into 5° intervals and treating $f(\phi)$ as a constant over each interval. $P[\phi - \Delta\phi < \phi < \phi + \Delta\phi]$ is found by multiplying the area between the small circles defined by $\phi - \Delta\phi$ and $\phi + \Delta\phi$ by $1/(2\pi)$. (As explained earlier, this area increases with ϕ .) The results are plotted in Figure A.4 as a histogram. If the size of the interval were reduced to the point where $\Delta\phi$ approached zero, the histogram would become $f(\phi)$ -- the curve shown in Figure A.4.

$$f(\phi) = \sin \phi \quad (\text{A.5})$$

The fact that $f(\phi = 0) = 0$ does not imply that there is zero probability that a joint pole will be situated in the differential area located at the bottom of the hemisphere. That area, like any other area, has a probability of $\frac{dA}{2\pi}$. $\phi = 0$ is a singularity because that one coordinate completely defines the point; all other points require both a ϕ and a θ .

Table A.1 Numerical Approximation of $f(\phi)$ --Uniform Distribution

Interval		$\Delta\phi$	Surface Area (10^{-1})	Density of pdf	$P[\phi_{\text{MIN}} < \phi < \phi_{\text{MAX}}]$ (10^{-2})	$f(\phi)$
ϕ_{MIN}	ϕ_{MAX}					
0	5	5	0.239	$1/(2\pi)$	0.381	0.044
5	10	"	0.716	"	1.139	0.131
10	15	"	1.187	"	1.889	0.217
15	20	"	1.648	"	2.623	0.301
20	25	"	2.097	"	3.338	0.383
25	30	"	2.531	"	4.028	0.462
30	35	"	2.945	"	4.687	0.537
35	40	"	3.337	"	5.311	0.609
40	45	"	3.703	"	5.894	0.675
45	50	"	4.041	"	6.432	0.737
50	55	"	4.349	"	6.921	0.793
55	60	"	4.623	"	7.358	0.843
60	65	"	4.862	"	7.738	0.887
65	70	"	5.064	"	8.060	0.924
70	75	"	5.228	"	8.320	0.953
75	80	"	5.351	"	8.517	0.976
80	85	"	5.434	"	8.649	0.991
85	90	"	5.476	"	8.715	0.999

$\Sigma = 2\pi$

$\Sigma = 1.00$

Table A.1 Numerical Approximation of $f(\phi)$
263

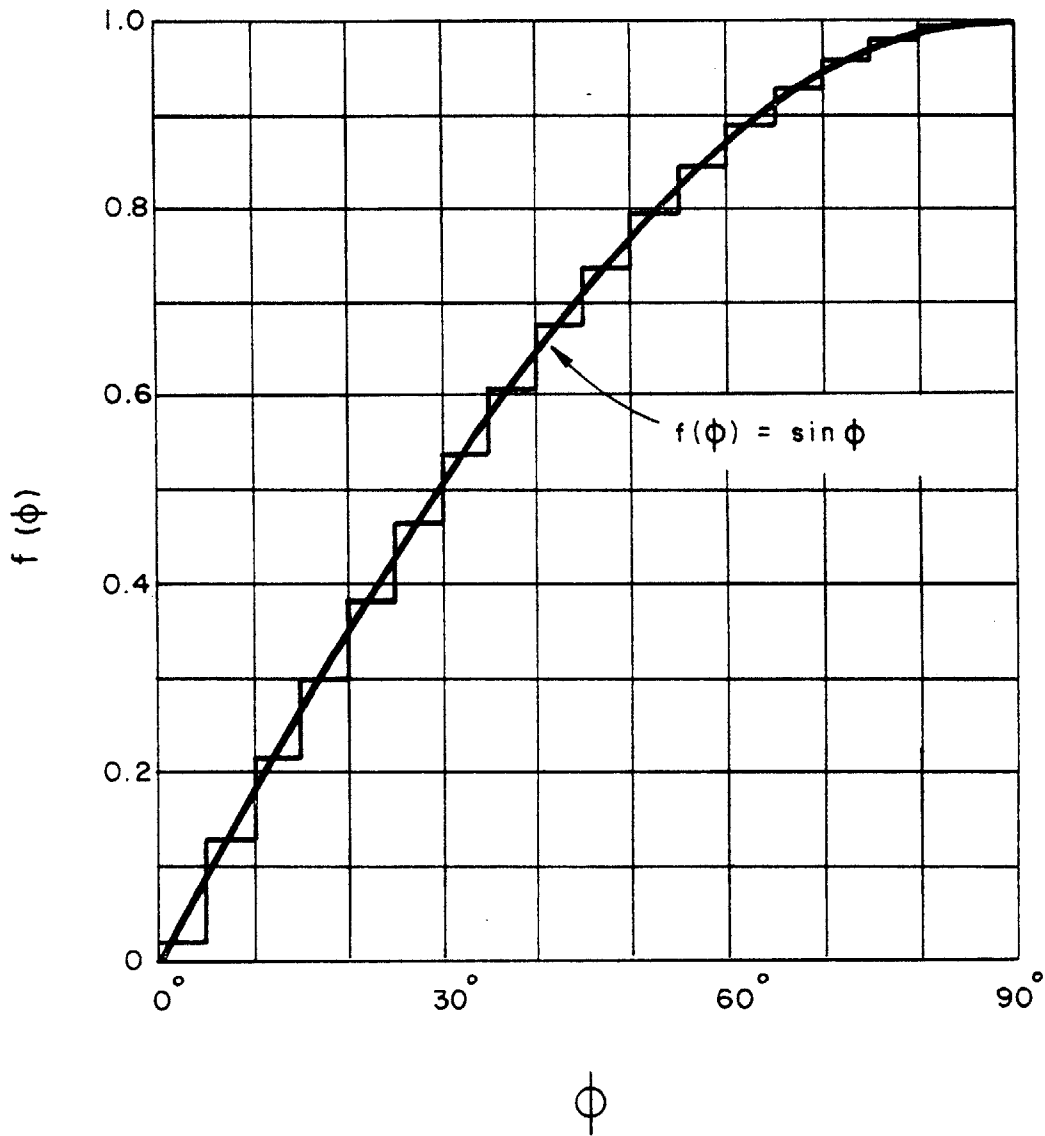


Figure A.4 $f(\phi)$ vs. ϕ for the Uniform Distribution
264

$\phi = 0$ is a unique point and the probability of finding a joint pole at that one point (or any other point) is zero. All other values of ϕ define small circles and there is a finite value of $f(\phi)$ for each circle. As ϕ increases the circles enlarge and $f(\phi)$ increases.

The remainder of the appendix will discuss the characteristics of specific distributions.

A.1 Uniform Distribution

The uniform distribution suggests that joint poles have no preferred orientation. The distribution has limited applicability with respect to real data but it does serve as a research tool because it represents the extreme limit of dispersion in orientation data.

As derived in the previous section:

$$f(\phi) = \sin \phi \quad (\text{A.5})$$

Since ϕ and θ are independent random variables:

$$f(\phi, \theta) = f(\phi)f(\theta) = \frac{1}{2\pi} \sin \phi \quad (\text{A.6})$$

Figure A.5 is a 3-dimensional representation* of the uniform distribution. It was developed by revolving the $\frac{1}{2\pi} \sin \phi$ curve through a θ angle of 2π about the $\phi = 0$ axis.

* For the sake of clarity, the curve is shown on an upper hemisphere. This same convention will be used for other pdf's in the appendix.

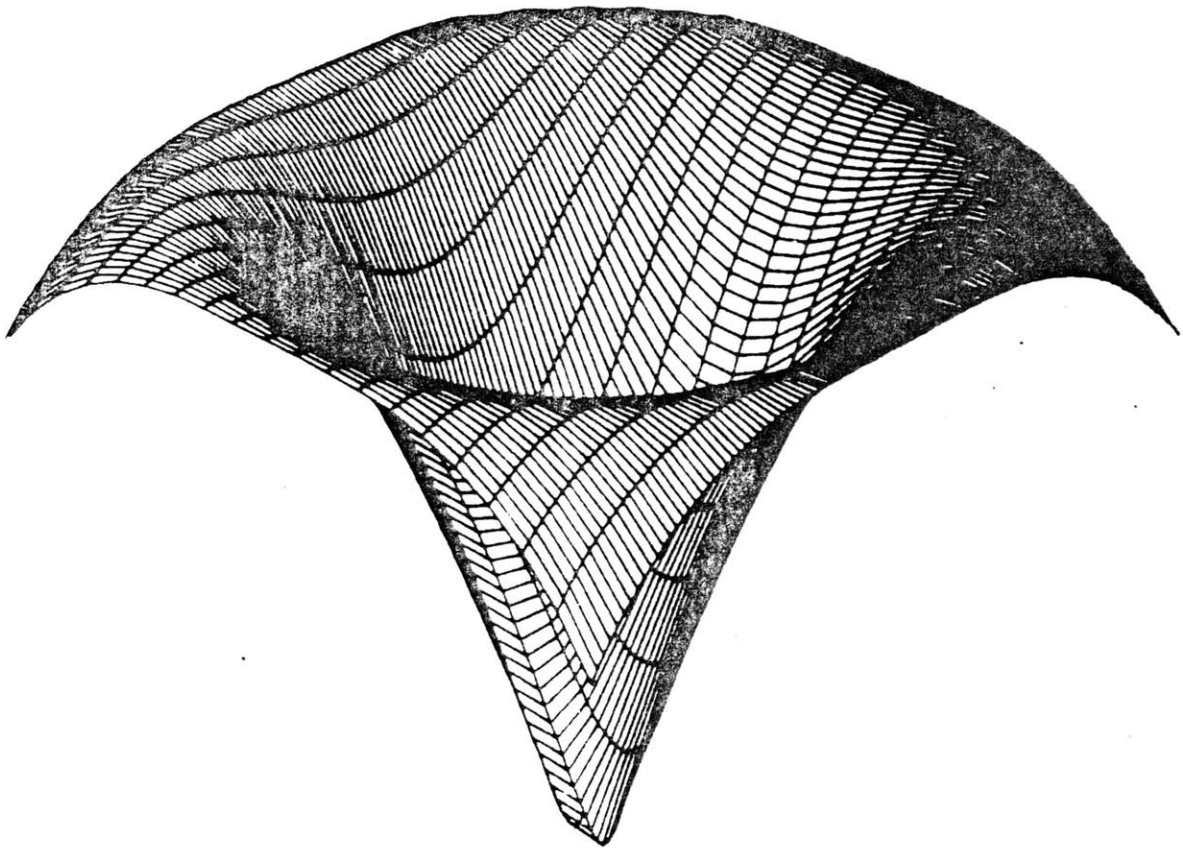


Figure A.5 Uniform Distribution

A.2 Fisher Distribution

The Fisher distribution is axially symmetric about its mean pole (θ_0, ϕ_0) .

$$f(\theta, \phi) = \frac{k}{4\pi \sinh(k)} e^{k \cos \eta} \sin \eta \quad (\text{A.7})$$

k is a dispersion coefficient and η is the angle between (θ, ϕ) and $(\theta_0, \phi_0)^*$. As indicated in Figure A.6, the density function begins at the origin, reaches a peak and then decays to 0 at high values of η . η can assume values up to π i.e., the distribution is defined over the entire sphere (not just a hemisphere). From a theoretical standpoint, the Fisher distribution is improper for joint data because pole diagrams only utilize a hemisphere i.e., $0 \leq \eta \leq \pi/2$. However, the distribution can be truncated at $\eta = \pi/2$ and normalized so that its integral over the hemisphere equals unity. λ , the normalizing constant, is the inverse of the cumulative distribution function at $\eta = \pi/2$.

$$\lambda = \frac{1}{1 - e^{-2k}} \quad (\text{A.8})$$

λ does not appreciably affect the pdf for values of k greater than 3. (A k of 3 corresponds to a λ of 1.0025.)

Figure A.7 shows a Fisher distribution with a k of 5.

* η can be found through vector algebra:

$$\eta = \cos^{-1} \left((\theta_0, \phi_0) \cdot (\theta, \phi) \right)$$

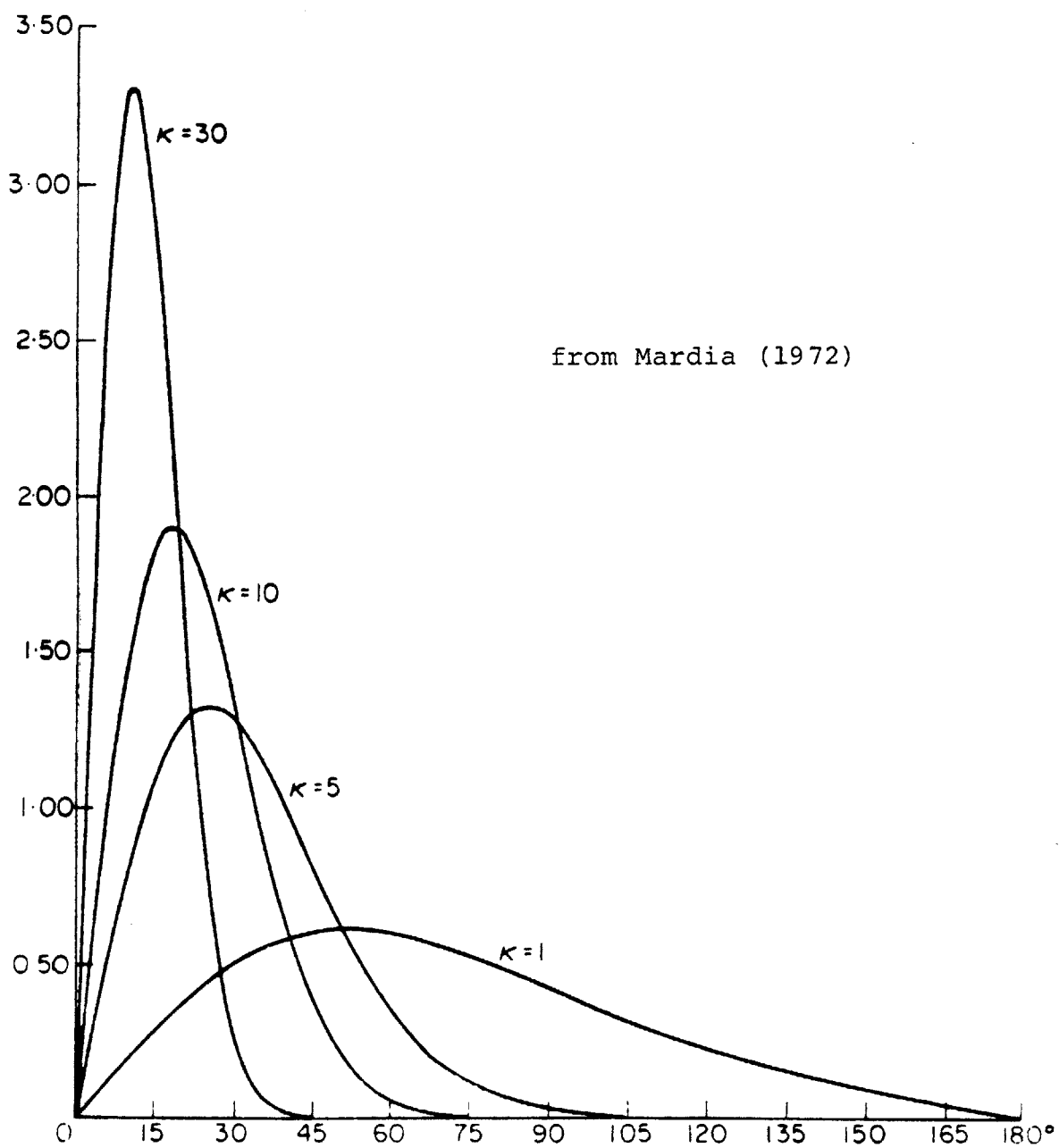


Figure A.6 $f(\eta)$ vs. η for the Fisher Distribution

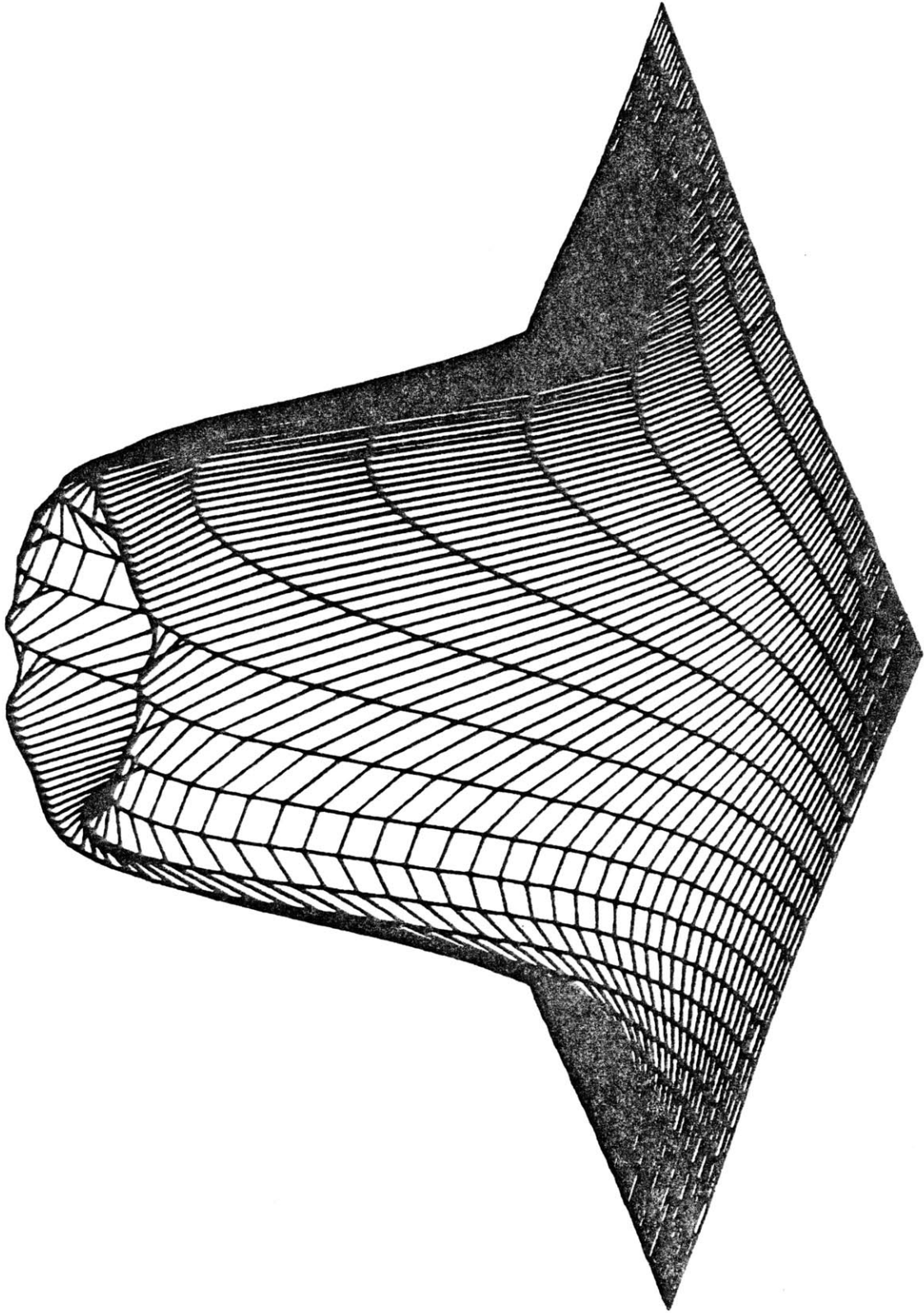


Figure A.7 Fisher Distribution ($k = 5$)

A.3 Arnold Distribution

The Arnold distribution is quite similar to the Fisher. Like the Fisher, it is axially symmetric about its mean pole; it does, however, have a slightly different form:

$$f(\theta, \phi) = \frac{k}{2\pi(e^k - 1)} e^{k \cos \eta} \sin \eta \quad (\text{A.9})$$

The Arnold distribution is antipodally symmetric* so only one half of the distribution is needed to describe orientation data. The normalizing constant is 2 and has been included in Equation (A.9).

Bridges (1977) pointed out that the Arnold and Fisher distributions are virtually identical for dispersion coefficients (k's) greater than 10.

A.4 Bingham Distribution

In general, the Bingham distribution is axially asymmetric; however, it is always symmetric with respect to two great circles termed the "major" and "minor" axes. The axes are orthogonal to each other as well as to the mean pole. The Bingham has five parameters: the orientation of the mean pole (θ_0, ϕ_0) , the orientation of the major axis $(\theta_1$ or $\phi_1)$ ** and two dispersion coefficients $(k_1$ and $k_2)$.

* Antipodal symmetry implies that the distribution is symmetric with respect to its equator.

** Since the mean pole and major axis are orthogonal, only θ_1 or ϕ_1 must be specified.

It is easier to work with the Bingham if the reference axes are rotated so that the new axes coincide with the major axis, minor axis and mean pole. (θ and ϕ define a direction with respect to the axes shown in Figure A.1; that same direction is described in the new system as θ^1 and ϕ^1 .) The direction ($\theta^1 = 0, \phi^1 = 90$) corresponds to the major axis while $\phi^1 = 0$ corresponds to the mean pole. In this new reference system the pdf has the following form:

$$f(\theta^1, \phi^1) = \lambda e^{(k_1 \cos^2 \theta^1 + k_2 \sin^2 \theta^1) \sin^2 \phi^1} \sin \phi^1 \quad (\text{A.10})$$

where λ is a normalizing constant.

The Bingham is antipodally symmetric; thus, λ should reflect the fact that joint poles are plotted in only one hemisphere.

Figure A.8 depicts an anisotropic Bingham distribution ($k_1 = -5, k_2 = -3$).

A.5 Dershowitz Distribution

From an analytic standpoint, the Dershowitz distribution resembles the Bingham*. The Dershowitz distribution decays as $\cos \phi$ rather than $\sin^2 \phi$. Like the Bingham, the Dershowitz involves a rotation of reference axes.

* From a probabilistic standpoint the Dershowitz distribution bears a closer resemblance to the Fisher than to the Bingham. Dershowitz (19xx) introduced the $(k_1 \cos^2 \theta^1 + k_2 \sin^2 \theta^1)$ term to make the Fisher anisotropic.

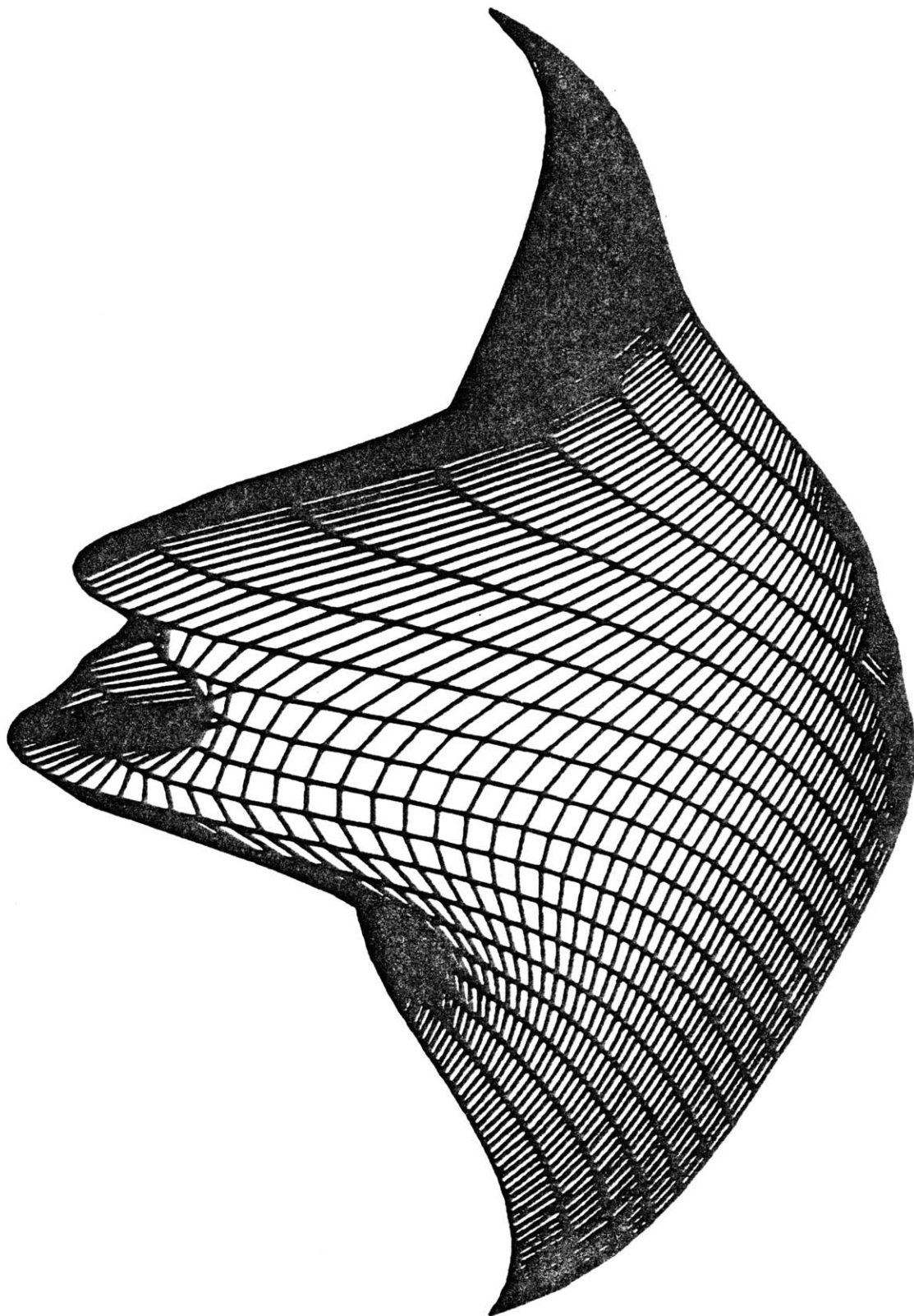


Figure A.8 Bingham Distribution ($k_1 = -5$; $k_2 = -3$)

$$f(\theta^1, \phi^1) = \lambda e^{(k_1 \cos^2 \theta^1 + k_2 \sin^2 \theta^1) \cos \phi^1 \sin \phi^1} \quad (\underline{\underline{A.11}})$$

Figure A.9 shows a Dershowitz distribution that has the same dispersion coefficients (k_1 and k_2) as the Bingham in Figure A.8.

A.6 Bivariate Normal Distribution

The bivariate normal is the Gaussian or normal distribution that describes the interrelationship of two random variables.

The distribution is not defined in terms of the points on the surface of a reference hemisphere but rather in terms of the projection of the points on a reference plane*. The distribution is first rotated so that its mean pole lies at the bottom of the reference hemisphere (Figure A.10). Next, all the points on the hemisphere are projected on to a horizontal reference plane through the relations

$$x = \cos \theta \quad (\text{A.12})$$

$$y = \sin \theta \quad (\text{A.13})$$

Finally, the x and y axes are rotated so that \bar{x} and \bar{y} coincide with the two axes of symmetry -- the major and minor axes.

* The distribution can be defined directly on ϕ and θ . For example, see Steffen and Jennings (1974).

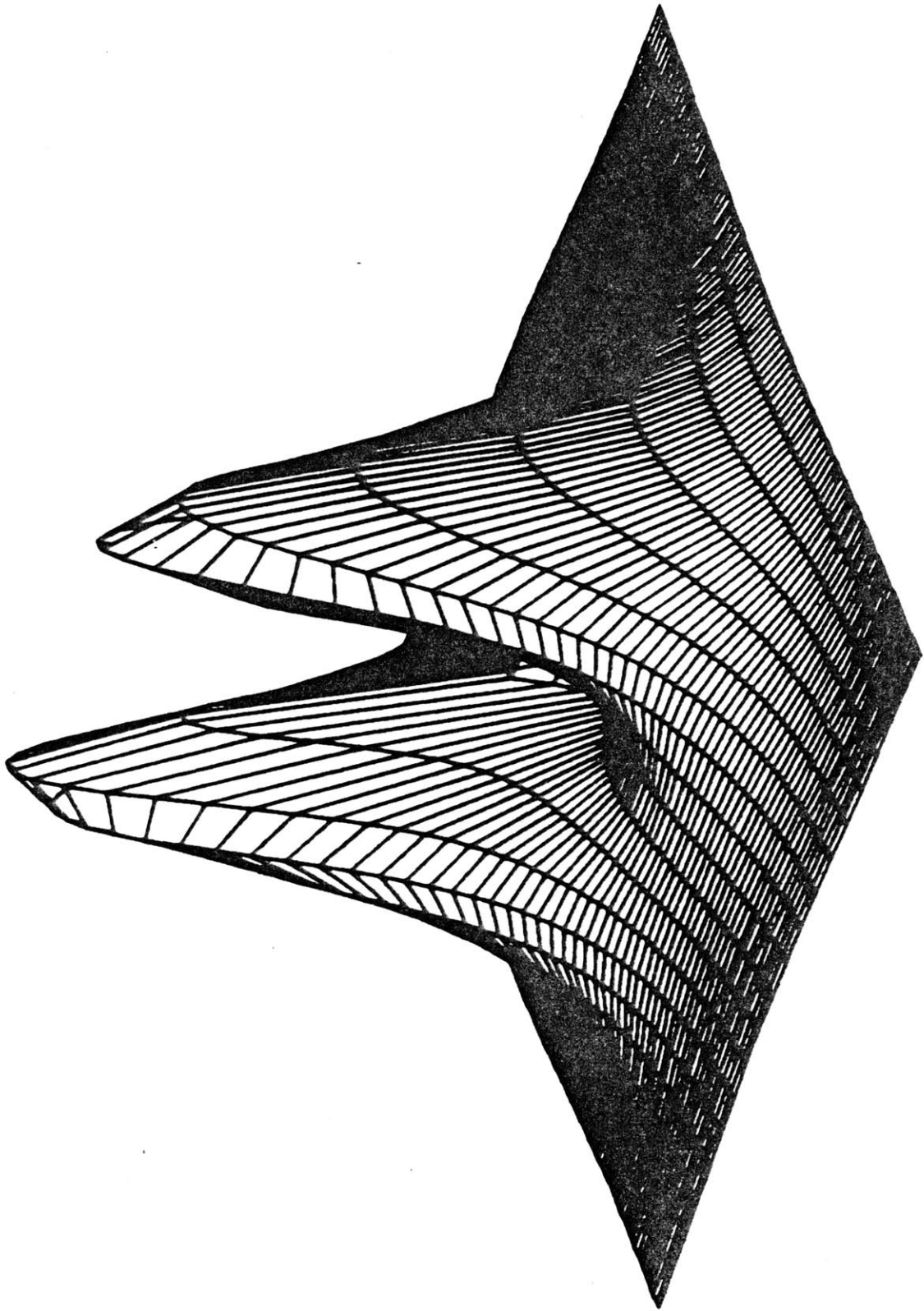


Figure A.9 Dershowitz Distribution ($k_1 = 5; k_2 = 3$)

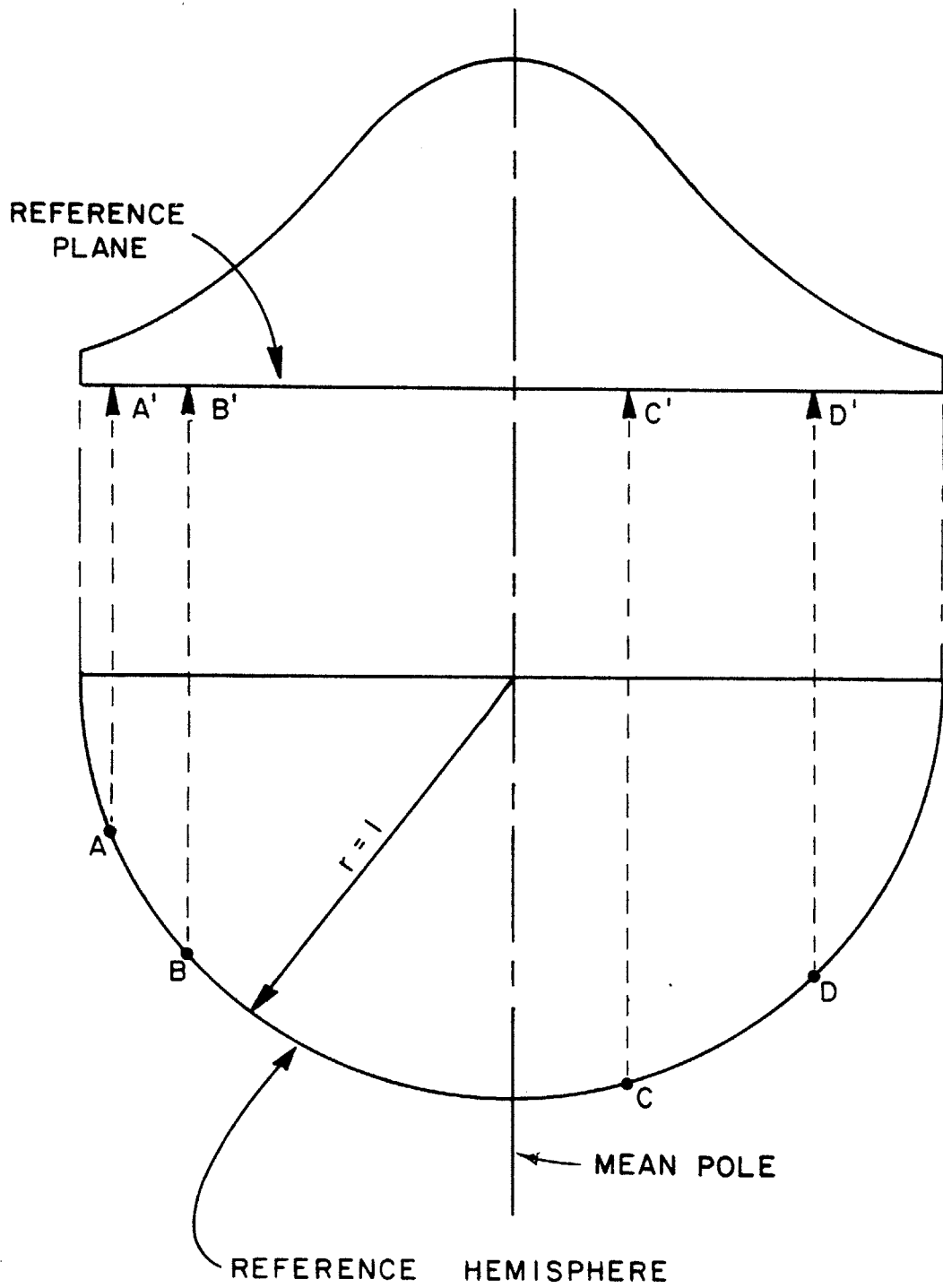


Figure A.10 Bivariate Normal Distribution--Projection on Plane

The distribution has the following form:

$$f(\bar{x}, \bar{y}) = \frac{1}{2\pi\sigma_{\bar{x}}\sigma_{\bar{y}}} e^{-\frac{1}{2} \left\{ \left(\frac{\bar{x}}{\sigma_{\bar{x}}} \right)^2 + \left(\frac{\bar{y}}{\sigma_{\bar{y}}} \right)^2 \right\}} \quad (\text{A.14})$$

The bivariate normal distribution involves five parameters: the orientation of the mean pole (θ_0, ϕ_0) , the orientation of the major axis $(\theta_1$ or $\phi_1)$ and the variances in the \bar{x} and \bar{y} directions $(\sigma_{\bar{x}}^2, \sigma_{\bar{y}}^2)$.

The bivariate normal is not an ideal distribution to use on orientation data because it assumes that both \bar{x} and \bar{y} are unbounded i.e., both \bar{x} and \bar{y} can range from $-\infty$ to ∞ . As suggested in Figure A.10, the distribution must be truncated at the locus of points $\bar{x}^2 + \bar{y}^2 = 1$. The normalization procedure is tedious because there is no closed form solution for the cumulative distribution function of a normal distribution. The pdf must be integrated numerically over the appropriate limits.

A.7 Summary

Table A.2 summarizes the six distributions described in this appendix.

Table A.2 Summary of Distributions

Distribution	Parameters			Total Number of Parameters	Antipodal Symmetry
	Vectors		Scalars		
	Mean Pole	Major Axis			
Uniform	--	--	--	0	yes
Fisher	θ_0, ϕ_0	--	k	3	no
Arnold	θ_0, ϕ_0	--	k	3	yes
Bivariate Normal	θ_0, ϕ_0	θ_1 or ϕ_1	$\sigma_{\bar{x}}^2, \sigma_{\bar{y}}^2$	5	no
Bingham	θ_0, ϕ_0	θ_1 or ϕ_1	k_1, k_2	5	yes
Dershowitz	θ_0, ϕ_0	θ_1 or ϕ_1	k_1, k_2	5	no

Table A.2 Summary of Distributions
277

Appendix B

Two Problems in Vector Algebra

This appendix solves two problems in vector algebra; the solutions are used in DAYLITE to locate points along the joint pole girdle (Section 3.2.4).

Problem 1

Given: the strike $(x_1, y_1, 0)$ and lower hemisphere pole (x_0, y_0, z_0) of plane A.

Find: the point (x, y, z) on A where a line L with a rake angle η pierces the unit hemisphere.

(Figure B.1)

\bar{A} , \bar{B} and \bar{C} are shown in Figure B.1 as the pole of the plane A, strike of plane A and direction of line L respectively. The three vectors have the following relationships:

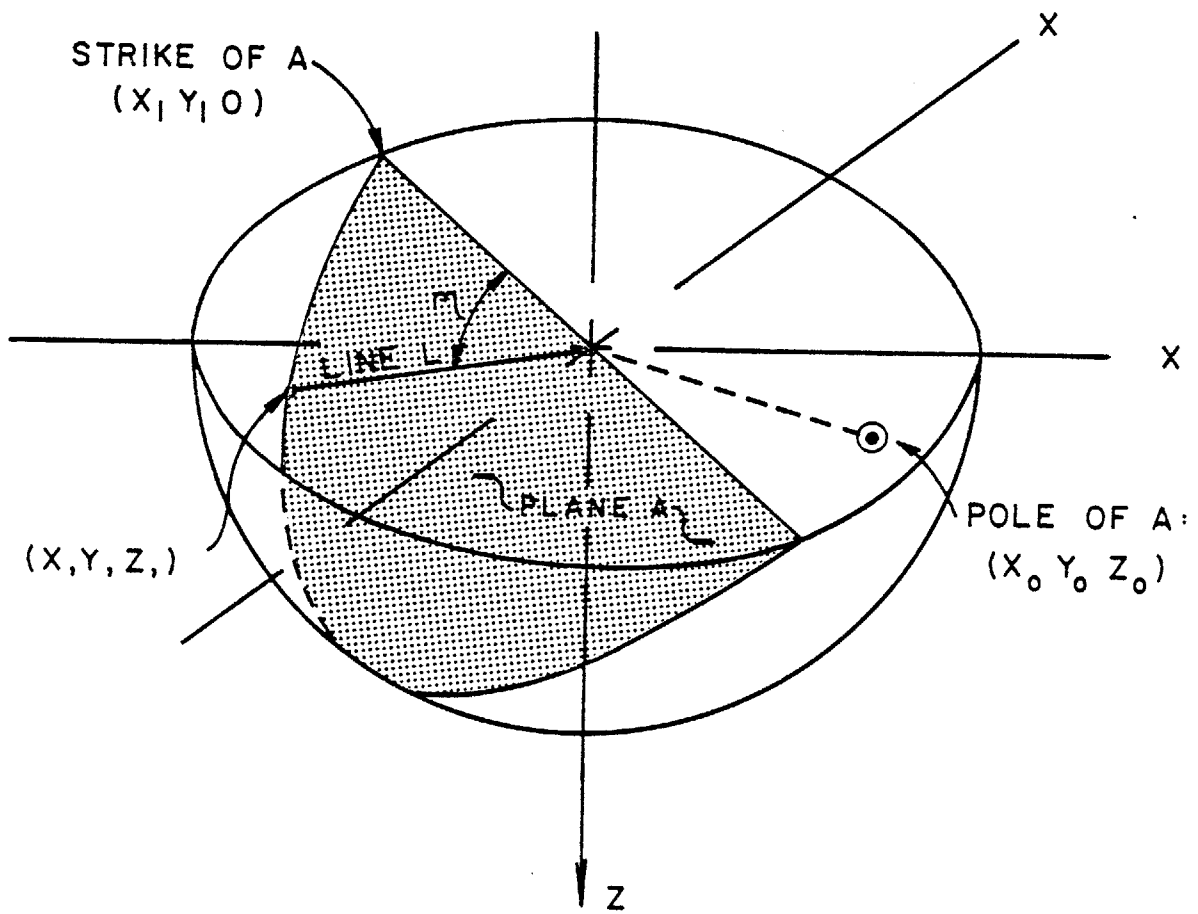
$$\bar{A} \cdot \bar{C} = x_0 x + y_0 y + z_0 z = \cos \pi/2 = 0 \quad (\text{B.1})$$

$$\bar{B} \cdot \bar{C} = x_1 x + y_1 y = \cos \eta \quad (\text{B.2})$$

Also, by definition, \bar{C} is a unit vector:

$$x^2 + y^2 + z^2 = 1 \quad (\text{B.3})$$

The problems can be solved by using the law of sines for spherical triangles. From Figure B.2:

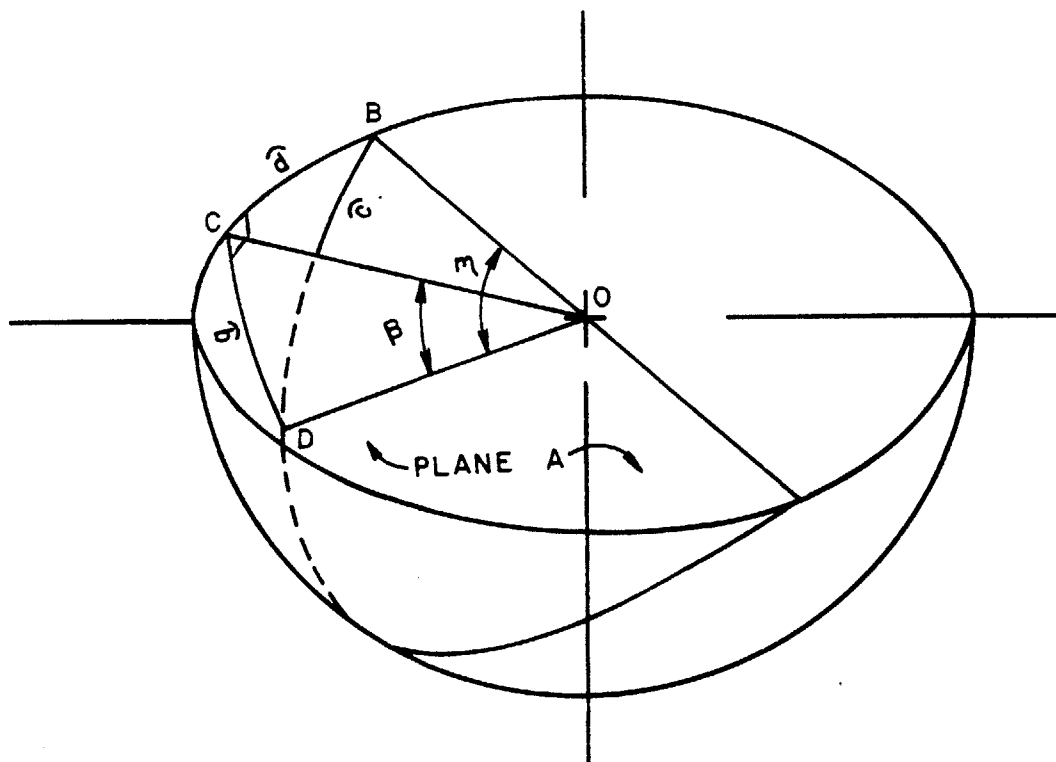


$$A = (X_0 \ Y_0 \ Z_0)$$

$$B = (X_1 \ Y_1 \ 0)$$

$$C = (X \ Y \ Z)$$

Figure B.1 Definition of η



SPHERICAL TRIANGLE BCD

B, C, D, : Spherical Angles at Corresponding Vertices

b, c, d, : Arc Lengths of sides

Law of Sines:

$$\frac{\sin B}{\widehat{b}} = \frac{\sin C}{\widehat{c}} = \frac{\sin D}{\widehat{d}}$$

Figure B.2 Law of Sines For Spherical Triangles

$$\frac{\sin B}{\tilde{b}} = \frac{\sin C}{\tilde{c}} = \frac{\sin D}{\tilde{d}} \quad (\text{B.4})$$

B, C and D are the spherical angles at the corresponding vertices of spherical triangle BCD. \tilde{b} , \tilde{c} and \tilde{d} are the arc lengths (in radians) of the respective opposite legs of the triangle; they are measured by their angles subtended at the center O of the sphere e.g., $\tilde{c} = \eta$

By definition (Figure B.2):

$$C = \pi/2 \quad (\text{B.5})$$

$$B = \text{Dip of Plane A} = (A)_{\text{Dip}} \quad (\text{B.6})$$

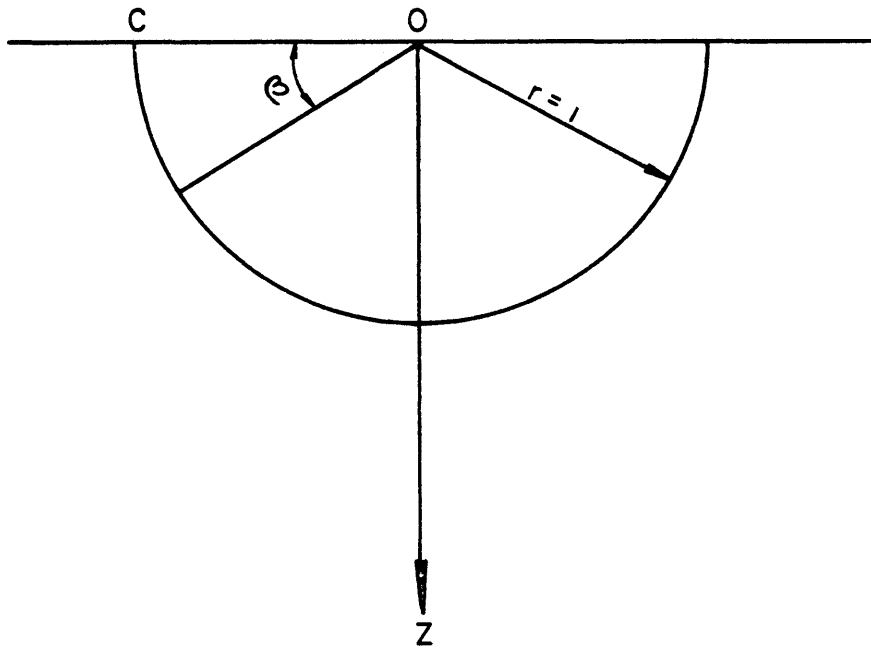
$$\frac{\sin C}{\tilde{c}} = \frac{1}{\eta} = \frac{\sin B}{\tilde{b}} = \frac{\sin (A)_{\text{Dip}}}{\tilde{b}} \quad (\text{B.7})$$

$$\tilde{b} = \sin (A)_{\text{Dip}} = \beta \quad (\text{B.7A})$$

Figure B.3 is a section along the line CO. From Figure B.3:

$$z = \sin \beta = \sin (\eta \sin (A)_{\text{Dip}}) \quad (\text{B.8})$$

From Equation B.2:



$$z = \sin \beta$$

Figure B.3 Derivation of z

$$y = \frac{\cos \eta - x_1 x}{y_1} \quad (\text{B.2A})$$

Substituting into Equation B.3:

$$x^2 + \frac{(\cos \eta - x_1 x)^2}{y_1^2} + z^2 = 1 \quad (\text{B.9})$$

$$x^2 + \frac{\cos^2 \eta - 2x_1 x \cos \eta + x_1^2 x^2}{y_1^2} + z^2 = 1 \quad (\text{B.10})$$

Collecting terms:

$$x^2 \left(1 + \frac{x_1^2}{y_1^2} \right) + x \left(\frac{-2x_1 \cos \eta}{y_1^2} \right) + z^2 - 1 + \frac{\cos^2 \eta}{y_1^2} = 0 \quad (\text{B.10A})$$

Equation (B.10A) can be solved with the quadratic formula.

$$x = \frac{-b \pm (b^2 - 4ac)^{1/2}}{2a} \quad (\text{B.11})$$

$$a = (1 + x_1^2 / y_1^2) \quad (\text{B.12})$$

$$b = (-2x_1 \cos \eta) / y_1^2 \quad (\text{B.13})$$

$$c = z^2 - 1 + \frac{\cos^2 \eta}{y_1^2} = \sin^2 \left(\eta \sin(A_{\text{Dip}}) \right) - 1 + \frac{\cos^2 \eta}{y_1^2} \quad (\text{B.14})$$

Finally, y can be found from Equation B.2A:

$$y = \frac{\cos \eta - xx_1}{y_1} \quad (\text{B.2A})$$

(The sign of the square root in Equation (B.11) can be determined by substituting the two roots into the relation $xx_0 + yy_0 + zz_0 = 0$ i.e., $A \cdot \bar{C} = 0$. The root which fulfills the equation is the correct one.)

Problem 2

Given: the point B with coordinates $(x_b, y_b, 0)$ and a point D with coordinates (x_d, y_d, z_d) that is η radians from point B on a unit hemisphere.

Find: the point E with coordinates (x, y, z) that is η radians from B and $\delta/2$ radians from D

(Figure B.4).

Points B, D and E are shown in Figure B.1. \bar{B}, \bar{D} and \bar{E} are the vectors from the origin to the respective points. The three vectors have the following relationships:

$$\bar{B} \cdot \bar{E} = x_b x + y_b y = \cos \eta \quad (\text{B.15})$$

$$\bar{D} \cdot \bar{E} = x_d x + y_d y + z_d z = \cos \delta/2 \quad (\text{B.16})$$

Also, by definition, E is a unit vector:

$$x^2 + y^2 + z^2 = 1 \quad (\text{B.17})$$

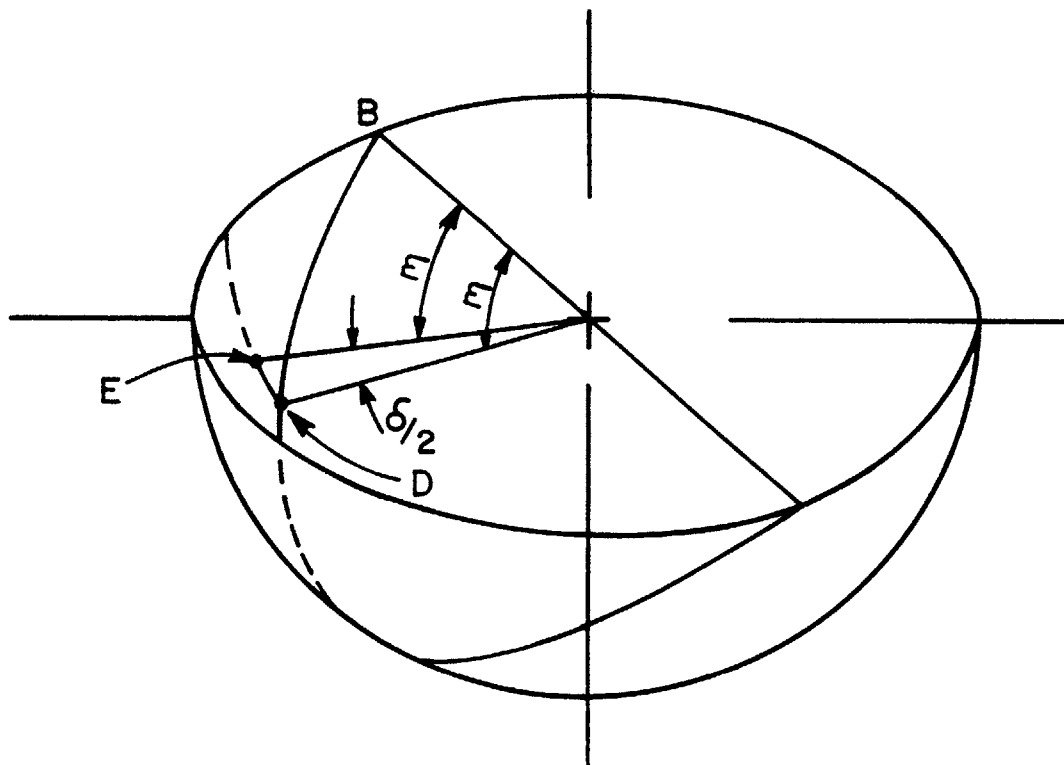


Figure B.4 Location of Points B, D and E

Multiplying Equation (B.15) by x_d and Equation (B.16) by x_b :

$$x_b x x_d + y_b y x_d = x_d \cos \eta \quad (\text{B.15A})$$

$$x_d x x_b + y_d y x_b + z_d z x_b = x_b \cos \delta/2 \quad (\text{B.16A})$$

Subtracting:

$$y(y_b x_d - y_d x_b) - z_d z x_b = x_d \cos \eta - x_b \cos \delta/2 \quad (\text{B.18})$$

Letting $P = x_d \cos \eta - x_b \cos \delta/2$ and solving for y ;

$$y = \frac{z_d z x_b + P}{(y_b x_d - y_d x_b)} \quad (\text{B.18A})$$

Multiplying Equation (B.15) by y_d and Equation (B.16) by y_b :

$$x_b x y_d + y_b y y_d = y_d \cos \eta \quad (\text{B.15B})$$

$$x_d x y_b + y_d y y_b + z_d z y_b = y_b \cos \delta/2 \quad (\text{B.16B})$$

Subtracting:

$$x(x_b y_d - x_d y_b) - z_d z y_b = y_d \cos \eta - y_b \cos \delta/2 \quad (\text{B.19})$$

Letting $q = y_d \cos \eta - y_b \cos \delta/2$ and solving for x :

$$x = \frac{z_d z y_b + q}{(x_b y_d - x_d y_b)} \quad (\text{B.19A})$$

Defining r as

$$r = \frac{1}{(y_b x_d - y_d x_b)^2} = \frac{1}{(x_b y_d - x_d y_b)^2} \quad (\text{B.20})$$

Substituting Equations (B.18A), (B.19A) and (B.20) into Equation (B.17):

$$r(z_d z x_b + p)^2 + r(z_d z y_b + q)^2 + z^2 = 1 \quad (\text{B.21})$$

$$\begin{aligned} r p^2 + r 2 p z_d z x_b + r z_d^2 z^2 x_b^2 \\ + r q^2 + r 2 q z_d z y_b + r z_d^2 z^2 y_b^2 \\ + z^2 - 1 = 0 \end{aligned} \quad (\text{B.21A})$$

Grouping terms:

$$\begin{aligned} z^2 \left[r z_d^2 (x_b^2 + y_b^2) + 1 \right] + z \left[2 r z_d (p x_b + q y_b) \right] + (r p^2 + r q^2 - 1) \\ = 0 \end{aligned} \quad (\text{B.21B})$$

$$\text{Since } z_b = 0, \quad x_b^2 + y_b^2 = 1 \quad (\text{B.22})$$

Thus, Equation (B.20) can be simplified to:

$$z^2(rz_d^2 + 1) + z\left(2rz_d(Px_b + qY_b)\right) + (rp^2 + rq^2 - 1) = 0 \quad \text{(B.21C)}$$

Equation (B.21C) can be solved with the quadratic formula:

$$z = \frac{-b \pm (b^2 - 4ac)^{\frac{1}{2}}}{2a} \quad \text{(B.23)}$$

$$a = rz_d^2 + 1 \quad \text{(B.24)}$$

$$b = 2rz_d(Px_b + qY_b) \quad \text{(B.25)}$$

$$c = rp^2 + rq^2 - 1 \quad \text{(B.26)}$$

x and y can be found by substituting z into Equations (B.19A) and (B.18A) respectively.

The positive and negative roots of Equation (B.23) correspond to solutions for point E $\delta/2$ radians above point D and $\delta/2$ radians below point D.

Appendix C

Computer Program DAYLITE

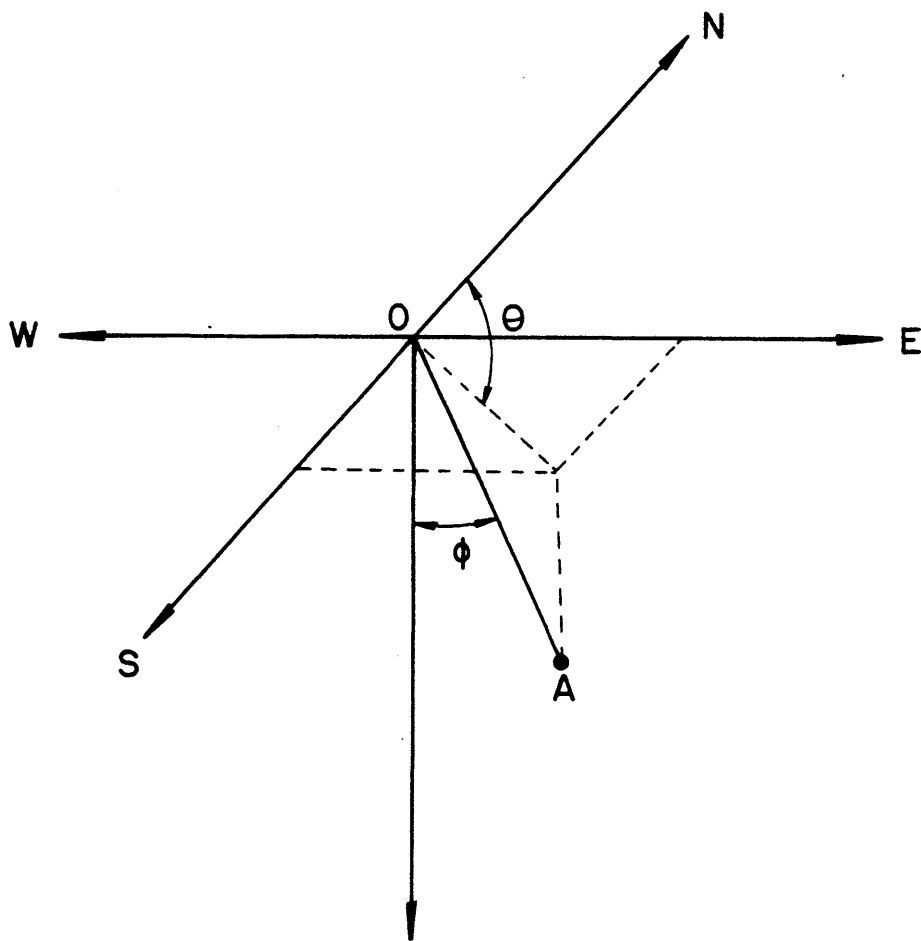
DAYLITE calculates the probability density function (pdf) for the orientation of the line of intersection of two joint planes. The orientations of the planes are characterized in terms of the spherical distributions discussed in Appendix A. The program uses the numerical integration technique that is presented in Chapter 3. The primary input parameters to the program are the pdf's of the two joint sets and the orientation of the slope face. The output consists of the various probabilities defined in Section 3.2.7:

$P[\theta_i, \phi_i]$ - the probability that a wedge (regardless of its shape) will have a line of intersection oriented in the (θ_i, ϕ_i) direction.

$P[\theta_i, \phi_i, \psi_j]$ - the probability that a wedge with a central angle of ψ_j (regardless of β_1) will have a line of intersection oriented in the (θ_i, ϕ_i) direction.

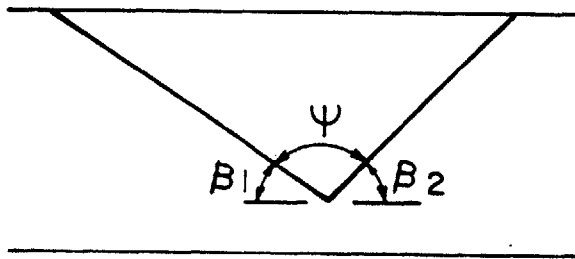
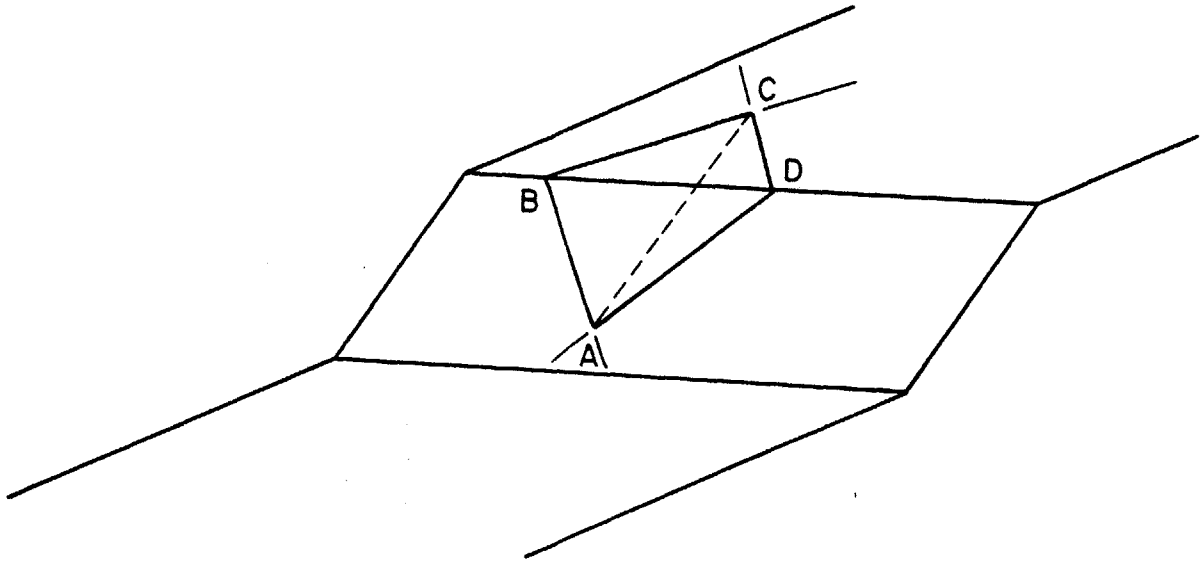
$P[\theta_i, \phi_i, \psi_j, (\beta_1)_k]$ - the probability that a wedge with a central angle of ψ_j and a β_1 of $(\beta_1)_k$ will have a line of intersection oriented in the (θ_i, ϕ_i) direction.

θ, ϕ, ψ and β_1 are defined in Figures C.1 and C.2.



OA = JOINT POLE

Figure C.1 Definitions of θ and ϕ



SECTION PERPENDICULAR TO AC

Figure C.2 Definitions of ψ and β_1
291

C.1 Coordinate System

All orientations are expressed in geologic notation: strike and dip for a plane; strike and plunge for a line. The directions of the lines of intersection are also defined in terms of the x,y,z coordinate system shown in Figure C.3. The computer program SWARS-2MC (Appendix F) uses this same Cartesian system so that the output from DAYLITE will be compatible with the input to SWARS-2MC.

C.2 Input

Unless otherwise noted the inputs do not have to be right justified in their respective columns. The term "integer" implies that the number is expressed without a decimal point.

Angular input is always in degrees.

Card #1

Strike of the Slope (S1S, STRS, S2S) is entered in geologic notation in columns 1 to 6. Geologic strike must be expressed in the northern quadrants and the angle is expressed with one decimal place. (Example: N45.0E)

Dip of the Slope (DIPS, D1S, D2S) is entered in geologic notation in columns 11 to 16. Dip directions must indicate a particular quadrant i.e., NE, NW, SE, SW. The angle is expressed with one decimal place. (Example: 36.0NE)

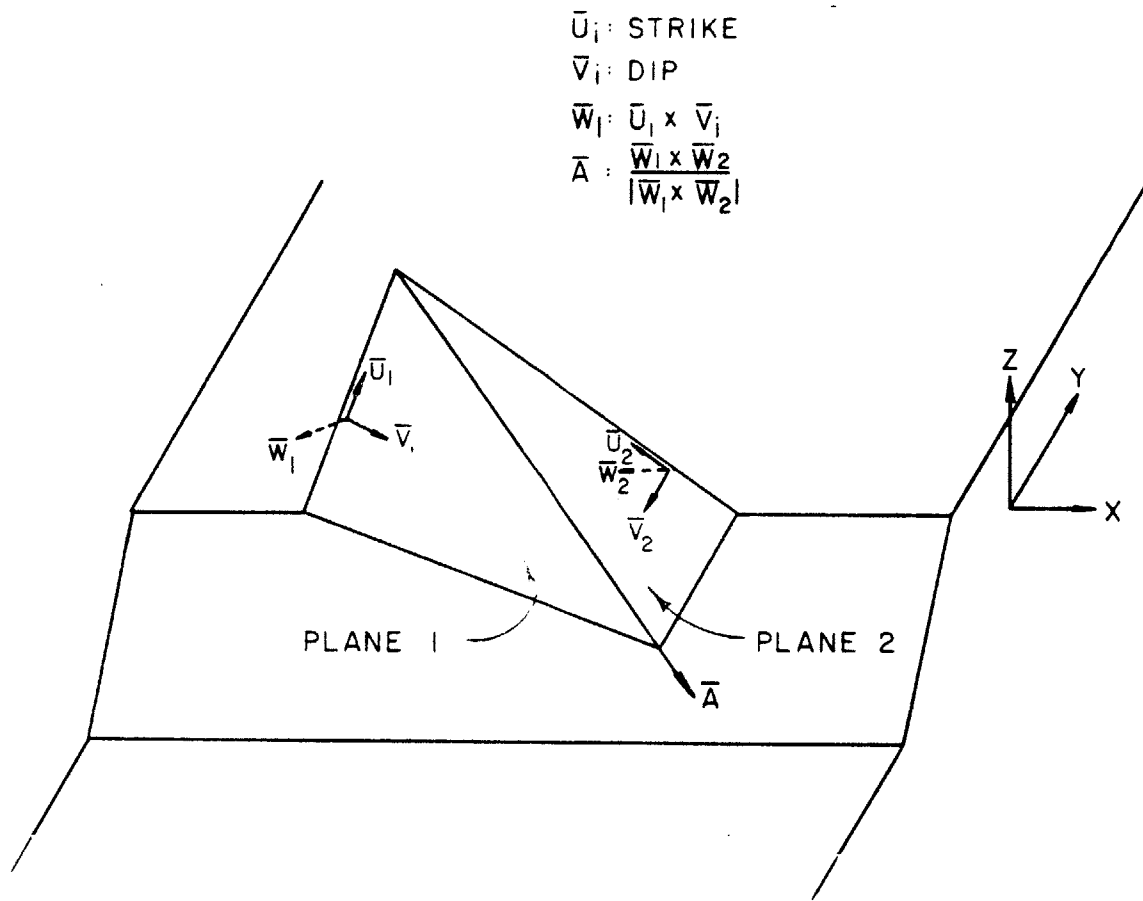


Figure C.3 Orientation of X, Y and Z Axes

Card #2

Card #2 inputs the analysis criteria discussed in Section 3.3.

$\underline{\epsilon}$ (DEGN) is an angular dimension which controls the size of the cells in the critical zone. It is entered in columns 1 to 10 with a maximum of 2 decimal places.

$\underline{\alpha}$ (FRIC) is an angular dimension which enables the user to shorten the analysis by ignoring lines of intersection with very shallow plunges. The program will not examine any lines of intersection that plunge at an angle less than α (Section 3.2.1). FRIC is entered in columns 11 to 20 with a maximum of two decimal places. The program will default to FRIC = 0.0 if those columns are left blank.

$\overline{\psi}$ (DEGMAN) is an angular dimension that enables the user to ignore very narrow wedges. The program will not examine any wedges that have a central angle less than $\overline{\psi}$ (Section 3.3). DEGMAN is entered in columns 21 to 30 with a maximum of 2 decimal places. The program will default to DEGMAN = DEGN if those columns are left blank.

$\underline{\Delta\psi}$ (WEDINC) is an angular dimension that enables the user to consolidate the output into ranges of β_1 angles rather than individual β_1 angles (Section 3.3). WEDINC is entered in columns 31 to 40 with a maximum of 2 decimal places. The program will default to WEDINC = DEGN if those columns are left blank.

Card #3

The first two parameters on card #3 specify the distributional forms* of the two joint sets. The code is as follows:

- 0 : Uniform Distribution
- 1 : Fisher Distribution
- 2 : Arnold Distribution
- 3 : Bingham Distribution
- 4 : Dershowitz Distribution
- 5 : Bivariate Normal Distribution

Pdf Code for Joint Set 1 (NDIST1) is entered as an integer in column 10.

Pdf Code for Joint Set 2 (NDIST2) is entered as an integer in column 20.

Wedge Code (NCODE) determines which sets of joints should be combined to form wedges. If a '1' is entered in column 30 the program will calculate the pdf of the line of intersection of wedges formed by two joints from set 1. If a '2' is entered in column 30 the program will calculate the pdf of wedges formed by two joints from set 2. If a '3' is entered in column 30 the program will calculate the pdf of wedges formed by a joint from set 1 and a joint from set 2. If any integer greater than 3 is entered in column 30 the program will examine all three cases.

* The six distributions are discussed in Appendix A.

Cards #4 and #5

Cards #4 and #5 must contain all the parameters required to analytically define the pdf's specified on Card #3.

Card #4 contains information relating to joint set 1 while Card #5 contains information relating to joint set 2. The information on the cards depends on the respective pdf's:

Uniform Distribution: The uniform distribution is nonparametric so the program needs no additional information. The input card i.e., Card #4 or Card #5 should be eliminated. (If joint set 1 has a uniform distribution the program will use the parameters on Card #4 to define joint set 2.)

Fisher Distribution: The Fisher distribution has the following form:

$$f(\theta, \phi) = \frac{K}{4 \sinh(K)} e^{K \cos \eta} \sin \eta \quad (C.1)$$

η is the angle between the mean pole of the distribution and the (θ, ϕ) direction. The distribution requires three input parameters - one is K, the dispersion coefficient, the other two define the orientation of the mean plane.

Mean Strike: (FA1S, STRFA, FA2S) is entered in geologic notation in columns 1 to 6 of Cards #4 and #5. Geologic strike must be expressed in the northern quadrants

* The program will compute the normalizing constant to ensure that the integral of the distribution over the surface of the hemisphere is unity.

and the angle is expressed with one decimal place. (Example: N45.0E)

Mean Dip: (DIPFA, D1FA, D2FA) is entered in geologic notation in columns 11 to 16 of Cards #4 and #5. Dip directions must indicate a particular quadrant i.e., NE, NW, SE, SW. The angle is expressed with one decimal place. (Example: 36.0NE)

Dispersion Coefficient: (FAK) is entered in columns 21 to 30 of Cards #4 and #5 with a maximum of 5 decimal places.

Arnold Distribution: The Arnold distribution is very similar to the Fisher:

$$f(\theta, \phi) = \frac{K}{2(e^K - 1)} e^{K \cos \eta} \sin \eta \quad (C.2)$$

Like the Fisher, the Arnold has three parameters: a dispersion coefficient and two parameters to define the orientation of the mean plane. The format for inputting the parameters is identical to that of the Fisher distribution.

Bingham Distribution: The Bingham distribution has the following form:

$$f(\theta', \phi') = K_1 e^{(K_2 \cos^2 \theta' + K_3 \sin^2 \theta')} \sin^2 \phi' \sin \phi' \quad (C.3)$$

where θ' and ϕ' are the colatitude and latitude in the spherical coordinate system in which $\phi' = 0$ is the mean pole and

($\theta' = 0$, $\phi' = 90^\circ$) is the major axis. In general, the (θ' , ϕ') system will not coincide with the conventional coordinate system i.e., the (θ , ϕ) system shown in Figure C.1. The program develops transformation relations so that the pdf in the direction expressed in the (θ , ϕ) system can be evaluated through Equation (C.3). The input parameters include three coefficients (K_1 , K_2 and K_3 as shown in Equation (C.3)), the orientations (in the (θ , ϕ) system) of the mean plane and the major plane. The major plane is the plane whose pole forms the major axis.

Mean Strike: (B1S, BS, B2S) is entered in geologic notation in columns 1 to 6 of cards #4 and #5. Geologic strike must be expressed in the northern quadrants and the angle is expressed with one decimal place. (Example: N45.OE)

Mean Dip: (BD, B1D, B2D) is entered in geologic notation in columns 11 to 16 of cards #4 and #5. Dip directions must indicate a particular quadrant i.e., NE, NW, SE, SW. The angle is expressed with one decimal place. (Example: 36.ONE)

Major Strike:* (AB1S, BAS, AB2S) is entered in columns 21 to 26 of cards #4 and #5 in a manner similar to the mean strike.

Major Dip:* (ABD, ABD1, ABD2) is entered in columns 31 to 36 of cards #4 and #5 in a manner similar to the mean dip.

* Since the mean pole and major axis are orthogonal, either the major strike or the major dip (in addition to the mean pole) will completely define the reference axes. As a precaution against inadvertent errors the user must input both the major dip and strike. The program will check that the input is consistent.

K₁: (DISCO (I,2)) is a normalizing constant that is entered in columns 41 to 50 of Cards #4 and #5 with a maximum of 3 decimal places. In selecting a value for K₁ the user should assure himself that the integral of the pdf over the unit hemisphere in unity. (See Section A.4.)

K₂: (DISCO (I,3)) is a dispersion coefficient that is entered in columns 51 to 60 of Cards #4 and #5 with a maximum of 3 decimal places.

K₃: (DISCO (I,4)) is a dispersion coefficient that is entered in columns 61 to 70 of Cards #4 and #5 with a maximum of 3 decimal places.

Dershowitz Distribution: The analytic form of the Dershowitz distribution is very similar to the Bingham:

$$f(\theta', \phi') = K_1 e^{(K_2 \cos^2 \theta' + K_3 \sin^2 \theta') \cos \phi' \sin \phi'} \quad (C.4)$$

Like the Bingham, the Dershowitz has 3 coefficients, a mean plane and a major plane. The format for inputting the parameters is identical to that of the Bingham distribution.

Bivariate Normal Distribution: The bivariate normal distribution has the following form:

$$f(\bar{X}, \bar{Y}) = K e^{-\frac{1}{2} \left((\bar{X}/\sigma_{\bar{X}})^2 + (\bar{Y}/\sigma_{\bar{Y}})^2 \right)} \quad (C.5)$$

As discussed in Appendix A (Section A.6) \bar{X} and \bar{Y} represent coordinates of projections from the reference hemisphere on to a plane. \bar{X} is the planar distance measured along the projection of the major axis while \bar{Y} is the distance along the projection of the minor axis. The input parameters include the 3 coefficients (K , $\sigma_{\bar{X}}$, and $\sigma_{\bar{Y}}$), the orientation of the mean plane and the orientation of the major plane. The major plane is the plane whose pole forms the major axis.

Mean Strike: (B1S, BS, B2S) is entered in geologic notation in columns 1 to 6 of cards #4 and #5. Geologic strike must be expressed in the northern quadrants and the angle is expressed with one decimal place. (Example: N45.0E)

Mean Dip: (BD, B1D, B2D) is entered in geologic notation in columns 11 to 16 of cards #4 and #5. Dip directions must indicate a particular quadrant i.e., NE, NW, SE, SW. The angle is expressed with one decimal place. (Example: 36.0NE)

Major Strike:* (AB1S, BAS, AB2S) is entered in columns 21 to 26 of cards #4 and #5 in a manner similar to the mean strike.

Major Dip:* (ABD, ABD1, ABD2) is entered in columns 31 to 36 of cards #4 and #5 in a manner similar to the mean dip.

K: (DISCO (I,2)) is a normalizing constant that is entered in columns 41 to 50 of cards #4 and #5 with a maximum
* Specifying both the major strike and the major dip is redundant. The subject is discussed in a footnote relating to the Bingham distribution.

of 3 decimal places. In selecting a value for K the user should assure himself that the integral of the pdf over the unit hemisphere is unity. As mentioned in Appendix A, the bivariate normal must be truncated when used to describe orientation data. (See Section A.6.)

$\sigma_{\bar{X}}^2$: (DISCO (I,3)) is the variance along the \bar{X} axis. It is entered in columns 51 to 60 of Cards #4 and #5 with a maximum of 3 decimal places.

$\sigma_{\bar{Y}}^2$: (DISCO (I,4)) is the variance along the \bar{Y} axis. It is entered in columns 61 to 70 of Cards #4 and #5 with a maximum of 3 decimal places.

DAYLITE Listing

C
C
C
C
C
C
C

DAYLITE

THIS PROGRAM CALCULATES THE PROBABILITY DENSITY FUNCTION
OF THE ORIENTATION OF THE LINE OF INTERSECTION OF TWO
JOINT PLANES. THE PROGRAM UTILIZES A LOWER HEMISPHERE
PROJECTION OF JOINT POLES. THE COLATITUDE (AZIM) IS
MEASURED CLOCKWISE FROM NORTH. THE LATITUDE (BETA)
EQUALS 90 - DIP.

REAL NO
DIMENSION DISCO(2,13), PJT(10,20), ZZ(91), PLINED(3,10,20)
DIMENSION X(5), Y(5), Z(5), PROB(2,5), SNBET(180)
DATA NO,SO,ET,WT/'N','S','E','W'/
NRD = 5
NWR = 6
NOPT = 0
PI = 3.14159265
PI2 = PI/2.0
PIF = PI/180.
TPRO1 = 0.0
TPRO2 = 0.0
TPRO3 = 0.0
PRO1M = 0.0
PRO2M = 0.0
PRO3M = 0.0
NN1 = 1
NN2 = 2

10 FORMAT (A1,F4.1,A1,4X,F4.1,A1,A1,4X,F10.5)
11 FORMAT (A1,F4.1,A1,4X,F4.1,A1,A1)
15 FORMAT (4F10.2)
20 FORMAT (3I10)
60 FORMAT (A1,F4.1,A1,4X,F4.1,A1,A1,4X,A1,F4.1,A1, 4X,F4.1,A1,A1,
1 4X,3F10.3)
1000 FORMAT ('1',29X,'***** SLOPE DATA *****',//
1 19X,'STRIKE:',15X,'N',F4.1,A1, 3X,'DIP:',15X,F4.1,A1,A1)
1002 FORMAT (////,30X,'***** ANALYSIS CRITERIA *****',//,34X,
1 'REFERENCE INTERVAL:',5X,F5.2,///,34X,'MINIMUM DIP:',12X,F5.2,//
2 34X,'MINIMUM WEDGE ANGLE:',4X,F5.2,///,34X,'WEDGE ANGLE ',

DYLT0001
DYLT0002
DYLT0003
DYLT0004
DYLT0005
DYLT0006
DYLT0007
DYLT0008
DYLT0009
DYLT0010
DYLT0011
DYLT0012
DYLT0013
DYLT0014
DYLT0015
DYLT0016
DYLT0017
DYLT0018
DYLT0019
DYLT0020
DYLT0021
DYLT0022
DYLT0023
DYLT0024
DYLT0025
DYLT0026
DYLT0027
DYLT0028
DYLT0029
DYLT0030
DYLT0031
DYLT0032
DYLT0033
DYLT0034
DYLT0035
DYLT0036

303

```

3 'INCREMENT:',2X,F5.2)
1003 FORMAT (///,10X,'INJUDICIOUS CHOICE OF ANALYSIS CRITERIA - ',
1 '(180)/(REFERENCE INTERVAL) MUST BE AN EVEN INTEGER - ',
2 'RUN TERMINATED')
1004 FORMAT (///,10X,'INJUDICIOUS CHOICE OF ANALYSIS CRITERIA - ',
1 '(DIP - MINIMUM DIP)/(REFERENCE INTERVAL) MUST BE AN INTEGER - ',
2 'RUN TERMINATED')
1005 FORMAT (///,10X,'INJUDICIOUS CHOICE OF ANALYSIS CRITERIA - ',
1 '(MINIMUM WEDGE ANGLE)/(REFERENCE INTERVAL) MUST BE AN INTEGER ',
2 '- RUN TERMINATED')
1006 FORMAT (///,10X,'INJUDICIOUS CHOICE OF ANALYSIS CRITERIA - ',
1 '(WEDGE ANGLE)/(REFERENCE INTERVAL) MUST BE AN INTEGER - ',
2 'RUN TERMINATED')
1008 FORMAT (////,32X,'***** JOINT SET ',I1,' *****',//
1 38X,'UNIFORM DISTRIBUTION',//,'+',37X,'-----')
1010 FORMAT (////,32X,'***** JOINT SET ',I1,' *****',//
1 39X,'FISHER DISTRIBUTION',//,'+',38X,'-----')
2 18X,'MEAN STRIKE:',11X,'N',F4.1,A1,3X,'MEAN DIP:',13X,F4.1,A1,A1)
1020 FORMAT (////,32X,'***** JOINT SET ',I1,' *****',//
1 39X,'ARNOLD DISTRIBUTION',//,'+',38X,'-----')
2 18X,'MEAN STRIKE:',11X,'N',F4.1,A1,3X,'MEAN DIP:',13X,F4.1,A1,A1)
1026 FORMAT (/,40X,'K FACTOR:',F8.2)
1030 FORMAT (////,20X,'***** LINE OF INTERSECTION: ',
1 '*****',//,18X,'STRIKE:',15X,A1,F5.2,A1,3X,'PLUNGE:',
2 20X,F5.2,//,18X,'X = ',F7.4,14X,'Y = ',F7.4,14X,'Z = ',F7.4,//
3 33X,'APPARENT DIP OF SLOPE:',F9.2,//,23X,'PDF INCLUDES ALL ',
4 'LINES THAT INTERSECT SPHERE FROM:',//,30X,'(',F5.2,' ',F5.2,
5 ') *** (',F5.2,' ',F5.2,')',//,37X,'*',21X,'*',//,37X,
6 '* (STRIKE : PLUNGE) *',//,37X,'*',21X,'*',//,30X,'(',
7 F5.2,' ',F5.2,') *** (',F5.2,' ',F5.2,')')
1035 FORMAT (////,32X,'***** JOINT SET ',I1,' *****',//
1 38X,'BINGHAM DISTRIBUTION',//,'+',37X,'-----')
2 18X,'MEAN STRIKE:',11X,'N',F4.1,A1,3X,'MEAN DIP:',13X,F4.1,A1,A1,
3 //,18X,'MAJOR STRIKE:',10X,'N',F4.1,A1,3X,'MAJOR DIP:',12X,
4 F4.1,A1,A1,//,18X,'K1 = ',F7.2,13X,'K2 = ',F7.2,11X,'K3 = ',F7.2)
1036 FORMAT (//,18X,'DISTRIBUTION ',I1,': MEAN POLE AND MAJOR ',

```

```

DYLT0037
DYLT0038
DYLT0039
DYLT0040
DYLT0041
DYLT0042
DYLT0043
DYLT0044
DYLT0045
DYLT0046
DYLT0047
DYLT0048
DYLT0049
DYLT0050
DYLT0051
DYLT0052
DYLT0053
DYLT0054
DYLT0055
DYLT0056
DYLT0057
DYLT0058
DYLT0059
DYLT0060
DYLT0061
DYLT0062
DYLT0063
DYLT0064
DYLT0065
DYLT0066
DYLT0067
DYLT0068
DYLT0069
DYLT0070
DYLT0071
DYLT0072

```

304

```

1 'AXIS ARE NOT ORTHAGONAL')
1040 FORMAT (////, 32X, '***** JOINT SET ', I1, ' *****', //
1 37X, 'DEKSHOWITZ DISTRIBUTION', //, '+',
1 36X, '-----', //
2 18X, 'MEAN STRIKE:', 11X, 'N', F4.1, A1, 3X, 'MEAN DIP:', 13X, F4.1, A1, A1,
3 //, 18X, 'MAJOR STRIKE:', 10X, 'N', F4.1, A1, 3X, 'MAJOR DIP:', 12X,
4 F4.1, A1, A1, //, 18X, 'K1 = ', F7.2, 13X, 'K2 = ', F7.2, 11X, 'K3 = ', F7.2)
1045 FORMAT (////, 32X, '***** JOINT SET ', I1, ' *****', //
1 34X, 'BIVARIATE NORMAL DISTRIBUTION', //, '+',
1 33X, '-----', //
2 18X, 'MEAN STRIKE:', 11X, 'N', F4.1, A1, 3X, 'MEAN DIP:', 13X, F4.1, A1, A1,
3 //, 18X, 'MAJOR STRIKE:', 10X, 'N', F4.1, A1, 3X, 'MAJOR DIP:', 12X,
4 F4.1, A1, A1, //, 18X, 'K1 = ', F7.2, 13X, 'K2 = ', F7.2, 11X, 'K3 = ', F7.2)
1055 FORMAT (//, 18X, 'WEDGE ANGLE', 5X, 'P (WEDGE FORMING ; TWO ',
1 'JOINTS ARE PRESENT)', //, 19X, 'MIN MAX', 4X, 'SET 1 & SET 1 ',
2 'SET 2 & SET 2 SET 1 & SET 2', //)
1060 FORMAT (18X, F5.1, 3X, F5.1, 3X, G13.7, 3X, G13.7, 3X, G13.7)
1065 FORMAT ('+', 34X, '-----', //
1 25X, 'TOTAL:', 3X, G13.7, 3X, G13.7, 3X, G13.7)
1070 FORMAT (////, 21X, '***** SUMMARY ',
1 '*****')
1075 FORMAT (////, 29X, '***** SET ', I1, ' & SET ', I1, ' *****',
1 //, 31X, 'TOTAL PROBABILITY: ', G13.7, //, 33X, 'FOR ALL LINES', //,
2 30X, 'MAXIMUM PROBABILITY: ', G13.7, //, 35X, 'AT STRIKE: ', A1,
3 F5.2, A1, //, 36X, 'AND DIP: ', F5.2)
1080 FORMAT (87X, 'BETA 1 BETA 2 PROB. COND.', //
1 88X, 'MIN. MAX. PROB.')
1085 FORMAT (87X, F6.2, 4X, F6.2, 2X, G10.4, 2X, G10.4)
READ (NRD, 11) S1S, STRS, S2S, DIPS, D1S, D2S
WRITE (NWR, 1000) STRS, S2S, DIPS, D1S, D2S
READ (NRD, 15) DEGN, FRIC, DEGMAN, WEDINC
IF ( WEDINC .LT. DEGN ) WEDINC = DEGN
IF ( DEGMAN .LT. DEGN ) DEGMAN = DEGN
WRITE (NWR, 1002) DEGN, FRIC, DEGMAN, WEDINC
READ (NRD, 20) NDIST1, NDIST2, NCODE
IF ( NCODE .GT. 4 ) NCODE = 4

```

```

DYLT0073
DYLT0074
DYLT0075
DYLT0076
DYLT0077
DYLT0078
DYLT0079
DYLT0080
DYLT0081
DYLT0082
DYLT0083
DYLT0084
DYLT0085
DYLT0086
DYLT0087
DYLT0088
DYLT0089
DYLT0090
DYLT0091
DYLT0092
DYLT0093
DYLT0094
DYLT0095
DYLT0096
DYLT0097
DYLT0098
DYLT0099
DYLT0100
DYLT0101
DYLT0102
DYLT0103
DYLT0104
DYLT0105
DYLT0106
DYLT0107
DYLT0108

```

305

```

DISCO (1,1) = NDIST1
DISCO (2,1) = NDIST2
DO 200 I = 1, 2
IF ( DISCO(I,1) .EQ. 0.0 ) WRITE (NWR,1008) I
IF ( DISCO(I,1) .EQ. 0.0 ) GO TO 200
IF ( DISCO(I,1) .GT. 2.0 ) GO TO 150
READ (NRD,10) FA1S, STRFA, FA2S, DIPFA, D1FA, D2FA, FAK
IF (DISCO(I,1) .EQ. 1.0) WRITE (NWR,1010) I, STRFA, FA2S, DIPFA, D1FA, D2FA
IF (DISCO(I,1) .EQ. 2.0) WRITE (NWR,1020) I, STRFA, FA2S, DIPFA, D1FA, D2FA
WRITE (NWR,1026) FAK
DISCO (I,2) = FAK
FFACT1 = (EXP(FAK) - 1.0)/(EXP(FAK) - EXP(-FAK))
DISCO (I,3) = FAK/(2.0*PI*FFACT1*(EXP(FAK) - EXP(-FAK)))
DISCO (I,4) = FAK/(2.0*PI*(EXP(FAK) - 1.0))
CALL STRIKE(PIF, STRFA, FA2S, DIPFA, D1FA, D2FA, DISCO(I,5), DISCO(I,6),
1 DISCO(I,7))
GO TO 200
150 READ(NRD,60) B1S, BS, B2S, BD, B1D, B2D, AB1S, BAS, AB2S, ABD,
1 ABD1, ABD2, DISCO (I,2), DISCO (I,3), DISCO (I,4)
IF ( DISCO (I,1) .EQ. 3.0 ) WRITE (NWR,1035) I, BS, B2S, BD, B1D, B2D,
1 BAS, AB2S, ABD, ABD1, ABD2, DISCO (I,2), DISCO (I,3), DISCO (I,4)
IF ( DISCO (I,1) .EQ. 4.0 ) WRITE (NWR,1040) I, BS, B2S, BD, B1D, B2D,
1 BAS, AB2S, ABD, ABD1, ABD2, DISCO (I,2), DISCO (I,3), DISCO (I,4)
IF ( DISCO (I,1) .EQ. 5.0 .AND. DISCO (I,4) .EQ. 0.0 )
1 DISCO (I,4) = 1.0/(2.0*PI*DISCO (I,2)*DISCO (I,3))
IF ( DISCO (I,1) .EQ. 5.0 ) WRITE (NWR,1045) I, BS, B2S, BD, B1D, B2D,
1 BAS, AB2S, ABD, ABD1, ABD2, DISCO (I,2), DISCO (I,3), DISCO (I,4)
CALL STRIKE(PIF, BS, B2S, BD, B1D, B2D, DISCO (I,5), DISCO (I,6),
1 DISCO (I,7))
CALL STRIKE(PIF, BAS, AB2S, ABD, ABD1, ABD2, DISCO (I,8),
1 DISCO (I,9), DISCO (I,10))
TESTO = DISCO (I,5)*DISCO (I,8) + DISCO (I,6)*DISCO (I,9) +
1 DISCO (I,7)*DISCO (I,10)
IF ( TESTO .GT. 0.01 ) WRITE (NWR,1036) I
DISCO (I,11) = DISCO (I,6)*DISCO (I,10) - DISCO (I,7)*DISCO (I,9)
DISCO (I,12) = DISCO (I,7)*DISCO (I,8) - DISCO (I,5)*DISCO (I,10)

```

```

DYLTO109
DYLTO110
DYLTO111
DYLTO112
DYLTO113
DYLTO114
DYLTO115
DYLTO116
DYLTO117
DYLTO118
DYLTO119
DYLTO120
DYLTO121
DYLTO122
DYLTO123
DYLTO124
DYLTO125
DYLTO126
DYLTO127
DYLTO128
DYLTO129
DYLTO130
DYLTO131
DYLTO132
DYLTO133
DYLTO134
DYLTO135
DYLTO136
DYLTO137
DYLTO138
DYLTO139
DYLTO140
DYLTO141
DYLTO142
DYLTO143
DYLTO144

```

```

DISCO (I,13) = DISCO (I,5)*DISCO (I,9) - DISCO (I,6)*DISCO (I,8)
IF ( DISCO (I,13) .LT. 0.0 ) DISCO (I,11) = -DISCO (I,11)
IF ( DISCO (I,13) .LT. 0.0 ) DISCO (I,12) = -DISCO (I,12)
IF ( DISCO (I,13) .LT. 0.0 ) DISCO (I,13) = -DISCO (I,13)
200 CONTINUE
IF (S2S .EQ. ET .AND. D2S .EQ. ET) AZIMTH = STRS*PI/180.0
IF (S2S .EQ. ET .AND. D2S .EQ. WT) AZIMTH = (180.0 + STRS)*PI/180.
IF (S2S .EQ. WT .AND. D2S .EQ. WT) AZIMTH = (180.0 - STRS)*PI/180.
IF (S2S .EQ. WT .AND. D2S .EQ. ET) AZIMTH = (360.0 - STRS)*PI/180.
IF (STRS .EQ. 90.0 .AND. D1S .EQ. NO) AZIMTH = 1.5*PI
IF (STRS .EQ. 90.0 .AND. D1S .EQ. SO ) AZIMTH = PI/2.0
FRIC = FRIC*PI/180.
NIDC = 1
NAZIM = 180./DEGN
FLT1 = NAZIM
IF (FLT1*DEGN .NE. 180. ) NIDC = 2
IF ( (-1.0)**NAZIM .LT. 0.0 ) NIDC = 2
NMAX = (DIPS - FRIC)/DEGN
FLT2 = NMAX
IF ( DIPS - FRIC .NE. FLT2*DEGN ) NIDC = 3
NMAXW = NAZIM - 1
NMINW = DEGMAN/DEGN
FLT3 = NMINW
IF ( FLT3*DEGN .NE. DEGMAN ) NIDC = 4
NPERWD = WEDINC/DEGN
FLT4 = NPERWD
IF ( FLT4*DEGN .NE. WEDINC ) NIDC = 5
IF ( NIDC .EQ. 1 ) GO TO 205
IF ( NIDC .EQ. 2 ) WRITE (NWR,1003)
IF ( NIDC .EQ. 3 ) WRITE (NWR,1004)
IF ( NIDC .EQ. 4 ) WRITE (NWR,1005)
IF ( NIDC .EQ. 5 ) WRITE (NWR,1006)
GO TO 9000
205 DEGN = DEGN*PI/180.
DEGN2 = DEGN/2.0
C AREAG IS THE SURFACE AREA OF THE GIRDLE BETWEEN FRIC AND DIPS

```

307

DYLTO145
DYLTO146
DYLTO147
DYLTO148
DYLTO149
DYLTO150
DYLTO151
DYLTO152
DYLTO153
DYLTO154
DYLTO155
DYLTO156
DYLTO157
DYLTO158
DYLTO159
DYLTO160
DYLTO161
DYLTO162
DYLTO163
DYLTO164
DYLTO165
DYLTO166
DYLTO167
DYLTO168
DYLTO169
DYLTO170
DYLTO171
DYLTO172
DYLTO173
DYLTO174
DYLTO175
DYLTO176
DYLTO177
DYLTO178
DYLTO179
DYLTO180

```

AREAG = 2.0*PI*(SIN(DIPS*PI/180.) - SIN(FRIC*PI/180.))
AREAIN = AREAG/FLI2
COZETA = 1.0 - (AREAIN*DEGN)/(4.0*PI**2)
SIZETA = SQRT(1.0 - COZETA**2)
ZETA = ATAN(SIZETA/COZETA)
AREAF IS ONE SIXTH THE AREA OF A GIPDLE COMPONENT
AREAF = 2.0*COZETA*(PI2 - ZETA)*DEGN/6.0
AREA = 2.0*PI*(1.0 - COS(PI2-PROC)) + AREAIN/2.0
BETA1 = FRIC
DO 500 J = 1, NMAX
AREA = AREA - AREAIN
COSDIP = (1.0 - AREA/(2.0*PI))
SINDIP = SQRT(1.0 - COSDIP**2)
DIP = ATAN(SINDIP/COSDIP)
BETA2 = (PI2 - DIP)*180./PI
AREAX = AREA - AREAIN/2.0
FIECOS = 1.0 - AREAX/(2.0*PI)
FIESIN = SQRT(1.0 - FIECOS**2)
BETA3 = (PI2 - ATAN(FIESIN/FIECOS))*180./PI
CHI = -DEGN2
DO 206 K = 1, 91
CHI = CHI + DEGN2
IF ( CHI .GT. PI2 ) GO TO 207
ZZ(K) = SIN(CHI*SINDIP)
206 CONTINUE
207 CONTINUE
ALPHAS = TAN(FROC)/TAN(DIP)
ALPHAC = SQRT(1.0 - ALPHAS**2)
ALPHA = ATAN(ALPHAS/ALPHAC) - DEGN2
NEGL = ALPHA/DEGN
NNEGL = NAZIM - NEGL
AZIM = AZIMTH - DEGN/2.0
ZETA = -DEGN/2.0
DO 400 I = NEGL, NNEGL
ZETA = ZETA + DEGN
AZIM = AZIM + DEGN

```

```

DYLTO181
DYLTO182
DYLTO183
DYLTO184
DYLTO185
DYLTO186
DYLTO187
DYLTO188
DYLTO189
DYLTO190
DYLTO191
DYLTO192
DYLTO193
DYLTO194
DYLTO195
DYLTO196
DYLTO197
DYLTO198
DYLTO199
DYLTO200
DYLTO201
DYLTO202
DYLTO203
DYLTO204
DYLTO205
DYLTO206
DYLTO207
DYLTO208
DYLTO209
DYLTO210
DYLTO211
DYLTO212
DYLTO213
DYLTO214
DYLTO215
DYLTO216

```

```

ADIP = ATAN(TAN(DIPS*PI/180.)*SIN(AZIM-AZIMTH))*180./PI
208 IF ( AZIM .LT. PI2 ) STRPT = AZIM*180./PI
IF ( AZIM .LT. PI2 ) STRPT1 = NO
IF ( AZIM .LT. PI2 ) STRPT2 = ET
IF ( AZIM .LT. PI2 ) GO TO 210
IF ( AZIM .LT. PI ) STRPT = (PI - AZIM)*180./PI
IF ( AZIM .LT. PI ) STRPT1 = SO
IF ( AZIM .LT. PI ) STRPT2 = ET
IF ( AZIM .LT. PI ) GO TO 210
IF ( AZIM .LT. 3.0*PI2 ) STRPT = (AZIM - PI)*180./PI
IF ( AZIM .LT. 3.0*PI2 ) STRPT1 = SO
IF ( AZIM .LT. 3.0*PI2 ) STRPT2 = WT
IF ( AZIM .LT. 3.0*PI2 ) GO TO 210
STRPT = (2.0*PI - AZIM)*180./PI
STRPT1 = NO
STRPT2 = WT
IF ( AZIM .GT. 2.0*PI ) AZIM = AZIM - 2.0*PI
IF ( AZIM .GT. 2.0*PI ) GO TO 208
309 210 STRMN = STRPT - DEGN*90./PI
STRMX = STRPT + DEGN*90./PI
C XPT, YPT, ZPT ARE THE UNIT VECTORS OF THE DAYLIGHTING LINE
XPT = SIN(DIP)*COS(AZIM)
YPT = SIN(DIP)*SIN(AZIM)
ZPT = COS(DIP)
C XR, YR ARE THE UNIT VECTORS OF THE STRIKE OF THE "JOINT POLE" PLANE
XR = COS(AZIM-PI2)
YR = SIN(AZIM-PI2)
IF ( NOPT .EQ. 1 ) GO TO 215
XSW = SIN(DIP)*COS(ZETA)
YSW = -SIN(DIP)*SIN(ZETA)
C XSW, ETC. ARE UNIT VECTORS OF DAYLT. LINE W.R.T. SWARS COOF. SYS.
WRITE (NWR, 1030) STRPT1, STRPT, STRPT2, BETA2, XSW, YSW, ZPT,
1 ADIP, STRMN, BETA1, STRMX, BETA1, STRMN, BETA3, STRMX, BETA3
WRITE ( NWR, 1055)
215 AA = (1.0 + (XR/YR)**2)
DO 250 K = 1, NAZIM

```

```

DYLT0217
DYLT0218
DYLT0219
DYLT0220
DYLT0221
DYLT0222
DYLT0223
DYLT0224
DYLT0225
DYLT0226
DYLT0227
DYLT0228
DYLT0229
DYLT0230
DYLT0231
DYLT0232
DYLT0233
DYLT0234
DYLT0235
DYLT0236
DYLT0237
DYLT0238
DYLT0239
DYLT0240
DYLT0241
DYLT0242
DYLT0243
DYLT0244
DYLT0245
DYLT0246
DYLT0247
DYLT0248
DYLT0249
DYLT0250
DYLT0251
DYLT0252

```

```

G = K - 1
CHI = -DEGN2 + G*DEGN
DO 225 L = 1, 3
CHI = CHI + DEGN2
IF ( K .NE. 1 .AND. L .EQ. 1 ) GO TO 225
COSCHI = COS (CHI)
IF ( L .EQ. 2 ) COSIN = COSCHI
CHO = CHI
IF ( CHO .GT. PI2 ) CHO = PI - CHO
NZ = 1.0 + CHO/DEGN2
Z (L) = ZZ (NZ)
BB = -2.0*XR*COSCHI/YR**2
CC = (COSCHI/YR)**2 + Z(L)**2 - 1.0
DD = SQRT (ABS (BB**2 - 4.0*AA*CC) )
X (L) = (-BB-DD)/(2.0*AA)
Y (L) = (COSCHI - XR*X (L) )/YR
EE = ATAN (X(L)*XPT + Y (L) *YPT + Z (L) *ZPT)
IF ( EE .LT. 0.0100 ) GO TO 225
X (L) = (-BB+DD)/(2.0*AA)
Y (L) = (COSCHI - XR*X (L) )/YR
225 CONTINUE
XRR = X (2)
YRR = Y (2)
ZRR = Z (2)
H = 1.0/((XRR*YR - XR*YRR)**2)
S = XRR*COSIN - XR*COZETA
T = YRR*COSIN - YR*COZETA
A = H*ZRR**2 + 1.0
B = 2.0*H*ZRR*(XR*S + YR*T)
C = H*(T**2 + S**2) - 1.0
D = SQRT (ABS (B**2 - 4.0*A*C) )
Z (4) = (-B+D)/(2.0*A)
Y (4) = (XR*ZRR*Z (4) + S)/(XRR*YR - XR*YRR)
X (4) = (COSIN - Y (4) *YR)/XR
Z (5) = (-B-D)/(2.0*A)
Y (5) = (XR*ZRR*Z (5) + S)/(XRR*YR - XR*YRR)

```

310

DYLTO253
DYLTO254
DYLTO255
DYLTO256
DYLTO257
DYLTO258
DYLTO259
DYLTO260
DYLTO261
DYLTO262
DYLTO263
DYLTO264
DYLTO265
DYLTO266
DYLTO267
DYLTO268
DYLTO269
DYLTO270
DYLTO271
DYLTO272
DYLTO273
DYLTO274
DYLTO275
DYLTO276
DYLTO277
DYLTO278
DYLTO279
DYLTO280
DYLTO281
DYLTO282
DYLTO283
DYLTO284
DYLTO285
DYLTO286
DYLTO287
DYLTO288

```

X(5) = (COSIN - Y(5)*YR)/XR
DO 245 L = 1, 2
IF ( DISCO(L,1) .EQ. 0.0 ) PJT(L,K) = AREA*3.0/PI
IF ( DISCO(L,1) .EQ. 0.0 ) GO TO 245
DO 240 LL = 1, 5
IF ( K .NE. 1 ) PROB(L,1) = PROB(L,3)
IF ( K .NE. 1 .AND. LL .EQ. 1 ) GO TO 240
IF ( DISCO(L,1) .GT. 2.0 ) GO TO 230
GAMMA = (DISCO(L,5)*X(LL)+DISCO(L,6)*Y(LL)+DISCO(L,7)*Z(LL))
GAMMA = ATAN((SQRT(1.0 - GAMMA**2))/GAMMA)
IF ( GAMMA .LT. 0.0 ) GAMMA = PI - GAMMA
IF ( DISCO(L,1) .EQ. 1.0 ) PROB(L,LL) = DISCO(L,3) *
1 SIN(GAMMA)*EXP(DISCO(L,2)*COS(GAMMA))
IF ( DISCO(L,1) .EQ. 2.0 ) PROB(L,LL) = DISCO(L,4) *
1 SIN(GAMMA)*EXP(DISCO(L,2)*COS(GAMMA))
GO TO 240
CMJ: COOR MAJOR AXIS, CMR: COOR MINOR AXIS, CMN: COOR MEAN AXIS
230 CMJ = X(LL)*DISCO(L,8) + Y(LL)*DISCO(L,9) + Z(LL)*DISCO(L,10)
CMR = X(LL)*DISCO(L,11) + Y(LL)*DISCO(L,12) + Z(LL)*DISCO(L,13)
IF ( DISCO(L,1) .EQ. 5.0 ) PROB(L,LL) = DISCO(L,4) *
1 EXP(0.5*(CMJ/DISCO(L,2) + CMR/DISCO(L,3)))
IF ( DISCO(L,1) .EQ. 5.0 ) GO TO 240
CMN = X(LL)*DISCO(L,5) + Y(LL)*DISCO(L,6) + Z(LL)*DISCO(L,7)
ANGPH = ATAN(CMN)
IF ( ANGPH .LT. 0.0 ) ANGPH = PI - ANGPH
ANGTH = ATAN(CMR/CMJ)
IF ( DISCO(L,1) .EQ. 3.0 ) PROB(L,LL) = DISCO(L,2)*SIN(ANGPH) *
1 EXP((SIN(ANGPH)**2)*(DISCO(L,3)*COS(ANGTH)**2 + DISCO(L,4) *
2 SIN(ANGTH)**2))
IF ( DISCO(L,1) .EQ. 4.0 ) PROB(L,LL) = DISCO(L,2)*SIN(ANGPH) *
1 EXP(COS(ANGPH)*(DISCO(L,3)*COS(ANGTH)**2 + DISCO(L,4) *
2 SIN(ANGTH)**2))
240 CONTINUE
PJT(L,K) = (PROB(L,1) + PROB(L,3) + PROB(L,4) + PROB(L,5) +
1 PROB(L,2)*2.0)*AREA*
245 CONTINUE

```

```

DYLT0289
DYLT0290
DYLT0291
DYLT0292
DYLT0293
DYLT0294
DYLT0295
DYLT0296
DYLT0297
DYLT0298
DYLT0299
DYLT0300
DYLT0301
DYLT0302
DYLT0303
DYLT0304
DYLT0305
DYLT0306
DYLT0307
DYLT0308
DYLT0309
DYLT0310
DYLT0311
DYLT0312
DYLT0313
DYLT0314
DYLT0315
DYLT0316
DYLT0317
DYLT0318
DYLT0319
DYLT0320
DYLT0321
DYLT0322
DYLT0323
DYLT0324

```

```

250 CONTINUE
270 NAZIM2 = NAZIM/2
DO 280 L = 1, 2
DO 278 K = 1, NAZIM2
NA2K = NAZIM2 + K
DUMP = PJT(L,K)
PJT(L,K) = PJT(L,NA2K)
PJT(L,NA2K) = DUMP
278 CONTINUE
280 CONTINUE
PRO1S = 0.0
PRO2S = 0.0
PRO3S = 0.0
PRO1 = 0.0
PRO2 = 0.0
PRO3 = 0.0
DEGMIN = DEGMAN
NNNN = 0
DO 325 N = NMINW, NMAXW
NNNN = NNNN + 1
NWEDGS = NAZIM - N
IF ( NCODE .EQ. 1 .OR. NCODE .EQ. 4 ) NSET1 = 1
IF ( NCODE .EQ. 1 .OR. NCODE .EQ. 4 ) NSET2 = 1
296 IF ( NCODE .EQ. 2 .OR. NCODE .EQ. 5 ) NSET1 = 2
IF ( NCODE .EQ. 2 .OR. NCODE .EQ. 5 ) NSET2 = 2
298 IF ( NCODE .EQ. 3 .OR. NCODE .EQ. 6 ) NSET1 = 1
IF ( NCODE .EQ. 3 .OR. NCODE .EQ. 6 ) NSET2 = 2
PRO = 0.0
NJEG = 1
MMM = 0
NBET1 = 0
PCBET = 0.0
SUMBT1 = 0.0
DO 300 M = 1, NWEDGS
N1 = NSET1
N2 = NSET2

```

```

DYLTO325
DYLTO326
DYLTO327
DYLTO328
DYLTO329
DYLTO330
DYLTO331
DYLTO332
DYLTO333
DYLTO334
DYLTO335
DYLTO336
DYLTO337
DYLTO338
DYLTO339
DYLTO340
DYLTO341
DYLTO342
DYLTO343
DYLTO344
DYLTO345
DYLTO346
DYLTO347
DYLTO348
DYLTO349
DYLTO350
DYLTO351
DYLTO352
DYLTO353
DYLTO354
DYLTO355
DYLTO356
DYLTO357
DYLTO358
DYLTO359
DYLTO360

```

```

MN = H + N
PROPT = PJT(N1,M)*PJT(N2,MN) + PJT(N1,MN)*PJT(N2,M)
PRO = PROPT + PRO
IF ( NCODE .GT. 3 ) GO TO 300
NBET1 = NBET1 + 1
PROBET = PROBET + PROPT
IF ( NBET1 .NE. NPERWD ) GO TO 300
MMM = MMM + 1
SNBET(MMM) = PROBET
SUMBT1 = SUMBT1 + PROBET
PROBET = 0.0
NBET1 = 0
300 CONTINUE
IF ( NCODE .GT. 3 .OR. PROBET .EQ. 0.0 ) GO TO 305
NJEG = 2
MMM = MMM + 1
SNBET(MMM) = PROBET
SWEGS = NWEDGS
DEGMAX = SWEGS*DEGN*180./PI
SUMBT1 = SUMBT1 + PROBET
305 IF ( NCODE .EQ. 3 .OR. NCODE .EQ. 6 ) PRO3 = PRO + PRO3
IF ( NCODE .EQ. 6 ) GO TO 310
IF ( NCODE .EQ. 2 .OR. NCODE .EQ. 5 ) PRO2 = PRO + PRO2
IF ( NCODE .EQ. 5 ) NCODE = 6
IF ( NCODE .EQ. 6 ) GO TO 298
IF ( NCODE .EQ. 1 .OR. NCODE .EQ. 4 ) PRO1 = PRO + PRO1
IF ( NCODE .EQ. 4 ) NCODE = 5
IF ( NCODE .EQ. 5 ) GO TO 296
310 IF ( NCODE .LT. 6 ) NCODE = 4
IF ( NNNN .NE. NPERWD ) GO TO 325
PRO1S = PRO1S + PRO1
PRO2S = PRO2S + PRO2
PRO3S = PRO3S + PRO3
DEGMAX = DEGMIN + WEDINC
IF ( NCPT .NE. 1 ) WRITE (NWR,1060) DEGMIN,DEGMAX,PRO1,PRO2,PRO3
IF ( NCODE .GT. 3 ) GO TO 316

```

```

DYLT0361
DYLT0362
DYLT0363
DYLT0364
DYLT0365
DYLT0366
DYLT0367
DYLT0368
DYLT0369
DYLT0370
DYLT0371
DYLT0372
DYLT0373
DYLT0374
DYLT0375
DYLT0376
DYLT0377
DYLT0378
DYLT0379
DYLT0380
DYLT0381
DYLT0382
DYLT0383
DYLT0384
DYLT0385
DYLT0386
DYLT0387
DYLT0388
DYLT0389
DYLT0390
DYLT0391
DYLT0392
DYLT0393
DYLT0394
DYLT0395
DYLT0396

```

```

WRITE (NWR,1080)
DO 315 IIII = 1, MMM
IF ( IIII .EQ. 1 ) EGMIN = 0.0
IF ( IIII .NE. 1 ) EGMIN = EGMAX
BEET1 = NPERWD*IIII
EGMAX = BEET1*DEGN/PIF
SSBET = SNBET (IIII)/SUMBT1
IF ( IIII .EQ. MMM .AND. NJEG .EQ. 2 ) EGMAX = EEGMAX
WRITE (NWR,1085) EGMIN,EGMAX,SNBET (IIII),SSBET
315 CONTINUE
316 CONTINUE
PRO1 = 0.0
PRO2 = 0.0
PRO3 = 0.0
DEGLIN = DEGMAX
NNNN = 0.0
314 325 CONTINUE
IF ( NGPT .NE. 1 ) WRITE (NWR,1065) PRO1S, PRO2S, PRO3S
PLINED (1,J,K) = PRO1S
PLINED (2,J,K) = PRO2S
PLINED (3,J,K) = PRO3S
TPRO1 = TPRO1 + PRO1S
TPRO2 = TPRO2 + PRO2S
TPRO3 = TPRO3 + PRO3S
IF ( PRO1S .LT. PRO1M ) GO TO 380
PRO1M = PRO1S
PRO1S1 = STRPT1
PRO1S2 = STRPT
PRO1S3 = STRPT2
PRO1D = BETA2
380 IF ( PRO2S .LT. PRO2M ) GO TO 390
PRO2M = PRO2S
PRO2S1 = STRPT1
PRO2S2 = STRPT
PRO2S3 = STRPT2
PRO2D = BETA2

```

```

DYLTO397
DYLTO398
DYLTO399
DYLTO400
DYLTO401
DYLTO402
DYLTO403
DYLTO404
DYLTO405
DYLTO406
DYLTO407
DYLTO408
DYLTO409
DYLTO410
DYLTO411
DYLTO412
DYLTO413
DYLTO414
DYLTO415
DYLTO416
DYLTO417
DYLTO418
DYLTO419
DYLTO420
DYLTO421
DYLTO422
DYLTO423
DYLTO424
DYLTO425
DYLTO426
DYLTO427
DYLTO428
DYLTO429
DYLTO430
DYLTO431
DYLTO432

```

390	IF (PRO3S .LT. PRO3M) GO TO 400	DYLT0433
	PRO3M = PRO3S	DYLT0434
	PRO3S1 = STRPT1	DYLT0435
	PRO3S2 = STRPT	DYLT0436
	PRO3S3 = STRPT2	DYLT0437
	PRO3D = BETA2	DYLT0438
400	CONTINUE	DYLT0439
	BETA1 = BETA3	DYLT0440
500	CONTINUE	DYLT0441
	WRITE (NWR,1070)	DYLT0442
	IF (NCODE .EQ. 1 .OR. NCODE .EQ. 4) WRITE (NWR,1075) NN1, NN1,	DYLT0443
	1 TPRO1, PRO1M, PRO1S1, PRO1S2, PRO1S3, PRO1D	DYLT0444
	IF (NCODE .EQ. 2 .OR. NCODE .EQ. 4) WRITE (NWR,1075) NN2, NN2,	DYLT0445
	1 TPRO2, PRO2M, PRO2S1, PRO2S2, PRO2S3, PRO2D	DYLT0446
	IF (NCODE .EQ. 3 .OR. NCODE .EQ. 4) WRITE (NWR,1075) NN1, NN2,	DYLT0447
	1 TPRO3, PRO3M, PRO3S1, PRO3S2, PRO3S3, PRO3D	DYLT0448
9000	CONTINUE	DYLT0449
	STOP	DYLT0450
	END	DYLT0451
	SUBROUTINE STRIKE(PIF,STRFA,FA2S,DIPFA,D1FA,D2FA,A,B,C)	DYLT0452
	REAL NO	DYLT0453
	DATA NO,SC,ET,WT/'N','S','E','W'/	DYLT0454
	IF (FA2S .EQ. WT .AND. D2FA .EQ. ET) THOM = (270. - STRFA)*PIF	DYLT0455
	IF (FA2S .EQ. WT .AND. D2FA .EQ. WT) THOM = (90. - STRFA)*PIF	DYLT0456
	IF (FA2S .EQ. ET .AND. D2FA .EQ. ET) THOM = (270. + STRFA)*PIF	DYLT0457
	IF (FA2S .EQ. ET .AND. D2FA .EQ. WT) THOM = (90. + STRFA)*PIF	DYLT0458
	IF (STRFA .EQ. 90.0 .AND. D1FA .EQ. NO) THOM = 180.0*PIF	DYLT0459
	IF (STRFA .EQ. 90.0 .AND. D1FA .EQ. SC) THOM = 0.0	DYLT0460
	PHOM = (90. - DIPFA)*PIF	DYLT0461
	A = SIN(PHOM)*COS(THOM)	DYLT0462
	B = SIN(PHOM)*SIN(THOM)	DYLT0463
	C = COS(PHOM)	DYLT0464
	RETURN	DYLT0465
	END	DYLT0466

315

Appendix D

A Generalization of the Stiffness Approach

The approach used by St. John to examine symmetric wedges can be extended to handle more general conditions. In particular, the extended solution considers asymmetrical wedges and arbitrary loadings as pictured in Figure D.1.

The approach is predicated on a number of basic assumptions:

1. The rock wedge and parent rock mass are rigid bodies compared to the joints. All the deformations in the system occur at joints which are idealized as thin, pliant mediums.
2. There is a linear relationship between the stresses and displacements in the joint planes. The shear and normal stresses can be related to the corresponding displacements through the following equations:

$$k_s = \frac{\text{shear stress}}{\text{shear displacement}} = \frac{\tau}{\delta_s} \quad (\text{D.1})$$

$$k_n = \frac{\text{normal stress}}{\text{normal displacement}} = \frac{\sigma_n}{\delta_n} \quad (\text{D.2})$$

3. When subjected to loads the wedge will experience translational (but not rotational) movements. These movements can be expressed in

X, Y: RESULTANT LOADS

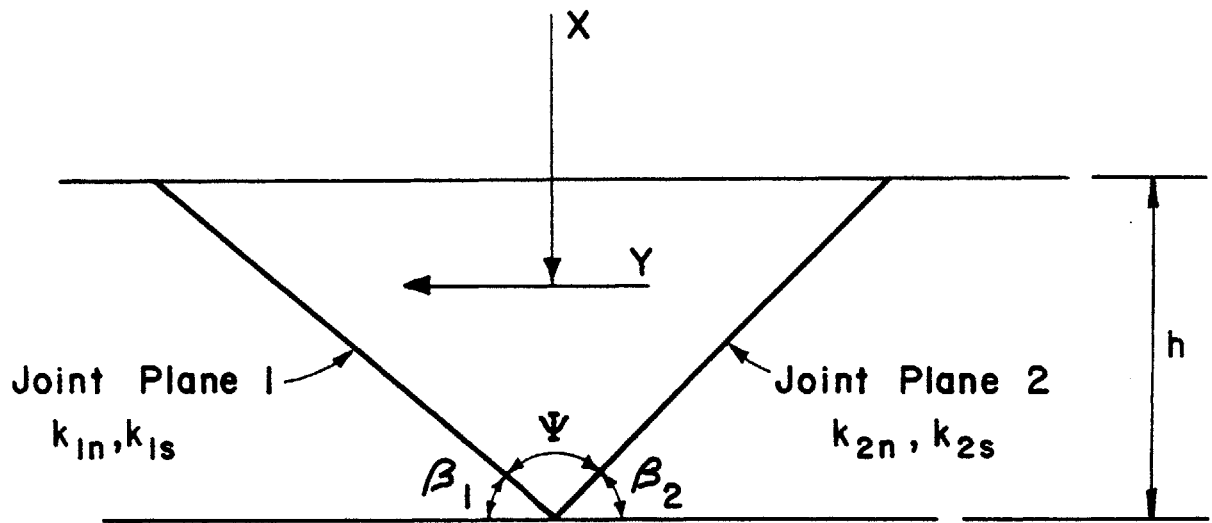


Figure D.1 Generalized Stiffness Approach--Known Parameters

terms of two parameters: δ_t , the magnitude of resultant displacement and α , the direction of resultant displacement (Figure D.2).

These assumptions make the problem statically determinate. The various reactions at the joint planes (as well as δ_t and α) can be obtained by solving a set of six simultaneous equations. The six unknowns ($N_1, T_1, N_2, T_2, \delta_t$ and α) are shown in Figure D.2).

δ_t can be resolved into horizontal and vertical components: $\delta_v = \delta_t \cos \alpha$ and $\delta_h = \delta_t \sin \alpha$.

The displacement pattern at the left joint (joint plane '1') is shown in Figure D.3. One can derive the following relationships:

$$\text{area of joint '1'} = h \csc \beta_1 \quad (D.3)$$

$$\begin{aligned} T_1 &= \tau_1 h \csc \beta_1 \\ &= (\delta_v \sin \beta_1 - \delta_h \cos \beta_1) k_{1s} h \csc \beta_1 \\ &= \delta_t (\cos \alpha \sin \beta_1 - \sin \alpha \cos \beta_1) k_{1s} h \csc \beta_1 \\ &= \delta_t (\cos \alpha - \sin \alpha \operatorname{ctn} \beta_1) k_{1s} h \end{aligned} \quad (D.4)$$

positive $T_1 \therefore$ ↙

$$\begin{aligned} N_1 &= \sigma_1 h \csc \beta_1 \\ &= (\delta_h \sin \beta_1 + \delta_v \cos \beta_1) k_{1n} h \csc \beta_1 \\ &= \delta_t (\sin \alpha \sin \beta_1 + \cos \alpha \cos \beta_1) k_{1n} h \csc \beta_1 \\ &= \delta_t (\sin \alpha + \cos \alpha \operatorname{ctn} \beta_1) k_{1n} h \end{aligned} \quad (D.5)$$

positive $N_1 \therefore$ ↗

$\delta_T = \text{Resultant Displacement}$

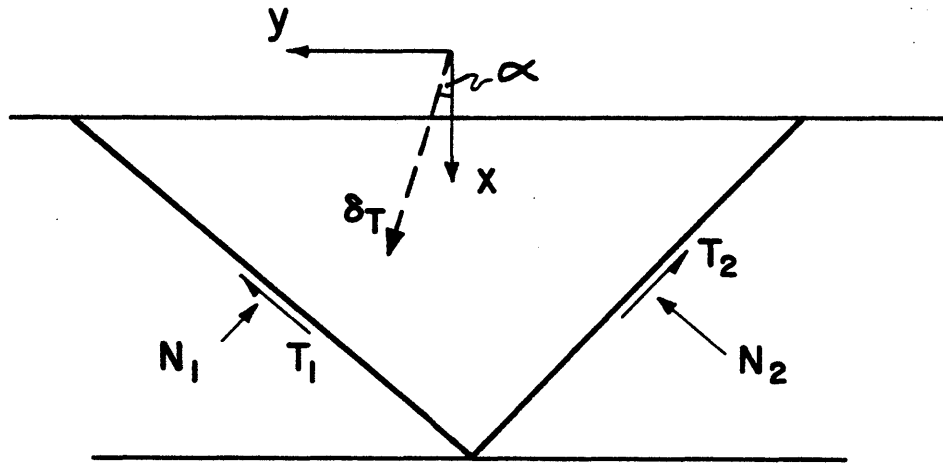
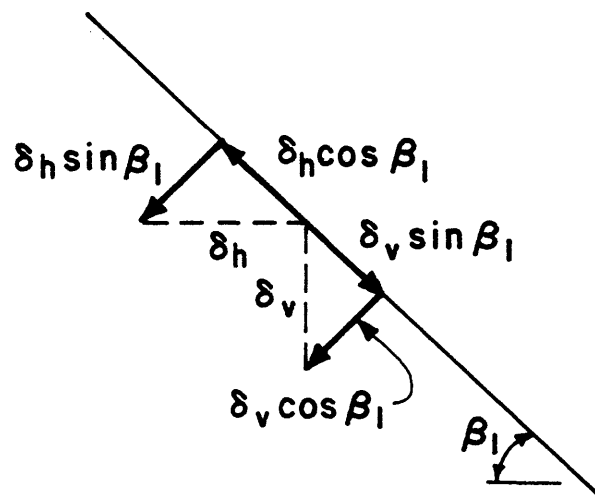


Figure D.2 Generalized Stiffness Approach--Unknown Parameters

Left Joint




$$\delta_v = \delta_T \cos \alpha$$
$$\delta_h = \delta_T \sin \alpha$$

Figure D.3 Displacements--Left Joint


The right joint (joint plane '2') can be analyzed in the same manner (Figure D.4):

$$\text{area of joint '2'} = h \csc \beta_2 \quad (\text{D.6})$$

$$\begin{aligned} T_2 &= \tau_2 h \csc \beta_2 \\ &= (\delta_v \sin \beta_2 + \delta_h \cos \beta_2) k_{2s} h \csc \beta_2 \\ &= \delta_t (\cos \alpha \sin \beta_2 + \sin \alpha \cos \beta_2) k_{2s} h \csc \beta_2 \\ &= \delta_t (\cos \alpha + \sin \alpha \operatorname{ctn} \beta_2) k_{2s} h \end{aligned} \quad (\text{D.7})$$

positive $T_2 \therefore$ 

$$\begin{aligned} N_2 &= \sigma_2 h \csc \beta_2 \\ &= (\delta_v \cos \beta_2 - \delta_h \sin \beta_2) k_{2n} h \csc \beta_2 \\ &= \delta_t (\cos \alpha \cos \beta_2 - \sin \alpha \sin \beta_2) k_{2n} h \csc \beta_2 \\ &= \delta_t (\cos \alpha \operatorname{ctn} \beta_2 - \sin \alpha) k_{2n} h \end{aligned} \quad (\text{D.8})$$

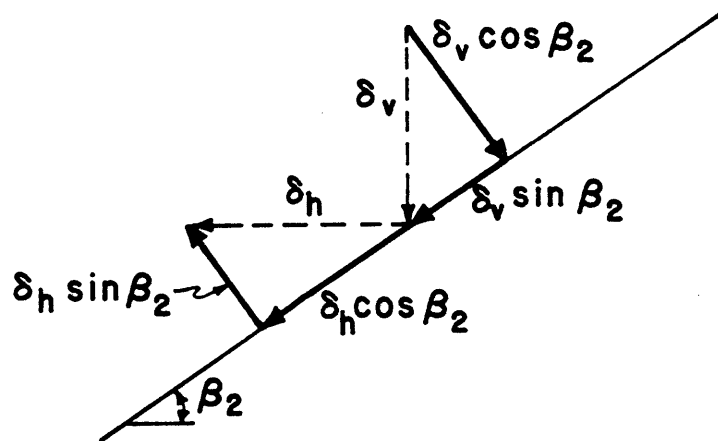
positive $N_2 \therefore$ 

The term $\delta_t h$ is common to Equations D.4, D.5, D.7, and D.8. The equations can be rewritten to isolate that term:

$$\delta_t h = \frac{T_1}{(\cos \alpha - \sin \alpha \operatorname{ctn} \beta_1) k_{1s}} \quad (\text{D.4A})$$

$$= \frac{N_1}{(\sin \alpha + \cos \alpha \operatorname{ctn} \beta_1) k_{1n}} \quad (\text{D.5A})$$

Right Joint



$$\delta_v = \delta_T \cos \alpha$$

$$\delta_h = \delta_T \sin \alpha$$

Figure D.4 Displacements--Right Joint

$$\delta_t h = \frac{T_2}{(\cos \alpha + \sin \alpha \operatorname{ctn} \beta_2) k_{2s}} \quad (\text{D.7A})$$

$$= \frac{N_2}{(\cos \alpha \operatorname{ctn} \beta_2 - \sin \alpha) k_{2n}} \quad (\text{D.8A})$$

Next, one can examine the equations for force equilibrium and sum forces in the x and y directions (Figure D.2):

$$N_1 \cos \beta_1 + T_1 \sin \beta_1 + N_2 \cos \beta_2 + T_2 \sin \beta_2 = X \quad (\text{D.9})$$

$$N_1 \sin \beta_1 - T_1 \cos \beta_1 - N_2 \sin \beta_2 + T_2 \cos \beta_2 = Y \quad (\text{D.10})$$

Equations D.4A, D.5A, D.7A D.8A, D.9 and D.10 constitute a set of six linear equations involving six unknowns: N_1 , T_2 , T_1 , N_2 , δ_t and α . The solution procedure can be simplified by expressing T_1 , N_2 and T_2 in terms of N_1 and substituting into D.9 and D.10.

From D.5A and D.4A:

$$T_1 = \frac{(\cos \alpha - \sin \alpha \operatorname{ctn} \beta_1) k_{1s}}{(\sin \alpha + \cos \alpha \operatorname{ctn} \beta_1) k_{1n}} N_1 \quad (\text{D.11})$$

From D.5A and D.8A

$$N_2 = \frac{(\cos \alpha \operatorname{ctn} \beta_2 - \sin \alpha) k_{2n}}{(\sin \alpha + \cos \alpha \operatorname{ctn} \beta_1) k_{1n}} N_1 \quad (\text{D.12})$$

From D5A and D.7A

$$T_2 = \frac{(\cos \alpha + \sin \alpha \operatorname{ctn} \beta_2) k_{2s}}{(\sin \alpha + \cos \alpha \operatorname{ctn} \beta_1) k_{1n}} N_1 \quad (D.13)$$

Substituting into D.9 and D.10:

$$N_1 \frac{(\cos \beta_1 + (\cos \alpha - \sin \alpha \operatorname{ctn} \beta_1) k_{1s}) \sin \beta_1 + (\cos \alpha \operatorname{ctn} \beta_2 - \sin \alpha) k_{2n} \cos \beta_2 + (\cos \alpha + \sin \alpha \operatorname{ctn} \beta_2) k_{2s} \sin \beta_2}{(\sin \alpha + \cos \alpha \operatorname{ctn} \beta_1) k_{1n}} = x \quad (D.14)$$

And

$$N_1 \frac{(\sin \beta_1 + (\sin \alpha \operatorname{ctn} \beta_1 - \cos \alpha) k_{1s}) \cos \beta_1 + (\sin \alpha - \cos \alpha \operatorname{ctn} \beta_2) k_{2n} \sin \beta_2 + (\cos \alpha + \sin \alpha \operatorname{ctn} \beta_2) k_{2s} \cos \beta_2}{(\sin \alpha + \cos \alpha \operatorname{ctn} \beta_1) k_{1n}} = y \quad (D.15)$$

Equations D.14 and D.15 are of the form

$$N_1 (f(\alpha)) = X \quad (D.14A)$$

$$N_1 (g(\alpha)) = Y \quad (D.15A)$$

where $f(\alpha)$ and $g(\alpha)$ are functions of the single unknown and numerous constants. The term N_1 can be isolated in both equations:

$$N_1 = \frac{X}{f(\alpha)} \quad (D.14B)$$

$$N_1 = \frac{Y}{g(\alpha)} \quad (D.15B)$$

Equating the right sides of Equations D.14B and D.15B:

$$\frac{X}{f(\alpha)} = \frac{Y}{g(\alpha)} \quad (D.16)$$

or

$$\frac{X}{Y} = \frac{f(\alpha)}{g(\alpha)} \quad (D.16A)$$

Thus,

$$\frac{X}{Y} = \frac{\cos\beta_1 + \frac{(\cos\alpha - \sin\alpha \operatorname{ctn}\beta_1)k_{1s} \sin\beta_1 + (\cos\alpha \operatorname{ctn}\beta_2 - \sin\alpha)k_{2n} \cos\beta_2 + (\cos\alpha + \sin\alpha \operatorname{ctn}\beta_2)k_{2s} \sin\beta_2}{(\sin\alpha + \cos\alpha \operatorname{ctn}\beta_1)k_{1n}}}{\sin\beta_1 + \frac{(\sin\alpha \operatorname{ctn}\beta_1 - \cos\alpha)k_{1s} \cos\beta_1 + (\sin\alpha - \cos\alpha \operatorname{ctn}\beta_2)k_{2n} \sin\beta_2 + (\cos\alpha + \sin\alpha \operatorname{ctn}\beta_2)k_{2s} \cos\beta_2}{(\sin\alpha + \cos\alpha \operatorname{ctn}\beta_1)k_{1n}}} \quad (D.16B)$$

Multiplying by $\frac{(\sin \alpha + \cos \alpha \operatorname{ctn} \beta_1)k_{1n}}{(\sin \alpha + \cos \alpha \operatorname{ctn} \beta_1)k_{1n}}$ and collecting terms:

$$\frac{X}{Y} = \frac{\sin\alpha(k_{1n} \cos\beta_1 - k_{1s} \cos\beta_1 - k_{2n} \cos\beta_2 + k_{2s} \cos\beta_2) + \cos\alpha(k_{1n} \frac{\cos^2 \beta_1}{\sin\beta_1} + k_{1s} \sin\beta_1 + k_{2n} \frac{\cos^2 \beta_2}{\sin\beta_2} + k_{2s} \sin\beta_2)}{\sin\alpha(k_{1n} \sin\beta_1 + k_{1s} \frac{\cos^2 \beta_1}{\sin\beta_1} + k_{2n} \sin\beta_2 + k_{2s} \frac{\cos^2 \beta_2}{\sin\beta_2}) + \cos\alpha(k_{1n} \cos\beta_1 - k_{1s} \cos\beta_1 - k_{2n} \cos\beta_2 + k_{2s} \cos\beta_2)} \quad (D.17)$$

$$\text{Therefore, } \frac{X}{Y} = \frac{A \sin \alpha + B \cos \alpha}{C \sin \alpha + A \cos \alpha} \quad (D.17A)$$

where

$$A = (k_{1n} - k_{1s}) \cos \beta_1 + (k_{2s} - k_{2n}) \cos \beta_2$$

$$B = k_{1n} \frac{\cos^2 \beta_1}{\sin \beta_1} + k_{1s} \sin \beta_1 + k_{2n} \frac{\cos^2 \beta_2}{\sin \beta_2} + k_{2s} \sin \beta_2$$

$$C = k_{1n} \sin \beta_1 + k_{1s} \frac{\cos^2 \beta_1}{\sin \beta_1} + k_{2n} \sin \beta_2 + k_{2s} \frac{\cos^2 \beta_2}{\sin \beta_2}$$

Finally,

$$\alpha = \tan^{-1} \left[\frac{YB - XA}{XC - YA} \right] \quad (D.18)$$

Once α is obtained the remaining unknowns can be evaluated through substitution:

$$\text{Equation D.14} \rightarrow N_1$$

$$\text{Equation D.11} \rightarrow T_1$$

$$\text{Equation D.12} \rightarrow N_2$$

$$\text{Equation D.13} \rightarrow T_2$$

$$\text{Equation D.4A} \rightarrow \delta_t$$

All of the equations derived in this appendix are also valid for wedges in which β_1 or β_2 is greater than 90° . The results for these cases must be examined quite closely because one of the normal forces may become tensile. This problem is discussed in Section 4.3.

Special Case

When $Y = 0$, Equation D.18 simplifies to:

$$\alpha = \tan^{-1} \frac{XA}{XC} \quad (D.19)$$

or

(D.19A)

$$\alpha = \tan^{-1} \frac{(k_{1s} - k_{1n}) \cos \beta_1 + (k_{2n} - k_{2s}) \cos \beta_2}{k_{1n} \sin \beta_1 + k_{1s} \frac{\cos^2 \beta_1}{\sin \beta_1} + k_{2n} \sin \beta_2 + k_{2s} \frac{\cos^2 \beta_2}{\sin \beta_2}}$$

Section 4.2 examines this special case in connection with some limiting values for the stiffnesses.

Appendix E

Computer Program SWARS-2PM

SWARS-2PM is an extended version of SWARS-2P that includes the effects of stiffnesses and in situ stresses as discussed in Chapter 4. The two programs have precisely the same options available for analyzing rock bolts, seismic loads, point loads, and groundwater conditions. Campbell (1974) documented the SWARS-2PM program; the SWARS-2P user should consult Campbell's work for additional information on the program logic and a more detailed description of the loading and groundwater options. The only major difference between SWARS-2P and SWARS-2PM is the manner in which they calculate the factor(s) of safety (FS). SWARS-2PM computes two FS's; FS_I , the factor of safety against initial movement, and FS_U , the factor of safety against ultimate failure. As indicated in Sections 4.3 and 4.4, FS_I is a function of the in situ stresses and the joint stiffnesses. FS_U applies to movement down the line of intersection and is independent of the original stresses and of the joint stiffness.* FS_U is analytically identical to the residual factor of safety (FS_R) computed by SWARS-2P. (SWARS-2P also computes another FS which is similar to (FS_R) but includes the effects of cohesion and asperities in calculating the resistance.)

* FS_I and FS_U are only defined for failure modes that consist of sliding on both planes. If the failure modes involve sliding along a single plane, SWARS-2PM will compute the factors of safety in exactly the same manner as SWARS-2P, i.e., a peak FS and a residual FS.

E.1 Coordinate System

The coordinate system used in SWARS-2PM is shown in Figure E.1. The positive X axis is horizontal to the right. The positive Y axis is horizontal and 90° counterclockwise from the positive X axis. (It is directed into the slope.) The positive Z axis is vertical upward.

E.2 Units

All units used in the input must be consistent. Units are generally in feet or pounds, but any other system may be employed as long as all other input is in consistent units. Angular input is always in degrees.

Unless otherwise noted, input data does not have to be right justified. The term "integer" implies that the parameter is expressed without a decimal point.

E.3 Inputs

Card #1

Case Number: (ICASE) is entered as an integer in columns 1 to 5. It must be right justified.

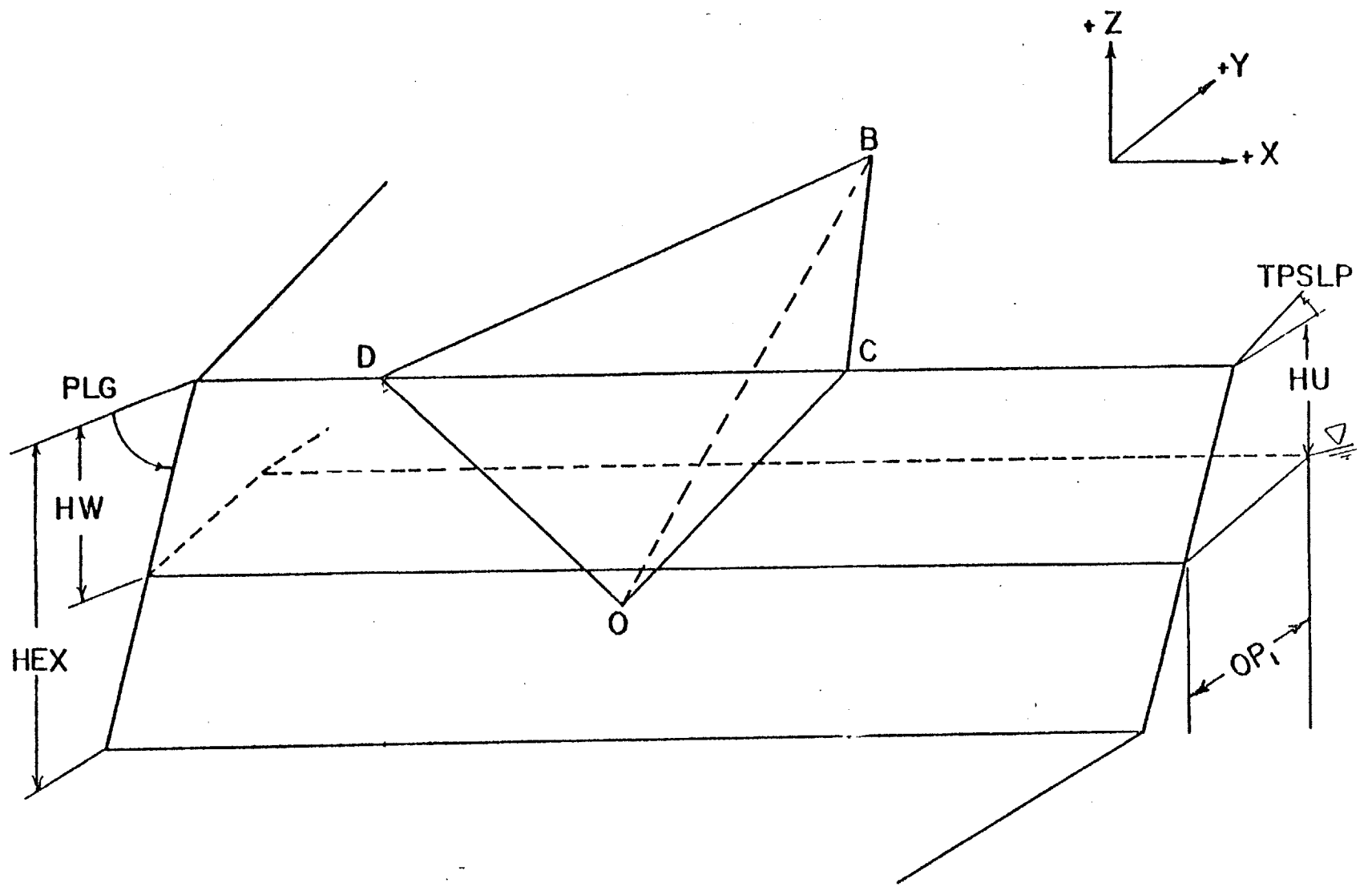
Number of Planes: (N) is entered as an integer in column 10. N may range from 2 to 8.

Cards #2 through #(N + 1)

Note: A separate card with the following data is entered for each joint plane being analyzed.

Strike of the Joint Plane: (H1STK, STK, H2STK) is entered in geologic notation in columns 1 to 4. Geologic strike must be expressed in the northern quadrants and the

Figure E.1 Model Slope
330



angle must be expressed as a two digit integer. (Examples: N45E, N06W)

Dip of the Joint Plane: (DIP, H1DIP, H2DIP) is entered in geologic notation in columns 6 to 9. Dip directions must indicate a particular quadrant i.e., NE, NW, SE, SW. The angle must be expressed as a two digit integer. (Examples: 30NW, 09NE)

Friction Angle: (PHX) on the joint planes is entered in columns 11 to 15 with a maximum of two decimal places.

Asperities: (AQ), the angular value of additional shearing resistance due to larger size irregularities of the joint planes, is entered in columns 16 to 20 with a maximum of two decimal places.

Cohesion of Intact Rock: (TAU) is entered in columns 21 to 30 with a maximum of two decimal places.

Normal Stiffness: (STIFFN) is entered in columns 31 to 40 with a maximum of three decimal places. STIFFN can also be entered in scientific notation with a maximum of three decimal places. (Examples: 173.2, 1.732E2) If columns 31 to 40 are left blank the program will default to STIFFN = 1000000.0.

Shear Stiffness: (STIFFS) is entered in columns 41 to 50 with a maximum of three decimal places. STIFFS can also be entered in scientific notation with a maximum of 3 decimal places. (Examples: 6789.6, 6.79E2) If the columns 41 to 50 are left blank the computer will default to STIFFS = 1.0.

Joint Persistence: (PCTJTG) is the percent of the area of the total joint that is not intact rock. PCTJTG is entered in columns 51 to 55 with a maximum of two decimal places.

Depth to Water: (HU) is measured from the crest of the excavation to a horizontal piezometric level (Figure E.1). It is used in conjunction with Piezometric Options 3 and 4 (Ref.: Piezometric Option). HU is entered in columns 56 to 60 with a maximum of one decimal place.

Uniform Water Pressure: (UAV) is entered in columns 61 to 70 with a maximum of three decimal places. UAV is used in conjunction with Piezometric Option 2 only (Ref.: Piezometric Option).

Piezometric Option: (IU) is a code that indicates how cleft water effects are to be incorporated into the analysis. 1: No effect from water; 2: Uniform pressure acting on the joint; 3: Pressure determined by a horizontal phreatic surface; 4: Pressure determined by an arbitrary phreatic surface. The code is entered in column 71 as an integer.

Card #(N + 2)

Strike of the Slope: (H1AZ1, AZ1, H2AZI) is entered in geologic notation in columns 1 to 4. Geologic strike must be expressed in the northern quadrants and the angle must be expressed as a two digit integer. (Examples: N45E, N06W)

Dip of the Slope: (PLG, H1PLG, H2PLG) is entered in geologic notation in columns 6 to 9. Dip directions must indicate a particular quadrant, i.e., NE, NW, SE, SW. The angle is expressed as a two digit integer. (Examples: 16NW, 07NE)

Height of the Slope: (HEX) is entered in columns 11 to 20 with a maximum of three decimal places. HEX is measured from the crest of the slope to the bottom of the slope (Figure E.1).

Length of the Slope: (XLEN) is entered in columns 21 to 30 with a maximum of three decimal places.

Angle of the Top Slope: (TPSLP) is entered in columns 31 to 40 with a maximum of three decimal places. TPSLP is shown in Figure E.1.

Unit Weight of Rock: (UNIWGT) is entered in columns 41 to 50 with a maximum of three decimal places.

Unit Weight of Water: (WWGT) is entered in columns 51 to 60 with a maximum of three decimal places.

Uniform Vertical Surcharge: (SUR) is the uniform vertical load acting per unit area on the top face of the wedge (face BCD in Figure E.1). SUR is entered in columns 61 to 70 with a maximum of three decimal places.

Surcharge Option: (IS) There are two options available to analyze the effects of the surcharge on the stability of the tetrahedron in the dynamic case. Option 1 assumes that the surcharge is a mass and that it is accelerated in the

same directions as the wedge under dynamic loading. The code 1 or 2 is entered in column 71 without a decimal.

Card # (N + 3)

Stress Ratio: (RATIO) is entered in columns 1 to 5 with a maximum of three decimal places. RATIO is the ratio of horizontal to vertical stresses within the wedge.

FS Option #1: (NDOP) is a code that indicates how the program should compute FS_I . As indicated in Section 4.4 (q.v.), FS_I is defined as

$$FS_I = \frac{\bar{R} \cdot \bar{\Delta}}{\bar{D} \cdot \bar{\Delta}} \quad (E.1)$$

where \bar{R} is the resultant of all resisting forces, \bar{D} is the resultant of all driving forces, and $\bar{\Delta}$ is the direction of impending movement. If a ' 0 ' is placed in column 15 $\bar{\Delta}$ is the displacement that would occur in response to a vertical load. If any other integer is placed in columns 11 to 15 $\bar{\Delta}$ is the displacement that occurs in response to the resultant of all external loads, i.e., all loads except the weight.

FS Option #2: (LOPT) is an option that allows the user to analyze all loads (including the weight of the wedge) with the stiffness approach. If a ' 1 ' is entered in column 20 the program will use this option. If any other integer is placed in columns 16 to 20 the program will analyze loads

according to the "standard" procedure presented in Section 4.3, i.e., stress approach for gravitational loads, stiffness approach for all other loads. If columns 16 to 20 are left blank the program will default to the standard procedure.

Card # (N + 4)

Depth to Piezometric Level on the Slope: (HW) is entered in columns 1 to 10 with a maximum of three decimal places. HW is shown in Figure E.1 and is used in conjunction with Piezometric Option 4.

Distance OPI: (OPl) is used in conjunction with Piezometric Option 4. As shown in Figure E.1, it is the horizontal distance from the face of the slope where the phreatic surface exits to the point where the phreatic surface becomes horizontal. OPl is entered in columns 11 to 20 with a maximum of three decimal places.

Seismic Coefficients X, Y, Z: (AKX, AKY, AKZ) Seismic forces are entered as decimal fractions of the gravitational force. Positive values will be forces acting at the centroid of the wedge in the direction of the appropriate positive coordinate, negative values act in the direction of the appropriate negative coordinate. AKX, AKY and AKZ are entered in columns 21 to 30, 31 to 40, and 41 to 50 respectively. The three coefficients are expressed with a maximum of three decimal places. If no seismic loads are to be considered columns 21 to 50 may be left blank--the computer will default

to $AKX = AKY = AKZ = 0$.

Point Loads: (PX, PY, PZ) can be used in the program. PX, PY, and PZ as point loads acting at the centroid of the wedge. PX, PY, and PZ are entered in columns 51 to 60, 61 to 70, and 71 to 80 respectively. They are expressed with a maximum of three decimal places. If no point loads are to be considered columns 51 to 80 may be left blank--the computer will default to $PX = PY = PZ = 0$.

Card # (N + 5)

Note: If no rock bolts are to be analyzed, a blank card is inserted.

Plane Numbers Supporting a Tetrahedron: (III,JJJ) It is anticipated that a user will run the program initially without any rock bolts. After the primary stability analysis, certain tetrahedrons may prove to need rock bolts. III and JJJ and the respective joint plane numbers specified by the user that support a particular tetrahedron that requires rock bolting. They are entered in columns 5 and 10 respectively as integers.

Number of Different Bolt Orientations: (NNN) The program is designed to accommodate up to sixteen different bolt orientations simultaneously; eight different orientations for face bolting, and eight different orientations for top bolting. The value of NNN may range from 1 to 8 and is entered in column 15 as an integer.

Card # (N + 6) Through # (NNN + N + 6)

Note: If no rock bolts are to be analyzed, these cards need not be entered.

Number of Top Bolts: (BTOP) is the total number of rock bolts at any particular orientation acting on the top side of the tetrahedron. BTOP may range in value from 1.0 to 9999.0 and is entered in columns 1 to 10 with a maximum of three decimal places.

Azimuth of Top Bolts: (ORT) is the angle projection in the XY plane of the angle the bolt set makes with the strike of the slope measured from 0 to 360 counterclockwise from the positive X-axis (Figure E.2). The value is entered in degrees with a maximum of three decimal places in columns 11 to 20.

Plunge of Top Bolts: (DPT) is the angle the bolt set makes with the positive Y axis measured from 0 to 360 in a clockwise direction (Figure E.2). The value is entered in degrees with a decimal in columns 21 to 30.

Load on a Top Bolt: (TEN) is the total working load of a top bolt. It is entered with a maximum of three decimal places in columns 31 to 40.

Number of Face Bolts: (BFAC) is the total number of rock bolts at any particular orientation load acting on the slope face of the tetrahedron. BFAC may range in value from 1.0 to 9999.0 and is entered in columns 41 to 50 with a maximum of three decimal places.

Azimuth of Face Bolts: (ORF) is defined in the same manner as ORT. It is entered in columns 51 to 60 with a maximum of three decimal places.

Plunge of Face Bolt: (DPF) is defined in the same manner as DPT. It is entered in columns 61 to 70 with a maximum of three decimal places.

Load on a Face Bolt: (FTEN) is the total working load of a face rock bolt. It is entered with a maximum of three decimal places in columns 71 to 80.

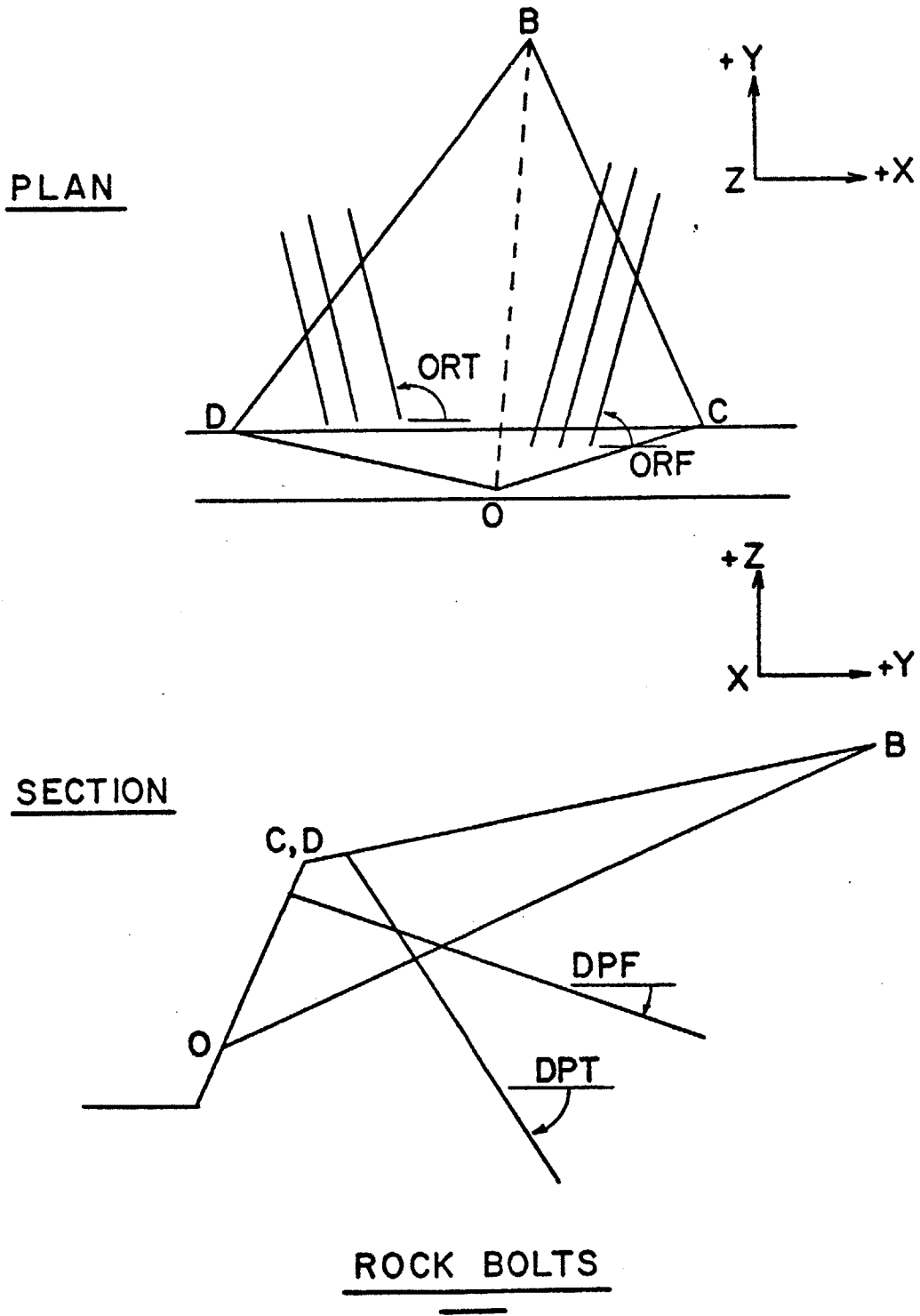


Figure E.2 Parameters For Rock Bolt Option
339

SWARS-2PM Listing

C		SWARS-PM	SWPM0001
C		SLIDING WEDGE ANALYSIS OF ROCK SLOPES -- TWO PLANES	26920030 SWPM0002
C		THIS IS THE ROUTINE TO TREAT FAILURE WHEN TWO PLANES ARE	26920040 SWPM0003
C		INVOLVED.	26920050 SWPM0004
		DIMENSION BETA (8), C (8), GAMMA (8), VX (8), VY (8), VZ (8), TAU (8), PCTJTG (8)	26920060 SWPM0005
		DIMENSION UX (8), UY (8), UZ (8), WX (8), WY (8), WZ (8), B (8)	26920070 SWPM0006
		DIMENSION T (8), TX (8), TY (8), TZ (8), EN (8), PHI (8)	26920080 SWPM0007
		DIMENSION SX (8), SY (8), SZ (8), RSS (8), RRX (8), RRY (8), RRZ (8)	26920090 SWPM0008
		DIMENSION H1STK (8), STK (8), H2STK (8), DIP (8), H1DIP (8), H2DIP (8)	26920100 SWPM0009
		DIMENSION INDEX (8), DUMMY (8), PHX (8), AP (8), AQ (8), CH (8)	26920110 SWPM0010
		DIMENSION WWX (8), WWY (8), WWZ (8), BET (8)	26920120 SWPM0011
		DIMENSION UAV (8), HU (8), UF (8), AREA (8), IU (8)	26920130 SWPM0012
		DIMENSION BTOP (8), ORT (8), DPT (8), TEN (8)	26920140 SWPM0013
		DIMENSION BFAC (8), ORF (8), DPF (8), FTEN (8)	26920150 SWPM0014
		DIMENSION STIFFN (8), STIFFS (8), RATIOK (8)	SWPM0015
		DIMENSION UI (8)	SWPM0016
		REAL NORD, HXX, HXY	SWPM0017
		LOGICAL FLIM	SWPM0018
		DATA NORD, SOTH, EAST, WEST/'N', 'S', 'E', 'W' /	26920160 SWPM0019
		NWR = 5	SWPM0020
		NRD = 8	SWPM0021
		FLIM = .TRUE.	SWPM0022
		PI=3.141593	26920180 SWPM0023
		PI2=PI/2.	26920190 SWPM0024
		FACT=180./PI	26920200 SWPM0025
10		FORMAT (3I5)	26920210 SWPM0026
11		FORMAT (2I5)	SWPM0027
15		FORMAT (A1, F2.0, A1, 1X, F3.0, A1, A1, 6G10.3, I1)	26920220 SWPM0028
16		FORMAT (F5.3, 2I5)	SWPM0029
20		FORMAT (8G10.3)	26920230 SWPM0030
25		FORMAT (A1, F2.0, A1, 1X, F2.0, A1, A1, 1X, 2F5.2, F10.3, 2G10.3, 2F5.2,	SWPM0031
		1 F10.3, I1)	SWPM0032
1001		FORMAT ('0', T20, 'FS =', F6.2, ' FOR SLIDING ON PLANE ', I1)	26920250 SWPM0033
1002		FORMAT ('1', T27, '***** CASE NUMBER IS ', I5, 3X, '*****', ///)	SWPM0034
		1 T30, '***** JOINT SETS ARE ', I1, ' AND ', I1, 2X, '*****', ///	SWPM0035
		2 T30, '***** JOINT DATA *****', ///)	SWPM0036

341

1004	FORMAT (29X,'***** JOINT SET ',I1,5X,'*****',///		SWPM0037
	1 18X,'STRIKE:',16X,'N',F3.0,A1,3X,'DIP:',18X,F3.0,A1,A1,///		SWPM0038
	2 18X,'PHI:',19X,F5.2,3X,'ASPERITIES:',11X,F5.2,///		SWPM0039
	3 18X,'COHESION:',9X,F10.2,3X,'PERSISTENCE:',10X,F5.2,///		SWPM0040
	4 18X,'NORMAL STIFFNESS:',G10.2,' SHEAR STIFFNESS:',G10.2,///		SWPM0041
	5 34X,'STIFFNESS RATIO:',F10.2,///		SWPM0042
	6 18X,'PIEZOMETRIC OPTION:',8X,I1)		SWPM0043
1006	FORMAT (37X,'SEISMIC ACCELERATIONS:',///,18X,'AKX =',F7.3,12X,		SWPM0044
	1 'AKY =',F7.3,11X,'AKZ =',F7.3,/))		SWPM0045
1007	FORMAT (40X,'POINT LOADS:',///,18X,'PX =',F9.2,12X,'PY =',F9.2,13X,		SWPM0046
	1 'PZ =',F9.2,/))		SWPM0047
1008	FORMAT('0',T20,'RESULTANT TENDS TO LIFT BLOCK OFF SUPPORTS')	26920480	SWPM0048
1009	FORMAT('0',T20,'FS IS NEG. SINCE THE DIRECTIONS OF ADDITIONAL'/	26920490	SWPM0049
	1T20,'LOADS OR SEISMIC FORCES TEND TO DISPLACE THE WEDGE'/	26920500	SWPM0050
	2T20,'UP THE LINE OF INTERSECTION OF THE TWO PLANES')	26920510	SWPM0051
1010	FORMAT('0',T20,'CHECK FOR TOPPLING ABOUT POINT 0')	26920520	SWPM0052
1011	FORMAT('0',42X,'SEISMIC DATA'///	26920530	SWPM0053
	1T20,'MINIMUM SEISMIC FORCE NEEDED IS ',F6.3/	26920540	SWPM0054
	2T20,'ACTING AT AN ORIENTATION OF ',F6.3,' ',F6.3,' ',F6.3)	26920550	SWPM0055
1012	FORMAT(T20,'NO ROTATIONS OCCUR ON EITHER PLANE')	26920560	SWPM0056
1013	FORMAT(T20,'FS =',F6.2,' FOR ROTATIONS ON PLANE ',I2)	26920570	SWPM0057
1014	FORMAT('0',T20,'LINE OF INTERSECTION AND EXCAVATION',	26920580	SWPM0058
	1' FACE ARE PARALLEL')	26920590	SWPM0059
1015	FORMAT('0',41X,'ROCK BOLT DATA')	26920600	SWPM0060
1016	FORMAT (T20,'FS(ULTIMATE) =',F6.2)		SWPM0061
1018	FORMAT ('0',T20,'FS(INITIAL) =',F6.2,' FOR SLIDING ON BOTH ',		SWPM0062
	1 'PLANES')		SWPM0063
1019	FORMAT('0',T20,'LINE OF INTERSECTION DOES NOT INTERSECT',	26920750	SWPM0064
	1' TOP OF SLOPE')	26920760	SWPM0065
1020	FORMAT('0',T20,'DIP OF THE LINE OF INTERSECTION',/	26920770	SWPM0066
	1T20,' IS GREATER THAN THE DIP OF THE EXCAVATION')	26920780	SWPM0067
1021	FORMAT('0',T20,'STRIKE OF PLANE AND EXCAVATION ARE THE SAME')	26920790	SWPM0068
1022	FORMAT('0',T20,'DIP AND STRIKE OF JOINT ARE IN THE SAME',	26920800	SWPM0069
	1' DIRECTION')	26920810	SWPM0070
1023	FORMAT('0',T20,'DIP AND STRIKE OF THE EXCAVATION ARE IN THE',	26920820	SWPM0071
	1' SAME DIRECTION')	26920830	SWPM0072

1024	FORMAT ('0',T20,'BOLT SET NO. ',I1,//	26920840	SWPM0073
	1T20,'TOP BOLTS ',F5.0,' LOAD = ',F10.0,//	26920850	SWPM0074
	2T20,'ORT = ',F5.1,' DPT = ',F5.1,//	26920860	SWPM0075
	3T20,'FACE BOLTS ',F5.0,' LOAD = ',F10.0,//	26920870	SWPM0076
	4T20,'ORF = ',F5.1,' DPF = ',F5.1)	26920880	SWPM0077
1030	FORMAT ('+',48X,'NO EFFECT FROM WATER',///)		SWPM0078
1031	FORMAT ('+',48X,'UNIFORM PRESSURE:',2X,F8.3,///)		SWPM0079
1032	FORMAT ('+',48X,'DEPTH TO WATER:',4X,F8.3,///)		SWPM0080
1033	FORMAT ('+',48X,'DEFINED PHREATIC SURFACE',///)		SWPM0081
1034	FORMAT (//,29X,'***** WEDGE DATA *****',//		SWPM0082
	1 18X,'BETA 1 = ',F6.2,8X,' PSI = ',F6.2,8X,' BETA 2 = ',F6.2,//		SWPM0083
	2 18X,'AREA: JT. PLANE 1:',F10.2,3X,' AREA: JT. PLANE 2:',F10.2,//		SWPM0084
	3 18X,'AREA: TOP FACE:',3X,F10.2,3X,' AREA: EXCAV. FACE:',F10.2,//		SWPM0085
	4 37X,'VOLUME:',F17.2,//		SWPM0086
	5 18X,'HEIGHT TO CREST:',2X,F10.2,3X,' HEIGHT ABOVE CREST:',F9.2,//		SWPM0087
	6 37X,'LINE OF INTERSECTION:',//,18X,' X = ',F6.3,15X,' Y = ',F6.3,		SWPM0088
	7 14X,' Z = ',F6.3,//)		SWPM0089
343 1035	FORMAT (29X,'***** LOAD DATA *****',//		SWPM0090
	1 18X,'UNIT WEIGHT OF ROCK:',F8.2,3X,' UNIT WEIGHT OF WATER: ',F6.2,		SWPM0091
	2 //,34X,' IN SITU STRESS RATIO:',F6.3,//		SWPM0092
	3 34X,'VERTICAL SURCHARGE:',F8.2,//)		SWPM0093
1036	FORMAT (29X,'***** EXCAVATION DATA *****',//		SWPM0094
	1 18X,'STRIKE:',16X,' N',F3.0,A1,3X,' DIP:',18X,F3.0,A1,A1,//		SWPM0095
	2 18X,'HEIGHT OF FACE:',F13.2,3X,' LENGTH OF FACE:',F12.2,//		SWPM0096
	3 31X,'INCLINATION OF TOP SLOPE:',F8.2,///)		SWPM0097
200	CONTINUE	26920890	SWPM0098
	READ (8,11) ICASE, N		SWPM0099
	IF (ICASF.EQ.0) GO TO 9000	26920910	SWPM0100
	DO 30 I=1,N	26920920	SWPM0101
	READ (8,25) H1STK(I),STK(I),H2STK(I),DIP(I),H1DIP(I),H2DIP(I),		SWPM0102
	1 PHX(I),AQ(I),TAU(I),STIFFN(I),STIFFS(I),PCTJTG(I),HU(I),		SWPM0103
	2 UAV(I),IU(I)		SWPM0104
	UI(I) = IU(I)		SWPM0105
	IF (PCTJTG(I) .EQ. 0.) PCTJTG(I) = 100.	26920950	SWPM0106
30	CONTINUE	26920960	SWPM0107
	READ (8,15) H1AZI,AZI,H2AZI,PLG,H1PLG,H2PLG,	26920970	SWPM0108

```

1 HEX,XLEN,TPSIP,UNIWGT,WWGT,SUR,IS
  READ (NRD,16) RATIO, LOPT, NDOP
  READ (8,20) HW,OP1,AKX,AKY,AKZ,PX,PY,PZ
  READ (8,10) III,JJJ,NNN
  IF (III.EQ.0) GO TO 65
  DO 80 I=1,NNN
  READ (8,20) BTOP (I),ORT (I),DPT (I),TEN (I),BFAC (I),ORF (I),
1 DPF (I),FTEN (I)
80 CONTINUE
65 IF (UNIWGT.EQ.0.) UNIWGT=1.0
  IF (UNIWGT.EQ.1.0) WWGT=0.0
  S=AZI+90.
  IF (H2AZI.EQ.WEST) S=90.-AZI
  DO 35 I=1,N
  BETA (I)=STK (I)+90.
  IF (H2STK (I).EQ.WEST) BETA (I)=90.-STK (I)
  GAMMA (I)=DIP (I)
  BET (I)=S-BETA (I)
  IF (BETA (I).GE.S) BET (I)=180.-BETA (I)+S
  IF (H1PLG.EQ.WEST.OR.H2PLG.EQ.WEST) GO TO 40
  IF (BETA (I).LT.S.AND.(H1DIP (I).EQ.WEST.OR.H2DIP (I).EQ.WEST))
1 GAMMA (I)=180.-DIP (I)
  IF (BETA (I).GT.S.AND.(H1DIP (I).EQ.EAST.OR.H2DIP (I).EQ.EAST))
1 GAMMA (I)=180.-DIP (I)
  GO TO 45
40 IF (BETA (I).LT.S.AND.(H1DIP (I).EQ.EAST.OR.H2DIP (I).EQ.EAST))
1 GAMMA (I)=180.-DIP (I)
  IF (BETA (I).GT.S.AND.(H1DIP (I).EQ.WEST.OR.H2DIP (I).EQ.WEST))
1 GAMMA (I)=180.-DIP (I)
45 CONTINUE
  B (I)=BET (I)/FACT
  C (I)=GAMMA (I)/FACT
  PHI (I)=PHX (I)/FACT
  AP (I)=AQ (I)/FACT
35 CONTINUE
  P=PLG/FACT

```

```

26920980 SWPM0109
          SWPM0110
26920990 SWPM0111
26921000 SWPM0112
26921010 SWPM0113
26921020 SWPM0114
26921030 SWPM0115
26921040 SWPM0116
26921050 SWPM0117
26921060 SWPM0118
26921070 SWPM0119
26921080 SWPM0120
26921090 SWPM0121
26921100 SWPM0122
26921110 SWPM0123
26921120 SWPM0124
26921130 SWPM0125
26921140 SWPM0126
26921150 SWPM0127
26921160 SWPM0128
26921170 SWPM0129
26921180 SWPM0130
26921190 SWPM0131
26921200 SWPM0132
26921210 SWPM0133
26921220 SWPM0134
26921230 SWPM0135
26921240 SWPM0136
26921250 SWPM0137
26921260 SWPM0138
26921270 SWPM0139
26921280 SWPM0140
26921290 SWPM0141
26921300 SWPM0142
26921310 SWPM0143
26921320 SWPM0144

```

```

D=TFSLP/FACT
CALL ORDER (N,B,INDEX)
CALL SWITCH (N,C,INDEX,DUMMY)
CALL SWITCH (N,BET,INDEX,DUMMY)
CALL SWITCH (N,PHX,INDEX,DUMMY)
CALL SWITCH (N,PHI,INDEX,DUMMY)
CALL SWITCH (N,AQ,INDEX,DUMMY)
CALL SWITCH (N,AP,INDEX,DUMMY)
CALL SWITCH (N,TAU,INDEX,DUMMY)
CALL SWITCH (N,PCTJTG,INDEX,DUMMY)
CALL SWITCH (N,UI,INDEX,DUMMY)
CALL SWITCH (N,UAV,INDEX,DUMMY)
CALL SWITCH (N,HU,INDEX,DUMMY)
CALL SWITCH (N,STK,INDEX,DUMMY)
CALL SWITCH (N,H2STK,INDEX,DUMMY)
CALL SWITCH (N,EIP,INDEX,DUMMY)
CALL SWITCH (N,H1DIP,INDEX,DUMMY)
CALL SWITCH (N,H2DIP,INDEX,DUMMY)
CALL SWITCH (N,STIFFN,INDEX,DUMMY)
CALL SWITCH (N,STIFFS,INDEX,DUMMY)
DO 105 I=1,N
IU(I) = UI(I)
UX(I)=COS(B(I))
UY(I)=SIN(B(I))
UZ(I)=0.
VX(I)=COS(C(I))*UY(I)
VY(I)=-COS(C(I))*UX(I)
VZ(I)=-SIN(C(I))
WX(I)=(UY(I)*VZ(I))-(UZ(I)*VY(I))
WY(I)=(UZ(I)*VX(I))-(UX(I)*VZ(I))
WZ(I)=(UX(I)*VY(I))-(UY(I)*VX(I))
UF(I)=0.
IF ( STIFFS(I) .NE. 0.0 ) RATIOK(I) = STIFFN(I)/STIFFS(I)
IF ( STIFFS(I) .EQ. 0.0 ) RATIOK(I) = 1000000.
IF ( RATIOK(I) .EQ. 1000000. ) STIFFS(I) = 1.
IF ( RATIOK(I) .EQ. 1000000. ) STIFFN(I) = 1000000.

```

345

```

26921330 SWPM0145
26921340 SWPM0146
26921350 SWPM0147
26921360 SWPM0148
26921370 SWPM0149
26921380 SWPM0150
26921390 SWPM0151
26921400 SWPM0152
26921410 SWPM0153
26921420 SWPM0154
                SWPM0155
26921440 SWPM0156
26921450 SWPM0157
26921460 SWPM0158
26921470 SWPM0159
26921480 SWPM0160
26921490 SWPM0161
26921500 SWPM0162
                SWPM0163
                SWPM0164
26921510 SWPM0165
                SWPM0166
26921520 SWPM0167
26921530 SWPM0168
26921540 SWPM0169
26921550 SWPM0170
26921560 SWPM0171
26921570 SWPM0172
26921580 SWPM0173
26921590 SWPM0174
26921600 SWPM0175
26921610 SWPM0176
                SWPM0177
                SWPM0178
                SWPM0179
                SWPM0180

```

105 CONTINUE

TAREX=0.

FAREX=0.

TEX=0.

TBY=0.

TBZ=0.

FBX=0.

FBY=0.

FBZ=0.

IF (III.NE.0) CALL BOLT (III,JJJ,NNN,WX,WY,WZ,HEX,C,B,P,XLEN,

1 PLG,D,TPSLP,ETOP,ORT,DPT,TEN,TAREX,TBX,TBY,TBZ,BFAC,ORF,DPF,PTEN,

2 FAREX,FBX,FBY,FBZ,FACT)

NN=N-1

DC 500 I=1,NN

II=I+1

DO 510 J=II,N

ID=J-I

WRITE (5,1002) ICASE,I,J

DO 210 K=I,J,ID

WRITE (5,1004) K,STK(K),H2STK(K),DIP(K),H1DIP(K),H2DIP(K),

1 PHX(K),AQ(K),TAU(K),PCTJTG(K),STIPFN(K),STIFFS(K),

2 RATIOK(K),IU(K)

IF (IU(K).EQ.1) WRITE (NWR,1030)

IF (IU(K).EQ.2) WRITE (NWR,1031) UAV

IF (IU(K).EQ.3) WRITE (NWR,1032) HU

IF (IU(K).EQ.4) WRITE (NWR,1033)

IF (H2STK(K).EQ.EAST.AND.H1DIP(K).EQ.SOTH.AND.H2DIP(K).EQ.WEST)

1 WRITE (5,1022)

IF (H2STK(K).EQ.EAST.AND.H1DIP(K).EQ.SOTH.AND.H2DIP(K).EQ.WEST)

1 GO TO 510

IF (H2STK(K).EQ.EAST.AND.H1DIP(K).EQ.NORD.AND.H2DIP(K).EQ.EAST)

1 WRITE (5,1022)

IF (H2STK(K).EQ.EAST.AND.H1DIP(K).EQ.NORD.AND.H2DIP(K).EQ.EAST)

1 GO TO 510

IF (H2STK(K).EQ.WEST.AND.H1DIP(K).EQ.NORD.AND.H2DIP(K).EQ.WEST)

1 WRITE (5,1022)

26921620 SWPM0181

26921630 SWPM0182

26921640 SWPM0183

26921650 SWPM0184

26921660 SWPM0185

26921670 SWPM0186

26921680 SWPM0187

26921690 SWPM0188

26921700 SWPM0189

26921710 SWPM0190

26921720 SWPM0191

26921730 SWPM0192

26921740 SWPM0193

26921750 SWPM0194

26921760 SWPM0195

26921770 SWPM0196

26921780 SWPM0197

26921790 SWPM0198

26921800 SWPM0199

SWPM0200

SWPM0201

SWPM0202

SWPM0203

SWPM0204

SWPM0205

SWPM0206

SWPM0207

SWPM0208

SWPM0209

SWPM0210

SWPM0211

SWPM0212

SWPM0213

SWPM0214

SWPM0215

SWPM0216

	IF(H2STK(K).EQ.WEST.AND.H1DIP(K).EQ.NORD.AND.H2DIP(K).EQ.WEST)	26921870	SWPM0217
	1 GO TO 510		SWPM0218
	IF(H2STK(K).EQ.WEST.AND.H1DIP(K).EQ.SOTH.AND.H2DIP(K).EQ.EAST)		SWPM0219
	1 WRITE (5,1022)		SWPM0220
	IF(H2STK(K).EQ.WEST.AND.H1DIP(K).EQ.SOTH.AND.H2DIP(K).EQ.EAST)		SWPM0221
	1 GO TO 510		SWPM0222
	IF(BET(K).EQ.0..OR.BET(K).EQ.180.) WRITE (5,1021)		SWPM0223
	IF(BET(K).EQ.0..OR.BET(K).EQ.180.) GO TO 510		SWPM0224
210	CONTINUE	26921920	SWPM0225
	WRITE (NWR,1036) AZI, H2AZI,PLG, H1PLG, H2PLG, HEX, XLEN, TPSLP		SWPM0226
	WRITE (5,1035) UNIWGT, WWGT, RATIO, SUR		SWPM0227
	IF(AKX.NE.0.0.OR.AKY.NE.0.0.OR.AKZ.NE.0.0)		SWPM0228
	1 WRITE (NWR,1006) AKX, AKY, AKZ		SWPM0229
	IF(PX.NE.0.0.OR.PZ.NE.0.0.OR.PZ.NE.0.0) WRITE (NWR,1007) PX,PY,PZ		SWPM0230
	IF(H2AZI.EQ.EAST.AND.H2PLG.EQ.EAST.AND.H1PLG.EQ.NORD) WRITE (5,1023)		SWPM0231
	IF(H2AZI.EQ.EAST.AND.H2PLG.EQ.EAST.AND.H1PLG.EQ.NORD) GO TO 510		SWPM0232
	IF(H2AZI.EQ.EAST.AND.H2PLG.EQ.WEST.AND.H1PLG.EQ.SOTH) WRITE (5,1023)		SWPM0233
	IF(H2AZI.EQ.EAST.AND.H2PLG.EQ.WEST.AND.H1PLG.EQ.SOTH) GO TO 510		SWPM0234
	IF(H2AZI.EQ.WEST.AND.H2PLG.EQ.WEST.AND.H1PLG.EQ.NORD) WRITE (5,1023)		SWPM0235
	IF(H2AZI.EQ.WEST.AND.H2PLG.EQ.WEST.AND.H1PLG.EQ.NORD) GO TO 510		SWPM0236
	IF(H2AZI.EQ.WEST.AND.H2PLG.EQ.EAST.AND.H1PLG.EQ.SOTH) WRITE (5,1023)		SWPM0237
	IF(H2AZI.EQ.WEST.AND.H2PLG.EQ.EAST.AND.H1PLG.EQ.SOTH) GO TO 510		SWPM0238
	IF (III .EQ. 0) GO TO 230		SWPM0239
	WRITE (5,1015)		SWPM0240
	DO 255 K=1,NNN	26922080	SWPM0241
	WRITE (5,1024) K,BTOP(K),TEN(K),ORT(K),DPT(K),BFAC(K),FTEN(K),	26922090	SWPM0242
	1 ORF(K),DPF(K)	26922100	SWPM0243
255	CONTINUE	26922110	SWPM0244
230	XX=(WY(J)*WZ(I)-WZ(J)*WY(I))	26922190	SWPM0245
	XY=(WZ(J)*WX(I)-WX(J)*WZ(I))	26922200	SWPM0246
	XZ=(WX(J)*WY(I)-WY(J)*WX(I))	26922210	SWPM0247
	X=SQRT(XX**2+XY**2+XZ**2)	26922220	SWPM0248
	XX1 = XX/X		SWPM0249
	XY1 = XY/X		SWPM0250
	XZ1 = XZ/X		SWPM0251
	ODX = -HEX/(TAN(C(I))*SIN(B(I))) + HEX/(TAN(P)*TAN(B(I)))		SWPM0252

	OCX = -HEX/(TAN(C(J))*SIN(B(J))) + HEX/(TAN(P)*TAN(B(J)))	SWPM0253
	ODY = HEX/TAN(P)	SWPM0254
	DC=OCX-ODX	26922260 SWPM0255
	IF(DC.LE.XLEN) GO TO 95	26922270 SWPM0256
	H=XLEN*HEX/DC	26922280 SWPM0257
	ODX = -H / (TAN(C(I))*SIN(B(I))) + H / (TAN(P)*TAN(B(I)))	SWPM0258
	OCX = -H/(TAN(C(J))*SIN(B(J))) + H/(TAN(P)*TAN(B(J)))	SWPM0259
	ODY = H/TAN(P)	SWPM0260
	DC=OCX-ODX	26922320 SWPM0261
	GO TO 100	26922330 SWPM0262
95	H=HEX	26922340 SWPM0263
100	CONTINUE	26922350 SWPM0264
	OCY=ODY	26922360 SWPM0265
	ODZ=H	26922370 SWPM0266
	OCZ=ODZ	26922380 SWPM0267
	IF(XY.EQ.0.)GO TO 50	26922390 SWPM0268
	TANE=XZ/XY	26922400 SWPM0269
	TAND=TAN(D)	26922410 SWPM0270
	IF(TANE.LE.TAND) GO TO 125	26922420 SWPM0271
	E=ATAN(TANE)	26922430 SWPM0272
	IF(E.LT.0.) E=E+PI	26922440 SWPM0273
	IF(E.GT.P) GO TO 155	26922450 SWPM0274
	GO TO 60	26922460 SWPM0275
125	WRITE(5,1019)	SWPM0276
	GO TO 510	26922480 SWPM0277
50	WRITE(5,1014)	SWPM0278
	GO TO 510	26922500 SWPM0279
155	WRITE(5,1020)	SWPM0280
	GO TO 510	26922520 SWPM0281
60	AAA=1.	26922530 SWPM0282
	IF(PLG.NE.90.) AAA=1.-TANE/TAN(P)	26922540 SWPM0283
	HH=H*AAA*TAND/(TANE-TAND)	26922550 SWPM0284
	CCC=(H+HH)/XZ	26922560 SWPM0285
	OBX = CCC*XX	26922570 SWPM0286
	OBY = CCC*XY	26922580 SWPM0287
	OBZ = CCC*XZ	26922590 SWPM0288

```

OD=SQRT (ODX**2+ODY**2+ODZ**2)
OC=SQRT (OCX**2+OCY**2+OCZ**2)
OB=SQRT (OBX**2+OBY**2+OBZ**2)
OBBY=OBY-ODY
IF (TPSLP.NE.0.) OBBY=HH/SIN(D)
TAREA=OBBY*DC/2.
AZ=H/SIN(P)
FAREA=DC*AZ/2.
BDX=ODX-OBX
IF (BDX.LT.0.) BDX=-BDX
DB=OBBY
R1=ATAN2 (BDX,OBBY)
IF (TAN(R1).NE.0.) DB=OBBY/COS(R1)
CBX=OCX-OBX
IF (CBX.LT.0.) CBX=-CBX
CE=OBBY
R=ATAN2 (CBX,OBBY)
IF (TAN(R).NE.0.) CB=OBBY/COS(R)
CCP=H/XZ
DEPY=CCP*XY-ODY
VOL=DBPY*DC*(H+HH)/6.
OSX=(OBX+OCX+OEX)/4.
OSY=(OBY+OCY+ODY)/4.
OSZ=(OBZ+OCZ+ODZ)/4.
TEMP=VOL*UNWGT
DUMMYT = TEMP*COS(E)*1.0E-10
SURG=SUR*TAREA/COS(D)
SUM1=(OD+OB+DB)/2.
SUM2=(OC+OB+CB)/2.
AREA(I)=SQRT(SUM1*(SUM1-OD)*(SUM1-OB)*(SUM1-DB))
AREA(J)=SQRT(SUM2*(SUM2-OC)*(SUM2-OB)*(SUM2-CB))
CH(I)=TAU(I)*(100.-PCTJTG(I))*(.01)*AREA(I)
CH(J)=TAU(J)*(100.-PCTJTG(J))*(.01)*AREA(J)
CH1=CH(I)
CH2=CH(J)
TAR=TAREA

```

349

```

26922600 SWPM0289
26922610 SWPM0290
26922620 SWPM0291
26922630 SWPM0292
26922640 SWPM0293
26922650 SWPM0294
26922660 SWPM0295
26922670 SWPM0296
26922680 SWPM0297
26922690 SWPM0298
26922700 SWPM0299
26922710 SWPM0300
26922720 SWPM0301
26922730 SWPM0302
26922740 SWPM0303
26922750 SWPM0304
26922760 SWPM0305
26922770 SWPM0306
26922780 SWPM0307
26922790 SWPM0308
26922800 SWPM0309
26922810 SWPM0310
26922820 SWPM0311
26922830 SWPM0312
26922840 SWPM0313
                SWPM0314
26922850 SWPM0315
26922860 SWPM0316
26922870 SWPM0317
26922880 SWPM0318
26922890 SWPM0319
26922900 SWPM0320
26922910 SWPM0321
26922920 SWPM0322
26922930 SWPM0323
26922940 SWPM0324

```

```

IF (TAREX.LT.TAREA) TAR=TAREX
FAR=FAREA
IF (FAREX.LT.FAREA) FAR=FAREX
RBX=TBX*TAR+FBX*FAR
RBY=TBY*TAR+FBY*FAR
RBZ=TBZ*TAR+FEZ*FAR
RX = RBX + PX + TEMP*AKX
RY = RBY + PY + TEMP*AKY
RZ = RBZ + PZ -SURG - TEMP*(1.0 - AKZ)
IF ( IS .EQ. 2 ) RX = RX + SURG*AKX
IF ( IS .EQ. 2 ) RY = RY + SURG*AKY
IF ( IS .EQ. 2 ) RZ = RZ + SURG*AKZ
CALL WATER (RX,RY,RZ,H,E,P,PLG,HU,IU,UAV,OP1,HW,UF,HH,PI,
1 ARFA,WWGT,I,J,ID,WX,WY,WZ,TPSLP)
OIRX=OSY*RZ-OSZ*RY
OIRY=OSZ*RX-OSX*RZ
OIRZ=OSX*RY-OSY*RX
EMX=XX*OIRX+XY*OIRY+XZ*OIRZ
DO 110 K=I,J,ID
EN(K) =RX*WX(K) +RY*WY(K) +RZ*WZ(K)
TX(K) =RX-EN(K) *WX(K)
TY(K) =RY-EN(K) *WY(K)
TZ(K) =RZ-EN(K) *WZ(K)
T(K) =SQRT(TX(K)**2+TY(K)**2+TZ(K)**2)
110 CONTINUE
ENN=0.
IF (EN(I).GT.0.0.OR.EN(J).LT.0.0) GO TO 120
WRITE (5,1008)
GO TO 400
120 DO 115 K=I,J,ID
SX(K) = (XY*WZ(K) -XZ*WY(K) )
SY(K) = (XZ*WX(K) -XX*WZ(K) )
SZ(K) = (XX*WY(K) -XY*WX(K) )
RSS(K) =RX*SX(K) +RY*SY(K) +RZ*SZ(K)
115 CONTINUE
T12 = RX*XX1 + RY*XY1 + RZ*XZ1

```

```

26922950 SWPM0325
26922960 SWPM0326
26922970 SWPM0327
26922980 SWPM0328
26922990 SWPM0329
26923000 SWPM0330
SWPM0331
SWPM0332
SWPM0333
SWPM0334
SWPM0335
SWPM0336
26923100 SWPM0337
26923110 SWPM0338
26923120 SWPM0339
26923130 SWPM0340
26923140 SWPM0341
26923150 SWPM0342
26923160 SWPM0343
26923170 SWPM0344
26923180 SWPM0345
26923190 SWPM0346
26923200 SWPM0347
26923210 SWPM0348
26923220 SWPM0349
26923230 SWPM0350
26923240 SWPM0351
SWPM0352
26923260 SWPM0353
26923270 SWPM0354
26923280 SWPM0355
26923290 SWPM0356
26923300 SWPM0357
26923310 SWPM0358
26923320 SWPM0359
SWPM0360

```

```

T12P = RX*XX1 + RY*XY1 + (RZ+TEMP)*XZ1
SILEN = SQRT(SX(I)**2 + SY(I)**2 + SZ(I)**2)
SJLEN = SQRT(SX(J)**2 + SY(J)**2 + SZ(J)**2)
ETACOS = (SX(J)*SX(I) + SY(J)*SY(I) + SZ(J)*SZ(I))/(SILEN*SJLEN)
ETA = ACOS(ETACOS)
IF ( ETA .LT. 0.0 ) ETA = PI + ETA
ETO = ETA*180./PI
HORIZL = SQRT(XX**2 + XY**2)
COSBT2 = (XY*SX(J) - XX*SY(J))/(SJLEN*HORIZL)
SINBT2 = SQRT(1.0 - COSBT2**2)
BETA2 = ATAN(SINBT2/COSBT2)
BETO2 = BETA2*180./PI
BETA1 = PI - BETA2 - ETA
BETO1 = BETA1*180./PI
SINBT1 = SIN(BETA1)
COSBT1 = COS(BETA1)
WRITE (NWR,1034) BETO1, ETO, BETO2, AREA(I), AREA(J), TAREA,
1 FAREA, VOL, H, HH, XX1, XY1, XZ1
IF (RSS(I).LT.0.0) GO TO 130
IF (RSS(J).LT.0.0) GO TO 140
PERP1 = 0.0
TANG1 = 0.0
PERP2 = 0.0
TANG2 = 0.0
IF ( LOPT .EQ. 1 ) GO TO 78
C THIS SECTION COMPUTES THE EFFECT OF IN SITU STRESSES
WTCO = TEMP*COS(E)
IF ( RATIO .NE. 1.0 ) GO TO 76
PERP2 = WTCO/(COSBT2 + SINBT2*COSBT1/SINBT1)
PERP1 = PERP2*SINBT2/SINBT1
GO TO 78
76 RAT1=(RATIO+(1.0-RATIO)*COSBT1**2)/((1.0-RATIO)*SINBT1*COSBT1)
RAT2=(RATIO+(1.0-RATIO)*COSBT2**2)/((1.0-RATIO)*SINBT2*COSBT2)
RAT12 = (RAT2*SINBT2 - COSBT2)/(RAT1*SINBT1 - COSBT1)
TANG2 = WTCO/(RAT12*(RAT1*COSBT1 + SINBT1) + (RAT2*COSBT2+SINBT2))
TANG1 = RAT12*TANG2

```

```

SWPM0361
SWPM0362
SWPM0363
SWPM0364
SWPM0365
SWPM0366
SWPM0367
SWPM0368
SWPM0369
SWPM0370
SWPM0371
SWPM0372
SWPM0373
SWPM0374
SWPM0375
SWPM0376
SWPM0377
SWPM0378
26923330 SWPM0379
26923340 SWPM0380
SWPM0381
SWPM0382
SWPM0383
SWPM0384
SWPM0385
SWPM0386
SWPM0387
SWPM0388
SWPM0389
SWPM0390
SWPM0391
SWPM0392
SWPM0393
SWPM0394
SWPM0395
SWPM0396

```

	PERP1 = RAT1*TANG1	SWPM0397
	PERP2 = TANG2*RAT2	SWPM0398
C	THIS PART COMPUTES THE EFFECT OF JOINT STIFFNESSES	SWPM0399
78	HXX = XY1/(SQRT(XX1**2 + XY1**2))	SWPM0400
	HXY = -XX1/(SQRT(XX1**2 + XY1**2))	SWPM0401
	RHORIZ = RX*HXX + RY*HXY	SWPM0402
	RVERT = -1.0*(RX*HXY*XZ1 - RY*HXX*XZ1 + RZ*(HXX*XY1 - XX1*HXY))	SWPM0403
	UR1A = RVERT/(COSBT1 + COSBT2*SINBT1/SINBT2)	SWPM0404
	UR2A = UR1A*SINBT1/SINBT2	SWPM0405
	UR1B = RHORIZ/(SINBT1 + SINBT2*COSBT1/COSBT2)	SWPM0406
	UR2B = UR1B*COSBT1/COSBT2	SWPM0407
C	FSLR IS THE 'ULTIMATE' F.S. FOR SLIDING DOWN THE LINE OF INTERSECTION	SWPM0408
	FSLR = ((UR1A + UR1B)*TAN(PHI(I)) + (UR2A + UR2B)*TAN(PHI(J))) /T12	SWPM0409
	RVERT1 = RVERT - TEMP*(HXX*XY1 - XX1*HXY)	SWPM0410
	IF (LOPT .EQ. 1) RVERT1 = RVERT	SWPM0411
	IF (RVERT1 .NE. 0.0 .OR. RHORIZ .NE. 0.0) GO TO 79	SWPM0412
167	RVERT1 = DUMMYT	SWPM0413
79	ST1N = STIFFN(I)*AREA(I)	SWPM0414
	ST1S = STIFFS(I)*AREA(I)	SWPM0415
	ST2N = STIFFN(J)*AREA(J)	SWPM0416
	ST2S = STIFFS(J)*AREA(J)	SWPM0417
	FACTAA = ST1N*SINBT1 + ST1S*COSBT1**2/SINBT1 +	SWPM0418
	1 ST2N*SINBT2 + ST2S*COSBT2**2/SINBT2	SWPM0419
	FACTBB = (ST1N-ST1S)*COSBT1 + (ST2S-ST2N)*COSBT2	SWPM0420
	FACTCC = ST1N*COSBT1**2/SINBT1 + ST1S*SINBT1 +	SWPM0421
	1 ST2N*COSBT2**2/SINBT2 + ST2S*SINBT2	SWPM0422
	ALPHA = ATAN((FACTCC*RHORIZ - FACTBB*RVERT1)/	SWPM0423
	1 (FACTAA*RVERT1 - FACTBB*RHORIZ))	SWPM0424
	COSALP = COS(ALPHA)	SWPM0425
	SINALP = SIN(ALPHA)	SWPM0426
	FACTDD = ST1N*(SINALP + COSALP*COSBT1/SINBT1)	SWPM0427
	FACTEE = ST1S*(COSALP*SINBT1 - SINALP*COSBT1)	SWPM0428
	FACTFF = ST2N*(COSALP*COSBT2**2/SINBT2 - SINALP*COSBT2)	SWPM0429
	FACTGG = ST2S*(COSALP*SINBT2 + SINALP*COSBT2/SINBT2)	SWPM0430
	PERP11 = RVERT1*FACTDD/(COSBT1 + FACTEE + FACTFF + FACTGG)	SWPM0431
	DISP = PERP11/FACTDD	SWPM0432

352

```

PERP1 = PERP11 + PERP1
TANG1 = PERP11*FACTIE/(SINBT1*FACTDD) + TANG1
PERP2 = PERP11*FACTFF/(COSBT2*FACTDD) + PERP2
TANG2 = PERP11*FACTGG/(SINBT2*FACTDD) + TANG2
IF (.NOT.FLIM) GO TO 166
IF ( NDOP .NE. 0 ) GO TO 166
PPERP1 = PERP1
PPERP2 = PERP2
TTANG1 = TANG1
TTANG2 = TANG2
FLIM = .FALSE.
RHORIZ = 0.0
GO TO 167

```

C THIS PART COMPUTES THE FACTOR OF SAFETY: THE RATIO OF THE
C COMPONENTS OF DRIVING TO RESISTING FORCES IN THE DISPLACEMENT DIRECTION

```

166 IF ( RVERT1 .EQ. DUMMYT ) T12P = DUMMYT*TAN(E)

```

```

ADISP = T12P/(ST1S + ST2S)
BDISP = DISP*SINALP
CDISP = -DISP*COSAIP
DISP = SQRT(ADISP**2 + BDISP**2 + CDISP**2)
ADISP = ADISP/DISP
BDISP = BDISP/DISP
CDISP = CDISP/DISP
IF (FLIM) GO TO 168
PERP1 = PPERP1
PERP2 = PPERP2
TANG1 = TTANG1
TANG2 = TTANG2

```

```

168 FLIM = .TRUE.

```

```

ADRF1 = T12*ST1S/(ST1S + ST2S)
BDRF1 = -TANG1*COSBT1
CDRF1 = -TANG1*SINBT1
ADRF2 = T12 - ADRF1
BDRF2 = TANG2*COSBT2
CDRF2 = -TANG2*SINBT2
DRF = (ADRF1+ADRF2)*ADISP + (BDRF1+BDRF2)*BDISP + (CDRF1+CDRF2)*CDISP

```

```

SWPM0433
SWPM0434
SWPM0435
SWPM0436
SWPM0437
SWPM0438
SWPM0439
SWPM0440
SWPM0441
SWPM0442
SWPM0443
SWPM0444
SWPM0445
SWPM0446
SWPM0447
SWPM0448
SWPM0449
SWPM0450
SWPM0451
SWPM0452
SWPM0453
SWPM0454
SWPM0455
SWPM0456
SWPM0457
SWPM0458
SWPM0459
SWPM0460
SWPM0461
SWPM0462
SWPM0463
SWPM0464
SWPM0465
SWPM0466
SWPM0467
SWPM0468

```

```

FACTHH = (ADRF1*ALISP+BDRF1*BDISP+CDRF1*CDISP)/
1 (SQRT (ADRF1**2+BDRF1**2+CDRF1**2))
FACTJJ = (ADRF2*ADISP+BDRF2*BDISP+CDRF2*CDISP)/
1 (SQRT (ADRF2**2+BDRF2**2+CDRF2**2))
REST2 = PERP2*TAN (PHI (J) +AP (J)) + CH2
REST1 = PERP1*TAN (PHI (I) +AP (I)) +CH1
FSL = (REST1*FACTHH + REST2*FACTJJ)/DRF
WRITE (5, 1018) FSL
IF (FSL.LT.0.) WRITE (5, 1009)
WRITE (NWR, 1016) FSLR
245 IF (FSL.LT.1.) GO TO 300
WWX (I) = -WX (I)
WWY (I) = -WY (I)
WWZ (I) = -WZ (I)
WWX (J) = WX (J)
WWY (J) = WY (J)
WWZ (J) = WZ (J)
DO 410 K=I, J, ID
COSP=COS (PHI (K) +AP (K))
SINP=SIN (PHI (K) +AP (K))
RRX (K) =WWX (K) *COSP-XX*SINP/X
RRY (K) =WWY (K) *COSP-XY*SINP/X
RRZ (K) =WWZ (K) *COSP-XZ*SINP/X
410 CONTINUE
CRPX=RRY (I) *RRZ (J) -RRZ (I) *RRY (J)
CRPY=RRZ (I) *RRX (J) -RRX (I) *RRZ (J)
CRPZ=RRX (I) *RRY (J) -RRY (I) *RRX (J)
CRR=SQRT (CRPX**2+CRPY**2+CRPZ**2)
CRRX=-CRPX/CRR
CRRY=-CRPY/CRR
CRRZ=-CRPZ/CRR
ENN=(RX*CRRX+RY*CRRY+RZ*CRRZ)/(TEMP)
GO TO 300
130 IF (EN(I).LT.0.0) GO TO 150
FLS = 0.0
K=I

```

```

SWPM0469
SWPM0470
SWPM0471
SWPM0472
SWPM0473
SWPM0474
SWPM0475
SWPM0476
SWPM0477
SWPM0478
26923500 SWPM0479
26923510 SWPM0480
26923520 SWPM0481
26923530 SWPM0482
26923540 SWPM0483
26923550 SWPM0484
26923560 SWPM0485
26923570 SWPM0486
26923580 SWPM0487
26923590 SWPM0488
26923600 SWPM0489
26923610 SWPM0490
26923620 SWPM0491
26923630 SWPM0492
26923640 SWPM0493
26923650 SWPM0494
26923660 SWPM0495
26923670 SWPM0496
26923680 SWPM0497
26923690 SWPM0498
26923700 SWPM0499
26923710 SWPM0500
26923720 SWPM0501
26923730 SWPM0502
SWPM0503
26923750 SWPM0504

```

355

GO TO 145	26923760	SWPM0505
140 IF (EN(J).GT.0.0) GO TO 150	26923770	SWPM0506
FSL=0.	26923780	SWPM0507
K=J	26923790	SWPM0508
EN(K)=-EN(K)	26923800	SWPM0509
145 CONTINUE	26923810	SWPM0510
FSS=(EN(K)*TAN(PHI(K)+AP(K))+CH(K))/T(K)	26923820	SWPM0511
WRITE(5,1001) FSS,K		SWPM0512
IF(CH1.NE.0..OR.CH2.NE.0..OR.AP(I).NE.0..OR.AP(J).NE.0.) GO TO 70	26923840	SWPM0513
GO TO 240	26923850	SWPM0514
70 FSSR=EN(K)*TAN(PHI(K))/T(K)	26923860	SWPM0515
WRITE(5,1016) FSSR		SWPM0516
GO TO 240	26923880	SWPM0517
150 WRITE(5,1010)		SWPM0518
GO TO 400	26923900	SWPM0519
240 IF(FSS.LT.1.) GO TO 300	26923910	SWPM0520
ENN=SIN(PHI(K)+AP(K)-ATAN2(T(K),EN(K)))	26923920	SWPM0521
AA=B(K)-90./FACT		SWPM0522
IF(TX(K).NE.0.) AA=B(K)-ATAN2(TY(K),TX(K))	26923940	SWPM0523
AB=C(K)	26923950	SWPM0524
IF(DIP(K).NE.90.) AB=ATAN(TAN(C(K))*SIN(AA))	26923960	SWPM0525
PLUN=PHI(K)-AB	26923970	SWPM0526
CRRH=SQRT(TX(K)**2+TY(K)**2)	26923980	SWPM0527
CRRZ=CRRH*TAN(PLUN)/T(K)	26923990	SWPM0528
CRRX=TX(K)/T(K)	26924000	SWPM0529
CRRY=TY(K)/T(K)	26924010	SWPM0530
300 IF(FSL.NE.0.) FSS=0.	26924020	SWPM0531
IF(FSS.NE.0.) GO TO 400	26924030	SWPM0532
IF(IU(I).NE.1 .AND. IU(J).NE.1) GO TO 400		SWPM0533
AK1COS = ((ODX*OBX+ODY*OBY+ODZ*OBZ)/(OD*OB))		SWPM0534
AK10 = ATAN(SQRT(1.0 - AK1COS**2)/AK1COS)		SWPM0535
AK2COS = ((OCX*OBX+OCY*OBY+OCZ*OBZ)/(OC*OB))	26924070	SWPM0536
AK20 = ATAN(SQRT(1.0 - AK2COS**2)/AK2COS)		SWPM0537
EM10=- (WX(I)*OIRX+WY(I)*OIRY+WZ(I)*OIRZ)	26924080	SWPM0538
EM20=- (WX(J)*OIRX+WY(J)*OIRY+WZ(J)*OIRZ)	26924090	SWPM0539
IF (EMX.LE.0.0.OR.EM10.LE.0.0) GO TO 310	26924100	SWPM0540

IF (AK20.GT.PI2) GO TO 310	26924110	SWPM0541
IF (ETA.LT.PI2.AND.AK10.GT.PI2.AND.	26924120	SWPM0542
1 (TAN(AK20)/TAN(PI-AK10)).GT.(1./COS(PI-ETA))) GO TO 310	26924130	SWPM0543
K=I	26924140	SWPM0544
305 TOP=OSX*WX(K)+OSY*WY(K)+OSZ*WZ(K)	26924150	SWPM0545
BOT=RX*WX(K)+RY*WY(K)+RZ*WZ(K)	26924160	SWPM0546
VJP=-TOP/BOT		SWPM0547
OQX=OSX+VJP*RX		SWPM0548
OQY=OSY+VJP*RY		SWPM0549
OQZ=OSZ+VJP*RZ		SWPM0550
OQWX=OQY*WZ(K)-OQZ*WY(K)	26924210	SWPM0551
OQWY=OQZ*WX(K)-OQX*WZ(K)	26924220	SWPM0552
OQWZ=OQX*WY(K)-OQY*WX(K)	26924230	SWPM0553
DET=-OQY*OQWZ+OQZ*OQWY	26924240	SWPM0554
C2=(-TZ(K)*OQY+TY(K)*OQZ)/DET	26924250	SWPM0555
TT=C2*SQRT(OQWX**2+OQWY**2+OQWZ**2)	26924260	SWPM0556
FSR=(EN(K)*TAN(PHI(K)+AP(K))+CH(K))/TT	26924270	SWPM0557
WRITE(5,1013)FSR,K		SWPM0558
IF(CH1.NE.0..OR.CH2.NE.0..OR.AP(I).NE.0..OR.AP(J).NE.0.) GO TO 75	26924290	SWPM0559
GO TO 420	26924300	SWPM0560
75 FSRR=EN(K)*TAN(PHI(K))/TT	26924310	SWPM0561
WRITE(5,1016)FSRR		SWPM0562
GO TO 420	26924330	SWPM0563
310 IF (EMX.GE.0.0.OR.EM20.LE.0.0) GO TO 320	26924340	SWPM0564
IF (AK10.GT.PI2) GO TO 320	26924350	SWPM0565
IF (ETA.LT.PI2.AND.AK20.GT.PI2.AND.	26924360	SWPM0566
1 (TAN(AK10)/TAN(PI-AK20)).GT.(1./COS(PI-ETA))) GO TO 320	26924370	SWPM0567
K=J	26924380	SWPM0568
EN(K)=-EN(K)	26924390	SWPM0569
GO TO 305	26924400	SWPM0570
320 WRITE(5,1012)		SWPM0571
FSR=).	26924420	SWPM0572
GO TO 400	26924430	SWPM0573
420 IF (FSR.LT.1.) GO TO 400	26924440	SWPM0574
ENNR=SIN(PHI(K)+AP(K)-ATAN2(TT,EN(K)))	26924450	SWPM0575
CHRRX=C2*OQWX/TT	26924460	SWPM0576

356

```

CRRRY=C2*OQWY/IT
CRRRZ=C2*OQWZ/IT
IF(ENNR.LT.ENN) GO TO 405
GO TO 400
405 ENN=ENNR
CRRX=CRRRX
CRRY=CRRRY
CRRZ=CRRRZ
400 CONTINUE
DCX=-ODX
DBX=OBX-ODX
IF(AKX.NE.0..OR.AKY.NE.0..OR.AKZ.NE.0.) GO TO 510
IF(ENN.EQ.0.) GO TO 510
WRITE(5,1011) ENN,CRRX,CRRY,CRRZ
510 CONTINUE
500 CONTINUE
GO TO 200
357 9000 CONTINUE
STOP
END
SUBROUTINE ORDER (N,B,INDEX)
DIMENSION B(8),INDEX(8)
LOGICAL FIN
DO 10 I=1,N
10 INDEX(I)=I
NN=N-1
DO 15 J=1,NN
M=N-J
FIN=.TRUE.
DO 20 I=1,M
IF (B(I).LE.B(I+1)) GO TO 20
FIN=.FALSE.
BF=B(I+1)
B(I+1)=B(I)
B(I)=BF
IN=INDEX(I)

```

```

26924470 SWPM0577
26924480 SWPM0578
26924490 SWPM0579
26924500 SWPM0580
26924510 SWPM0581
26924520 SWPM0582
26924530 SWPM0583
26924540 SWPM0584
26924550 SWPM0585
26924560 SWPM0586
26924570 SWPM0587
26924620 SWPM0588
26924630 SWPM0589
SWPM0590
26924650 SWPM0591
26924660 SWPM0592
26924670 SWPM0593
26924680 SWPM0594
26924690 SWPM0595
26924700 SWPM0596
26924710 SWPM0597
26924720 SWPM0598
26924730 SWPM0599
26924740 SWPM0600
26924750 SWPM0601
26924760 SWPM0602
26924770 SWPM0603
26924780 SWPM0604
26924790 SWPM0605
26924800 SWPM0606
26924810 SWPM0607
26924820 SWPM0608
26924830 SWPM0609
26924840 SWPM0610
26924850 SWPM0611
26924860 SWPM0612

```

```

INDEX (I) = INDEX (I + 1)
INDEX (I + 1) = IN
20 CONTINUE
IF (FIN) RETURN
15 CONTINUE
RETURN
END
SUBROUTINE SWITCH (N, A, INDEX, DUMMY)
DIMENSION A (8), INDEX (8), DUMMY (8)
DO 10 I = 1, N
10 DUMMY (I) = A (I)
DO 15 I = 1, N
II = INDEX (I)
15 A (I) = DUMMY (II)
RETURN
END
SUBROUTINE WATER (RX, RY, RZ, H, E, P, PLG, HU, IU, UAV, OP1, HW, UF, HH, PI,
1 AREA, WWGT, I, J, ID, WX, WY, WZ, TPSLP)
DIMENSION HU (8), IU (8), UAV (8), AREA (8), UF (8), WX (8), WY (8), WZ (8)
DO 15 K = 1, J, ID
KK = IU (K)
HHH = HU (K)
IF (TPSLP.LT.0..AND.HHH.LT.-HH) HHH = -HH
DH = H - HHH
IF (DH.LE.0.) GO TO 15
TEM = (DH/H) * (DH/(H+HH))
GO TO (15, 20, 25, 30), KK
20 UF (K) = AREA (K) * UAV (K)
GO TO 35
25 PER = 1.
GO TO 40
30 AZZ = DH/SIN (P)
AXX = 0.
IF (PLG.NE.90.) AXX = DH/TAN (P)
AX = DH/TAN (E) - AXX
PA = PI - P

```

```

26924870 SWPM0613
26924880 SWPM0614
26924890 SWPM0615
26924900 SWPM0616
26924910 SWPM0617
26924920 SWPM0618
26924930 SWPM0619
26924940 SWPM0620
26924950 SWPM0621
26924960 SWPM0622
26924970 SWPM0623
26924980 SWPM0624
26924990 SWPM0625
26925000 SWPM0626
26925010 SWPM0627
26925020 SWPM0628
26925030 SWPM0629
26925040 SWPM0630
26925050 SWPM0631
26925060 SWPM0632
26925070 SWPM0633
26925080 SWPM0634
26925090 SWPM0635
26925100 SWPM0636
26925110 SWPM0637
26925120 SWPM0638
26925130 SWPM0639
26925140 SWPM0640
26925150 SWPM0641
26925160 SWPM0642
26925170 SWPM0643
26925180 SWPM0644
26925190 SWPM0645
26925200 SWPM0646
26925210 SWPM0647
26925220 SWPM0648

```

358

```

ART=AZZ*AX*SIN(PA)/2.
IF(HW.NE.0.) GC TO 45
EA=P/2.
IF(EA.LE.E) GO TO 15
ARA=AZZ*AZZ*SIN(PA)/2.
ARB=ART-ARA
PER=ARB/ART
GO TO 40
45 HP=HW-HU(K)
AY=OP1-AXX
AZW=HP/SIN(P)
IF(HP.GT.DH) GO TO 50
ARA1=AZW*AY*SIN(PA)/2.
ARB1=ART-ARA1
IF(AY.GT.AX) GO TO 55
PER=ARB1/ART
GO TO 40
359 55 IF(HP.EQ.DH.AND.AY.GE.AX) GO TO 15
    AYY=AXX*AZW/AZZ
    ZA=ATAN2(HP,(AY+AYY))
    ZE=AY-AX
    ZC=PI-E
    ZD=PI-ZC-ZA
    ARF=ZB*ZB*SIN(ZA)*SIN(ZC)/(2.*SIN(ZD))
    PFR=(ARB1+ARF)/ART
    GO TO 40
50 IF(AY.GE.AX) GO TO 15
    ZG=AX-AY
    ZE=ATAN2(OP1,HP)+PI/2.
    ZF=PI-ZE-ZG
    ARB2=ZG*ZG*SIN(ZE)*SIN(E)/(2.*SIN(ZF))
    PER=ARB2/ART
40 CONTINUE
UF(K)=PER*TEM*AREA(K)*WWGT*DH/3.
35 IF(K.EQ.J) UF(K)=-UF(K)
    UFX=WX(K)*UF(K)

```

```

26925230 SWPM0649
26925240 SWPM0650
26925250 SWPM0651
26925260 SWPM0652
26925270 SWPM0653
26925280 SWPM0654
26925290 SWPM0655
26925300 SWPM0656
26925310 SWPM0657
26925320 SWPM0658
26925330 SWPM0659
26925340 SWPM0660
26925350 SWPM0661
26925360 SWPM0662
26925370 SWPM0663
26925380 SWPM0664
26925390 SWPM0665
26925400 SWPM0666
26925410 SWPM0667
26925420 SWPM0668
26925430 SWPM0669
26925440 SWPM0670
26925450 SWPM0671
26925460 SWPM0672
26925470 SWPM0673
26925480 SWPM0674
26925490 SWPM0675
26925500 SWPM0676
26925510 SWPM0677
26925520 SWPM0678
26925530 SWPM0679
26925540 SWPM0680
26925550 SWPM0681
26925560 SWPM0682
26925570 SWPM0683
26925580 SWPM0684

```

	UFY=WY(K)*UF(K)	26925590	SWPM0685
	UFZ=WZ(K)*UF(K)	26925600	SWPM0686
	RX=RX-UFX	26925610	SWPM0687
	RY=RY-UFY	26925620	SWPM0688
	RZ=RZ-UFZ	26925630	SWPM0689
15	CONTINUE	26925640	SWPM0690
	RETURN	26925650	SWPM0691
	END	26925660	SWPM0692
	SUBROUTINE BOLT(III,JJJ,NNN,WX,WY,WZ,HEX,C,B,P,XLEN,PLG,D,TPSLP,	26925670	SWPM0693
1	BTOP,ORT,DPT,TEN,TAREX,TEX,TBY,TBZ,BFAC,ORF,DPF,FTEN,FAREX,	26925680	SWPM0694
2	FBX,FBY,FBZ,FACT)	26925690	SWPM0695
	DIMENSION BTOP(8),ORT(8),DPT(8),TEN(8),BFAC(8),ORF(8)	26925700	SWPM0696
	DIMENSION DPF(8),FTEN(8),WX(8),WY(8),WZ(8),C(8),B(8)	26925710	SWPM0697
	IF(III.GT.JJJ) GO TO 20	26925720	SWPM0698
	GO TO 25	26925730	SWPM0699
20	TE=III	26925740	SWPM0700
	III=JJJ	26925750	SWPM0701
	JJJ=TE	26925760	SWPM0702
25	CONTINUE	26925770	SWPM0703
	XY=WZ(JJJ)*WX(III)-WX(JJJ)*WZ(III)	26925780	SWPM0704
	XZ=WX(JJJ)*WY(III)-WY(JJJ)*WX(III)	26925790	SWPM0705
	ODX = -HEX/(TAN(C(III))*SIN(B(III))) + HEX/(TAN(P)*TAN(B(III)))		SWPM0706
	OCX = -HEX/(TAN(C(JJJ))*SIN(B(JJJ))) + HEX/(TAN(P)*TAN(B(JJJ)))		SWPM0707
	ODY = HEX/TAN(P)		SWPM0708
	DC=OCX-ODX	26925830	SWPM0709
	IF(DC.LE.XLEN) GO TO 30	26925840	SWPM0710
	H=XLEN*HEX/DC	26925850	SWPM0711
	ODX = -H/(TAN(C(III))*SIN(B(III))) + H/(TAN(P)*TAN(B(III)))		SWPM0712
	OCX = -H/(TAN(C(JJJ))*SIN(B(JJJ))) + H/(TAN(P)*TAN(B(JJJ)))		SWPM0713
	ODY = H/TAN(P)		SWPM0714
	DC=OCX-ODX	26925890	SWPM0715
	GO TO 35	26925900	SWPM0716
30	H=HEX	26925910	SWPM0717
35	CONTINUE	26925920	SWPM0718
	TANE=XZ/XY	26925930	SWPM0719
	TAND=TAN(D)	26925940	SWPM0720

360

361

```

AAA=1.
IF (PLG.NE.90.) AAA=1.-TANE/TAN (P)
HH=H*AAA*TANB/(TANE-TAND)
CCC=(H+HH)/XZ
OBY = CCC*XY
OBBY=OBY-ODY
IF (TPSLP.NE.0.) OBBY=HH/SIN (D)
TAREX=OBBY*DC/2.
AZ1=H/SIN (P)
FAREX=DC*AZ1/2.
AX=0.
AY=0.
AZ=0.
AFX=0.
AFY=0.
AFZ=0.
DO 10 K=1,NNN
BT=BTOP (K) *TEN (K)
IF (BT.EQ.0.) GO TO 15
BXY=BT*COS (DPT (K) /FACT)
IF (BXY.LT.0.) BXY=-BXY
BX=BXY*COS (ORT (K) /FACT)
BY=BXY*SIN (ORT (K) /FACT)
BZ=BT*SIN (DPT (K) /FACT)
AX=AX+BX
AY=AY+BY
AZ=AZ-BZ
15 CONTINUE
BF=BFAC (K) *FTEN (K)
IF (BF.EQ.0.) GO TO 10
BFXY=BF*COS (DPF (K) /FACT)
IF (BFXY.LT.0.) BFXY=-BFXY
BFX=BFXY*COS (ORF (K) /FACT)
BFY=BFXY*SIN (ORF (K) /FACT)
BFZ=BF*SIN (LPF (K) /FACT)
AFX=AFX+BFX

```

```

26925950 SWPM0721
26925960 SWPM0722
26925970 SWPM0723
26925980 SWPM0724
26925990 SWPM0725
26926000 SWPM0726
26926010 SWPM0727
26926020 SWPM0728
26926030 SWPM0729
26926040 SWPM0730
26926050 SWPM0731
26926060 SWPM0732
26926070 SWPM0733
26926080 SWPM0734
26926090 SWPM0735
26926100 SWPM0736
26926110 SWPM0737
26926120 SWPM0738
26926130 SWPM0739
26926140 SWPM0740
26926150 SWPM0741
26926160 SWPM0742
26926170 SWPM0743
26926180 SWPM0744
26926190 SWPM0745
26926200 SWPM0746
26926210 SWPM0747
26926220 SWPM0748
26926230 SWPM0749
26926240 SWPM0750
26926250 SWPM0751
26926260 SWPM0752
26926270 SWPM0753
26926280 SWPM0754
26926290 SWPM0755
26926300 SWPM0756

```

AFY=AFY+BFY
AFZ=AFZ-BFZ
10 CONTINUE
TBX=AX/TAREX
TBY=AY/TAREX
TBZ=AZ/TAREX
FBX = AFX/FAREX
FBY = AFY/FAREX
FBZ = AFZ/FAREX

RETURN
END

26926310 SWPM0757
26926320 SWPM0758
26926330 SWPM0759
26926340 SWPM0760
26926350 SWPM0761
26926360 SWPM0762
SWPM0763
SWPM0764
SWPM0765
SWPM0766
26926400 SWPM0767
26926410 SWPM0768

362

Appendix F

Computer Program SWARS-2MC

SWARS-2MC is a modified version of SWARS-2PM that enables the user to determine the probability of failure (P_f) through Monte Carlo simulation. The program will compute the factor of safety (FS) for many sets of input parameters-- P_f is the proportion of FS values that fall below 1.0. Any (or all) of the parameters that define the shape and size of the wedge or characterize the shear resistance along the joint planes can be considered random variables. The values for these random variables should be selected in accordance with their respective probability density functions. (Section 2.2 outlines the principles of Monte Carlo simulation.)

SWARS-2MC is virtually identical to SWARS-2PM with respect to its computational algorithms. Both programs compute two FS's: FS_I , the factor of safety against initial movement, and FS_U , the factor of safety against ultimate failure. (The distinction between the two values is discussed in Section 4.4.)

There are three major differences between SWARS-2PM and SWARS-2MC.

1. In SWARS-2PM the user inputs individual planes. He can specify up to 8 planes. Some combinations of planes will form kinematically stable wedges; the program will

indicate that these combinations do not constitute stability problems. The user does not specify the size of the wedges. The program identifies (and analyzes) the largest wedge that can form given the overall height and width of the slope. In SWARS-2MC the user inputs pairs of planes and the height of the resulting wedge. In effect, the user specifies the shape and size of the wedge to be analyzed. Thus, SWARS-2MC is based on wedges rather than individual planes. SWARS-2MC is designed to complement the computer program DAYLITE (Appendix C) in that the input for SWARS-2MC uses the same format as the output from DAYLITE. Since DAYLITE only considers kinematically unstable wedges, the input for SWARS-2MC will not identify any wedges which are kinematically stable.

2. In SWARS-2PM the user identifies planes by their strike and dip. As indicated above, SWARS-2MC is concerned with wedges rather than planes, so the user inputs the orientation of the line of intersection of planes (XX,XY, XZ) and the central angle of the

wedge (ψ). (XX, XY, and XZ) and ψ can be obtained from DAYLITE.

3. The input from SWARS-2PM includes a detailed description of the wedges formed by each pair of planes and the two FS values for each wedge. Since the SWARS-2MC user prescribes the size and slope of each wedge, the output from the program consists of just the two FS values (as well as a recapitulation of the input parameters).

SWARS-2MC maintains most of the versatility of SWARS-2PM with respect to loading conditions and ground water conditions but not all the conditions can be varied in each set of input parameters. In particular,

1. SWARS-2MC will not consider rock bolt loads.
2. SWARS-2MC will compute cleft water pressures with respect to a specified phreatic surface; however, (unlike SWARS-2PM) both planes which bound the wedge must have the same surface. In addition, all the wedges in any one computer run* must have the same phreatic surface. (The user can specify "Piezometric Option 2" i.e., the same uniform hydrostatic pressure on both joints, and then let the pressure vary for each wedge.)

* A computer run consists of a series of FS calculations based on a single set of computer cards as prescribed in Section F.3.

3. SWARS-2MC will consider pseudo-static seismic loadings but the same seismic coefficients must be used for all wedges in a particular run.
4. SWARS-2MC (unlike SWARS-2PM) will not compute the minimum seismic accelerations required to cause failure.
5. SWARS-2MC will consider point loads but the same loads will be applied to all wedges in a particular run.

Some of these restrictions can be circumvented by conditioning the results on the loading condition. For example, suppose there is a 0.05 probability that a design earthquake will occur. Two computer runs can be made: one with the appropriate seismic accelerations and one without. If one assumes that the design earthquake is the only earthquake that can occur, P_f can be calculated as:

$$P_f = (0.05)P_f^1 + (0.95)P_f^2 \quad (\text{F.1})$$

where P_f^1 is the probability of failure with the seismic loads and P_f^2 is the probability of failure without the seismic loads.

The user must specify the number of wedges to be analyzed and he must provide input data for each wedge. This input is listed on cards #5 and #6 (see Section F.3) so a pair of

cards must be provided for each wedge (or "realization"). The lone exception to this rule occurs when the user only wishes to investigate FS_U . If this is the case, he inputs ' 1 ' for ISTIFF (card #4) and can disregard card #6 for each realization. (Card #6 contains information on the in situ stress ratio and joint stiffnesses--none of the data is required for the FS_U computations.)

The format for inputting data is designed so that the user can vary one parameter at a time. In analyzing the i^{th} wedge the program will use all the parameters from the $(i - 1)^{\text{th}}$ wedge except those parameters which are specified on the i^{th} pair of cards #5 and #6. For example, if H, the height of the wedge, is specified as 15.0 for the first realization, the computer will continue to use $H = 15.0$ for all subsequent wedges until the user specifies another value for H. If in analyzing two consecutive realizations the user wishes to change the value of a parameter from a non-zero number to zero he must input ' -1.0 '. For example, in the i^{th} realization the uniform hydrostatic pressure might be 124.8. If the uniform hydrostatic pressure in the $(i + 1)^{\text{th}}$ realization should be zero, the user must input ' -1.0 ' in the appropriate columns in the $(i + 1)^{\text{th}}$ pair of cards #5 and #6.

F.1 Coordinate System

The coordinate system used in SWARS-2MC is shown in Figure F.1. The positive X axis is horizontal to the right.

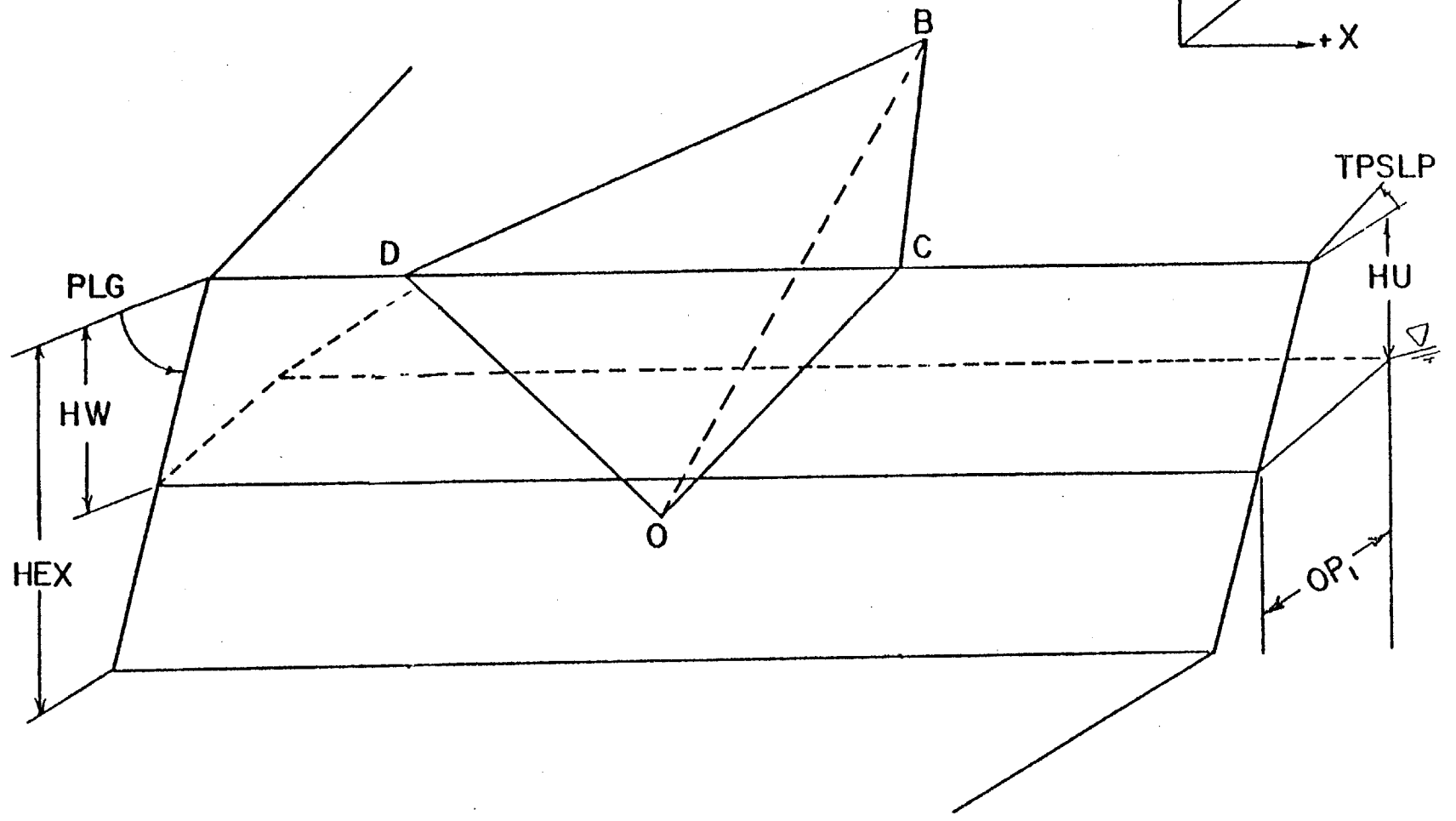
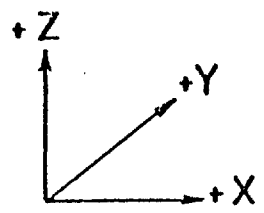


Figure F.1 Model Slope
368

The positive Y axis is horizontal and 90° counterclockwise from the positive X axis. (The positive Y direction is directed into the slope.) The positive Z axis is vertical upward.

DAYLITE uses this same coordinate system in describing the orientation of the line of intersection.

F.2 Units

All units used in the input must be consistent. Units are generally in feet or pounds but any other system may be employed as long as all the other input is in consistent units. Angular input is always in degrees.

Unless otherwise noted, input data does not have to be right justified. The term "integer" implies that the parameter is expressed without a decimal point.

F.3 Inputs

Card #1

Strike of the Slope: (H1AZI, AZI, H2AZI) is entered in geologic notation in columns 1 to 4. Geologic strike must be expressed in the northern quadrants and the angle must be expressed as a two digit integer. (Examples: N45E, N06W)

Dip of the Slope: (PLG, H1PLG, H2PLG) is entered in geologic notation in columns 6 to 9. Dip directions must indicate a particular quadrant i.e., NE, NW, SE, SW. The angle is expressed as a two digit integer. (Examples: 16NW, 07NE)

Height of the Slope: (HEX) is entered in columns 11 to

20 with a maximum of three decimal places. HEX is measured from the crest of the slope to the bottom of the slope (Figure F.1).

Length of the Slope: (XLEN) is entered in columns 21 to 30 with a maximum of three decimal places.

Angle of the Top Slope: (TPSLP) is entered in columns 31 to 40 with a maximum of three decimal places. TPSLP is shown in Figure F.1.

Unit Weight of Rock: (UNIWGT) is entered in columns 41 to 50 with a maximum of three decimal places.

Unit Weight of Water: (WWGT) is entered in columns 51 to 60 with a maximum of three decimal places.

Uniform Vertical Surcharge: (SUR) is the uniform vertical load acting per unit area on the top face of the wedge (face BCD in Figure F.1). SUR is entered in columns 61 to 70 with a maximum of three decimal places.

Surcharge Option: (IS) There are two options available to analyze the effects of the surcharge on the stability of the tetrahedron in the dynamic case. Option 1 assumes that the surcharge is accelerated only in the vertical direction. Option 2 assumes that the surcharge is a mass and that it is accelerated in the same directions as the wedge under dynamic loading. The code 1 or 2 is entered in column 71.

Card #2

X Coordinate of the Line of Intersection: (XX) is entered in columns 1 to 10 with a maximum of five decimal places.

Y Coordinate of the Line of Intersection: (XY) is entered in columns 11 to 20 with a maximum of 5 decimal places.

Z Coordinate of the Line of Intersection: (XZ) is entered in columns 21 to 30 with a maximum of 5 decimal places.

Note: (XX, XY, XZ) should be a unit vector i.e., $(XX^2 + YX^2 + XZ^2)^{\frac{1}{2}} = 1.0$.

Card #3

Piezometric Option: (IU) is a code that indicates how cleft water effects are to be incorporated into the analysis.

1. No effect from water;
2. Uniform pressure acting on the joint;
3. Pressure defined by a horizontal phreatic surface;
4. Pressure determined by an arbitrary phreatic surface.

IU is entered in column 5 as an integer. (Unlike SWARS-2P or SWARS-2PM, SWARS-2MC requires that the same code be used for both planes. In addition, the phreatic surfaces defined in Options 3 and 4 must be identical for both planes.)

Depth to Water: (HU) is measured from the crest of the slope to a horizontal phreatic surface (Figure F.1). HU is used in conjunction with Piezometric Options 3 and 4. HU is entered in columns 6 to 10 with a maximum of 1 decimal place.

Depth to Piezometric Level on the Slope: (HW) is entered in columns 11 to 15 with a maximum of 1 decimal place. HW is shown in Figure F.1 and is used in conjunction with Piezometric Option 4.

Distance OP1: (OP1) is used in conjunction with Piezo-metric Option 4. As shown in Figure F.1, it is the horizontal distance from the face of the slope where the phreatic surface exits to the point where the phreatic surface becomes horizontal. OP1 is entered in columns 16 to 20 with a maximum of 1 decimal place.

Seismic Coefficients X,Y,Z: (AKX, AKY, AKZ) Seismic forces are entered as decimal fractions of the gravitational force. Positive values will be forces acting at the centroid in the direction of the appropriate positive coordinate, negative values set in the direction of the appropriate negative coordinates. AKX is entered in columns 21 to 25, AKY is entered in columns 26 to 30, and AKZ is entered in columns 31 to 35. The three values are expressed with a maximum of three decimal places. If no seismic loads are to be considered columns 21 to 35 may be left blank--the computer will default to $AKX = AKY = AKZ = 0$.

Point Loads: (PX, PY, PZ) can be used in the program. PX, PY, and PZ are the X, Y, and Z components of a point load. The program treats PX, PY and PZ as point loads acting at the centroid of the wedge. PX is entered in columns 36 to 45, PY is entered in columns 46 to 55 and PZ is entered in columns 56 to 65. The three values are expressed with a maximum of three decimal places. If not point loads are to be considered columns 36 to 65 may be left blank--the computer will default to $PX = PY = PZ = 0$.

Card #4

Number of Realizations: (NOREAL) is entered as an integer in columns 1 to 5. NOREAL must be right justified. Note: The user must provide a set of input parameters i.e., cards #5 and #6 for each realization.

FS Option #1: (ISTIFF) If a ' 1 ' is entered in column 10 the program will compute FS_U only. If any integer greater than 1 is entered in columns 6 to 10 the program will compute both FS_I and FS_U .

FS Option #2: (NDOP) is a code that indicates how the program should compute FS_I . As indicated in Section 4.4 (g.v.), FS_I is defined as:

$$FS_I = \frac{\bar{R} \cdot \bar{\Delta}}{\bar{D} \cdot \bar{\Delta}} \quad (F.2)$$

where \bar{R} is the resultant of all resisting forces, \bar{D} is the resultant of all driving forces, and $\bar{\Delta}$ is the direction of impending movement. If a ' 0 ' is placed in column 15, $\bar{\Delta}$ is the displacement that would occur in response to a vertical load. If any other integer is placed in columns 11 to 15 $\bar{\Delta}$ is the displacement that occurs in response to the resultant of all external loads i.e., all loads except the weight.

FS Option #3: (LOPT) is an option that allows the user to analyze all loads (including the weight of the wedge) with

the stiffness approach. If a ' 1 ' is entered in column 20 the program will use this option. If any other integer is placed in columns 16 to 20 the program will treat loads according to the "standard" procedure presented in Section 4.3 i.e., stress approach for gravitational loads, stiffness approach for all other loads. If columns 16 to 20 are left blank the program will default to the standard procedure.

Card #5

Note: A separate card is used for each of the NREAL realizations--see the introductory discussion to this appendix.

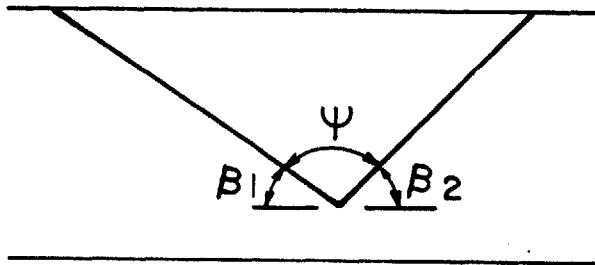
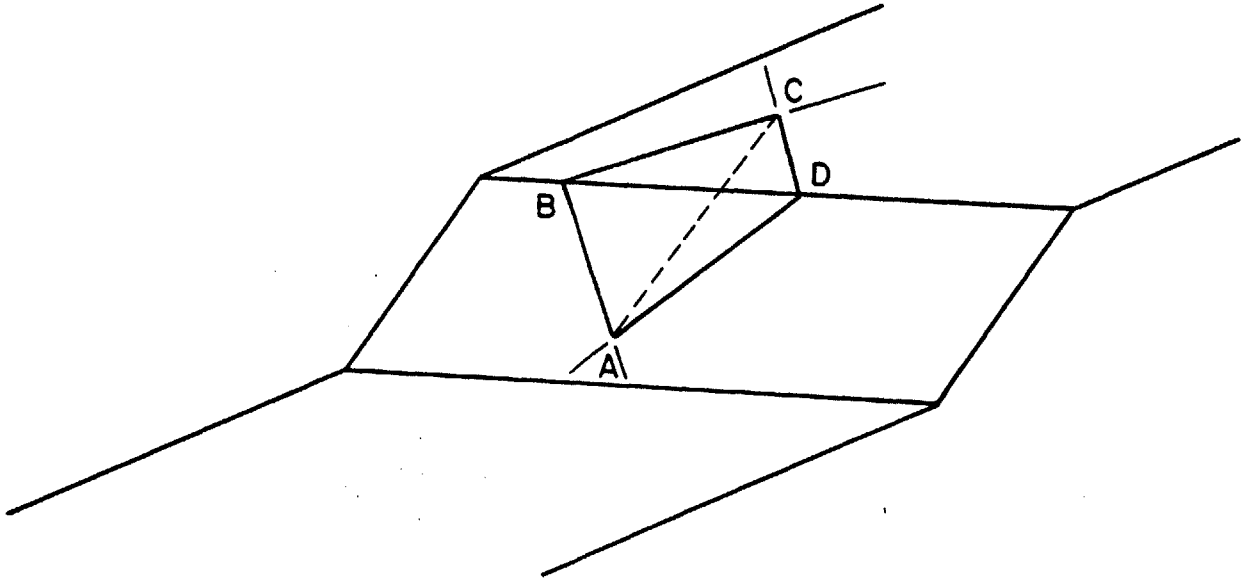
Central Wedge Angle: (PSI) is entered in columns 1 to 5 with a maximum of 1 decimal place. PSI is shown in Figure F.2 as ψ .

Orientation Angle #1: (BETA1) is entered in columns 6 to 10 with a maximum of 1 decimal place. BETA1 is shown in Figure F.2 as β_1 .

Height of Wedge: (H) is entered in columns 11 to 15 with a maximum of 1 decimal place. H is measured from the crest of the slope to the vertex of the wedge i.e., in the same manner as HEX in Figure F.1.

Friction Angle on Joint Plane 1: (PHX(1)) is entered in columns 16 to 20 with a maximum of 1 decimal place.

Asperities on Joint Plane 1: (AQ(1)), the angular value of additional shearing resistance due to larger size



SECTION PERPENDICULAR TO AC

Figure F.2 Definitions of ψ and β_1

irregularities on the joint plane, is entered in columns 21 to 25 with a maximum of 1 decimal place.

Cohesion of Intact Rock on Joint Plane 1: (TAU(1)) is entered in columns 26 to 33 with a maximum of 1 decimal place.

Joint Persistence on Joint Plane 1: (PCTJTG(1)) is the percent of the area of the total joint plane that is not intact rock. PCTJTG(1) is entered in columns 33 to 38 with a maximum of 1 decimal place.

Uniform Water Pressure on Joint Plane 1: (UAV(1)) is entered in columns 39 to 45 with a maximum of 1 decimal place. UAV(1) is used in conjunction with Piezometric Option 2.

Friction Angle on Joint Plane 2: (PHX(2)) is entered in columns 46 to 50 with a maximum of 1 decimal place.

Asperities on Joint Plane 2: (AQ(2)), the angular value of additional shearing resistance due to larger size irregularities on the joint plane, is entered in columns 51 to 55 with a maximum of 1 decimal place.

Cohesion of Intact Rock on Joint Plane 2: (TAU(2)) is entered in columns 56 to 62 with a maximum of 1 decimal place.

Joint Persistence on Joint Plane 2: (PCTJTG(2)) is the percent of the area of the total joint plane that is not intact rock. PCTJTG(2) is entered in columns 63 to 67 with a maximum of 1 decimal place.

Uniform Water Pressure on Joint Plane 2: (UAV(2)) is entered in columns 68 to 72 with a maximum of 1 decimal place. UAV(2) is used in conjunction with Piezometric Option 1.

Card #6

Note: A separate card is used for each of the NREAL realizations unless ISTIFF = 1 in which case Card #6 is deleted for each realization.

Stress Ratio: (RATIO) is entered in columns 1 to 10 with a maximum of 5 decimal places. RATIO is the ratio of horizontal to vertical stresses within the wedge.

Shear Stiffness on Joint Plane 1: (STIFFS(1)) is entered in columns 11 to 20 with a maximum of two decimal places. STIFFS(1) can also be entered in scientific notation with a maximum of two decimal places. (Examples: 678.54, 6.78E2)

Normal Stiffness on Joint Plane 1: (STIFFN(1)) is entered in columns 21 to 30 with a maximum of two decimal places. STIFFN(1) can also be entered in scientific notation with a maximum of two decimal places. (Examples: 45678.2, 4.57E4)

Shear Stiffness on Joint Plane 2: (STIFFS(2)) is entered in columns 31 to 40 with a maximum of two decimal places. STIFFS(2) can also be entered in scientific notation with a maximum of two decimal places. (Examples: 567.9, 5.68E3)

Normal Stiffness on Joint Plane 2: (STIFFN(2)) is entered in columns 41 to 50 with a maximum of two decimal places. STIFFN(2) can also be entered in scientific notation with a maximum of two decimal places. (Examples: 10000.0, 10.0E4)

SWARS-2MC Listing

C
C

SWARS-MC

SLIDING WEDGE ANALYSIS OF ROCK SLOPES -- MONTE CARLO

DIMENSION BICP (8), ORT (8), DPT (8), TEN (8), UAV (8), UF (8), AREA (8), IU (8)		SWMC0001
DIMENSION TAU (2), PCTJTG (2), PUFFY (30), WX (2), WY (2), WZ (2)		SWMC0002
DIMENSION T (8), TX (8), TY (8), TZ (8), EN (8), PHI (8)	26920080	SWMC0003
DIMENSION SX (8), SY (8), SZ (8), RSS (8), RRX (8), RRY (8), RRZ (8)	26920090	SWMC0004
DIMENSION INDEX (8), DUMMY (8), PHX (8), AP (8), AQ (8), CH (8)	26920110	SWMC0005
DIMENSION WWX (8), WWY (8), WWZ (8), BET (8), B (2), C (2)		SWMC0006
DIMENSION BFAC (8), ORF (8), DPF (8), FTEN (8)	26920150	SWMC0007
DIMENSION STIFFN (8), STIFFS (8), RATIOK (8)		SWMC0008
REAL NORD, HXX, HXY		SWMC0009
LOGICAL FLIM		SWMC0010
DATA NORD, SOTH, EAST, WEST/'N', 'S', 'E', 'W'/	26920160	SWMC0011
NWR = 6		SWMC0012
NFD = 5		SWMC0013
FLIM = .TRUE.		SWMC0014
PI=3.141593	26920180	SWMC0015
PI2=PI/2.	26920190	SWMC0016
FACT=180./PI	26920200	SWMC0017
10 FORMAT (4I5)		SWMC0018
11 FORMAT (2I5)		SWMC0019
12 FORMAT (3F10.5)		SWMC0020
13 FORMAT (5F5.1, F8.1, F5.1, F7.1, 2F5.1, F7.1, F5.1, F7.1)		SWMC0021
14 FORMAT (F10.5, 4G10.2)		SWMC0022
15 FORMAT (A1, F2.0, A1, 1X, F2.0, A1, A1, 1X, 6F10.3, I1)		SWMC0023
16 FORMAT (F5.3, 2I5)		SWMC0024
17 FORMAT (6F10.5)		SWMC0025
20 FORMAT (I5, 3F5.1, 3F5.3, 3F10.3)		SWMC0026
25 FORMAT (A1, F2.0, A1, 1X, F2.0, A1, A1, 1X, 2F5.2, F10.3, 2G10.3, 2F5.2, 1 F10.3, I1)		SWMC0027
1001 FORMAT ('0', T20, 'FS =', F6.2, ' FOR SLIDING ON PLANE ', I1)	26920250	SWMC0028
1006 FORMAT (37X, 'SEISMIC ACCELERATIONS:', //, 18X, 'AKX =', F7.3, 12X, 1 'AKY =', F7.3, 11X, 'AKZ =', F7.3, ///)		SWMC0029
1007 FORMAT (40X, 'POINT LOADS:', //, 18X, 'PX =', F9.2, 12X, 'PY =', F9.2, 13X, 1 'PZ =', F9.2, ///)		SWMC0030
1008 FORMAT ('0', T20, 'RESULTANT TENDS TO LIFT BLOCK OFF SUPPORTS')	26920480	SWMC0031

380

1010	FORMAT ('0',T20,'CHECK FOR TOPPLING ABOUT POINT 0')	26920520	SWMC0037
1013	FORMAT(T20,'FS =',F6.2,' FOR ROTATIONS ON PLANE ',I2)	26920570	SWMC0038
1016	FORMAT (3F6.2)		SWMC0039
1018	FORMAT (3F6.2)		SWMC0040
1019	FORMAT ('0',T20,'LINE OF INTERSECTION DOES NOT INTERSECT',	26920750	SWMC0041
	1 ' TOP OF SLOPE')	26920760	SWMC0042
1030	FORMAT ('+',48X,'NO EFFECT FROM WATER',///)		SWMC0043
1031	FORMAT ('+',48X,'UNIFORM PRESSURE',///)		SWMC0044
1032	FORMAT ('+',48X,'DEPTH TO WATER:',4X,F8.3,///)		SWMC0045
1033	FORMAT ('+',48X,'DEFINED PHREATIC SURFACE: HU = ',F6.2,' HW = ',		SWMC0046
	1 F6.2,' OP1 = ',F6.2,///)		SWMC0047
1035	FORMAT (29X,'***** LOAD DATA *****',//		SWMC0048
	1 18X,'UNIT WEIGHT OF ROCK:',F8.2,3X,'UNIT WEIGHT OF WATER: ',F6.2,		SWMC0049
	2 //,34X,'VERTICAL SURCHARGE:',F8.2,//)		SWMC0050
1036	FORMAT (29X,'***** EXCAVATION DATA *****',//		SWMC0051
	1 18X,'STRIKE:',16X,'N',F3.0,A1,3X,'DIP:',18X,F3.0,A1,A1,//		SWMC0052
	2 18X,'HEIGHT OF FACE:',F13.2,3X,'LENGTH OF FACE:',F12.2,//		SWMC0053
	3 31X,'INCLINATION OF TOP SLOPE:',F8.2,//		SWMC0054
	4 37X,'LINE OF INTERSECTION:',//,18X,'X = ',F6.3,15X,'Y = ',F6.3,		SWMC0055
	5 14X,'Z = ',F6.3,//,18X,'PIEZOMETRIC OPTION:',8X,I1)		SWMC0056
1040	FORMAT (' NO. PSI BETA1 H PHI(1) AQ(1) TAU',		SWMC0057
	1 '(1) PJ(1) UA(1) PHI(1) AQ(1) TAU(1) PJ(2)',		SWMC0058
	2 ' UA(2) FS(I) FS(U)')		SWMC0059
1041	FORMAT (I5,3X,F5.1,3X,F5.1,3X,F5.1,3X,F5.1,3X,F5.1,3X,F7.1,		SWMC0060
	1 3X,F5.1,2X,F7.1,2X,F5.1,3X,F5.1,3X,F7.1,3X,F5.1,2X,F7.1,		SWMC0061
	2 2X,F6.4,2X,F6.4)		SWMC0062
1045	FORMAT (29X,'* NUMBER OF REALIZATIONS: ',I5,' *',///,		SWMC0063
	1 29X,'* ISTIFF: ',I5,' *',///,		SWMC0064
	2 29X,'* NDOP: ',I5,' *',///,		SWMC0065
	3 29X,'* LOPT: ',I5,' *',///)		SWMC0066
	DO 1 I = 1, 30		SWMC0067
	1 PUFFY(I) = 0.0		SWMC0068
	READ(NRD,15) H1AZI, AZI, H2AZI, PLG, H1PLG, H2PLG,		SWMC0069
	1 HEX, XLEN, TPSLP, UNIWGT, WWGT, SUR, IS		SWMC0070
	READ (NRD,12) XX, XY, XZ		SWMC0071
	READ (NRD,20) IU(1), HU, HW, OP1, AKX, AKY, AKZ, PX, PY, PZ		SWMC0072

	READ (NRD,10) NREAL, ISTIFF, NDOP, LOPT		SWMC0073
	READ (NRD,13) PSI,BETA1,H,PHX(1),AQ(1),TAU(1),PCTJTG(1),UAV(1),		SWMC0074
	1 PHX(2),AQ(2),TAU(2),PCTJTG(2),UAV(2)		SWMC0075
	IF (ISTIFF.NE.1) READ (NRD,14) RATIO, STIFFS(1), STIFFN(1),		SWMC0076
	1 STIFFS(2), STIFFN(2)		SWMC0077
65	IF (UNIWT.EQ.0.) UNIWT=1.0	26921060	SWMC0078
	IF (UNIWT.EQ.1.0) WWGT=0.0	26921070	SWMC0079
	IU(2) = IU(1)		SWMC0080
	WRITE (NWR,1036) AZI, H2AZI,PLG, H1PLG, H2PLG, HEX, XLEN, TPSLP,		SWMC0081
	1 XX, XY, XZ, IU(1)		SWMC0082
	IF (IU(1) .EQ. 1) WRITE (NWR,1030)		SWMC0083
	IF (IU(1) .EQ. 2) WRITE (NWR,1031)		SWMC0084
	IF (IU(1) .EQ. 3) WRITE (NWR,1032) HU		SWMC0085
	IF (IU(1) .EQ. 4) WRITE (NWR,1033) HU, HW, OP1		SWMC0086
	WRITE (NWR,1035) UNIWT, WWGT, SUR		SWMC0087
	IF(AKX.NE.0.0.OR.AKY.NE.0.0.OR.AKZ.NE.0.0)		SWMC0088
	1 WRITE (NWR,1006) AKX, AKY, AKZ		SWMC0089
	IF(PX.NE.0.0.OR.PZ.NE.0.0.OR.PZ.NE.0.0) WRITE (NWR,1007) PX, PY, PZ		SWMC0090
	WRITE (NWR,1045) NREAL, ISTIFF, NDOP, LOPT		SWMC0091
	IF (ISTIFF .EQ. 1) RATIO = 1.0		SWMC0092
	P=PLG/FACT	26921320	SWMC0093
	D=TPSLP/FACT	26921330	SWMC0094
	TANE=XZ/XY	26922400	SWMC0095
	TAND=TAN(D)	26922410	SWMC0096
	IF (TANE .LT. TAND) WRITE (NWR,1018)		SWMC0097
	IF (TANE .LT. TAND) GO TO 9000		SWMC0098
	E=ATAN(TANE)	26922430	SWMC0099
	IF(E.LT.0.) E=E+PI	26922440	SWMC0100
	NREAL = 0		SWMC0101
	WRITE (NWR,1040)		SWMC0102
	DO 5000 IJOHN =1, NREAL		SWMC0103
	NREAL = NREAL + 1		SWMC0104
	IF (IJOHN .EQ. 1) GO TO 50		SWMC0105
	READ (NRD,13) (PUFFY(I),I=1,13)		SWMC0106
	IF (PUFFY(1) .NE. 0.0) PSI = PUFFY(1)		SWMC0107
	IF (PUFFY(2) .NE. 0.0) BETA1 = PUFFY(2)		SWMC0108

```

IF ( PUFFY (3) .NE. 0.0 ) H = PUFFY (3)
IF ( PUFFY (4) .NE. 0.0 ) PHI (1) = PUFFY (4)
IF ( PUFFY (5) .NE. 0.0 ) AQ (1) = PUFFY (5)
IF ( PUFFY (6) .NE. 0.0 ) TAU (1) = PUFFY (6)
IF ( PUFFY (7) .NE. 0.0 ) PCTJTG (1) = PUFFY (7)
IF ( PUFFY (8) .NE. 0.0 ) UAV (1) = PUFFY (8)
IF ( PUFFY (9) .NE. 0.0 ) PHI (2) = PUFFY (9)
IF ( PUFFY (10) .NE. 0.0 ) AQ (2) = PUFFY (10)
IF ( PUFFY (11) .NE. 0.0 ) TAU (2) = PUFFY (11)
IF ( PUFFY (12) .NE. 0.0 ) PCTJTG (2) = PUFFY (12)
IF ( PUFFY (13) .NE. 0.0 ) UAV (2) = PUFFY (13)
IF ( BETA1 .EQ. -1.0 ) BETA1 = 0.0
IF ( PHI (1) .EQ. -1.0 ) PHI (1) = 0.0
IF ( PHI (2) .EQ. -1.0 ) PHI (2) = 0.0
IF ( AQ (1) .EQ. -1.0 ) AQ (1) = 0.0
IF ( AQ (2) .EQ. -1.0 ) AQ (2) = 0.0
IF ( TAU (1) .EQ. -1.0 ) TAU (1) = 0.0
IF ( TAU (2) .EQ. -1.0 ) TAU (2) = 0.0
IF ( PCTJTG (1) .EQ. -1.0 ) PCTJTG (1) = 0.0
IF ( PCTJTG (2) .EQ. -1.0 ) PCTJTG (2) = 0.0
IF ( UAV (1) .EQ. -1.0 ) UAV (1) = 0.0
IF ( UAV (2) .EQ. -1.0 ) UAV (2) = 0.0
IF ( ISTIFF .EQ. 1 ) GO TO 50
READ (NRD,14) (PUFFY (I), I=14,18)
IF ( PUFFY (14) .NE. 0.0 ) RATIO = PUFFY (14)
IF ( PUFFY (15) .NE. 0.0 ) STIFFS (1) = PUFFY (15)
IF ( PUFFY (16) .NE. 0.0 ) STIFFN (1) = PUFFY (16)
IF ( PUFFY (17) .NE. 0.0 ) STIFFS (2) = PUFFY (17)
IF ( PUFFY (18) .NE. 0.0 ) STIFFN (2) = PUFFY (18)
IF ( RATIO .EQ. -1.0 ) RATIO = 0.0
IF ( STIFFS (1) .EQ. -1.0 ) STIFFS (1) = 0.0
IF ( STIFFS (2) .EQ. -1.0 ) STIFFS (2) = 0.0
IF ( STIFFN (1) .EQ. -1.0 ) STIFFN (1) = 0.0
IF ( STIFFN (2) .EQ. -1.0 ) STIFFN (2) = 0.0
50 CONTINUE
DO 60 I = 1, 2

```

```

SWMC0109
SWMC0110
SWMC0111
SWMC0112
SWMC0113
SWMC0114
SWMC0115
SWMC0116
SWMC0117
SWMC0118
SWMC0119
SWMC0120
SWMC0121
SWMC0122
SWMC0123
SWMC0124
SWMC0125
SWMC0126
SWMC0127
SWMC0128
SWMC0129
SWMC0130
SWMC0131
SWMC0132
SWMC0133
SWMC0134
SWMC0135
SWMC0136
SWMC0137
SWMC0138
SWMC0139
SWMC0140
SWMC0141
SWMC0142
SWMC0143
SWMC0144

```

	IF (I .EQ. 1) ANGLE = BETA1/FACT	SWMC0145
	IF (I .EQ. 2) ANGLE = PI - (BETA1 + PSI)/FACT	SWMC0146
	SINGLE = SIN(ANGLE)*SQRT(XX**2 + XY**2)/XY	SWMC0147
	AA = XX/XY	SWMC0148
	BB = XX*AA + XY	SWMC0149
	CC = BB**2 + XZ**2 + XZ**2*AA**2	SWMC0150
	DD = 2.0*SINGLE*(BB*XX + AA*XZ**2)	SWMC0151
	EE = (XX*SINGLE)**2 - XZ**2 + (XZ*SINGLE)**2	SWMC0152
	WY(I) = (-DD - SQRT(DD**2 - 4.0*CC*EE))/(2.0*CC)	SWMC0153
	WX(I) = SINGLE + WY(I)*AA	SWMC0154
	WZ(I) = -SQRT(1.0 - WX(I)**2 - WY(I)**2)	SWMC0155
	IF (I .EQ. 1 .AND. ANGLE .GT. PI2) WZ(I) = -WZ(I)	SWMC0156
	IF (I .EQ. 2 .AND. ANGLE .LT. PI2) WZ(I) = -WZ(I)	SWMC0157
	AATEST = ABS(XX*WX(I) + XY*WY(I) + XZ*WZ(I))	SWMC0158
	IF (AATEST .LT. 0.01) GO TO 59	SWMC0159
	WY(I) = (-DD + SQRT(DD**2 - 4.0*CC*EE))/(2.0*CC)	SWMC0160
	WX(I) = SINGLE + WY(I)*AA	SWMC0161
	WZ(I) = -SQRT(1.0 - WX(I)**2 - WY(I)**2)	SWMC0162
	IF (I .EQ. 1 .AND. ANGLE .GT. PI2) WZ(I) = -WZ(I)	SWMC0163
	IF (I .EQ. 2 .AND. ANGLE .LT. PI2) WZ(I) = -WZ(I)	SWMC0164
59	CONTINUE	SWMC0165
	B(I) = ATAN((-WX(I))/WY(I))	SWMC0166
	IF (WY(I) .LT. 0.0) B(I) = PI - ATAN(WX(I)/WY(I))	SWMC0167
	C(I) = ATAN((SQRT(1.0 - WZ(I)**2))/(-WZ(I)))	SWMC0168
	IF (WZ(I) .GT. 0.0) C(I) = ATAN(WZ(I)/(SQRT(1.0-WZ(I)**2)))	SWMC0169
	PHI(I)=PHX(I)/FACT	SWMC0170
	AP(I)=AQ(I)/FACT	26921300 SWMC0171
	IF (ISTIFF .EQ. 1) GO TO 60	SWMC0172
	IF (STIFFS(I) .NE. 0.0) RATIOK(I) = STIFFN(I)/STIFFS(I)	SWMC0173
	IF (STIFFS(I) .EQ. 0.0) RATIOK(I) = 1000000.	SWMC0174
	IF (RATIOK(I) .EQ. 1000000.) STIFFS(I) = 1.	SWMC0175
	IF (RATIOK(I) .EQ. 1000000.) STIFFN(I) = 1000000.	SWMC0176
60	CONTINUE	SWMC0177
	I = 1	SWMC0178
	J = 2	SWMC0179
	XX1 = XX	SWMC0180

	XY1 = XY	SWMC0181
	XZ1 = XZ	SWMC0182
	HEX = H	SWMC0183
	ODX = -HEX/(TAN(C(I))*SIN(B(I))) + HEX/(TAN(P)*TAN(B(I)))	SWMC0184
	OCX = -HEX/(TAN(C(J))*SIN(B(J))) + HEX/(TAN(P)*TAN(B(J)))	SWMC0185
	ODY = HEX/TAN(P)	SWMC0186
	DC=CCX-ODX	26922260 SWMC0187
	IF(DC.LE.XLEN) GO TO 95	26922270 SWMC0188
	H=XLEN*HEX/DC	26922280 SWMC0189
	ODX = -H/(TAN(C(I))*SIN(B(I))) + H/(TAN(P)*TAN(B(I)))	SWMC0190
	OCX = -H/(TAN(C(J))*SIN(B(J))) + H/(TAN(P)*TAN(B(J)))	SWMC0191
	ODY = H/TAN(P)	SWMC0192
	DC=OCX-ODX	26922320 SWMC0193
95	CONTINUE	SWMC0194
	OCY=ODY	26922360 SWMC0195
	ODZ=H	26922370 SWMC0196
	OCZ=ODZ	26922380 SWMC0197
	AAA = 1.0	SWMC0198
	IF (PLG.NE.90.) AAA=1.-TANE/TAN(P)	26922540 SWMC0199
	HH=H*AAA*TAND/(TANE-TAND)	26922550 SWMC0200
	CCC=(H+HH)/XZ	26922560 SWMC0201
	OBX = CCC*XX	26922570 SWMC0202
	OBY = CCC*XY	26922580 SWMC0203
	OBZ = CCC*XZ	26922590 SWMC0204
	OD=SQRT(ODX**2+ODY**2+ODZ**2)	26922600 SWMC0205
	OC=SQRT(OCX**2+OCY**2+OCZ**2)	26922610 SWMC0206
	OB=SQRT(OBX**2+OBY**2+OBZ**2)	26922620 SWMC0207
	OBBY=OBY-ODY	26922630 SWMC0208
	IF(TPSLP.NE.0.) OBBY=HH/SIN(D)	26922640 SWMC0209
	TAREA=OBBY*DC/2.	26922650 SWMC0210
	AZ=H/SIN(P)	26922660 SWMC0211
	FAREA=DC*AZ/2.	26922670 SWMC0212
	BDX=ODX-OBX	26922680 SWMC0213
	IF(BDX.LT.0.) BDX=-BDX	26922690 SWMC0214
	DR=OBBY	26922700 SWMC0215
	R1=ATAN2(BDX,OBBY)	26922710 SWMC0216

```

IF (TAN (R1) .NE. 0.) DB=OBBY/COS (R1)
CBX=OCX-OBX
IF (CBX.LT. 0.) CBX=-CBX
CB=OBBY
R=ATAN2 (CBX, OBBY)
IF (TAN (R) .NE. 0.) CB=OBBY/COS (R)
CCP=H/XZ
DBPY=CCP*XY-ODY
VOL=DBPY*DC*(H+HH)/6.
OSX=(OBX+OCX+ODX)/4.
OSY=(OBY+OCY+ODY)/4.
OSZ=(OBZ+OCZ+ODZ)/4.
TEMP=VOL*UNIWT
DUMMYT = TEMP*COS (E) *1.0E-10
SURG=SUR*TAREA/COS (D)
SUM1=(OD+OB+DB)/2.
SUM2=(OC+OB+CB)/2.
AREA (I) =SQRT (SUM1*(SUM1-OD)*(SUM1-OB)*(SUM1-DB))
AREA (J) =SQRT (SUM2*(SUM2-OC)*(SUM2-OB)*(SUM2-CB))
CH (I) =TAU (I) * (100.-PCTJTG (I) ) * (.01) *AREA (I)
CH (J) =TAU (J) * (100.-PCTJTG (J) ) * (.01) *AREA (J)
CH1=CH (I)
CH2=CH (J)
RX = PX + TEMP*AKX
RY = PY + TEMP*AKY
RZ = PZ - SURG - TEMP*(1.0 - AKZ)
IF ( IS .EQ. 2 ) RX = RX + SURG*AKX
IF ( IS .EQ. 2 ) RY = RY + SURG*AKY
IF ( IS .EQ. 2 ) RZ = RZ + SURG*AKZ
CALL WATER (RX, RY, RZ, H, E, P, PLG, HU, IU, UAV, OP1, HW, UF, HH, PI,
1 AREA, WWGT, WX, WY, WZ, TPSLP)
OIRX=OSY*RZ-OSZ*RY
OIRY=OSZ*RX-OSX*RZ
OIRZ=OSX*RY-OSY*RX
EMX=XX*OIRX+XY*OIRY+XZ*OIRZ
DO 110 K=1,2
26922720 SWMC0217
26922730 SWMC0218
26922740 SWMC0219
26922750 SWMC0220
26922760 SWMC0221
26922770 SWMC0222
26922780 SWMC0223
26922790 SWMC0224
26922800 SWMC0225
26922810 SWMC0226
26922820 SWMC0227
26922830 SWMC0228
26922840 SWMC0229
SWMC0230
26922850 SWMC0231
26922860 SWMC0232
26922870 SWMC0233
26922880 SWMC0234
26922890 SWMC0235
26922900 SWMC0236
26922910 SWMC0237
26922920 SWMC0238
26922930 SWMC0239
SWMC0240
SWMC0241
SWMC0242
SWMC0243
SWMC0244
SWMC0245
26923100 SWMC0246
SWMC0247
26923120 SWMC0248
26923130 SWMC0249
26923140 SWMC0250
26923150 SWMC0251
SWMC0252

```

EN(K) = RX*WX(K) + RY*WY(K) + EZ*WZ(K)	26923170	SWMC0253
TX(K) = RX - EN(K)*WX(K)	26923180	SWMC0254
TY(K) = RY - EN(K)*WY(K)	26923190	SWMC0255
TZ(K) = RZ - EN(K)*WZ(K)	26923200	SWMC0256
T(K) = SQRT(TX(K)**2 + TY(K)**2 + TZ(K)**2)	26923210	SWMC0257
110 CONTINUE	26923220	SWMC0258
ENN=0.	26923230	SWMC0259
IF (EN(I).GT.0.0.OR.EN(J).LT.0.0) GO TO 120	26923240	SWMC0260
WRITE (5,1008)		SWMC0261
GO TO 5000		SWMC0262
120 DO 115 K=1,2		SWMC0263
SX(K) = (XY*WZ(K) - XZ*WY(K))	26923280	SWMC0264
SY(K) = (XZ*WX(K) - XX*WZ(K))	26923290	SWMC0265
SZ(K) = (XX*WY(K) - XY*WX(K))	26923300	SWMC0266
RSS(K) = RX*SX(K) + RY*SY(K) + RZ*SZ(K)	26923310	SWMC0267
115 CONTINUE	26923320	SWMC0268
T12 = RX*XX1 + RY*XY1 + RZ*XZ1		SWMC0269
T12P = RX*XX1 + RY*XY1 + (RZ+TEMP)*XZ1		SWMC0270
IF (RSS(I).LT.0.0) GO TO 130	26923330	SWMC0271
IF (RSS(J).LT.0.0) GO TO 140	26923340	SWMC0272
SINBT1 = SIN(BETA1/FACT)		SWMC0273
COSBT1 = COS(BETA1/FACT)		SWMC0274
BETA2 = 180. - BETA1 - PSI		SWMC0275
SINBT2 = SIN(BETA2/FACT)		SWMC0276
COSBT2 = COS(BETA2/FACT)		SWMC0277
PERP1 = 0.0		SWMC0278
TANG1 = 0.0		SWMC0279
PERP2 = 0.0		SWMC0280
TANG2 = 0.0		SWMC0281
IF (LOPT .EQ. 1) GO TO 78		SWMC0282
C THIS SECTION COMPUTES THE EFFECT OF IN SITU STRESSES		SWMC0283
WTCO = TEMP*COS(E)		SWMC0284
IF (RATIO .NE. 1.0) GO TO 76		SWMC0285
PERP2 = WTCO/(COSBT2 + SINBT2*COSBT1/SINBT1)		SWMC0286
PERP1 = PERP2*SINBT2/SINBT1		SWMC0287
GO TO 78		SWMC0288

```

76 RAT1=(RATIO+(1.0-RATIO)*COSBT1**2)/((1.0-RATIO)*SINBT1*COSBT1)
RAT2=(RATIO+(1.0-RATIO)*COSBT2**2)/((1.0-RATIO)*SINBT2*COSBT2)
RAT12 = (RAT2*SINBT2 - COSBT2)/(RAT1*SINBT1 - COSBT1)
TANG2 = WTCC/(RAT12*(RAT1*COSBT1 + SINBT1)+(RAT2*COSBT2+SINBT2))
TANG1 = RAT12*TANG2
PERP1 = RAT1*TANG1
PERP2 = TANG2*RAT2
C THIS PART COMPUTES THE EFFECT OF JOINT STIFFNESSES
78 HXX = XY1/(SQRT(XX1**2 + XY1**2))
HXY = -XX1/(SQRT(XX1**2 + XY1**2))
RHORIZ = RX*HXX + RY*HXY
RVERT = -1.0*(RX*HXY*XZ1 - RY*HXX*XZ1 + RZ*(HXX*XY1 - XX1*HXY) )
UR1A = RVERT/(COSBT1 +COSBT2*SINBT1/SINBT2)
UR2A = UR1A*SINBT1/SINBT2
UR1B = RHORIZ/(SINBT1 + SINBT2*COSBT1/COSBT2)
UR2B = UR1B*COSBT1/COSBT2
C FSLR IS THE 'ULTIMATE' F.S. FOR SLIDING DOWN THE LINE OF INTERSECTION
FSLR = ((UR1A + UR1B)*TAN(PHI(I)) +(UR2A + UR2B)*TAN(PHI(J))) /T12
IF ( ISTIFF .EQ. 1 ) GO TO 400
RVERT1 = RVERT - TEMP*(HXX*XY1 - XX1*HXY)
IF ( LOPT .EQ. 1 ) RVERT1 = RVERT
IF ( RVERT1 .NE. 0.0 .OR. RHORIZ .NE. 0.0 ) GO TO 79
167 RVERT1 = DUMMYT
79 ST1N = STIFFN(I)*AREA(I)
ST1S = STIFFS(I)*AREA(I)
ST2N = STIFFN(J)*AREA(J)
ST2S = STIFFS(J)*AREA(J)
FACTAA = ST1N*SINBT1 + ST1S*COSBT1**2/SINBT1 +
1 ST2N*SINBT2 + ST2S*COSBT2**2/SINBT2
FACTBB = (ST1N-ST1S)*COSBT1 + (ST2S-ST2N)*COSBT2
FACTCC = ST1N*COSBT1**2/SINBT1 + ST1S*SINBT1 +
1 ST2N*COSBT2**2/SINBT2 + ST2S*SINBT2
ALPHA = ATAN((FACTCC*RHORIZ - FACTBB*RVERT1)/
1 (FACTAA*RVERT1 - FACTBB*RHORIZ))
COSALP = COS(ALPHA)
SINALP = SIN(ALPHA)
SWMC0289
SWMC0290
SWMC0291
SWMC0292
SWMC0293
SWMC0294
SWMC0295
SWMC0296
SWMC0297
SWMC0298
SWMC0299
SWMC0300
SWMC0301
SWMC0302
SWMC0303
SWMC0304
SWMC0305
SWMC0306
SWMC0307
SWMC0308
SWMC0309
SWMC0310
SWMC0311
SWMC0312
SWMC0313
SWMC0314
SWMC0315
SWMC0316
SWMC0317
SWMC0318
SWMC0319
SWMC0320
SWMC0321
SWMC0322
SWMC0323
SWMC0324

```

```

FACTDD = ST1N*(SINALP + COSALP*COSBT1/SINBT1)
FACTEE = ST1S*(COSALP*SINBT1 - SINALP*COSBT1)
FACTFF = ST2N*(COSALP*COSBT2**2/SINBT2 - SINALP*COSBT2)
FACTGG = ST2S*(COSALP*SINBT2 + SINALP*COSBT2/SINBT2)
PERP11 = RVERT1*FACTDD/(COSBT1 + FACTEE + FACTFF + FACTGG)
DISP = PERP11/FACTDD
PERP1 = PERP11 + PERP1
TANG1 = PERP11*FACTEE/(SINBT1*FACTDD) + TANG1
PERP2 = PERP11*FACTFF/(COSBT2*FACTDD) + PERP2
TANG2 = PERP11*FACTGG/(SINBT2*FACTDD) + TANG2
IF (.NOT.FLIM) GO TO 166
IF ( NDOP .NE. 0 ) GO TO 166
PPERP1 = PERP1
PPERP2 = PERP2
TTANG1 = TANG1
TTANG2 = TANG2
FLIM = .FALSE.
RHORIZ = 0.0
GO TO 167
C THIS PART COMPUTES THE FACTOR OF SAFETY: THE RATIO OF THE
C COMPONENTS OF DRIVING TO RESISTING FORCES IN THE DISPLACEMENT DIRECTION
166 IF ( RVERT1 .EQ. DUMMYT ) T12P = DUMMYT*TAN (E)
ADISP = T12P/(ST1S + ST2S)
BDISP = DISP*SINALP
CDISP = -DISP*COSALP
DISP = SQRT (ADISP**2 + BDISP**2 + CDISP**2)
ADISP = ADISP/DISP
BDISP = BDISP/DISP
CDISP = CDISP/DISP
IF (FLIM) GO TO 168
PERP1 = PPERP1
PERP2 = PPERP2
TANG1 = TTANG1
TANG2 = TTANG2
168 FLIM = .TRUE.
ADRF1 = T12*ST1S/(ST1S + ST2S)

```

```

SWMC0325
SWMC0326
SWMC0327
SWMC0328
SWMC0329
SWMC0330
SWMC0331
SWMC0332
SWMC0333
SWMC0334
SWMC0335
SWMC0336
SWMC0337
SWMC0338
SWMC0339
SWMC0340
SWMC0341
SWMC0342
SWMC0343
SWMC0344
SWMC0345
SWMC0346
SWMC0347
SWMC0348
SWMC0349
SWMC0350
SWMC0351
SWMC0352
SWMC0353
SWMC0354
SWMC0355
SWMC0356
SWMC0357
SWMC0358
SWMC0359
SWMC0360

```

	BDRF1 = -TANG1*COSBT1	SWMC0361
	CDRF1 = -TANG1*SINBT1	SWMC0362
	ADRF2 = T12 - ADRF1	SWMC0363
	BDRF2 = TANG2*COSBT2	SWMC0364
	CDRF2 = -TANG2*SINBT2	SWMC0365
	DRF = (ADRF1+ADRF2)*ADISP+(BDRF1+BDRF2)*BDISP+(CDRF1+CDRF2)*CDISP	SWMC0366
	FACTHH = (ADRF1*ADISP+BDRF1*BDISP+CDRF1*CDISP)/	SWMC0367
	1 (SQRT(ADEF1**2+BDRF1**2+CDRF1**2))	SWMC0368
	FACTJJ = (ADRF2*ADISP+BDRF2*BDISP+CDRF2*CDISP)/	SWMC0369
	1 (SQRT(ADRF2**2+BDRF2**2+CDRF2**2))	SWMC0370
	REST2 = PERP2*TAN(PHI(J)+AP(J))+CH2	SWMC0371
	REST1 = PERP1*TAN(PHI(I)+AP(I))+CH1	SWMC0372
	FSL = (REST1*FACTHH + REST2*FACTJJ)/DRF	SWMC0373
245	IF(FSL.LT.1.) GO TO 300	26923500 SWMC0374
	WWX(I)=-WX(I)	26923510 SWMC0375
	WWY(I)=-WY(I)	26923520 SWMC0376
	WWZ(I)=-WZ(I)	26923530 SWMC0377
	WWX(J)=WX(J)	26923540 SWMC0378
	WWY(J)=WY(J)	26923550 SWMC0379
	WWZ(J)=WZ(J)	26923560 SWMC0380
	DO 410 K=I,J,1D	26923570 SWMC0381
	COSP=COS(PHI(K)+AP(K))	26923580 SWMC0382
	SINP=SIN(PHI(K)+AP(K))	26923590 SWMC0383
	RRX(K)=WWX(K)*COSP-XX*SINP/X	26923600 SWMC0384
	RRY(K)=WWY(K)*COSP-XY*SINP/X	26923610 SWMC0385
	RRZ(K)=WWZ(K)*COSP-XZ*SINP/X	26923620 SWMC0386
410	CONTINUE	26923630 SWMC0387
	CRPX=RRY(I)*RRZ(J)-RRZ(I)*RRY(J)	26923640 SWMC0388
	CRPY=RRZ(I)*RRX(J)-RRX(I)*RRZ(J)	26923650 SWMC0389
	CRPZ=RRX(I)*RRY(J)-RRY(I)*RRX(J)	26923660 SWMC0390
	CRR=SQRT(CRPX**2+CRPY**2+CRPZ**2)	26923670 SWMC0391
	CRRX=-CRPX/CRR	26923680 SWMC0392
	CRRY=-CRPY/CRR	26923690 SWMC0393
	CRRZ=-CRPZ/CRR	26923700 SWMC0394
	ENN=(RX*CRRX+RY*CRRY+RZ*CRRZ)/(TEMP)	26923710 SWMC0395
	GO TO 300	26923720 SWMC0396

130	IF (EN(I).LT.0.0) GO TO 150	26923730	SWMC0397
	FLS = 0.0		SWMC0398
	K=I	26923750	SWMC0399
	GO TO 145	26923760	SWMC0400
140	IF (EN(J).GT.0.0) GO TO 150	26923770	SWMC0401
	FSL=0.	26923780	SWMC0402
	K=J	26923790	SWMC0403
	EN(K)=-EN(K)	26923800	SWMC0404
145	CONTINUE	26923810	SWMC0405
	FSS=(EN(K)*TAN(PHI(K)+AP(K))+CH(K))/T(K)	26923820	SWMC0406
	WRITE(5,1001) FSS,K		SWMC0407
	IF(CH1.NE.0..OR.CH2.NE.0..OR.AP(I).NE.0..OR.AP(J).NE.0.) GO TO 70	26923840	SWMC0408
	GO TO 240	26923850	SWMC0409
70	FSSE=EN(K)*TAN(PHI(K))/T(K)	26923860	SWMC0410
	GO TO 240	26923880	SWMC0411
150	WRITE(5,1010)		SWMC0412
	GO TO 400	26923900	SWMC0413
240	IF(FSS.LT.1.) GO TO 300	26923910	SWMC0414
300	IF(FSL.NE.0.) FSS=0.	26924020	SWMC0415
	IF(FSS.NE.0.) GO TO 400	26924030	SWMC0416
	IF(IU(I).NE.1.AND.IU(J).NE.1) GO TO 400		SWMC0417
	AK1COS = ((ODX*OBX+ODY*OBY+ODZ*OBZ)/(OD*OB))		SWMC0418
	AK10 = ATAN(SQRT(1.0 - AK1COS**2)/AK1COS)		SWMC0419
	AK2COS = ((OCX*OBX+OCY*OBY+OCZ*OBZ)/(OC*OB))	26924070	SWMC0420
	AK20 = ATAN(SQRT(1.0 - AK2COS**2)/AK2COS)		SWMC0421
	EM10=- (WX(I)*OIRX+WY(I)*OIRY+WZ(I)*OIRZ)	26924080	SWMC0422
	EM20=- (WX(J)*OIRX+WY(J)*OIRY+WZ(J)*OIRZ)	26924090	SWMC0423
	IF (EMX.LE.0.0.OR.EM10.LE.0.0) GO TO 310	26924100	SWMC0424
	IF (AK20.GT.PI2) GO TO 310	26924110	SWMC0425
	IF (ETA.LT.PI2.AND.AK10.GT.PI2.AND.	26924120	SWMC0426
	1 (TAN(AK20)/TAN(PI-AK10)).GT.(1./COS(PI-ETA))) GO TO 310	26924130	SWMC0427
	K=I	26924140	SWMC0428
305	TOP=OSX*WX(K)+OSY*WY(K)+OSZ*WZ(K)	26924150	SWMC0429
	BOT= RX*WX(K)+ RY*WY(K)+ RZ*WZ(K)	26924160	SWMC0430
	VJP=-TOP/BOT		SWMC0431
	OQX=OSX+VJP*RX		SWMC0432

	OQY=OSY+VJP*RY		SWMC0433
	OQZ=OSZ+VJP*RZ		SWMC0434
	OQWX=OQY*WZ (K) -OQZ*WY (K)	26924210	SWMC0435
	OQWY=OQZ*WX (K) -OQX*WZ (K)	26924220	SWMC0436
	OQWZ=OQX*WY (K) -OQY*WX (K)	26924230	SWMC0437
	DET=-OQY*OQWZ+OQZ*OQWY	26924240	SWMC0438
	C2= (-TZ (K) *OQY+TY (K) *OQZ)/DET	26924250	SWMC0439
	TT=C2*SQRT (OQWX**2+OQWY**2+OQWZ**2)	26924260	SWMC0440
	FSR= (EN (K) *TAN (PHI (K) +AP (K)) +CH (K))/TT	26924270	SWMC0441
	WRITE (5,1013) FSR,K		SWMC0442
	IF (CH1.NE.0..OR.CH2.NE.0..OR.AP (I) .NE.0..OR.AP (J) .NE.0.) GO TO 75	26924290	SWMC0443
	GO TO 420	26924300	SWMC0444
75	FSRB=EN (K) *TAN (PHI (K))/TT	26924310	SWMC0445
	GO TO 420	26924330	SWMC0446
310	IF (EMX.GE.0.0.OR.EM20.LE.0.0) GO TO 320	26924340	SWMC0447
	IF (AK10.GT.PI2) GO TO 320	26924350	SWMC0448
	IF (ETA.LT.PI2.AND.AK20.GT.PI2.AND.	26924360	SWMC0449
	1 (TAN (AK10)/TAN (PI-AK20)) .GT. (1./COS (PI-ETA))) GO TO 320	26924370	SWMC0450
	K=J	26924380	SWMC0451
	LN (K) =-EN (K)	26924390	SWMC0452
	GO TO 305	26924400	SWMC0453
320	CONTINUE		SWMC0454
400	CONTINUE		SWMC0455
405	CONTINUE		SWMC0456
420	CONTINUE		SWMC0457
510	CONTINUE	26924650	SWMC0458
500	CONTINUE	26924660	SWMC0459
	WRITE (NWR,1041) NREAL,PSI,BETA1,H,PHX (1),AQ (1),TAU (1),		SWMC0460
	1 PCTJTG (1),UAV (1),PHX (2),AQ (2),TAU (2),PCTJTG (2),UAV (2),		SWMC0461
	2 FSL,FSLR		SWMC0462
5000	CONTINUE		SWMC0463
9000	CONTINUE	26924680	SWMC0464
	STOP	26924690	SWMC0465
	END	26924700	SWMC0466
	SUBROUTINE WATER (RX,RY,RZ,H,E,P,PLG,HU,IU,UAV,OP1,HW,UF,HH,PI,		SWMC0467
	1 AREA,WWGT,I,J,ID,WX,WY,WZ,TPSLP)		SWMC0468

	DIMENSION	IU (8) , UAV (8) , AREA (8) , UF (8) , WX (8) , WY (8) , WZ (8)	SWMC0469
	DO 15 K = 1, 2		SWMC0470
	KK=IU (K)		26925070 SWMC0471
	HHH=HU (K)		26925080 SWMC0472
	IF (TPSLP.LT.0..AND.HHH.LT.-HH) HHH=-HH		26925090 SWMC0473
	DH=H-HHH		26925100 SWMC0474
	IF (DH.LE.0.) GO TO 15		26925110 SWMC0475
	TEM=(DH/H) *(DH/(H+HH))		26925120 SWMC0476
	GO TO (15,20,25,30) ,KK		26925130 SWMC0477
20	UF (K) =AREA (K) *UAV (K)		26925140 SWMC0478
	GO TO 35		26925150 SWMC0479
25	PER=1.		26925160 SWMC0480
	GO TO 40		26925170 SWMC0481
30	AZZ=DH/SIN (P)		26925180 SWMC0482
	AXX=0.		26925190 SWMC0483
393	IF (PLG.NE.90.) AXX=DH/TAN (P)		26925200 SWMC0484
	AX=DH/TAN (E) -AXX		26925210 SWMC0485
	PA=PI-P		26925220 SWMC0486
	ART=AZZ*AX*SIN (PA) /2.		26925230 SWMC0487
	IF (HW.NE.0.) GO TO 45		26925240 SWMC0488
	EA=P/2.		26925250 SWMC0489
	IF (EA.LE.E) GO TO 15		26925260 SWMC0490
	ARA=AZZ*AZZ*SIN (PA) /2.		26925270 SWMC0491
	ARB=ART-ARA		26925280 SWMC0492
	PER=ARB/ART		26925290 SWMC0493
	GO TO 40		26925300 SWMC0494
45	HP=HW-HU (K)		26925310 SWMC0495
	AY=OP1-AXX		26925320 SWMC0496
	AZW=HP/SIN (P)		26925330 SWMC0497
	IF (HP.GT.DH) GO TO 50		26925340 SWMC0498
	ARA1=AZW*AY*SIN (PA) /2.		26925350 SWMC0499
	ARB1=ART-ARA1		26925360 SWMC0500
	IF (AY.GT.AX) GO TO 55		26925370 SWMC0501
	PER=ARB1/ART		26925380 SWMC0502
	GO TO 40		26925390 SWMC0503
55	IF (HP.EQ.DH.AND.AY.GE.AX) GO TO 15		26925400 SWMC0504

```

    AYY=AXX*AZW/AZZ
    ZA=ATAN2 (HP, (AY+AYY))
    ZB=AY-AX
    ZC=PI-E
    ZD=PI-ZC-ZA
    ARF=ZB*ZB*SIN(ZA)*SIN(ZC)/(2.*SIN(ZD))
    PER=(ARB1+ARF)/ART
    GO TO 40
50 IF (AY.GE.AX) GO TO 15
    ZG=AX-AY
    ZE=ATAN2(OP1,HP)+PI/2.
    ZF=PI-ZE-ZG
    ARB2=ZG*ZG*SIN(ZE)*SIN(E)/(2.*SIN(ZF))
    PER=ARB2/ART
40 CONTINUE
    UF(K)=PER*TEM*AREA(K)*WWGT*DH/3.
35 IF(K.EQ.J) UF(K)=-UF(K)
    UFX=WX(K)*UF(K)
    UFY=WY(K)*UF(K)
    UFZ=WZ(K)*UF(K)
    RX=RX-UFX
    RY=RY-UFY
    RZ=RZ-UFZ
15 CONTINUE
    RETURN
    END

```

```

26925410 SWMC0505
26925420 SWMC0506
26925430 SWMC0507
26925440 SWMC0508
26925450 SWMC0509
26925460 SWMC0510
26925470 SWMC0511
26925480 SWMC0512
26925490 SWMC0513
26925500 SWMC0514
26925510 SWMC0515
26925520 SWMC0516
26925530 SWMC0517
26925540 SWMC0518
26925550 SWMC0519
26925560 SWMC0520
26925570 SWMC0521
26925580 SWMC0522
26925590 SWMC0523
26925600 SWMC0524
26925610 SWMC0525
26925620 SWMC0526
26925630 SWMC0527
26925640 SWMC0528
26925650 SWMC0529
26925660 SWMC0530

```

Appendix G

Strength Derivations for Mechanical Model

The mechanical model described in Chapter 5 uses a Griffith-Modified Griffith envelope to define the strength of intact rock. The orientation of the failure surface is a critical feature in the strength determination. The model investigates numerous paths with different orientations in order to find the one with the minimum strength. Figure G.1 shows a typical path from Point A to Point B inclined at an angle θ . The objective is to find the resistance which must be overcome to create a failure path between the two points. The Mohr stress circle is used in solving this problem. The Mohr circle for the state of stress at failure must be tangent to the Griffith-Modified Griffith envelope at a point such that the failure plane develops in the direction θ (Figure G.1). The critical stress condition is obtained by superimposing upon the ambient stress field both negative horizontal normal stresses ($\Delta\sigma_h$) and shear stresses ($\Delta\tau$) in the horizontal and vertical planes.* (The vertical normal stress is assumed to be constant.) The problem is essentially a geometrical exercise in which the Mohr circle at failure is the unknown while θ , the failure envelope, σ_{vo} and σ_{ho} (the ambient stress field) are the knowns.

* Intact rock will generally fail in tension given the relatively low range of stresses encountered in most engineering problems.

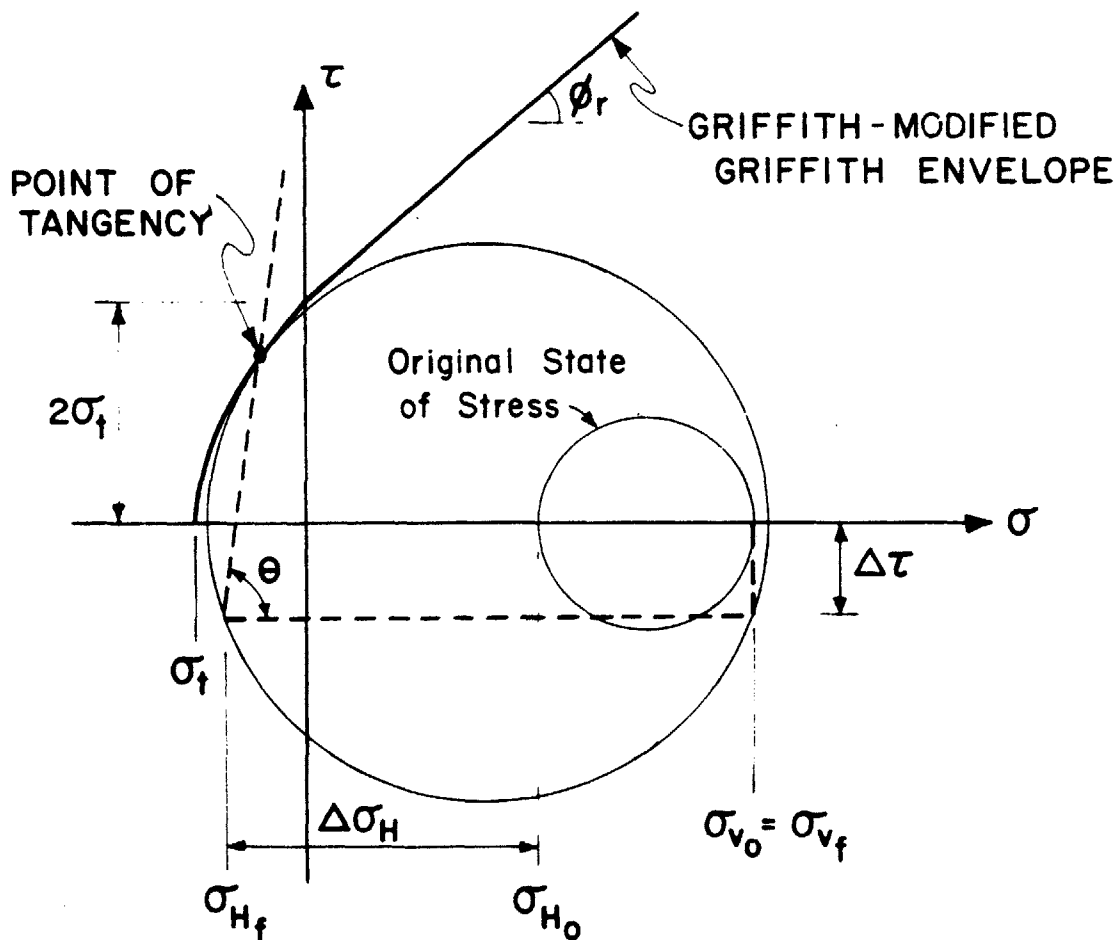
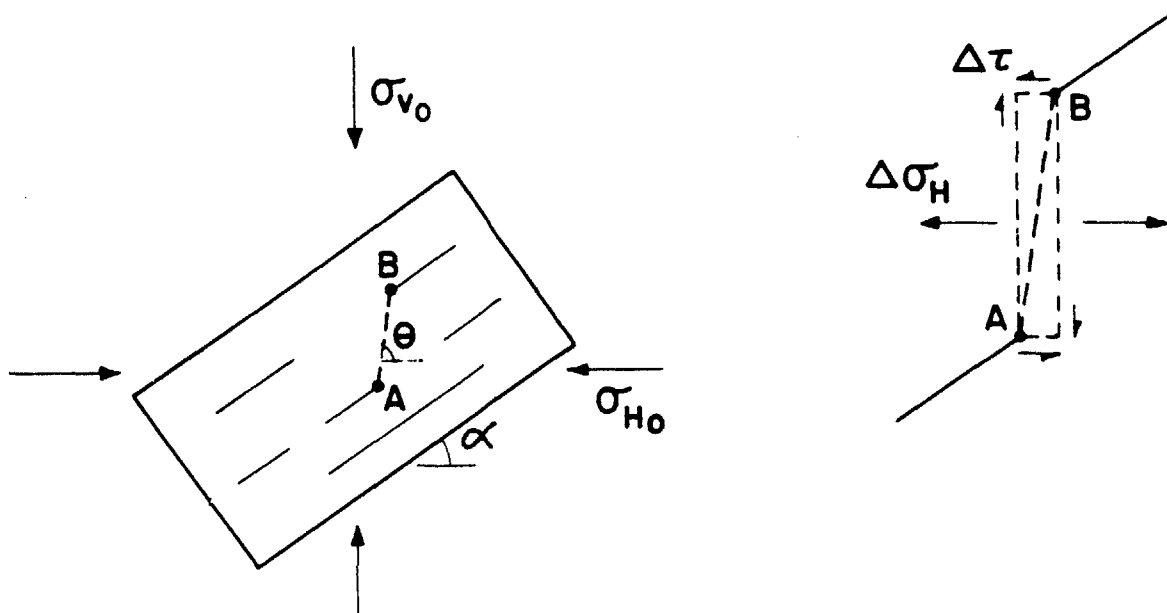


Figure G.1 Failure Conditions--Intact Rock
396

The mechanical model places some constraints on the values that θ can assume. The angle the failure path makes with the lower joint plane must be less than or equal to 90° (Figure G.2). However, the joint planes are inclined at an angle α relative to the horizontal so that the maximum value that θ can reach is $90^\circ + \alpha$.

The formation of a failure path potentially lets the upper portion of the rock mass slide down the direction of the joint planes. When $\theta \leq 90^\circ$ this impending movement implies that the shear stresses on the failure path are counterclockwise; hence, the point of tangency for the Mohr circle at failure will be above the σ axis. Similarly, when $\theta \geq 90^\circ$, the point of tangency will be below the σ axis.

G.1 Griffith-Modified Griffith Envelope (Figure G.1)

The Griffith-Modified Griffith Envelope is composed of a parabola in the tensile range and a straight line in the compression range. It is completely defined by two parameters: σ_t , the tensile strength of the intact rock, and ϕ_r , the friction angle. The envelope intercepts the τ axis at $2|\sigma_t|$.

Circles tangent to the parabola can be characterized by an angle γ where γ is the acute angle between the horizontal and line of tangency (Figure G.3). There is a unique one-to-one correspondence between γ values and failure circles.

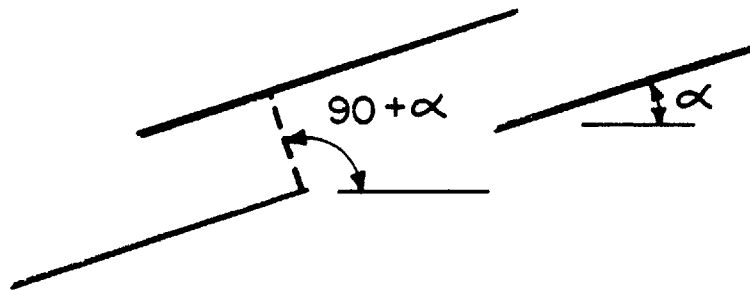
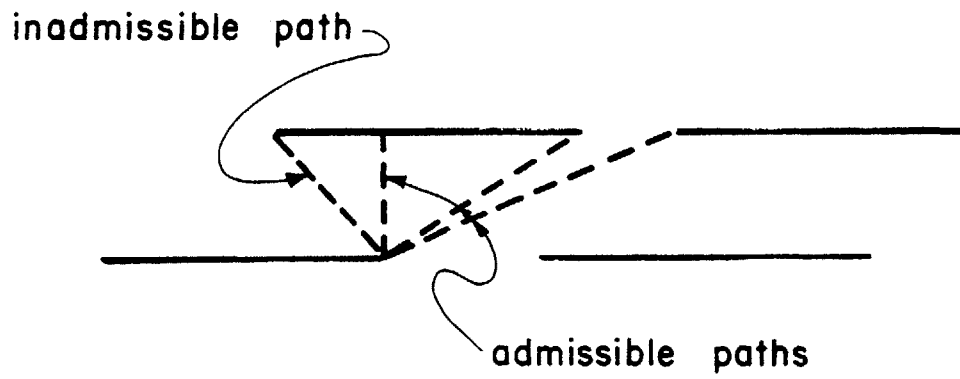


Figure G.2 Limitation on the Maximum Value of θ

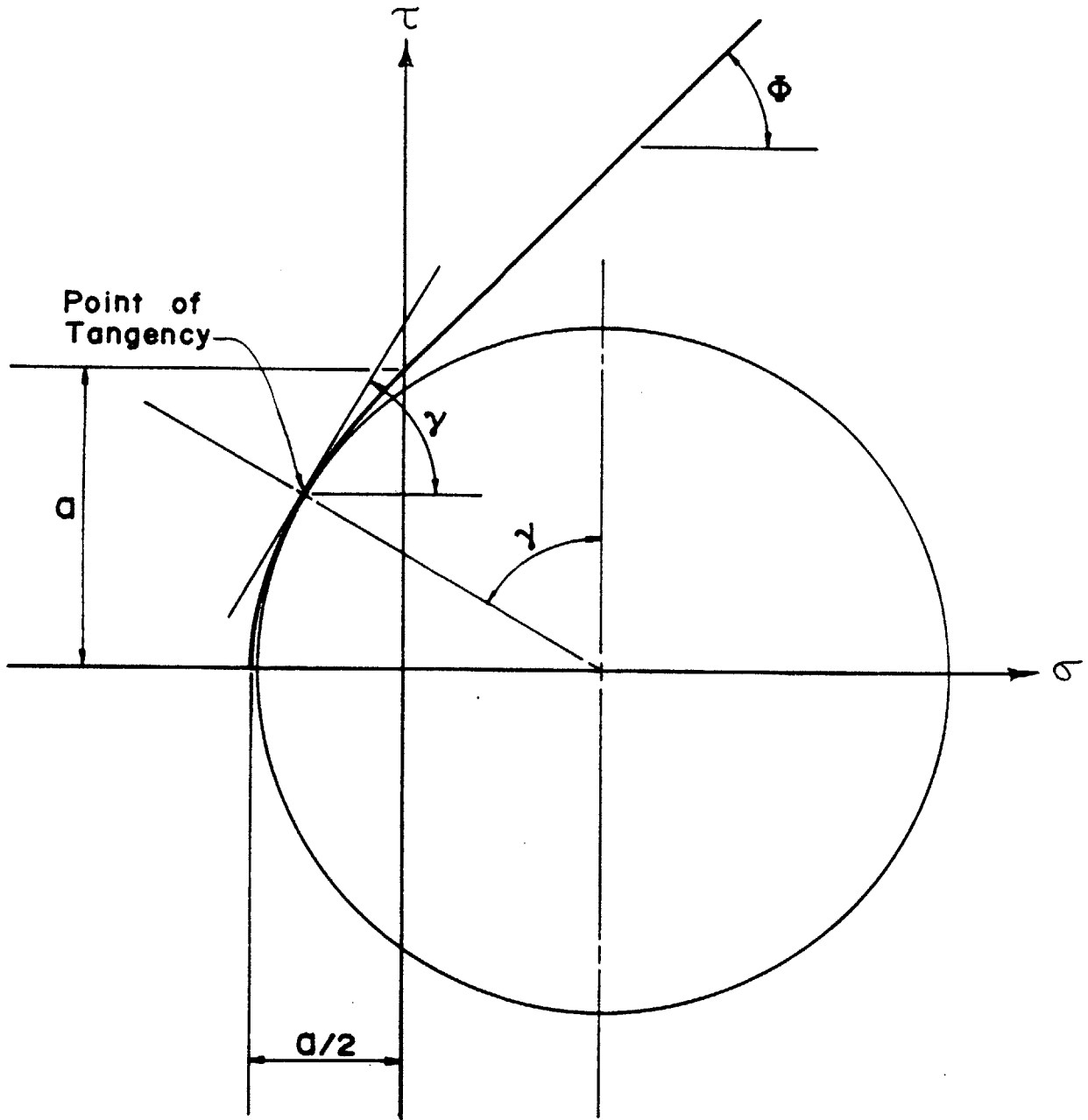


Figure G.3 Definition of γ

The circle tangent at $\sigma = \sigma_t$ and $\tau = 0$ has a $\gamma = 90^\circ$. Similarly, the circle tangent at $\sigma = 0$ and $\tau = 2|\sigma_t|$ has a $\gamma = 45^\circ$.

The point $(0, 2|\sigma_t|)$ is common to both the linear and parabolic portions of the envelope. The change from parabola to line is not necessarily a smooth transition. The tangent to the parabola at $(0, 2|\sigma_t|)$ is inclined at 45° . If $\phi_r = 45^\circ$, the envelope will be smooth, i.e., its first derivative will be continuous. On the other hand, if $\phi_r \neq 45^\circ$, the first derivative will be discontinuous and the envelope will be kinked. The implications of the singularity are discussed in the two succeeding sections.

G.1.1 $\phi_r < 45^\circ$

For $\phi < 45^\circ$ ^{*}, there is one circle which is tangent to both the straight line and the parabola. It is important to analytically define this circle because it serves as a transition between two distinct families of failure circles--those that are tangent to the parabola and those that are tangent to the line. The circle with dual tangency can be characterized by two parameters: r , the radius, and x , the distance along the σ axis from the origin to the center of the circle.

* For the sake of convenience the "r" subscript will subsequently be dropped from ϕ_r .

Figure G.4 shows a typical circle with dual tangency. As noted in Figure G.4, $a = -2\sigma_t$. The equation of the parabola is:

$$\tau^2 = 4\sigma_t(\sigma_t - \sigma_n) \quad (G.1)$$

since $\sigma_t = -a/2$

$$\tau^2 = a^2 + 2a\sigma_n \quad (G.1A)$$

Hoek (1969) derived the following relation:

$$x - \sigma_n = 2\sigma_t \quad (G.2)$$

or

$$x - \sigma_n = -a$$

or

$$\sigma_n = x - a \quad (G.2A)$$

Substituting into Equation (G.1A):

$$\tau^2 = a^2 + 2a(x - a) = 2ax - a^2 \quad (G.3)$$

Using the Pythagorean Theorem:

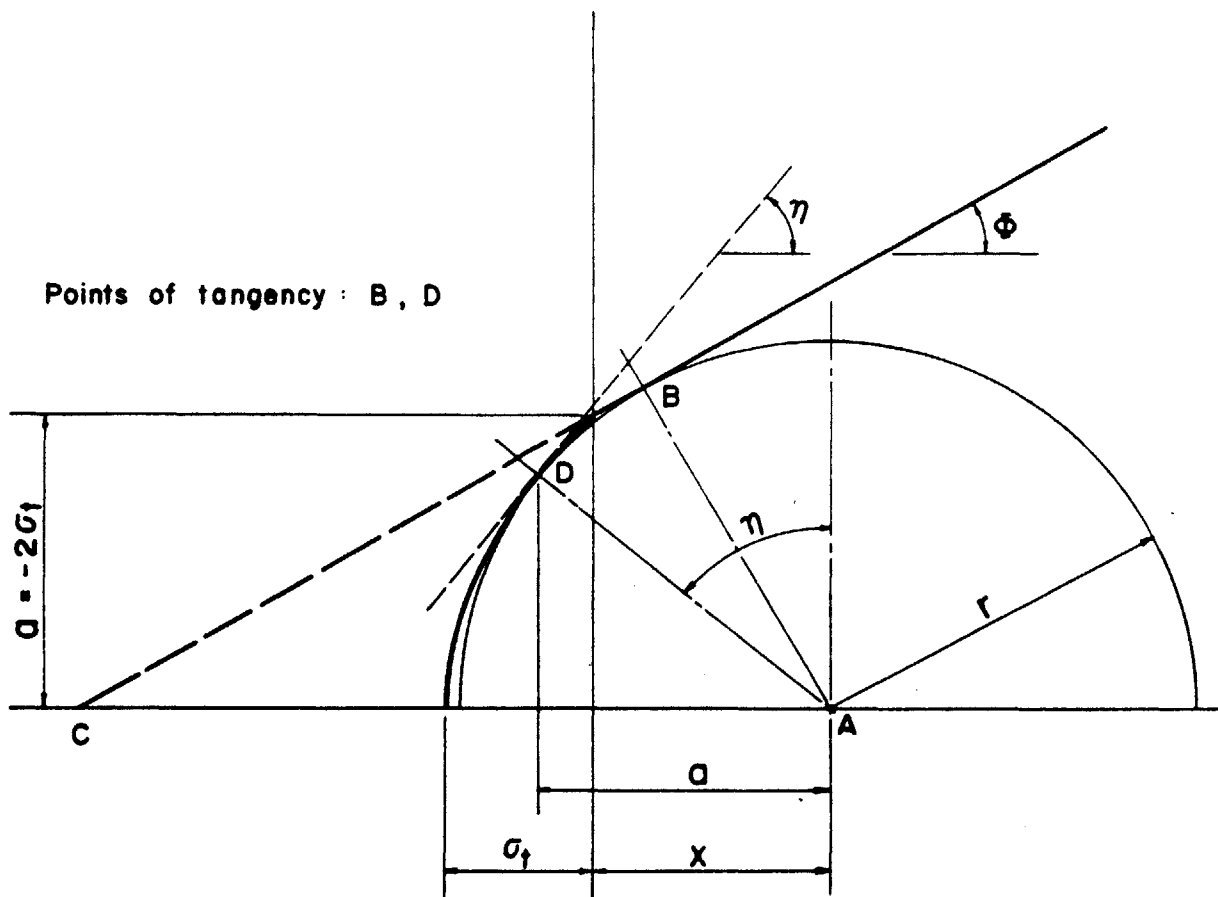


Figure G.4 Circle With Dual Tangency

$$r^2 = \tau^2 + (x - \sigma_n)^2 \quad (G.4)$$

or

$$r^2 = \tau^2 + a^2 \quad (G.4A)$$

Combining Equations (G.4A) and (G.3):

$$r^2 = 2ax - a^2 + a^2 = 2ax \quad (G.5)$$

r and x are also related to the parameters defining the linear envelope:

Examining the triangle ABC:

$$r = \sin \phi (x + a/\tan \phi) \quad (G.6)$$

$$r^2 = \sin^2 \phi (x + a/\tan \phi)^2 \quad (G.6A)$$

Combining Equations (G.5) and (G.6A):

$$2ax = \sin^2 \phi (x + a/\tan \phi)^2 \quad (G.7)$$

Equation (G.7) is a quadratic equation which can be solved for x:

$$x = \frac{a[(1 - \sin \phi \cos \phi) - (1 - 2 \sin \phi \cos \phi)^{\frac{1}{2}}]}{\sin^2 \phi} \quad (G.8)$$

The γ value for the circle with dual tangency has particular interest and is defined as η .

From Figure G.4:

$$\sin \eta = \frac{a}{r} \quad (G.9)$$

From Equation (G.5):

$$r = (2ax)^{\frac{1}{2}} \quad (G.5A)$$

Substituting for r in Equation (G.9):

$$\sin \eta = \frac{a}{(2ax)^{\frac{1}{2}}} \quad (G.10)$$

$$= \left(\frac{a}{2x}\right)^{\frac{1}{2}} \quad (G.10A)$$

ϕ and η are uniquely related:

ϕ	η
25°	54.93°
30°	52.05°
35°	49.49°
40°	47.16°
45°	45.00°

G.1.2 $\phi > 45^\circ$

For $\phi > 45^\circ$, the failure envelope has a cusp (Figure G.5). As indicated in the figure there is a family of failure circles which touch the envelope at the point $(0,a)$. The family includes all circles whose centers lie between the points x_p and x_L

ϕ	x_p^*	x_L^*
45°	1.0	1.0
50°	1.0	1.192
55°	1.0	1.428
60°	1.0	1.732
65°	1.0	2.145
70°	1.0	2.747

* x_p and x_L are expressed as multiples of a .

G.2 Classes of Failure Circles

All failure circles fall within one of four generic classes:

1. Circles tangent to the linear envelope.
2. Circles tangent to the parabolic envelope ($\gamma < 90^\circ$)
3. Circles tangent to the parabolic envelope at $(\sigma_t, 0)$,
i.e., $\gamma = 90^\circ$.
4. Circles touching the cusp.

Class 4 is applicable only when $\phi > 45^\circ$. Circles with dual tangency are exceptional cases in that they qualify for

both Classes 1 and 2.

The succeeding sections will examine each of the classes and derive general solutions to the fundamental problem:

Given: θ (the inclination of the failure surface)
 σ_v (vertical stress)

Find: x }
 r } (center and radius of the failure circle)

G.2.1 Circles Tangent to the Linear Envelope

Figure G.6 shows a failure circle with $45 + \phi/2 \leq \theta \leq 90^\circ$.

From triangle ABC:

$$r = (a \text{ ctn } \phi + x) \sin \phi \quad (\text{G.11})$$

From triangle ADE:

$$r^2 - r^2 (\sin^2 (2\theta - 90 - \phi)) = (\sigma_v - x)^2 \quad (\text{G.12})$$

$$r^2 (1 - \sin^2 (2\theta - 90^\circ - \phi)) = (\sigma_v - x)^2 \quad (\text{G.12A})$$

$$(1 - \sin^2 (2\theta - 90 - \phi)) = \cos^2 (2\theta - 90 - \phi) = \sin^2 (2\theta - \phi) \quad (\text{G.13})$$

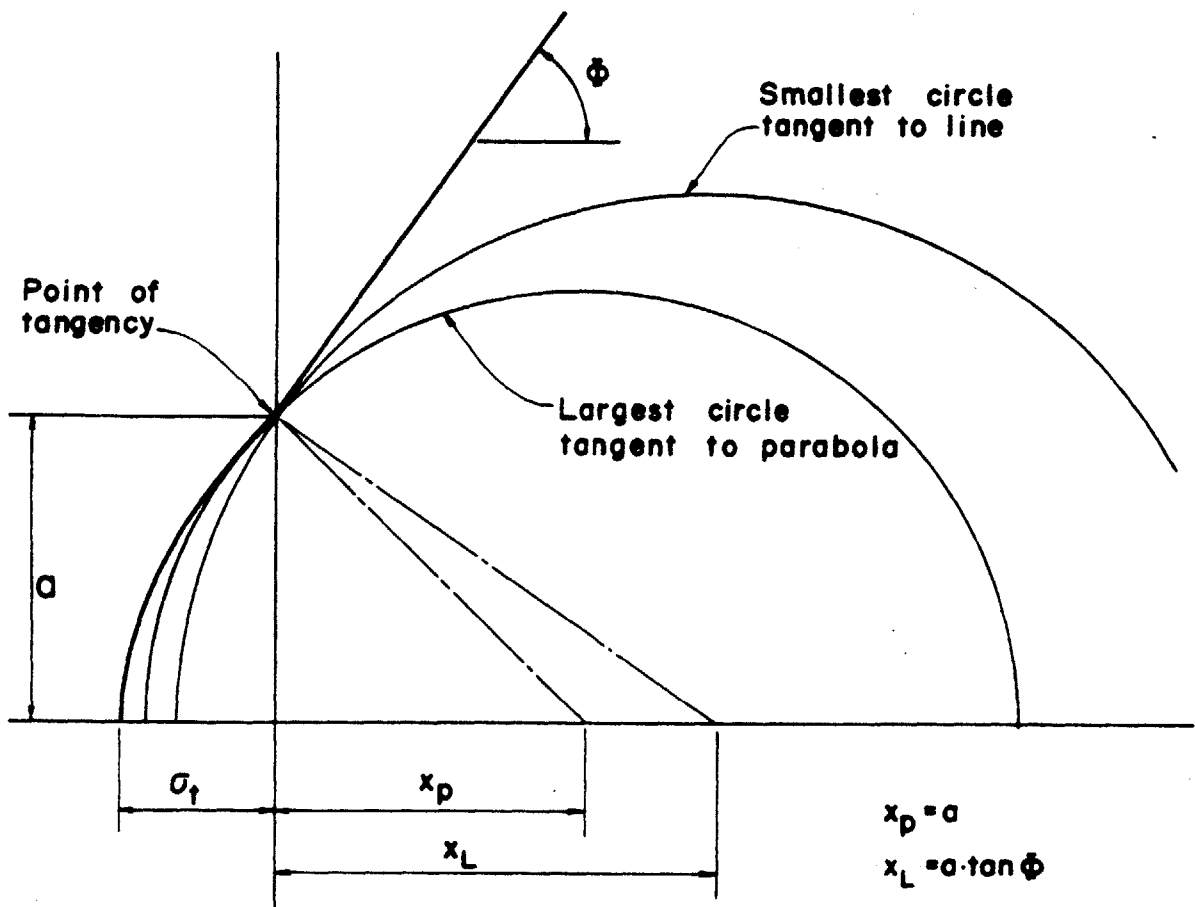


Figure G.5 Failure Envelope With a Cusp

Letting $\lambda = \sin (2\theta - \phi)$ and substituting into (G.12A):

$$\lambda^2 r^2 = (\sigma_v - x)^2 \quad (\text{G.14})$$

$$\lambda r = \sigma_v - x \quad (\text{G.14A})$$

Combining Equations (G.11) and (G.14A):

$$\lambda(a \operatorname{ctn} \phi + x) \sin \phi = \sigma_v - x \quad (\text{G.15})$$

Finally,

$$x = \frac{\sigma_v - \lambda a \cos \phi}{1 + \lambda \sin \phi} \quad (\text{G.15A})$$

$$\tau^2 = r^2 + (\sigma_v - x)^2 \quad (\text{G.16})$$

A similar analysis can be performed for other ranges of θ . In all cases, the solution has the same general form as Equation (G.16); however, the expression for λ varies.

<u>range of θ</u>	<u>λ</u>	<u>sign of τ^*</u>
$0 \leq \theta \leq 45 + \phi/2$	$\sin(2\theta - \phi)$	+
$45 + \phi/2 \leq \theta \leq 90$	$\sin(2\theta - \phi)$	-
$90 \leq \theta \leq 135 - \phi/2$	$-\sin(2\theta + \phi)$	+
$135 - \phi/2 \leq \theta \leq 180$	$-\sin(2\theta + \phi)$	-

G.2.2 Circles Tangent to the Parabolic Envelope at $(\sigma_t, 0)$;
 $\gamma = 90^\circ$

Figure G.7 shows a typical failure circle tangent to the envelope at $(\sigma_t, 0)$. The geometric relations shown in Figure G.7 and the equations derived below are valid for θ between 0° and 45° .

From triangle ABC:

$$2r = \frac{\tau}{\sin \theta \cos \theta} \quad (\text{G.17})$$

$$\text{diameter of circle} = \sigma_1 + \frac{a}{2} = \frac{\tau}{\sin \theta \cos \theta} \quad (\text{G.18})$$

From Figure G.7:

$$x - \sigma_v = \frac{\tau}{\tan \theta} - \frac{\tau}{2 \sin \theta \cos \theta} = \frac{\tau}{2 \sin \theta \cos \theta} - \frac{a}{2} - \sigma_v \quad (\text{G.19})$$

* A positive τ implies shear stresses on horizontal planes that tend to rotate an element counterclockwise.

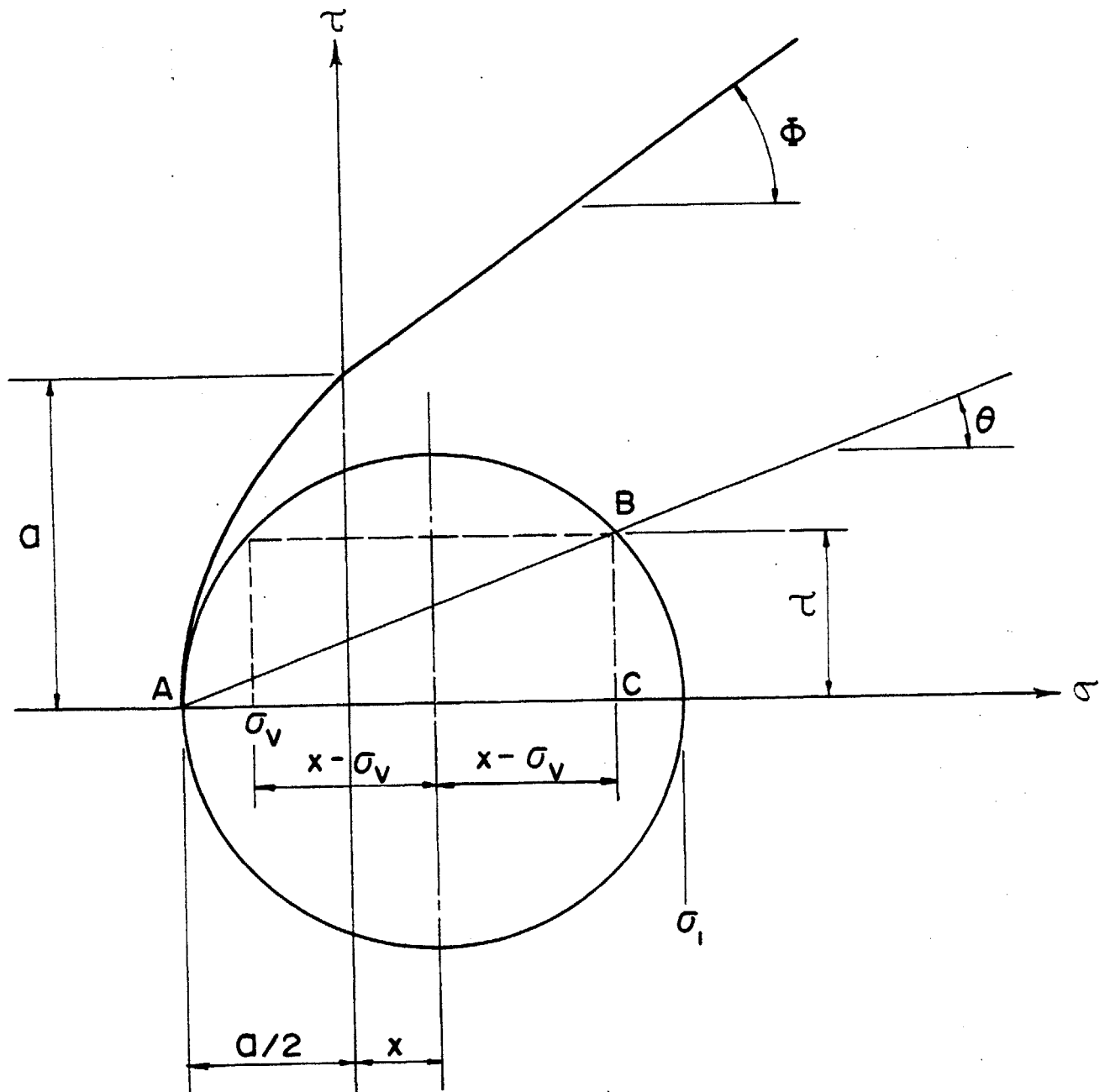


Figure G.7 Failure Circle Tangent to Parabolic Envelope
 at $\sigma = -a/2$ and $\tau = 0$

$$\tau = \frac{\frac{a}{2} + \sigma_v}{\left(\frac{1}{\sin \theta \cos \theta} - \frac{1}{\tan \theta}\right)} \quad (\text{G.20})$$

$$r = x + \frac{a}{2} = \frac{\tau}{2 \sin \theta \cos \theta} \quad (\text{G.21})$$

Substituting τ from Equation (G.20) into Equation (G.21):

$$x + \frac{a}{2} = \frac{1}{2 \sin \theta \cos \theta} \frac{\frac{a}{2} + \sigma_v}{\left(\frac{1}{\sin \theta \cos \theta} - \frac{1}{\tan \theta}\right)} \quad (\text{G.22})$$

$$x + \frac{a}{2} = \frac{\frac{a}{2} + \sigma_v}{2 \sin^2 \theta} \quad (\text{G.22A})$$

Finally,

$$x = \frac{1}{2} \left(\frac{\frac{a}{2} + \sigma_v}{\sin^2 \theta} - a \right) \quad (\text{G.23})$$

A similar analysis can be performed for other ranges of θ . The results indicate that Equation (G.23) is valid for all values of θ between 0° and 180° . The general expression for τ , the shear stress on a horizontal plane is

$$\tau = \frac{\sigma_v + \frac{a}{2}}{\left(\frac{1}{|\sin \theta \cos \theta|} - \frac{1}{|\tan \theta|}\right)} \quad (\text{G.24})$$

<u>Range of θ</u>	<u>Sign of τ</u>
$0 \leq \theta \leq 90^\circ$	+
$90 \leq \theta \leq 180^\circ$	-

G.2.3 Circles Tangent to the Parabolic Envelope $\eta < \gamma < 90^\circ$

There is no closed form solution to relate x to θ and σ_v when the circle is tangent to the parabola. The problem must be solved by using iterative techniques. Various points of tangency and their corresponding failure circles are examined. For a given θ value one can calculate the " σ_v " associated with each circle. The circle whose " σ_v " corresponds to the true σ_v is the requisite circle. The convergence on the solution is very rapid and a good ($\pm 0.1\%$) approximation can be found within 5 trials.

The parameter γ is a convenient way of identifying the trial circles. As noted earlier, $\eta < \gamma < 90^\circ$. Once a trial value for γ is chosen the problem reduces to an analysis involving a circle tangent to a straight line whose slope is $\tan \gamma$. This analysis was discussed in Section G.2.1. The relations used to obtain the results below are borrowed in part from that section with the modification that η replaces ϕ and that the unknown is " σ_v " rather than x .

From Figure G.6 and as derived in Section G.2.1:

$$r^2 - r^2 (\sin^2 (2\theta - 90 - \phi))^{1/2} = (\sigma_v - x)^2 \quad (G.12)$$

$$r \sin (2\theta - \phi) = \sigma_v - x \quad (G.14A)$$

Substituting γ for ϕ and " σ_V " for σ_V ,

$$r \sin (2\theta - \gamma) = \sigma_V - x \quad (G.25)$$

From Figure G.4:

$$\sin \gamma = \frac{a}{r} \quad (G.26)$$

$$r = a \csc \gamma \quad (G.26A)$$

As shown earlier,

$$r^2 = 2ax \quad (G.5)$$

$$\sin^2 \gamma = \frac{a^2}{r^2} = \frac{a^2}{2ax} = \frac{a}{2x} \quad (G.27)$$

Solving for x:

$$x = \frac{a}{2 \sin^2 \gamma} = \frac{a \csc^2 \gamma}{2} \quad (G.28)$$

Substituting Equations (G.26A) and (G.28) into Equation (G.25):

$$a \csc \gamma \sin (2\theta - \gamma) = \sigma_V - \frac{a \csc^2 \gamma}{2} \quad (G.29)$$

Rearranging terms:

$$"σ_v" = \frac{a}{2} \csc^2 \gamma + a \csc \gamma \sin (2\theta - \gamma) \quad (G.29A)$$

Equation (G.29A) is valid for θ between 0 and 90°. Equation (G.30) is valid for θ between 90° and 180°.

$$"σ_v" = \frac{a}{2} \csc^2 \gamma - a \csc \gamma \sin (2\theta + \gamma) \quad (G.30)$$

Once the proper γ is found, all the remaining properties of the failure circle can be found. Equation (G.26) can be used to find r while (G.28) will yield x . τ is a function of r :

$$\tau^2 = r^2 + a^2 \quad (G.31)$$

$$\tau = (r^2 + a^2)^{\frac{1}{2}} \quad (G.31A)$$

The sign of τ depends on θ and γ :

θ	<u>Sign of γ</u>
$0 \leq \theta \leq 45 + \gamma/2$	+
$45 + \gamma/2 \leq \theta \leq 90$	-
$90 \leq \theta \leq 135 - \gamma/2$	+
$135 - \gamma/2 \leq \theta \leq 180$	-

G.2.4 Circle Touching the Cusp

If the requisite failure circle touches the cusp its center must lie between the limits x_p and x_L discussed in Section G.2.1. The solution requires iterative techniques. Numerous circles must be examined to find the one with the proper " σ_v ." Figure G.8 shows a typical trial circle. Once a value for x is chosen the procedures developed for linear envelopes are applicable. The parameter ω replaces ϕ of the linear envelope solution.

$$\tan \omega = x/a \quad (G.32)$$

Since x can vary from a to $a \cdot \tan \phi$, ω will vary from 45° to ϕ . All the equations of Section G.2.1 are valid:

$$x = \frac{(\sigma_v - a\lambda \cos \phi)}{(1 + \lambda \sin \phi)} \quad (G.15A)$$

Substituting ω for ϕ and rearranging the equations to reflect the fact that " σ_v " rather than x is the unknown:

$$\sigma_v = a\lambda \cos \omega + x(1 + \lambda \sin \omega) \quad (G.33)$$

$$\begin{array}{ll} \frac{\theta}{0^\circ < \theta \leq 90^\circ} & \frac{\lambda}{\sin (2\theta - \omega)} \\ \frac{\theta}{90^\circ \leq \theta \leq 180^\circ} & -\sin (2\theta + \omega) \end{array}$$

Once the proper ω is obtained r can be calculated.

$$r = (a \operatorname{ctn} \omega + x) \sin \omega \quad (\text{G.34})$$

G.3 General Solution Procedure

As indicated in Section G.1, the most general form of the problem is:

Given: $a, \phi, \sigma_V, \theta$

Find: x and r (or x and τ)

One typically does not know a priori which part of the envelope the requisite circle touches. Part of the solution is to determine into which of the four categories listed in Section G.2 the problem falls.

The solution procedure outlined below provides a logical means of identifying the critical circle based solely on the "given" information described above.

**** For $\phi \leq 45^\circ$ ****

Step 1: Find the circle with dual tangency.

x_η = center of circle with dual tangency

$$x_\eta = \frac{a[(1 - \sin \phi \cos \phi) - (1 - 2 \sin \phi \cos \phi)^{\frac{1}{2}}]}{\sin^2 \phi} \quad (\text{G.35})$$

$$\eta = \sin^{-1} \left(\frac{a}{2x_\eta} \right)^{\frac{1}{2}} \quad (G.36)$$

Step 2: Compute " σ_v " for the circle with dual tangency. The equations are similar to Equations (G.29) and (G.30) except η replaces γ .

$$" \sigma_v " = (a/2) \csc^2 \eta - a\delta \csc \eta \quad (G.37)$$

$$\begin{array}{ll} \underline{\theta} & \underline{\delta} \\ 0 \leq \theta \leq 90 & \sin (2\theta - \eta) \\ 90 \leq \theta < 180 & -\sin (2\theta + \eta) \end{array}$$

Step 3: If $\sigma_v > " \sigma_v "$ the requisite circle must be tangent to the linear envelope. Therefore, go to Step 6.

Step 4: Examine circles tangent to the parabola at $x = -a/2$; $y = 0$.

$$x = 1/2 \left(\frac{\sigma_v + \frac{a}{2}}{\sin^2 \theta} - a \right) \quad (G.38)$$

Compute the maximum principal stress for that circle (see Figure G.7).

$$\sigma_1 = x + \left(x + \frac{a}{2} \right) = 2x + \frac{a}{2} \quad (G.39)$$

If $\sigma_1 \leq 1.5 a$, the circle centered at x is the requisite circle. τ can be found from Equation (G.24).

If $\sigma_1 > 1.5 a$, go to Step 5.

Step 5: The requisite circle must be tangent to the parabola with $\eta < \gamma < 90^\circ$. Use the iterative technique described in Section G.2.3 to find γ and x .

Step 6: The requisite circle is tangent to the linear envelope.

$$x = \frac{(\sigma_v - a\lambda \cos \phi)}{(1 + \lambda \sin \phi)} \quad (G.40)$$

θ	λ
$0 < \theta \leq 90^\circ$	$\sin (2\theta - \phi)$
$90 \leq \theta \leq 180^\circ$	$-\sin (2\theta + \phi)$

$$r = (a \operatorname{ctn} \phi + x) \sin \phi \quad (G.6)$$

**** For $\phi > 45^\circ$ ****

Step 1: Compute " σ_{vp} " for the largest circle tangent to the parabola. The circle has a γ of 45° .

$$" \sigma_{vp} " = \frac{a}{2} \operatorname{csc}^2 45^\circ - \delta a \operatorname{csc} 45^\circ \quad (G.41)$$

$$= a - (1.414)a\delta \quad (G.41A)$$

$$\begin{array}{ll} 0 < \theta \leq 90 & \sin (2\theta - 45) \\ 90 \leq \theta < 180 & -\sin (2\theta + 45) \end{array}$$

Compute the " σ_{v_L} " for the smallest circle tangent to the straight line. Use Equation (G.33) with $\omega = \phi$.

$$x = a \cdot \tan \phi \quad (G.42)$$

$$" \sigma_{v_L} " = a\lambda \cos \phi + x(1 + \lambda \sin \phi) \quad (G.43)$$

$$\begin{array}{ll} 0 < \theta < 90 & \sin (2\theta - \phi) \\ 90 \leq \theta \leq 180 & -\sin (2\theta + \phi) \end{array}$$

Step 2: If $\sigma_v > " \sigma_{v_L} "$ the requisite circle must be tangent to the linear envelope. Go to Step 6 described for $\phi \leq 45^\circ$.

If $\sigma_v < " \sigma_{v_p} "$ the requisite circle must be tangent to the parabola. Go to Step 4 described for $\phi \leq 45^\circ$. If

" σ_{v_p} " $\leq \sigma_v \leq " \sigma_{v_L} "$, the requisite circle must touch the cusp. Use the iterative technique described in Section G.2.3 to find x and r.

G.4 Failure Along Joints

Failure along joints is easier to analyze than failure through intact rock. Continuous joints cannot maintain a tensile stress so the failure envelope is defined solely in the compression region. The failure envelope is assumed to be linear and is characterized by a friction angle, ϕ_j , and a cohesion, c_j (Figure G.9). The problem is to find the failure circle whose failure plane is oriented at the proper θ angle. For joints, θ equals α (Figure G.9). The requisite circle is found by reducing the horizontal stress while holding the vertical stress (σ_v) constant. (Unlike the intact rock, no shear stresses need to be introduced in the horizontal and vertical planes.) The problems can be stated as:

Given: $\phi_j, c_j, \theta = \alpha, \sigma_v = \sigma_{v_0}$

Find: the failure circle.

Figure G.10 shows a typical failure circle.

$$u + v + w = c \operatorname{ctn} \phi_j + \sigma_v \quad (\text{G.44})$$

Examining the line AB, one can express its length two ways:

$$A - B = w \tan (90 - \theta) \quad (\text{G.45})$$

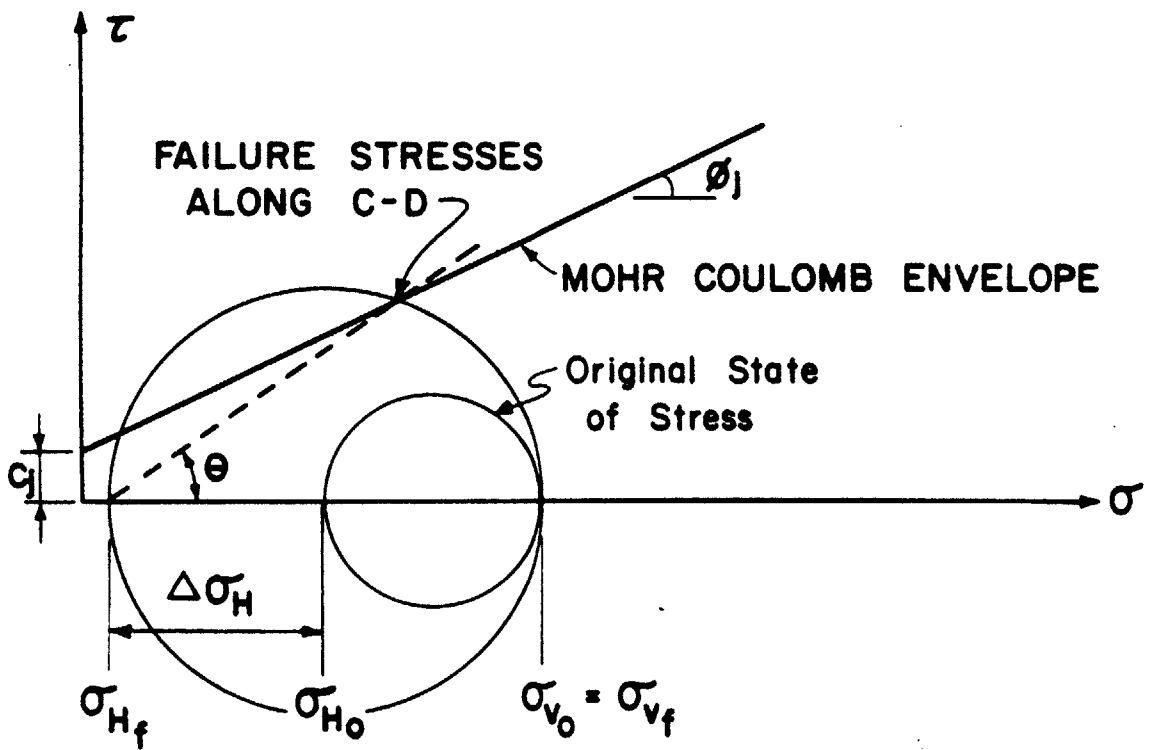
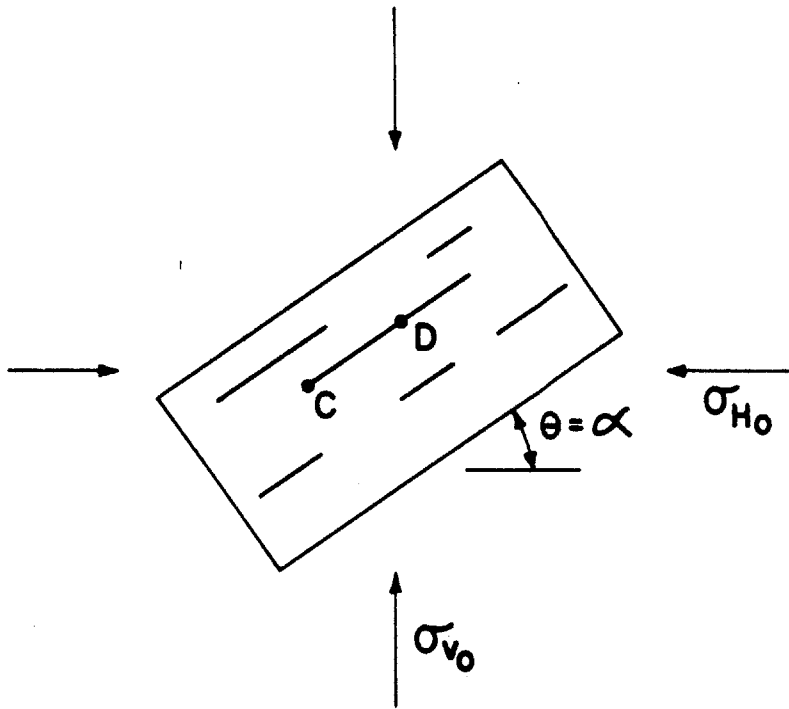


Figure G.9 Failure Conditions--Joint

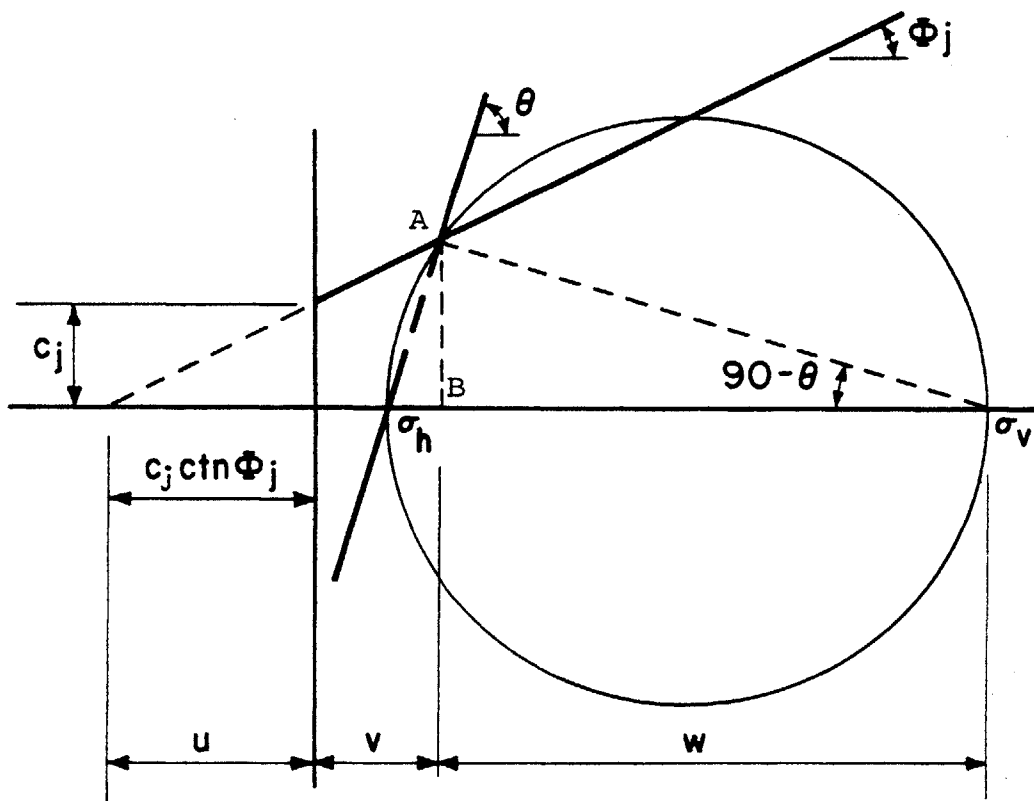


Figure G.10 Typical Failure Circle for Joint

$$A - B = (c_j \text{ ctn } \phi_j + \sigma_v - w) \tan \phi_j \quad (\text{G.46})$$

Combining Equations (G.45) and (G.46) and solving for
w:

$$w = \frac{(c_j \text{ ctn } \phi_j + \sigma_v) \tan \phi_j}{\tan (90 - \theta) + \tan \phi_j} \quad (\text{G.47})$$

$$\sigma_v - \sigma_h = \text{diameter} = \frac{w}{\cos^2 (90 - \theta)} \quad (\text{G.48})$$

Substituting w into Equation (G.48):

$$(\sigma_v - \sigma_h) \cos^2 (90 - \theta) = \frac{(c_j \text{ ctn } \phi_j + \sigma_v) \tan \phi_j}{\tan (90 - \theta) + \tan \phi_j} \quad (\text{G.49})$$

Rearranging terms:

$$\sigma_h = \sigma_v - \frac{(c_j \text{ ctn } \phi_j + \sigma_v) \tan \phi_j}{(\tan (90 - \theta) + \tan \phi_j) \cos^2 (90 - \theta)} \quad (\text{G.50})$$

Equation (G.50) is valid for all values of θ between
 0° and 90° .

Appendix H

Computer Program JOINTSIM

JOINTSIM (Joint Simulation) is designed to assess the strength of a jointed rock mass. The geometry of the jointing pattern is treated as a random variable. The results of the analysis are expressed in terms of the mean and standard deviation of an "apparent persistence" parameter. The program simulates a specified number of jointing patterns and calculates the minimum strength of each pattern. Jointing is modeled as a multi-dimensional Poisson process that can be characterized by three parameters: mean joint plane spacing, mean joint length, mean length of rock bridges. The dimensions and orientation of the block, the strength parameters of the joint and intact rock and the in situ stress field are deterministic inputs.

H.1 Coordinate System

JOINTSIM uses a coordinate system as shown in Figure H.1. The origin is located at the upper right corner of the block. α is the inclination angle of the joints.

H.2 Units

All units used in the input must be consistent. Units are generally in feet or pounds, but any other consistent system may be employed.

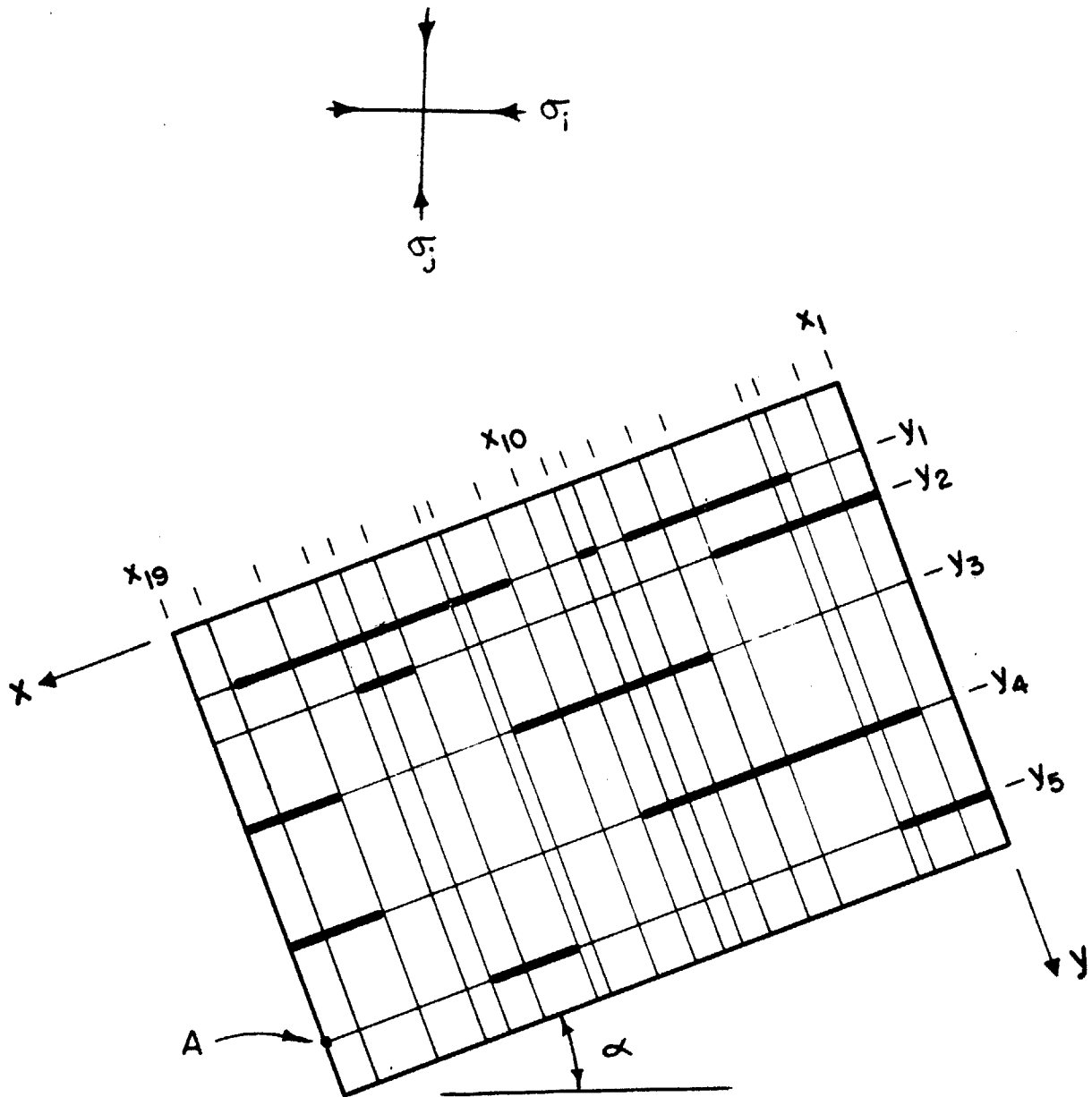


Figure H.1 Coordinate System for JOINTSIM

H.3 Inputs

Unless otherwise noted the inputs do not have to be right justified in their respective columns. The term "integer" implies the number is expressed without a decimal point.

Card #1:

Width of Block (XDIM) is entered in Columns 1 through 10 with a maximum of two decimal places.

Height of Block (YDIM) is entered in Columns 11 through 20 with a maximum of two decimal places.

Inclination of Block (ALPHA) is entered in Columns 21 through 30 with a maximum of two decimal places. The angle is expressed in degrees.

Card #2:

Joint Friction Angle (PHIJT) is entered in Columns 1 through 10 with a maximum of two decimal places. The angle is expressed in degrees.

Joint Cohesion (COJT) is entered in Columns 11 through 20 with a maximum of two decimal places.

Intact Rock Friction Angle (PHIRK) is entered in Columns 21 through 30 with a maximum of two decimal places. The angle is expressed in degrees.

Intact Rock Cohesion (CORK) is entered in Columns 31 through 40 with a maximum of two decimal places. In the 'Griffith-Modified Griffith' envelope used by the program the cohesion is twice the tensile strength of the rock.

Card #3:

Initial Vertical Stress (SIG1) is entered in Columns 1 through 10 with a maximum of 2 decimal places.

Initial Horizontal Stress (SIG3) is entered in Columns 11 through 20 with a maximum of 2 decimal places.

NOTE: The program assumes that the initial principal stresses are in the horizontal and vertical directions (see Figure H.1). The major principal stress can be in either direction.

Card #4:

Mean Joint Spacing (SP3) is entered in Columns 1 through 10 with a maximum of two decimal places.

Mean Joint Length (SPJTLN) is entered in Columns 11 through 20 with a maximum of two decimal places.

Mean Length of Rock Bridges (SPRKBR) is entered in Columns 21 through 30 with a maximum of two decimal places.

Card #5:

This card designates which technique or techniques should be used to evaluate the results. The user can select any one (or all) of three different methods.

Method #1 (Enter '-1' in Columns 9 and 10). The results are expressed in terms of the percent continuity (or persistence) required on a hypothetical joint if that joint were to have the same resistance as the weakest path

through the rock mass. The hypothetical joint is inclined at the same angle as the real joint planes.

Method #2: (Enter '0' in Column 10). This method also computes the persistence of a hypothetical joint with the same minimum resistance as the rock mass. However, the hypothetical joint is inclined at the same angle as the net failure path.

Method #3: (Enter '1' in Column 10). This method is based on the concept that the jointed rock mass can be treated as a homogenous medium whose strength parameters can be related to those of the intact rock through a reduction factor. This material has the same friction angle as the intact rock. Method #3 computes the ratio of cohesion of homogeneous material to cohesion of intact rock in order for the homogeneous material to have the same minimum resistance as the jointed rock mass.

NOTE: The program will compute the results according to all three methods if any positive integer greater than 1 is entered in Columns 1 through 10.

Card #6:

Seed Number (ISEED) for the routine to generate random numbers is entered in Columns 1 through 10. The number can be chosen arbitrarily but must be an integer less than 2147473647.

Card #7:

This card controls the amount of information given in the output. The user must enter 3 integers in Columns 1 through 10, 11 through 20 and 21 through 30 respectively. In deciding which options to use, the user should refer to the sample output included in this appendix.

Integer #1 (NOTPOP): If a 1 is entered in Column 10 the program will print the coordinates of the left and right ends of each joint segment and a sequential listing of the X coordinates. (See "Section A1" and Section A2" in the sample output.) None of this information will be printed if any other number or numbers are printed in Columns 1 through 10. (Blanks in Columns 1 through 10 will also suppress the information.)

Integer #2 (NOTPOT): If a 2 is entered in Column 20 the program will print the detailed strength data labeled "Section B1" , "Section B2" and "Section B3" in the sample output. "Section B1" lists the strengths for all points along the row $y = 1$ while "Section B3" details the location of the path with the minimum strength. "Section B2" is a summary of all possible failure paths that originate from the point at the lower left corner of the joint grid. (See Point A in Figure H.1). If a 1 is entered in Column 20 the program will print failure path summaries similar to

"Section B2" for all points in the joint grid. None of this information will be printed if any other number or numbers are printed in Columns 11 through 20. (Blanks in Columns 11 through 20 will also suppress the information.)

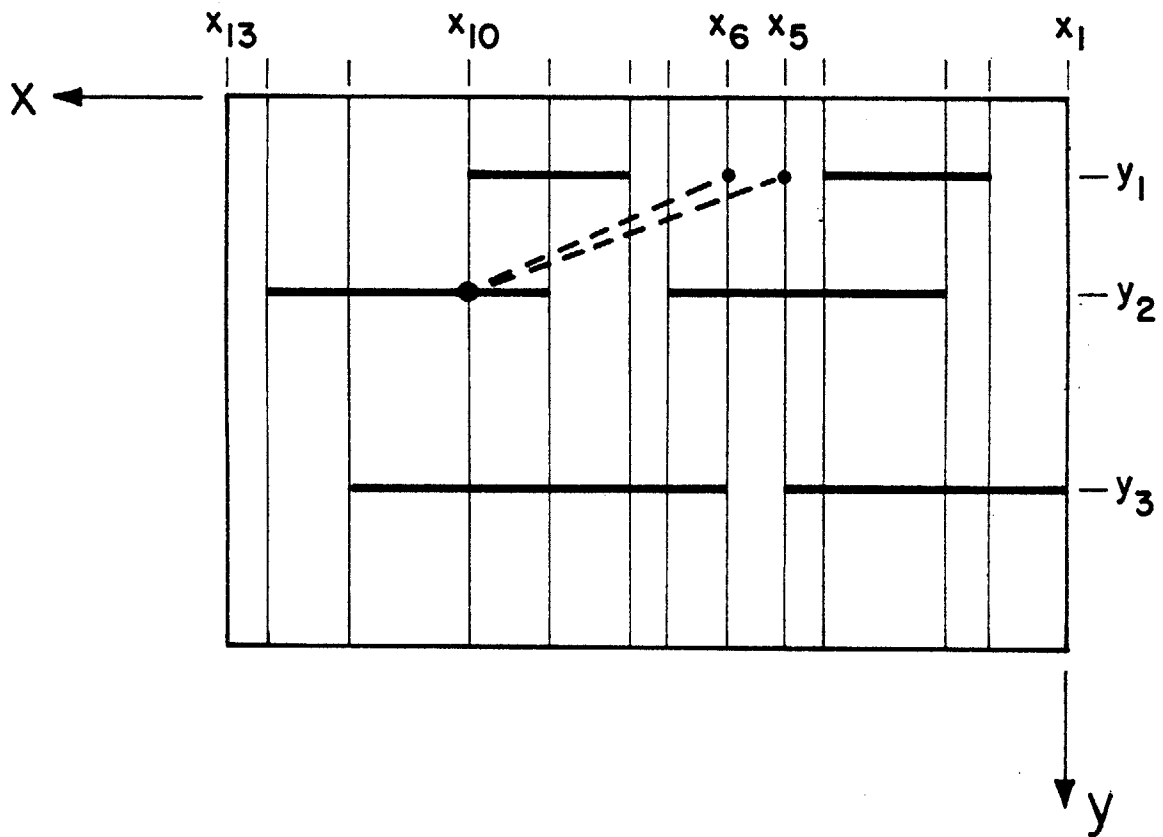
Integer #3 (NOTPOD): Serves as a safety mechanism to eliminate undesired output. The volume of output can be enormous if the number of realizations (see card #8) is large and Integers #1 and #2 are both 1. A 1 entered in Column 30 will print all information as prescribed by Integer #1 and Integer #2. None of the information will be printed if any other number or numbers is printed in Columns 21 through 30. (Blanks in Columns 21 through 30 will also suppress the information.)

Card #8:

Number of Realizations (NOREAL) may range from 1 to 400. This integer must be right justified in Columns 8, 9, and 10. A minimum of 200 realizations is usually required to get a good estimate of the mean and standard deviation of apparent persistence.

The next two parameters (DMIN and NJUMP) are used to reduce the number of failure paths the program must examine at each grid point.

Minimum Distance (DMIN) is entered in Columns 11 through 20 with a maximum of 2 decimal places. The program will not



(y_2, x_{10}) : Point Under Consideration
 Program will not examine path to
 (y_1, x_6) unless $x_6 - x_5 > \text{DMIN}$

Figure H.2 Definition of DMIN

examine a failure path whose transition point is within DMIN of the previous transition point (Figure H.2). If, however, the point happens to be the left or right end of a joint segment the program will check it anyway. If Columns 11 through 20 are left blank the program will default to DMIN = 0.00001 and check essentially every point.

Maximum Joint Plane Transition (NJUMP) is entered as an integer in Column 30. The program will not examine any failure paths that jump more than NJUMP planes in one transition. If Column 30 is left blank the program will check failure paths with transitions to all the eligible joint planes.

Sample Output

THE DIMENSIONS OF THE BLOCK ARE 10.00 HIGH BY 20.00 WIDE

THE INCLINATION OF THE JOINTS IS 40.0 DEGREES

STRENGTH PARAMETERS:

PHI (JOINT) = 30.00 DEGREES
COHESION (JOINT) = 5.00
PHI (ROCK) = 30.00 DEGREES
COHESION (ROCK) = 50.00

THE VERTICAL CONFINING STRESS IS 50.00
THE HORIZONTAL CONFINING STRESS IS 50.00

DISTRIBUTIONAL PARAMETERS FOR JOINTS:

MEAN SPACING BETWEEN PLANES = 2.00
MEAN SPACING BETWEEN JOINTS = 5.00
MEAN JOINT LENGTH = 2.50

THE INITIAL RANDOM NUMBER IS 124513

THE NUMBER OF REALIZATIONS IS 1

PATH CRITERIA:

MINIMUM SPACING = 2.00
MAXIMUM TRANSITION = 3

JOINT PLANE	Y COOR	NUMBER OF JOINTS	PERCENT CONTINUITY	RANDOM NUMBERS USED
1	1.06	3	3.4	8
2	6.38	3	42.3	8
3	7.31	4	58.0	10
4	8.66	3	22.5	8
Y COOR IS	1.055	X COOR OF RIGHT END IS	4.110	
		X COOR OF LEFT END IS	4.263	
Y COOR IS	1.055	X COOR OF RIGHT END IS	9.768	
		X COOR OF LEFT END IS	10.232	
Y COOR IS	1.055	X COOR OF RIGHT END IS	16.218	
		X COOR OF LEFT END IS	16.284	
Y COOR IS	6.377	X COOR OF RIGHT END IS	0.000	
		X COOR OF LEFT END IS	3.824	
Y COOR IS	6.377	X COOR OF RIGHT END IS	11.816	
		X COOR OF LEFT END IS	14.368	
Y COOR IS	6.377	X COOR OF RIGHT END IS	15.058	
		X COOR OF LEFT END IS	17.144	
Y COOR IS	7.314	X COOR OF RIGHT END IS	0.000	
		X COOR OF LEFT END IS	0.738	
Y COOR IS	7.314	X COOR OF RIGHT END IS	5.233	
		X COOR OF LEFT END IS	8.289	
Y COOR IS	7.314	X COOR OF RIGHT END IS	9.801	
		X COOR OF LEFT END IS	13.971	
Y COOR IS	7.314	X COOR OF RIGHT END IS	15.914	
		X COOR OF LEFT END IS	19.559	
Y COOR IS	8.658	X COOR OF RIGHT END IS	3.179	
		X COOR OF LEFT END IS	7.390	
Y COOR IS	8.658	X COOR OF RIGHT END IS	13.648	
		X COOR OF LEFT END IS	13.770	
Y COOR IS	8.658	X COOR OF RIGHT END IS	13.897	
		X COOR OF LEFT END IS	14.056	

*** THE NUMBER OF INDEPENDENT X COORDINATES IS 26 ***

Section A1

THE ORDERED X COORDINATES:

0.000
 0.738
 3.179
 3.824
 4.110
 4.263
 5.233
 7.390
 8.289
 9.768
 9.801
 10.232
 11.816
 13.648
 13.770
 13.897
 13.971
 14.056
 14.363
 15.058
 15.914
 16.218
 16.284
 17.144
 19.559
 20.000

438

THE MINIMUM TOTAL STENGTH FOR Y COOR =	1.055	AND X COOR =	0.000	IS	0.00
THE MINIMUM TOTAL STENGTH FOR Y COOR =	1.055	AND X COOR =	0.738	IS	48.70
THE MINIMUM TOTAL STENGTH FOR Y COOR =	1.055	AND X COOR =	3.179	IS	209.82
THE MINIMUM TOTAL STENGTH FOR Y COOR =	1.055	AND X COOR =	3.824	IS	252.36
THE MINIMUM TOTAL STENGTH FOR Y COOR =	1.055	AND X COOR =	4.110	IS	271.24
THE MINIMUM TOTAL STENGTH FOR Y COOR =	1.055	AND X COOR =	4.263	IS	276.42
THE MINIMUM TOTAL STENGTH FOR Y COOR =	1.055	AND X COOR =	5.233	IS	340.48
THE MINIMUM TOTAL STENGTH FOR Y COOR =	1.055	AND X COOR =	7.390	IS	482.84
THE MINIMUM TOTAL STENGTH FOR Y COOR =	1.055	AND X COOR =	8.289	IS	542.12
THE MINIMUM TOTAL STENGTH FOR Y COOR =	1.055	AND X COOR =	9.768	IS	639.75
THE MINIMUM TOTAL STENGTH FOR Y COOR =	1.055	AND X COOR =	9.801	IS	640.85
THE MINIMUM TOTAL STENGTH FOR Y COOR =	1.055	AND X COOR =	10.232	IS	655.48
THE MINIMUM TOTAL STENGTH FOR Y COOR =	1.055	AND X COOR =	11.816	IS	760.00

Section A2

Section B1

THE MINIMUM TOTAL STENGTH FOR Y COOR =	1.055	AND X COOR =	13.643 IS	880.90
THE MINIMUM TOTAL STENGTH FOR Y COOR =	1.055	AND X COOR =	13.770 IS	888.97
THE MINIMUM TOTAL STENGTH FOR Y COOR =	1.055	AND X COOR =	13.897 IS	897.36
THE MINIMUM TOTAL STENGTH FOR Y COOR =	1.055	AND X COOR =	13.971 IS	902.21
THE MINIMUM TOTAL STENGTH FOR Y COOR =	1.055	AND X COOR =	14.056 IS	907.84
THE MINIMUM TOTAL STENGTH FOR Y COOR =	1.055	AND X COOR =	14.368 IS	928.40
THE MINIMUM TOTAL STENGTH FOR Y COOR =	1.055	AND X COOR =	15.058 IS	973.94
THE MINIMUM TOTAL STENGTH FOR Y COOR =	1.055	AND X COOR =	15.914 IS	1030.48
THE MINIMUM TOTAL STENGTH FOR Y COOR =	1.055	AND X COOR =	16.218 IS	1050.51
THE MINIMUM TOTAL STENGTH FOR Y COOR =	1.055	AND X COOR =	16.284 IS	1052.74
THE MINIMUM TOTAL STENGTH FOR Y COOR =	1.055	AND X COOR =	17.144 IS	1109.52
THE MINIMUM TOTAL STENGTH FOR Y COOR =	1.055	AND X COOR =	19.559 IS	1268.89
THE MINIMUM TOTAL STENGTH FOR Y COOR =	1.055	AND X COOR =	20.000 IS	1298.00

POINT CONSIDERED:

JOINT PLANE = 4
 Y COORDINATE = 8.658
 X COORDINATE = 20.000

PATH NO.	-- JUNCTION POINT --		ANGLE TO JCT.	STRENGTH TO JT PT	STRENGTH TO EDGE	STRENGTH TOTAL	MINOR PRIN. STRESS	TANGENT TO	
	JT. PL.	Y COOR							X COOR
1	4	8.658	19.559	40.60	29.10	966.21	995.31	-24.54	PARABOLA
2	1	1.055	0.000	60.81	1436.22	0.00	1436.22	-25.00	POINT
3	1	1.055	3.179	64.32	1296.55	209.82	1508.37	-25.00	POINT
4	1	1.055	4.110	65.57	1250.26	271.24	1529.50	-25.00	POINT
5	1	1.055	4.263	65.78	1251.64	276.42	1528.05	-25.00	POINT
6	1	1.055	7.390	71.09	1115.20	482.84	1599.04	-25.00	POINT
7	1	1.055	9.768	76.61	1013.26	639.73	1653.00	-25.00	POINT
8	1	1.055	10.232	77.90	993.14	655.48	1648.62	-25.00	POINT
9	1	1.055	13.648	90.12	845.24	880.90	1726.14	-25.00	POINT
10	2	6.377	0.000	40.51	1340.18	0.00	1340.18	-24.88	PARABOLA
11	2	6.377	3.179	47.72	1132.10	107.67	1239.77	-24.91	PARABOLA
12	2	6.377	3.824	48.03	1090.07	129.50	1219.57	-24.92	PARABOLA
13	2	6.377	7.390	50.25	857.48	364.90	1222.38	-24.96	PARABOLA
14	2	6.377	9.768	52.57	702.99	521.80	1224.79	-24.99	PARABOLA
15	2	6.377	11.816	55.57	569.74	656.99	1226.73	-25.00	PARABOLA
16	2	6.377	13.897	60.49	435.31	727.48	1162.79	-25.00	POINT
17	2	6.377	14.368	62.05	414.95	743.40	1158.35	-25.00	POINT
18	2	6.377	15.058	64.77	385.07	788.95	1174.02	-25.00	POINT
19	2	6.377	17.144	78.61	294.73	859.61	1154.33	-25.00	POINT
20	3	7.314	0.000	43.84	1329.19	0.00	1329.19	-24.78	PARABOLA
21	3	7.314	0.738	43.99	1280.61	24.99	1305.60	-24.79	PARABOLA
22	3	7.314	3.179	44.57	1120.17	183.80	1303.97	-24.81	PARABOLA
23	3	7.314	5.233	45.20	985.14	260.81	1245.95	-24.84	PARABOLA
24	3	7.314	7.390	46.08	843.62	333.87	1177.48	-24.87	PARABOLA
25	3	7.314	8.289	46.55	784.84	364.28	1149.12	-24.88	PARABOLA
26	3	7.314	9.801	47.51	685.94	464.07	1150.01	-24.91	PARABOLA
27	3	7.314	11.816	49.33	554.31	532.33	1086.64	-24.95	PARABOLA
28	3	7.314	13.897	52.42	418.98	662.82	1021.80	-24.98	PARABOLA
29	3	7.314	13.971	52.57	414.22	605.31	1019.53	-24.99	PARABOLA
30	3	7.314	15.914	58.21	287.23	733.57	1020.81	-25.00	PARABOLA
31	3	7.314	19.559	111.83	119.89	857.01	976.90	-25.00	POINT

THE MINIMUM TOTAL STRENGTH FOR Y COOR = 8.658 AND X COOR = 20.000 IS 476.90

440

Section B2

THE MINIMUM STRENGTH IS: 886.11

THE NUMBER SHOULD BE BETWEEN:

946.99 (THE VALUE FOR A 58.0% CONTINUOUS JOINT)
 AND 677.35 (THE VALUE FOR A CONTINUOUS JOINT)

THE FAILURE PATH PROCEEDS FROM:

(LEFT END)	Y COOR =	7.314	X COOR =	20.000
	TO Y COOR =	7.314	X COOR =	13.559
	TO Y COOR =	7.314	X COOR =	17.144
	TO Y COOR =	7.314	X COOR =	16.284
	TO Y COOR =	7.314	X COOR =	16.213
	TO Y COOR =	7.314	X COOR =	15.914
	TO Y COOR =	7.314	X COOR =	15.058
	TO Y COOR =	7.314	X COOR =	14.368
	TO Y COOR =	7.314	X COOR =	14.056
	TO Y COOR =	7.314	X COOR =	13.971
	TO Y COOR =	7.314	X COOR =	13.897
	TO Y COOR =	7.314	X COOR =	13.770
	TO Y COOR =	7.314	X COOR =	13.648
	TO Y COOR =	7.314	X COOR =	11.816
	TO Y COOR =	7.314	X COOR =	10.232
	TO Y COOR =	7.314	X COOR =	9.801
	TO Y COOR =	7.314	X COOR =	9.768
	TO Y COOR =	7.314	X COOR =	8.289
	TO Y COOR =	7.314	X COOR =	7.390
	TO Y COOR =	7.314	X COOR =	5.233
	TO Y COOR =	6.377	X COOR =	3.824
	TO Y COOR =	6.377	X COOR =	3.179
	TO Y COOR =	6.377	X COOR =	0.738
	TO Y COOR =	6.377	X COOR =	0.000
(RIGHT END)	TO Y COOR =	6.377	X COOR =	0.000

THE AVERAGE INCLINATION OF THE FAILURE PATH IS 42.68 DEGREES

REALIZATION NUMBER	NO. OF JT PLS	PERSISTENCE		ANGLE OF FAIL. PATH	MINIMUM STRENGTH	REDUCTION OPTIONS			UPDATED MEAN VALUES			TRANSITIONS UNIT::TOTAL	
		MIN.	MAX.			(1)	(2)	(3)	(1)	(2)	(3)		
1	4	3.4	58.0	42.7	886.11	67.5	68.1	29.0	67.5	68.1	29.0	1	1

CODE FOR REDUCTION OPTIONS:

- (1) PERCENT CONTINUITY FOR A FAILURE SURFACE INCLINED AT THE SAME ANGLE AS THE JOINTS
- (2) PERCENT CONTINUITY FOR A FAILURE SURFACE INCLINED AT THE SAME ANGLE AS THE FAILURE PATH
- (3) PERCENT COHESION OF INTACT ROCK FOR A FAILURE SURFACE INCLINED AT THE SAME ANGLE AS THE FAILURE PATH

441

Section 83

JOINTSIM Listing

C		JOINTSIM	JTSM0001
C		THIS PROGRAM EVALUATES THE MINIMUM STRENGTH OF A RANDOMLY GENERATED	JTSM0002
C		JOINTING PATTERN AS DEFINED IN D. VENEZIANO'S MODEL	JTSM0003
C		PROGRAM LIMIT: 400 REALIZATIONS	JTSM0004
		DIMENSION R(400), IIR(400), REALBD(400), PSI(400), JJPL(400),	JTSM0005
	1	APPER1(400), APPER2(400), APPER3(400), PERMIN(400), PERMAX(400),	JTSM0006
	2	AP1MEN(400), AP2MEN(400), AP3MEN(400), STALSM(400), NTRANS(400),	JTSM0007
	3	NTRAN(400)	JTSM0008
C		PROGRAM LIMIT: 20 JOINT PLANES	JTSM0009
		DIMENSION YRAND(20), Y(20), NPT(20), IR(21)	JTSM0010
C		PROGRAM LIMIT: 50 X COORDINATES PER JOINT PLANE	JTSM0011
		DIMENSION CJOINT(20,50)	JTSM0012
C		PROGRAM LIMIT: (20 X 300) PATH GRID	JTSM0013
		DIMENSION AISM(20,300), TAUSM(20,300), MINPTH(20,300), XCOOR(300)	JTSM0014
		EQUIVALENCE (IIR(400), REALBD(400)), (XCOOR(300), IR(21))	JTSM0015
		LOGICAL FIN, FAM, FLIM, FLAM, FAD, FUD	JTSM0016
		READ (5, 1000) XDIM, YDIM, ALPHA	JTSM0017
		READ (5, 1001) PHIJT, COJT, PHIRK, CORK	JTSM0018
		READ (5, 1002) SIG1, SIG3	JTSM0019
		READ (5, 1000) SP3, SPJTLN, SPRKBR	JTSM0020
		READ (5, 1004) NREDOP	JTSM0021
		READ (5, 1004) ISEED	JTSM0022
		READ (5, 1006) NOTPOP, NOTPOT, NOTPOD	JTSM0023
		READ (5, 1007) NOREAL, DISTMN, NJUMP	JTSM0024
	1000	FORMAT (F10.2, F10.2, F10.2)	JTSM0025
	1001	FORMAT (F10.2, F10.2, F10.2, F10.2)	JTSM0026
	1002	FORMAT (F10.2, F10.2)	JTSM0027
	1004	FORMAT (I10)	JTSM0028
	1006	FORMAT (I10, I10, I10)	JTSM0029
	1007	FORMAT (I10, F10.2, I10)	JTSM0030
	1010	FORMAT ('1', 10X, 'THE DIMENSIONS OF THE BLOCK ARE ', F8.2,	JTSM0031
		1 ' HIGH BY ', F8.2, ' WIDE')	JTSM0032
	1011	FORMAT ('0', 10X, 'THE INCLINATION OF THE JOINTS IS ', F4.1,	JTSM0033
		1 ' DEGREES')	JTSM0034
	1012	FORMAT ('0', 10X, 'STRENGTH PARAMETERS: '//	JTSM0035
		1 T20, 'PHI (JOINT) = ', T50, F10.2, ' DEGREES'//	JTSM0036

443

2	T20,'COHESION (JOINT) = ',T50,F10.2,/'	JTSM0037
3	T20,'PHI (ROCK) = ',T50,F10.2,' DEGREES'/'	JTSM0038
4	T20,'COHESION (ROCK) = ',T50,F10.2)	JTSM0039
1013	FORMAT ('0',10X,'THE VERTICAL CONFINING STRESS IS ',T50,F10.2,/'	JTSM0040
1	11X,'THE HORIZONTAL CONFINING STRESS IS ',T50,F10.2)	JTSM0041
1014	FORMAT ('0',10X,'DISTRIBUTIONAL PARAMETERS FOR JOINTS:'//	JTSM0042
1	T20,'MEAN SPACING BETWEEN PLANES =',T50,F10.2,/'	JTSM0043
2	T20,'MEAN SPACING BETWEEN JOINTS = ',T50,F10.2,/'	JTSM0044
3	T20,'MEAN JOINT LENGTH = ',T50,F10.2)	JTSM0045
1015	FORMAT (//,10X,'PATH CRITERIA:'//	JTSM0046
1	T20,'MINIMUM SPACING =',T50,F10.2,/'	JTSM0047
2	T20,'MAXIMUM TRANSITION =',T50,I10)	JTSM0048
1016	FORMAT (//,10X,'THE NUMBER OF REALIZATIONS IS ',T50,I10)	JTSM0049
1017	FORMAT (//,10X,'THE INITIAL RANDOM NUMBER IS ',T50,I10)	JTSM0050
1018	FORMAT ('1',T10,'JOINT',14X,'Y',12X,'NUMBER OF',10X,' PERCENT ',	JTSM0051
1	10X,'RANDOM NUMBERS'/'	JTSM0052
2	T10,'PLANE',13X,'COOR',11X,'JOINTS',12X,'CONTINUITY',14X,'USED')	JTSM0053
1020	FORMAT ('0',T10,I3,14X,F6.2,11X,I3,17X,F4.1,17X,I3)	JTSM0054
1021	FORMAT (T10,'REALIZATION NO. ',I4,': NOT ENOUGH RANDOM NUMBERS',	JTSM0055
1	' AVAILABLE TO DEFINE ALL THE JOINT SEGMENTS ON A PLANE')	JTSM0056
1022	FORMAT (T10,'REALIZATION NO. ',I4,': NOT ENOUGH RANDOM NUMBERS',	JTSM0057
1	' AVAILABLE TO DEFINE ALL THE JOINT PLANES')	JTSM0058
1024	FORMAT (T10,'REALIZATION NO. ',I4,': NO JOINT PLANES WITHIN THE ',	JTSM0059
1	'BLOCK')	JTSM0060
1025	FORMAT (T10,'REALIZATION NO. ',I4,': REDUCTION OPTION NO. 2 ',	JTSM0061
1	'REQUIRES THE TENSILE STRENGTH OF THE JOINT - NOT COMPUTED')	JTSM0062
1050	FORMAT ('0','Y COOR IS ',F10.3,' X COOR OF RIGHT END IS ',	JTSM0063
1	F10.3)	JTSM0064
1060	FORMAT (T27,'X COOR OF LEFT END IS ',F10.3)	JTSM0065
1061	FORMAT ('0','Y COOR IS ',F10.3,5X,'*** NO JOINTS IN THIS ',	JTSM0066
1	'PLANE ***')	JTSM0067
1070	FORMAT (///,27X,'*** THE NUMBER OF INDEPENDENT X COORDINATES',	JTSM0068
1	' IS ',I4,' ***',///,44X,'THE ORDERED X COORDINATES:'//)	JTSM0069
1072	FORMAT (T50,F10.3)	JTSM0070
1080	FORMAT (///,'FAILURE ALONG JOINT REQUIRES TENSILE STRENGTH OF',	JTSM0071
1	' JOINT - UNDEFINED CONDITION - RUN TERMINATED')	JTSM0072

444

```

1090 FORMAT ('1',10X,'POINT CONSIDERED:',//,T20,'JOINT PLANE = ',12X,
1 I5,/,T20,'Y COORDINATE = ', 9X,F10.3,/,T20,'X COORDINATE = ',9X,
2 F10.3,///,' PATH NO.',8X,'-- JUNCTION POINT --',7X,'ANGLE ',
3 4X,'STRENGTH',4X,'STRENGTH',4X,'STRENGTH',06X,'MINOR PRIN.',4X,
4 'TANGENT TO',/,14X,'JT. PL.',3X,'Y COOR',4X,'X COOR',3X,
5 'TO JCT.',4X,'TO JT PT',4X,'TO EDGE',6X,'TOTAL',10X,'STRESS',/)
1092 FORMAT (I5,7X,I5,2X,F10.3,F10.3,5X,F6.2,4X,F8.2,4X,F8.2,4X,F8.2,
1 7X,F7.2)
1093 FORMAT ('+',T110,'POINT')
1094 FORMAT ('+',T109,'PARABOLA')
1095 FORMAT ('+',T111,'LINE')
1096 FORMAT ('+',T109,'* JOINT *')
1097 FORMAT ('+',T111,'CUSP')
1098 FORMAT ('0','THE MINIMUM TOTAL STENGTH FOR Y COOR = ',
1 F10.3,' AND X COOR = ',F10.3,' IS ',F10.2)
1100 FORMAT ('1','THE MINIMUM STRENGTH IS: ',F10.2,///,'THE NUMBER ',
1 'SHOULD BE BETWEEN:',//,T20,F10.2,' (THE VALUE FOR A ',F4.1,
2 '% CONTINUOUS JOINT)',//,T16,'AND ',F10.2,
3 ' (THE VALUE FOR A CONTINUOUS JOINT) ')
1101 FORMAT ('0','THE FAILURE PATH PROCEEDS FROM:',//
1 T10,' (LEFT END)',T31,'Y COOR = ',F10.3,T61,'X COOR = ',F10.3)
1102 FORMAT (T25,'TO',T31,'Y COOR = ',F10.3,T61,'X COOR = ',F10.3)
1103 FORMAT ('+',T10,' (RIGHT END) ')
1104 FORMAT ('0','THE AVERAGE INCLINATION OF THE FAILURE PATH IS ',
1 F6.2,' DEGREES',//)
1110 FORMAT (///,' REALIZATION NO. OF PERSISTENCE ANGLE OF ',
1 ' MINIMUM REDUCTION OPTIONS UPDATED MEAN VALUES',
2 ' TRANSITIONS' /
3 ' NUMBER JT PLS MIN. MAX. FAIL. PATH ',
4 'STRENGTH (1) (2) (3) (1) (2) (3) ',
5 ' UNIT::TOTAL',//)
1111 FORMAT (3X,I4,10X,I2,6X,F5.1,2X,F5.1,6X,F4.1,7X,F7.2,3X,F5.1,2X,
1 F5.1,2X,F5.1,4X,F5.1,1X,F5.1,1X,F5.1,7X,I2,2X,I2)
1112 FORMAT (3X,I4,T30,'***** SEE BELOW *****')
1113 FORMAT (///,T40,'CODE FOR REDUCTION OPTIONS:',//,T10,
1 '(1) PERCENT CONTINUITY FOR A FAILURE SURFACE INCLINED AT',

```

```

JTSM0073
JTSM0074
JTSM0075
JTSM0076
JTSM0077
JTSM0078
JTSM0079
JTSM0080
JTSM0081
JTSM0082
JTSM0083
JTSM0084
JTSM0085
JTSM0086
JTSM0087
JTSM0088
JTSM0089
JTSM0090
JTSM0091
JTSM0092
JTSM0093
JTSM0094
JTSM0095
JTSM0096
JTSM0097
JTSM0098
JTSM0099
JTSM0100
JTSM0101
JTSM0102
JTSM0103
JTSM0104
JTSM0105
JTSM0106
JTSM0107
JTSM0108

```

2	' THE SAME ANGLE AS THE JOINTS',/,T10,' (2) PERCENT CONTINUITY',	JTSM0109
3	' FOR A FAILURE SURFACE INCLINED AT THE SAME ANGLE AS THE ',	JTSM0110
4	' FAILURE PATH',/,T10,' (3) PERCENT COHESION OF INTACT ROCK FOR',	JTSM0111
5	' A FAILURE SURFACE INCLINED AT THE SAME ANGLE AS THE FAILURE',	JTSM0112
6	' PATH',////////)	JTSM0113
1122	FORMAT (///,45X,'***** INCLINATION OF FAILURE PATH *****',///	JTSM0114
1	52X,'NO. OF REALIZATIONS: ',I4,//	JTSM0115
2	52X,'MEAN VALUE:',13X,F4.1,/,52X,'MINIMUM VALUE:',10X,F4.1,/,	JTSM0116
3	52X,'MAXIMUM VALUE:',10X,F4.1,/,52X,'STANDARD DEVIATION:',5X,	JTSM0117
4	F4.1,//////////)	JTSM0118
1123	FORMAT ('0',45X,'***** MAXIMUM PERSISTENCE *****',///	JTSM0119
1	52X,'NO. OF REALIZATIONS: ',I4,//	JTSM0120
2	52X,'MEAN VALUE:',13X,F4.1,/,52X,'MINIMUM VALUE:',10X,F4.1,/,	JTSM0121
3	52X,'MAXIMUM VALUE:',10X,F4.1,/,52X,'STANDARD DEVIATION:',5X,	JTSM0122
4	F4.1)	JTSM0123
1124	FORMAT (///,45X,'***** REDUCTION OPTION NUMBER ',I2,' *****',	JTSM0124
1	///,52X,'NUMBER OF REALIZATIONS: ',I4,//	JTSM0125
2	52X,'MEAN VALUE:',13X,F4.1,/,52X,'MINIMUM VALUE:',10X,F4.1,/,	JTSM0126
3	52X,'MAXIMUM VALUE:',10X,F4.1,/,52X,'STANDARD DEVIATION:',5X,	JTSM0127
4	F4.1,/,52X,'COEFF. OF CORRELATION',/,52X,	JTSM0128
5	'WITH INCLINATION ANGLE: ',F6.3)	JTSM0129
	PI = 3.14159265	JTSM0130
	PI4 = PI/4.0	JTSM0131
	PI2 = PI/2.0	JTSM0132
	ALPHO = ALPHA*PI/180.	JTSM0133
	PHOJT = PHIJT*PI/180.	JTSM0134
	TANJT = TAN(PHIJT*PI/180.)	JTSM0135
	PHORK = PHIRK*PI/180.	JTSM0136
	SINRK = SIN(PHORK)	JTSM0137
	COSRK = COS(PHORK)	JTSM0138
	TANRK = TAN(PHORK)	JTSM0139
	P = SPJTLN/(SPJTLN + SPRKBR)	JTSM0140
	CORK2K = COEK/2000.	JTSM0141
	IF (NJUMP .EQ. 0) NJUMP = 1000	JTSM0142
	IF (DISTMN .EQ. 0.0) DISTMN = 0.00001	JTSM0143
C	ETA AND XCTETA DEFINE THE CIRCLE WITH DUAL TANGENCY	JTSM0144

446

XCTETA = CORK*((1.0-SINRK*COSRK) - (1.0-(2.0*COSRK*SINRK))**0.5)	JTSM0145
1 /SINRK**2.0	JTSM0146
IF (PHIRK .GT. 45.0) ETA = PI4	JTSM0147
IF (PHIRK .GT. 45.0) ETASIN = SIN(PI4)	JTSM0148
IF (PHIRK .LE. 45.0) ETASIN = (CORK/(2.0*XCTETA))**0.5	JTSM0149
IF (PHIRK .LE. 45.0) ETA = ATAN(ETASIN/((1.0 - ETASIN**2.0)	JTSM0150
1 **0.5))	JTSM0151
AFACT = 0.5*CORK/ETASIN**2	JTSM0152
BFACT = CORK/ETASIN	JTSM0153
XCTPTF = CORK/2.0	JTSM0154
IF (COJT .EQ. 0.0) THETAJ = PI2	JTSM0155
IF (COJT .NE. 0.0) THETAJ = ATAN(SIG1/COJT)	JTSM0156
IF (ALPHO .GT. THETAJ) WRITE (6, 1080)	JTSM0157
IF (ALPHO .GT. THETAJ) GO TO 2000	JTSM0158
WRITE (6, 1010) YDIM, XDIM	JTSM0159
WRITE (6, 1011) ALPHA	JTSM0160
WRITE (6, 1012) PHIJT, COJT, PHIRK, CORK	JTSM0161
WRITE (6, 1013) SIG1, SIG3	JTSM0162
WRITE (6, 1014) SP3, SPRKBR, SPJTLN	JTSM0163
WRITE (6, 1017) ISEED	JTSM0164
WRITE (6, 1016) NOREAL	JTSM0165
WRITE (6,1015) DISTMN, NJUMP	JTSM0166
FLAM = .TRUE.	JTSM0167
IF (NOTPOD .EQ. 1) FLAM = .FALSE.	JTSM0168
CALL GGUB(ISEED,NOREAL,R)	JTSM0169
DO 17 I = 1, NOREAL	JTSM0170
17 IIR(I) = R(I)*10**8.0	JTSM0171
TAN90 = 5.0	JTSM0172
NREAL = 0	JTSM0173
NBUM = 0	JTSM0174
NNBUM = 0	JTSM0175
SUMAP1 = 0.0	JTSM0176
SUMAP2 = 0.0	JTSM0177
SUMAP3 = 0.0	JTSM0178
PSISUM = 0.0	JTSM0179
CONSUM = 0.0	JTSM0180

AP1MAX = 0.0	JTSM0181
AP2MAX = 0.0	JTSM0182
AP3MAX = 0.0	JTSM0183
PSIMAX = 0.0	JTSM0184
CONMAX = 0.0	JTSM0185
AP1MIN = 100.0	JTSM0186
AP2MIN = 100.0	JTSM0187
AP3MIN = 100.0	JTSM0188
PSIMIN = 180.	JTSM0189
CONMIN = 100.0	JTSM0190
DO 1950 MM = 1, NOREAL	JTSM0191
YSUM = 0.0	JTSM0192
PERCMN = 100.0	JTSM0193
PERCMX = 0.0	JTSM0194
NREAL = NREAL + 1	JTSM0195
ISEED = IIR (MM)	JTSM0196
CALL GGUB (ISEED, 21, R)	JTSM0197
DO 20 I = 1, 21	JTSM0198
20 IR(I) = R(I)*10**8.0	JTSM0199
ISEED = IR(21)	JTSM0200
CALL GGUB (ISEED, 20, R)	JTSM0201
DO 30 I = 1, 20	JTSM0202
30 YRAND (I) = R (I)	JTSM0203
IF (.NOT. FLAM) WRITE (6, 1018)	JTSM0204
31 DO 200 I = 1, 20	JTSM0205
YSUM = YSUM + (SP3)*ALOG (1.0/(1.0-YRAND (I)))	JTSM0206
Y(I) = YSUM	JTSM0207
IF (Y(I) .GT. YDIM) GO TO 250	JTSM0208
ISEED = IR (I)	JTSM0209
CALL GGUB (ISEED, 51, R)	JTSM0210
IF (R(51) .LT. P) CJOINT (I, 1) = 0.0	JTSM0211
IF (R(51) .GE. P) CJOINT (I, 1) = SPRKBR*ALOG (1.0/R (1))	JTSM0212
IF (CJOINT (I, 1) .GE. XDIM) CJOINT (I, 1) = XDIM	JTSM0213
C FOR ODD N: CJOINT (I, N) IS THE RIGHT END OF THE (N+1)/2 JOINT	JTSM0214
C IN THE I TH JOINT PLANE	JTSM0215
C FOR EVEN N: CJOINT (I, N) IS THE LEFT END OF THE N/2 JOINT	JTSM0216

448

C	<pre> IN THE I TH JOINT PLANE DO 80 J = 2, 50, 2 CJOINT(I,J) = CJOINT(I,J-1) + SPJTLN*ALOG(1.0/R(J)) IF (CJOINT(I,J) .GE. XDIM) GO TO 90 CJOINT(I,J+1) = CJOINT(I,J) + SPRKBR*ALOG(1.0/R(J+1)) IF (CJOINT(I,J+1) .GE. XDIM) GO TO 120 80 CONTINUE REALBD(MM) = 1.0 GO TO 1948 90 CJOINT(I,J) = XDIM NPT(I) = J NJOINT = J/2.0 NRN = J + 1 GO TO 150 120 CJOINT(I,J+1) = XDIM NPT(I) = J + 1 NJOINT = J/2.0 NRN = J + 2 150 CONTINUE SUMJTL = 0.0 DO 160 J = 1, NJOINT NNJT = 2*J 160 SUMJTL = SUMJTL + CJOINT(I,NNJT) - CJOINT(I,NNJT - 1) PERCON = SUMJTL*100.0/XDIM IF (PERCON .GE. PERCMX) PERCMX = PERCON IF (PERCON .LE. PERCMN) PERCMN = PERCON 190 IF (FLAM) GO TO 200 IF (CJOINT(I,1) .EQ. XDIM) NJOINT = 0 WRITE (6, 1020) I, Y(I), NJOINT, PERCON, NRN 200 CONTINUE REALBD(MM) = 2.0 GO TO 1948 250 JJPL(MM) = I - 1 IF (JJPL(MM) .EQ. 0) REALBD(MM) = 4.0 IF (JJPL(MM) .EQ. 0) GO TO 1948 JPL = JJPL(MM) </pre>	<pre> JTSM0217 JTSM0218 JTSM0219 JTSM0220 JTSM0221 JTSM0222 JTSM0223 JTSM0224 JTSM0225 JTSM0226 JTSM0227 JTSM0228 JTSM0229 JTSM0230 JTSM0231 JTSM0232 JTSM0233 JTSM0234 JTSM0235 JTSM0236 JTSM0237 JTSM0238 JTSM0239 JTSM0240 JTSM0241 JTSM0242 JTSM0243 JTSM0244 JTSM0245 JTSM0246 JTSM0247 JTSM0248 JTSM0249 JTSM0250 JTSM0251 JTSM0252 </pre>
---	--	--

449

255	IF (FLAM) GO TO 310	JTSM0253
	IF (NOTPOP .NE. 1) GO TO 310	JTSM0254
	DO 300 I = 1, JPL	JTSM0255
	NOPT = NPT(I)	JTSM0256
	DO 280 J =1, NOPT	JTSM0257
	IF ((-1.0)**J) 260, 260, 270	JTSM0258
260	IF (CJCINT(I,1) .EQ. XDIM) WRITE (6, 1061) Y(I)	JTSM0259
	IF (CJOINT(I,J) .EQ. XDIM) GO TO 280	JTSM0260
	IF (CJOINT(I,1) .NE. XDIM) WRITE (6, 1050) Y(I), CJOINT(I,J)	JTSM0261
	GO TO 280	JTSM0262
270	IF (CJOINT(I,1) .NE. XDIM) WRITE (6, 1060) CJOINT(I,J)	JTSM0263
280	CONTINUE	JTSM0264
300	CONTINUE	JTSM0265
C	THE FOLLOWING ROUTINE ARRANGES THE X COORDINATES IS ASCENDING' ORDER	JTSM0266
310	NXCORS = 0	JTSM0267
	DO 345 I = 1, JPL	JTSM0268
	NPTI = NPT(I) - 1	JTSM0269
	DO 345 J = 1, NPTI	JTSM0270
	IF (CJOINT(I,J) .EQ. 0.0 .OR. CJOINT(I,J) .EQ. XDIM) GO TO 345	JTSM0271
	NXCORS = NXCORS + 1	JTSM0272
	XCOOR(NXCORS) = CJOINT(I,J)	JTSM0273
345	CONTINUE	JTSM0274
	NXCORS = NXCORS + 1	JTSM0275
	XCOOR(NXCORS) = XDIM	JTSM0276
	NN = NXCORS - 1	JTSM0277
	DO 390 J = 1, NN	JTSM0278
	M = NXCORS - J	JTSM0279
	FIN = .TRUE.	JTSM0280
	DO 380 I = 1, M	JTSM0281
	IF (XCOOR(I) .LE. XCOOR(I+1)) GO TO 380	JTSM0282
	FIN = .FALSE.	JTSM0283
	XX = XCOOR(I+1)	JTSM0284
	XCOOR(I+1) = XCOOR(I)	JTSM0285
	XCOOR(I) = XX	JTSM0286
380	CONTINUE	JTSM0287
	IF (FIN) GO TO 400	JTSM0288

```

390 CONTINUE
400 DO 410 I = 1, NXCORS
    L = NXCORS + 1 - I
410 XCOORD(L+1) = XCOORD(L)
    XCOORD(1) = 0.0
    NXCORS = NXCORS + 1
    PERMIN(MM) = PERCMN
    PERMAX(MM) = PERCMX
    IF ( PERCMX .LE. CONMIN ) CONMIN = PERCMX
    IF ( PERCMX .GE. CONMAX ) CONMAX = PERCMX
    IF (FLAM) GO TO 431
    WRITE (6, 1070) NXCORS
    DO 427 I = 1, NXCORS
427 WRITE (6, 1072) XCOORD(I)
C     THE FOLLOWING ROUTINE COMPUTES THE VALUES OF AISM(I,J) - THE
C     MINIMUM APPARENT INCREMENTAL SAFETY MARGIN REQUIRED TO INITIATE
C     A FAILURE CRACK FROM THE ITH JOINT PLANE AT THE JTH X COORDINATE.
431 DO 450 I = 1, JPL
    TAUSM(I,1) = 0.0
450 AISM(I,1) = 0.0
C     THIS PART COMPUTES THE AISM FOR A UNIT LENGTH OF
C     JOINT (AISMJT) AND INTACT ROCK (AISMRK).
    IF ( NREAL .GT. 1 .AND. PSISUM .NE. 0.0 ) GO TO 499
457 SINALP = SIN(ALPHO)
    COSALP = COS(ALPHO)
    DENOMJ = SINALP*COSALP + (SINALP**2)*TANJT
    SIG3FJ = SIG1*(1.0 - TANJT/DENOMJ) - COJT/DENOMJ
    DLTNJT = (SIG3 - SIG3FJ)*SINALP*COSALP
    DLNOJT = (SIG3 - SIG3FJ)*SINALP**2
    AISMJT = DLNOJT*TANJT + DLTNJT
    CALL ROCK(CORK,PHORK,SINRK,COSRK,TANRK,SIG1,SIG3,PI4,PI2,
1CORK2K,ALPHO,AFACT,BFACT,ETA,XCTPTF,DELTA3,TAUFR,TANIDY,PRIM3R)
    F3FR = DELTA3*SINALP + TAUFR*COSALP
    F1FR = TAUFR*SINALP
    DLNORK = F3FR*SINALP + F1FR*COSALP
    DLTNRK = F3FR*COSALP - F1FR*SINALP

```

```

JTSM0289
JTSM0290
JTSM0291
JTSM0292
JTSM0293
JTSM0294
JTSM0295
JTSM0296
JTSM0297
JTSM0298
JTSM0299
JTSM0300
JTSM0301
JTSM0302
JTSM0303
JTSM0304
JTSM0305
JTSM0306
JTSM0307
JTSM0308
JTSM0309
JTSM0310
JTSM0311
JTSM0312
JTSM0313
JTSM0314
JTSM0315
JTSM0316
JTSM0317
JTSM0318
JTSM0319
JTSM0320
JTSM0321
JTSM0322
JTSM0323
JTSM0324

```

	AISMRK = DLNORK*TANJT + DLTNRK	JTSM0325
C	THIS PART COMPUTES THE VALUES OF AISM(1,J)	JTSM0326
	499 STR = 0.0	JTSM0327
	TAU = 0.0	JTSM0328
	NPT1 = NPT(1)	JTSM0329
	INDX = 1	JTSM0330
	DO 570 I = 2, NXCORS	JTSM0331
	IF (XCOOR(I) .GT. CJOINT(1,1)) GO TO 510	JTSM0332
	STR = STR + AISMRK*(XCOOR(I) - XCOOR(I-1))	JTSM0333
	TAU = TAU + DLTNRK*(XCOOR(I) - XCOOR(I-1))	JTSM0334
	AISM(1,I) = STR	JTSM0335
	TAUSM(1,I) = TAU	JTSM0336
	GO TO 570	JTSM0337
	510 CONTINUE	JTSM0338
	NPT0 = INDX	JTSM0339
	DO 560 J = NPT0, NPT1	JTSM0340
	IF (XCOOR(I) .GT. CJOINT(1,J)) GO TO 560	JTSM0341
	IF ((-1.0)**J) 520, 520, 530	JTSM0342
452	520 STR = STR + AISMRK*(XCOOR(I) - XCOOR(I-1))	JTSM0343
	TAU = TAU + DLTNRK*(XCOOR(I) - XCOOR(I-1))	JTSM0344
	GO TO 550	JTSM0345
	530 STR = STR + AISMJT*(XCOOR(I) - XCOOR(I-1))	JTSM0346
	TAU = TAU + DLTNJT*(XCOOR(I) - XCOOR(I-1))	JTSM0347
	550 AISM(1,I) = STR	JTSM0348
	TAUSM(1,I) = TAU	JTSM0349
	INDX = J	JTSM0350
	GO TO 570	JTSM0351
	560 CONTINUE	JTSM0352
	570 CONTINUE	JTSM0353
	STRXXX = AISM(1,NXCORS)	JTSM0354
	INDY = 1	JTSM0355
	IF (FLAM) GO TO 590	JTSM0356
	IF (NOTPOT .NE. 1 .AND. NOTPOT .NE. 2) GO TO 590	JTSM0357
	DO 580 J = 1, NXCOES	JTSM0358
	580 WRITE (6, 1098) Y(1), XCOOR(J), AISM(1,J)	JTSM0359
	590 IF (JPL .EQ. 1) GO TO 703	JTSM0360

C	THIS PART COMPLETES THE AISM(I,J) MATRIX. EACH POINT (I,J)	JTSM0361
C	HAS N FAILURE PATHS - EACH PATH HAS AN APPARENT INCREMENTAL	JTSM0362
C	SAFETY MARGIN, STRCSE, ASSOCIATED WITH IT. AISM(I,J) IS	JTSM0363
C	THE MINIMUM OF ALL THE STRCSE VALUES	JTSM0364
	NTRAN (MM) = 0	JTSM0365
	DO 700 J = 2, JPL	JTSM0366
	IF (CJOINT(J,1) .EQ. XDIM) GO TO 700	JTSM0367
	DO 680 I = 2, NXCORS	JTSM0368
	FLIM = .TRUE.	JTSM0369
	IF (NOTPOT .EQ. 1) FLIM = .FALSE.	JTSM0370
	IF (NOTPOT .EQ. 2 .AND. J .EQ. JPL .AND. I .EQ. NXCORS)	JTSM0371
	1 FLIM = .FALSE.	JTSM0372
	IF (.NOT.FLIM .AND. .NOT.FLAM) WRITE (6,1090) J, Y(J), XCOOR(I)	JTSM0373
C	THE FIRST PATH TO CONSIDER IS THE ONE THAT PROCEEDS FROM	JTSM0374
C	(J,I) TO (J,I-1) -- IT IS OFTEN THE CRITICAL PATH --	JTSM0375
C	IT IS ALSO THE ONLY PATH THAT NEED BE EVALUATED	JTSM0376
C	IN THE JTH ROW	JTSM0377
	NCASE = 1	JTSM0378
	IF (XCOOR(I) .GT. CJOINT(J,1)) GO TO 593	JTSM0379
	PRIMIN = PRIM3R	JTSM0380
	STR = AISMRK*(XCOOR(I) - XCOOR(I-1))	JTSM0381
	STRLOW = STR + AISM(J,I-1)	JTSM0382
	TAUCSE = TAUSM(J,I-1) + DLTNRK*(XCOOR(I) - XCOOR(I-1))	JTSM0383
	ITHCSE = J*NXCORS + I - 1	JTSM0384
	GO TO 603	JTSM0385
593	NPTI = NPT(J)	JTSM0386
	DO 602 K = 1, NPTI	JTSM0387
	IF (XCOOR(I) .GT. CJOINT(J,K)) GO TO 602	JTSM0388
	IF ((-1.0)**K) 600, 600, 598	JTSM0389
598	STR = AISMJT*(XCOOR(I) - XCOOR(I-1))	JTSM0390
	PRIMIN = SIG3FJ	JTSM0391
	GO TO 601	JTSM0392
600	STR = AISMRK*(XCOOR(I) - XCOOR(I-1))	JTSM0393
	PRIMIN = PRIM3R	JTSM0394
601	STRLOW = STR + AISM(J,I-1)	JTSM0395
	IF (PRIMIN .EQ. SIG3FJ)	JTSM0396

453

	1 TAUCSE = TAUSM(J,I-1) + DLTNJT*(XCOOR(I) - XCOOR(I-1))	JTSM0397
	IF (PRIMIN .EQ. PRIM3R)	JTSM0398
	1 TAUCSE = TAUSM(J,I-1) + DLTNRK*(XCOOR(I) - XCOOR(I-1))	JTSM0399
	ITHCSE = J*NXCORS + I - 1	JTSM0400
	GO TO 603	JTSM0401
602	CONTINUE	JTSM0402
603	IF (FLIM .OR. FLAM) GO TO 604	JTSM0403
	WRITE (6, 1092) NCASE, J, Y(J), XCOOR(I-1), ALPHA, STR,	JTSM0404
	1 AISM(J,I-1), STRLOW, PRIMIN	JTSM0405
	IF (PRIMIN .EQ. SIG3FJ) WRITE (6,1096)	JTSM0406
	IF (PRIMIN .NE. SIG3FJ .AND. TANIDY .EQ. -1.0) WRITE (6,1093)	JTSM0407
	IF (PRIMIN .NE. SIG3FJ .AND. TANIDY .EQ. 0.0) WRITE (6,1094)	JTSM0408
	IF (PRIMIN .NE. SIG3FJ .AND. TANIDY .EQ. 1.0) WRITE (6,1095)	JTSM0409
	IF (PRIMIN .NE. SIG3FJ .AND. TANIDY .EQ. 2.0) WRITE (6,1097)	JTSM0410
604	J1 = J - 1	JTSM0411
	I1 = I	JTSM0412
	IF (I .EQ. NXCORS) I1 = I - 1	JTSM0413
	DO 635 N = 1, J1	JTSM0414
	IF (J - N .GT. NJUMP) GO TO 635	JTSM0415
	IF (CJOINT(N,1) .EQ. XDIM) GO TO 635	JTSM0416
	INDEX = 1	JTSM0417
	DO 634 M = 1, I1	JTSM0418
	IF (M .EQ. I .AND. N .NE. J1) GO TO 635	JTSM0419
	IF (STRLOW .LT. AISM(N,M)) GO TO 634	JTSM0420
	IF (M .EQ. I1 .AND. N .EQ. J1) GO TO 608	JTSM0421
	NPT0 = INDEX	JTSM0422
	NPTN = NPT(N)	JTSM0423
	IF (M .EQ. 1) GO TO 608	JTSM0424
	DO 605 K = NPT0, NPTN	JTSM0425
	IF (CJOINT(N,K) .EQ. XCOOR(M)) INDEX = K	JTSM0426
	IF (CJOINT(N,K) .EQ. XCOOR(M)) GO TO 608	JTSM0427
605	CONTINUE	JTSM0428
	IF ((XCOOR(M) - XCOOR(INXLPT)) .LT. DISTMN) GO TO 634	JTSM0429
608	NCASE = NCASE + 1	JTSM0430
	XDIST = XCOOR(I) - XCOOR(M)	JTSM0431
	IF (XDIST .EQ. 0.0 .AND. TAN90 .NE. 5.0) GO TO 627	JTSM0432

454

```

YDIST = Y(J) - Y(N)
IF ( XDIST .NE. 0.0 ) CHI = ATAN((Y(J) - Y(N))/XDIST)
IF ( XDIST .EQ. 0.0 ) CHI = PI2
XYDIST = (Y(J) - Y(N))/SIN(CHI)
BETAR = CHI + ALPHO
VERTZ = XYDIST*SIN(BETAR)
HORIZ = XYDIST*COS(BETAR)
IF ( XDIST .NE. 0.0 ) GO TO 610
CALL ROCK(CORK,PHORK,SINRK,COSRK,TANRK,SIG1,SIG3,PI4,PI2,
1CORK2K,BETAR,AFACT,BFACT,ETA,XCTPTF,DELTA3,TAUFR,TAN90,PRI90)
TAU90 = ((DELTA3*VERTZ+TAUFR*HORIZ)*COSALP - TAUFR*VERTZ*SINALP)/
1 YDIST
STR90 = ((DELTA3*VERTZ+TAUFR*HORIZ)*SINALP + TAUFR*VERTZ*COSALP)*
1 TANJT/YDIST + TAU90
GO TO 627
610 BETA = (CHI + ALPHO)*180.0/PI
CALL ROCK(CORK,PHORK,SINRK,COSRK,TANRK,SIG1,SIG3,PI4,PI2,
1CORK2K,BETAR,AFACT,BFACT,ETA,XCTPTF,DELTA3,TAUFR,TANIDX,PRIMIN)
F3FR = DELTA3*VERTZ + TAUFR*HORIZ
F1FR = TAUFR*VERTZ
TAU = F3FR*COSALP - F1FR*SINALP
PER = F3FR*SINALP + F1FR*COSALP
STR = PER*TANJT + TAU
GO TO 628
627 BETA = 90.0 + ALPHA
PRIMIN = PRI90
TANIDX = TAN90
STR = STR90*YDIST
TAU = TAU90*YDIST
628 STRCSE = STR + AISM(N,M)
IF ( STRCSE .LE. STRLOW ) STRLOW = STRCSE
IF ( STRCSE .EQ. STRLOW ) TAUCSE = TAU + TAUSM(N,M)
IF ( STRCSE .EQ. STRLOW ) ITHCSE = N*NXCORS + M
IF ( STRCSE .EQ. STRLOW .AND. J-N .GT. NTRAN(MM) ) NTRAN(MM) = J-N
INXLPT = M
IF ( FLIM .OR. FLAM ) GO TO 634

```

```

JTSM0433
JTSM0434
JTSM0435
JTSM0436
JTSM0437
JTSM0438
JTSM0439
JTSM0440
JTSM0441
JTSM0442
JTSM0443
JTSM0444
JTSM0445
JTSM0446
JTSM0447
JTSM0448
JTSM0449
JTSM0450
JTSM0451
JTSM0452
JTSM0453
JTSM0454
JTSM0455
JTSM0456
JTSM0457
JTSM0458
JTSM0459
JTSM0460
JTSM0461
JTSM0462
JTSM0463
JTSM0464
JTSM0465
JTSM0466
JTSM0467
JTSM0468

```

455

	WRITE (6, 1092) NCASE, N, Y(N), XCOOR(M), BETA, STR, AISM(N,M),	JTSM0469
	1 STRCSE, PRIMIN	JTSM0470
	IF (TANIDX .EQ. -1.0) WRITE (6,1093)	JTSM0471
	IF (TANIDX .EQ. 0.0) WRITE (6,1094)	JTSM0472
	IF (TANIDX .EQ. 1.0) WRITE (6,1095)	JTSM0473
	IF (TANIDX .EQ. 2.0) WRITE (6,1097)	JTSM0474
634	CONTINUE	JTSM0475
635	CONTINUE	JTSM0476
	AISM(J,I) = STRLOW	JTSM0477
	MINPTH(J,I) = ITHCSE	JTSM0478
	TAUSM(J,I) = TAUCSE	JTSM0479
	IF (I .EQ. NXCORS .AND. AISM(J,I) .LE. STRXXX) STRXXX=AISM(J,I)	JTSM0480
	IF (I .EQ. NXCORS .AND. AISM(J,I) .LE. STRXXX) INDY = J	JTSM0481
	IF (FLIM .OR. FLAM) GO TO 680	JTSM0482
	WRITE (6, 1098) Y(J), XCOOR(I), AISM(J,I)	JTSM0483
680	CONTINUE	JTSM0484
700	CONTINUE	JTSM0485
	THIS PART FINDS THE MINIMUM VALUE OF STRENGTH FOR THE	JTSM0486
	SECTION AND THE CORRESPONDING FAILURE PATH.	JTSM0487
703	FIN = .FALSE.	JTSM0488
	FAM = .FALSE.	JTSM0489
	STAISM(MM) = STRXXX	JTSM0490
	INDYY = INDY	JTSM0491
	INDX = NXCORS	JTSM0492
	IF (FLAM) GO TO 720	JTSM0493
	STRREP = AISMJT*XDIM	JTSM0494
	STREG = STRREF*PERCMX/100.0 + AISMRK*XDIM*(1.0-PERCMX/100.0)	JTSM0495
	WRITE (6, 1100) STRXXX, STREG, PERCMX, STRREF	JTSM0496
	WRITE (6,1101) Y(INDY), XCOOR(NXCORS)	JTSM0497
720	IF (INDY .EQ. 1) GO TO 725	JTSM0498
	INDPTH = MINPTH(INDY,INDX)	JTSM0499
	INDY = INDPTH/NXCORS	JTSM0500
	INDX = INDPTH - INDY*NXCORS	JTSM0501
	IF (.NOT. FLAM) WRITE (6,1102) Y(INDY), XCOOR(INDX)	JTSM0502
725	IF (INDY .EQ. 1) FIN = .TRUE.	JTSM0503
	IF (INDX .EQ. 1) FAM = .TRUE.	JTSM0504

	IF (FIN .AND. .NOT. FLAM) WRITE (6,1102) Y(1), XCOOR(1)	JTSM0505
	IF (FIN) GO TO 775	JTSM0506
	IF (FAM .AND. .NOT. FLAM) WRITE (6,1102) Y(INDY), XCOOR(1)	JTSM0507
	IF (FAM) GO TO 775	JTSM0508
	GO TO 720	JTSM0509
775	IF (.NOT.FLAM) WRITE (6, 1103)	JTSM0510
	DO 780 I = 1, JPL	JTSM0511
	IF (Y(INDY) .EQ. Y(I)) NTRAN1 = I	JTSM0512
	IF (Y(INDYY) .EQ. Y(I)) NTRAN2 = I	JTSM0513
780	CONTINUE	JTSM0514
	NTRANS(MM) = NTRAN2 - NTRAN1	JTSM0515
	RHO = ATAN((Y(INDYY) - Y(INDY))/XDIM)	JTSM0516
	PSO = RHO + ALPHO	JTSM0517
	SINPSO = SIN(PSO)	JTSM0518
	COSPSO = COS(PSO)	JTSM0519
	PSI(MM) = PSO*180./PI	JTSM0520
	IF (PSI(MM) .LE. PSIMIN) PSIMIN = PSI(MM)	JTSM0521
	IF (PSI(MM) .GT. PSIMAX) PSIMAX = PSI(MM)	JTSM0522
	PSISUM = PSISUM + PSI(MM)	JTSM0523
	CONSUM = CONSUM + PERMAX(MM)	JTSM0524
	IF (.NOT. FLAM) WRITE (6,1104) PSI(MM)	JTSM0525
	PER = (STAIISM(MM) - TAUSM(INDYY,NXCORS))/TANJT	JTSM0526
	FORTAN = TAUSM(INDYY,NXCORS)*COS(RHO) - PER*SIN(RHO)	JTSM0527
	FORNOR = TAUSM(INDYY,NXCORS)*SIN(RHO) + PER*COS(RHO)	JTSM0528
	DISTFD = XDIM/COS(RHO)	JTSM0529
	APPER1(MM) = 0.0	JTSM0530
	APPER2(MM) = 0.0	JTSM0531
	APPER3(MM) = 0.0	JTSM0532
	AP1MEN(MM) = 0.0	JTSM0533
	AP2MEN(MM) = 0.0	JTSM0534
	AP3MEN(MM) = 0.0	JTSM0535
	IF (NREDOP .GT. 1) GO TO 790	JTSM0536
	IF (NREDOP) 790, 820, 850	JTSM0537
790	NRED1 = -1	JTSM0538
	APPER1(MM) = 100.*{(STRXXX /XDIM)-AISM RK)/(AISMJT-AISM RK)	JTSM0539
	SUMAP1 = SUMAP1 + APPER1(MM)	JTSM0540

457

```

AP1MEN(MM) = SUMAP1/(NREAL-NBUM)
IF ( APPER1(MM) .LE. AP1MIN ) AP1MIN = APPER1(MM)
IF ( APPER1(MM) .GE. AP1MAX ) AP1MAX = APPER1(MM)
IF ( NREDOP .LT. 1 ) GO TO 860
820 NRED2 = 0
IF ( PSO .GT. THETAJ ) REALBD(MM) = 3.0
IF ( PSO .GT. THETAJ ) GO TO 840
DENOMJ = SINPSO*COSPSO + (SINPSO**2)*TANJT
SIG3JJ = SIG1*(1.0 - TANJT/DENOMJ) - COJT/DENOMJ
AISMJJ = (SIG3 - SIG3JJ)*(TANJT*SINPSO**2 + SINPSO*COSPSO)
CALL ROCK(CORK,PHORK,SINRK,COSRK,TANRK,SIG1,SIG3,PI4,PI2,
1CORK2K,PSO,AFACT,BFACT,ETA,XCTPTF,DELTA3,TAUFR,TANIDX,PRIMIN)
DLNORR = DELTA3*SINPSO**2 + 2.0*TAUFR*SINPSO*COSPSO
DLTNRR = DELTA3*SINPSO*COSPSO + TAUFR*(COSPSO**2 - SINPSO**2)
AISMRR = DLNORR*TANJT + DLTNRR
825 STR2DX = FORTAN + FORNOR*TANJT
APPER2(MM) = 100.*((STR2DX/DISTFD) - AISMRR)/(AISMJJ - AISMRR)
SUMAP2 = SUMAP2 + APPER2(MM)
AP2MEN(MM) = SUMAP2/(NREAL-NBUM-NNBUM)
IF ( APPER2(MM) .GE. AP2MAX ) AP2MAX = APPER2(MM)
IF ( APPER2(MM) .LE. AP2MIN ) AP2MIN = APPER2(MM)
840 IF ( NREDOP .LE. 1 ) GO TO 860
850 NRED3 = 1
STRTAN = FORTAN/DISTFD
STRNOR = FORNOR/DISTFD
TANPSO = (SIG1 - SIG3)*SINPSO*COSPSO
PERPSO = SIG1*COSPSO**2 + SIG3*SINPSO**2
TSTTAN = TANPSO + STRTAN
TSTPER = PERPSO - STRNOR
PHOCMB = P*PHOJT + (1.0 - P)*PHORK
APPER3(MM) = (TSTTAN - TSTPER*TAN(PHOCMB))*100./CORK
SUMAP3 = SUMAP3 + APPER3(MM)
AP3MEN(MM) = SUMAP3/(NREAL - NBUM)
IF ( APPER3(MM) .GE. AP3MAX ) AP3MAX = APPER3(MM)
IF ( APPER3(MM) .LE. AP3MIN ) AP3MIN = APPER3(MM)
860 IF ( PSO .LE. THETAJ .OR. NREDOP .EQ. -1 .OR. NREDOP .EQ. 1 )

```

```

JTSM0541
JTSM0542
JTSM0543
JTSM0544
JTSM0545
JTSM0546
JTSM0547
JTSM0548
JTSM0549
JTSM0550
JTSM0551
JTSM0552
JTSM0553
JTSM0554
JTSM0555
JTSM0556
JTSM0557
JTSM0558
JTSM0559
JTSM0560
JTSM0561
JTSM0562
JTSM0563
JTSM0564
JTSM0565
JTSM0566
JTSM0567
JTSM0568
JTSM0569
JTSM0570
JTSM0571
JTSM0572
JTSM0573
JTSM0574
JTSM0575
JTSM0576

```

```

1 REALBD(MM) = 0.0
GO TO 1950
1948 NBUM = NBUM + 1
1950 CONTINUE
WRITE ( 6, 1110)
DO 1960 MM = 1, NOREAL
IF ( REALBD(MM) .NE. 0.0 ) WRITE (6,1112) MM
IF ( REALBD(MM) .EQ. 0.0 .OR. REALBD(MM) .EQ. 3.0 )
1 WRITE (6,1111) MM, JJPL(MM), PERMIN(MM), PERMAX(MM), PSI(MM),
2 STAISM(MM), APPER1(MM), APPER2(MM), APPER3(MM), AP1MEN(MM),
3 AP2MEN(MM), AP3MEN(MM), NTRAN(MM), NTRANS(MM)
1960 CONTINUE
WRITE (6, 1113)
DO 1970 MM = 1, NOREAL
IF ( REALBD(MM) .EQ. 0.0 ) GO TO 1970
IF ( REALBD(MM) .EQ. 1.0 ) WRITE (6, 1021) MM
IF ( REALBD(MM) .EQ. 2.0 ) WRITE (6, 1022) MM
IF ( REALBD(MM) .EQ. 3.0 ) WRITE (6, 1025) MM
IF ( REALBD(MM) .EQ. 4.0 ) WRITE (6, 1024) MM
1970 CONTINUE
NREAL1 = NOREAL - NBUM
NREAL2 = NOREAL - NBUM - NNBUM
IF ( NREAL2 .LT. 3 ) GO TO 2000
IF ( NREDOP .EQ. -1 .OR. NREDOP .GT. 1 ) AP1MAN = SUMAP1/(NREAL1)
IF ( NREDOP .EQ. 0 .OR. NREDOP .GT. 1 ) AP2MAN = SUMAP2/(NREAL2)
IF ( NREDOP .GE. 1 ) AP3MAN = SUMAP2/(NREAL1)
1974 PSIMAN = PSISUM/(NREAL1)
CONMAN = CONSUM/NREAL1
VARAP1 = 0.0
VARAP2 = 0.0
VARAP3 = 0.0
VARPSI = 0.0
VARCON = 0.0
CCAP1 = 0.0
CCAP2 = 0.0
CCAP3 = 0.0

```

```

JTSM0577
JTSM0578
JTSM0579
JTSM0580
JTSM0581
JTSM0582
JTSM0583
JTSM0584
JTSM0585
JTSM0586
JTSM0587
JTSM0588
JTSM0589
JTSM0590
JTSM0591
JTSM0592
JTSM0593
JTSM0594
JTSM0595
JTSM0596
JTSM0597
JTSM0598
JTSM0599
JTSM0600
JTSM0601
JTSM0602
JTSM0603
JTSM0604
JTSM0605
JTSM0606
JTSM0607
JTSM0608
JTSM0609
JTSM0610
JTSM0611
JTSM0612

```

```

DO 1980 I = 1, NREAL
IF ( REALBD(I) .EQ. 1.0 .OR. REALBD(I) .EQ. 2.0 .OR.
1 REALBD(I) .EQ. 4.0 ) GO TO 1980
VARPSI = VARPSI + (PSI(I) - PSIMAN)**2
VARCON = VARCON + (CONMAN - PERMAX(I))**2
IF ( NREDOP .EQ. -1 .OR. NREDOP .GT. 1 )
1VARAP1 = VARAP1 + (APPER1(I) - AP1MAN)**2
IF ( NREDOP .EQ. -1 .OR. NREDOP .GT. 1 )
1CCAP1 = (APPER1(I) - AP1MAN)*(PSI(I) - PSIMAN) + CCAP1
IF ( NREDOP .GE. 1 )
1VARAP3 = VARAP3 + (APPER3(I) - AP3MAN)**2
IF ( NREDOP .GE. 1 )
1CCAP3 = (APPER3(I) - AP3MAN)*(PSI(I) - PSIMAN) + CCAP3
IF ( REALBD(I) .EQ. 3.0 ) GO TO 1980
IF ( NREDOP .EQ. 0 .OR. NREDOP .GT. 1 )
1VARAP2 = VARAP2 + (APPER2(I) - AP2MAN)**2
IF ( NREDOP .EQ. 0 .OR. NREDOP .GT. 1 )
1CCAP2 = (APPER2(I) - AP2MAN)*(PSI(I) - PSIMAN) + CCAP2
1980 CONTINUE
SD1 = (VARAP1/NREAL1)**0.5
SD2 = (VARAP2/NREAL2)**0.5
SD3 = (VARAP3/NREAL1)**0.5
SDPSI = (VARPSI/NREAL1)**0.5
SDCON = (VARCON/NREAL1)**0.5
IF ( SDPSI .EQ. 0.0 ) GO TO 1983
IF ( VARAP1 .NE. 0.0 ) CC1 = CCAP1/(SD1*SDPSI*NREAL1)
IF ( VARAP2 .NE. 0.0 ) CC2 = CCAP2/(SD2*SDPSI*NREAL2)
IF ( VARAP3 .NE. 0.0 ) CC3 = CCAP3/(SD3*SDPSI*NREAL1)
1983 WRITE (6,1122) NREAL1, PSIMAN, PSIMIN, PSIMAX, SDPSI
WRITE (6,1123) NREAL1, CCONMAN, CONMIN, CONMAX, SDCON
IF ( NREDOP .EQ. -1 .OR. NREDOP .GT. 1 )
1WRITE (6, 1124) NRED1, NREAL1, AP1MAN, AP1MIN, AP1MAX, SD1, CC1
IF ( NREDOP .EQ. 0 .OR. NREDOP .GT. 1 )
1WRITE (6, 1124) NRED2, NREAL2, AP2MAN, AP2MIN, AP2MAX, SD2, CC2
IF ( NREDOP .GE. 1 )
1WRITE (6, 1124) NRED3, NREAL1, AP3MAN, AP3MIN, AP3MAX, SD3, CC3

```

```

JTSM0613
JTSM0614
JTSM0615
JTSM0616
JTSM0617
JTSM0618
JTSM0619
JTSM0620
JTSM0621
JTSM0622
JTSM0623
JTSM0624
JTSM0625
JTSM0626
JTSM0627
JTSM0628
JTSM0629
JTSM0630
JTSM0631
JTSM0632
JTSM0633
JTSM0634
JTSM0635
JTSM0636
JTSM0637
JTSM0638
JTSM0639
JTSM0640
JTSM0641
JTSM0642
JTSM0643
JTSM0644
JTSM0645
JTSM0646
JTSM0647
JTSM0648

```

460

```

2000 CONTINUE
      STOP
      END
      SUBROUTINE ROCK (CORK, PHORK, SINRK, COSRK, TANRK, SIG1, SIG3, PI4, PI2,
1CORK2K, BETAR, AFACT, BFACT, ETA, XCTPTF, DELTA3, TAUFR, TANIDX, PRIMIN)
      LOGICAL FAM
      FAM = .FALSE.
      IF ( BETAR .LE. PI2 ) XMNTLN = AFACT + BFACT*SIN(2.0*BETAR - ETA)
      IF ( BETAR .GT. PI2 ) XMNTLN = AFACT - BFACT*SIN(2.0*BETAR + ETA)
      IF ( SIG1 .GT. XMNTLN ) GO TO 619
C          THIS PART EXAMINES CIRCLES WITH PURE TENSILE FAILURES
      TANIDX = -1.0
      IF ( BETAR .EQ. PI2 ) XCTR = (SIG1 - XCTPTF)*0.5
      IF ( BETAR .NE. PI2 ) XCTR = 0.5*((SIG1 + XCTPTF)/
1 ((SIN(BETAR))**2.0) - CORK)
      IF ( XCTR .GT. XCTPTF ) GO TO 614
      RADIUS = XCTPTF + XCTR
      IF ( BETAR .GT. PI2 ) FAM = .TRUE.
      GO TO 625
C          THIS PART EXAMINES CIRCLES TANGENT TO THE PARABOLA
614 TANIDX = 0.0
      ZETA1 = PI2
      VERT1 = 2.0*CORK*(SIN(BETAR))**2.0 - XCTPTF
      ZETA2 = ETA
      VERT2 = XMNTLN
615 ZETA = (ZETA1 + ZETA2)/2.0
      XCTR = (CORK*0.5)/((SIN(ZETA))**2.0)
      IF ( BETAR .LE. PI2 ) VERT = XCTR + CORK*SIN(2.0*BETAR - ZETA)/
1 SIN(ZETA)
      IF ( BETAR .GT. PI2 ) VERT = XCTR - CORK*SIN(2.0*BETAR + ZETA)/
1 SIN(ZETA)
      IF ( SIG1 .GT. VERT .AND. SIG1 .LE. VERT2 ) VERT1 = VERT
      IF ( SIG1 .GT. VERT1 .AND. SIG1 .LE. VERT2 ) ZETA1 = ZETA
      IF ( SIG1 .GT. VERT1 .AND. SIG1 .LE. VERT ) VERT2 = VERT
      IF ( SIG1 .GT. VERT1 .AND. SIG1 .LE. VERT ) ZETA2 = ZETA
      ADVERT = ABS(VERT - SIG1)

```

```

JTSM0649
JTSM0650
JTSM0651
JTSM0652
JTSM0653
JTSM0654
JTSM0655
JTSM0656
JTSM0657
JTSM0658
JTSM0659
JTSM0660
JTSM0661
JTSM0662
JTSM0663
JTSM0664
JTSM0665
JTSM0666
JTSM0667
JTSM0668
JTSM0669
JTSM0670
JTSM0671
JTSM0672
JTSM0673
JTSM0674
JTSM0675
JTSM0676
JTSM0677
JTSM0678
JTSM0679
JTSM0680
JTSM0681
JTSM0682
JTSM0683
JTSM0684

```

```

IF ( ABVERT .GE. CORK2K ) GO TO 615
RADIUS = CORK/SIN(ZETA)
ZETA45 = ZETA*0.5 + PI4
ZETA35 = 3.0*PI4 - ZETA*0.5
IF ( BETAR .GT. ZETA45 .AND. BETAR .LE. PI2 ) FAM = .TRUE.
IF ( BETAR .GT. ZETA35 ) FAM = .TRUE.
GO TO 625

```

```

JTSM0685
JTSM0686
JTSM0687
JTSM0688
JTSM0689
JTSM0690
JTSM0691
JTSM0692
JTSM0693
JTSM0694
JTSM0695
JTSM0696
JTSM0697
JTSM0698
JTSM0699
JTSM0700
JTSM0701
JTSM0702
JTSM0703
JTSM0704
JTSM0705
JTSM0706
JTSM0707
JTSM0708
JTSM0709
JTSM0710
JTSM0711
JTSM0712
JTSM0713
JTSM0714
JTSM0715
JTSM0716
JTSM0717
JTSM0718
JTSM0719
JTSM0720

```

C

THIS PART EXAMINES CIRCLES TANGENT TO THE STRAIGHT LINE

```

619 IF ( BETAR .LE. PI2 ) QFACT = SIN(2.0*BETAR - PHORK)
IF ( BETAR .GT. PI2 ) QFACT = -SIN(2.0*BETAR + PHORK)
XMXTLN = CORK*QFACT*COSRK + CORK*TANRK*(1.0 + QFACT*SINRK)
IF ( PHORK .LE. PI4 .OR. SIG1 .GT. XMXTLN ) GO TO 624
TANIDX = 2.0
ZETA1 = PI4
VERT1 = XMNTLN
ZETA2 = PHORK
VERT2 = XMXTLN
622 ZETA = (ZETA1 + ZETA2)/2.0
IF ( BETAR .LE. PI2 ) RFACT = SIN(2.0*BETAR - ZETA)
IF ( BETAR .GT. PI2 ) RFACT = -SIN(2.0*BETAR + ZETA)
VERT = CORK*RFACT*COS(ZETA)+CORK*TAN(ZETA)*(1.0+RFACT*SIN(ZETA))
IF ( SIG1 .GT. VERT .AND. SIG1 .LE. VERT2 ) VERT1 = VERT
IF ( SIG1 .GT. VERT .AND. SIG1 .LE. VERT2 ) ZETA1 = ZETA
IF ( SIG1 .GT. VERT1 .AND. SIG1 .LE. VERT ) VERT2 = VERT
IF ( SIG1 .GT. VERT1 .AND. SIG1 .LE. VERT ) ZETA2 = ZETA
ABVERT = ABS(VERT - SIG1)
IF ( ABVERT .GE. CORK2K ) GO TO 622
XCTR = CORK*TAN(ZETA)
RADIUS = (XCTR**2.0 + CORK**2.0)**0.5
ZETA45 = ZETA*0.5 + PI4
ZETA35 = 3.0*PI4 - ZETA*0.5
IF ( BETAR .GT. ZETA45 .AND. BETAR .LE. PI2 ) FAM = .TRUE.
IF ( BETAR .GT. ZETA35 ) FAM = .TRUE.
GO TO 625
624 TANIDX = 1.0
XCTR = (SIG1 - CORK*QFACT*COSRK)/(1.0 + QFACT*SINRK)

```

462

```
RADIUS = (CORK/TANRK + XCTR)*SINRK
IF ( BETAR .GT. PI4 +PHORK*0.5 .AND. BETAR .LE. PI2 ) FAM = .TRUE.
IF ( BETAR .GT. 3*PI4 - PHORK*0.5 ) FAM = .TRUE.
625 TAUFR = ( ABS(RADIUS**2 - (SIG1-XCTR)**2) )**0.5
PRIMIN = XCTR - RADIUS
626 IF (FAM) TAUFR = (-1.0)*TAUFR
DELTA3 = SIG3 - (2.0*XCTR - SIG1)
RETURN
END
```

```
JTSM0721
JTSM0722
JTSM0723
JTSM0724
JTSM0725
JTSM0726
JTSM0727
JTSM0728
JTSM0729
```